Characterisation of T cell specificity, functional, activation and memory profiles associated with QuantiFERON TB Gold conversion and reversion.

Cheleka Anne-Marie Mpande

Thesis Presented for the Degree of

DOCTOR OF PHILOSOPHY

in the Department of Pathology

Faculty of Health Sciences

UNIVERSITY OF CAPE TOWN

On the 7th of April 2021

Supervisor: Associate Professor Elisa Nemes

Co-supervisors: Professor Thomas J. Scriba and Dr Virginie Rozot

University of Cape Town

The copyright of this thesis vests in the author. No quotation from it or information derived from it is to be published without full acknowledgement of the source. The thesis is to be used for private study or non-commercial research purposes only.

Published by the University of Cape Town (UCT) in terms of the non-exclusive license granted to UCT by the author.

University of Cape Town

The copyright of this thesis vests in the author. No quotation from it or information derived from it is to be published without full acknowledgement of the source. The thesis is to be used for private study or non- commercial research purposes only.

Published by the University of Cape Town (UCT) in terms of the non-exclusive license granted to UCT by the author.

Declaration

I, Cheleka Anne-Marie Mpande, hereby declare that the work on which this thesis is based is my original work (except where acknowledgements indicate otherwise) and that neither the whole work nor any part of it has been, is being, or is to be submitted for another degree in this or any other university.

I empower the university to reproduce, for the purpose of research, either the whole or any portion of the contents in any manner whatsoever.

Signature: Signed by candidate

Date: 7th April 2021

I confirm that I have been granted permission by the University of Cape Town's Doctoral Degrees Board to include the following publication(s) in my PhD thesis, and where co-authorships are involved, my co-authors have agreed that I may include the publications:

Mpande, C.A.M., Dintwe, O.B., Musvosvi, M., et al. (2018). Functional, Antigen-Specific Stem Cell Memory (TSCM) CD4+ T Cells Are Induced by Human Mycobacterium tuberculosis Infection. Front Immunol *9*, 324.

Mpande, C.A.M., Rozot, V., Mosito, B., et al. (2021). Immune profiling of Mycobacterium tuberculosis-specific T cells in recent and remote infection. EBioMedicine 64, 103233.

Mpande, C.A.M., Musvosvi, M., Rozot, V., et al. (2021). Antigen-specific T Cell Activation Distinguishes Between Recent and Remote Tuberculosis Infection. Am J Resp Crit Care *148*, 1292–1297.

Signature: Signed by candidate

Student Name: Cheleka Anne-Marie Mpande Student Number: MPNCHE001

Date: 7th April 2021

Acknowledgments

Gaawsh it's finally over, mini-me envisioned this 20 years ago and it has finally happened. It may not have been the journey I had planned but it's definitely been a journey I am very proud of taking.

Ukutangila teku fika

(Bemba proverb, translation: Finishing ahead, does not mean you have reached)

This mantra has kept me going through the last 3 years, during the times I felt my progress was not good enough.

It takes a village to raise a child, and it definitely has taken one to raise this scientist. There are so many people who have contributed in some way, who have advised, mentored, and supported me. I thank you all very much, these words are not enough to express my gratitude.

I would like to thank my family for supporting me through this, and most importantly my Mother. From the moment I told you I wanted to pursue a medical research career, you ensured I had a plan and I was aware of the sacrifices and choices I was making. The reasons I have plans A to C is because of you. Thank you, Mum, for being my number one supporter.

Koloma Son, honorary SATVI member ☺, you have seen all the ups and downs of this journey. You have been my companion during late nights of lab work and helped me figure out ways to stop FlowJo from crashing. Without you, this would have been a bleak journey.

To my supervisors, Elisa, Virginie and Tom, thank you for the opportunity to take on this project. It's been 7 years and I am so *shooketh* and overwhelmed at how much work we have accomplished. Thank you for challenging, trusting and guiding me through this journey. It's been great learning from you and becoming a TB immunologist under your mentorship. **I believe there is no other place that would have given me as much exposure to top class TB research.**

Boitumelo, Constance and Tim, thank you for contributing your time and helping with the last stretch of lab work. Munya, there are no words to express my gratitude for all the help you gave me. The only reason I can *flake* through R is because of you.

The Corner Office ☺, you really made my PhD journey so much easier and happier. Our random chats were literally the highlight of my long lab days, thank you so much. Sherazaan, thank you for always reminding me to be patient with myself.

Everyone at SATVI in Cape Town and Worcester, thank you for being part of this journey. I am glad that my project gave me the opportunity to work with almost every *arm of SATVI* from the CRWs, the Worcester/Cape town Lab members to Ethics and Admin.

Last but not least, The PARTICIPANTs, none of this would have been possible without your consent and enthusiasm to take part in the research projects, thank you. Thank you to all the funders: SA MRC, SA NRF, US NIH, UCT and many more institutions who have provided financial assistance to do this research.

Summary

Recent acquisition of *Mycobacterium tuberculosis* (M.tb) infection is associated with a higher risk of tuberculosis disease, compared with remote, asymptomatic infection. M.tb infection, defined by a positive tuberculin skin test (TST) and/or IFN-γ-release assay [IGRA e.g. QuantiFERON TB GOLD (QFT)], is commonly thought to be a chronic state. However, longitudinal studies have demonstrated the dynamic nature of M.tb infection, whereby TSTs and IGRAs revert from a positive to a negative test in some individuals, possibly an indication of bacterial clearance. Despite the first observation of discordant serial TST results over 80 years ago and the wide use of TSTs/IGRAs, there is still a limited understanding of immunological features associated with different stages of M.tb infection and discordant serial TST/IGRA results. Most studies of M.tb-specific immune responses in humans are based on cross-sectional comparisons between M.tb infection and active disease, with very few large cohort studies enabling a longitudinal assessment of different phases of infection. Thus, the main objective of this thesis was to gain a better understanding of changes in M.tb-specific CD4 T cell functional, memory and activation profiles associated with QFT conversion (acquisition of M.tb infection) and reversion (potential M.tb clearance).

Our first aim was to characterise the homing, cytotoxic and functional capacity of M.tb-specific memory CD4+ T cells during recent and remote M.tb infection, with a special focus on stem cell memory T (T_{SCM}) cells. T_{SCM} cells play a critical role in maintaining long-lasting immunity, demonstrated by their superior longevity, proliferation and differentiation capacity compared to central memory (T_{CM}) and effector (T_E) cells. Before this study, our knowledge of T_{SCM} cells was primarily based on virus-specific CD8+ T_{SCM} cells. We demonstrate that M.tb-specific CD4+ T_{SCM} cells are induced upon recent M.tb infection and maintained at steady-state during established infection. Despite being the least differentiated M.tb-specific memory subset and representing <10% of total memory cells, M.tb-specific CD4+ T_{SCM} cells expressed CXCR3, TNF and IL-2, as well as IFN-γ, granzyme A and granzyme K, molecules expressed during high antigen exposure. These results suggest that CD4+ T_{SCM} cells are a suitable T cell population that could be targeted by vaccination.

We then focused on gaining a broader understanding of T cell immunobiology associated with recent acquisition of M.tb infection. Since tuberculosis risk is highest within the first two years

of recent compared to remote (>2 years) M.tb infection, we also aimed to define an M.tb-specific T cell biomarker that can distinguish between the two infection states as current diagnostics fail to do so. Our second major finding demonstrated that recently infected individuals have lower proportions of highly differentiated IFN-γ+TNF+KLRG-1+ CD4+ T_E cells and higher proportions of early differentiated IFN-γ-TNF+IL2+KLRG-1- CD4+ T cells than remotely infected individuals in response to M.tb lysate but not CFP-10/ESAT-6 stimulation. Akin to their recent M.tb exposure, recently infected individuals had higher levels of T cell activation, regardless of M.tb antigen specificity, than remotely infected individuals. The degree of M.tb-specific CD4 T cell activation was identified as the best candidate biomarker for recent infection. The very same biomarker could also distinguish between progressors and non-progressors and identify individuals with active tuberculosis disease among healthy individuals with remote M.tb infection. We propose that, upon large-scale clinical validation, the T cell activation biomarker could be used as a screening test in conjunction with current tuberculosis diagnostics to guide the provision of either preventive or full tuberculosis therapy. These results have very important implications for targeting provision of preventive treatment to M.tb infected individuals at high-risk of tuberculosis, which is one of the top 10 strategies required to achieve tuberculosis elimination targets.

Based on data from observational studies conducted during the pre-antibiotic era and guinea pig tuberculosis models, TST/IGRA reversion in humans is hypothesised to be associated with spontaneous (natural) clearance of infection. Similarly, individuals recently exposed to patients with tuberculosis who did not convert TST/IGRA (termed resistors) nor develop disease had M.tb-specific T cell responses that did not include IFN-γ production. However, clearance of M.tb infection is virtually impossible to demonstrate in healthy individuals. We clearly illustrated that acquisition infection is associated with induction of CD4+ Th1 functional and memory T cell subsets associated with increased antigen burden. We thus hypothesised that if reversion represents natural M.tb infection clearance then immune responses post-QFT reversion, if detectable, would be predominantly T_{SCM}/T_{CM} cells that have an IFN-γ independent cytokine expression profile and low T cell activation levels. Interestingly, QFT reversion was not associated with a decrease in CFP-10/ESAT-6-specific IFN-γ+ CD4 T cell responses detected by flow cytometry. Overall, CD4 T cell responses to CFP-10/ESAT-6 in

reverters were of intermediate magnitude between non-converters and remotely infected individuals. These responses were very low in most reverters (regardless of QFT status), which may explain fluctuations around the QFT assay cut-off resulting in reversion of the test. In the reverters who had low but robustly detectable responses, CFP-10/ESAT-6-specific CD4 T cells showed low levels of M.tb-specific T cell activation, maintenance of both IFN-γ dependent and independent Th1 cytokine co-expressing profiles and a predominantly T_{TM}/T_E phenotype. Memory and functional profiles detected in reverters in response to M.tb lysate shared more characteristics with non-converters than persistently infected (QFT+) individuals. Based on these results, we conclude that QFT reverters represent a heterogenous population in the tuberculosis spectrum who may experience very low or no *in vivo* antigen exposure.

Altogether, these results indicate that not everyone with a QFT+ test likely experiences on-going *in vivo* M.tb exposure, as suggested by much lower T cell activation observed during remote M.tb infection and QFT reversion compared to recent M.tb infection. Whether ongoing *in vivo* antigen exposure is required to maintain memory responses against M.tb remains to be determined. It is possible that key features of T cell responses against M.tb, including magnitude and differentiation, are shaped by the antigen load experienced during primary infection, regardless of whether infection is subsequently cleared. Answering these questions is critical to inform the interpretation of the current immunodiagnostic assays and to determine who could be spared from preventive tuberculosis therapy. On the other hand, here we defined a biomarker of recent infection and tuberculosis disease, which could enable the provision of targeted treatment to those who would benefit the most.

List of Abbreviations

ACS:	Adolescent cohort study
APC:	Antigen-presenting cell
AU(ROC):	Area under the (receiver operator curve)
BCG:	Bacille Calmette Guerin
BD:	Becton Dickinson
BS:	Brilliant stain
BV:	Brilliant violet
CD:	Cluster of differentiation
CFP-10:	10 kDa culture filtrate antigen
CI:	Confidence Interval
COMPASS:	Combinatorial polyfunctionality analysis of antigen-specific T-cell subsets
DCs:	Dendritic cells
dH_2O:	Distilled water
DURTs:	Donor unrestricted T cells
DMSO:	Dimethyl sulfoxide
DNA:	Deoxyribonucleic acid
EDTA:	Ethylenediaminetetraacetic acid
ELISA:	Enzyme-linked immunosorbent assay
ELISpot:	Enzyme-linked immunospot assay
ESAT-6:	6 kDa early secretory antigenic target
et al.,:	and others
FACS:	Fluorescence activated cell sorting
FBS:	Fetal bovine serum
Fc:	Crystallizable fragment
FCS:	Flow cytometry standard
FMO:	Fluorescence minus one
Grn:	Granzyme
HHC:	Household contacts
HIV:	Human immunodeficiency virus
HLA:	Human leukocyte antigen
HREC:	Human research ethics committee
IFN:	Interferon
Ig:	Immunoglobulin
IGRA:	IFN-γ release assay
IL:	Interleukin
IQR:	Interquartile range
IU/mL:	International units per mL
KLRG-1:	Killer cell lectin-like receptor G1
LAMP:	Lysosomal-associated membrane glycoprotein
LTBI:	Latent tuberculosis infection
MAIT:	Mucosal-associated invariant T
MFI:	Median fluorescent intensity
MHC:	Major histocompatibility complex
MHC I:	MHC class I
MHC II:	MHC class II
MIMOSA:	Mixture models for single-cell assays
µL:	microlitre
mL:	millilitre
mm:	millimetre
MSMD:	Mendelian susceptibility to mycobacterial disease

M.tb:	*Mycobacterium tuberculosis*
MVA-85A:	Modified vaccinia virus Ankara expressing antigen 85A
NAATs:	Nucleic acid amplification tests
NTM:	Non-tuberculous mycobacteria
NK:	Natural Killer
PAMPs:	Pathogen-associated molecular patterns
PBMC:	Peripheral blood mononuclear cells
PBS:	Phosphate buffer saline
PCR:	Polymerase chain reaction
PFA:	Paraformaldehyde
PFC:	Polychromatic flow cytometry
PLHIV:	People living with human immunodeficiency virus
PPD:	Purified M.tb protein derivatives
PRRs:	Pattern recognition receptors
Qdot:	Quantum dots
QFT(-G):	QuantiFERON TB Gold
QFT-GIT:	QuantiFERON TB Gold in tube test
RCF:	Relative centrifugal force
RPMI:	Roswell Park Memorial Institute
RT:	Room temperature
SATVI:	South African Tuberculosis Vaccine Initiative
SDG:	Sustainability Development Goal
SSC:	Side scatter
TCR:	T cell receptor
TB:	Tuberculosis
TBI:	*Mycobacterium tuberculosis* infection
T_{CM}:	Central memory T cell
T_{CNP}:	Cytokine-producing T cells with a naïve phenotype
T_E:	Effector memory T cell
Tfh:	Follicular T helper T cells
Th:	T helper cell
T_N:	Naïve T cell
TNF:	Tumour necrosis factor
T_{NLM}:	Naïve-like memory T cells
TPT:	Tuberculosis preventive therapy
T-reg:	Regulatory T cell
T_{RM}:	Tissue resident T cell
T_{SCM}:	Stem cell memory T cell
T_{TE}/T_{EMRA}:	terminally differentiated effector
T_{TM}:	transitional memory T cell
TST:	Tuberculin skin test
v:	Version
v/v:	Volume per volume
WHO:	World Health Organisation
xg:	Times gravity

List of Figures

Figure 1: Tuberculous granulomas are heterogenous. 8
Figure 2: Commonly known CD4 Th lineages. 11
Figure 3: Functional and phenotypic characteristics of M.tb-specific T cells localised in the lung parenchyma (tissue) and vasculature. 18
Figure 4: Linear model of T cell differentiation. 20
Figure 5: Graphical illustration of the hypothesised spectrum of TBI defined by IGRA/TST responses. 28
Figure 6: Antibody staining temperature does not affect detection of CCR4 and CXCR3 on cryopreserved PBMC.. 47
Figure 7: Comparison of chemokine receptor detection on whole blood and fresh PBMC.. 48
Figure 8: Gating strategy utilised to identify CD4+ dump-(CD8-CD14-CD19-dead-) T cells prior to gating of tetramer signal. 49
Figure 9: BS buffer improves resolution of BV-conjugated markers. 50
Figure 10: Detection of high background in tetramer+ CD4+ T cell population. 51
Figure 11: Flow cytometry plots of tetramer channel (PE) vs combination of memory marker and chemokine receptor antibody staining of total CD4+ T cells (n=2). 52
Figure 12: Dual tetramer staining improves the specificity of tetramer+ signal.. 54
Figure 13: Optimisation of the lineage and memory marker staining protocol for the cytotoxic T cell panel. 56
Figure 14: Longitudinal (A) QFT and (B) TST results of recent M.tb infected adolescents. 61
Figure 15: Gating strategy for M.tb-tetramer+ sorting and functional characterisation. 65
Figure 16: Defining the limit of detection of tetramer+ CD4 T cells. 67
Figure 17: Detection of memory markers and subsets on M.tb-tetramer+ is affected by cryopreservation and/or antibody fluorochrome. 68
Figure 18: Detection of M.tb-tetramer+ cells in recent QFT converters.. 69
Figure 19: M.tb-specific T_{SCM} cells are detected in recently M.tb infected adolescents. 70
Figure 20: M.tb-specific T_{CM} cells are the predominant memory subset once TBI is established. 71
Figure 21: Distribution of M.tb-specific memory subsets is not affected by cryopreservation. 72
Figure 22: M.tb-specific T_{SCM} cells are not naïve cells and express distinct homing and cytotoxic profiles from bulk T_{SCM} cells.. 74
Figure 23: M.tb-specific T_{SCM} cells share some chemokine receptor and cytotoxic molecule expression profiles with bulk memory T cells.. 75
Figure 24: M.tb-specific T_{SCM} cells have the least differentiated chemokine receptor co-expression profile.. 77
Figure 25: M.tb-specific T_{SCM} cells have the least differentiated cytotoxic co-expression profile.. 78
Figure 26: Gating strategy to detect Th1 cytokine by CD4+ T cells in response to M.tb antigen stimulation. .79
Figure 27: M.tb-specific T_{SCM} cells can be defined using CD45RA and CCR7 staining only. 80
Figure 28: M.tb-specific T_{SCM} cells express Th1 cytokines.). 81
Figure 29: BCG-specific T_{SCM} cells are associated with long-term CD4+ T cell proliferation after vaccination. 82
Figure 30: Stain index for each detector.. 100
Figure 31: (A) Spillover spread matrix, spillover spread of fluorochromes contributed into each (B) and received by each (C) LSR II detector. 101
Figure 32: T cell lineage and functional markers are better detected after treatment with Cytofix/Cytoperm compared to FACS Lyse/Perm II. 103
Figure 33: Comparison of PBMC intracellular cytokine staining protocols for the detection of live CD3, CD4 and CD8 T cells. 105
Figure 34: Comparison of PBMC intracellular cytokine staining protocols for the detection of memory and phenotypic markers on CD4 T cells.. 106
Figure 35: Comparison of PBMC intracellular cytokine staining protocols for the detection of antigen-specific CD4+ T cell functional markers. 106
Figure 36: Frequencies of functional CD4 and CD8 T cells in response to different concentrations of M.tb antigens.. 108
Figure 37: Stimulation in the presence of serum free media did not reduce detection of non-specific background responses nor increase detection of antigen-specific responses. 109
Figure 38: Use of AB serum does not improve detection of functional responses. 110
Figure 39: Use of co-stimulatory molecules suggestively increases CD4 T cell background functional activity.). 111
Figure 40: Use of co-stimulatory molecules did not significantly improve induction of functional responses. 112

Figure 41: Cohort QFT Kinetics. 120
Figure 42: Gating strategy used to identify M.tb-lysate responsive T cells in the TB progressor cohort.. 124
Figure 43: Analysis pipeline.. 126
Figure 44: Gating strategy used to identify live M.tb-responsive CD3, CD4 and CD8 T cells. 127
Figure 45: Recent vs remote TBI CITRUS analysis result. 131
Figure 46: Analysis pipeline used to confirm CITRUS cluster co-expression profiles. 132
Figure 47: Representative flow cytometry histogram overlay of HLA-DR expression levels by IFN-γ+TNF+ CD3+ T cells (black) and total CD3 T cells (blue), and how Δ (Delta) HLA-DR MFI was calculated. 133
Figure 48: Acute TBI is associated with high proportions of activated M.tb-specific CD4 T cells which significantly decrease once TBI is established. 135
Figure 49: CFP-10/ESAT-6-specific IFN-γ+ CD4 T cells detected by flow cytometry correlate with QFT responses. 7. 136
Figure 50: Remote TBI is associated with persistent detection of IFN-γ+ and IFN-γ-independent functional CD4 T cell responses.. 137
Figure 51: Polyfunctional cytokine co-expression capacity is stable during remote TBI. 138
Figure 52: Remote TBI is associated with low levels of CD4 T cell activation.. 139
Figure 53: T_{TM} and T_E cells are the predominant memory phenotype during remote TBI. 140
Figure 54: Recent TBI is associated with induction of functional responses which are observed in similar ranges as remote TBI. 142
Figure 55: Recent TBI is associated with a decrease in less differentiated T cell subsets, and predominantly differentiated polyfunctional and memory T cell subsets which are similar between recent and remote TBI. 144
Figure 56: Recent TBI in associated with a decrease in less differentiated IFN-γ+-independent TSCM and TCM subsets, and an increase in T_E polyfunctional T cell subsets. 147
Figure 57: TBI is associated with higher levels T cell activation compared with remote TBI. 148
Figure 58: T cell activation is a potential biomarker of recent TBI. 150
Figure 59: M.tb-specific IFN-γ+TNF+ CD3+ T cell activation biomarker distinguishes recent and remote TBI. 153
Figure 60: ΔHLA-DR MFI biomarker distinguishes remote TBI from recent TBI or tuberculosis. 155
Figure 61: Mycobacteria-specific T cells in tuberculosis progressors are more activated than those in non-progressors. 156
Figure 62: QFT results. 168
Figure 63: Gating strategy for detection of functional responses by lymphocytes. 169
Figure 64: Calculation of median responses based on QFT status.. 171
Figure 65: Analysis pipeline used to define a single FCS file per participant-QFT status.. 172
Figure 66: Lymphocyte and CD4 T cell Analysis Pipeline.. 174
Figure 67: TST results. 175
Figure 68: CD4 T cells are the main source of IFN-γ in QFT+ individuals.. 177
Figure 69: QFT reversion is not associated with a decrease in IFN-γ+ CD4 T cells detected by flow cytometry. 179
Figure 70: Immunodominant M.tb-specific IFN-γ+ CD4 T cells are maintained at similar frequencies during QFT reversion.. 181
Figure 71: QFT reverters maintain expression of TNF and IL-2 cytokines. 182
Figure 72: M.tb-specific CD154+ and CD107+ responses are detected similar levels regardless of stage of M.tb infection. 184
Figure 73: Polyfunctionality score and polyfunctional profiles are not significantly diffe rent between pre- and post- reversion. 185
Figure 74: Reverters have lower CFP-10/ESAT-6-specific functional differentiation than remote M.tb infected individuals. 188
Figure 75: Reversion is not associated with a shift in T cell memory composition. 190
Figure 76: M.tb-specific CXCR3 expression levels are not different between groups. 190
Figure 77: M.tb lysate-specific memory/functional profiles induced upon M.tb infection are sustained once TBI is established even upon QFT reversion. 193
Figure 78: CFP-10/ESAT-6-specific memory/functional co-expression patterns are different between LTBI and reverters.. 194
Figure 79: Reverters have low T cell activation. 195

Figure 80: Magnitude and duration of M.tb exposure shape M.tb-specific immune responses.. 200
Figure 81: Length of M.tb-exposure governs the composition of M.tb-specific memory subsets, which follows a predominantly linear T cell differentiation model.. 202
Figure 82: M.tb-specific T cell activation tracks the tuberculosis spectrum.. 206

List of Table

Table 1: T cell features that distinguish between TBI and tuberculosis diseases and may track antigen load. 30
Table 2: Participant inclusion criteria. 38
Table 3: BD LSR Fortessa Configuration. 41
Table 4: PBMC phenotypic marker panel. 42
Table 5: Chemokine receptor antibody cocktail. 42
Table 6: HLA-class II tetramer-peptide conjugates. 43
Table 7: Phenotypic antibody cocktail. 43
Table 8: Phenotypic markers antibody cocktail. 45
Table 9: Anti-chemokine receptor antibodies used to detect chemokine receptor expression profiles of CD4+ T cells from fresh PBMC stained using flow cytometry panel 2. 62
Table 10: Distribution of HLA-class II tetramer-peptides stained for each flow cytometry panel. 63
Table 11: Lineage and memory markers used across different panels. 63
Table 12: Antibodies used to detect cytotoxic molecule co-expression profiles of CD4+ T cells from cryopreserved PBMC stained using flow cytometry panel 3. 64
Table 13: BD LSR II Flow Cytometer Configuration. 90
Table 14: Phenotypic molecules used to stain flow cytometry panel 1. 91
Table 15: Phenotypic molecule flow cytometry panel 2. 91
Table 16: Phenotypic antibodies used for permeabilisation optimisation experiment. 93
Table 17: Phenotypic antibodies used in antibody cocktail for protocol 1. 95
Table 18: Phenotypic and functional antibodies used in antibody cocktail for protocol 2. 96
Table 19: Antibody-fluorochrome and detector combinations measured to determine stain index and spillover spread. 100
Table 20: Final flow cytometry panel designed to achieve aims outlined Chapters 5 and 6. 102
Table 21: Cohort demographics. 122
Table 22: Antibody clones and volumes for staining lineage and phenotypic markers. 123
Table 23: Antibody clones and volumes used for staining functional markers. 123
Table 24: mRNA transcripts targeted by single cell phenotyping primers. 124
Table 25: Number of differentially expressed clusters identified between 2 groups using CITRUS. 145
Table 26: Memory-cytokine expression profile of differentially expressed clusters between 2 groups. 146
Table 27: AUROC comparison of potential biomarkers of recent TBI 151
Table 28: Interpretation of ΔHLA-DR MFI biomarker test results. 154
Table 29: Interpretation of Δ HLA-DR MFI biomarker on the test cohort. 156
Table 30: Cohort Demographics. 168
Table 31: QFT and TST concordance. 175
Table 32: Proportions of M.tb-specific IFN-γ+ lymphocyte responders. 176
Table 33: Antigen-specific Th1+ CD4 T cell responders. 187
Table 34: Number of differentially expressed clusters identified between 2 groups using CITRUS. 192

List of Equations

Equation 1: Calculation of stain index 46
Equation 2: Calculation of signal:noise ratio 46
Equation 3: Functional Differentiation Score calculation. 132
Equation 4: HLA-DR MFI ratio calculation. 133
Equation 5: ΔHLADR MFI calculation. 133

Table of Contents

Declaration ..... ***ii***

Acknowledgments ..... ***iv***

Summary ..... ***vi***

List of Abbreviations ..... ***ix***

List of Figures ..... ***xi***

List of Table ..... ***xiv***

List of Equations ..... ***xv***

Chapter 1: General Introduction ***1***

Tuberculosis is a global threat. **1**
Diagnosis and treatment of tuberculosis 3
Plans to reduce tuberculosis burden 4

Infection and Immunity: An overview of M.tb-specific T cell immunity **7**
Innate cells: first responders 7
Role of CD4 T cells in tuberculosis pathogenesis 9
Do other adaptive immune cells, CD8 T cells and B cells, play a role in TBI and disease? 21

Immunodiagnostics for TBI **22**
TST 23
IGRAs 23

Clinical use of TBI diagnostics for monitoring acquisition and clearance of TBI **24**
Challenges with serial IGRA (and TST) testing 24

Spectrum of TBI **26**
Absence of TBI 26
Resisters 26
Classical TBI: recent and established infection 29
Reverters 31

Aims and objectives of this thesis **34**
Thesis objectives and hypotheses. 34

Chapter 2: Optimisation of chemokine receptor and cytotoxic molecule staining to detect M.tb-tetramer+ CD4 T cells ***36***

Introduction **36**
Specific Objectives 37

Materials and Methods **38**
Participant samples and ethics 38
Sample preparation 38
Optimisation of flow cytometry staining protocols 40
Data Analysis 45

Results and Discussion **46**
Chemokine receptor antibody staining of cryopreserved PBMC at 37°C does not improve detection. 46
Comparison of chemokine receptor detection on whole blood and fresh PBMC samples 47
BD Brilliant Stain Buffer improves resolution of BV-conjugated antibodies 49
Detection of tetramer+ CD4+ T cells is improved by dual tetramer staining 53
Optimisation of cytotoxic molecule staining 55

Conclusion **56**

Contributions **57**

Chapter 3: Phenotypic and functional characterisation of M. tuberculosis-specific stem cell memory (T_{SCM}) CD4+ T cells. *58*

Introduction **58**
Objectives 60

Materials and Methods **60**
Participant samples and ethics 60
PBMC isolation and cryopreservation 61
Flow cytometry staining protocol 61
Data Analysis 64

Results **66**
Tetramer Detection limit 66
Definition of T_{SCM} phenotypes 67
M.tb-specific T_{SCM} cells are induced by primary TBI 68
M.tb-specific T_{SCM} cells express chemokine receptor and cytotoxic profiles distinct from bulk T_N and T_{SCM} CD4 T cells. 72
M.tb-specific CD4 T_{SCM} are the least differentiated M.tb-specific memory subset 75
M.tb-specific T_{SCM} CD4 T cells express Th1 cytokines 79
BCG-Specific T_{SCM} cell frequencies are associated with CD4+ T Cell proliferative capacity 81

Discussion **82**

Contributions **86**

Chapter 4: Optimisation of PBMC stimulation and intracellular cytokine staining assay to measure mycobacteria-specific functional responses. *87*

Introduction **87**
Objectives 89

Materials and Methods **89**
Participant samples and ethics 89
BD LSR II flow cytometer configuration 89
Antibodies 90
Defining the stain index and spillover spreading of the BD LSR II flow cytometer 90
Antigens 91
Optimisation of intracellular cytokine staining protocol 92
Optimisation of PBMC stimulation protocol 97
Data analysis 99

Results and Discussion **99**
Panel design: Marker selection 99
Fixation and permeabilisation with Cytofix/Cytoperm is better than FACS Lyse/Perm II Solution 102
Extracellular staining of phenotypic markers has the best resolution 104
Antigen titration 107
Serum free and complete media induce equivalent T cell responses 107
RPMI supplemented with antibody serum does not improve detection of cytokines compared to fetal bovine serum 109
Co-stimulatory molecules anti-CD28/CD49d do not improve induction of mycobacteria-specific functional responses in an 18 hour stimulation assay. 110

Conclusion **112**

Chapter 5: Recent and remote TBI can be distinguished by T cell activation and less differentiated T cell memory phenotypes. *114*

Introduction **114**
Objectives 118

Materials and Methods **118**
Study Design 118

Participant samples and ethics 118
Adolescents 118
PBMC stimulation and staining protocol 122
Biomarker discovery cohort data analysis pipeline 125
Progressor and non-progressors transcriptomic analysis 133
Statistical analysis pipeline 133

Results 134
M.tb-specific T cell activation peaks during acute M.tb infection. 134
Concordance of QFT and PBMC-ICS 135
Remote TBI is associated with maintenance of polyfunctional M.tb-specific CD4 T cells and a predominantly transitional and effector memory CD4 T cell phenotype. 136
Recent TBI is associated with higher T cell activation but lower T cell functional differentiation compared to remote TBI. 141
Potential biomarkers of recent M.tb infection 149
T cell activation as a biomarker of recent TBI and TB 152

Discussion 157

Contributions 161

Chapter 6: QFT reversion is associated with M.tb-specific functional, memory and activation profiles suggestive of very low in vivo exposure M.tb. 162

Introduction and Rationale 162
Objectives 166

Methodology 166
Study Design 166
PBMC stimulation and intracellular cytokine staining protocol 168
Data analysis pipeline 169

Results and Discussion 174
TST and QFT concordance 174
T cells are the main source of IFN-γ by mycobacteria-specific lymphocytes 175
QFT reversion is not associated with decrease in IFN-γ production detected by flow cytometry 178
Responses to immunodominant M.tb antigens are sustained in QFT reverters 179
QFT reversion is associated with maintenance of functional M.tb-specific CD4+ T cells. 181
Reversion is associated with the maintenance of predominantly T_{TM} and T_E cells. 189
Reversion is not associated with a decrease in T cell activation 195

Conclusion 195

Chapter 7: General Discussion and Concluding Remarks 199

References 212

Appendix 227

Chapter 1: General Introduction

Tuberculosis is a global threat.

Tuberculosis is an ancient disease caused by *Mycobacterium tuberculosis* (M.tb). Despite our long history of co-evolution, an estimated 10 million individuals developed tuberculosis and 1.41 million individuals died from the disease in 2019, making it one of the top causes of mortality due to a single infectious agent (Geneva: World Health Organization, 2020a). Tuberculosis is an airborne disease that can manifest anywhere in the human body, however, pulmonary tuberculosis is the predominant form of disease. Fortunately, we have a vaccine against tuberculosis, Bacille Calmette Guerin (BCG), that is very efficacious against the development of severe tuberculosis in children (Colditz et al., 1995; Roy et al., 2014) but has variable and limited efficacy in adults (Colditz et al., 1994; Mangtani et al., 2014). Tuberculosis is also a curable disease, however, treatment is lengthy, ranging from 6-36 months depending on the antibiotic resistance profile of the disease-causing M.tb strain. Despite these successful interventions, the reality of tuberculosis management has many challenges. According to the latest World Health Organisation's (WHO) Tuberculosis Global Report, only 71% of estimated tuberculosis cases were actually diagnosed, of whom 71% received treatment and, among those treated, 85% were successfully cured globally (Geneva: World Health Organization, 2020a). Unfortunately, individuals who have been successfully cured are still at high risk of disease recurrence (Hermans et al., 2020). Due to this and other challenges associated with the cascade of care, tuberculosis remains a major global health problem.

The global distribution of disease burden is not uniform, with most cases (> 87%) occurring in Africa, Asia and Western Pacific (Geneva: World Health Organization, 2020a). South Africa is among the top eight tuberculosis burden countries, accounting for approximately 3% of the global tuberculosis cases, of which an estimated 58% of tuberculosis patients are people living with HIV (PLHIV). Additionally, South Africa is also one of the top 20 multi-drug resistant tuberculosis burden countries. This highlights the negative impact tuberculosis has on the national population, as well as the multifaceted approach South Africa needs to undertake to curb the tuberculosis epidemic. According to the recent WHO Tuberculosis Global Report, South Africa is on track to reach the 2020 milestone of a 20% reduction in TB incidence (compared to 2015 baseline) (Geneva: World Health Organization, 2020a). However, we still have many hurdles to overcome, some of which include improving the tuberculosis cure

success rate, which is estimated to be just over 50% of tuberculosis patients (Naidoo et al., 2017). The distribution of tuberculosis in high burden countries is unequal, with most cases occurring in areas with high poverty, low socio-economic status and poor access to adequate health care, thus highlighting the role of social determinants in the tuberculosis crisis. Reduction of tuberculosis morbidity and mortality is a key priority of the United Nations (UN) highlighted under the sustainability development goal (SDG) 3: target 3.3:

By 2030, end the epidemics of AIDS, tuberculosis, malaria and neglected tropical diseases and combat hepatitis, water-borne diseases and other communicable diseases [Source: (UN General Assembly, 2015)].

Over the past two decades, tuberculosis incidence has been decreasing at a steady annual rate of 1.6% (2000-2018) and 2.3% (2018/19) (Geneva: World Health Organization, 2019a, 2020a). This is much lower than the estimated annual decline of 10% by 2025, which is required to achieve a 90% reduction in tuberculosis incidence in 2035 compared to 2015 (Geneva: World Health Organization, 2014). This highlights major hurdles we need to overcome to achieve SDG 3. WHO has identified priority areas of improvement needed to achieve a 90% reduction of tuberculosis, some of which include the development of better diagnostics, improved access to preventive and full tuberculosis therapy, and vaccine development. At the South African Tuberculosis Vaccination Initiative (SATVI) our research primarily focuses on tuberculosis vaccine development, advancement of prevention strategies and investigating immune responses associated with M.tb infection and disease progression that could guide the development of novel immunodiagnostics and vaccines.

Development of tuberculosis disease does not always occur after infection, most individuals are thought develop an asymptomatic chronic infection, which then progresses to disease in 5-10% of immunocompetent persons (Geneva: World Health Organization, 2020a). This suggests that there are mechanisms of natural protection against disease progression, which are not fully understood. Lack of progression from infection to disease has been attributed to immune-mediated containment of M.tb replication, which may cause M.tb to enter a dormant metabolic phase that is hypothesised not to cause disease. However, in some individuals M.tb eventually re-activates to cause disease much later in life, when immune responses are weakened, likely due to other diseases, precipitating factors or old-age (predominantly in low tuberculosis burden regions) (Ai et al., 2019). For these reasons, M.tb infection is often referred to as latent tuberculosis infection (LTBI). Updated WHO documents

have revised the term LTBI to TBI (Geneva: World Health Organization, 2020b) because "latent" assumes that everyone with asymptomatic TBI harbours life-long M.tb bacilli at a metabolically dormant state. Recent studies revealed that this may not be the case, suggesting that a substantial proportion of individuals classified as LTBI may have cleared infection (Behr et al., 2019). On the other hand, some individuals classified as LTBI may have asymptomatic sub-clinical disease, indicative of metabolically active M.tb bacilli (Esmail et al., 2016; Pai et al., 2016). This gives a glimpse as to why the term LTBI is "*problematic*", as it oversimplifies the dynamic nature of infection and demonstrates our limited understanding of basic tuberculosis pathogenesis.

Thus, the overall aim of this thesis was to characterise M.tb-specific immune responses associated with different stages of non-progressing TBI, to ultimately expand our current understanding of the spectrum of TBI.

Diagnosis and treatment of tuberculosis

Tuberculosis disease is generally diagnosed based on self-reported symptoms (such as recent unexpected weight loss, night sweats, persistent cough for more than two weeks etc.) and the ability to detect M.tb in human samples, predominantly sputum for pulmonary tuberculosis, or abnormalities in the lungs. M.tb is either detected using microbiological assays or nucleic acid amplification tests (NAATs). Though widely used, microbiological tests do have shortfalls, mostly the inability to detect very low bacterial burden and a long waiting period between the isolation of samples and availability of results, particularly for culture-based tests. NAATs, on the other hand, can yield results within hours of sample collection. Unfortunately, incorporation of NAATs in clinical settings has not hastened tuberculosis diagnosis, treatment initiation nor improved morbidity and mortality compared to microbiological diagnostics (Agizew et al., 2019; Chawla et al., 2016; Churchyard et al., 2015; Tanna et al., 2019; Theron et al., 2014). This lack of improvement could be due to empirical (symptomatic) treatment of a significant proportion of individuals who have challenges producing sputum, such as immunocompromised individuals and children. This suggests that sample type, rather than diagnostic (microbiology *versus* NAATs) is the limiting factor to hastening tuberculosis diagnosis and highlights the need for new diagnostics that circumvent this challenge (discussed later).

Once diagnosed, treatment of tuberculosis is very lengthy, with the shortest standard course of treatment being six months. This treatment regimen comprises two months with rifamycin (or other derivatives), isoniazid, pyrazinamide and ethambutol, followed by four months of rifamycin and isoniazid only. Use of multiple drugs targets different microbial metabolic pathways and aims to prevent the development of drug resistance. In most cases (85%), disease is treated successfully if treatment is well adhered to (Geneva: World Health Organization, 2020a). However, treatment is associated with several side effects, which are even worse for individuals that must go on lengthy treatment for drug-resistant tuberculosis. Ongoing studies aim to shorten treatment of drug susceptible and resistant tuberculosis (Conradie et al., 2020; Grace et al., 2018; Silva et al., 2020).

Since the focus of this thesis is to understand immune responses associated with TBI and not disease, no additional details on disease progression, diagnosis and treatment will be provided in the following sections.

Plans to reduce tuberculosis burden

The STOP-TB partnership proposed a 90-(90)-90 model that aims to diagnose and treat 90% of all tuberculosis cases, with a special focus on providing full or preventive treatment to at least 90% of *vulnerable, underserved, at-risk populations*, and ensuring that 90% of treated individuals are compliant and complete the full course of treatment (STOP TB Partnership, 2019). To achieve this, we need new and improved tuberculosis diagnostics that can identify high risk asymptomatic individuals and diagnose active (including multidrug resistant) tuberculosis in individuals who cannot produce sputum (Silveira-Mattos et al., 2019).

Development of new tuberculosis diagnostics that utilise venous blood, urine or any other easily accessible sample would revolutionise tuberculosis management, as it circumvents the need for sputum collection. Urine-based diagnostics that measure M.tb antigens, e.g. lateral flow urine lipoarabinomannan assays, are recommended for PLHIV and are being tested for utility in children (Nicol and Zar, 2020; Nicol et al., 2020; Geneva: World Health Organization, 2019b). Diagnostics based on blood may measure the host immune responses as a proxy for bacterial burden. Ideally, such tests would also enable the diagnosis of individuals with sub-clinical tuberculosis before they develop symptoms, or before the mycobacterial load is high enough to be detectable by microbiological tests. The importance of developing such tests was recently highlighted by the First National TB Prevalence survey in South Africa, which

demonstrated that approximately 57% of individuals diagnosed with microbiologically confirmed disease had no symptoms (sub-clinical tuberculosis) that would normally trigger tuberculosis investigation (Knowledge HUB, 2021). Similar findings were also reported by a recent metanalysis of tuberculosis prevalence surveys, which demonstrated that 50.4% of microbiologically confirmed tuberculosis patients had sub-clinical disease (Frascella et al., 2020). Accordingly, many groups have developed putative blood-based transcriptomic biomarkers that can identify individuals before they progress to symptomatic disease (Gupta et al., 2020a; Mulenga et al., 2019; Turner et al., 2020; Warsinske et al., 2019; Zak et al., 2016). These biomarkers perform best closer to the time of confirmed tuberculosis diagnosis and could thus be used to identify both subclinical and ongoing disease (Scriba et al., 2021).

Besides providing antibiotic therapy to all individuals with tuberculosis, WHO is promoting increased uptake of tuberculosis preventive therapy (TPT) to high-risk individuals, such as those with known contact with a person with active disease, PLHIV, individuals on anti-TNF treatment, among others. This policy is based on evidence from observational studies demonstrating the positive impact of TPT, which significantly lowers tuberculosis risk (Erkens et al., 2016; Mølhave and Wejse, 2020; Morán-Mendoza et al., 2010; Reichler et al., 2019). Administration of TPT even in the absence of other risk factors, is usually performed in wealthy countries, while in settings with low resources and high disease burden, the risk of re-infection after TPT is very high, thus provision of TPT to all infected individuals would be infeasible and unaffordable (Churchyard et al., 2017; Mathema et al., 2017; Scriba et al., 2021). Therefore, despite current WHO recommendation for TPT for all known tuberculosis contacts, TPT in these regions is reserved for high-risk individuals such as children with known tuberculosis contact and PLHIV. A test that can identify individuals with TBI who are at risk of progressing to tuberculosis disease is needed to guide the provision of TPT to those who would benefit the most. Our research group has recently demonstrated that a blood biomarker of tuberculosis risk, RISK-11 (Darboe et al., 2018; Zak et al., 2016), identified HIV uninfected individuals and PLHIV at high risk of tuberculosis through community-based screening (Mendelsohn et al., 2021; Scriba et al., 2021). Provision of TPT to RISK-11**+** HIV uninfected individuals did not reduce the likelihood of incident tuberculosis during the 15-month follow-up (Scriba et al., 2021). This study was the first demonstration of the utility of a blood-based biomarker to identify high-risk individuals in a community setting and

highlights the need for a more accurate biomarker of risk and better TPT regimens for high transmission settings.

Recently infected individuals are also at higher risk of developing tuberculosis compared to individuals with established TBI (Wiker et al., 2010). Since TBI is asymptomatic, these individuals can only be identified by mass serial TBI testing, which is infeasible. Development of a simple biomarker that can identify recently infected individuals cross-sectionally could guide the provision of TPT in low resourced settings. Accordingly, one of the aims of this thesis was to define immune features associated with recent TBI that could be used to define such a biomarker (Chapter 5; discussed in detail later).

Vaccination is one of most effective public health interventions, therefore improved vaccination strategies are also required to reduce tuberculosis burden (Abu-Raddad et al., 2009; Harris et al., 2020). Infant BCG vaccination, universally administered in countries with high tuberculosis burden, is generally very efficacious (>70%) and has greatly reduced tuberculosis incidence in infants and children (Abubakar et al., 2013; Colditz et al., 1995; Roy et al., 2014). However, BCG efficacy is variable in adults (Mangtani et al., 2014), from as high as 80% (Colditz et al., 1994) to no protection (Geneva: World Health Organization, 1979, 1980). The latter has been attributed to a decline in BCG-induced protection (Abubakar et al., 2013) and waning immunity (Orme, 2010). New and improved vaccines that will either boost existing BCG-immunity or induce *de novo* responses specific for antigens in M.tb that are absent in BCG are needed.

Multiple trials have tested the safety and immunogenicity of vaccines designed to prevent disease progression but only a few have measured efficacy in phase 2b trials. One such vaccine is the modified vaccinia virus Ankara expressing antigen 85A (MVA85A), which showed non-significant efficacy of 17.3% [95% confidence interval (CI): -31.09 to 48.2%] when tested as prime (BCG)-boost (MVA85A) vaccine regimen in infants, and therefore showed no benefit over BCG vaccination alone (Tameris et al., 2013). MVA85A was also tested in PLHIV and demonstrated an efficacy of 32·8% [95% CI: -111·5 to 80·3; (Ndiaye et al., 2015)], also not significant.

More recently, the sub-unit candidate vaccine M72/AS01E, which contains a recombinant fusion protein (M72) of the two M.tb antigens Mtb32A and Mtb39A adjuvanted in AS01E, demonstrated 49.7% (95% CI: 2.1 to 74.2%) efficacy against progression to tuberculosis in M.tb infected adults. This vaccine had an acceptable safety profile and induced robust

humoral and cellular adaptive immune responses (Tait et al., 2019). These results represent a major success in the advancement of the tuberculosis vaccine pipeline, with the potential licensure of a M.tb vaccine within the next 10-20 years, should efficacy be confirmed in a planned phase 3 trial.

Additionally, other vaccine candidates and strategies are being tested to prevent the acquisition of TBI (discussed later), development of primary tuberculosis disease and recurrence of disease, as well as therapeutic vaccines that are co-administered with antibiotic treatment (Andersen and Urdahl, 2015; Hatherill et al., 2020).

Infection and Immunity: An overview of M.tb-specific T cell immunity

In this section we shall provide a general overview of immune responses associated with TBI, with a special focus on the role CD4 T cells play in immune responses against M.tb. We acknowledge that some sub-sections, such as Innate cells: first responses, are not detailed. However, since the main immune cells investigated in this thesis were classical T cells, we decided to rather focus on M.tb-specific classical T cell immunology as it is important for defining stages of TBI.

Innate cells: first responders

Inhalation of M.tb in aerosol droplets can cause an infection, which is generally either cleared or contained by immune cells. If bacterial replication supersedes and overpowers immune cells, then TBI can progress to disease. The canonical feature of tuberculosis disease is the development of granulomas, structured organisations of cells that aim to contain bacterial replication and prevent dissemination. Granuloma physiology is characterised by a centre enriched in either cell-free M.tb or M.tb-infected atypical alveolar macrophages, which are surrounded by innate cells (monocytes, neutrophils and dendritic cells (DCs)] and a lymphocytic cuff of mostly B and T cells on the exterior (Kaufmann, 2001; Ndlovu and Marakalala, 2016; Ramakrishnan, 2012). Granulomas are very heterogenous *e.g.* caseous, necrotic, non-necrotising or calcified granulomas etc., and can exhibit great intra-host variability [Figure 1; (Ehlers and Schaible, 2013; Flynn et al., 2011; Pagán and Ramakrishnan, 2015)].

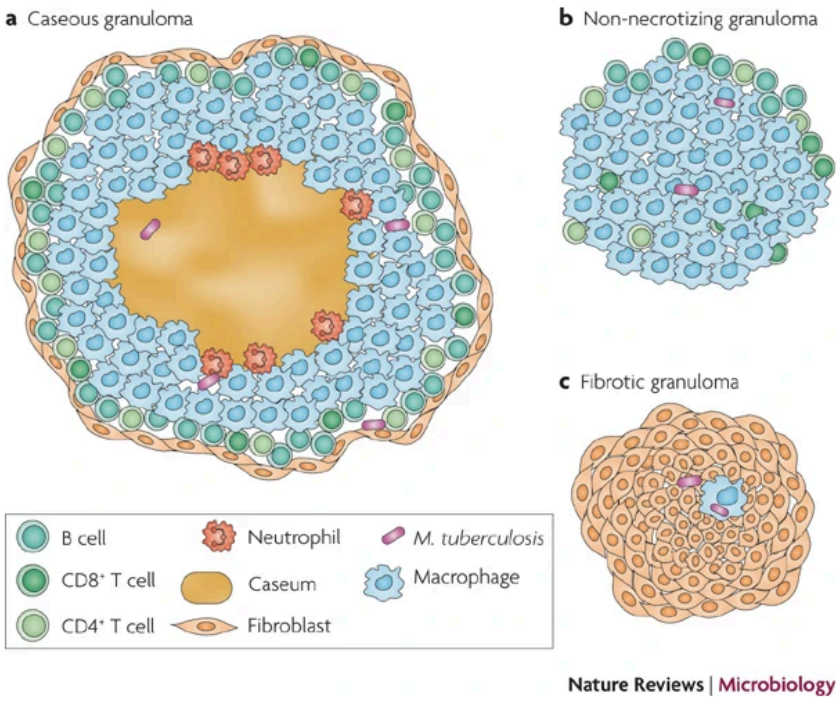

Figure 1: Tuberculous granulomas are heterogenous. Multiple tuberculosis granuloma types have been observed. One of the most defined granuloma type is the (A) caseous granuloma, characterised by caseous centre which contains M.tb surrounded by macrophages, followed by other innate cells including neutrophils, DCs and NK cells and a lymphocytic cuff of predominantly B and T cells. Other granuloma types included (B) non-necrotizing granuloma, consisting of predominantly macrophages and some lymphocytes, and (C) fibrotic granulomas lesions which are mostly composed of fibroblasts and few macrophages surrounding M.tb. Adapted from (Barry et al., 2009).

Development of granulomas requires complex interactions between different immune cells. The first immune cells to typically come in contact with M.tb in a naïve host are innate cells. These cells use pattern recognition receptors (PRRs) to recognise pathogen-associated molecular patterns (PAMPs) expressed on the M.tb cell surface, such as carbohydrates, glycolipids, glycoproteins and lipoproteins. Binding of PAMPs by PRRs initiates immunological responses that aim to contain and eliminate M.tb. Examples of these processes include phagocytosis, autophagy, apoptosis and inflammasome maturation. The main immunological niche for initial M.tb replication is the alveolar macrophage. Upon M.tb recognition, alveolar macrophages also release chemokines and cytokines that create a pro-inflammatory micro-environment, recruit and activate other innate cells such as recruited macrophages, neutrophils, DCs and natural killer (NK) cells (Algood et al., 2005). Together innate cells play an essential role in containing initial M.tb replication (Sia et al., 2015), and in some cases can clear M.tb without the help from adaptive immune cells (Simmons et al., 2018; Verrall et al., 2014). Unfortunately, M.tb can escape and interfere with various aspects of innate immune

cell activity (Liu et al., 2017), resulting in a gradual increase in bacterial burden which facilitates dissemination of infection to other immune cells. Assistance from adaptive immune cells is required to improve bacterial killing by innate immune cells. Although alveolar macrophages can present antigens to T cells, the primary antigen-presenting cell (APC) responsible for linking innate and adaptive immunity in the context of TBI are DCs. M.tb is known to delay induction of adaptive immune cells in lymphoid tissues by interfering with DC activation, maturation and lymphoid tissue homing (Baena and Porcelli, 2009; Liu et al., 2017). Eventually, M.tb infected DCs drain to nearby lymph nodes where they prime and activate naïve T (T_N) cells.

The focus of this thesis is to understand T cell immune responses associated with different stages of TBI, which are described in more details in the following sections.

Role of CD4 T cells in tuberculosis pathogenesis

The importance of antigen-specific, particularly IFN-γ-secreting, CD4 T cells in the control of M.tb burden has been clearly illustrated using murine models, which demonstrate an association between dysfunctions in CD4 T cell priming, activation and functionality and rapid progression to fatal disease. In humans, characterisation of Mendelian susceptibility to mycobacterial disease (MSMD) has also demonstrated the importance of CD4 T cells in immune responses against M.tb. Individuals with MSMD have genetic mutations in key genes associated with priming (innate immunity) and induction of functional IFN-γ-producing CD4 T cells [reviewed in (Bustamante et al., 2014)]. This is associated with high susceptibility to mycobacterial disease caused by weakly virulent species such as BCG and environmental non-tuberculous mycobacteria (NTM). Further, depletion of CD4 T cells in PLHIV is associated with a higher tuberculosis risk than HIV uninfected individuals (Jones et al., 1993; Kwan and Ernst, 2011).

Many aspects of CD4 T cell-mediated immune responses during different stages of TBI in humans are not fully understood and are addressed in this thesis.

Activation and differentiation of CD4 T helper cells

T cell priming in the lymph nodes requires three signals: (1) antigen presentation to the T cell receptor (TCR), (2) co-stimulation to activate T cell proliferation and effector functions, and (3) release of cytokines by APCs to direct polarisation of T cells. APCs process antigens for

presentation on major histocompatibility complex [MHC; also known as human leukocyte antigens (HLA)] class I (MHC-I) and II (MHC-II) molecules to CD8 and CD4 T cells, respectively. The interaction between MHC-antigen complexes (on APCs) and TCRs induces a signalling cascade which activates T cells. The interaction between co-stimulatory molecules (CD70, CD80, CD86 and CD40 on APCs) and their ligands (CD27/28 and CD40L on T cells) amplifies this activation signal and initiates induction of proliferation and effector functions. Without this signal, T cells may become unresponsive (anergic) despite recognising MHC-antigen complexes. Classical markers of T cell activation are CD38 and HLA-DR. For this thesis, our T cell activation marker of choice was HLA-DR. HLA-DR is a member of the MHC class II family expressed by APCs, notwithstanding T cells also express HLA-DR (Aversa and Hall, 1991). Although the exact functional role and mechanisms of HLA-DR expression by T cells are not fully understood, some studies suggest that during high antigen burden T cell expression of HLA-DR facilitates antigen presentation to other T cells (Aversa and Hall, 1991; Mangalam et al., 2006). This additional source of *de novo* antigen presentation may contribute to the activation of more T cells that can enhance pathogen clearance. As described above, activation of T cells by APCs also induces T cell proliferation. Ki-67, a molecule upregulated during all stages of active cell division and mitosis and downregulated when cells are resting, is a widely used cell proliferation marker for *in vitro* and direct *ex vivo* assays (Elias et al., 2019; Gerdes et al., 1984; Scholzen and Gerdes, 2000; Soares et al., 2010). Comparative studies between TBI and disease have demonstrated significantly higher proportions of M.tb-specific HLA-DR+, Ki-67+ and CD38+ T cells during tuberculosis disease compared with infection (Adekambi et al., 2015; Musvosvi et al., 2018; Wilkinson et al., 2016). These findings likely reflect high *in vivo* antigen exposure during disease, which results in activation of memory and effector T cells. In this thesis, we investigated whether distinct stages of TBI (*i.e.* acquisition of recent TBI, persistent infection and potential M.tb clearance) are associated with differential M.tb-specific T cell activation.

In addition to presenting antigens and providing co-stimulation signal, APCs also release cytokines that activate specific transcription factors in T cells, which polarise T cells to differentiate into different T helper (Th) lineages, such as Th1, Th2, Th9, Th17, Th22, regulatory cells (Tregs) and follicular helper T (Tfh) cells. The specific functional profiles and effector functions characteristic of these T helper lineages have been extensively reviewed (Geginat et al., 2013; Kara et al., 2014; Zhu et al., 2010) and are summarised in Figure 2.

Th lineage				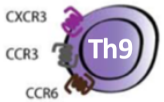			
Cytokines driving polarisation	IL-12 , IL-18	IL-4	TGFβ, IL-6	TGFβ, IL-4	IL-6, TNF, IL-1β	TGFβ, IL-2	IL-21, IL-6
Major transcription regulator	T-bet	GATA-3	RORγt	PU.1	AhR?	FoxP3	Bcl-6
Major Cytokine	IFN-γ	IL-4	IL-17	IL-9	IL-22	IL-10, TGFβ	IL-21
Major function	Clearance of intercellular pathogens e.g. bacteria, viruses	Clearance of extracellular pathogens e.g. parasites; allergic immune responses	Clearance of extracellular pathogens e.g. fungi, bacteria	Clearance of extracellular pathogens e.g. parasites; auto-immunity	Extracellular pathogens e.g. fungi, bacteria; epidermal immunity	Anti-inflammatory immune regulation	Provide help for B cell maturation
Major site of effector function	Peripheral tissues	Peripheral tissues	Peripheral tissues	Peripheral tissues	Peripheral tissues	Peripheral tissues and secondary lymphoid organs	Secondary lymphoid organs
Defining chemokine receptor	CXCR3	CCR4	CCR6	?	CCR10	?	CXCR5

Figure 2: Commonly known CD4 Th lineages. Figure summarises cytokines released by APCs during priming of naïve T cells that drive T cell polarisation to specific Th lineages by inducing specific master transcription factors. These Th lineages: Th1, Th2, Th17, Th9, Th22, Tregs and Tfh T cells have specific effector functions, which include secretion of cytokines required to assist in anti-pathogenic immune responses, expression of chemokine receptor molecules that facilitate homing to peripheral sites where infection is taking place [Figure adapted from (Geginat et al., 2013, 2014; Kara et al., 2014; Mousset et al., 2019)].

When APCs recognise M.tb, a predominantly intracellular pathogen, they release lL-12 and IL-18. Binding of these cytokines to their respective receptors on T cells activates the T-bet transcription factor, which drives polarisation towards the Th1 functional lineage. Th1 cells primarily release IFN-γ and TNF, cytokines essential for intracellular pathogen clearance (discussed in detail later).

Ex vivo identification of antigen-specific T cells

Activation of T_N cells by APCs leads to clonal expansion and differentiation to effector and memory T cells that recognise a specific epitope. Antigen-experienced T cells can be detected *ex vivo* using multimeric peptide-MHC molecules (*e.g.* tetramers, since most reagents make use of streptavidin and thus multimerise 4 peptide-MHC molecules) or by measuring functional responses induced by *in vitro* antigenic re-stimulation (Elias et al., 2019; Nepom et al., 2002). Tetramers directly bind to TCRs by mimicking T cell receptor-peptide-MHC binding complexes that form during antigen presentation to T cells (Altman et al., 1996; Nepom, 2012). Tetramer staining is typically a short procedure that does not markedly alter T cell transcription and protein expression levels, making it an ideal technique for measuring and tracking expression patterns of T cell phenotypic markers directly *ex vivo*. However, tetramer staining requires prior knowledge of the individual's HLA expression repertoire and epitopes that could be presented on the HLA molecules. As a result, a single tetramer can only measure specificity to a single epitope in the subset of the population that carries the relevant HLA allele. Further, detection of HLA genes, achieved by HLA-typing, does not always translate to *in vivo* induction of a T cell that is restricted to that HLA-peptide complex. Therefore, tens to hundreds of MHC-peptide complexes would be required to comprehensively capture CD4 T cells specific for a single M.tb protein, this highlights a major limitation of tetramer applications.

To capture a more holistic representation of antigen-specific T cells, *in vitro* stimulation of cells with saturating concentrations of antigens are typically used. This circumvents the need for knowing an individual's HLA background and allows detection of a broader repertoire of antigen-specific T cells. During *in vitro* antigenic stimulation, saturating concentrations of peptides facilitate the formation of immunological synapses, which provide sufficient signal required to induce cytokine production. If the stimulant is a complex molecule, *e.g.* proteins

or entire microorganisms, APCs process and present antigens to T cells, which activates production of cytokines and other effector molecules. Further, antigen-experienced T cells also upregulate CD40L (CD154), OX40 (CD134), PD-L1 (CD274), 4-1BB (CD137), among other markers upon *in vitro* antigen stimulation (Elias et al., 2019). Of these molecules, detection of CD154 upregulation is one of the most used cytokine-independent methods for measuring antigen-specificity and CD154 has been shown to be also up-regulated by Th1, Th2 and IL-10 cytokine+ CD4 T cells (Frentsch et al., 2005).

In this thesis, we utilised both MHC-II tetramers and *in vitro* antigen stimulations followed by intra-cellular cytokine staining to detect M.tb-specific CD4 T cells.

Th1 T cells are the main players in T cell responses to M.tb.

Animal models of TBI have demonstrated the importance of CD4 T cells to control M.tb infection, particularly their ability to produce IFN-γ and TNF. CD4 T cells are not the sole source of IFN-γ and TNF, however, depletion of CD4 T cells does lead to loss of M.tb control, despite production of these cytokines by other cells (Scanga et al., 2000). Upon activation by DCs, M.tb-specific CD4 T cells home to the lung, potentially in a CCR2 or CXCR3 chemotactic dependent manner, and provide help to innate cells by secreting IFN-γ and TNF (Peters et al., 2001; Sakai et al., 2014a, 2014b). IFN-γ activates macrophages (and other innate cells) to produce anti-microbial molecules and undergo phagosome maturation [reviewed in (Domingo-Gonzalez et al., 2017)]. TNF induces phagocyte activation and contributes to the creation of a pro-inflammatory microenvironment, which facilitates recruitment of immune cells required for M.tb control and granuloma formation (Bean et al., 1999; Domingo-Gonzalez et al., 2017; Flynn et al., 1995). In humans, an association between increased risk of tuberculosis and anti-TNF therapy has further demonstrated the importance of TNF in immune responses against M.tb (Keane, 2005). However, excessive TNF production can contribute to tuberculosis pathogenesis by damaging host cells. This highlights the need to regulate TNF production in favour of M.tb control and prevent tipping the scale towards excessive TNF production which favour of tuberculosis pathogenesis (Domingo-Gonzalez et al., 2017). In addition, Th1 cells produce IL-2, a cytokine that plays a critical role in T cell differentiation and homeostatic proliferation (Boyman and Sprent, 2012; Liao et al., 2013; Morgan et al., 1976). Th1 cells are also identifiable based on expression CXCR3 and in some

cases CCR5, chemokine receptors associated with homing to inflammatory sites [Figure 2; (Becattini et al., 2015; Bonecchi et al., 1998; Lindestam Arlehamn et al., 2013; Qin et al., 1998; Strickland et al., 2017)].

T cell differentiation and Th1 cytokine co-expression profiles are affected by *in vivo* antigen burden. During low or no antigen exposure memory Th1 cells maintain an early differentiation stage and preferentially co-express TNF and IL-2, while IFN-γ, TNF and IL-2 cytokines are preferentially co-expressed by more differentiated cells in response to high antigen burden. Further, chronic exposure to high antigen load is associated with differentiation of Th1 cells to an IFN-γ-monofunctional profile (Appay et al., 2008; Seder et al., 2008).

Many researchers hypothesised that polyfunctional T cells that co-express IFN-γ, TNF and IL-2 would be associated with protection from tuberculosis, as it has been observed in many other infectious diseases (Seder et al., 2008). Interestingly, several human studies have found no association nor correlation between the magnitude of polyfunctional CD4 T cell responses and risk of disease [(Kagina et al., 2010); also reviewed in (Caccamo and Dieli, 2012; Lewinsohn et al., 2017)]. Others suggested that polyfunctional T cells could be a potential correlate of tuberculosis risk in some individuals (Fletcher et al., 2016). On the other hand, animal models have demonstrated that polyfunctional T cells are induced by vaccination and may play an important role in M.tb control (Lewinsohn et al., 2017). Specifically, recent studies in non-human primates showed that BCG-induced protection against TBI and disease was associated with the accumulation of lung infiltrating polyfunctional Th1 CD4 T cells that also co-expressed IL-17 (Darrah et al., 2020; Dijkman et al., 2019). These results suggest that bi-functional and polyfunctional T cells potentially play a favourable role in immune responses against M.tb, but whether they are necessary and sufficient for protection remains to be established.

Since TBI and disease are likely associated with different levels of *in vivo* antigen burden, researchers hypothesised that patterns of Th1 cytokine co-expression profiles could distinguish between infection and disease. Unfortunately, studies thus far have reported conflicting data, with some suggesting that disease is associated with higher proportions of IFN-γ+TNF+ (Day et al., 2011) or single-positive TNF (Harari et al., 2011) M.tb-specific CD4 T cells than asymptomatic infection, while many others have shown no difference in CD4 T cells Th1 cytokine co-expression profiles between disease and infection [reviewed in (Caccamo and

Dieli, 2012; Jasenosky et al., 2015; Lewinsohn et al., 2017; Lyadova and Nikitina, 2019)]. However, to our knowledge only one study has investigated Th1 cytokine co-expression during different stages of TBI i.e. recent *versus* established TBI (Halliday et al., 2017). Halliday and colleagues showed that proportions of M.tb-specific single-positive TNF CD4 T cells with an effector phenotype were significantly lower in individuals with established TBI compared with recent TBI, and were highest in patients with active disease. These results suggest that this T cell subset may track antigen load.

One of our aims was to determine whether different stages of TBI are associated with distinct Th1 (IFN-γ, TNF and IL-2) cytokine co-expression patterns, since an improved understanding of T cell functional profiles could guide the development of novel biomarkers of recent and cleared infection.

Another cytokine produced by M.tb-specific CD4 T cells is IL-17, the canonical cytokine of Th17 cells (Scriba et al., 2008). Th17 cells are very heterogenous, as shown by their ability to co-express IFN-γ or IL-10 depending on the type of infection (Zielinski et al., 2012). Cells that co-expresses both IFN-γ and IL-17, referred to as Th1/17 cells, are phenotypically identifiable based on co-expression of CCR6 and CXCR3 (Acosta-Rodriguez et al., 2007; Becattini et al., 2015). In humans, Th1/17 CXCR3+CCR6+ cells are one of the most prevalent M.tb-specific CD4 T cells subsets, and, in most cases, the proportional contribution of these cells outnumbers Th1 CXCR3+ CCR6- cells (Lindestam Arlehamn et al., 2013; Nikitina et al., 2018; Strickland et al., 2017). IL-17 has many functions, including playing a role in granulopoiesis and neutrophil recruitment to the airways [reviewed in (Khader and Cooper, 2008; Ouyang et al., 2008)]. In animal models, infection and vaccine-induced IL-17-producing CD4 T cells contribute to rapid pathogen clearance, likely by recruiting and potentiating Th1 immune cells (Cooper and Khader, 2008; Dijkman et al., 2019; Khader et al., 2007; Sia and Rengarajan, 2019). In humans, TBI has been associated with higher levels of circulating IL-17+ CD4 T cells compared to disease (Scriba et al., 2008), while others have reported a correlation between IL-17 (and IFN-γ) producing CD4 T cells and disease severity (Jurado et al., 2012). It is likely that during the early stages of (controlled) TBI, IL-17 plays a critical role in anti-mycobacterial immune responses. However, if and when M.tb continues to persist, continued expression of Th1/17 associated cytokines in response to increasing bacterial burden likely over-stimulates innate

cells and contributes to excessive inflammation, which causes lung damage (Cruz et al., 2010; Lyadova and Panteleev, 2015; Torrado and Cooper, 2010).

T-regs that produce the anti-inflammatory cytokine IL-10 (Jankovic et al., 2010) also play a role in immune responses against M.tb by dampening excessive pro-inflammatory responses that could damage host cells (Moore et al., 2001; Redford et al., 2011). However, excessive T-reg activity can favour uncontrolled bacterial replication by inhibiting favourable pro-inflammatory activity (Shafiani et al., 2010). A pre-clinical M.tb vaccine challenge model has recently shown an association between IL-10 levels and reduced pathology and protective immunity, however, the cellular source of IL-10 was not defined (Dijkman et al., 2019; Scriba and Nemes, 2019).

M.tb-specific T helper functions described above point towards the duality of Th1/Th17 and T-reg mediated M.tb-specific immunity, whereby too little or too much of a specific response could contribute to reduced M.tb control and immunopathology depending on the stage of infection and disease. Unfortunately, in our experience, intra-cellular expression of IL-17 and IL-10 have been very difficult to detect upon stimulation of cryopreserved peripheral blood mononuclear cells (PBMC), and therefore were not measured in the experiments for this thesis.

Cytotoxic CD4 T cells

Cytotoxic activity, a lesser-studied effector function of CD4 T cells, is induced by expression of RunX3, the main transcription factor responsible for regulating cytotoxic potential in T cells (Anderson, 2013; Mucida et al., 2013). Expression of RunX3 by CD4 T cells is activated by repeated MHC-antigen-TCR interaction during high antigen burden (Cheroutre and Husain, 2013). Cytotoxic CD4 T cells, which usually exhibit Th1 functional capacity, are detectable during viral infections, autoimmune diseases and bacterial infections, including M.tb (Cheroutre and Husain, 2013; Kobayashi et al., 2007; Leeuwen et al., 2004; MacArthur et al., 2007; Sun et al., 2002). These cells release cytotoxic molecules that can mediate killing of M.tb infected cells (perforins and granzymes) or kill M.tb directly (granulysin) (Aerts et al., 2019; Canaday et al., 2001; Martirosyan et al., 2013; Mueller et al., 2011).

Unlike cytokines, cytotoxic molecules are pre-formed and stored intracellularly in cytotoxic granules that contain lysosomal-associated membrane glycoproteins (LAMPs), such as CD107a (LAMP-1), in their lipid bilayer. Upon T cell activation, the lipid bilayer of the cytotoxic

granules fuses with cell membrane releasing cytotoxic molecules, and LAMPs become temporarily detectable on the surface cell membrane. Researchers thus developed a technique to measure cell surface CD107a expression, upon *in vitro* antigen stimulation, as a proxy for cytotoxic potential (Betts and Koup, 2004).

In this thesis, we defined cytotoxic CD4 T cells by directly measuring granzymes, perforin and granulysin in PBMC stained *ex vivo* with MHC-II tetramers or by measuring CD107a+ T cells upon *in vitro* antigen stimulation.

CD4 T cell homing capacity

Migration of immune cells, including T cells, is facilitated by interactions between chemokines, specialised cytokines and signalling proteins, and chemokine receptors expressed on all immune cells via a process called chemotaxis. Expression of chemokine receptors varies depending on the cell activation state, type of infection and the localisation of the immune response. Chemokines and their roles in immunity and migration to specific organs have been extensively reviewed (Bachelerie et al., 2013; Griffith et al., 2014). Early studies demonstrated the role of chemokine receptors CCR2 and CXCR3 in T cell lung homing (Peters et al., 2001; Sakai et al., 2014a, 2014b). However, blocking of chemokine receptors did not entirely abrogate T cell homing to the lung (Hoft et al., 2019), thus highlighting that other mechanisms contribute to T cell recruitment to the lung. More recently, the development of intravascular staining protocols in animal models has enabled in-depth characterisation of T cells that reside in tissues and organs, referred to as tissue-resident (T_{RM}) memory T cells. Using this technique, murine TBI models have demonstrated that CD4+ cells that express CXCR3 home to the lung parenchyma (where gaseous exchange takes place), while T cells that do not express CXCR3 or those that express CX3CR1 (fractalkine receptor) are predominantly found in the lung vasculature and have limited ability to egress into the lung tissue (Sakai et al., 2014a; Sallin et al., 2017). Further, CX3CR1 expression by CD4 T cells is associated with terminal T cell differentiation, characterised by higher expression of the T-bet transcription factor, killer cell lectin-like receptor G1 (KLRG-1; terminal T cell differentiation marker) and single-positive IFN-γ expression, T cell features associated with poor control of M.tb replication in these models [Figure 3; (Hoft et al., 2019; Sakai et al., 2014a, 2014b, 2016; Sallin et al., 2017; Woodworth et al., 2016)]. These findings demonstrated that not all Th1 cells mediate immune responses associated with bacterial

clearance. Further, these studies suggest that CXCR3+ M.tb-specific CD4 T cells in circulation could potentially home to the lung.

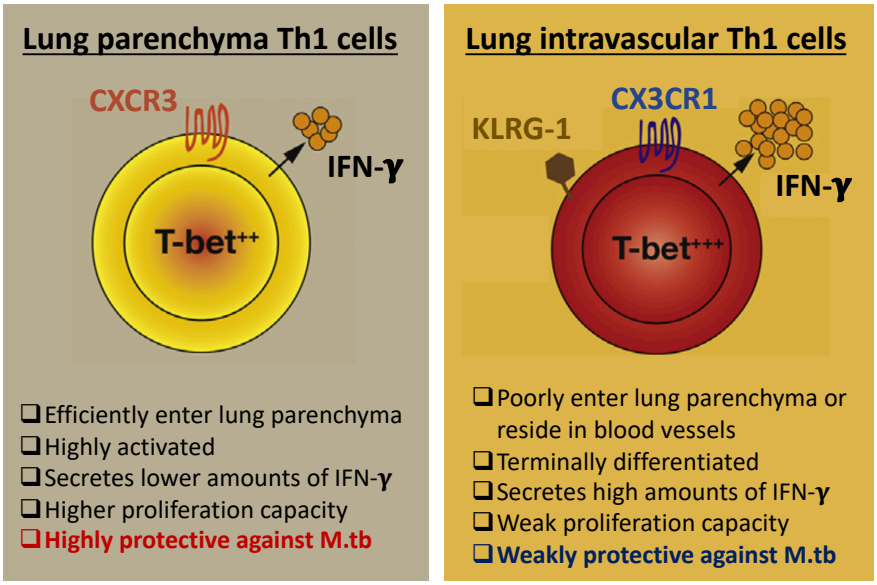

Figure 3: Functional and phenotypic characteristics of M.tb-specific T cells localised in the lung parenchyma (tissue) and vasculature. Th1 cells that home to lung parenchyma express high levels of CXCR3 and moderate levels IFN-γ and are associated with immune responses that contribute to containing M.tb burden. T cells that remain in the lung vasculature exhibit terminal differentiation characterised by high levels of KLRG-1, CX3CR1 and IFN-γ, immune responses associated with poor M.tb control. [Adapted from (Sakai et al., 2014b; Sallin et al., 2017)]

Based on these studies in animal models, we included the measurement of CXCR3 and KLRG-1 expression along with Th1 cytokines during different stages of TBI, as a proxy for potential homing to different compartments of the lung.

CD4 T cell differentiation and expression of other phenotypic markers

In addition to delineating T cell lineages based on cytokine and chemokine receptor expression, T cells can also be characterised based on their memory differentiation state, defined by co-expression of the following markers: CD45RA, CCR7, CD27, KLRG-1 and CD95 (Figure 4), among others. Antigen-inexperienced T_N cells co-express CD45RA, CCR7 and CD27, but do not express CD95 and KLRG-1. Upon priming and activation of T_N cells by APCs, these cells differentiate into antigen-experienced short-lived effector cells and long-lived memory cells. Antigen-experienced cells express CD95 and undergo alternative splicing of CD45 resulting in the expression of CD45RO instead of CD45RA (Lugli et al., 2007). There are exceptions to this rule, early differentiated T cell memory subsets known as stem cell memory (T_{SCM}) cells maintain expression of CD45RA (Gattinoni et al., 2011), and T cells at terminal

stages of differentiation re-express CD45RA instead of CD45RO (Appay et al., 2008). Interaction between CCR7 and its ligands CCL21 and CCL19 facilitates homing to lymphoid tissues, the main site for antigen presentation. Thus, expression of CCR7 by T_N cells ensures that these cells are at the optimal site for initial T cell priming and activation. T_{SCM} and central memory (T_{CM}) cells, long-lived memory T cell subsets associated with high proliferation and T cell differentiation capacity but reduced effector functions, also express CCR7 (Gattinoni et al., 2011; Sallusto et al., 1999). Maintenance of CCR7 expression by T_{SCM}/T_{CM} cells ensures preferential homing to lymphoid organs, where they get activated by APCs upon secondary antigen exposure. Such activation usually induces T cell proliferation and differentiation into transitional (T_{TM}) and effector (T_E) cells. These cell subsets are endowed with enhanced effector functions and homing to peripheral tissues, facilitated by down-regulation of CCR7 (Fritsch et al., 2005) and upregulation of other chemokine receptors, as detailed in the previous section. CD27, a member of the TNF receptor superfamily, is a co-stimulatory molecule required for induction of T cell responses. As cells become exposed to increasing antigen load, their ability to produce cytokines and perform other effector functions increases, resulting in a lower reliance of co-stimulation to maintain their functional capacity. Accordingly, T_N, T_{SCM}, T_{CM} and T_{TM} cells express high levels of CD27, while T_E cells do not (Fritsch et al., 2005; Okada et al., 2008). Lastly, as cells gain more effector functions and transition to a more differentiated state, they up-regulate expression of KLRG-1, lose the capacity to produce IL-2 and TNF and to proliferate (Henson et al., 2009; Sarkar et al., 2008). Studies predominantly focused on virus-specific CD8 T cells have associated the expression of KLRG-1 to T cell exhaustion, senescence and terminal differentiation (Akbar and Henson, 2011; Henson and Akbar, 2009). As a result, expression of KLRG-1 is typically associated with late stage effector T cell differentiation such as terminally differentiated effector T (T_{TE}; also referred to as T_{EMRA}) cells. The summary provided above describes a linear model of T cell memory differentiation where, upon secondary antigen exposure, memory cells differentiate along a linear continuum: (T_N →) T_{SCM} → T_{CM} → T_{TM} →T_E →T_{TE}. This differentiation is associated with decreasing lymphoid homing, proliferation and T cell differentiation potential, and an increase in effector functions and homing to inflamed tissues (Figure 4).

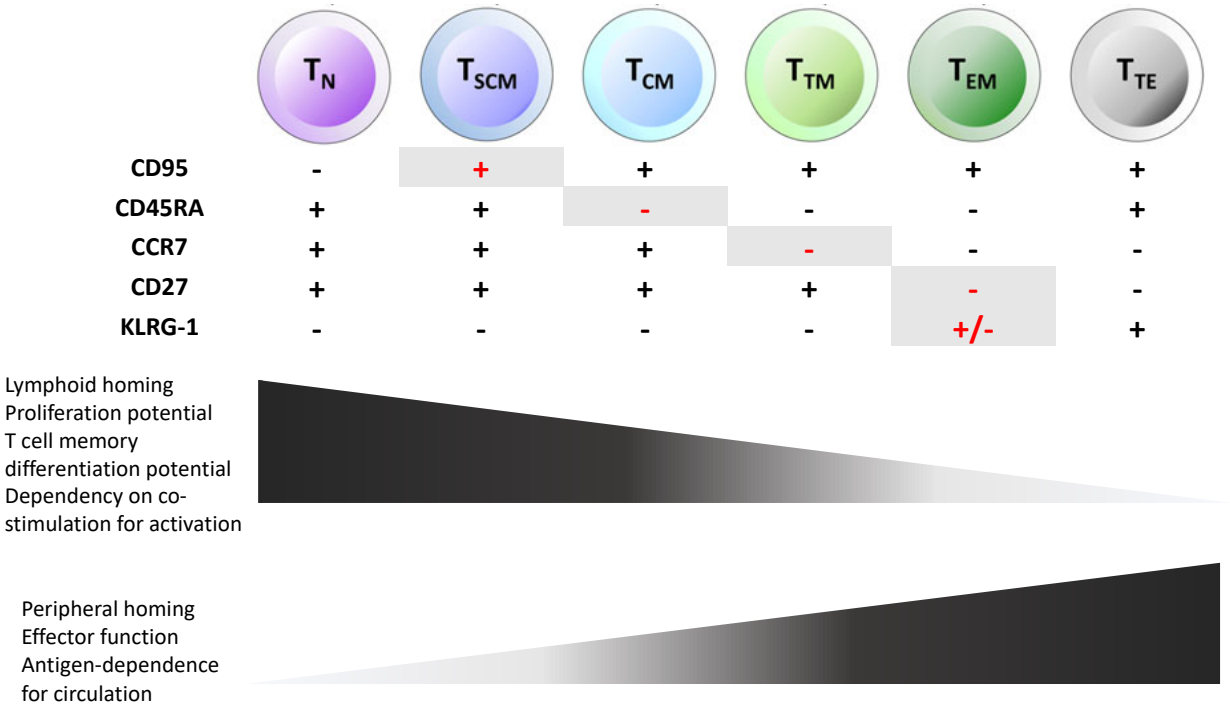

Figure 4: Linear model of T cell differentiation. T cell memory subsets can be delineated based on the expression of CD45RA, CCR7, CD27, KLRG-1 and CD95. Upon antigen-exposure naïve T cells defined as CD45RA+CCR7+CD27+KLRG-1-CD95- expressing cells, differentiate into CD95+ memory cells. The least differentiated memory subset is T_{SCM} (CD45RA+CCR7+CD27+KLRG-1-CD95+) cells. As cells become more differentiated, they first down-regulate CD45RA: T_{CM} (CD45RA-CCR7+CD27+KLRG-1-CD95+) cells, followed by down-regulation of CCR7: T_{TM} (CD45RA-CCR7-CD27+KLRG-1-CD95+) cells, which enables homing to non-lymphoid tissue and organs. The next memory marker to be down-regulated is CD27: T_E (CD45RA-CCR7-CD27-) followed by up-regulation of KLRG-1. T cell differentiation is associated with a reduction in lymphoid homing, proliferation and T cell differentiation potential, while their capacity for peripheral homing, effector functions and antigen-dependence to maintain the memory subset increases. Adapted from (Mahnke et al., 2013).

As described above, not all memory cells are equivalent. Studies predominantly using viral infection models have demonstrated that chronic infection is associated with persistent detection of IFN-γ producing T cells (mainly T_E cells), while cleared or low antigen burden is associated with T_{SCM}/T_{CM} cells that predominantly produce TNF and IL-2 (Fuertes Marraco et al., 2015; Lugli et al., 2013a; Seder et al., 2008; Wu et al., 2002). In the context of TBI, polyfunctional T_E cells that produce IFN-γ, TNF and IL-2 are the predominant memory phenotype during both infection and disease (Jasenosky et al., 2015; Orme and Henao-Tamayo, 2018). It is assumed that ongoing antigen exposure, albeit at potentially lower levels during infection compared to disease, maintains this functional subset.

Generally, protection from developing infection or disease upon secondary antigen exposure is mediated by pre-existing adaptive immunity. *Does this principle also apply to M.tb re-exposure*? Non-human primate models (Cadena et al., 2018) and longitudinal human studies

(Andrews et al., 2012) have demonstrated that pre-existing immune responses induced by prior infection are associated with partial protection against re-infection and/or disease progression upon M.tb re-exposure. *Is this partial protection mediated by T_E or T_{SCM}/T_{CM} cells?* Murine models have suggested that pre-existing M.tb-specific T_{CM} cells rather than T_E cells are associated with superior M.tb control upon M.tb challenge (Andersen and Smedegaard, 2000; Cruz et al., 2015). This is likely attributed to the ability of T_{CM} cells to differentiate into IFN-γ+ T_{TM}/T_E cells with limited terminal differentiation, while upon secondary challenge T_E cells proliferate poorly and likely undergo terminal differentiation, a phenotype associated with poor M.tb control. In reality, both $T_{E/RM}$ and T_{SCM}/T_{CM} cells are probably required for optimal M.tb control. T_{SCM}/T_{CM} cells are likely important for maintaining the overall memory pool and replenishing early effector cells, while T_E are more likely to quickly migrate to infected tissues and contribute to M.tb control at the site of infection, together with T_{RM} cells. To our knowledge, no study has interrogated longitudinal memory T cell responses in M.tb infected individuals at different stages of non-progressing infection. We thus aimed to contribute to filling this knowledge gap, by conducting a longitudinal study to investigate memory, activation and functional T cell properties during different stages of TB.

Do other adaptive immune cells, CD8 T cells and B cells, play a role in TBI and disease?

CD8 T cells, well known for their cytotoxic functional properties, produce Th1 associated cytokines IFN-γ and TNF and, to a lesser extent, IL-2 (Prezzemolo et al., 2014; Serbina and Flynn, 1999). Murine models have demonstrated that CD8 T cells are important for M.tb control, however, they may not be as critical as CD4 T cells (Mogues et al., 2001; North and Jung, 2004). In humans, active disease is associated with a higher probability of detecting M.tb-specific cytotoxic and cytokine-producing CD8 T cells than TBI (Prezzemolo et al., 2014; Rozot et al., 2015). These findings suggest that CD8 T cells are induced during high levels of M.tb antigen exposure, *e.g.* in disease. In addition to CD8 T cells, researchers have also investigated the role of donor unrestricted T cells (DURTs), such as mucosal-associated invariant T (MAIT) and γδ T cells, in tuberculosis pathogenesis (Gold et al., 2015; Libero et al., 2014; Ruibal et al., 2021). Thus far studies have demonstrated the anti-mycobacterial capacity of DURTs. An example of this is the consistent detection of lower levels of circulating MAIT cells and γδ T cells during tuberculosis compared with TBI (Libero et al., 2014). These cells

likely home to the site of infection (lung) to limit M.tb growth by complementing anti-M.tb classical T cell immune responses. However, the exact protective role of these and other DURT cells remains to be defined. For the purpose of this thesis, we shall not discuss these cell subsets further, since we primarily focused on understanding memory, function and activation profiles of classical CD4 T cells during different stages of TBI.

Although B cells are involved in immune responses against M.tb, we have a limited understanding of which aspects of B cell and antibody-mediated responses may be critical for M.tb control (Jacobs et al., 2016). Many studies have suggested a protective role of M.tb-specific antibody responses, while others suggest that high levels of M.tb-specific antibodies are driven by high antigen burden during disease and are not associated with protection [reviewed by (Achkar et al., 2015; Glatman-Freedman and Casadevall, 1998)]. Recent studies focused on understanding antibody-mediated effector functions demonstrated that modifications to the crystallizable fragment (Fc-region) of the antibody, such as glycosylation, digalactosylation and sialylation, likely play a larger role in antibody-mediated immune responses to M.tb than antibody titres (Lu et al., 2016, 2019). Further, they showed that antibody-mediated NK activation, cellular-mediated cytotoxic activity via antibody binding to the FcγRIII, and antibody-mediated inflammasome activation were enhanced in M.tb infected individuals compared to those with disease (Li and Javid, 2018; Lu et al., 2016). Further investigations are warranted to gain a better understanding of the role of B cells and antibodies during tuberculosis pathogenesis. Analysis of M.tb-specific antibody-responses during different stages of TBI was beyond the scope of this thesis.

Immunodiagnostics for TBI

TBI is assumed to cause a life-long infection in many individuals which maintains immunological memory without causing any pathology or symptoms. Bacterial burden during TBI is thought to be too low to be detectable in tissues using current tools. TBI is thus solely detected using immunodiagnostics that measure immunological sensitisation to M.tb, designed on the principle: detectable immune responses (memory) = viable TBI (bacterial persistence. The two types of TBI immunodiagnostics in use are tuberculin skin test(s) [TST(s)] and IFN-γ release assay(s) [IGRA(s)].

TST

TST measures a delayed cell-mediated hypersensitivity reaction induced upon intradermal injection with purified M.tb proteins, usually purified M.tb protein derivatives (PPD). TST can also measure immune responses to cross-reactive mycobacteria because antigens in PPD are also present in other mycobacterial *sp.* including BCG and NTMs. TST is administered by intradermal injection of PPD, which induces a local hypersensitivity reaction in M.tb-sensitised individuals that is measured using a calliper or ruler 48-72 hours later. This relatively long period (48-72 hours) between administration and recording of TST results enables activation of mycobacteria-specific effector and resting memory cells, which are recruited to the injection site where they release cytokines that activate other cells to release inflammatory mediators, leading to a hypersensitivity reaction (induration). A positive TST result is defined as an induration of ≥ 5mm, 10mm or 15mm, depending on age, epidemiological risk factors, geographical location, among other factors (Jasmer et al., 2002; Nayak and Acharjya, 2012).

IGRAs

IGRA predominantly measures adaptive T cell responses, specifically the release of IFN-γ by T cells upon stimulation with M.tb antigens, most commonly CFP-10 and ESAT-6. These antigens are highly immunodominant, expressed by M.tb and are absent from BCG and most NTMs, making IGRAs more specific for M.tb than TST. IGRAs are performed by stimulation of whole blood or PBMC with M.tb antigens for 16-24 hours, followed by measurement of IFN-γ either by enzyme-linked immunosorbent assay (ELISA) or enzyme-linked immunosorbent spot (ELISpot) assay.

QuantiFERON TB Gold (QFT, QIAGEN, Germany) is the most widely used ELISA-based IGRA and was the assay of choice to define TBI in the studies described in this thesis. In the QFT assay, whole blood is stimulated with M.tb antigens (CFP-10, ESAT-6), mitogen (positive control) or no antigen (negative control) at 37°C for 16-24 hours. This short stimulation period is likely to predominantly activate circulating T_E cells. Upon completion of stimulation, IFN-γ is measured using the sandwich ELISA technique and quantified as a concentration of IFN-γ international units (IU)/mL. Quantitative IGRA results are interpreted qualitatively as either positive or negative based on a positivity threshold of 0.35 IU/mL. The QFT platform has

evolved from its original inception. The first iterations of QFT [QFT-G and QuantiFERON TB Gold in Tube test (QFT-GIT)] used peptide pools of CFP-10, ESAT-6 and TB 7.7 proteins that were 20 mer long and preferentially induced IFN-γ expression by CD4 T cells (Mori et al., 2004). The latest version of QFT, QFT-Plus, has two separate M.tb-specific stimulant tubes, TB-1 and TB-2, which contain peptide pools that stimulate predominantly CD4 T cells and both CD4 and CD8 T cells, respectively (Petruccioli et al., 2016). Addition of TB-2, which includes shorter peptides, aims to improve the sensitivity of the QFT-plus because disease is associated with induction of M.tb-specific CD8 T cells to a larger extent than TBI (Petruccioli et al., 2017).

Clinical use of TBI diagnostics for monitoring acquisition and clearance of TBI

Although some studies showed that higher magnitude of M.tb-specific responses measured by IGRAs is associated with higher risk of disease (Andrews et al., 2017; Gupta et al., 2019a; Winje et al., 2018), these tests have a low (2-6%) positive predictive value for tuberculosis, and are mostly used for their excellent negative predictive value (>99%) (Gupta et al., 2019b, 2020b). As mentioned above, IGRAs are more specific for detecting TBI than TSTs. However, TSTs use is more widespread because they are significantly cheaper, require less equipment and technical expertise than the IGRAs. Thus, in low resourced clinical settings IGRAs are primarily used for research purposes, while IGRA testing is a common practice for tuberculosis management in high resourced settings. Serial IGRA/TST testing can be used to monitor acquisition of TBI in individuals with known tuberculosis risk, such as healthcare workers. IGRAs are better suited for serial testing than TSTs because they measure responses *ex vivo*, while TSTs inoculate individuals with M.tb antigens. Repeated inoculation has been shown to cause a boosting effect in individuals with low positive TST responses (Andrews et al., 2015; Menzies, 1999).

Challenges with serial IGRA (and TST) testing

A positive IGRA/TST technically means that an individual has detectable M.tb-specific memory responses induced by historical or current TBI, i.e. *in vivo* exposure to M.tb antigens. Clinically, individuals with positive IGRA/TST results are interpreted as harbouring an ongoing TBI and are thus at risk of developing tuberculosis and would benefit from TPT. Unlike for disease cure, no biomarker of infection clearance exists, and this makes defining a successful

outcome of TPT challenging. In addition, IGRA and TST cannot measure the occurrence of re-infection upon completion of TPT, and therefore cannot guide the decision to offer TPT again in high transmission settings.

Interpretation of IGRAs is generally simplified by the translation of IFN-γ levels to a qualitative positive/negative result, however quantitative detection of IFN-γ is not bimodal around the IGRA positivity threshold. Instead, IFN-γ expression in response to M.tb-specific antigenic stimulation has a wide dynamic range (Penn-Nicholson et al., 2015). Based on the QFT positivity threshold (0.35IU/mL), quantitative QFT values of 0.34IU/mL and 0.36IU/mL are defined as QFT negative and positive, respectively. *Is the difference between the two QFT values immunologically significant? Further, if IGRAs performed serially or in duplicate yield such results, is the difference due to biological or technical variability?* Multiple longitudinal studies have tested the utility of serial IGRA testing to monitor the acquisition of TBI in health care workers and household contacts (HHC). Most individuals were either persistently QFT negative or positive, or showed a robust QFT conversion signal from negative to persistent positive IGRA results. However, some participants showed discordant serial IGRA test results (Joshi et al., 2014; Pai et al., 2012; Veerapathran et al., 2008; Zyl-Smit et al., 2009):

- positive → negative
- positive → negative → positive
- negative → positive→ negative

Most individuals with discordant IGRA results had low quantitative IGRA responses that fluctuated around the assay cut-off, while robust conversion was associated with higher IFN-γ values (Nemes et al., 2017a; Pai et al., 2012; Ringshausen et al., 2010; Zanetti et al., 2012; Zyl-Smit et al., 2009). These studies highlight the importance of considering IFN-γ values and the epidemiological/risk context when interpreting serial IGRA results. However, there is still a limited understanding of the immunological significance of low quantitative IGRA responses. In most cases, fluctuations of low IFN-γ values are likely due technical variability, however, variability could also be due to biological reasons. Researchers have tried to account for technical variability by defining a QFT uncertainty zone (0.2IU/mL – 0.7IU/mL) to guide clinical interpretation of QFT results (Brown et al., 2017; Nemes et al., 2017a; Nienhaus et al., 2014; Ringshausen et al., 2012).

Nonetheless, robust IGRA conversion and reversion outside of the QFT uncertainty zone have been widely reported (Hawn et al., 2014; Hill et al., 2007; Joshi et al., 2014; Nemes et al., 2017a; Pai and O'Brien, 2007; Pai et al., 2009, 2012), and serial TST/IGRA testing can help delineate different stages of TBI, as discussed below.

Spectrum of TBI

The observations briefly reported above illustrate that TBI comprises a spectrum of different scenarios and does not necessarily represent a static state of chronic infection (Figure 5). Accurate identification of individuals who are truly uninfected, those who have a low-grade or possibly cleared infection, those who recently acquired TBI and those with established TBI who are at risk of disease progression is essential to provide appropriate clinical care, and could offer opportunities to delineate immune responses associated with natural protection from tuberculosis. Such knowledge could guide the development of tests for M.tb clearance as well as guide the interpretation of discordant serial QFT results.

Absence of TBI

M.tb uninfected individuals (defined by negative IGRA/TST result) have either not been exposed to M.tb or, if they did, their innate immune cells cleared M.tb rapidly without inducing adaptive immune responses detectable by IGRA or TST (Figure 5).

If they are truly uninfected, TST/IGRA- individuals cannot develop disease and should not have any detectable M.tb-specific immune responses. However, a few IGRA/TST- individuals do have detectable M.tb-specific responses (measured by flow cytometry or Luminex), albeit at a lower magnitude than IGRA/TST+ individuals (Adankwah et al., 2019; Penn-Nicholson et al., 2015). This suggests that some TST/IGRA- individuals were infected with M.tb at some point in their life (Dahlstrom, 1940; Hawn et al., 2014).

Resisters

Resisters were first described in a large epidemiological study that aimed to determine the dynamics of TBI and disease progression in highly exposed HHCs (Mahan et al., 2012; Stein et al., 2018a). Even though most HHC enrolled in the study acquired infection, defined by IGRA/TST conversion, some individuals remained IGRA/TST-. Initially, non-conversion was assumed to be due to low level or no M.tb exposure. However, analysis of epidemiological

data demonstrated that some M.tb uninfected individuals had similar duration and intensity of exposure to index cases as IGRA/TST converters and persistent IGRA/TST+ . Thus, resistance to acquisition of TBI was potentially due to host resistance or immunological reasons. The resister clinical phenotype has been observed in many other studies, as extensively reviewed by Simmons and colleagues (Simmons et al., 2018). Characterisation of antibody-mediated immune responses from these individuals demonstrated that resisters had similar levels of functional M.tb-specific antibodies, including those specific for CFP-10/ESAT-6, as M.tb infected (QFT/TST+) individuals. Surprisingly, these antibodies had markers of long-term maturation, such as class-switched sub-classes (IgG, IgA) including those associated with chronic infection (IgG2, IgG3), as well as antibody modifications such as glycosylation of the Fc region. Further, these M.tb-specific antibodies were also able to induce cellular activity including antibody-dependent cellular phagocytosis and neutrophil phagocytosis (Lu et al., 2019). Interestingly, resisters did have low but detectable levels of M.tb-specific CD154(40L)+TNF+IL-2+ CD4 T cells, a functional phenotype associated with low to no antigen exposure (Lu et al., 2019). These results demonstrated that resisters were at some point infected with M.tb, resulting in the induction of adaptive immune cells (Figure 5). However, TBI may have been transient but sufficient to induce robust long-lived cellular and humoral immune cells, but not prolonged enough to sustain a sizeable population of IFN-γ T_E cells, which mediate responses detected by IGRA. These observations highlight a major short-coming of IGRAs, specifically the inability to detect M.tb-specific IFN-γ-independent T cell functional responses. However, this does not fully explain why resisters were TST negative. Although a higher threshold to TST positivity (≥ 10mm) was used, almost all resistors had an induration of 0 mm. Inability to detect TST responses in resisters could be because T cell-mediated pro-inflammatory responses induced by TST were too low to recruit other cells and result in an induration at the injection site within the 2 days of TST read-out. It remains unclear whether the resister phenotype described here is characteristic of rapid clearance of TBI without the induction of long-lived IFN-γ producing cells, or sustained TBI with a very low M.tb burden that does not to drive T cell differentiation towards production of IFN-γ.

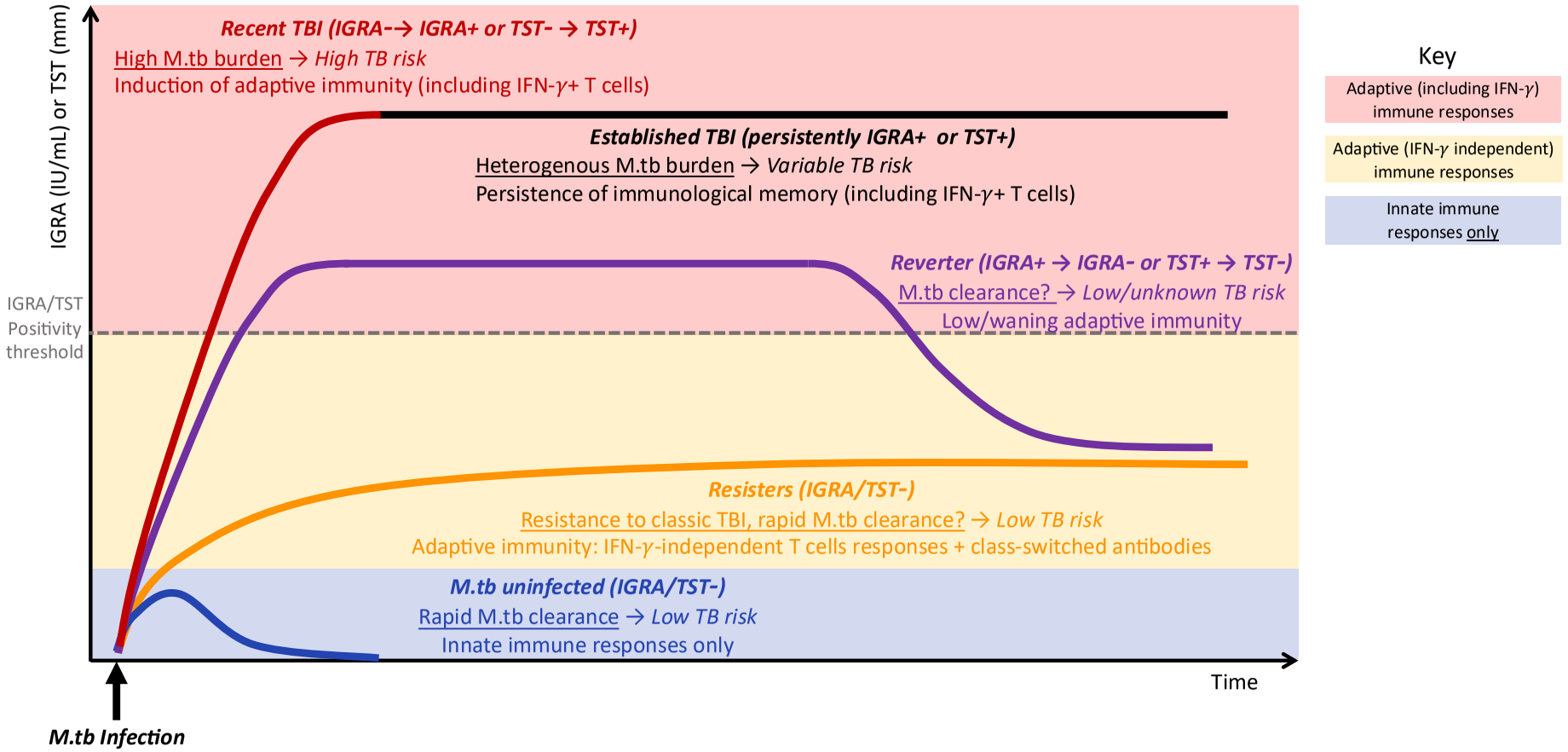

Figure 5: Graphical illustration of the hypothesised spectrum of TBI defined by IGRA/TST responses. There are many gaps in our understanding of immune responses associated with the spectrum of TBI (defined by IGRA/TST responses), some of which are highlighted in the figure. After initial M.tb infection, M.tb may be rapidly cleared by innate immune cells (**M.tb uninfected**) or adaptive IFN-γ-independent immune responses (**resisters**). In both situations, immune responses are not detectable by IGRA/TST and individuals are thus defined as IGRA/TST-. If M.tb persists, infection is generally associated with induction of adaptive (including IFN-γ) T cell responses that are detectable by IGRA/TST conversion (**recent TBI**), which in most cases leads to persisting IGRA/TST positivity (**established TBI**). However, a few individuals, who generally have a lower magnitude of IGRA/TST responses than individuals with established TBI, can revert their IGRA/TST responses from positive to negative (**reverters**). The magnitude of quantitative IGRA/TST responses associated with different stages of TBI (illustrated above) is depicted by the coloured lines. Dotted line represents the IGRA/TST positivity threshold. Shaded areas in the graph indicate induction of innate (light blue), adaptive IFN-γ-independent (orange) and adaptive (including IFN-γ+; pink) immune responses.

Classical TBI: recent and established infection

Robust TST/IGRA conversion is indicative of acquisition of TBI, which in most cases results in sustained TST/IGRA positivity (established TBI) (Figure 5).

How long does TBI last? Historical epidemiological studies showed that TBI can re-activate and progress to disease many years after primary infection, even in settings with extremely low exposure to re-infection (Ai et al., 2019; Yoshikawa, 1992). Accordingly, TBI is thought to be a state of chronic low-grade infection, where persistent expression of antigens maintains IFN-γ+ T_E cells (Figure 5). Several studies postulate that in many individuals detectable M.tb-specific immune responses are simply due to immunological memory and not indicative of ongoing bacterial replication (Behr et al., 2019; Emery et al., 2021).

I*s there a clinical difference in recent and established TBI?* Yes, recent IGRA conversion is associated with a higher risk of disease progression than remote infection (Behr et al., 2018; Wiker et al., 2010). *Is this increased risk due to a difference in antigen burden or immune responses between the two TBI states? Additionally, what does persistent IGRA positivity in individuals that do not progress to disease indicate? Is it a favourable response, indicative of long-term immunity that protects against re-infection as suggested by some* (Andrews et al., 2012; Cadena et al., 2018) *or is it indicative of a chronic low-grade infection that warrants provision of TPT?* Unfortunately, we are unable to definitively answer these questions based on the evidence we have thus far. It is likely that even this stage of TBI of persistent IGRA positivity is heterogenous and includes a mixture of both scenarios. In addition, even persistently IGRA/TST+ individuals (established TBI) can get re-infected, which would shift them to the recent TBI stage.

Murine and non-human primate models have demonstrated that M.tb rapidly grows during the primary stages of acute TBI and that the number of M.tb-containing lesions is established very early, while adaptive immune cells are being primed (Cooper and Khader, 2008; Lin et al., 2014; North and Jung, 2004). Thus, increased tuberculosis risk upon recent TBI in humans could be either due to a delay in priming adaptive immune cells that contribute to M.tb control or very high and uncontrolled M.tb replication, or a combination of both, which facilitates dissemination and potentially the establishment of tuberculosis lesions with high M.tb burden. On the other hand, individuals with established TBI have robust detectable memory immune cells, which likely controls M.tb growth upon secondary M.tb exposure (Andrews et al., 2012; Cadena et al., 2018). Levels of M.tb replication *in vivo* are likely higher

during recent compared to established TBI. If this is true, then provision of TPT to individuals with no other risk factors would likely benefit individuals with recent rather than established TBI. Unfortunately, we cannot distinguish between these two TBI states using our current diagnostic arsenal, except by serial testing. We have provided evidence that T cell function, memory and activation track antigen burden. To date, no study has compared longitudinal T cell responses between recent and established TBI. However, many studies have cross-sectionally compared immune responses between TBI and disease (Table 1), including one study that included recent and remotely infected individuals (Halliday et al., 2017). Despite defining a potential biomarker of recent TBI, TNF only T_E CD4 T cells, Halliday and colleagues did not perform an in-depth characterisation of immune response associated with recent and remote TBI.

Table 1: T cell features that distinguish between TBI and tuberculosis diseases and may track antigen load.

Category of the T cell feature	Cell Population	T cell feature	Comment	Studies
T cell activation	IFN-γ+ or Total Th1 cytokine+ CD4 T cells	HLA-DR+ and/ or CD38+ CD4 T cells	Higher during disease	(Adekambi et al., 2015; Riou et al., 2017; Wilkinson et al., 2016)
	IFN-γ+TNF+ CD3 T cells	HLA-DR+ CD3 and CD4 T cells	Higher in disease	(Musvosvi et al., 2018)
T cell proliferation	IFN-γ+ or Total Th1 cytokine+ CD4 T cells	Ki-67+ CD4 T cells	Higher in disease	(Adekambi et al., 2015; Riou et al., 2017; Wilkinson et al., 2016)
T cell memory	CD4 T cells	CD27 Median fluorescence intensity (MFI) = $\frac{\text{CD27 MFI of total CD4 T cells}}{\text{IFN-γ+ CD4 T cell CD27 MFI}}$	Higher in TBI	(Portevin et al., 2014)
Cytokine producing CD4 (and CD8 T cells)	CD4 T cells	Frequencies of IL-2+ CD4 T cells	Higher during TBI	(Sargentini et al., 2009)
	CD4 T cells	Frequencies of TNF only CD4 T cell	Higher in disease	(Harari et al., 2011)
	CD8 T cells	CD8 T cell responder rate	Higher in disease	(Rozot et al., 2013, 2015)

In these studies, the magnitude of IFN-γ+ and total Th1 cytokine+ T cells were not different between TBI and disease, however, specific T cell properties such as activation (Adekambi et al., 2015; Musvosvi et al., 2018; Riou et al., 2017; Wilkinson et al., 2016), memory phenotype (Portevin et al., 2014) and Th1 cytokine co-expression profiles (Harari et al., 2011; Rozot et al., 2013, 2015) did distinguish between TBI and disease (Table 1). All these biomarkers are based on T cell features associated with high antigen exposure (discussed in detail in the "CD4

T cell functions during tuberculosis pathogenesis" section). *If these properties can distinguish between TBI and disease, can they also distinguish between recent and remote TBI*? We aimed to answer this question by conducting an in-depth characterisation of CD4 and CD8 T cell functional, memory and activation profiles to determine T cell features that can distinguish between recent and established TBI.

Reverters

Detection of transient IGRA/TST conversion followed by robust reversion illustrates the dynamic nature of TBI and challenges the common assumption that TBI causes lifelong infection. If detectable immune responses indicate ongoing bacterial replication, *does IGRA/TST reversion suggest clearance of infection*? Studies conducted during the pre-antibiotic era demonstrated that TST reversion was associated with a lower risk of disease progression and reported the detection of calcified lung lesions suggestive of contained and cleared disease in TST-negative individuals who had no recorded history of tuberculosis (Dahlstrom, 1940). Additionally, animal models demonstrated that guinea pigs that acquired TBI (defined by recent TST conversion) and then reverted to a negative TST had sterile lung lesions indicative of cured infection (Dharmadhikari et al., 2011; Riley et al., 1959, 1962). These findings provided evidence that some individuals can spontaneously cure TBI and gave rise to the **reversion = clearance hypothesis**, which contradicts the common assumption that TBI is a life-long chronic condition.

Reversion has been observed naturally (Adams et al., 1959; Dahlstrom, 1940; Hawn et al., 2014; Hill et al., 2007; Jenum et al., 2014; Medawar et al., 2019; Pai et al., 2009, 2012; Xin et al., 2019a; Zhang et al., 2019; Zyl-Smit et al., 2012), in association with antibiotic treatment (Ewer et al., 2006; Hill et al., 2007; Johnson et al., 2014; Zhang et al., 2019) and BCG-revaccination (discussed later) (Nemes et al., 2018). Despite multiple reports of natural or intervention-induced reversion, very few studies have investigated M.tb-specific immunological responses associated with reversion, besides a decrease in M.tb-specific IFN-γ (Jenum et al., 2014; Medawar et al., 2019). Medawar and colleagues showed that QFT reverters had significantly lower magnitudes of M.tb-specific IFN-γ, IFN-α, IL-2 and matrix metalloproteinase-3 (MMP-3) post-reversion than remotely infected individuals, and were in range with those detected in non-converters (Medawar et al., 2019). A study by Jenum and colleagues partially contradicted these findings, by showing that magnitude and cytokine co-

expression profile of M.tb-specific Th1 CD4 T cells were not significantly different between QFT reverters (n=6) and remotely infected individuals [n=14, (Jenum et al., 2014)]. However, this study had a small sample size (n=20) and was likely underpowered to detect any meaningful statistical differences. A study by Xin and colleagues that measured direct *ex vivo* cytokines and chemokines (12 analytes) in reverters and remotely infected individuals, observed lower serum levels of monocyte chemoattractant protein-1 (MCP-1/CCL2) and IL-8 in QFT/TST reverters compared with remote TBI (Xin et al., 2019a). These results suggest that reverters are distinct from persistently QFT+ individuals and could be more similar to QFT non-converters. However, immunological data available does not provide conclusive evidence for lower or no *in vivo* antigen load in reverters compared to remotely infected individuals.

Does reversion indicate a reduction of in vivo antigen exposure or loss of recognition of CFP-10/ESAT-6? Low *in vivo* antigen exposure or loss of antigen recognition is associated with a drastic increase in T_{SCM}/T_{CM} cells, lower IFN-γ production and T cell activation, compared to high *in vivo* antigen exposure (Appay et al., 2008; Lugli et al., 2013a; Seder et al., 2008). Further, resisters maintain low but robustly detectable M.tb-specific IFN-γ-independent Th1 CD4+ T cells (Lu et al., 2019). However, since TST measures immune responses to multiple M.tb antigens (PPD), reversion may indicate a true reduction in immune responses, likely due to antigen clearance. Unfortunately, addressing this hypothesis by detecting *in vivo* antigen load in humans is virtually impossible, therefore tracking the kinetics of T cell features shaped by antigen burden seems an appropriate alternative option. We thus aimed to answer some of these questions by characterising M.tb-specific CD4 and CD8 T cell functional, memory and activation kinetics associated with QFT reversion.

Prevention of TBI by vaccination

Researchers hypothesise that reduced efficacy of BCG against tuberculosis in adolescents and adults is partly due to waning immunity (Orme, 2010). Therefore, several vaccination strategies aimed at boosting newborn BCG-induced immunity during adolescence are being tested (Hatherill et al., 2020). In high transmission settings where rates of TBI and disease increase during adolescence, measuring vaccine efficacy to prevent TBI rather than disease has been proposed as an efficient trial design to provide proof-of-concept prior to larger efficacy trials testing protection against disease (Ellis et al., 2015). This is because TBI occurs

much more frequently than disease, and if the efficacy in preventing infection is high, then likely the same vaccine could be successful at preventing disease. In these prevention of TBI trials, the efficacy end-points include IGRA conversion from negative to positive, and sustained QFT conversion without reversion to a negative test. Since IGRA conversion usually results in persistent QFT positivity (sustained conversion) and is the defining feature of established TBI, the inverse transient conversion followed by a reversion (QFT- → QFT+ → QFT-) could be indicative of M.tb clearance that does not result sustained (established) TBI.

A recent BCG revaccination trial of M.tb-uninfected adolescents, who were vaccinated with BCG at birth, demonstrated partial vaccine-induced protection [45.4% (95% CI 6.4 to 68.1%) efficacy] against the acquisition of sustained TBI, defined as transient QFT conversion followed by a swift reversion (QFT- → QFT+ → QFT-) within a 6-month period (Nemes et al., 2018). The partial efficacy of BCG revaccination against sustained acquisition of TBI could be attributed to boosting of already existing immune responses, which rapidly cleared infection upon M.tb-exposure (Rakshit et al., 2019; Rozot et al., 2020). These results suggest that vaccine-induced QFT reversion may be biologically meaningful, but we still have a limited understanding of the immunological significance of reversion beyond a decrease in IFN-γ levels below the QFT threshold. Therefore, another main objective of this thesis is to comprehensively characterise immune responses in a cohort of adolescents experiencing spontaneous QFT reversion, to inform the interpretation of the clinical trial results.

Trials performed in other settings did not show significant protection of BCG revaccination against tuberculosis disease (Barreto et al., 2011; Geneva: World Health Organization, 2017). These trials did not stratify individuals based on TST/IGRA status and had a different endpoint (disease). In subgroup analyses among younger children with negative TST, partial protection against disease was indeed observed (Barreto et al., 2011). Therefore, since infection is required for progression to tuberculosis, BCG-revaccination of M.tb uninfected individuals might be protective against the development of tuberculosis, a hypothesis that needs to be tested. Nonetheless, these studies have shown that testing vaccine efficacy for prevention of TBI is a feasible and biologically meaningful approach to identify vaccine candidates that should be tested for efficacy to prevent disease progression.

Aims and objectives of this thesis

As described in detail above, there are gaps in our understanding of immunological responses associated with recent QFT conversion and reversion. An improved understanding of immunological features associated with these TBI states, as well as sustained QFT positive and non-conversion states, is needed to guide the development of novel diagnostics for TBI and the interpretation of serial discordant QFT results. We thus measured Th1 cytokine, memory and activation profiles of M.tb-specific CD4 and CD8 T cells induced by natural infection in recent QFT converters and reverters, as well as in persistent QFT+ individuals and non-converters, to achieve the objectives listed below.

All methodology and statistical analyses described in Chapters 2-6 were performed by Cheleka Anne-Marie Mpande, unless stated otherwise.

Thesis objectives and hypotheses.

I. **To optimise MHC class II tetramer staining protocols to detect chemokine receptor, cytotoxic molecule and memory marker co-expression profiles of M.tb-specific CD4 T cells directly *ex vivo* (Chapter 2).**

II. **To determine if M.tb-specific CD4+ T_{SCM} cells are induced by TBI and characterise the chemokine receptor, cytotoxic molecule and cytokine co-expression profiles of M.tb-specific CD4+ T_{SCM} cells (Chapter 3).**

    i. *We hypothesise that M.tb-specific CD4+ T_{SCM} cells are induced by primary TBI and are sustained throughout established TBI.*

    ii. *We hypothesise that M.tb-specific CD4+ T_{SCM} cells are the least differentiated M.tb-specific memory subsets and have functional features characteristic of M.tb memory cells, such as expression of CXCR3 and Th1 cytokines, despite their naïve phenotype.*

III. **To optimise a PBMC stimulation and intracellular cytokine staining assay that enables reliable detection of M.tb-specific T cell functional, memory and activation profiles (Chapter 4).**

IV. To define a simplified biomarker of recent TBI based on differential expression of M.tb-specific CD4 and CD8 T cell functional, memory and activation profiles during recent and remote TBI (Chapter 5).

i. We hypothesise that individuals with recent TBI have higher proportions of activated (HLA-DR+) and Th1 functional/memory phenotypes associated with high antigen burden than remote TBI.

ii. We hypothesise that remote (established) TBI is associated with higher proportions of terminally differentiated T_E cells with IFN-γ-monofunctional activity and express higher levels of KLRG-1 than recent infection.

V. To characterise M.tb-specific CD4 and CD8 T cell functional, memory and activation kinetics associated with QFT reversion (Chapter 6).

i. We hypothesise that QFT reversion represents a true reduction in IFN-γ expression by M.tb-specific T cells rather than an artefact due to technical assay variability.

ii. We hypothesise that QFT reversion is associated with a relative enrichment T_{SCM} and T_{CM} CD4+ T cells, memory subsets associated with low antigen load.

Chapter 2: Optimisation of chemokine receptor and cytotoxic molecule staining to detect M.tb-tetramer+ CD4 T cells

Introduction

M.tb-specific CD4 T cells play an important role in the control of TBI (summarised in Chapter 1: General Introduction). Though widely studied, characterisation of M.tb-specific CD4 T cell responses has predominantly focused on co-expression patterns of Th1 cytokines, IFN-γ, TNF and IL-2. However, comparison of Th1 cytokine co-expression profiles between TBI and tuberculosis disease has not resulted in improved knowledge of the role of T cell functional phenotypes in disease progression. This highlights the need for improved understanding of other T cell characteristics such as memory phenotype, homing capacity and cytotoxic function induced by TBI.

Antigen-specific CD4 and CD8 T cells are typically detected by measuring functional responses induced by *in vitro* whole blood or PBMC antigenic stimulation. Though widely used, *in vitro* stimulation can also affect the expression pattern of phenotypic markers that may not reflect profiles observed *in vivo*. Alternatively, antigen-specific T cell responses can be detected directly *ex vivo* without the need of antigenic stimulation using specialised multimeric peptide-MHC molecules, such as tetramers (discussed in detail in the "Ex vivo identification of antigen-specific T cells" section). MHC I tetramers have been widely used to detect and immunophenotype classical CD8 T cell properties and kinetics during viral infections or cancer (Klenerman et al., 2002; Lechner et al., 2001; Mami-Chouaib et al., 2002). Over the past two decades, MHC II tetramer technology has advanced to accurately detect CD4 T cells (Nepom, 2012; Sims et al., 2014). Additionally, the use of tetramers to detect antigen-specific T cells circumvents the need to measure multiple functional responses induced by antigen stimulation to define the T cell specificity. This facilitates the design of flow cytometry panels that solely focus on detecting cytokine-independent features of antigen-specific T cells.

Our research group has successfully used MHC II tetramers to detect, sort and determine direct *ex vivo* M.tb-specific CD4 T cell memory and functional transcriptional profiles during TBI and in response to vaccination (Dintwe et al., 2013; Moguche et al., 2017; Mpande et al., 2018). Additionally, we were able to accurately detect antigen-specific CD4 T cells with a naïve phenotype using tetramers (Dintwe, 2014; Dintwe et al., 2013). These cells have also been detected using *in vitro* antigen stimulation (Soares et al., 2008). However, this population has

been largely disregarded because researchers considered them an artefact of *in vitro* stimulation and not true memory T cells because T_N cells are not known to readily produce effector molecules upon brief re-stimulation (Mitra et al., 1999; Rosa et al., 2001). Transcriptomic analysis of naïve-like memory tetramer+ CD4 T cells by Dintwe and colleagues suggested that these cells possessed functional features such as expression of cytokines (IFN-γ, TNF, IL-2), chemokine receptors (CCR4, CCR5, CCR6, CCR9) and cytotoxic molecules [granzymes (A,B,K), granulysin, perforin], suggestive of true memory responses (Dintwe, 2014; Mpande et al., 2018). We therefore aimed to determine the cytokine, chemokine receptor and cytotoxic molecule co-expression patterns of naïve-like memory T cells induced by recent TBI, outlined in Chapter 3.

Before my research project, our in-house tetramer staining protocol predominantly measured the co-expression pattern of memory markers or integrins and adhesion molecules on tetramer+ CD4 T cells in a flow cytometry panel of not more than 9 fluorochromes (Dintwe, 2014; Dintwe et al., 2013; Moguche et al., 2017). Increasing the number fluorochromes detected in a single flow cytometry panel increases potential spill-over and spread issues which could result in detection of non-specific tetramer responses, as well as negatively impact the resolution of co-expression phenotypes on tetramer+ CD4 T cells. Additionally, modifying the staining protocol to include measurement of intracellular cytotoxic markers could disrupt the tetramer-TCR binding interaction, further decreasing resolution of tetramer+ signal.

This chapter summarises the optimisation processes conducted to develop tetramer staining protocols required to accurately detect the co-expression of up to 11 phenotypic and/or intracellular markers in a single experiment without decreasing the resolution of tetramer detection.

Specific Objectives

I. **Optimise MHC II tetramer staining protocol to detect co-expression patterns of up to 11 molecules on MHC II tetramer+ CD4 T cells.**
II. **Optimise antibody staining protocol to detect chemokine receptor and memory marker co-expression profiles of MHC II tetramer+ CD4 T cells.**

III. **Optimise antibody staining protocol to detect intracellular cytotoxic molecule and memory marker co-expression profiles of MHC II tetramer+ CD4 T cells.**

Materials and Methods

Participant samples and ethics

HLA-typed participants were selected from the SATVI biorepository [Human research ethics committee (HREC) 126/2006; (Mahomed et al., 2011a)], and recruited from our research sites in Cape Town or Worcester, Western Cape, South Africa (HREC 753/2014). All participants provided written informed consent and were enrolled based on inclusion criteria summarised in table 2. QFT assay was performed on all participants when possible.

Table 2: Participant inclusion criteria.

Inclusion Criteria	Cape Town	Worcester
Above 18 years of age	Yes	Yes
No self-reported previous history of tuberculosis	Yes	Yes
Not on any tuberculosis medication or have current tuberculosis	Yes	Yes
HIV seronegative determined by HIV rapid test	Not tested	Yes
Participant does not have low blood pressure	Not tested	Yes
Not pregnant if female	Not tested	Yes*

*Self-reported pregnancy

HLA-typing

Prior to staining PBMC with tetramers, HLA-typing is required to determine which tetramers could be used to measure M.tb-specific T cells. Experimental protocols used to perform HLA-typing were conducted by Dintwe and Musvosvi [described in detail in (Dintwe, 2014; Nyasha, 2016)] and collated into a participant HLA database. Briefly, deoxyribonucleic acid (DNA) was extracted from PBMC to determine high resolution HLA class I and II genotypes by polymerase chain reaction (PCR) using sequence-specific primers (Sidney et al., 1999). HLA allele ambiguities were resolved by allele-specific DNA sequencing (Moguche et al., 2017; Wang et al., 2008).

Sample preparation

Isolation of PBMC from whole blood

We isolated PBMC from whole blood using the Ficoll-density gradient centrifugation method. Whole blood was collected from participants in sodium-heparinised tubes (Becton Dickinson (BD) Vacutainer®) or blood bags (Mediclinic, Worcester), diluted at a ratio of 1:1 in 1X

phosphate buffer saline solution (PBS, Lonza). PBMC were then isolated from diluted whole blood within 4 hours using either 50mL Falcon tubes or Leucosep tubes [50mL tube with filter (Greiner Bio-One)]. 15mL of Ficoll-Histopaque1077 (Ficoll, Sigma Aldrich) solution was added to 50mL Falcon or Leucosep tubes, followed by centrifugation of Leucosep tubes only at 1000 Relative centrifugal force [RCF; times gravity (xg)] for 1 minute to ensure that Ficoll was below the filter. 30mL of diluted blood was either layered into 50mL Falcon tube using a 25mL pipette ensuring that Ficoll and blood do not mix, or added to Leucosep tube. PBMC were separated from granulocytes by centrifugation at 1100 xg for 15 minutes, at 21°C with 0 deceleration. The buffy coat layer of PBMC suspended in plasma supernatant was then transferred to a 50mL Falcon tube and resuspend to a final volume of 50mL in PBS. This tube was then centrifuged at 931xg for 10 minutes, at 21°C with maximum deceleration. Cells were further washed twice by discarding supernatant, re-suspension of cells in 50mL of PBS and centrifugation for 10 minutes. After the second wash, supernatant was discarded, and cells were used either fresh or cryopreserved.

Cryopreservation of freshly isolated PBMC

Isolated PBMC were resuspended to a total volume of 5mL in 10% fetal bovine serum (FBS, Hyclone) in Roswell Park Memorial Institute (RPMI, Lonza) solution, enumerated and resuspended in 10% FBS/RMPI to a final concentration of 20 million PBMC/mL. 500µL of cells in 10% FBS/RPMI were then transferred to cryovials, followed by dropwise addition of cold (4°C) 500µL of 20% dimethyl sulfoxide (DMSO, Sigma Aldrich)/FBS solution. Cryovials containing cells in cryopreservation solution were then transferred to -80°C for not more than 3 days and finally transferred to liquid nitrogen tanks for long term storage.

Thawing of cryopreserved PBMC

Cryovials containing cryopreserved PBMC were retrieved from liquid nitrogen tanks and transferred to a rack in dry ice. Cryovials were partially thawed at 37°C by shaking of cryovial in a water bath, followed by addition of 1mL of thawing solution [10% FBS, 1% volume/volume (v/v) of L-glutamine and penicillin-streptomycin (Lonza) in RPMI]. Cells were then transferred to a total of 10mL thawing solution and centrifuged at 460xg for 7 minutes at 21°C. Upon completion of centrifugation, supernatant was discarded, cells were resuspended in 1mL PBS

containing 50μL of DNAse (2000IU/mL, Sigma Aldrich) and incubated at 37°C for 15 minutes (cryopreserved within 2 years) or 30 minutes (cryopreserved for more than 2 years). After incubation cells were enumerated for viability and washed by resuspension in a total volume of 10mL of PBS and centrifugation. Supernatant was then discarded, and cells diluted to a final volume of 100μL with PBS in preparation of antibody staining.

Optimisation of flow cytometry staining protocols

Antibodies

Antibodies were all titrated and optimum volumes were selected based on the best compromise between high stain index, signal: noise ratio and frequency of positive population, and low fluorescence spread into other channels. This was followed by fluorescence minus one (FMO) experiments, which were used to determine the spill over effect of antibodies into other detectors and determine possible compensation issues. In brief, cells were stained with all antibodies except one, this was repeated for each antibody in the panel.

BD LSR Fortessa Configuration

The BD Bioscience LSR Fortessa was set up with the configuration below (Table 3). Daily quality checks were performed to monitor performance of the machine and determine optimum voltages for each detector (Perfetto et al., 2012). In addition to daily quality checks, we used single-stained compensation beads (BD Biosciences) to create a compensation matrix for each experiment. Briefly, a specified volume of antibody was added to equal volumes of positive [immunoglobulin (Ig) K containing beads] and negative compensations beads and incubated for 10 minutes. Antibody stained compensation beads were then washed by addition of 1mL PBS and centrifugated for 5 minutes at 931xg. Supernatant was then discarded, and beads fixed with 1% paraformaldehyde (Kimix) in PBS (1% PFA).

Table 3: BD LSR Fortessa Configuration.

Laser	Detector	First Filter (Long Pass)	Second Filter (Band Pass)	Fluorochrome
Violet Laser 405 nm	A	750LP	780/60	BV785
	B	685LP	710/40	BV711
	C	630LP	670/30	BV650
	D	585LP	605/30	BV605
	E	550LP	572/36	BV570
	F	535LP	560/40	Qdot545
	G	505LP	525/50	BV510
	H		450/50	BV421
Blue Laser 488 nm	A	670LP	685/35	PerCP-Cy5.5
	B	505LP	515/20	FITC
	C		488/10	SSC
Green Laser 544 nm	A	750LP	780/60	PE-Cy7
	B	685LP	710/50	PE-Cy5.5
	C	635LP	670/30	PE-Cy5
	D	610LP	610/20	PE-CF594
	E		575/26	PE
Red Laser 633 nm	A	750LP	780/60	APC-H7
	B	685LP	730/45	Alexa Fluor 700
	C		660/20	APC

Abbreviations: BV- brilliant violet; Qdot- Quantum dots; SSC- side scatter

Optimisation of chemokine receptor flow cytometry staining.

To determine the optimal sample type and antibody staining temperature for detection of chemokine receptors, cells were stained with anti-chemokine receptor antibodies in the following conditions.

Chemokine receptor staining of cryopreserved or fresh PBMC

Cryopreserved PBMC were prepared according to the protocol above. PBMC in 100μL of PBS were first incubated with viability marker Aqua (0.5μL, ThermoScientific) for 20 minutes. Cells were then washed with 1mL of PBS and centrifuged at 930xg for 5 minutes at 21°C. Supernatant was then discarded and cells resuspended in 100μL of PBS. Cryopreserved or fresh PBMC were then stained with anti-CCR4 BV421 (cryopreserved: 1.25μL, fresh: 2.5μL, Clone: 1G1, BD Biosciences), anti-CXCR3 PE-Cy5 (cryopreserved: 5μL, fresh: 2.5μL, Clone: 1C6/CXCR3, BD Biosciences) or anti-CCR6 BV605 (fresh: 1.25μL, Clone: 11A9, BD Biosciences). Unless specified, the same clones and volumes were used for all experiments. Cryopreserved cells were then incubated for 30 minutes at either room temperature (RT) or 37°C, while fresh cells were only incubated at 37°C.

Following chemokine receptor staining incubation, a 50μL antibody cocktail containing only phenotypic markers in PBS (Table 4) was added to the cells and incubated for 20 minutes at RT. After completion of antibody staining incubation, cells were washed by centrifugation, supernatant discarded, resuspended in 100μL of PBS, acquired on the BD LSR Fortessa.

Table 4: PBMC phenotypic marker panel.

Marker	Clone	Manufacturer	Fluorochrome	Volume
CD3	UCHT1	BD Biosciences	Alexa Fluor 700	0.6 μL
CD4	SK3	BD Biosciences	BV786	1 μL
CD8	RPA-T8	BD Biosciences	PE	1 μL
CD45RA	HI100	eBioscience	PE-Cy7	0.075μL

Chemokine receptor staining of whole blood

A 50μL antibody cocktail containing only phenotypic markers in distilled water (dH_2O, Table 4) was added to whole blood in combination with either anti-CCR4 BV421 (1.25μL), anti-CCR6 BV605 (2μL) or anti-CXCR3 PE-Cy5 (5μL) and incubated for 30 minutes at RT. 1mL of 1X FACS Lysing solution (BD Biosciences) was then added to antibody-stained cells, vortexed and incubated for 15 minutes at RT. This was followed by centrifugation of cells at 930xg for 5 minutes, supernatant discarded, cells resuspended in 100μL PBS and acquired on the BD LSR Fortessa.

Optimisation of antibody staining buffers

Cryopreserved PBMC were thawed as specified above, PBMC were either resuspended in 50μL of PBS or BD brilliant stain (BS, BD Biosciences) buffer after which an antibody cocktail of chemokine receptor markers (Table 5) diluted in PBS was added to cells and incubated for 30 minutes at 37°C.

Table 5: Chemokine receptor antibody cocktail.

Marker	Clone	Manufacturer	Fluorochrome	Volume
CCR2	K036C2	BioLegend	APC	1.25 μL
CCR4	1G1	BD Biosciences	BV421	1.25 μL
CCR5	2D7		BV711	1.25 μL
CCR6	11A9		BV605	1.25 μL
CCR7	150503	eBioscience	PE-CF594	1 μL
CXCR3	IC6/CXCR3	BD Biosciences	PE-Cy5	2.5 μL

Cells were then washed in 2mL of tetramer staining buffer (2% FBS, 2mM ethylenediaminetetraacetic acid (EDTA) in PBS) by centrifugation. Supernatant was discarded and cells resuspended in 100μL of tetramer staining buffer, this was followed by single tetramer staining by addition of either M.tb-tetramer-PE or CLIP-control (CLIP)-tetramer-PE (2μg/mL, NIH Tetramer facility, Table 6) to cells and incubated for 1 hour at RT.

Table 6: HLA-class II tetramer-peptide conjugates.

Tetramer	HLA Sequence	Protein	Peptide Sequence
M.tb	DPB1*04:01	$Ag85B_{128-144}$	GKAGCQTYKWETFLTSE
M.tb	DRB1*03:01	$Ag85A_{56-75}$	VPSPSMGRDIKVQFQSGGAN
M.tb	DRB1*04:01	$CFP\text{-}10_{71-85}$	EISTNIRQAGVQYSR
M.tb	DRB5*01:01	$CFP\text{-}10_{51-65}$	AQAAVVRFQEAANKQ
M.tb	DQB1*06:02	$ESAT\text{-}6_{31-45}$	EGKQSLTKLAAAWGG
CLIP-Control	DPB1*04:01; DRB1*03:01; DRB1*04:01; DRB5*01:01; DQB1*06:02	$CLIP_{87-101}$	PVSKMRMATPLLMQA

Cells were then washed in 1mL of PBS by centrifugation. Cells previously resuspended in BS buffer or PBS, were resuspend in 50μL of BS buffer or PBS, respectively, and stained with an antibody cocktail containing viability marker and phenotypic markers (Table 7) for 30 minutes at RT. Cells were then washed in 1mL of PBS by centrifugation and supernatant discarded. Cells that were stained in the presence of BS buffer or PBS were resuspended in 100μL 1% PFA or PBS, respectively.

Table 7: Phenotypic antibody cocktail.

Marker	Clone	Manufacturer	Fluorochrome	Volume
CD3	UCHT1	BD Biosciences	Alexa Fluor 700	0.5 μL
CD4	OKT4	BioLegend	BV785	0.5 μL
CD45RA	HI100	eBioscience	PE-Cy7	0.075 μL
CD27	L128	BD Biosciences	BV650	1.25 μL
CD95	DX2	BioLegend	FITC	0.075 μL
CD8	RPA-T8	BD Bioscience	BV510*	0.6 μL
CD14	M5E2	BioLegend	BV510*	1.25 μL
CD19	SJ25C1	BD Biosciences	BV510*	0.6 μL
CD335	9E2	BD Biosciences	BV510*	2.5 μL
Viability	(Ref L34957)	Thermo-Fisher Scientific	Aqua*	1 μL

*Dump channel: multiple reagents conjugated with fluorochromes detected by the same detector are used to exclude undesirable cell populations that could create artefacts in tetramer staining (Chattopadhyay et al., 2008; Dolton et al., 2015; Scriba et al., 2005).

Optimisation of tetramer staining protocol

PBMC were thawed according to the protocol above and cells diluted to a final volume of 100μL with PBS. Cells were then incubated at 37°C for 30 minutes with anti-CCR7 PE-CF594 (0.5μL) and where applicable anti-CCR2 PE (0.3μL, Clone: K036C2, BioLegend). Cells were then washed by addition of 2mL of tetramer staining buffer by centrifugation. Supernatant was then discarded and cells diluted to a final volume of 100μL with tetramer staining buffer. The following tetramer staining conditions were compared in parallel:

I. Single tetramer staining of cells for 1 hour at RT with either M.tb-tetramer-APC or CLIP-tetramer-APC at 2μg/mL in separate tubes.
II. Cells were pre-incubated for 15 minutes at RT with either CLIP-tetramer-APC or CLIP-tetramer-PE (2μg/mL). This was followed by addition of M.tb-tetramer-PE or M.tb-tetramer-APC (2μg/mL) to cells pre-stained with either CLIP-tetramer-APC or CLIP-tetramer-PE respectively, and incubation for 1 hour.
III. Dual tetramer staining of cells by co-staining with both CLIP-tetramer-APC and CLIP-tetramer-PE or M.tb-tetramer-APC and M.tb-tetramer-PE, followed by an (1) hour incubation at RT.

Upon completion of tetramer staining incubation, cells were washed in 2mL of PBS by centrifugation. Cells were then resuspended in a final volume of 50μL with BS buffer, and a 50μL antibody master mix of viability and lymphocyte lineage markers of interest (Table 7) was added and incubated for 30 minutes at RT. Upon completion of incubation cells were washed in 1mL of PBS by centrifugation, supernatant discarded and cells were resuspended in 1% PFA.

Optimisation of cytotoxic molecules staining protocol

PBMC were thawed according to the protocol above and cells diluted to a final volume of 100μL with PBS. Phenotypic markers were stained in parallel either before [protocol 1 (stain then)] or after **[protocol 2 (fix then stain)]** fixation and permeabilisation of cells. In both protocols, cells were incubated at 37°C for 30 minutes with anti-CCR7 BV711 (1μL; Clone: 150503, BD Biosciences), while viability marker (Aqua, 0.5μL) was added to **protocol 2 (fix then stain)** only. Cells were then washed in 2mL of tetramer staining buffer, supernatant discarded and diluted to a final volume of 100μL with tetramer staining buffer. Cells were

either incubated with no tetramer or identical M.tb-tetramers conjugated to either -PE or -APC (dual staining) for 1 hour at RT. Cells were washed in 3mL of PBS by centrifugation and supernatant discarded. Cells stained according to protocol 1 (stain then fix) were then resuspended to a final volume of 50μL with BS buffer, followed by addition of a cocktail of viability and phenotypic antibodies (Table 8) and a 30-minute incubation at RT. Cells were then washed in 1mL of PBS by centrifugation and supernatant discarded.

Table 8: Phenotypic markers antibody cocktail.

Marker	Clone	Manufacturer	Fluorochrome	Volume
CD3	UCHT1	BD Biosciences	Alexa Fluor 700	0.5 μL
CD4	SK3	BD Bioscience	BV786	0.5 μL
CD45RA	HI100	eBioscience	APC-H7	2 μL
CD27	L128	BD Biosciences	BV650	1.25 μL
CD95	DX2	BD Biosciences	BV605	1 μL
CD8	RPA-T8	BD Bioscience	BV510	0.6 μL
CD14	M5E2	BioLegend	BV510	1.25 μL
CD19	SJ25C1	BD Biosciences	BV510	0.6 μL
CD335	9E2	BD Biosciences	BV510	2.5 μL
Viability	(Ref L34957)	Thermo-Fisher Scientific	Aqua	0.5 μL

250μL of Cytofix/Cytoperm solution (BD Biosciences) was then added to cells (stained using both protocols), vortexed and incubated for 20 minutes on ice. Cells were then washed twice with 1mL of 1X Perm/Wash [BD Perm/Wash 10X (BD Biosciences) concentration diluted to 1X in dH_2O] by centrifugation, supernatant discarded and resuspended with 50μL of 1X Perm/Wash. Cells stained according to protocol 1 (stain then fix) were incubated with no antibodies, while a cocktail of phenotypic antibodies (Table 8, excluding viability marker) was added to cells stained according to **protocol 2 (fix then stain)** and incubated for 30 minutes at RT. Cells were then washed with 2mL of Perm/Wash by centrifugation, supernatant discarded, resuspended in 100μL of 1% PFA and acquired on the BD LSR Fortessa.

Data Analysis

Flow cytometry analysis was conducted using FlowJo version(v)9.4 - v9.9. Compensation was calculated using single stained compensation beads, and then applied to all samples in the FlowJo workspace. Where applicable, the median fluorescence intensity (MFI) of the positive and negative cell populations, and the robust standard deviation of the negative cell population were calculated in FlowJo. These parameters were then used to calculate the stain

index (equation 1) and signal: noise ratio (equation 2) to assess separation between positive and negative signal.

$$Stain\ Index = \frac{(MFI\ of\ positive\ population) - (\ MFI\ of\ negative\ population\ )}{2\ X\ robust\ standard\ deviation\ of\ the\ negative\ population}$$

Equation 1: Calculation of stain index

$$Signal{:}\ Noise\ Ratio = \frac{MFI\ of\ positive\ population}{MFI\ of\ negative\ population}$$

Equation 2: Calculation of signal: noise ratio

Statistical analyses were performed using GraphPad Prism v7. Specific statistical analyses are clearly defined for each experiment in the results section where applicable. Differences in protein expression were computed using Wilcoxon signed-rank or Mann-Whitney U statistical tests. The Bonferroni or Benjamini-Hochberg (false discovery rate <0.05) methods were used to correct for multiple comparisons for up to 4 comparisons or more than 4 comparisons, respectively.

Results and Discussion

Chemokine receptors expressed on the cell membrane are continuously internalised, recycled and re-expressed if they are not bound to chemokines (Neel et al., 2005). Detection of chemokine receptors is affected by sample type (Berhanu et al., 2003) and antibody staining temperature (Brodie et al., 2013). Whole blood has been shown to be the best sample type to detect chemokine receptor expression (Berhanu et al., 2003) and would be the optimal sample to use to achieve our outlined objectives. However, detection of antigen-specific tetramer+ CD4 T cells using whole blood would require staining of large volumes of blood to detect and phenotype naïve-like memory T cells. As a result, all experimental protocol using tetramers would have to be conducted on PBMC and not whole blood.

Chemokine receptor antibody staining of cryopreserved PBMC at 37℃ does not improve detection.

To characterise chemokine receptor expression patterns on a historical cohort, we only had access to cryopreserved PBMC, however, detection of some chemokine receptors is affected by cryopreservation (Brodie et al., 2013). Staining cryopreserved cells at 37°C has been shown

to greatly improve detection of chemokine receptors, such as CCR7. Thus, to ensure that we could optimally detect chemokine receptor expression on cryopreserved PBMC, we compared the effect of antibody staining temperature (RT vs 37°C) on detection of chemokine receptors (n = 1) on live CD4+ T cells (Figure 6A-B). Approximately, 20-30% and 30-60% of CD4+ T cells are expected to express CCR4 and CXCR3, respectively (Rivino et al., 2004; Yamamoto et al., 2000). Overall detection and resolution of CCR4+ and CXCR3+ T cells, determined by similar stain index and signal: noise ratio, was not affected by antibody staining temperature (Figure 6C-D). The proportion of CD4+ T cells that expressed CCR4 (≅ 22%) was within the expected range, however, we detected very low levels of CXCR3 expression (≅ 8%). These results suggested that detection of CXCR3 but not CCR4 was greatly affected by cryopreservation. We therefore decided to use freshly isolated PBMC to detect chemokine receptors, in order to prevent under-estimation of CXCR3 and potentially other chemokine receptor expression on CD4+ T cells.

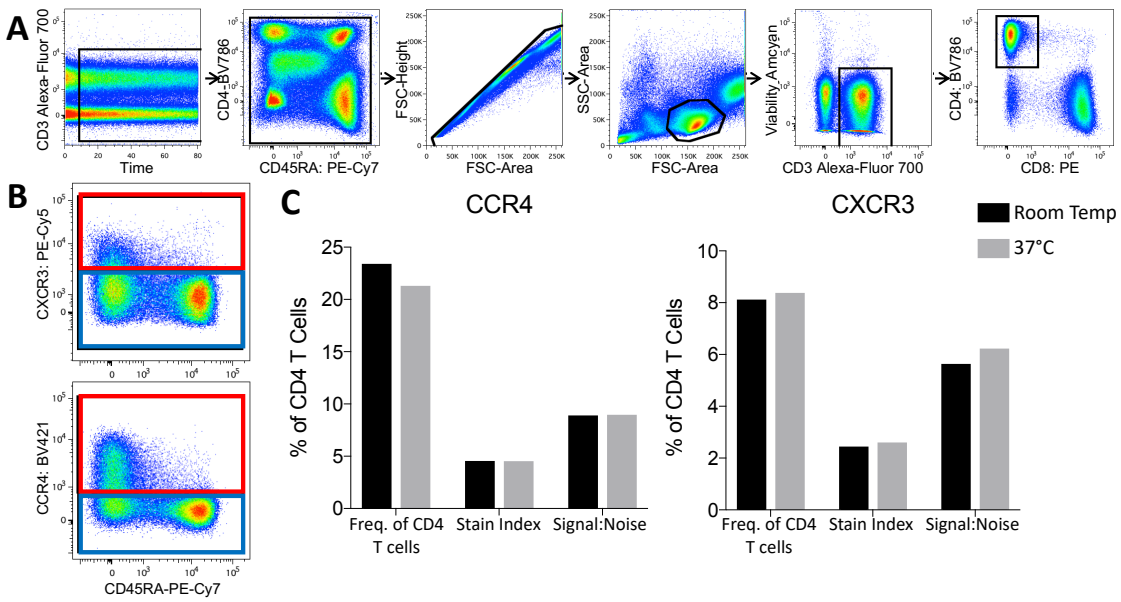

Figure 6: Antibody staining temperature does not affect detection of CCR4 and CXCR3 on cryopreserved PBMC. (A) Gating strategy used to identify live CD4+ T cells. We first gated total cells based on acquisition consistency over time (time gate), this was followed by exclusion of cell staining aggregates and cell doublets (singlet gate). We then gated CD4+ T cells on total live lymphocytes. (B) Graphical illustration of CCR4 and CXCR3 positive (red boxes) and negative (blue boxes) CD4+ T cell populations. (C) Proportion of CD4+ T cells, stain index and signal: noise ratio of CCR4 and CXCR3 expressing CD4+ T cells stained at RT (black bar) or 37°C (grey bar) (n =1).

Comparison of chemokine receptor detection on whole blood and fresh PBMC samples

PBMC isolation method has been shown to affect optimal detection of chemokine receptors, where detection of CCR2, CCR5 and CXCR3 is better when cells are isolated with Ficoll density centrifugation compared to BD Vacutainer® CPT™ tubes (Berhanu et al., 2003). To determine

whether our method of PBMC isolation (Ficoll density centrifugation) resulted in substantial (>20%) loss of chemokine receptors detection, we compared expression level of chemokine receptors in fresh whole blood and PBMC (n=1), stained at RT and 37°C respectively. We chose 37°C because the sensitivity of chemokine receptor detection is greater than RT staining of PBMC (Berhanu et al., 2003; Brodie et al., 2013). We observed minor differences in the proportion of CCR4+ (whole blood= 39.1% vs PBMC = 37.2%) and CCR6+ (whole blood= 49.7% vs PBMC = 44.6%) CD4+ T cells, and the resolution of CCR4+ and CCR6+ CD4+ T cells from total CD4+ T cells (Figure 7A-B). We did, however, observe lower detection and resolution of CXCR3+ CD4+ T cell population in fresh PBMC (35.4%) compared with whole blood (46.2%) (Figure 7C). We acknowledge that a sample size of 1 and a difference in CXCR3+ expression levels of ≅ 10% does not provide sufficient evidence to demonstrate the inferiority of PBMC as a sample type. Since our M.tb tetramer staining protocol (Dintwe et al., 2013; Moguche et al., 2017) was optimised for PBMC and not whole blood, and the overall detection of chemokine receptors was not different between whole blood and PBMC, we decided to proceed with fresh PBMC and not further optimise the chemokine receptor staining protocols.

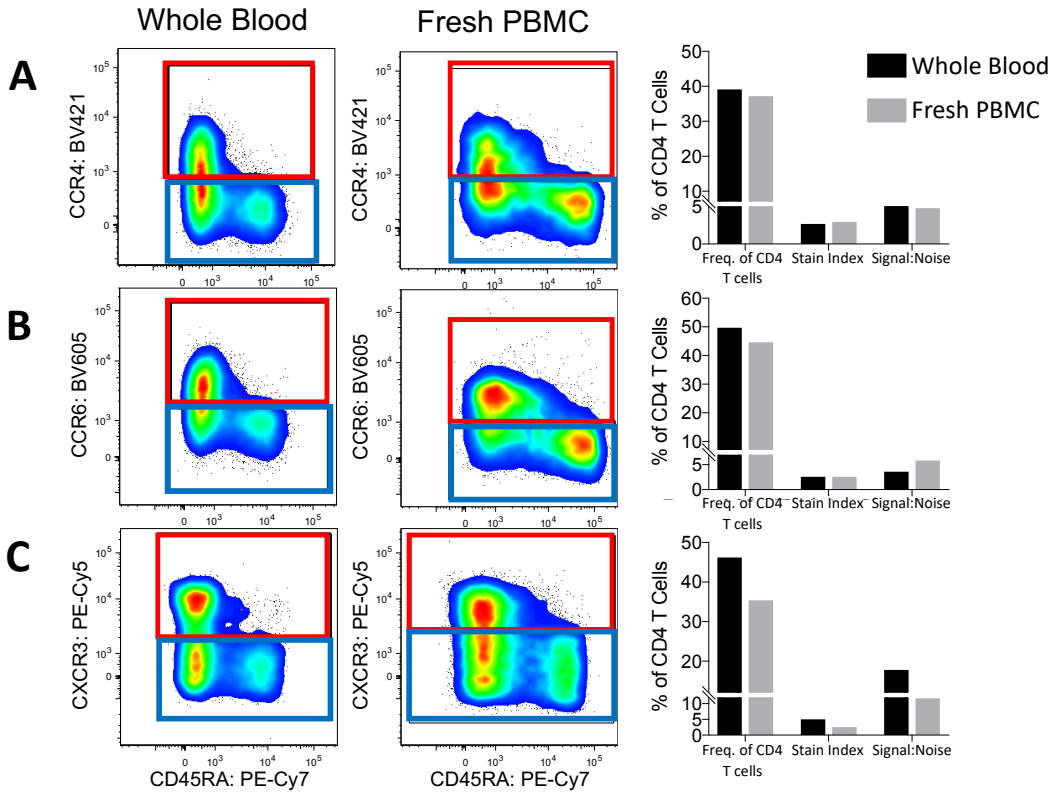

Figure 7: Comparison of chemokine receptor detection on whole blood and fresh PBMC. Staining pattern, frequency of CD4+ T cells, stain index and signal: noise ratio of (A) CCR4, (B) CCR6 and (C) CXCR3 expressing CD4+ T cells (n=1).

BD Brilliant Stain Buffer improves resolution of BV-conjugated antibodies

BD Biosciences recommends the use of BS buffer for antibody staining of flow cytometry panels with two or more brilliant violet (BV) conjugated antibodies. Our proposed flow cytometry panel for detection of chemokine receptor and memory co-expression patterns had 6 BV fluorochromes (BV421, BV510, BV605, BV650, BV711 and BV786) conjugated antibodies. To determine whether BS buffer does indeed improve the resolution of the positive signal of BV-conjugated antibodies in our flow cytometry panel and enables accurate detection of cell populations that co-express multiple markers, we visually compared the resolution of phenotypic markers stained in the presence of either BS buffer or PBS. We measured expression levels of chemokine receptors and memory markers on CD4+ T cells, after exclusion of CD8+ T cells, monocytes (CD14+) and B cells (CD19+) (Figure 8), which have been shown to non-specifically bind tetramers.

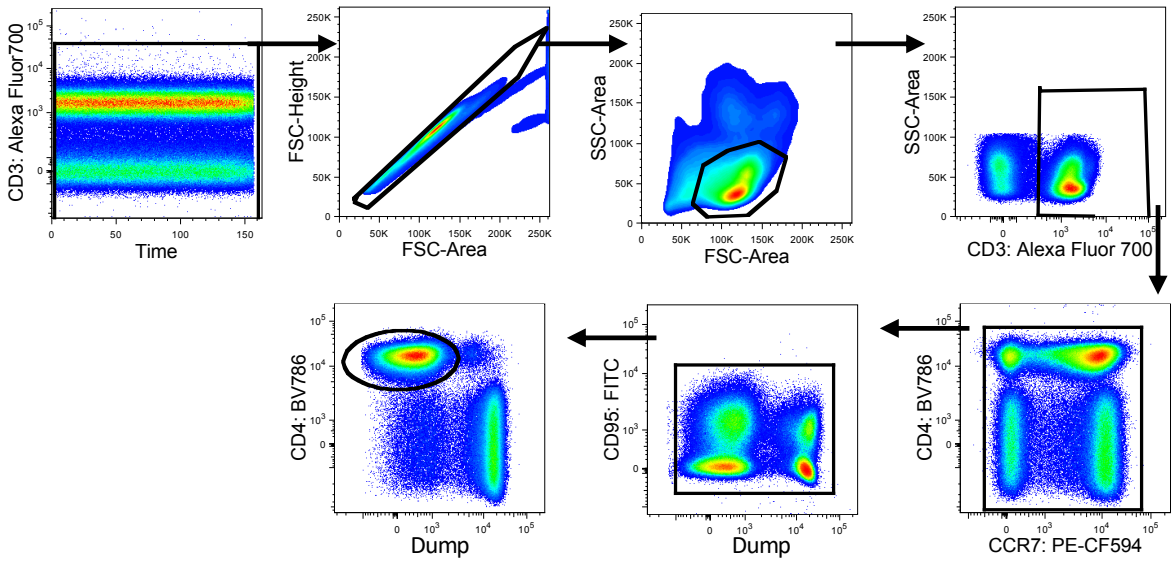

Figure 8: Gating strategy utilised to identify CD4+ dump- (CD8-CD14-CD19-dead-) T cells prior to gating of tetramer signal. We first gated on total cells based on fluorescence consistency over acquisition time (time gate) and then gated on single cells, total lymphocytes and CD3+ T cells, followed by exclusion of antibody aggregates. CD4+ (CD3+) T cells were gated by excluding dead cells, CD8+, CD14+ and CD19+ cells, collectively referred as *Dump*, and CD4- cells.

We observed similar separation patterns of chemokine receptor populations between the buffers (Figure 9). However, we observed better separation of memory markers when BS buffer was used compared to PBS (n=1). Specifically, we observed two distinct populations of CD45RA+ CD4+ T cells: CD45RA^{hi} and CD45RA$^{intermediate\ (int)}$ which is atypical of this population,

when we stained with PBS (Figure 9). Detection of the CD45RA^{int} was due to poor resolution of CD27 expression when PBS was used as the staining buffer. Staining with BS buffer improved the resolution of CD45RA and CD27 co-expression patterns and did not result in detection of a CD45RA^{int} population. Based on these results we decided to use BS buffer instead of PBS as our staining buffer for the rest of the experiments and incorporated it into our final staining protocol.

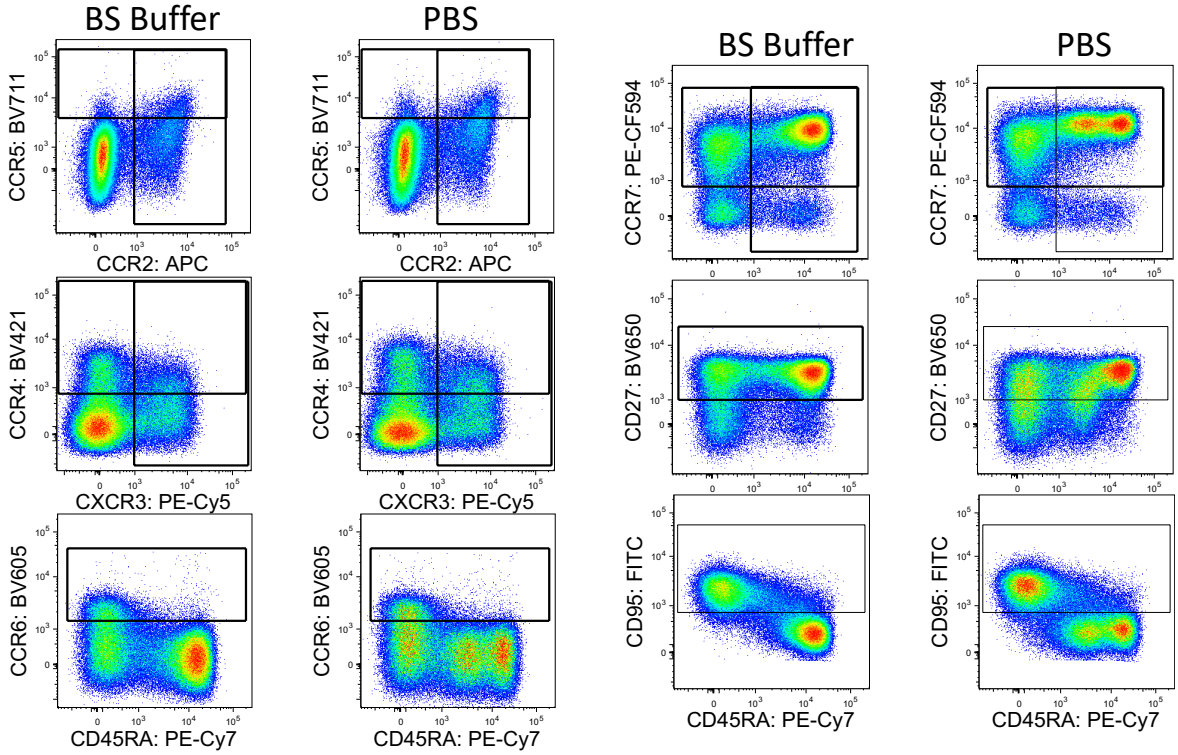

Figure 9: BS buffer improves resolution of BV-conjugated markers. Graphical illustration of memory marker and chemokine receptor co-expression patterns of CD4+ T cells (n=1).

After completion of staining protocol optimisation, we tested the final panel on a few healthy donors. For each M.tb-tetramer stain, we included the corresponding CLIP-control-tetramer (CLIP-tetramer) stain, where CLIP-self peptide was loaded on the identical MHC molecule instead of M.tb peptide, as a negative control. Both M.tb- and CLIP- tetramers were conjugated to the same fluorochrome, which enabled us to determine how much of the tetramer stain could be due to non-specific tetramer binding. We unexpectedly detected similar levels of M.tb-tetramer+ and CLIP-tetramer+ CD4+ T cell responses (Figure 10, n=4 donors, 7 M.tb-tetramer :Clip-tetramer combinations), and in some individuals even higher frequencies of CLIP-tetramer+ CD4+ T cells compared to M.tb-tetramer+ CD4+ T cells were observed (Figure 10B).

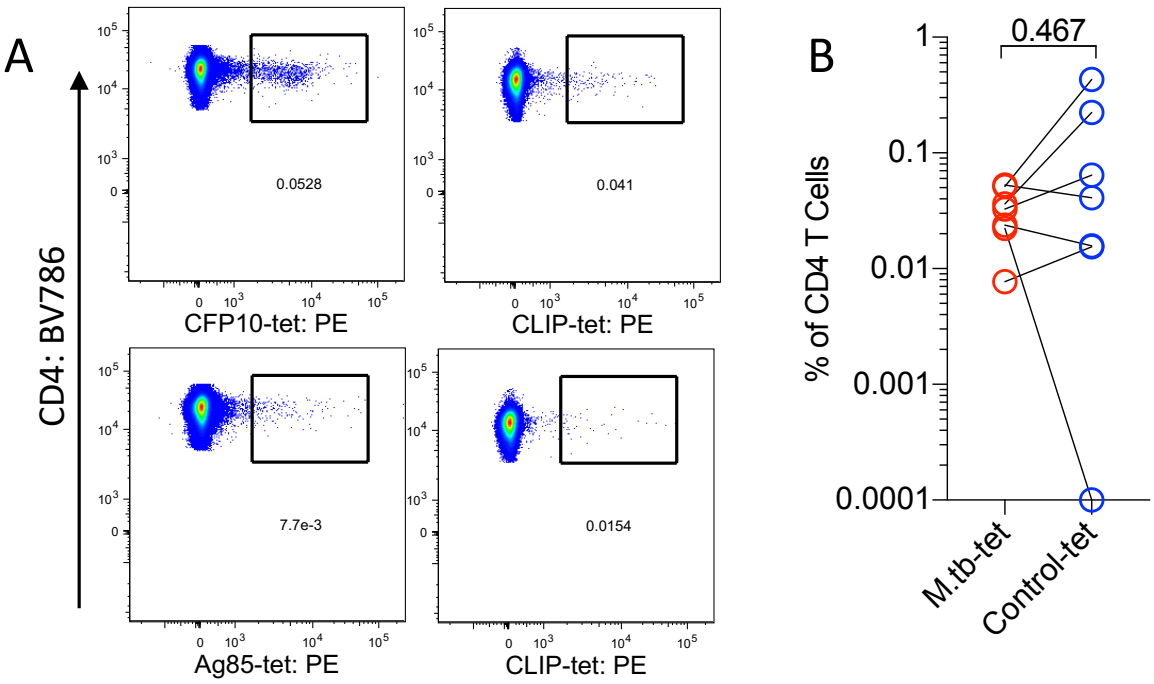

Figure 10: Detection of high background in tetramer+ CD4+ T cell population. (A) Representative example of M.tb- and CLIP-tetramer+ CD4+ T cell staining. (B) Percentage of M.tb-(red circles) and CLIP- (blue circles) tetramer+ CD4+ T cells detected. P value was calculated using Wilcoxon signed-rank test, and p-value < 0.05% is considered significant (n=4 donors, 7 M.tb-tetramer: Clip-tetramer combinations).

To determine if non-specific signal from other antibodies were responsible for high detection of background responses, we visually compared the contribution of each memory marker and chemokine receptor antibody-fluorochrome conjugate to the tetramer signal (Figure 11). Signal from CD45RA PE-Cy7, CCR7 PE-CF594 and CD27 BV605, and to a lesser extent CCR2 APC and CXCR3 PE-Cy5 contributed to non-specific signal in the tetramer-PE channel. It should be noted that, despite detection of high control-tetramer+ CD4+ T cells, the majority of M.tb-tetramer+ (CFP-10-tetramer+, Figure 11) CD4+ T cells expressed chemokine receptors (CCR2+, CCR4-, CXCR3+) and memory (CD45RA-, CD95+) markers characteristic of M.tb-specific T cells.

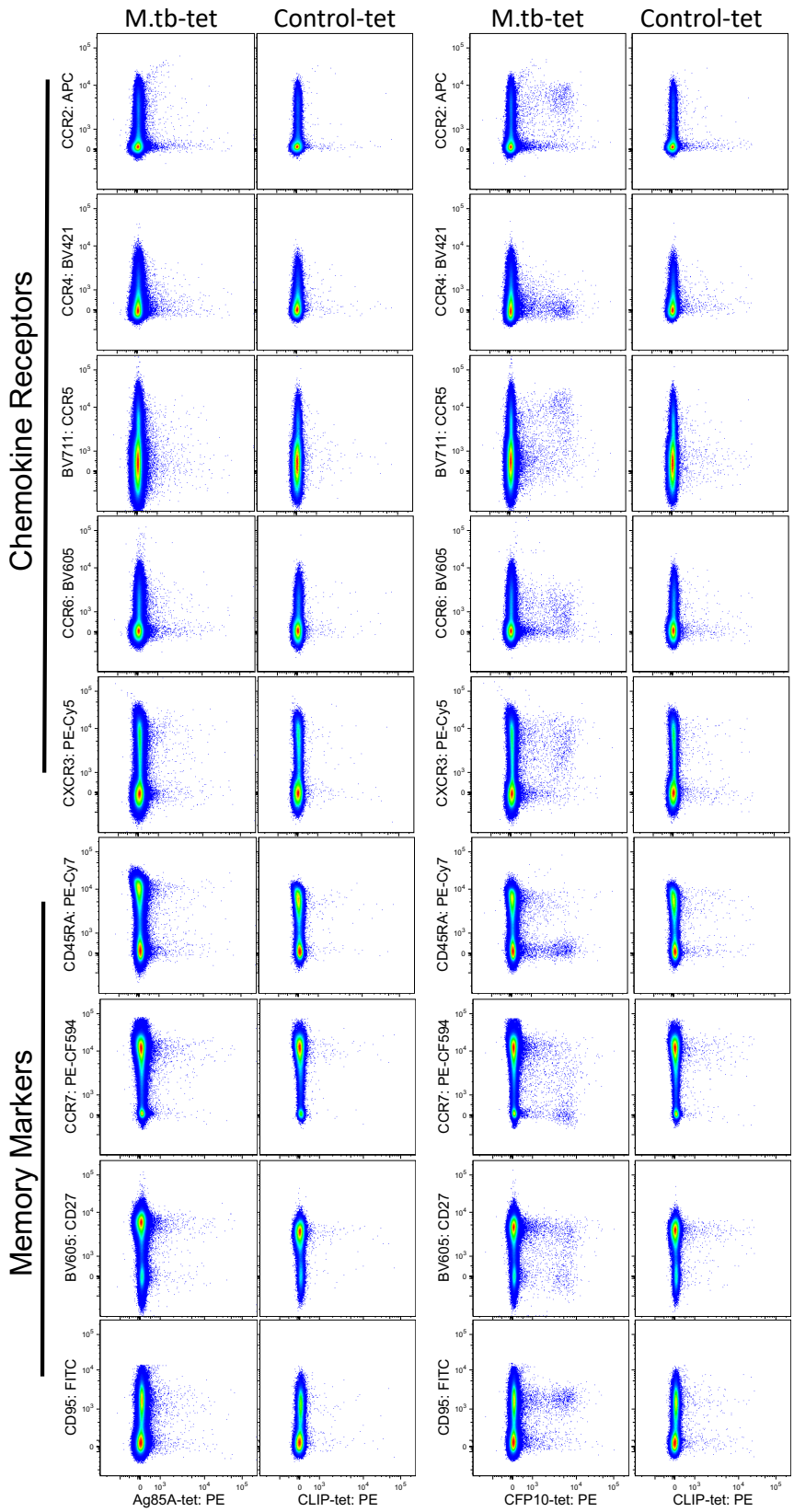

Figure 11: Flow cytometry plots of tetramer channel (PE) vs combination of memory marker and chemokine receptor antibody staining of total CD4+ T cells (n=2). Flow cytometry plots are of the same individuals as in Figure 5 A.

Detection of tetramer+ CD4+ T cells is improved by dual tetramer staining

To improve the specificity of detection of M.tb-tetramer+ CD4+ T cells, we compared different combinations of single and dual tetramer staining protocols:

- Single tetramer staining with tetramer-conjugated to APC (instead of PE)
- 15-minute pre-incubation with CLIP-tetramer-PE or -APC prior to addition of M.tb-tetramer-APC or -PE, respectively (to saturate unspecific binding sites)
- Dual staining with M.tb-tetramers or CLIP-tetramers conjugated to both -APC and -PE (to improve staining specificity)

We also ensured that tetramers used to stain PBMC matched the individuals HLA-type. When we stained with a single tetramer-APC in the presence of CCR2 PE, we observed minimal background staining (Figure 12A). Unfortunately, we did not perform single tetramer-PE staining, thus we were unable to determine if high background observed in Figure 10 & 11 was partially due to the use of a tetramer conjugated to PE. Additionally, similar levels of M.tb-tetramer+ CD4+ T cells were detected regardless of tetramer staining combination (Figure 12B). Control staining with CLIP-tetramer-PE resulted in detection of higher non-specific signal compared to CLIP-tetramer-APC (Figure 12C). Overall, dual staining with M.tb- or control-tetramer conjugated to both APC and PE, provided the best visual resolution and specificity of tetramer+ CD4+ T cells (Figure 12A), as well as lower detection of non-specific CLIP-tetramer signal (Figure 12C). Based on these results, we decided to perform dual tetramer staining of identical M.tb- or CLIP- tetramers conjugated to -PE and -APC for all subsequent experiments.

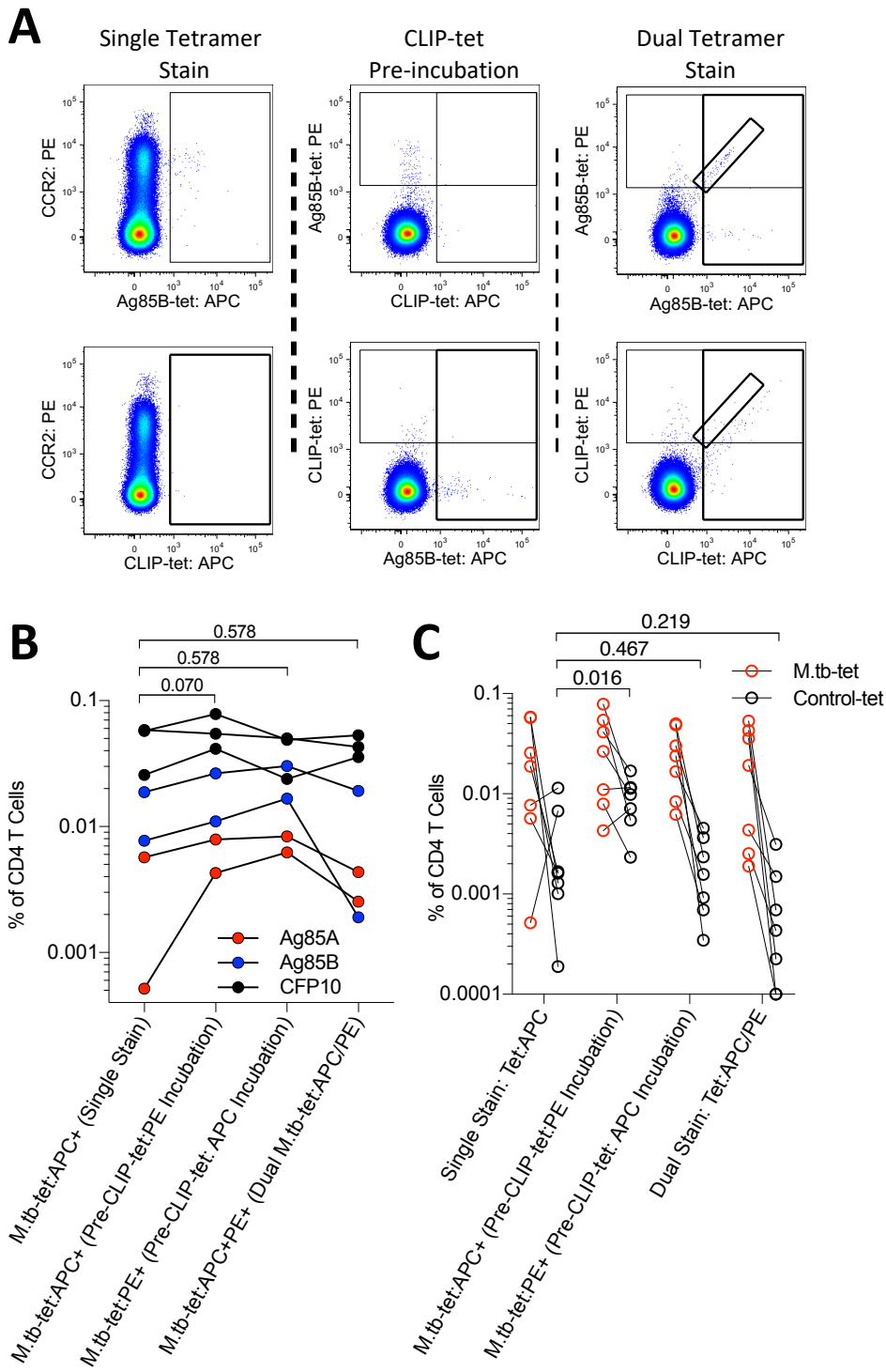

Figure 12: Dual tetramer staining improves the specificity of tetramer+ signal. (A) Representative example of single and dual tetramer staining tested. (B) Proportion of M.tb-tetramer+ (M.tb-tet) CD4+ T cells detected in each tetramer staining combination. (C) Proportion of M.tb- and CLIP-tetramer+ (tet) CD4+ T cells detected for each staining combination. Lines represent paired samples. P-value was calculated using Wilcoxon signed-rank test, using M.tb-tetramer-APC for (B) or CLIP-tetramer-APC for (C) staining as the reference comparator. P-values < 0.0167 were considered significant after correction for multiple comparison using Bonferroni method (n=4 donors, 7 M.tb-tetramer: Clip-tetramer combinations).

Optimisation of cytotoxic molecule staining

One of our aims was to determine the co-expression of cytotoxic molecules of tetramer+ CD4+ memory T cell subsets. To achieve this, fixation and permeabilisation of cells was required to detect intracellular expression of cytotoxic molecules. Furthermore, we aimed to detect both chemokine receptor and cytotoxic molecule expression of memory cell subsets from the same donor using two different panels. We, therefore, wanted to harmonise experimental protocols required to reduce experimental bias in the detection of M.tb-specific memory T cell subsets. Thus, we aimed to determine which staining protocol would result in optimal resolution of memory (CD45RA, CD27, CD95) and phenotypic (CD3, CD4, CD8, CD14, CD19) markers, by staining memory and phenotypic markers either before or after fixation and permeabilisation of PBMC. Staining of CCR7 and viability probe, followed by tetramer staining, were always conducted before permeabilisation of PBMC in both comparisons.

Staining of surface markers after fixation and permeabilisation resulted in visually lower resolution of CD3+, CD4+ and CD95+ T cell populations (Figure 13). Resolution of CD95+ T cells was greatly affected by permeabilisation before staining, which made it very difficult to discern CD95+ CD4+ T cells, as well as to identify “naïve” CD95- T cell populations (Figure 13). Additionally, high spread of the BV785 fluorochrome conjugated to CD4 resulted in spill over into the BV510 dump channel (Figure 13). Staining of phenotypic markers before permeabilisation improved poor resolution detected when we stained after permeabilisation (Figure 13). Additionally, we did not observe differences in detection of tetramer+ CD4+ T cell populations when either staining protocol was used (Figures 13). We therefore opted to stain phenotypic markers before permeabilisation and fixation of PBMC, to improve resolution of populations and have a similar staining protocol as the chemokine receptor staining protocol (Figure 13).

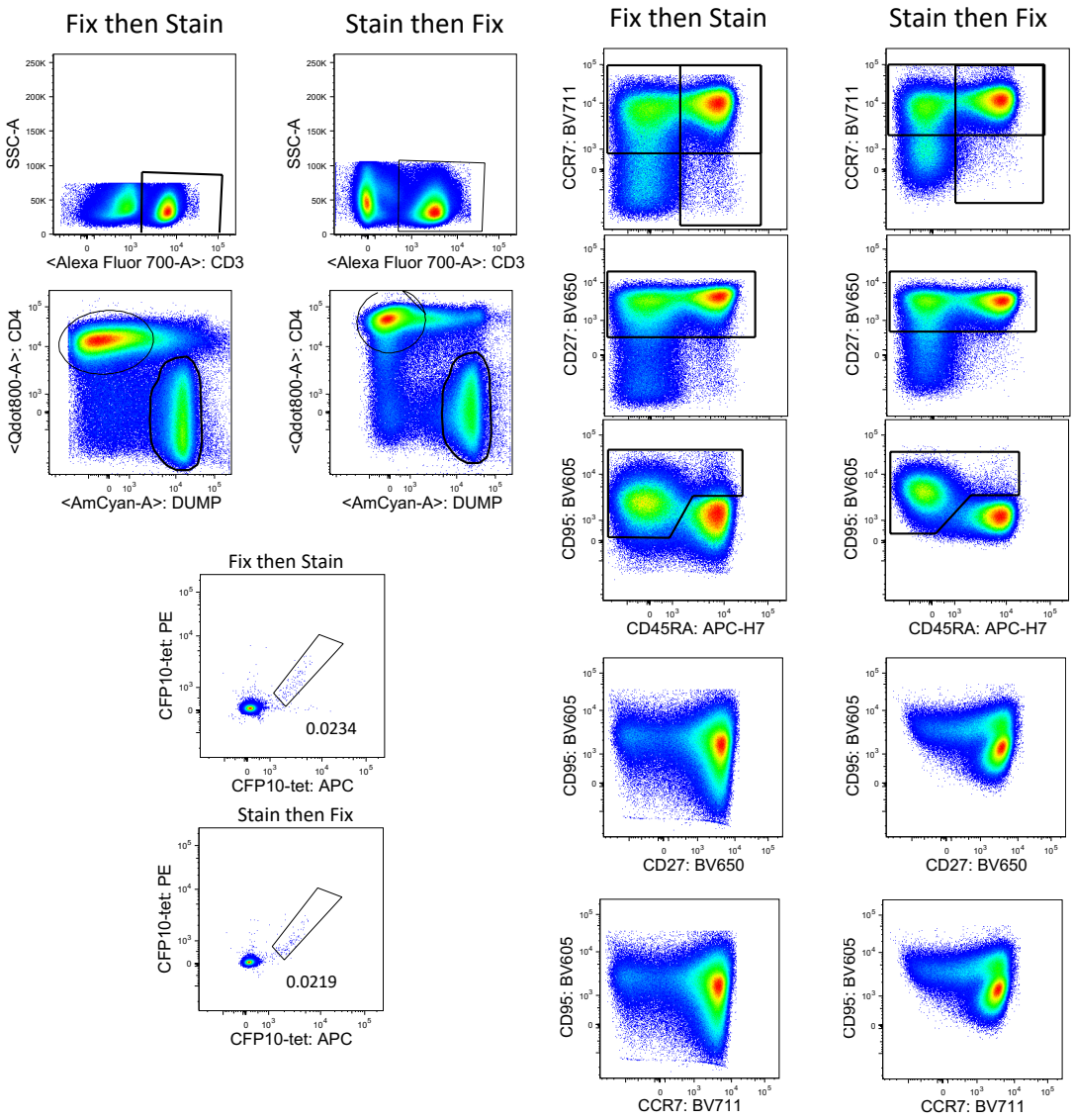

Figure 13: Optimisation of the lineage and memory marker staining protocol for the cytotoxic T cell panel. Graphical illustration of lineage populations (CD3, CD4 and CD8 T cells), memory population (CCR7, CD27, CD45RA, CD95) and M.tb-tetramer+ T stained either before (stain then fix) or after (fix then stain) permeabilisation and fixation of cells.

Conclusion

This chapter summarises the optimisation experiments we conducted to ensure robust detection of chemokine receptor and cytotoxic molecule co-expression patterns of M.tb-tetramer+ CD4+ memory T cells. We successfully demonstrated that dual tetramer staining with identical tetramers conjugated to both -PE and -APC resulted in lower background and superior resolution of M.tb-specific tetramer+ signal compared with single tetramer staining. Thus, enabling optimal detection of M.tb-tetramer+ CD4+ T cells from PBMC samples stained with flow cytometry panels measuring up to 14 parameters. We also demonstrated that staining of fresh PBMC was the best sample type to detect chemokine receptor co-expression

of M.tb-tetramer+ CD4+ T cells. Further, we illustrated that antibody staining in presence of BS buffer was required to improve resolution of BV-conjugated fluorochromes and optimally detect chemokine receptor and memory marker co-expression profiles. Finally, phenotypic marker and M.tb-tetramer staining prior to permeabilisation and fixation of PBMC resulted in the best resolution of lineage, memory and M.tb-tetramer+ populations. The final optimised protocol outlined in Chapter 3, demonstrates that we were able to optimise flow cytometry panels that enabled optimal detection of tetramer+ CD4+ T cells, as well as optimally detect co-expression of memory and chemokine receptors or cytotoxic molecules on M.tb-tetramer+ CD4 T cells.

Contributions

HLA-typing, curation of the HLA-typing database and selection of the panel of M.tb-tetramers available for use in this thesis were conducted by One B Dintwe (Dintwe, 2014) and Munyaradzi Musvosvi (Nyasha, 2016).

All methodology and statistical analyses were performed by Cheleka Anne-Marie Mpande, unless stated otherwise.

Chapter 3: Phenotypic and functional characterisation of *M. tuberculosis*-specific stem cell memory (T_{SCM}) CD4+ T cells.

Results reported in this chapter were partially published in the Frontiers of Immunology Journal.

Title: Functional, antigen-specific stem cell memory (T_{SCM}) CD4+ T cells are induced by human M. tuberculosis infection

Authors: Cheleka AM Mpande[#], One B Dintwe[#], Munyaradzi Musvosvi, Simbarashe Mabwe, Nicole Bilek, Mark Hatherill, Elisa Nemes and Thomas J Scriba and the SATVI Clinical Immunology Team[$].

#: Co-first authorship

$: The SATVI Clinical Immunology Team: Cynthia Ontong, Elizabeth Filander, Rachel Oelfose, Noncedo Xoyana, Sindile Matiwane, Lungisa Jaxa, Janelle Botes, Fadia Alexander, Hadn Africa, Marcia Steyn, Lebohang Makhethe

Year: 2018

Doi: 10.3389/fimmu.2018.00324

Introduction

Memory T cells have been classified into subsets, according to their phenotypes, functions and homing potential (Sallusto et al., 1999). Antigen-specific T_{CM} cells have been considered the main mediators of maintenance and expansion of T cell immunity, following secondary antigen exposure, due to their ability to differentiate into T_E cells, as well as their increased proliferative capacity and longevity compared to T_E cells. This ontology of memory T cells has recently been revised to include a recently discovered T_{SCM} cells. T_{SCM} cells typically express CD45RA, CCR7 and CD27, and thus phenotypically resemble T_N cells, but their co-expression of memory markers, such as CD95 and CXCR3, distinguish them from T_N cells (Gattinoni et al., 2011; Lugli et al., 2013a). Functional characterisation of antigen-specific T_{SCM} cells has predominantly focused on viral, parasitic and tumour-specific CD8 T cells, identified by MHC I tetramers, or by non-specific and/or antigen-specific stimulation (Gattinoni et al., 2011, 2017; Hong et al., 2016; Lugli et al., 2013a; Mateus et al., 2015) These studies showed that T_{SCM} cells characteristically possess excellent self-renewing capacity, longevity and

proliferative capacity, relative to T_{CM} and T_E cells. Importantly, T_{SCM} cells can also differentiate into T_{CM} and T_E cells (Gattinoni et al., 2011). CD8+ T_{SCM} cells are preferentially enriched in the absence of antigen (Lugli et al., 2013a), non-chronic states of infection (Mateus et al., 2015) and among long-lived T cells induced by vaccination (Fuertes Marraco et al., 2015). CD8+ T_{SCM} cells are also essential for the re-establishment of antigen-specific memory responses after T cell depletion in cancer patients (Biasco et al., 2015; Oliveira et al., 2015). As a result, T_{SCM} cells are considered a potential target for vaccination against infectious diseases and T cell therapy for autoimmunity, to induce and maintain long lasting T cell immunity capable of replenishing all T cell memory subsets.

Newborn vaccination against tuberculosis disease with BCG vaccine is efficacious against severe forms of tuberculosis in young children (Colditz et al., 1995; Roy et al., 2014). However, BCG efficacy is variable and mostly poor against pulmonary tuberculosis in adults (Colditz et al., 1994; Mangtani et al., 2014). Therefore, it has been proposed that waning of mycobacteria-specific T cell memory responses and insufficient maintenance of protective CD4+ T cells may underlie the limited durability of BCG-induced protection (Henao-Tamayo et al., 2014; Orme, 2010).

Newborn BCG vaccination induces antigen-specific T_{CM} and T_E CD4+ T cells (Soares et al., 2008), but the role of CD4+ T_{SCM} cells in immune responses induced by vaccination against tuberculosis or by natural TBI, in humans has not been extensively explored. In fact, prior to our publication (Mpande et al., 2018), there was very limited knowledge about the functional capacity and persistence of CD4+ T_{SCM} cells that are specific for bacterial antigens. We and others have reported that in humans a considerable proportion of cytokine-expressing or tetramer+ mycobacteria-specific CD4 T cells displayed a memory phenotype characteristic of T_N cells (CD45RA+CCR7+) and termed them naïve-like CD4+ T cells (Kagina et al., 2009; Lindestam Arlehamn et al., 2013; Orlando et al., 2018; Soares et al., 2008, 2013; Strickland et al., 2017; Tena-Coki et al., 2010; Yuan et al., 2019). In a clinical trial that tested boosting of mycobacteria-specific responses with the tuberculosis vaccine candidate, MVA85A, low but detectable Ag85A-specific CD45RA+CCR7+CD27+CD95- naive-like CD4 T cell responses were observed before MVA85A vaccination and frequencies of these cells were unaffected by vaccination (Dintwe et al., 2013). In mice, BCG-induced naïve-like ($CD44^{hi}CD62L^{hi}$) memory T (T_{NLM}) cells have been shown to play a role in the control of TBI, where these cells were capable of replenishing effector ($CD44^{hi}CD62L^{lo}$) T cells with superior functional activity and

protective potential against TBI, compared to those originating from T_E cells (Kipnis et al., 2005; Yuan et al., 2019).

In this chapter we aimed to determine the kinetics of M.tb-specific CD4+ T_{SCM} cell generation, and characterise the homing and functional profiles of mycobacteria-specific CD4+ T_{SCM} cells. Phenotypic and functional properties of M.tb-specific T_{SCM} cells were then compared to those of M.tb-specific T_{CM} and T_E cells, to determine their ontology. To achieve this, we developed flow cytometry staining protocols to detect mycobacteria-specific tetramer+ memory T cell populations as well as the chemokine receptor and cytotoxic molecules expression levels (Chapter 2).

We hypothesized that M.tb-specific CD4+ T_{SCM} cells are induced by primary infection with M.tb in humans and are sustained throughout established TBI. Our findings summarised below contribute to the current knowledge of the M.tb-specific T cell memory repertoire and highlight the need for a better understanding of CD4+ T_{SCM} cells in natural TBI, tuberculosis disease and vaccine-induced immune responses.

Objectives

I. **To determine whether M.tb-specific CD4+ T_{SCM} cells are induced by primary TBI.**
II. **To characterise the chemokine receptor, cytotoxic molecule and cytokine co-expression profile of M.tb-specific CD4+ T_{SCM} cells, as well as compare these profiles to well characterised memory phenotypes.**

Materials and Methods

Participant samples and ethics

Longitudinal natural TBI studies

Participants were selected from the Adolescent Cohort Study [ACS, HREC 045/2005, (Mahomed et al., 2011a)], which aimed to determine the prevalence and incidence of TBI and tuberculosis disease in adolescents in the Worcester area of the Western Cape, South Africa. Participants in the ACS were between 12 and 18 years of age and were followed-up for a 2-year period. Parents or legal guardians of adolescents provided written, informed consent and adolescents provided written, informed assent. TST and QFT were performed annually and bi-annually, respectively. TST was performed by intradermal injection with 0.1 mL dose

of purified protein derivative (RT-23, 2-TU, Statens Serum Institut), and induration recorded using a ruler 48-72 hours later.

We retrieved cryopreserved PBMC from 19 (HLA-typed) out of 6363 participants with evidence of newly acquired TBI. Primary TBI was defined as a negative QFT test (IFN-γ <0.35 IU/mL, Figure 14A) and negative TST (induration = 0mm, Figure 14B), followed by at least 3 positive QFT tests 6, 12 and 18 months later and a positive TST (induration >5mm) at 12 and 24 months (Figure 14).

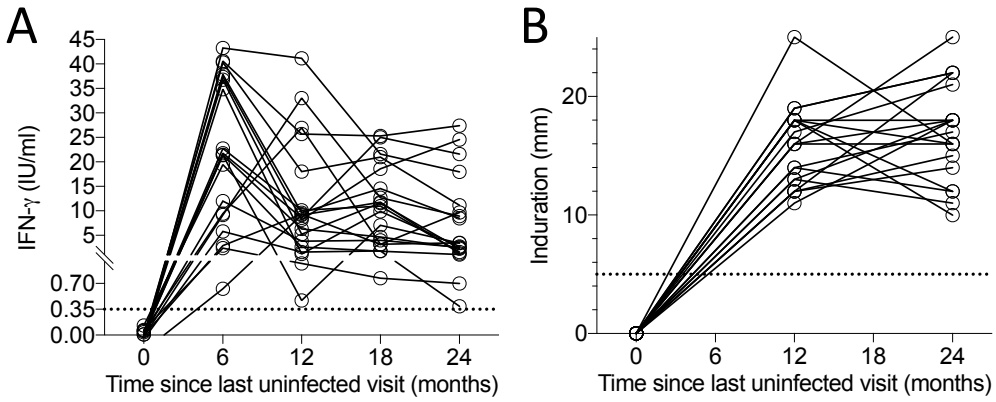

Figure 14: Longitudinal (A) QFT and (B) TST results of recent M.tb infected adolescents. Dotted lines in graph represent the QFT and TST positive threshold of (A) 0.35 IU/mL and (B) 5mm, respectively (n=19 participants).

Cross-sectional natural TBI studies

Participants were selected from the SATVI database of HLA-typed individuals, as described in Chapter 2: Participants samples and ethics.

PBMC isolation and cryopreservation

Blood was collected from participants in sodium-heparinised blood collection bags and PBMC were isolated within 4 hours of collection and stained fresh or after cryopreservation, as described in Chapter 2: Sample preparation.

Flow cytometry staining protocol

In Chapter 2, we demonstrated that fresh PBMC was the best sample type to detect chemokine receptor co-expression of M.tb-tetramer+ CD4+ T cells. We thus used fresh PBMC to detect M.tb-specific CD4+ T cell chemokine receptor co-expression profiles, while other experimental protocols were performed using cryopreserved PBMC.

We designed three flow cytometry panels to detect M.tb-specific CD4+ T cells, as well as phenotype CD4+ T cells at different stages of TBI, namely:

1. Detection of M.tb-specific CD4+ T cell profiles induced by primary TBI (Panel 1): CD3, CD4, CD45RA, CCR7, CD27, CD95, HLA-DR and dump channel (viability dye, CD8, CD14, CD19).
2. Detection of M.tb-specific CD4+ T cell chemokine receptor co-expression profiles in a cross-sectional cohort of remote M.tb infected individuals (Panel 2). PBMC stained with this panel were fresh and included: CD3, CD4, CD45RA, CCR7, CD27, CD95, CCR4, CCR6, CCR5, CCR7, CXCR3 and dump channel.
3. Detection of M.tb-specific CD4+ T cell cytotoxic molecule co-expression profiles in a cross-sectional cohort of remote M.tb infected individuals (Panel 3). Panel 3 was used on cryopreserved PBMC and included: CD3, CD4, CD45RA, CCR7, CD27, CD95, granzyme A, granzyme B, granzyme K, granulysin, perforin and dump channel.

Chemokine receptor staining: Fresh PBMC were stained with an anti-chemokine receptor antibody cocktail (Table 9) in total volume of 100µl of cells with BS buffer, while cryopreserved PBMC were stained with anti-CCR7 PE-CF594 (Panel 1: 1.5µL) or anti-CCR7-BV711 (Panel 3: 2µL) by incubation in a water bath at 37°C for 30 minutes.

Table 9: Anti-chemokine receptor antibodies used to detect chemokine receptor expression profiles of CD4+ T cells from fresh PBMC stained using flow cytometry panel 2.

Marker	Clone	Manufacturer	Fluorochrome	Volume
CCR4	1G1	BD Biosciences	BV421	1.25 µL
CCR5	2D7	BD Biosciences	BV711	5 µL
CCR6	11A9	BD Biosciences	BV605	2 µL
CCR7	150503	eBioscience	PE-CF594	2 µL
CXCR3	IC6/CXCR3	BD Biosciences	PE-Cy5	5 µL

MHC II tetramer staining: Upon completion of chemokine receptor staining and incubation, stained PBMC were washed in 2mL of tetramer staining buffer by centrifugation and supernatant discarded. Cells from each participant were stained in parallel with all available tetramers that matched their HLA (Table 10). Cells were then dual tetramer stained with identical M.tb-tetramer conjugated to PE or APC fluorochromes at a concentration of 2µg/mL (each tetramer) in final volume of 100µL for 1 hour at RT. Cells were washed in 3 mL of PBS by centrifugation and supernatant discarded.

Table 10: Distribution of HLA-class II tetramer-peptides stained for each flow cytometry panel.

			Number of participants per panel		
HLA Sequence	**Protein**	**Peptide Sequence**	**Panel 1**	**Panel 2**	**Panel 3**
DPB1*04:01	$Ag85B_{128-144}$	GKAGCQTYKWETFLTSE	4	2	2
DRB1*03:01	$Ag85A_{56-75}$	VPSPSMGRDIKVQFQSGGAN	2	2	1
DRB1*04:01	$CFP\text{-}10_{71-85}$	EISTNIRQAGVQYSR	7	9	8
DRB5*01:01	$CFP\text{-}10_{51-65}$	AQAAVVRFQEAANKQ	8	7	5
DQB1*06:02	$ESAT\text{-}6_{31-45}$	EGKQSLTKLAAAWGG	8	8	4
Total (n) tetramer staining			31	28	20
Total (n) participants			19	20	16

Phenotypic marker staining: PBMC were stained with antibodies to phenotypic extracellular markers and viability marker (Table 11) in total volume of 100μl of cells with BS buffer for 30 minutes at RT. Upon completion of incubation cells were washed in 1 mL of PBS buffer by centrifugation. If no further staining steps were required, cells were re-suspended and fixed with 100μl of 1% PFA and acquired on the BD LSR Fortessa cytometer.

Table 11: Lineage and memory markers used across different panels.

Marker	Clone	Manufacturer	Fluorochrome	PBMC Type	Panel	Volume
CD3	UCHT1	BD Biosciences	Alexa Fluor 700	Cryopreserved	1	1 μL
				Fresh	2	1.5 μL
				Cryopreserved	3	3.5 μL
CD4	L200	BioLegend	BV785	Cryopreserved/Fresh	1,2	1 μL
	SK3	BD Bioscience	BV786	Cryopreserved	3	1 μL
CD45RA	HI100	eBioscience	PE-Cy7	Cryopreserved	1	0.156 μL
				Fresh	2	0.51 μL
		BD Biosciences	APC H7	Cryopreserved	3	2.5 μL
CD27	L128	BD Biosciences	BV650	Cryopreserved/Fresh	1-3	2.5 μL
CD95	DX2	BioLegend	FITC	Cryopreserved	1	0.156 μL
				Fresh	2	0.5 μL
		BD Biosciences	BV605	Cryopreserved	3	2.5 μL
HLA-DR	L243	BioLegend	BV421	Cryopreserved	1	1.25 μL
CD8	RPA-T8	BioLegend	BV510	Cryopreserved/Fresh	1,2	0.6 μL
				Cryopreserved	3	1 μL
CD14	M5E2	BioLegend	BV510	Cryopreserved/Fresh	1,2	1.25 μL
				Cryopreserved	3	0.62 μL
CD19	SJ25C1	BD Biosciences	BV510	Cryopreserved/Fresh	1,2	0.6 μL
				Cryopreserved	3	1.25 μL
Viability	(Ref L34957)	Thermo-Fisher Scientific	Aqua	Cryopreserved/Fresh	1-3	1 μL

Intracellular cytotoxic molecule staining: To stain for cytotoxic molecules PBMC were fixed and permeabilised by addition of 250μL of Cytofix/Cytoperm solution, vortexed and incubated on ice for 20 minutes. Cells were then washed twice with 1mL of Perm/Wash by centrifugation, supernatant discarded and resuspended with 50μL of Perm/Wash. Permeabilised PBMC were then stained with anti-cytotoxic molecule antibodies (Table 12),

for 30 min at RT. This was followed by washing in 1mL of Perm/Wash and fixation with 1% PFA. Samples were then acquired on the BD Bioscience LSR Fortessa.

Table 12: Antibodies used to detect cytotoxic molecule co-expression profiles of CD4+ T cells from cryopreserved PBMC stained using flow cytometry panel 3.

Marker	Clone	Manufacturer	Fluorochrome	Volume
Granzyme A	CB9	eBioscience	PE-Cy 7	2.5 μL
Granzyme B	GB11	BioLegend	Pac Blue	3 μL
Granzyme K	GM6C3	Santa Cruz Biotechnology	FITC	5 μL
Granulysin	Polyclonal: Ref AF3138	R & D Systems	PE-Cy 5 (in-house conjugation)	3 μL
Perforin	δG9	BD Bioscience	PE-CF594	0.5 μL

Data Analysis

Flow Cytometry Analysis

Flow cytometry analysis was conducted using FlowJo version v9.7 to v10.1r.1. Compensation was calculated using single stained compensation beads, and then applied to all samples in the FlowJo workspace. CD4+ T cells and M.tb-tetramer+ T cells were gated according to the grating strategy outlined in Figure 15. Gated identifying memory markers, chemokine receptors and cytotoxic molecules were first gated on bulk CD4+ T cells and identical gates applied to M.tb-tetramer+ CD4+ T cells (Figure 15). To determine the cytokine expression profile and the proliferation capacity of TBI and vaccine-induced *mycobacteria*-specific naïve-like and other memory phenotypes, respectively, we reanalysed raw flow cytometry data from previously published research (Luabeya et al., 2015; Nemes et al., 2017b), UCT HREC 179/2011]. Specifically, we re-analysed baseline (Day 0) M.tb-specific T cell responses from healthy M.tb infected (QFT+) individuals included in the Phase I H56:IC31 vaccine trial (Luabeya et al., 2015) and the proliferation capacity of BCG-specific CD4 T cells in healthy infants 10-months post BCG vaccination (Nemes et al., 2017b).

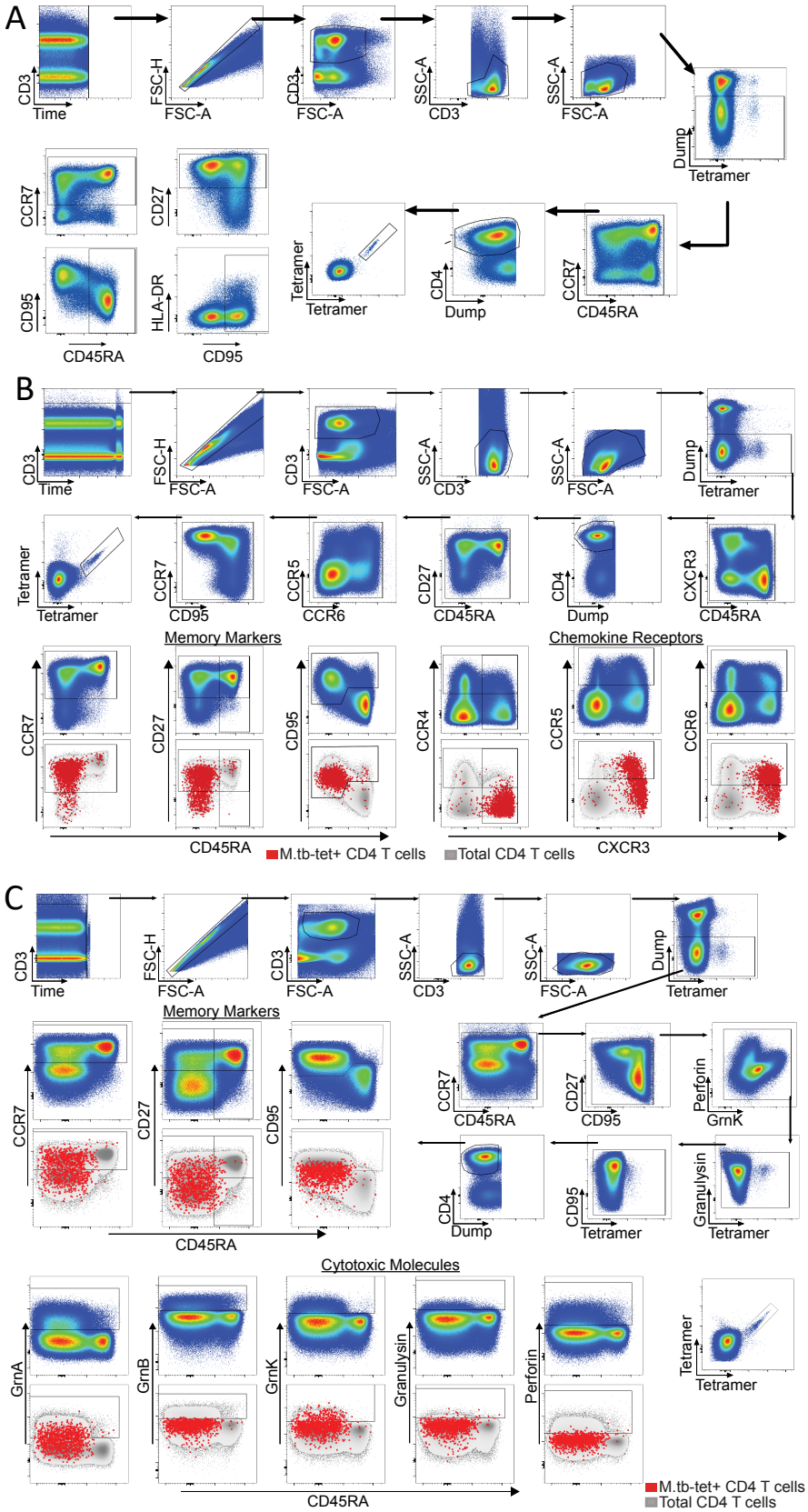

Figure 15: Gating strategy for M.tb-tetramer+ sorting and functional characterisation. Cryopreserved PBMC from recent M.tb-infected adolescents (A) and freshly isolated (B) and cryopreserved (C) PBMC from remote M.tb-infected adults were gated according to the illustration. M.tb-tetramer+ responses were defined on CD4+CD3+CD8-CD14- CD19- live lymphocytes. Gates identifying memory markers (A-C), chemokine receptors (B) and cytotoxic molecules (C) were defined on bulk CD4+ T cells, and then applied on M.tb-tetramer+ CD4+ T cells.

Statistical Analysis

Statistical analyses were performed using GraphPad Prism v6/7, R version 3.0.1, Pestle and/or SPICE version 5.2 to 5.3 (Roederer et al., 2011). Specific statistical analyses are clearly defined where applicable. Differences in protein expression were computed using Kruskal-Wallis, Wilcoxon signed-rank or Mann-Whitney U statistical tests. The Bonferroni or Benjamini-Hochberg [false discovery rate (FDR) <0.05] methods were used to correct for multiple comparisons for up to 4 comparisons or more than 4 comparisons, respectively. Differences in pie charts depicting memory, chemokine receptor and cytotoxic molecule co-expression profiles were calculated using nonparametric pair permutations comparing the overall distribution between median subset proportions using SPICE (Roederer et al., 2011).

Results

Tetramer Detection limit

We utilised M.tb-specific and CLIP-control tetramer staining of CD4+ T cells in our cohort of recent M.tb infected individuals to define the detection limit of tetramer+ CD4 T cell as 0.0021% measured by flow cytometry (Figure 16). This detection limit was calculated as the median frequency of negative control tetramer+ CD4 T cells plus the 95% CI of the median absolute deviation of negative control tetramer proportions. In addition, frequencies of tetramer+ CD4+ T cells had to be at least 5-fold higher (arbitrary cut-off) than frequencies of the corresponding control tetramer+ CD4+ T cells. This was to ensure that we only performed phenotypic analyses on "true" M.tb-tetramer+ CD4+ T cells and not non-specific tetramer+ cells that were above tetramer frequency threshold. Based on these criteria we were able to phenotype and analyse tetramer+ CD4 T cell responses in 8 (12 tetramer responses) of the 19 recently M.tb infected adolescents. Additionally, chemokine receptor and cytotoxic molecule co-expression analysis was performed on memory subsets (i.e. tetramer+ T_{SCM}, T_{CM} or T_E cells) that had a count threshold of at least 20 cells per subset.

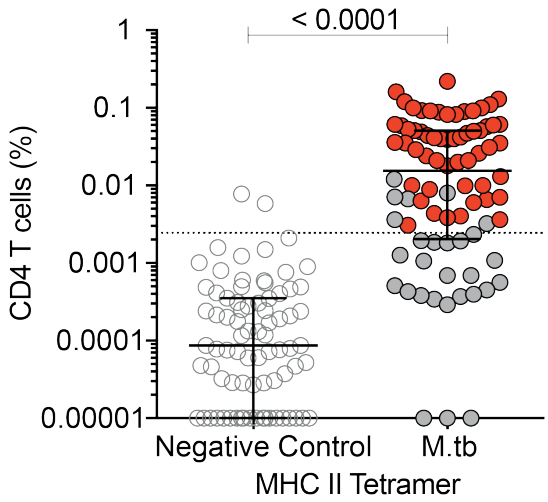

Figure 16: Defining the limit of detection of tetramer+ CD4 T cells. Frequencies of individual negative control (CLIP)- and M.tb-tetramer responses from 79 and 84 samples (19 participants with pooled time points), respectively. Median and interquartile range (IQR) are indicated by solid black lines. Red dots denote tetramer+ responses that met criteria for further phenotyping (tetramer+ cells > 0.0021% of CD4+ T cells (dotted line) and 5-fold higher than negative control). P-values were calculated with the Wilcoxon signed-rank, p-value < 0.05 was considered significant.

Definition of T_{SCM} phenotypes

To evaluate the effect of cryopreservation and different staining protocols on the detection of phenotypic markers, we compared PBMC that were stained fresh with surface markers only (chemokine receptor analysis) or after cryopreservation with surface and intracellular markers (cytotoxic molecule analysis), using different flow cytometry antibody panels (Figure 17). Cryopreservation and staining protocol significantly affected detected levels of CD45RA (higher on cryopreserved cells), CCR7 (lower on cryopreserved cells) and CD95 (markedly lower on cryopreserved cells), but not CD27 on M.tb-tetramer+ CD4+ cells (Figure 17A) and bulk CD4 cells (data not shown), which resulted in detecting different proportions of M.tb-tetramer+ CD4+ memory subsets (Figure 17B). Expression of CD95, a typical marker of T_{SCM} (Gattinoni et al., 2011), showed the highest variability between the different methodologies (Figure 17C). We therefore used CD45RA+CCR7+CD27+ CD4+ T cells to define M.tb-specific T_{SCM} CD4+ T cells and ignored expression of CD95, because tetramer+ cells are by definition antigen-experienced and not naïve (frequency of antigen-specific naïve T cells is too low to be detected by this method). On the other hand, we had to consider CD95 expression to differentiate bulk naïve (CD45RA+CCR7+CD27+CD95-) and T_{SCM} (CD45RA+CCR7+CD27+CD95+) CD4 T cells because it is the only marker that can differentiate these two bulk populations.

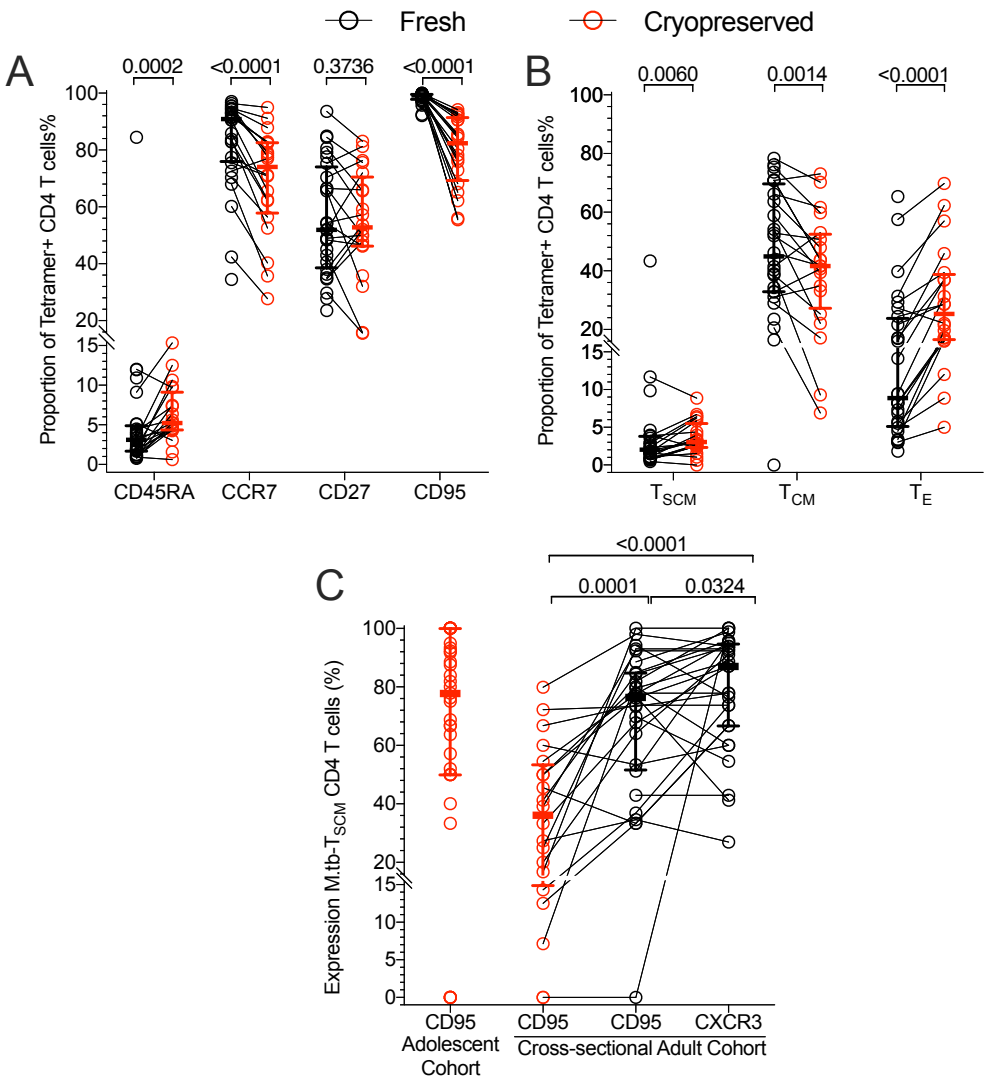

Figure 17: Detection of memory markers and subsets on M.tb-tetramer+ is affected by cryopreservation and/or antibody fluorochrome. Median (error bars denote IQR) (A) expression of memory markers CD45RA, CCR7, CD27 and CD95 on M.tb-tetramer+ and (B) proportions of M.tb-specific T_{SCM} (CD45RA+CCR7+CD27+), T_{CM} (CD45RA-CCR7+CD27+) and T_E (CD45RA-CCR7-) cells detected in remotely M.tb infected adults using either fresh PBMC (n=28) or matched cryopreserved PBMC (n=20). (C) Expression of CD95+ and CXCR3 on M.tb-specific T_{SCM} T cells. Symbols represents M.tb-specific T_{SCM} detected in recently M.tb infected adolescents (adolescent cohort, pooled time points, C only) and cross-sectional cohort of remotely M.tb infected adults [fresh PBMC (n=28) and matched cryopreserved PBMC (n=20)]. PBMC stained fresh or cryopreserved according to staining protocol (see methods) are illustrated by red or black symbols. P-values were calculated using Wilcoxon singed-rank test and p-values < 0.0125 (A and C) and < 0.0167 (B Only) were considered significant upon correction for multiple comparisons (Bonferroni method).

M.tb-specific T_{SCM} cells are induced by primary TBI

We next determined whether antigen-specific CD4+ T_{SCM} cells are induced during primary TBI. To track M.tb-specific CD4 T cells during acquisition of TBI, we utilised MHC II tetramers loaded with peptides of the M.tb complex-specific antigens, CFP-10 and ESAT-6, as well as a cross-reactive mycobacterial antigen, Ag85. Unfortunately, we were only able to detect Ag85-tetramer+ responses in one donor, as a result, all our analysis focused on CFP-10-tetramer+

and ESAT-6- tetramer+ CD4 T cells responses, collectively termed M.tb-tetramer+ CD4 T cells. Frequencies of M.tb-tetramer+ CD4+ T cells were below the limit of reliable detection before TBI in 11 out of 12 stained PBMC samples (representing 8 participants) and increased significantly upon QFT conversion 6 months later, when this response also peaked. Thereafter, frequencies of M.tb-tetramer+ CD4+ T cells decreased but were maintained at detectable levels throughout established TBI, at months 12-24 (Figure 18).

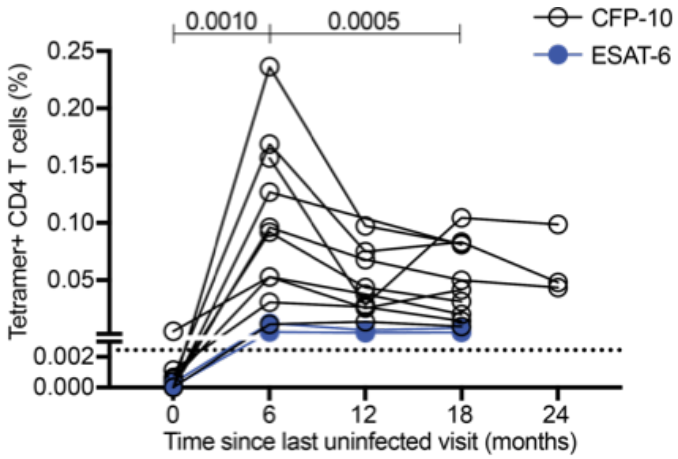

Figure 18: Detection of M.tb-tetramer+ cells in recent QFT converters. Frequencies of CFP-10-tetramer+ (black) and ESAT-6-tetramer+ (blue) CD4+ T cells detected in each participant (n=8; n = 12 PBMC samples). P-values were calculated with the Wilcoxon-singed-rank test, p-values < 0.025 were considered significant and are shown (corrected for multiple testing using the Bonferroni method).

Frequencies of M.tb-specific tetramer+ T_{SCM} (CD45RA+CCR7+CD27+), T_{CM} (CD45RA-CCR7+) and T_E (CD45RA-CCR7-) cells were below the limit for reliable detection at enrolment (month 0), demonstrating that circulating M.tb-specific T_N cells are too rare to detect by direct *ex vivo* tetramer staining (Figure 19). After M.tb infection, all three M.tb-specific memory subsets increased to detectable levels and remained detectable throughout established infection (Figure 19B). Interestingly, frequencies of M.tb-specific T_{SCM} and T_{CM} cells remained relatively consistent throughout primary (month 6) and established (month 18) TBI, while M.tb-specific T_E cells peaked during the primary TBI phase and thereafter steadily decreased (Figure 19B). These data suggest that M.tb-specific T_{SCM} cells are induced by primary TBI and maintained at low but consistent levels in the peripheral blood once TBI has been established.

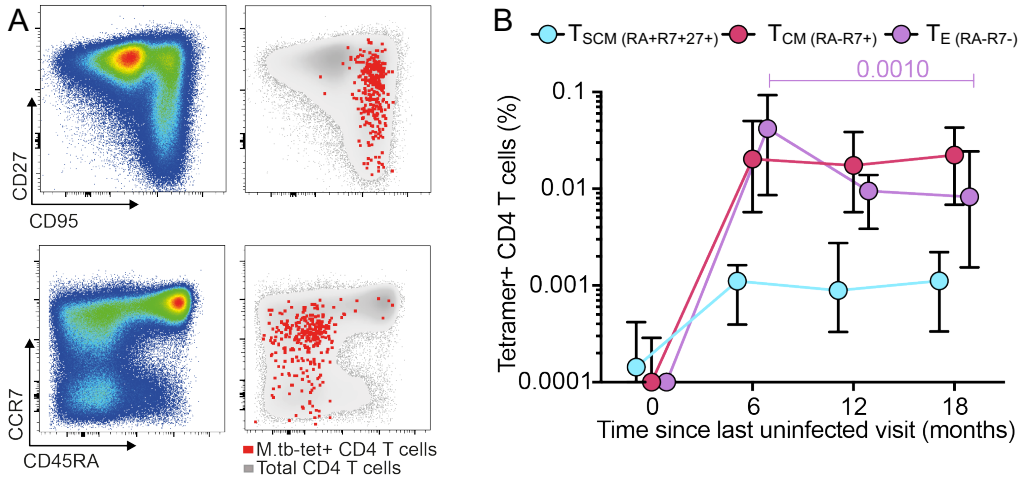

Figure 19: M.tb-specific T_{SCM} cells are detected in recently M.tb infected adolescents. (A) Representative flow cytometry plots for memory markers CD45RA, CCR7, CD27 and CD95 gated on bulk (pseudo-colour and grey) and M.tb-specific CD4+ T cells (red dots). (B) Median (error bars denote IQR) frequencies of M.tb-specific T_{SCM} (CD45RA+CCR7+CD27+, light blue), T_{CM} (CD45RA-CCR7+, magenta) and T_E (CD45RA-CCR7-, purple) during primary TBI. (n= 8 participants, n=12 tetramer+ CD4 T cell responses).

To further determine if the overall composition of memory subsets changed between primary and established TBI, we compared proportions of each memory subset between these two timepoints. We expanded the definition of memory subsets to include T_{CM} (CD45RA-CCR7+CD27+), more differentiated CD27- T_{CM*} (CD45RA-CCR7+CD27-), T_{TM} (CD45RA-CCR7-CD27+), T_E (CD45RA-CCR7-CD27-), and T_{TE} (CD45RA+CCR7-CD27-) T cells (Figure 20). Defining memory subsets based on these co-expression profiles ensured that we accounted for all "measurable" heterogenous memory populations. As illustrated in Figure 19B, the proportions of M.tb-specific+ T_{SCM} cells remained unchanged once TBI was established (Figure 20). Interestingly, despite no change in the overall frequencies of T_{CM} and/or T_{CM*} (CD45RA-CCR7+CD27±) cells once infection was established (Figure 19B), the proportional contribution of M.tb-specific+ T_{CM} and T_{CM*} cells increased during established TBI, while the proportion of M.tb-specific+ T_{TM} and T_E cells decreased (Figure 20). These results suggest that once infection is established the predominant memory phenotypes are T_{CM} and T_{CM*} (CD45RA-CCR7+CD27±) cells, potentially facilitating the long term maintenance of M.tb-specific T cells.

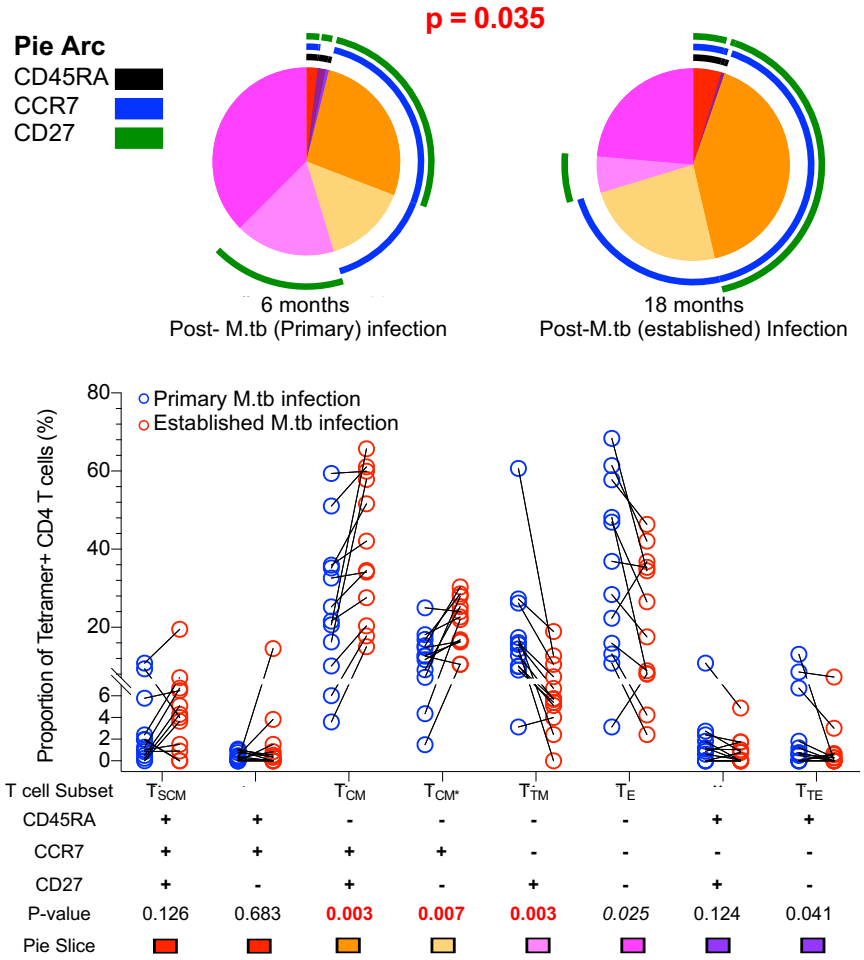

Figure 20: M.tb-specific T_{CM} cells are the predominant memory subset once TBI is established. Pie chart showing the median proportions (slices) of M.tb-specific CD4+ memory subsets T cells detected during primary and established TBI (6 and 18 months since last QFT negative visit, respectively). Arcs denote expression of CD45RA, CCR7 or CD27 memory markers. P-value was calculated using nonparametric pairs permutations comparing the overall distribution between pies. Dot plots denote proportions of each M.tb-specific memory subset: T_{SCM}, T_{CM}, T_{CM*}, T_{TM}, T_E and T_{TE} detected in 12 samples (from 8 participants) during primary (blue dots) and established (red dots) TBI. P-values were calculated using the Wilcoxon signed-rank test and corrected for multiple comparisons using the Benjamini-Hochberg method with an FDR of 0.05. Significant p-values are highlighted in **bold red** and p-values italicised had an FDR < 0.1.

Since we observed significant differences in CD45RA and CCR7 expression, as well as proportions of the simplified memory subsets cells in fresh and cryopreserved PBMC, (Figure 17A), we compared the distribution of the expanded memory (T_{SCM}, T_{CM}, T_{CM*}, T_{TM}, T_E, T_{TE}) subsets detected in fresh and cryopreserved PBMC from the same donors. As observed in Figure 17, higher proportions of M.tb-specific T_{SCM}, T_{TM}, T_E and T_{TE} and lower proportions of M.tb-specific T_{CM} and T_{CM*}cells were detected in cryopreserved PBMC compared to fresh PBMC (Figure 21). Difference in proportional contribution of memory subset in fresh and cryopreserved PBMC is likely due to higher proportions of CD45RA+ tetramer cells and lower proportions CCR7+ tetramer cells (Figure 17) in cryopreserved PBMC compared to fresh PBMC. Regardless, relative proportions of memory subsets maintained the same hierarchy

across sample types and panels, with T_{CM} and T_{CM*} cells being the most abundant during remote TBI, followed by T_{TM}, T_E and T_{SCM} cells and no overall difference in the total cell composition (pie comparison).

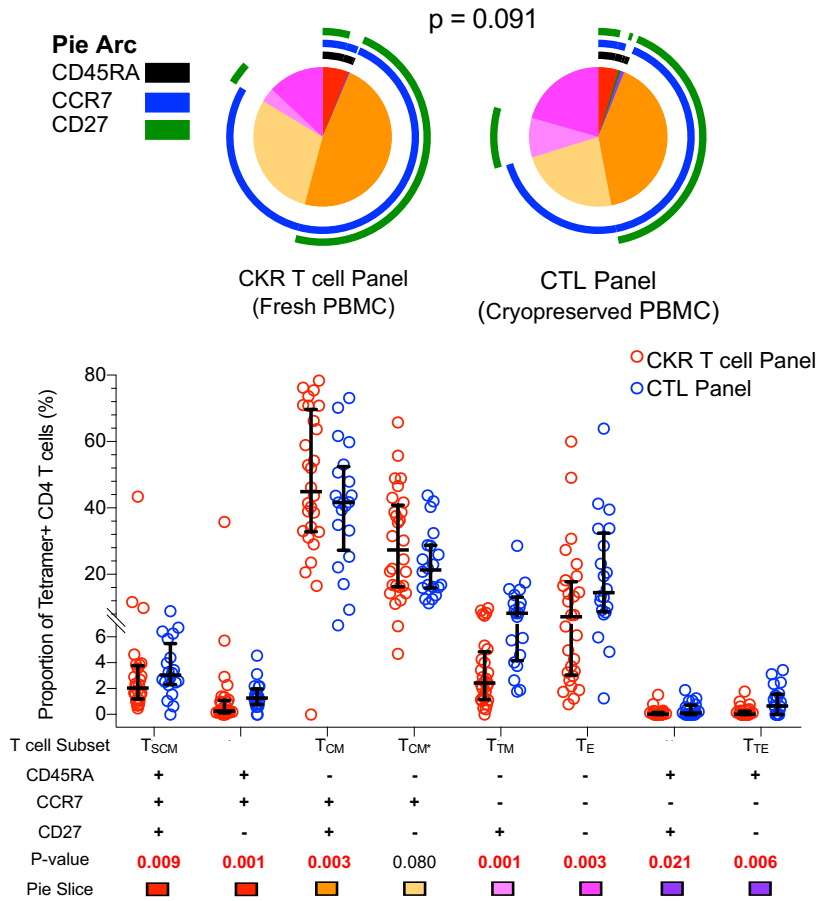

Figure 21: Distribution of M.tb-specific memory subsets is not affected by cryopreservation. Pie chart showing the median proportions (slices) and co-expression of CD45RA, CCR7 and/or CD27 denoted by pie arcs and dot plots showing median and IQR of proportions of memory subsets detected in fresh PBMC (n=28, red symbols) and cryopreserved PBMC (n=20, blue symbols). Statistical analysis was performed as in Figure 20.

M.tb-specific T_{SCM} cells express chemokine receptor and cytotoxic profiles distinct from bulk T_N and T_{SCM} CD4 T cells.

Chemokine receptors mediate tissue homing and allow classification of memory CD4 T cells into Th1, Th2, Th17 lineages (Acosta-Rodriguez et al., 2007; Becattini et al., 2015; Mahnke et al., 2013). Expression of cytotoxic mediators by CD4+ T cells indicates highly differentiated cells typically associated with high antigen exposure and effector T cell properties (Cheroutre and Husain, 2013). Expression of chemokine receptors: CCR4, CCR5, CCR6 and CXCR3, and cytotoxic molecules: granzymes A, B and K, granulysin and perforin by M.tb-specific T_{SCM} (CD45RA+CCR7+CD27+) cells were compared with bulk T_N (CD45RA+CCR7+CD27+CD95-) and T_{SCM} (CD45RA+CCR7+CD27+CD95+) cells. Despite differences in CD95 expression in fresh and

cryopreserved PBMC, we still used CD95 to define bulk T_{SCM} cells because this was the only marker that could distinguish bulk T_N from T_{SCM} cells.

Virtually all M.tb-tetramer+ CD4+ T cells expressed CXCR3 [median (IQR): 96.2% (86.2-97.8%) of tetramer+ cells), with relatively high proportions also expressing CCR5 and CCR6 (Figure 22A). A very small proportion of tetramer+ CD4 T cells expressed CCR4 (Figure 22A). By contrast, expression of all chemokine receptors were negligible or not detected on bulk T_N cells, as expected of T_N cells (Figure 22B), while CXCR3, CCR6 and CCR5 were expressed by a small proportion of bulk T_{SCM} cells (Figure 22B). Co-expression of these chemokine receptors by bulk T_{SCM} and M.tb-specific T_{SCM} cells revealed interesting patterns. Bulk T_{SCM} cells mostly expressed only a single chemokine receptor, whereas M.tb-specific T_{SCM} cells displayed more diverse co-expression profiles with single (CXCR3+), double (CCR5+CXCR3+ or CCR6+CXCR3+) and a small proportion of triple (CCR5+CCR6+CXCR3+) chemokine receptor co-expressing cells (Figure 22C). Importantly, a small subset of M.tb-specific T_{SCM} and >50% of bulk T_{SCM} cells did not express any of the chemokine receptors measured (Figure 22C), a profile suggestive of early T cell differentiation (Mahnke et al., 2013). Virtually all M.tb-specific CD4 T_{SCM} cells expressed CXCR3, while CD95, a typical marker of CD8 T_{SCM} cells (Gattinoni et al., 2011; Lugli et al., 2013b), was expressed by approximately 75% of tetramer+ CD4+ T_{SCM} cells (Figure 22C). Approximately 40% (range: 4.38-86.9%) of M.tb-tetramer+ CD4 T cells expressed granzyme A and/or granzyme K. Very few M.tb-tetramer+ CD4 T cells expressed granzyme B, granulysin or perforin (Figure 22D). Interestingly, about a quarter of M.tb-specific CD4+ T_{SCM} cells expressed cytotoxic molecules, also dominated by granzyme A and granzyme K (Figure 22E-F), which were generally not co-expressed by M.tb-specific CD4+ T_{SCM} cells. By contrast, bulk T_{SCM} cells expressed very low levels of cytotoxic molecules (Figure 22E-F).

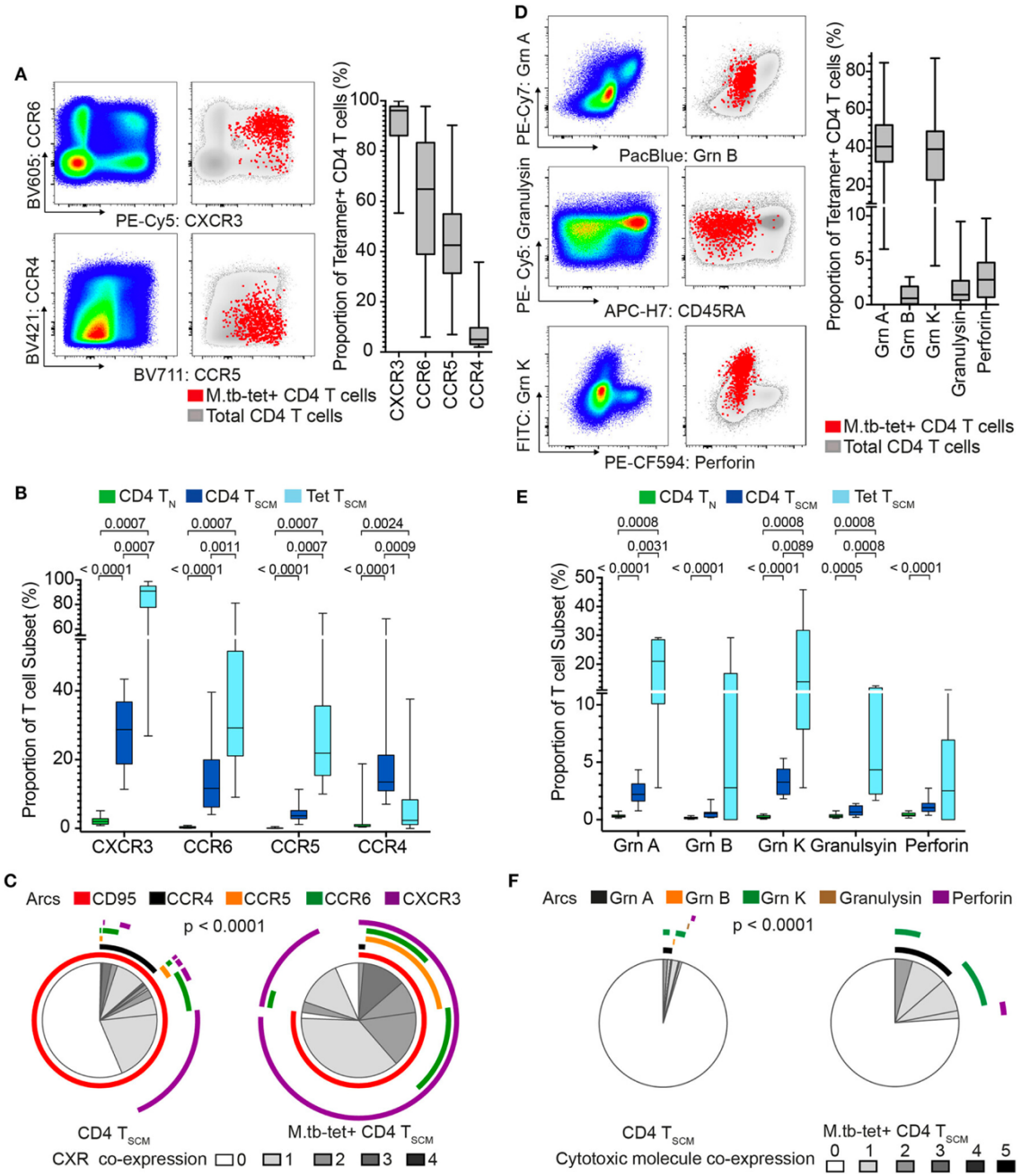

Figure 22: M.tb-specific T_{SCM} cells are not naïve cells and express distinct homing and cytotoxic profiles from bulk T_{SCM} cells. Expression of chemokine receptors and cytotoxic molecules was measured in remote M.tb infected (QFT+) adults (n = 28) when at least 20 events were detected in each tetramer+ memory subset. Representative flow cytometry plots of chemokine receptor (B, n=28) and cytotoxic molecule (D, n=20) expression on bulk (pseudo-colour and grey) and M.tb-specific (red dots) CD4+ T cells. Box and whisker plots represent the median proportion, IQR and range of chemokine receptor expression (n = 28). (B) Box and whisker plot and (C) pie chart showing the median proportions (slices) of expression CCR4, CCR5, CCR6, CXCR3 and/or CD95 by bulk T_N (CD45RA+ CCR7+ CD27+ CD95−, n = 28, green), T_{SCM} (CD45RA+ CCR7+ CD27+ CD95+, n = 28, blue), and M. tb-specific T_{SCM} (CD45RA+ CCR7+ CD27+, n = 15, light blue) CD4+ T cells. (E) Box and whisker plot and (F) pie chart showing the median proportions (slices) of granzyme (grn) A, B and K, granulysin, and perforin expression in bulk T_N (n = 20, green), T_{SCM} (n = 20, blue), and M.tb-specific T_{SCM} (n = 5, light blue) CD4+ T cells. p-values were calculated using Wilcoxon signed-rank test (chemokine receptor analysis) or Mann–Whitney U test (cytotoxic molecule analysis) and corrected for multiple comparisons using the Benjamini–Hochberg method with an FDR of 0.05. Adjusted p-values <0.05 were considered significant. P-value analysis of pie-charts was calculated using a non-parametric permutation test comparing the overall distribution between pies.

Increased expression of some chemokine receptors and cytotoxic molecules by M.tb-specific T_{SCM} cells compared to bulk T_{SCM} cells suggested that M.tb-specific T_{SCM} cells are more phenotypically differentiated than bulk T_{SCM} cells. We thus also compared chemokine receptor and cytotoxic molecule expression patterns by M.tb-specific T_{SCM} cells with bulk T_{CM} and T_E cells. M.tb-specific T_{SCM} cells expressed higher levels of CXCR3 than both bulk-T_{CM} and T_E cells, further supporting their T_{SCM} identity. Surprisingly, M.tb-specific T_{SCM} cells had similar expression levels of CCR5 and CCR6 to bulk T_E cells, but significantly lower expression of CCR4 than bulk T_{CM} and T_E cells (Figure 23A). M.tb-specific T_{SCM} also expressed significantly higher levels of granzyme A and granzyme K than bulk T_{CM} (Figure 23B). However, M.tb-specific T_{SCM} cells expressed lower levels of all cytotoxic molecules except granzyme K than bulk T_E cells (Figure 23B). These data further support the finding that M.tb-specific T_{SCM} cells are antigen-experienced memory cells with unique phenotypic and functional attributes that distinguish them from bulk T_{SCM} cells and are more similar to highly differentiated bulk T_{CM} and T_E cells.

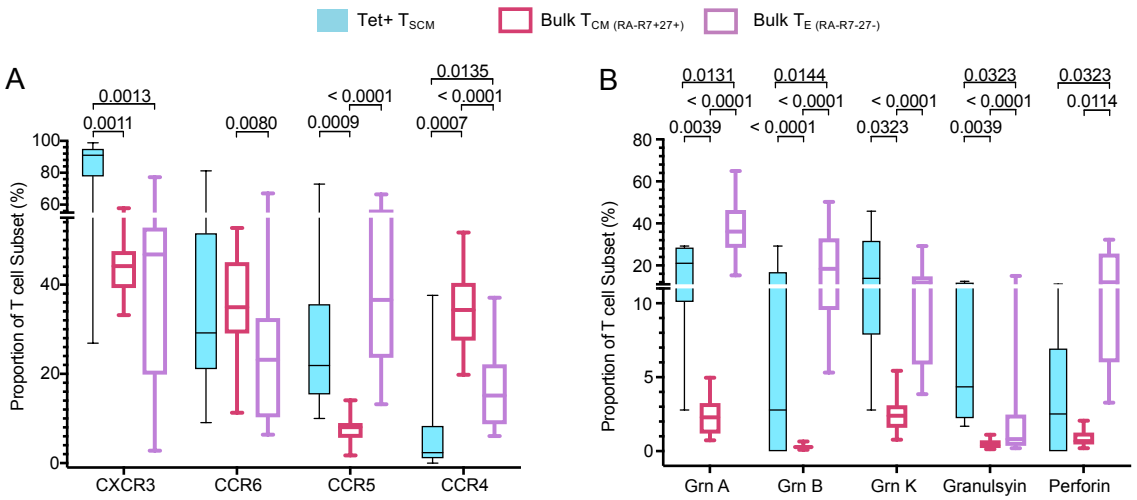

Figure 23: M.tb-specific T_{SCM} cells share some chemokine receptor and cytotoxic molecule expression profiles with bulk memory T cells. Box and whiskers plots depicting the proportion of M.tb-specific T_{SCM} (light blue, n=15), T_{CM} (magenta, n= 28) and T_E (purple n= 28) expressing (A) CCR4, CCR5, CCR6 and CXCR3 and (B) granzymes (grn) A, B and K; granulysin, and perforin. Statistical analysis was performed as in Figure 22.

M.tb-specific CD4 T_{SCM} are the least differentiated M.tb-specific memory subset

We then compared the expression of chemokine receptors and cytotoxic molecules between M.tb-specific tetramer+ CD4+ T_{SCM} cells and the other tetramer+ CD4+ T cell memory subsets. Virtually all cells among the five M.tb-specific memory subsets expressed CXCR3, as has been previously reported for M.tb-specific CD4+ T cells, although M.tb-specific T_{CM} cells displayed the highest proportion of CXCR3+ cells, compared to M.tb-specific T_{SCM}, T_{CM*}, T_{TM} and T_E cells (Figure 24A). A significantly lower proportion of M.tb-specific T_{SCM} cells expressed CCR6 than

either M.tb-specific T_{CM}, T_{CM*}, T_{TM} and T_E cells, while a minority of M.tb-specific T_{SCM} and T_{CM} expressed CCR5 or CCR4 (Figure 24A). Expression of CCR5 by M.tb-specific T_{CM*} cells was higher than T_{CM} but lower than both T_{TM} and T_E cells, suggesting that T_{CM*} are distinct from T_{CM} and could be more differentiated and/or activated (Figure 24A). Virtually all M.tb-specific T_E cells were CCR5+ and CCR4- (Figure 24A). An increase from single to triple chemokine receptor co-expression profiles was observed when M.tb memory cells were ordered according to their expected differentiation sequence, from T_{SCM} to T_{CM} to T_{CM*} to T_{TM} to T_E cells (Figure 24B-C). This was also observed when expression of the cytotoxic molecules granzyme A and K, was assessed (Figure 25). Proportions of M.tb-specific T_{SCM} cells expressing granzyme A and/or granzyme K were lower than other memory subsets, however, due to the low samples size (M.tb-specific T_{SCM} cells = 5 participants) the differences in expression levels were not significant. Overall proportion of granzyme A and K, were highest in M.tb-specific T_{TM} and T_E cells (Figure 25A), and significantly higher than T_{CM} and T_{CM*} populations. Proportions of M.tb-specific T_{TM} and T_E cells expressing both granzyme A and K were also higher than those observed in M.tb-specific T_{SCM} and T_{CM} but not T_{CM*} CD4+ T cells (Figure 25B-C).

Taken together, these data show that M.tb-specific T_{SCM} cells possess the least differentiated M.tb-specific phenotypic and functional profile, and suggest that M.tb-specific T_{CM} and T_{CM*} cells appear as an intermediate subset before cells differentiate into M.tb-specific T_{TM} and T_E CD4+ T cells.

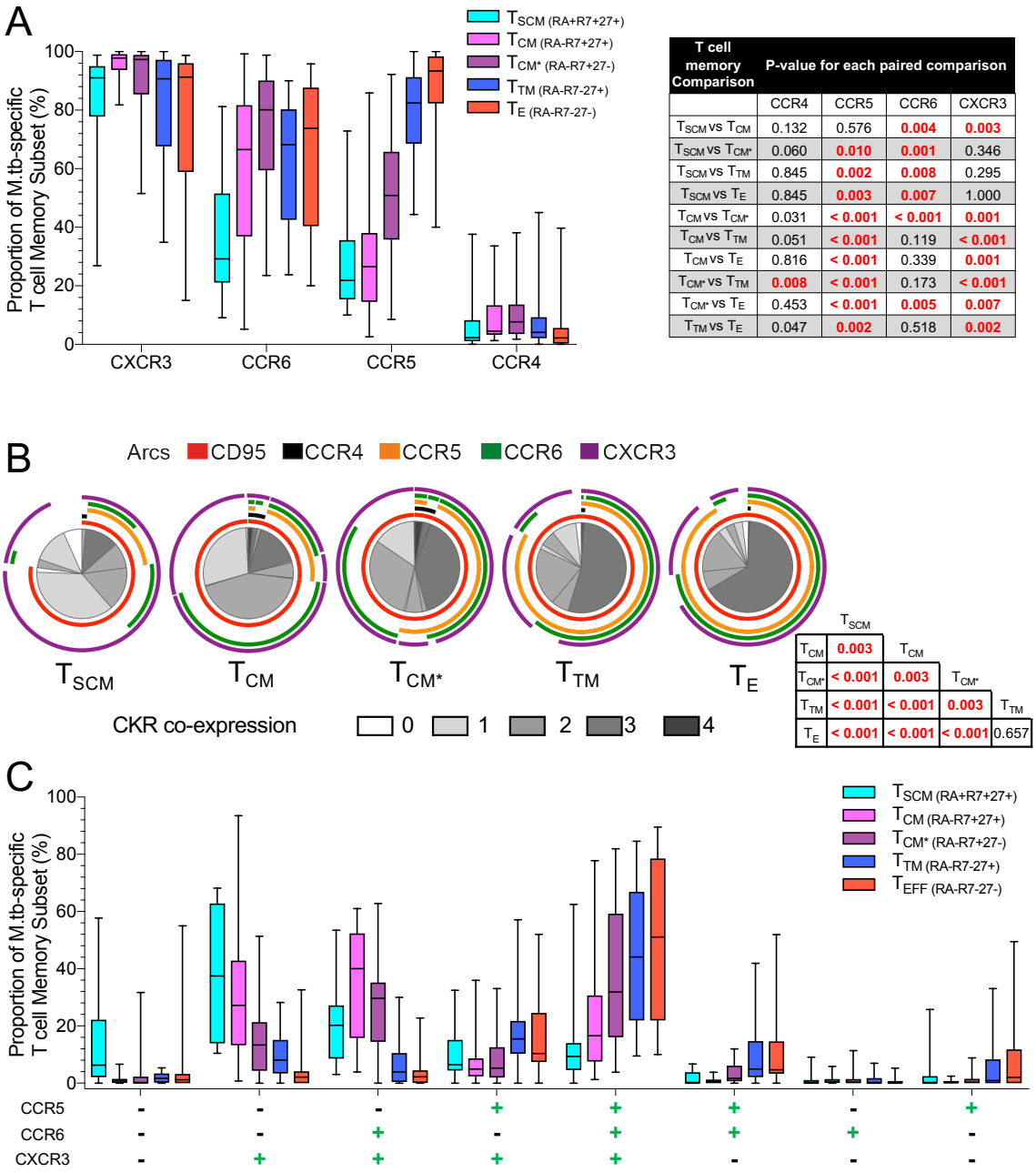

T cell memory Comparison	P-value for each paired comparison			
	CCR4	CCR5	CCR6	CXCR3
T_{SCM} vs T_{CM}	0.132	0.576	**0.004**	**0.003**
T_{SCM} vs T_{CM*}	0.060	**0.010**	**0.001**	0.346
T_{SCM} vs T_{TM}	0.845	**0.002**	**0.008**	0.295
T_{SCM} vs T_{E}	0.845	**0.003**	**0.007**	1.000
T_{CM} vs T_{CM*}	0.031	**< 0.001**	**< 0.001**	**0.001**
T_{CM} vs T_{TM}	0.051	**< 0.001**	0.119	**< 0.001**
T_{CM} vs T_{E}	0.816	**< 0.001**	0.339	**0.001**
T_{CM*} vs T_{TM}	**0.008**	**< 0.001**	0.173	**< 0.001**
T_{CM*} vs T_{E}	0.453	**< 0.001**	**0.005**	**0.007**
T_{TM} vs T_{E}	0.047	**0.002**	0.518	**0.002**

	T_{SCM}	T_{CM}	T_{CM*}	T_{TM}
T_{CM}	**0.003**			
T_{CM*}	**< 0.001**	**0.003**		
T_{TM}	**< 0.001**	**< 0.001**	**0.003**	
T_{E}	**< 0.001**	**< 0.001**	**< 0.001**	0.657

T cell memory Comparison	P-value for each paired comparison							
T_{SCM} vs T_{CM}	**0.007**	0.258	**0.001**	0.414	0.069	0.196	0.315	0.889
T_{SCM} vs T_{CM*}	**0.024**	**0.007**	0.530	0.451	**0.012**	0.043	0.307	0.224
T_{SCM} vs T_{TM}	**0.004**	**0.003**	**0.011**	**0.005**	**0.003**	**0.014**	0.726	0.058
T_{SCM} vs T_{E}	0.036	**0.002**	**0.003**	**0.014**	**0.002**	**0.002**	0.944	**0.009**
T_{CM} vs T_{CM*}	0.578	**0.000**	**0.000**	0.166	**0.000**	**0.000**	0.563	**0.002**
T_{CM} vs T_{TM}	0.060	**0.001**	**0.000**	**0.002**	**0.001**	**0.001**	0.798	**0.008**
T_{CM} vs T_{E}	**0.030**	**0.000**	**0.000**	**0.001**	**0.000**	**0.000**	0.041	**0.000**
T_{CM*} vs T_{TM}	0.268	0.047	**0.001**	**0.001**	0.036	**0.008**	0.045	**0.010**
T_{CM*} vs T_{E}	0.240	**0.000**	**0.000**	**0.001**	**0.003**	**0.000**	**0.007**	**0.000**
T_{TM} vs T_{E}	0.798	**0.005**	**0.007**	0.623	0.623	**0.016**	0.236	**0.014**

Figure 24: M.tb-specific T_{SCM} cells have the least differentiated chemokine receptor co-expression profile. Expression of chemokine receptors was measured in remote M.tb infected (QFT+) adults (n=28) when at least 20 events were detected in each tetramer+ memory subset. (A) Box and whiskers plots depicting the proportion of chemokine receptors expression of M.tb-specific T_{SCM} (n=15, light blue), T_{CM} (n=27, light purple), T_{CM*} (n=26, dark purple), T_{TM} (n=16, blue) and T_{E} (n=22, red). CD4+ T cells. (B) Pie chart showing the median proportions (slices) and (C) box and whisker plots depicting proportions of M.tb-specific T_{SCM}, T_{CM}, T_{CM*}, T_{TM} and T_{E} cells co-expressing CD95, CCR4, CCR5, CCR6 and/or CXCR3. Statistical analysis was performed as in Figure 22.

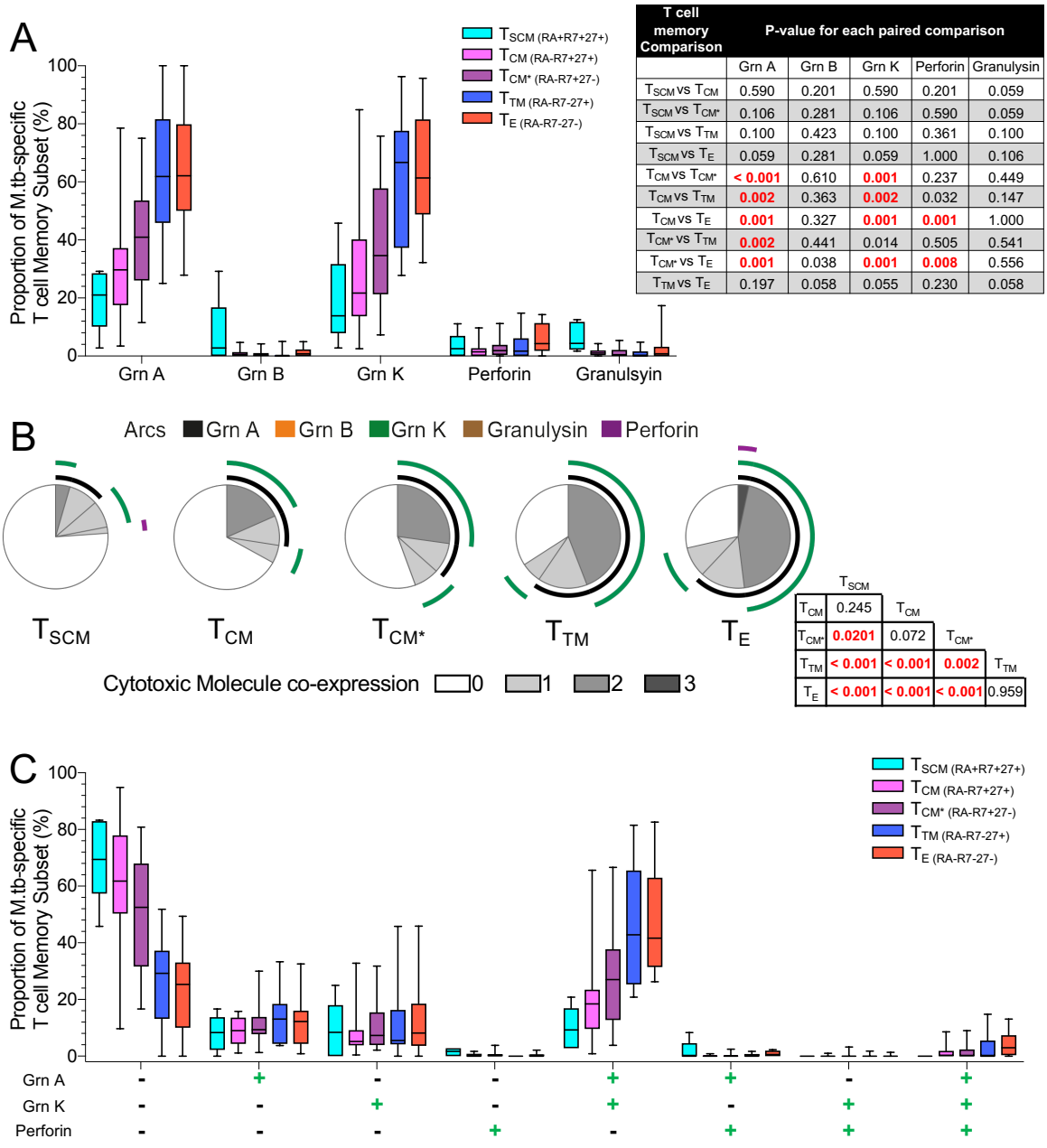

T cell memory Comparison	P-value for each paired comparison				
	Grn A	Grn B	Grn K	Perforin	Granulysin
T_{SCM} vs T_{CM}	0.590	0.201	0.590	0.201	0.059
T_{SCM} vs T_{CM*}	0.106	0.281	0.106	0.590	0.059
T_{SCM} vs T_{TM}	0.100	0.423	0.100	0.361	0.100
T_{SCM} vs T_{E}	0.059	0.281	0.059	1.000	0.106
T_{CM} vs T_{CM*}	**< 0.001**	0.610	**0.001**	0.237	0.449
T_{CM} vs T_{TM}	**0.002**	0.363	**0.002**	0.032	0.147
T_{CM} vs T_{E}	**0.001**	0.327	**0.001**	**0.001**	1.000
T_{CM*} vs T_{TM}	**0.002**	0.441	0.014	0.505	0.541
T_{CM*} vs T_{E}	**0.001**	0.038	**0.001**	**0.008**	0.556
T_{TM} vs T_{E}	0.197	0.058	0.055	0.230	0.058

	T_{SCM}	T_{CM}	T_{CM*}	T_{TM}
T_{CM}	0.245			
T_{CM*}	**0.0201**	0.072		
T_{TM}	**< 0.001**	**< 0.001**	**0.002**	
T_{E}	**< 0.001**	**< 0.001**	**< 0.001**	0.959

T cell memory Comparison	P-value for each paired comparison							
T_{SCM} vs T_{CM}	1.000	0.676	1.000	0.517	0.530	0.724	0.424	0.424
T_{SCM} vs T_{CM*}	0.210	0.531	0.675	0.387	0.402	0.724	0.424	0.180
T_{SCM} vs T_{TM}	**0.061**	0.312	0.885	0.067	**0.059**	0.878	0.453	0.453
T_{SCM} vs T_{E}	**0.022**	0.403	0.675	0.387	**0.012**	0.656	0.424	0.025
T_{CM} vs T_{CM*}	0.033	0.602	0.327	0.946	0.074	0.888	1.000	0.973
T_{CM} vs T_{TM}	**0.001**	0.166	0.505	0.008	**0.002**	0.512	0.644	0.458
T_{CM} vs T_{E}	**0.000**	0.281	0.281	0.174	**0.000**	0.067	0.609	0.030
T_{CM*} vs T_{TM}	0.021	0.305	0.758	**0.003**	0.091	0.599	0.579	0.596
T_{CM*} vs T_{E}	**0.002**	0.852	0.950	0.292	0.010	0.052	1.000	0.066
T_{TM} vs T_{E}	0.470	0.488	0.564	0.079	0.707	0.318	0.374	0.280

Figure 25: M.tb-specific T_{SCM} cells have the least differentiated cytotoxic co-expression profile. (A) Box and whiskers plots depicting the proportion of grnA, grnB, grnK, granulysin and perforin expression in M.tb-specific T_{SCM} (n=5, light blue), T_{CM} (n=19, light purple), T_{CM*} (n=18, dark purple), T_{TM} (n=13, blue) and T_{E} (n=15, red) CD4+ T cells (B) Pie chart showing the median proportions (slices) and (C) box and whisker plots depicting proportions of M.tb-specific T_{SCM}, T_{CM}, T_{CM*}, T_{TM} and T_{E} cells co-expressing of granzymes (grn) A, B and K; granulysin, and/or perforin. Statistical analysis was performed as in Figure 22, however p-values for (A) and (C) were calculated with Mann-Whitney U test.

M.tb-specific T_{SCM} CD4 T cells express Th1 cytokines

Studies of CD8+ (and CD4+) T_{SCM} cells have shown that T_{SCM} cells have limited cytokine expression capacity that is dominated by IL-2, and to a lesser extent TNF, in responses to non-specific stimulation (Gattinoni et al., 2011; Hong et al., 2016; Lugli et al., 2013a). To determine if this is also true for mycobacteria-specific T_{SCM} cells, we re-analysed available data from mycobacterial antigen stimulated whole blood from a previously published cohort of QFT+ adults [Figure 26; (Luabeya et al., 2015)].

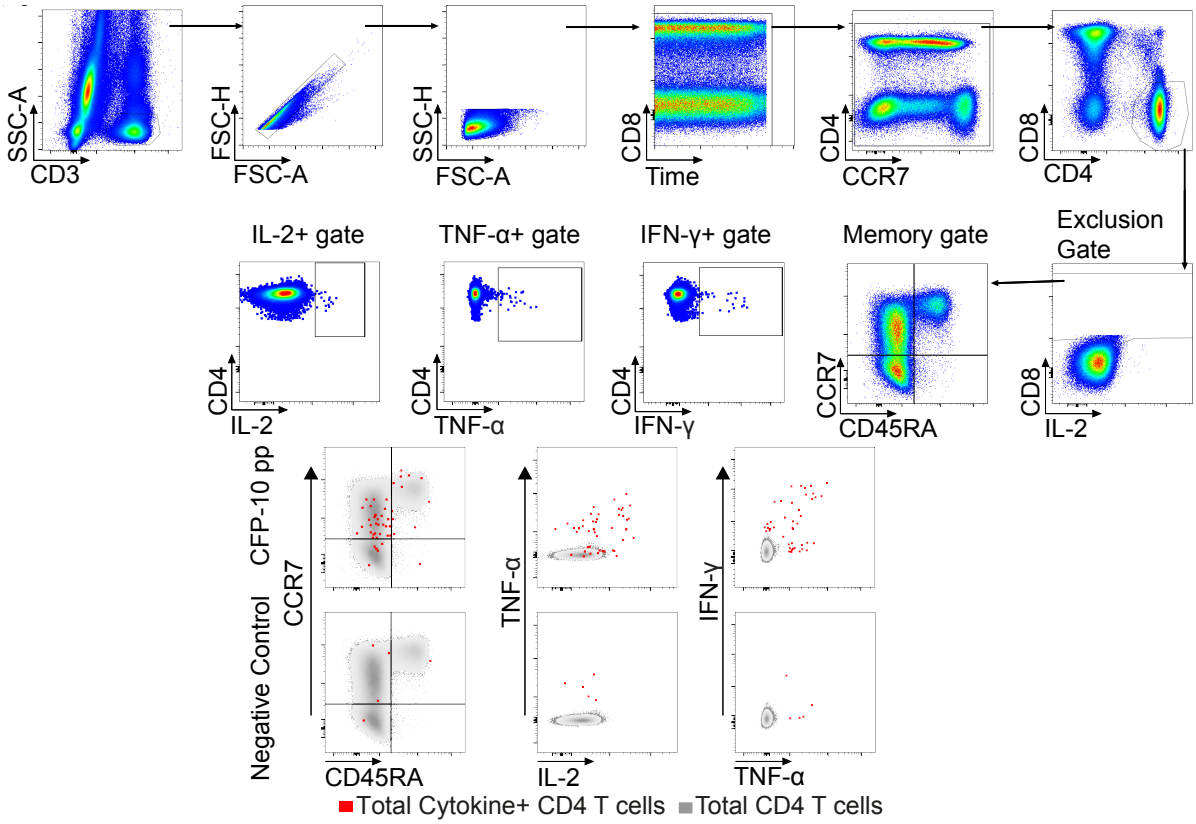

Figure 26: Gating strategy to detect Th1 cytokine by CD4+ T cells in response to M.tb antigen stimulation. Cells from stimulated whole blood were gated according to the illustration. Antigen-specific cytokine responses were defined on CD4+CD3+CD8- lymphocytes, setting the gates on unstimulated cells. Gates identifying memory subsets, based on CD45RA and CCR7 expression, were set on bulk CD4+ T cells and applied to cytokine+ cells.

Unfortunately, the flow cytometry panel published by Luabeya and colleagues did not contain CD27 as a memory marker (Luabeya et al., 2015). Thus, to determine whether CD45RA and CCR7 in the absence of CD27 are sufficient markers of to define M.tb-specific T_{SCM} cells, we compared protein expression levels (MFI) of the T_{SCM} markers CD27, CD95 and CXCR3 between CD45RA+CCR7+ and CD45RA+CCR7+CD27+ M.tb-tetramer+ T_{SCM} cells (Figure 27). No differences in the expression of these T_{SCM} markers were observed between the M.tb-specific T_{SCM} cells defined by the two phenotypes, suggesting that CD45RA and CCR7 are sufficient to define CD4+ M.tb-specific T_{SCM} cells.

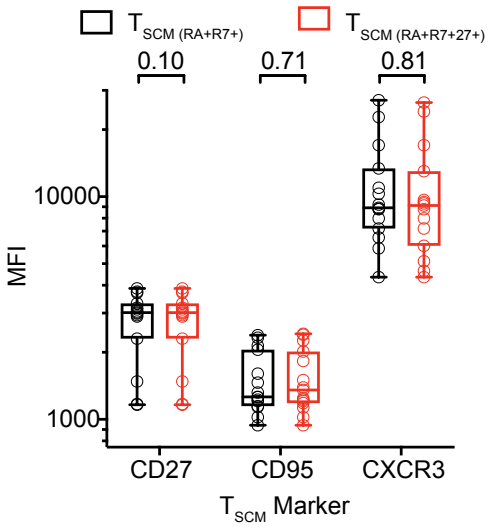

Figure 27: M.tb-specific T_{SCM} cells can be defined using CD45RA and CCR7 staining only. Comparison of protein expression (MFI) of CD27, CD95 and CXCR3 T_{SCM} markers between M.tb-specific T_{SCM} cells defined as CD45RA+CCR7+ (black) and CD45RA+CCR7+ CD27+ (red, n=15 participants). Statistical analysis was performed as in figure 14, p-values < 0.0167 were considered significant.

Mycobacterial antigen-specific cytokine+ cells expressing a T_{SCM} (CD45RA+CCR7+) phenotype were typically very infrequent and, in some donors, less than 10 T_{SCM} cells were detected per sample (Luabeya et al., 2015). As a result, we did not perform in-depth cytokine co-expression or Boolean analyses, and we report frequencies of CD4+ T_{SCM} cells that express total IFN-γ, TNF and IL-2 in unstimulated and antigen-stimulated samples (Figure 28). We detected significantly higher frequencies of BCG- and CFP-10- specific IFN-γ+, TNF+ and IL-2+ T_{SCM} cells, and only Ag85B-specific IL-2+ T_{SCM} cells compared to non-specific (unstimulated) T_{SCM} cells (Figure 28). This was however not observed in blood stimulated with ESAT-6. These results demonstrate cytokine production by mycobacteria-specific CD4+ T_{SCM} cells is not restricted to IL-2 but includes TNF and IFN-γ.

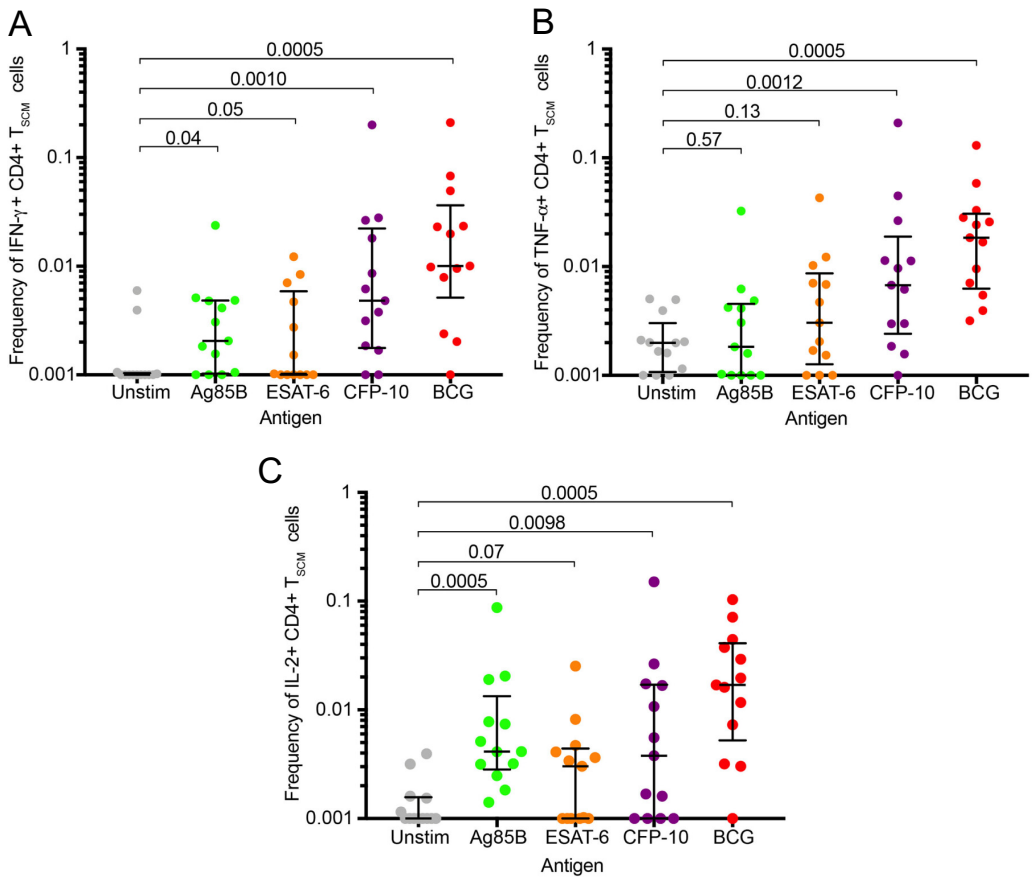

Figure 28: M.tb-specific T_{SCM} cells express Th1 cytokines. Fresh whole blood from remotely infected (QFT+) adults (n=13) was left unstimulated (grey) or stimulated with peptide pools spanning M.tb antigens, Ag85B (green), ESAT-6 (orange) or CFP-10 (purple), or whole BCG (red) for 12 hours. Box and whisker plots depict frequencies of CD4+ T_{SCM} (RA+R7+) cells expressing (A) IFN-γ,(B) TNF or (C) IL-2, calculated out of total CD4.+T_{SCM} cells. P-values were calculated using the Wilcoxon signed-rank test and p-values <0.0125 were considered significant (corrected for multiple testing using the Bonferroni method).

BCG-Specific T_{SCM} cell frequencies are associated with CD4+ T Cell proliferative capacity

A key feature of T_{SCM} cells is long-term maintenance of proliferative capacity in the absence of antigenic stimulation (Gattinoni et al., 2011). To determine whether vaccine-induced CD4+ T_{SCM} cells contribute to T cell long-term proliferative potential, we analysed available data: BCG vaccine-induced cytokine expression profiles and proliferative capacity of BCG-specific CD4+ T cells from a completed clinical trial in infants who received BCG vaccination (Nemes et al., 2017b). Frequencies of BCG-specific CD4+ T_{SCM} and T_{CM} cells, but not T_E cells, positively correlated with proliferative potential of BCG-stimulated CD4+ T cells 10 months after BCG vaccination (Figure 29). These results suggest that vaccine-induced T_{SCM} cells contribute to long-term memory and proliferative capacity of the vaccine-induced T cell response to mycobacteria.

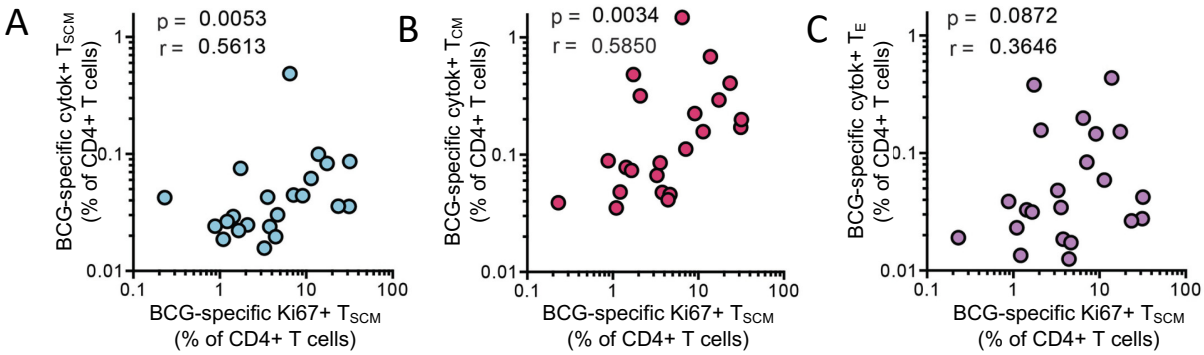

Figure 29: BCG-specific T_{SCM} cells are associated with long-term CD4+ T cell proliferation after vaccination. Whole blood from 1-year-old infants (n = 23) was stimulated with BCG for 12 hours to measure the frequencies of cytokine-producing (A) T_{SCM} (CD45RA+CCR7+), (B) T_{CM} (CD45RA-CCR7+), and (C) T_E (CD45RA-CCR7-) cells. In parallel, whole blood was stimulated with BCG for 7 days, and the frequency of proliferating CD4+ T cells was assessed by upregulation of Ki-67. Correlations between the frequencies of BCG-specific CD4+ memory T cell subsets and those of proliferating CD4+ T cells were calculated by Spearman test at 10 months post-vaccination.

Discussion

We performed in-depth analyses of the kinetics, phenotype and functional characteristics of M.tb-specific CD4+ T_{SCM} cells during natural TBI. Our data show that CD4+ T_{SCM} cells are induced by TBI in humans, predominantly express CD95 and CXCR3, are distinct from T_N cells and possess phenotypic and functional profiles consistent with M.tb-specific CD4+ T cells at an early stage of differentiation (Mahnke et al., 2013). These data supplement our current knowledge of T_{SCM} cells, which has primarily been derived from studies of virus-specific CD8 T cells (Fuertes Marraco et al., 2015; Gattinoni et al., 2011, 2017; Lugli et al., 2013a).

CD4+ M.tb-specific T_{SCM} cells were induced during primary TBI and maintained throughout established TBI at low frequencies. This phenomenon is highly characteristic of the stem cell nature of long-term memory cells such as T_{CM} and potentially T_{SCM} cells, where asymmetrical cell division maintains both the overall proportions of these memory cells and the pool of more differentiated effector memory subsets (Ciocca et al., 2012; Graef et al., 2014).

Consistent with published findings (Lindestam Arlehamn et al., 2013), we found that M.tb-specific cells were predominantly CXCR3+, a Th1 associated chemokine receptor (Rivino et al., 2004). This was accompanied with relatively high CCR5 and CCR6 expression, chemokine receptors associated with activation (Castellino et al., 2006) and Th1/17 T cells (Singh et al., 2008), respectively, but low expression of the Th2 associated CCR4 (Rivino et al., 2004). The predominant CXCR3 expression by M.tb-specific T_{SCM} cells is suggestive of Th1 lineage, which we confirmed on a functional level by showing that mycobacteria-specific T_{SCM} cells not only produced, IL-2, but also TNF and IFN-γ and, to a lesser extent, cytotoxic molecules.

Our data suggested that M.tb-specific T_{SCM} cells had different cytokine expression patterns depending on the M.tb antigen recognised. For example, Ag85B-specific T_{SCM} cells produced only IL-2, while BCG- and CFP-10- specific T_{SCM} cells produced TNF and IFN-γ in addition to IL-2. Despite the early stage of T cell memory differentiation of T_{SCM} cells, these findings may reflect different degrees of antigen exposure *in vivo*. A murine study showed that Ag85B mRNA expression peaks during early stages of TBI and significantly reduces during established infection, whereas ESAT-6 mRNA was maintained at high levels throughout these infection stages (Shi et al., 2004). Our research group recently also showed differential degrees of T cell differentiation of Ag85B and ESAT-6-specific CD4 T cells in M.tb infected mice and humans (Moguche et al., 2017). Expression of only IL-2, a cytokine associated with homeostatic proliferation and early T cell differentiation (Jaleco et al., 2003; Marrack et al., 2000), by Ag85B-specific T_{SCM} cells may reflect lower exposure of T cells to this antigen. By contrast, expression of TNF and IFN-γ, cytokines typically produced by more differentiated T cells, by CFP-10 and BCG-specific T_{SCM} cells is consistent with higher *in vivo* recognition or exposure to these antigens (Mahnke et al., 2013). However, in light of the low frequencies of M.tb-specific T_{SCM} cells these data on functional profiles should be interpreted conservatively. The nature of cytokine expression by M.tb-specific T_{SCM} cells requires more attention in future studies. Expression of other cytokines besides IFN-γ, suggests that T_{SCM} cells we described here, could be distinct from T_{NLM} described by Yuan and colleagues, which predominantly solely expressed IFN-γ (Yuan et al., 2019). However, Yuan and colleagues did not measure IL-2 expression, thus these T_{NLM} could potentially express IL-2 as well (Yuan et al., 2019). Besides T_{SCM} and T_{NLM} cells, another population of cytokine-producing cells with a naïve phenotype, termed T_{CNP} cells, were recently defined and detected during tuberculosis disease (Orlando et al., 2018). Interestingly, M.tb-specific T_{NLM} cells detected in mice and humans produced IFN-γ but not TNF (Yuan et al., 2019). Whereas M.tb-specific T_{CNP} cells, similar to M.tb-specific T_{SCM} cells, are capable of producing IFN-γ, TNF and IL-2, which surprisingly were the predominant triple-cytokine producing memory phenotype during tuberculosis disease (Orlando et al., 2018). It was proposed that T_{CNP} cells can suggestively track antigen load, where proportions of T_{CNP} cells were significantly higher in tuberculosis patients compared to individuals with remote TBI, and significantly decreased upon successful M.tb treatment (Orlando et al., 2018). This finding contradicts results from NHP studies (Lugli et al., 2013a),

which show that proportions of CD8+ T_{SCM} cells increase during antigen clearance. Differences observed between these two studies could be due to differences in species (human vs NHPs), infection model (bacterial vs viral), T cell lineage (CD4 vs CD8) and/or method of T cell detection (cytokine producing vs tetramer+ T cells). The characteristics of such mycobacteria-specific T_{NLM} and/or T_{CNP} CD4+ T cells are partly consistent with those of CD4+ T_{SCM} cells. However, lack of CD95 expression could suggest that these cell subsets might be at different stages of T cell differentiation and could be part of a heterogenous pool of phenotypically naïve memory cells, which also include T_{SCM} cells.

In addition to high CXCR3 expression, about a third of M.tb-specific T_{SCM} cells co-expressed CCR6, suggestive of early polarisation towards a Th1/Th17 lineage. This lineage has been described as the major CD4+ T cell subset responding to M.tb and associated with protection against TBI and tuberculosis disease in NHPs (Darrah et al., 2020; Dijkman et al., 2019; Lindestam Arlehamn et al., 2013). Finally, CCR5 expression, observed in about 20% of M.tb-specific T_{SCM} cells, suggests that at least some M.tb-specific T_{SCM} cells may have the potential to migrate to sites of infection (Kunkel et al., 2002; Qin et al., 1998) and are not confined to the circulatory and lymphoid compartments, despite CCR7 expression.

The ability of CD4+ T cells to produce cytotoxic molecules has been associated with high antigen exposure resulting in increased MHC-antigen-T cell receptor interaction and is mostly associated with late differentiated T cells with increased effector functions (Brown, 2010; Cheroutre and Husain, 2013; Juno et al., 2017). Cytotoxic CD4+ T cells have been well characterized in contexts of viral infections, where cytotoxic CD4+ T cells either utilise granzyme B and perforin or Fas-FasL interactions to mediate killing of infected cells (Brown, 2010; Juno et al. 2017). Surprisingly, we found that CD4+ M.tb-specific T cells, including M.tb-specific T_{SCM} cells, predominantly expressed granzyme A and/or granzyme K. Unlike granzyme B and perforin that mediate cytotoxic killing of infected cells, granzyme A and K, have been described as pro-inflammatory and cytokine-inducing cytotoxic molecules (Irmler et al., 1995; Joeckel et al., 2011; Metkar et al., 2008; Sower et al., 1996). In fact, expression of grnA by γδ T cells mediated increased M.tb killing by macrophages (Spencer et al., 2013). Thus, expression of these cytotoxic molecules by M.tb-specific memory subsets, including T_{SCM} cells, in absence of granzyme B and perforin, may induce pro-inflammatory responses in macrophages at the site of infection, rather than mediate direct killing of M.tb infected macrophages, which would require perforin to mediate entry of granzymes into infected cells.

We primarily employed MHC II tetramers loaded with M.tb-epitopes to identify M.tb-specific CD4+ T cells directly *ex vivo* for phenotypic profiling. MHC tetramers provide a method for detecting antigen-specific T cells directly *ex vivo* without the need for antigen stimulation, which can alter the function, phenotype, and gene expression profiles of T cells. However, an important limitation to using MHC class II tetramers is that only T cells that bear the cognate TCR for a single peptide in the context of a single MHC allele can be studied. To address this, we employed several tetramers that allowed detection of CFP-10, ESAT-6 and Ag85-specific CD4+ T cells restricted by DRB1*0301, DRB1*0401, DRB5*0101, DPB1*0401 or DQB1*0602, providing better coverage of the M.tb-specific CD4 T cell response and cohort compared to utilising a single MHC II tetramer-peptide. We do acknowledge that the tetramer panel we utilised is limited, and the HLA-distribution of tetramers may confound results presented. Unfortunately, due to limited sample availability and resources, we were unable to stain PBMC with tetramers that present the same M.tb-epitope on different HLA molecules.

Additionally, the majority of experimental protocols were performed on cryopreserved PBMC, while fresh PBMC were only used to assess chemokine co-expression patterns of M.tb-specific T cell memory subsets. Despite these differences in sample type, we observed no difference in the distribution of M.tb-specific T cell memory profiles between fresh and cryopreserved PBMC stained from the same persons.

Another limitation was our inability to characterise the proliferation and differentiation potential of purified M.tb-specific CD4+ T_{SCM} cells, because a very large number of cells (approximately 500 million PBMC per participant) would be required to sort at least 1000 M.tb-specific tetramer+ CD4 T_{SCM} cells. This is only achievable by leukapheresis, which was not available at our clinical site. We provided indirect evidence for this by showing that the precursor frequencies of BCG-specific T_{SCM} and T_{CM} CD4+ T cells correlated with proliferative potential of BCG-specific CD4+ T cells 10 months post infant BCG vaccination. Further studies measuring vaccine-induced T_{SCM} and long-term persistence of memory T cells are required to define the role of antigen-specific CD4+ T_{SCM} cells after vaccination.

In summary, these results demonstrate that M.tb-specific CD4+ T_{SCM} cells are induced by primary TBI and exhibit phenotypic and functional features that are distinct from bulk CD4+ T_N and T_{SCM} cells and consistent with early differentiation of M.tb-specific CD4+ T cells, possibly shaped by antigen exposure. Our findings have important implications in the study of the M.tb-specific T cell memory repertoire, and raises numerous unanswered questions.

For example, determining the functional role of M.tb-specific T_{SCM} cells in long-term immune responses, how their functional features differ between asymptomatic TBI and disease, as well as during tuberculosis treatment. Some of these questions are currently being explored, and recently published work suggests that M.tb-specific CD4+ T_{SCM} cells potentially track antigen load (Orlando et al., 2018). Additionally, future work should determine whether long-lived CD4+ T_{SCM} cells are associated with long-term memory responses and protection, as observed for CD8+ T_{SCM} upon yellow fever vaccination (Fuertes Marraco et al., 2015) as well as in adoptive immune-therapy (Biasco et al., 2015; Gattinoni et al., 2017; Oliveira et al., 2015). Our data on BCG-specific T_{SCM} cells provide evidence that T_{SCM} cells are an important component of vaccine-induced immune responses, and possibly play a role in maintaining the T cell memory population.

Contributions

Analysis of results of BCG vaccine-induced cytokine expression profiles and proliferative capacity of BCG-specific CD4+ T cells was performed by Elisa Nemes (Nemes et al., 2017b).
All methodology and statistical analyses were performed by Cheleka Anne-Marie Mpande, unless stated otherwise.

Chapter 4: Optimisation of PBMC stimulation and intracellular cytokine staining assay to measure mycobacteria-specific functional responses.

Introduction

The QFT assay is one of the most widely used TBI diagnostics. QFT is an ELISA-based immuno-diagnostic that detects IFN-γ in supernatant from whole blood stimulated overnight with M.tb-specific antigens, CFP-10, ESAT-6 and TB7.7, that are absent in BCG. As a result, QFT is highly specific for detection of M.tb-specific IFN-γ responses and does not cross-react with BCG-induced immunity.

The assay defines a positive QFT result as net detection of IFN-γ greater or equal to 0.35 IU/mL (QFT-G ELISA Package Insert 06/2018; https://www.quantiferon.com/wp-content/uploads/2019/03/L1075115-QuantiFERON-TB-Gold-ELISA-IFU-CE-rev07.pdf).

Quantitative detection of IFN-γ, which is calculated using a standard curve with a relatively narrow range, 0 - 4 IU/mL, is converted to a qualitative result. Biologically the distribution of quantitative IFN-γ measurements is not bimodal and detection of IFN-γ with alternative methods, such as flow cytometry, does not correspond with the QFT positivity threshold point, where IFN-γ expression might be detectable even in defined QFT "negative" individuals (Adankwah et al., 2019; Penn-Nicholson et al., 2015).

One of the caveats of QFT is the inability to distinguish the cellular source of IFN-γ. Flow cytometry enables the simultaneous detection of functional and phenotypic molecules at a single cell level in one assay. Due to this, it is one of the most utilised tools to phenotype and characterise immune cells. Measurement of antigen-specific responses by flow cytometry provides a wider dynamic range of IFN-γ detection than QFT, enabling reliable quantification of IFN-γ positive cells as well as their identity. QFT-antigen (CFP-10/ESAT-6)-specific IFN-γ responses detected by whole blood intracellular cytokine staining (flow cytometry) and QFT (ELISA) have been shown to be highly correlated (Penn-Nicholson et al., 2015), suggesting that flow cytometry is a suitable tool for confirming QFT responses. Further, using flow cytometry our research group has demonstrated that *in vitro* stimulation with CFP-10/ESAT-6 peptide pools preferentially induces IFN-γ production by CD4+ T cells in HIV uninfected individuals, but can also induce IFN-γ production by non T cells, which may be a result of by-stander activation (Penn-Nicholson et al., 2015).

One of the aims of this research project was to determine if QFT reversion represents a true reduction of IFN-γ production in response to M.tb-specific antigenic stimulation. To achieve this aim, we accessed cryopreserved PBMC from individuals that had undergone QFT reversion, as well as relevant control groups: QFT non-converters, QFT converters and persistently QFT+ adolescents. Inclusion of these control groups allowed us to compare immune dynamics of reverters to other TBI states. PBMC were stored at the same study visits as the QFT assay, which was conducted in real-time, allowing us to retrieve and stimulate cells with mycobacterial antigens and measure functional and phenotypic antigen-specific responses at a later stage. Our research group has qualified a whole blood stimulation and intracellular cytokine staining protocol (Kagina et al., 2015), which is widely used in our clinical trials and exploratory studies. However, we do not have an in-house standardised PBMC stimulation and intracellular cytokine staining protocol, we thus aimed to design and optimise such a protocol and measure immune responses using flow cytometry.

The QFT assay is performed on fresh whole blood, while we had access to cryopreserved PBMC. Whole blood and PBMC differ in composition, where cell populations such as granulocytes and plasma, which contains cytokines, chemokines, antibodies, and other soluble factors are present in whole blood but not PBMC. Additionally, cryopreservation of cells can also affect their functionality, whereby antigen presenting cells and T cells may partially lose their function upon cryopreservation (Smith et al., 2015). Such functional impairment can be partly mitigated by resting cells at 37°C prior to stimulation (Horton et al., 2007; Lamoreaux et al., 2006; Ramachandran et al., 2012), which allows compromised cells to continue the cell death process and the rest of the cells to stabilise, thus improving the overall viability of cells. None withstanding, since the ACS study was conducted almost 10 years ago, cryopreserved PBMC were the only sample type available. Multiple considerations are required to design a PBMC stimulation and intracellular cytokine staining assay, some of which include: (1) duration of stimulation, (2) stimulation conditions, and (3) intracellular staining protocol (Smith et al., 2015).

The aim of this chapter was to develop and optimise a PBMC stimulation and intracellular cytokine staining assay to measure the expression of functional markers by CD4+ and CD8+ T cells in response to stimulation with mycobacterial antigens. Below, we describe considerations made and optimisations conducted to develop the assay.

Objectives

I. **Design a flow cytometry antibody panel to enable reliable detection of phenotypic and functional markers on CD4+ and CD8+ T cells.**
II. **Optimise PBMC stimulation and intracellular cytokine staining conditions that would enable reliable detection of M.tb-specific functional responses.**

Materials and Methods

Participant samples and ethics

Adolescent and adult participants were selected from the SATVI biorepository (HREC 045/2005, HREC 753/2014; (Mahomed et al., 2011a)). Inclusion criteria for the adolescent cohort were:

- Between 12 and 18 years old
- Reside in the greater areas of Worcester, Western Cape, South Africa
- Attend public schools

Each adolescent participant completed informed assent, and informed consent was also obtained from parents or legal guardians. HREC only approved HIV testing of adolescents who developed tuberculosis during the follow-up period, none of which were included in this study, as a result the HIV status of adolescent participants was unknown. Since PBMC isolation methods and long-term sample cryopreservation could affect the assay performance, we conducted some of the optimisations on samples selected from the same adolescent cohort studied to test hypotheses outlined in Chapter 5 and 6**.** Adult participants were recruited based on inclusion criteria outlined in Chapter 2: Participant samples and ethics section.

BD LSR II flow cytometer configuration

The BD Bioscience LSR II flow cytometer was set according to the configuration outlined in Table 13. Once optimised, daily quality checks were performed to monitor performance of the machine, ensure day to day standardisation and determine optimum voltages for each detector [as described in Chapter 2 and (Perfetto et al., 2012)].

Table 13: BD LSR II Flow Cytometer Configuration.

Laser	Detector	First Filter (Long Pass)	Second Filter (Band Pass)	Fluorochrome
Violet Laser 405 nm	A	740 LP	780/60	BV785
	B	670 LP	705/70	BV711
	C	630 LP	660/20	BV650
	D	595 LP	610/20	BV605
	E	570 LP	585/42	BV570
	F	557 LP	560/40	Qdot545
	G	505 LP	515/20	BV510
	H		450/50	BV421
Blue Laser 488nm	A	685 LP	710/50	PerCP-Cy5.5
	B	505 LP	515/20	FITC
	C		488/10	SSC
Green Laser 544 nm	A	740 LP	780/40	PE-Cy7
	B	690 LP	710/50	PE-Cy5.5/ PerCP-eFlour710
	C	640 LP	660/40	Pe-Cy5
	D	600 LP	610/20	PE-CF594
	E		575/26	PE
Red Laser 633 nm	A	740 LP	780/60	APC-H7/FAR IR
	B	685 LP	710/50	Alexa Fluor 700
	C		660/20	APC

Antibodies

Antibodies were all titrated and optimum volumes were selected based on the best compromise between a high stain-index, signal-noise ratio, frequency of positive population and low fluorescence spread into other channels. Once the final flow cytometry antibody panel was optimised, FMO experiments were conducted to determine the spill over spread of antibody-fluorochromes into other detectors and to determine possible compensation issues.

Defining the stain index and spillover spreading of the BD LSR II flow cytometer

We determined the stain index and spillover spreading for each detector to rationally guide antibody panel design (Nguyen et al., 2013; Perfetto et al., 2012). To perform this experiment, we used two flow cytometry panels to ensure that we acquired a strong signal in all possible cytometer detectors, regardless of the biological meaning of marker expression. PBMC (n=1) were thawed as described in Chapter 2: Thawing of cryopreserved PBMC section and stained as described below:

I. **Panel 1:** Cells were stained with anti-CCR7 PE-CF594 (1μL) and anti-CXCR3 PE-Cy5 (7.5μL) in a total volume of 50μL of PBS for 30 minutes at 37°C. An antibody cocktail

of phenotypic markers (Table 14) in total volume of 50μL BS buffer was then added to the cells and incubated for 30 minutes at RT.

Table 14: Phenotypic molecules used to stain flow cytometry panel 1.

Marker	Clone	Manufacturer	Fluorochrome	Volume
CD3	UCHT1	BD Biosciences	BV421	2 μL
CD4	OKT4	BioLegend	BV785	2 μL
CD8	SK1	BD Biosciences	PerCP Cy5.5	5 μL
CD19	SJ25C1	BioLegend	BV510	1.5 μL
CD45RA	HI100	BioLegend	BV570	1.5 μL
CD57	NK-1	BioLegend	BV605	1.5 μL
CD95	DX2	BD Biosciences	FITC	1 μL

II. **Panel 2:** Cells were stained with anti-CCR7 PE (3μL, Clone 150503, BD Biosciences) in a total volume of 50μL of PBS for 30 minutes at 37°C. An antibody cocktail of phenotypic markers (Table 15) in total volume of 50μL BS buffer was then added to the cells and incubated for 30 minutes at RT.

Table 15: Phenotypic molecule flow cytometry panel 2.

Marker	Clone	Manufacturer	Fluorochrome	Volume
CD3	SK7	BD Biosciences	APC H7	2 μL
CD4	RPA-T4	BD Biosciences	PE Cy5.5	1 μL
CD8	RPA-T8	BD Biosciences	BV650	2.5 μL
CD26	BA5b	BioLegend	APC	1.5
CD45RA	Hl100	BD Biosciences	PE-Cy7	0.2 μL
CD56	HCD56	BioLegend	BV711	2 μL
HLA-DR	L243	BioLegend	PacBlue	1 μL

After completion of phenotypic antibody staining, cells were washed by centrifugation in 1 mL of PBS at 931xg for 5 minutes, supernatant discarded and resuspended in 100 μL of 1% PFA prior to acquisition on the LSR II.

Antigens

To measure mycobacteria-specific T cell responses, we either utilised peptide pools containing M.tb-specific antigens or M.tb lysate. We had access to 15mer peptides, overlapping by 9-10 amino-acids spanning the protein sequence of CFP-10 and ESAT-6 (GeneScript Biotechnology, 100μg/mL in PBS) that were utilised by Penn-Nicholson and colleagues (Penn-Nicholson et al., 2015) and stored long-term at -80°C. We also made an additional M.tb-specific peptide pool, referred to as the Esp peptide pool that contained

15mer peptides (overlapping by 9-10 amino acids) spanning the entire EspC, EspF and Rv2348A/B proteins (Nemes et al., 2019; Ruhwald et al., 2017). EspC, EspF and Rv2348A/B peptides were designed in-house and manufactured by GeneScript Biotechnology at a minimum purity of 80% for each peptide. We then diluted each peptide in DMSO (Sigma Aldrich) in final concentration between 39.47mg/mL to 50mg/mL depending on solubility of the peptide. Individual EspC, EspF and Rv2348A/B peptides were then pooled to a final concentration of 100μg/mL in RPMI with a final concentration of 11.82% DMSO and stored at -80°C. We obtained lyophilised whole cell M.tb (strain H37Rv) lysate from BEI Resources. Lyophilised M.tb lysate was diluted to a final concentration of 500μg/mL in PBS and stored at -80°C. Our positive control stimulant was Staphylococcal enterotoxin B (SEB, Sigma Aldrich), which was diluted in PBS to a final concentration of 100μg/mL and stored at -20°C.

Optimisation of intracellular cytokine staining protocol

Optimisation of fixation and permeabilisation protocol.

Cells can be fixed and permeabilised using different reagents. We compared the BD FACS™ Lysing solution and Permeabilizing Solution 2 (referred to FACS Lyse/Perm II), which are used in our qualified whole blood intracellular cytokine staining protocol and the HVTN PBMC intracellular cytokine staining validated protocol (Horton et al., 2007) to the BD Cytofix/Cytoperm kit (Lamoreaux et al., 2006; Papagno et al., 2007). To determine which protocol was better for our PBMC stimulation and intracellular cytokine staining assay, we compared the effect of permeabilisation solution on the detection of phenotypic and functional markers.

PBMC stimulation: Cells were thawed as defined in Chapter 2, however, we rested cells in 5mL of complete media [10% FBS (Gibco), 1% penicillin-streptomycin (Gibco), 1% L-glutamine (Gibco)] with DNAse (2000IU/mL) in a 37°C, 5% carbon-dioxide (CO_2) incubator for 4 hours. Cells were centrifuged at 754xg for 10 minutes, enumerated for viability and diluted to final concentration of 20 million cells/mL in complete media. Cells were stimulated with either no antigen (unstimulated), M.tb lysate (25μg/mL) or SEB (1μg/mL) in a total volume of 200μL complete media with BD Fastimmune™ CD28/CD49d (anti-CD28: Clone L293; CD49d: Clone L25, 1μg/mL, BD Biosciences), in a 37°C, 5% CO_2 incubator. After 3 hours, brefeldin A

(5μg/mL, Sigma Aldrich) and monensin (2.5μg/mL, Sigma Aldrich) were added to stimulating cells, gently vortexed and cells were incubated for a further 15 hours.

Phenotypic staining: After completion of stimulation, cells were incubated in 2mM EDTA for 10 minutes, centrifuged at 930xg for 10 minutes and supernatant discarded. Cells were stained with anti-CCR7 PE (2μL) and anti-CXCR3 PE-Cy5 (7.5μL) in a total volume of 50μL of PBS for 30 minutes at 37°C. An antibody cocktail of viability and phenotypic markers (Table 16, prepared in 50μL of BS buffer) was added and cells were incubated for a further 30 minutes at RT.

Table 16: Phenotypic antibodies used for permeabilisation optimisation experiment.

Marker	Clone	Manufacturer	Fluorochrome	Volume
CD3	UCHT1	BD Biosciences	BV421	2 μL
CD4	OKT4	BioLegend	BV785	2 μL
CD45RA	HI100	BioLegend	BV570	1.5 μL
Viability	N/A	Thermo-Fisher Scientific	FAR IR	1.5 μL

Fixation and permeabilisation of cells and intracellular cytokine staining: Cells were washed and permeabilised with either (I) BD FACS Lyse/PermII solution or (II) Cytofix/Cytoperm as defined below, followed by intracellular cytokine staining:

I. Fixation and permeabilisation with BD FACS Lyse/PermII solution

Cells were washed in 200μL of FACS wash (2% FBS, 2mM EDTA) by centrifugation and supernatant discarded. Cells were then fixed in 100μL of BD FACS Lysing solution [BD FACS™ Lysing Solution 10X concentrate (BD Biosciences), diluted to 1X in distilled water (dH_2O)] and incubated for 10 minutes in the dark, followed by a centrifugation wash step in 100μL of FACS wash. Supernatant was then discarded and cells permeabilised in 200μL of FACS PermII solution [BD FACS™ Permeabilizing Solution 2 10X (BD Biosciences) diluted to 1X in dH_2O] and incubated at RT for 10 minutes. This was followed by centrifugation and discarding of supernatant, and a final wash in 200μL of FACS wash by centrifugation and supernatant discarded.

Intracellular cytokine staining: Cells were stained in a final volume of 100μL with anti-IFNγ Alexa Fluor700 (1μL, Clone: B27, BD Biosciences), anti-IL-2 FITC (2μL, Clone: 5344.111, BD Biosciences) and anti-TNF PE-Cy7 (0.04μL, Clone Mab11, eBioscience) for 30 minutes at RT. Cells were then washed twice, first with 150μL and then with 200μL of FACS wash by

centrifugation. After completion of second wash, supernatant was discarded, and cells were resuspended in 190μL of 1% PFA and then acquired on the LSR II flow cytometer.

II. Fixation and permeabilisation with BD Cytofix/Cytoperm Kit

Cells were washed in 200μL of PBS then fixed and permeabilised in 100μL of Cytofix/Cytoperm solution and incubated for 20 minutes at RT, after which cells were washed in 100μL of Perm/Wash and centrifugation. Cells were then washed again in 200μL Perm/Wash by centrifugation and supernatant discarded.

Intracellular cytokine staining: Cells were then stained as indicated in (I. Fixation and permeabilisation with BD FACS Lyse/PermII solution) except the final washes were performed in Perm/Wash instead of FACS wash.

Optimisation of staining protocol

In our whole blood intracellular cytokine staining protocol phenotypic and intracellular molecules are all stained in a single step after fixation and permeabilisation of cells, but it was not clear if this was optimal for this PBMC protocol. To determine the best sequence of cell permeabilisation and staining of lineage, phenotypic and functional markers that would result in optimal detection of all markers, we compared 3 staining protocols described below. Protocol 1 (surface staining before fix/perm) was designed based on previous experience outlined in Chapter 2, which is also common practice for PBMC intracellular cytokine staining assays (Lamoreaux et al., 2006). Protocol 2 (surface staining after fix/perm) was developed due to its similarity to the validated HIV vaccine trials network (HVTN) PBMC intracellular cytokine staining protocol and our qualified in-house whole blood intracellular cytokine staining protocol (Horton et al., 2007; Kagina et al., 2015). We additionally, wanted to determine if reduced resolution of phenotypic and lineage markers observed in Chapter 2 also applies to stimulated PBMC. We designed Protocol 3 (surface stain before stimulation) to capture the memory profiles prior to stimulation, and to prevent detection of stimulation-induced effects on surface marker expression. However, we did not stain with anti-KLRG-1 and anti-HLA-DR antibodies before stimulation, because their expression does not appear to be affected by short-term stimulation (Robbins et al., 2003).

Protocol 1: Staining of phenotypic and lineage markers prior to permeabilisation

PBMC stimulation: Cells were thawed, rested, and enumerated as described above. Cells were then stimulated in total volume of 200µL complete media containing anti-CD107a PE-CF594 (0.1µL, Clone: H4A3, BD Biosciences) with no antigen, SEB (1µg/mL) or M.tb lysate (25µg/mL). Cells were then incubated for 3 hours at 37°C with 5% CO_2, after which brefeldin A and monensin were added, gently vortexed and cells incubated for a further 15 hours.

Phenotypic marker staining: After completion of PBMC antigen stimulation, 1mL of 2mM EDTA was added to the cells and incubated for 10 minutes. This was followed by centrifugation at 930xg for 10 minutes and discarding of supernatant. Cells were then stained with anti-CCR7 PE (3µL) and anti-CXCR3 PE-Cy5 (5µL) in a total volume of 50µL of PBS for 30 minutes at 37°C. An antibody cocktail of viability, phenotypic and lineage markers (Table 17, prepared in 50µL BS buffer) was then added to cells and incubated for 30 minutes at RT. Cells were then washed in 1mL of FACS wash by centrifugation.

Table 17: Phenotypic antibodies used in antibody cocktail for protocol 1.

Marker	Clone	Manufacturer	Fluorochrome	Volume
CD3	UCHT1	BD Biosciences	BV650	1 µL
CD4	OKT4	BioLegend	BV785	0.75 µL
CD8	RPA-T8	BD Biosciences	BV711	0.5 µL
CD45RA	HI100	eBioscience	BV570	1.5 µL
CD27	L128	BD Biosciences	BV510	0.25 µL
HLA-DR	L243	BD Biosciences	FITC	1.25 µL
KLRG-1	13F12F2	BD Biosciences	PerCP-eFluor 710	1 µL
Viability		Thermo-Fisher Scientific	FAR IR	0.2 µL

Fixation and permeabilisation: After washing, cells were fixed and permeabilised in 100µL of CytoFix/CytoPerm, incubated for 20 minutes at RT, washed in 1mL of Perm/Wash by centrifugation and supernatant discarded.

Intracellular cytokine staining: Cells were stained with anti-IFNγ Alexa Fluor 700 (1µL), anti-IL-2 APC (0.1µL, Clone: MQ1-17H12, BD Biosciences), anti-TNF PE-Cy7 (0.38µL) and anti-CD154 BV421 (0.5µL, Clone: TRAP-1, BD Biosciences) in a total volume of 50µL of Perm/Wash for 30 minutes at RT. Cells were then washed in 2mL Perm/Wash by centrifugation, supernatant discarded and resuspended in 100µL of 1% PFA and then acquired on the LSR II.

Protocol 2: Staining of all markers after permeabilisation

PBMC stimulation: Cells were stimulated as described in protocol 1.

Viability staining: After completion of stimulation incubation and EDTA treatment as in protocol 1, cells were stained with the viability marker (Live/Dead FAR IR, 0.2μL, Thermo-Fisher Scientific) in a total volume of 50μL of PBS for 30 minutes at RT. Cells were then washed in 1mL of FACS wash by centrifugation and supernatant discarded.

Permeabilisation, fixation and intracellular cytokine staining: Cells were permeabilised and fixed according to protocol 1. Cells were first stained with anti-CCR7 PE (3μL) and anti-CXCR3 PE-Cy5 (5μL) in a total volume of 50μL of Perm/Wash for 30 minutes at 37°C, followed by addition of an antibody cocktail of phenotypic, lineage and functional markers (Table 18, prepared in 50μL Perm/Wash) and a 30 minute incubation at RT. Cells were then washed in 2mL of Perm/Wash by centrifugation, supernatant discarded and resuspended 100μL of 1% PFA.

Table 18: Phenotypic and functional antibodies used in antibody cocktail for protocol 2.

Marker	Clone	Manufacturer	Fluorochrome	Volume
CD3	UCHT1	BD Biosciences	BV650	1 μL
CD4	OKT4	BioLegend	BV785	0.75 μL
CD8	RPA-T8	BD Biosciences	BV711	0.5 μL
CD45RA	HI100	eBioscience	BV570	1.5 μL
CD27	L128	BD Biosciences	BV510	0.25 μL
HLA-DR	L243	BD Biosciences	FITC	1.25 μL
KLRG-1	13F12F2	BD Biosciences	PerCP-eFluor 710	1 μL
IFN-γ	B27	BD Biosciences	Alexa Flour 700	0.5 μL
IL-2	MQ1-17H12	BD Biosciences	APC	1 μL
TNF	Mab11	BD Biosciences	Pe-Cy7	0.38 μL
CD154	TRAP-1	BD Biosciences	BV421	0.5 μL

Protocol 3: Staining of lineage and phenotypic markers before stimulation

Pre-staining of PBMC: After cells were thawed, rested and enumerated, they were stained with anti-CD3 BV650 (1μL), anti-CD4 BV785 (0.75μL), anti-CD8 BV711 (0.5μL), anti-CXCR3 PE-Cy5 (5μL), anti-CCR7 PE (3μL), anti-CD45RA BV570 (1.25μL) and anti-CD27 BV510 (0.25μL) in a total volume of 50μL of BS buffer for 30 minutes at 37°C. Cells were first washed in 1mL of FACS by centrifugation, then in 1mL of complete media by centrifugation.

PBMC stimulation: Cell were then stimulated as described in Protocol 1.

Viability and phenotypic staining: After completion of stimulation, 1mL of 2mM EDTA was added to the cells and incubated for 10 minutes. This was followed by centrifugation at

930xg for 10 minutes and discarding of supernatant. Cells were then stained with viability marker (Live/Dead-FAR IR, 0.2μL), anti-HLA-DR FITC (1.25 μL) and anti-KLRG-1 PerCP-eFlour710 (1μL) in a total volume of 50μL of PBS for 30 minutes at RT. Cells were then washed in 1mL of FACS by centrifugation and supernatant discarded.

Permeabilisation, fixation and intracellular cytokine staining: Cells were fixed, permeabilised and stained for functional markers (IFN-γ, IL-2, TNF, CD154) according to Protocol 1.

Optimisation of PBMC stimulation protocol

Optimisation of antigen stimulant concentration

We aimed to detect mycobacterial antigen-specific CD4+ and CD8+ T cell responses following PBMC stimulation with CFP-10/ESAT-6 peptide pools, Esp peptide pools and M.tb lysate. To ensure that the stimulant concentration was optimal for our 18 hours stimulation protocol, we compared production of Th1 cytokines (IFN-γ, IL-2 and TNF) following stimulation with various antigen concentrations.

PBMC stimulation: Cells were thawed, rested, and enumerated as described above. Cells were then stimulated in total volume of 200μL complete media with no antigen, SEB (1μg/mL) or mycobacterial antigens at varying concentrations: CFP-10/ESAT-6 or Esp peptide pools at 0.5μg/mL, 1μg/mL and 2μg/mL; and M.tb lysate at 5μg/mL, 10μg/mL and 25μg/mL. Cells were then incubated for 3 hours at 37°C with 5% CO_2, after which brefeldin A and monensin were added, gently vortexed and incubated for a further 15 hours.

Phenotypic marker staining: After completion of stimulation incubation, 1 mL of 2mM EDTA was added to the cells, incubated for 10 minutes, centrifuged at 930xg for 10 minutes and supernatant discarded. Cells in a total volume of 50μL of PBS were incubated for 30 minutes at 37°C, followed by addition of an antibody cocktail containing anti-CD3 BV421 (1μL), anti-CD4 BV785 (2μL) and viability marker (Live-Dead-Aqua/BV510, 0.2μL) in total volume of 50μL BS buffer to the cells and a 30 minute incubation at RT.

Permeabilisation and fixation of cells, and intracellular cytokine staining*:* Cells were then permeabilised, fixed, washed, and stained for functional markers according to Protocol 1 and acquired on the LSR II.

Optimisation of stimulation media

PBMC stimulation is generally conducted in the presence of serum free media or complete media containing either FBS or human (AB) serum. We therefore conducted two optimisation experiments that aimed to determine (I) if stimulation in the presence of serum free media results in lower non-specific background responses than complete media containing FBS, and (II) whether stimulation in the presence complete media containing AB/Serum induces higher mycobacteria-specific responses than complete media containing FBS.

Comparison of immune responses induced by complete media and serum free media

PBMC stimulation: Cells were thawed, rested, and enumerated as described above. Cells were then stimulated in total volume of 200μL of either complete media, OpTmizer™ CTS™ T-Cell Expansion media [OpT (Gibco) containing 1% v/v, L-Glutamine, 1% v/v Penicillin-Streptomycin and 26%v/v OpTmizer™ T-Cell Expansion Supplement (Gibco)] or X-VIVO™ 15 (Lonza) serum free media containing anti-CD107a (0.1μL) with no antigen, SEB (1μg/mL), CFP-10/ESAT-6 peptide pools (2μg/mL), Esp peptide pools (2μg/mL) or M.tb lysate (25μg/mL). Cells were stimulated for 3 hours at 37°C with 5% CO_2, after which brefeldin A and monensin were added, gently vortexed and incubated for a further 15 hours.

Phenotypic and functional marker staining: After completion of stimulation, cells were then processed according to Protocol 1, with the following modification. Cells were stained with anti-CCR7 PE and anti-CXCR3 PE-Cy5 in a total volume of 20μL of PBS for 30 minutes at 37°C, followed by addition of an antibody cocktail, containing anti-CD3 BV650 (1μL), anti-CD4 BV785 (0.75μL), anti-CD8 BV711 (0.5μL) and viability marker (Live/Dead-FAR IR 0.2μL) in total volume of 50μL of BS buffer, to the cells and a 30 minute incubation at RT. Cells were then washed, supernatant discarded, permeabilised, fixed and stained with functional markers.

Comparison of immune responses induced by complete media and media containing AB serum

We repeated the experiment described above: "*Comparison of immune responses induced by complete media and serum free media*", however, we only stimulated cells with no antigen, CFP-10/ESAT-6pp (2μg/mL) or M.tb lysate (25μg/mL) in the presence of complete media or AB stimulation media (10% AB serum in RPMI). The rest of the phenotypic, permeabilisation, fixation and functional staining protocol was conducted as described above.

Optimisation of use co-stimulatory antibodies for 18 hour stimulation

BD Fastimmune™ CD28/CD49d co-stimulatory molecules are often used to enhance induction of T cell functional responses in short-term stimulation (<12 hours) assays (Waldrop et al., 1998). Our research group uses these co-stimulatory molecules in the 12-hour whole blood intracellular cytokine staining assay (Kagina et al., 2015). To determine if the use of co-stimulatory molecules improved induction of functional markers in our 18 hour PBMC stimulation and intracellular cytokine staining assay, we either stimulated cells in the presence or absence of costimulatory molecules BD Fastimmune™ CD28/CD49d.

PBMC Stimulation: Cells were thawed, rested, and enumerated as described above. Cell were then stimulated in total volume of 200μL of complete media, containing anti-CD107a (0.1μL) with no antigen, SEB (1μg/mL), CFP-10/ESAT-6 peptide pools (2μg/mL), Esp peptide pools (2μg/mL) or M.tb lysate (25μg/mL) and either with or without BD Fastimmune™ CD28/CD49d (1μg/mL). Cells were stimulated for 3 hours at 37°C with 5% CO_2, after which brefeldin A and monensin were added, gently vortexed and incubated for a further 15 hours. After completion of stimulation cells were processed and stained according to Protocol 1.

Data analysis

Flow cytometry analysis was conducted as defined in Chapter 2, except for using FlowJo V10 instead of V9. Due to limited sample size, we did not perform any statistical analysis.

Results and Discussion

Panel design: Marker selection

To ensure that voltages set for the newly acquired flow cytometer were optimal, as well as to determine the stain index and spillover spread of each detector, we measured the signal of abundantly expressed molecules on PBMC. Unfortunately, we did not have non-overlapping antibody-fluorochrome conjugates detecting abundantly expressed markers that could be combined in a single panel. We therefore stained PBMC with two different panels (Table 14 and 15), utilised FlowJo to determine the optimal compensation for each panel and concatenated both flow cytometry standard (FCS) files into one, so that we had one FCS file

with signal in all parameters. For simplicity, we shall refer to the stain index and spillover spread of each detector/fluorochrome and not the molecule stained, because in some cases the same molecule was stained with two different antibodies in separate panels (Table 19).

Table 19: Antibody-fluorochrome and detector combinations measured to determine stain index and spillover spread.

Marker	Fluorochrome	Detector		Marker	Fluorochrome	Detector
Violet Laser				*Green Laser*		
HLA-DR	PacBlue	V450		CCR7	PE	G560
CD19	BV510	V545		CCR7	PE-CF594	G610
CD45RA	BV570	V565		CXCR3	PE-Cy5	G660
CD57	BV605	V605		CD4	PE-Cy5.5	G710
CD8	BV650	V655		CD45RA	PE-Cy7	G780
CD56	BV711	V705		*Red Laser*		
CD4	BV786	V800		CD26	APC	R660
Blue Laser				CD3	Alexa Fluor 700	R710
CD95	FITC	B515		CD3	APC-H7	R780
CD8	PerCPCy5.5	B710				

The stain index represents the resolution of the positive antibody-fluorochrome signal from the negative population. Ideally, fluorochromes that have high resolution are conjugated to antibodies that bind molecules that have low cellular expression, and vice-versa. This is to ensure that the positive signal of detection separates well from the population that does not express the molecule. Thus, we firstly compared the stain index for each detector and ranked them from highest to lowest (Figure 30). The PacBlue (V450), BV510 (V545), PE-Cy5.5 (G710) and PE-Cy7 (G780) fluorochromes exhibited the highest stain index, while PE (G560), FITC (B515), APC (R660), PE-Cy5 (G660) and PerCPCy5.5 (B710) fluorochromes had the lowest stain index. Based on these results we would assign antibodies that detected lowly expressed molecules to fluorochromes that would be detected using V450, V545, G710 and G780 detectors.

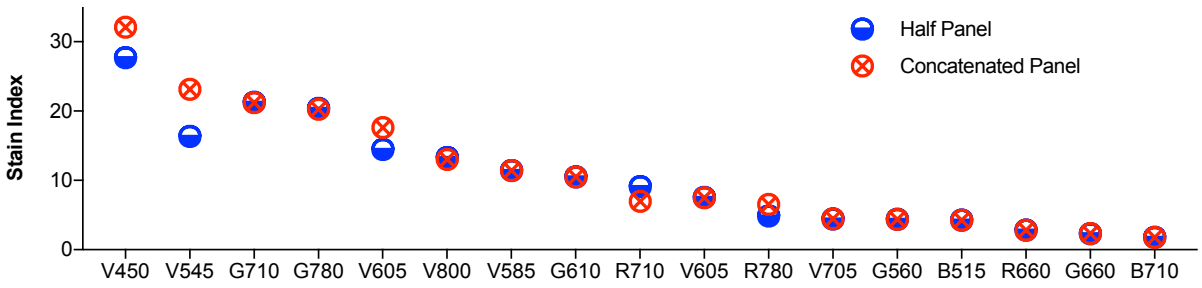

Figure 30: Stain index for each detector. Stain index for each flow cytometry panel analysed independently (half panel) and concatenated panels are depicted by the blue and red symbols, respectively.

We then calculated the spillover spread matrix (Figure 31A) using FlowJo. The output of the spillover spread matrix gives a value of how much spillover spread each fluorochrome contributes into each detector (sum of row spillover spread values) and total spillover spread received by each detector from all fluorochromes (sum of column spillover spread values) (Nguyen et al., 2013). Based on these values, we ranked the total spillover spread each fluorochrome contributes (Figure 31B) and each detector receives (Figure 31C) from highest to lowest. Since we wanted to measure functional, memory and activation profiles on classical T cells, we aimed to design a flow cytometry panel of antibody-fluorochrome combinations that enabled very good resolution of lowly expressed activation and functional markers by T cells, as well as prevent the spillover spread of highly expressed memory and lineage markers into detectors of lowly expressed markers. The final panel (Table 20) was designed considering instrument performance, fluorochrome brightness, reagent availability and previous experience with specific antibody-fluorochrome combinations.

A

	Detector																	
Fluorochrome	B515	B710	G560	G610	G660	G710	G780	R660	R710	R780	V450	V545	V585	V605	V655	V705	V800	Total spread each fluorochrome exhibits
B515	0.00	1.15	1.04	0.56	1.02	0.89	0.28	0.32	0.44	0.00	0.00	1.21	0.68	0.41	0.46	0.02	0.00	**8.48**
B710	0.00	0.00	2.63	0.30	1.96	4.95	1.12	0.67	1.90	0.55	1.00	0.00	0.01	0.28	1.30	4.21	3.36	**24.23**
G560	0.05	1.10	0.00	0.92	0.97	1.05	0.26	0.00	0.00	0.00	0.44	0.00	0.62	0.00	0.00	0.00	0.44	**5.86**
G610	0.00	3.01	1.49	0.00	2.45	2.63	0.67	0.20	0.33	0.00	0.01	0.00	0.00	0.70	0.75	1.50	0.72	**14.46**
G660	0.00	4.23	2.08	0.20	0.00	3.87	0.90	1.04	0.96	0.26	0.01	0.00	0.27	0.00	0.79	2.04	0.93	**17.57**
G710	0.39	6.48	4.33	0.68	1.78	0.00	1.38	0.25	0.98	0.23	0.28	0.22	0.53	0.31	0.46	3.11	1.34	**22.75**
G780	0.24	0.95	0.59	0.23	0.40	0.78	0.00	0.00	0.14	0.44	0.56	0.24	0.00	0.00	0.00	0.40	1.62	**6.60**
R660	0.04	1.05	0.03	0.00	2.35	1.90	0.62	0.00	2.50	0.72	0.50	0.00	0.00	0.00	1.34	1.43	0.95	**13.43**
R710	0.81	2.30	1.24	0.00	0.96	2.67	0.83	0.41	0.00	1.30	0.00	0.00	0.00	0.00	0.00	1.48	1.55	**13.56**
R780	1.28	0.00	0.02	0.00	1.88	1.04	2.05	0.90	1.00	0.00	1.07	0.00	0.00	0.00	0.46	0.01	2.77	**12.48**
V450	0.00	0.00	0.31	0.00	0.12	0.00	0.00	0.00	0.00	0.00	0.00	0.61	0.43	0.18	0.20	0.20	0.22	**2.28**
V545	0.00	0.76	1.70	0.53	1.56	0.93	0.27	0.90	1.34	0.34	1.03	0.00	2.80	2.01	2.08	1.58	1.56	**19.38**
V585	0.82	1.17	3.44	1.27	1.24	1.13	0.28	0.37	0.44	0.00	1.16	0.31	0.00	2.77	2.02	1.94	1.46	**19.81**
V605	0.33	2.68	1.80	2.06	2.41	2.33	0.66	0.55	0.87	0.17	1.08	0.60	2.39	0.00	4.79	4.69	2.97	**30.38**
V655	1.06	1.88	0.60	0.40	1.81	1.43	0.00	1.03	1.13	0.28	0.80	0.00	0.00	1.37	0.00	4.68	3.38	**19.84**
V705	0.00	3.81	1.29	0.46	0.81	2.39	0.37	0.00	2.04	0.71	1.96	0.77	0.36	0.00	0.97	0.00	6.25	**22.19**
V800	0.64	0.68	0.44	0.20	0.55	0.43	0.37	0.25	0.41	0.36	3.24	0.36	0.41	0.26	0.70	1.18	0.00	**10.47**
Total spread received by each detector	**5.65**	**31.24**	**23.03**	**7.80**	**22.27**	**28.42**	**10.05**	**6.91**	**14.48**	**5.34**	**13.14**	**4.34**	**8.49**	**8.29**	**16.32**	**28.47**	**29.52**	

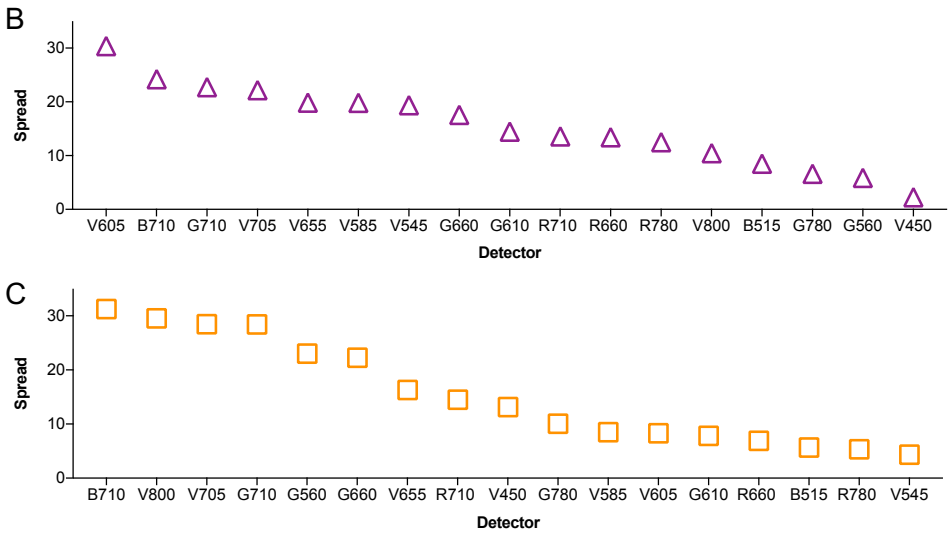

Figure 31: (A) Spillover spread matrix, spillover spread of fluorochromes contributed into each (B) and received by each (C) LSR II detector. (B-C) Detectors depicted in the x-axis are ranked from highest to lowest spillover spread.

Table 20: Final flow cytometry panel designed to achieve aims outlined Chapters 5 and 6.

Marker	Function	Fluorochrome
Viability	Viability	APC-H7
CD3	T cell lineages	BV650
CD4		BV785
CD8		BV711
IFN-γ	Th1 Cytokines	Alexa Fluor 700
IL-2		APC
TNF-α		PE-Cy7
CD154 (CD40L)	Most Th Cells	BV421
CD107	CTL	PE-CF594
CD45RA	T cell differentiation	BV570
CCR7		PE
CD27		BV510
HLA-DR	Activation	FITC
CXCR3	Inflammation homing/ Th1 associated CXR	PE-Cy5
KLRG-1	Exhaustion/Senescence	PercP-eFlour710

Fixation and permeabilisation with Cytofix/Cytoperm is better than FACS Lyse/Perm II Solution

As described in the introduction, we did not have an optimised PBMC intracellular cytokine staining flow cytometry protocol. We used the HVTN validated PBMC intracellular cytokine staining and our qualified whole blood intracellular cytokine staining protocols as references for our optimisation (Horton et al., 2007; Kagina et al., 2015). In these assays stimulated PBMC or whole blood is fixed and permeabilised using BD FACS lyse and/or BD FACS Perm II solution (PBMC only). BD FACS lyse preserves the cell structural integrity, enabling cryopreservation and detection of protein expression at a much later stage. As a result, stimulation experiments can be conducted on different days, but the intracellular cytokine staining-staining and flow cytometry acquisition can be batched per participant, reducing experimental protocol technical variability. A widely used alternative is the BD Cytofix/Cytoperm kit [also used in Chapter 2 and 3, (Lamoreaux et al., 2006; Papagno et al., 2007)]. Thus, our first aim was to optimise the fixation and permeabilisation step, and to determine which protocol was better for stimulated PBMC in our experiment. We compared detection of live CD3+ and CD4+ T cells, memory phenotype and T cell function, fixed and permeabilised with either FACS lyse/Perm II or Cytofix/Cytoperm (Figure 32). Overall, we experienced lower cell recovery and detected lower proportions of live CD3+ and CD4+ T cells using FACS Lyse/Perm II compared with the Cytofix/Cytoperm (Figure 32A). Detection of CXCR3+ and T_E (RA-R7-) CD4+ T cells was suggestively better using the FACS lyse/Perm II than Cytofix/Cytoperm. However, detection of T_N (RA+R7+) and T_{CM} (RA-R7+) appeared to be better using the Cytofix/Cytoperm kit (Figure

32B). Interestingly, we observed higher background responses which resulted in lower antigen-specific responses when cells were fixed and permeabilised with FACS lyse/Perm II compared to Cytofix/Cytoperm (Figure 32C). Lower background responses and higher recovery of live CD3+ and CD4+ T cells motivated us to choose Cytofix/Cytoperm instead of FACS lyse/Perm II as the fixation and permeabilisation reagents for our PBMC intracellular cytokine staining protocol. This was further supported by the fact that we intended to acquire cells on the flow cytometer immediately after staining, thus would have gained no additional benefits using FACS lyse/Perm II over Cytofix/Cytoperm.

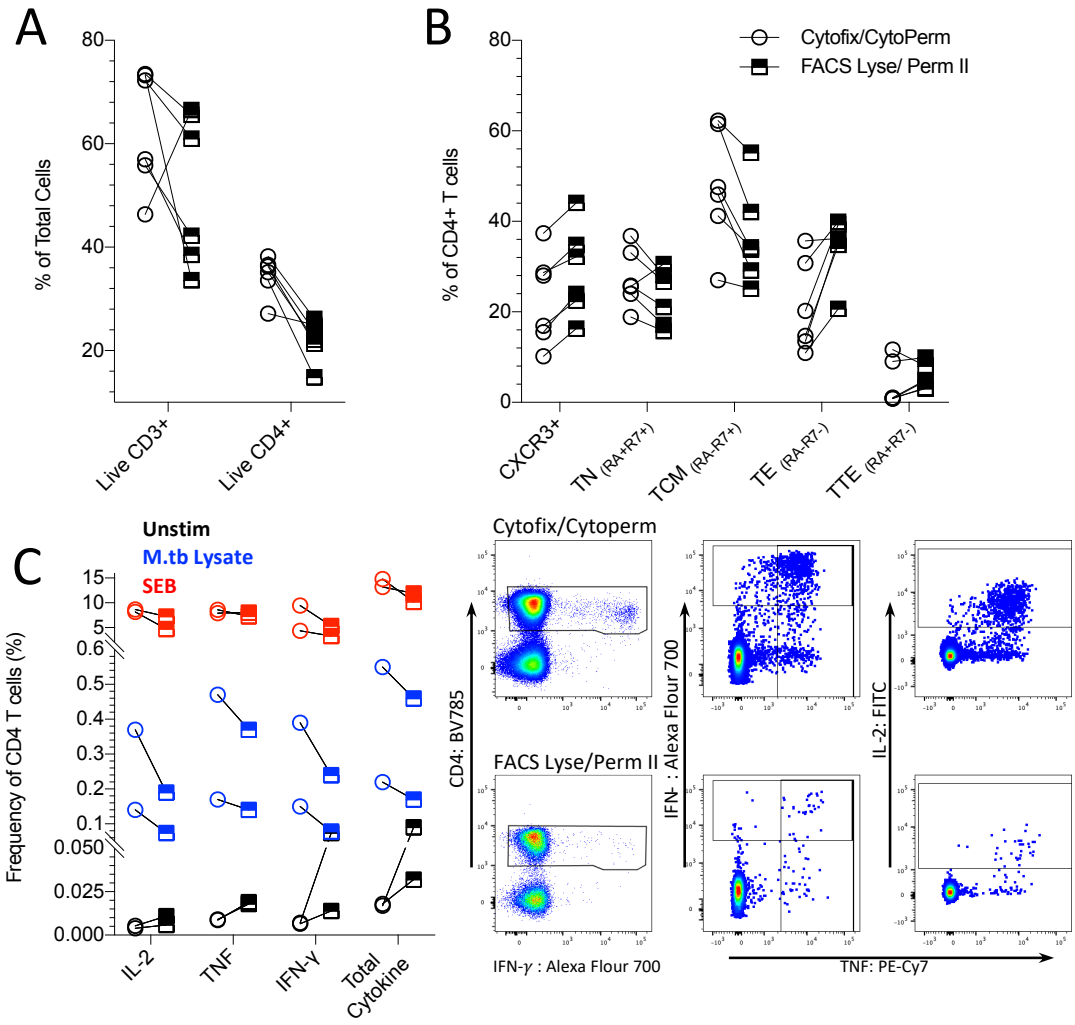

Figure 32: T cell lineage and functional markers are better detected after treatment with Cytofix/Cytoperm compared to FACS Lyse/Perm II. (A) CD3+ and CD4+ live T cells, (B) phenotypic and (C) functional marker expression were detected after permeabilisation with either Cytofix/Cytoperm or FACS lyse/Perm II solution, depicted by circle and half-filled boxes, respectively. (C) Cytokine-expressing T cells were detected in response to either no-stimulation (Unstimulated, black symbols), M.tb Lysate (blue symbols) or positive control (SEB, red symbols). Representative flow cytometry plots obtained from one donor are shown in (C) and display cytokine production in responses to M.tb lysate and permeabilisation with either Cytofix/Cytoperm or FACS lyse solution (n=2).

Extracellular staining of phenotypic markers has the best resolution

In the whole blood intracellular cytokine staining protocol, whole blood is fixed and cryopreserved before staining. At thawing, cells are permeabilised and stained, so detection of lineage markers is both extracellular (membrane bound) and intracellular. Based on our experience (discussed in Chapter 2), staining of lineage markers after permeabilisation of cryopreserved PBMC decreases the resolution of detection, and in some cases results in increased spectral overlap and spillover spread. We therefore compared 3 staining protocols:

- Protocol 1: Staining of lineage, phenotypic and memory markers before cell fixation, and functional markers after permeabilisation.
- Protocol 2: Staining of all markers after cell fixation and permeabilisation.
- Protocol 3: Pre-staining of all lineage and phenotypic markers except HLA-DR and KLRG-1 prior to stimulation. HLA-DR and KLRG-1 stained before cell fixation and functional markers after permeabilisation.

Rationale for the design of the 3 protocols is outlined above in the methodology. We hypothesised that protocol 1 would be the best protocol to detect T cell lineages and memory profiles because it is common practice in PBMC intracellular cytokine staining assays [HVTN Protocol; (Lamoreaux et al., 2006)]. Protocol 2 was designed because of similarity with our qualified whole blood intracellular cytokine staining assay (Horton et al., 2007; Kagina et al., 2015). Protocol 3 was designed to prevent detection of *in vitro* stimulation-induced effects such as down-regulation of lineage markers, CD3, CD4 or CD8, or up-regulation of phenotypic markers CCR7 and CXCR3 (Nakajima et al., 2002; Sallusto et al., 1999).

We firstly wanted to determine if a specific protocol was associated with detection of lower frequencies of live T cells. Overall, we did not observe a protocol-specific effect on detection of total live cells or CD3+ and CD8+ T cells. However, to our surprise we were unable detect to CD4+ T cells when we stained cells after permeabilisation (Protocol 2; Figure 33). We repeated this experiment to ensure that absence of CD4+ T cells when stained after permeabilisation was not due to pipetting error. Additionally, we observed increased frequencies of CD4+ T cells when we stained this molecule before stimulation (Protocol 3) compared to antibody staining after stimulation (Protocol 1). We also observed high spillover spread when lineage and phenotypic markers were stained prior to stimulation (Protocol 3), however, this did not significantly affect the proportion of cells detected. Based on these

results, we decided to not further investigate *protocol 2: staining markers after permeabilisation* because we were unable to detect CD4 T cells.

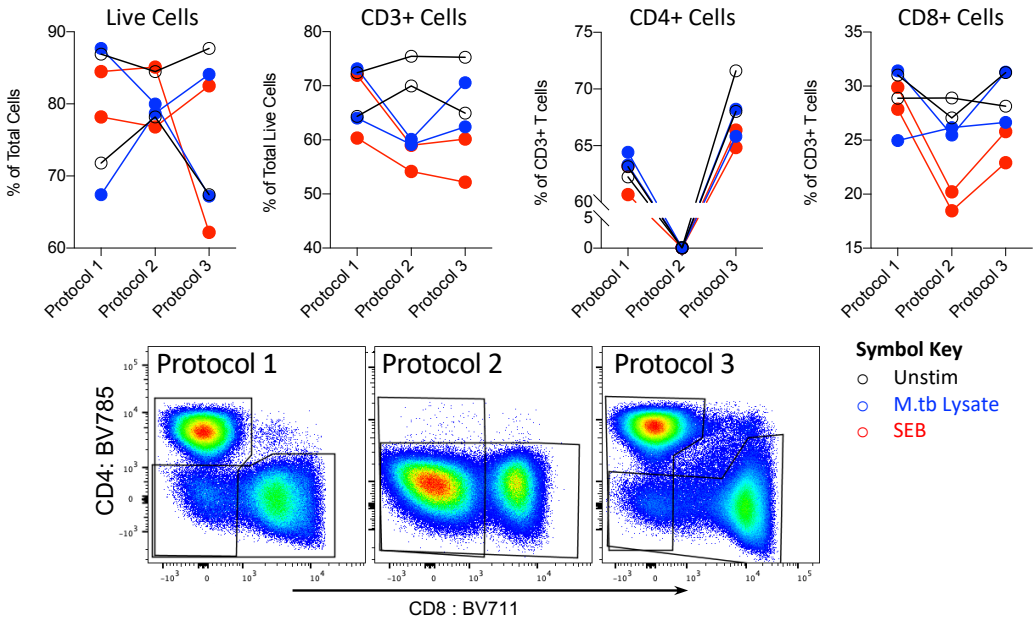

Figure 33: Comparison of PBMC intracellular cytokine staining protocols for the detection of live CD3, CD4 and CD8 T cells. Each graphs depicts proportion of cells detected in Unstimulated (black circles), M.tb lysate (blue symbols) and SEB (red symbols) stimulated PBMC. Representative flow cytometry plots illustrate detection of CD4 and CD8 T cells in each protocol (n= 2 participants, 3 stimulations).

We then focused our comparative analysis of the effect of PBMC intracellular cytokine staining protocol on the detection of memory and phenotypic molecule expression by CD4 T cells, because they were our main cells of interest. We observed lower detection of CD45RA, CCR7, CD27, CXCR3 and HLA-DR, but higher detection of KLRG-1 when cells were stained with Protocol 3 compared to Protocol 1 (Figure 34). Lower detection of these molecules could be due to the degradation of antibodies when these molecules get internalised during the stimulation process. We also observed high spillover spread and spillover into the B515 (FITC) detector when we pre-stained cells. This spillover spread reduced the resolution of the HLA-DR+ population and required us to have a higher HLA-DR positive threshold when we stained with protocol 3 compared to protocol 1. Overall detection of Th1 cytokines, IFN-γ, TNF and IL-2 was better when lineage and phenotypic markers were pre-stained before stimulation (Figure 35). However, we observed high non-specific spillover spread into the G610 (PE-CF594) detector when we pre-stained cells, which significantly affected detection of CD107 (Figure 35). Despite the low sample size, detection of high spillover spread into the B515 (FITC) and G610 (PE-CF594) detectors, as well lower detection of memory markers CD45RA and CCR7, and phenotypic markers CXCR3 and HLA-DR, provided sufficient evidence against

pursuing protocol 3. Thus, we opted to stain phenotypic and lineage markers after stimulation but before permeabilisation (protocol 1).

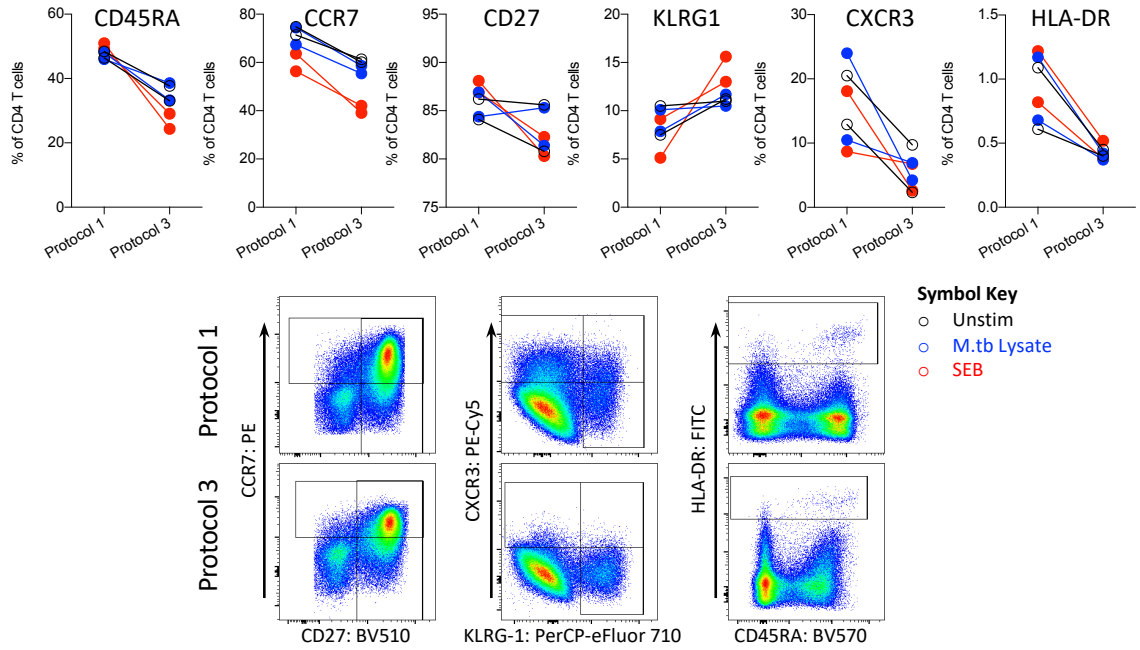

Figure 34: Comparison of PBMC intracellular cytokine staining protocols for the detection of memory and phenotypic markers on CD4 T cells. Each graph depicts proportions of cells detected in Unstimulated (black circles), M.tb lysate (blue symbols) and SEB (red symbols) stimulated PBMC (n= 2 participants, 3 stimulations). Representative flow cytometry plots illustrate detection of CD45RA, CCR7, CD27, KLRG-1, CXCR3 and HLA-DR using the two protocols.

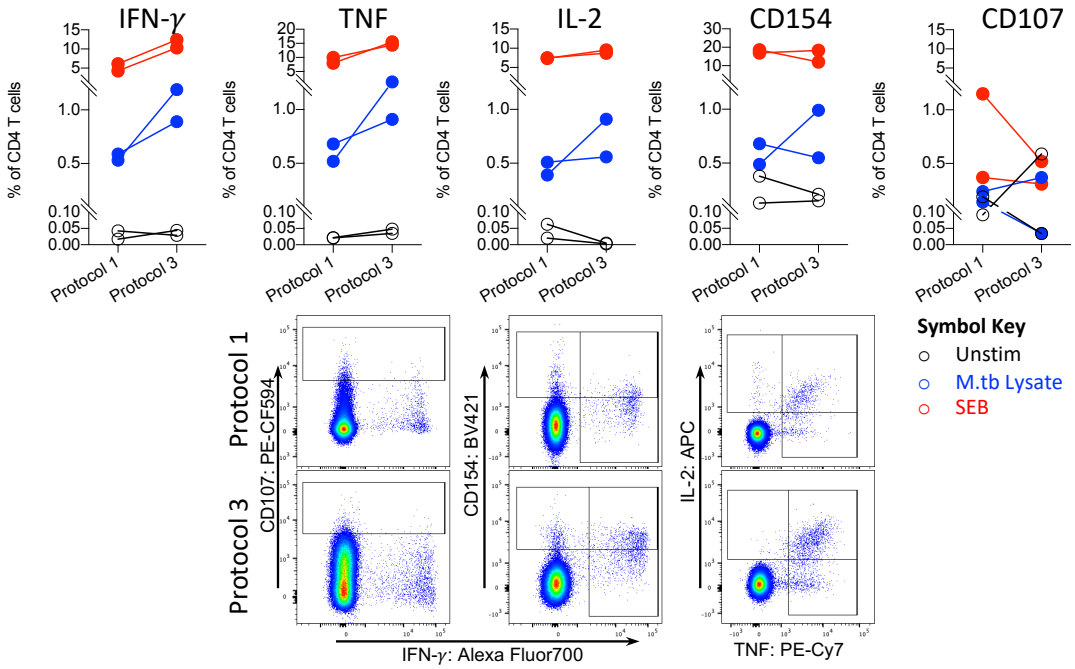

Figure 35: Comparison of PBMC intracellular cytokine staining protocols for the detection of antigen-specific CD4+ T cell functional markers. Each graph depicts frequencies of IFN-γ, TNF, IL-2-, CD154 or CD107 expressing CD4+ T cells [n= 2 participants, 3 stimulations: Unstimulated (black), M.tb lysate (blue), SEB (red)]. Representative flow cytometry plots illustrate detection of functional markers using the two protocols.

Antigen titration

Upon finalisation of our PBMC intracellular cytokine staining protocol, we then titrated the antigen concentration required for optimal detection of mycobacteria-specific T cell responses. We stimulated PBMC with varying concentrations of peptide pools (0.5-2μg/mL) and M.tb lysate (5-25μg/mL). CD4 T cell expression of most functional markers plateaued at 1μg/mL for peptide pools and 10μg/mL for M.tb lysate (Figure 36A). We also compared the MFI of each functional marker, indicative of the amount of expression per cell, and this appeared to be unaffected by antigen concentration (Figure 36B). Overall, we detected very low levels of CD8 Th1 cytokine expression regardless of mycobacterial stimulant. Detection of functional activity when stimulated with SEB (positive control) confirmed that cells were functional. Thus, lack of functional reactivity when stimulated with mycobacterial antigens is most likely due to undetectable presence of mycobacteria-specific CD8 T cells. (Figure 36A). Based on these results, we decided to use stimulant concentrations of 1μg/mL and 10μg/mL for peptide pools and M.tb lysate, respectively.

Serum free and complete media induce equivalent T cell responses

We tested serum free media from different manufacturers to determine if background responses were lower when stimulated in the presence of serum free media compared with complete media. We therefore compared functional responses from mycobacterial antigen-stimulated PBMC in the presence of either complete media (R10), OpT or XVIVO serum free media. Overall, we observed no stimulation media-induced difference in levels of background or mycobacteria-specific functional (IFN-γ, TNF, IL-2, CD154 and CD107) CD4 and CD8 T cell responses (Figure 37). Thus, based on these results we decided to use complete media because it did not significantly induce higher levels of background responses compared to serum free media nor did we observed higher proportions of functional responses when stimulated in the presence of serum free media.

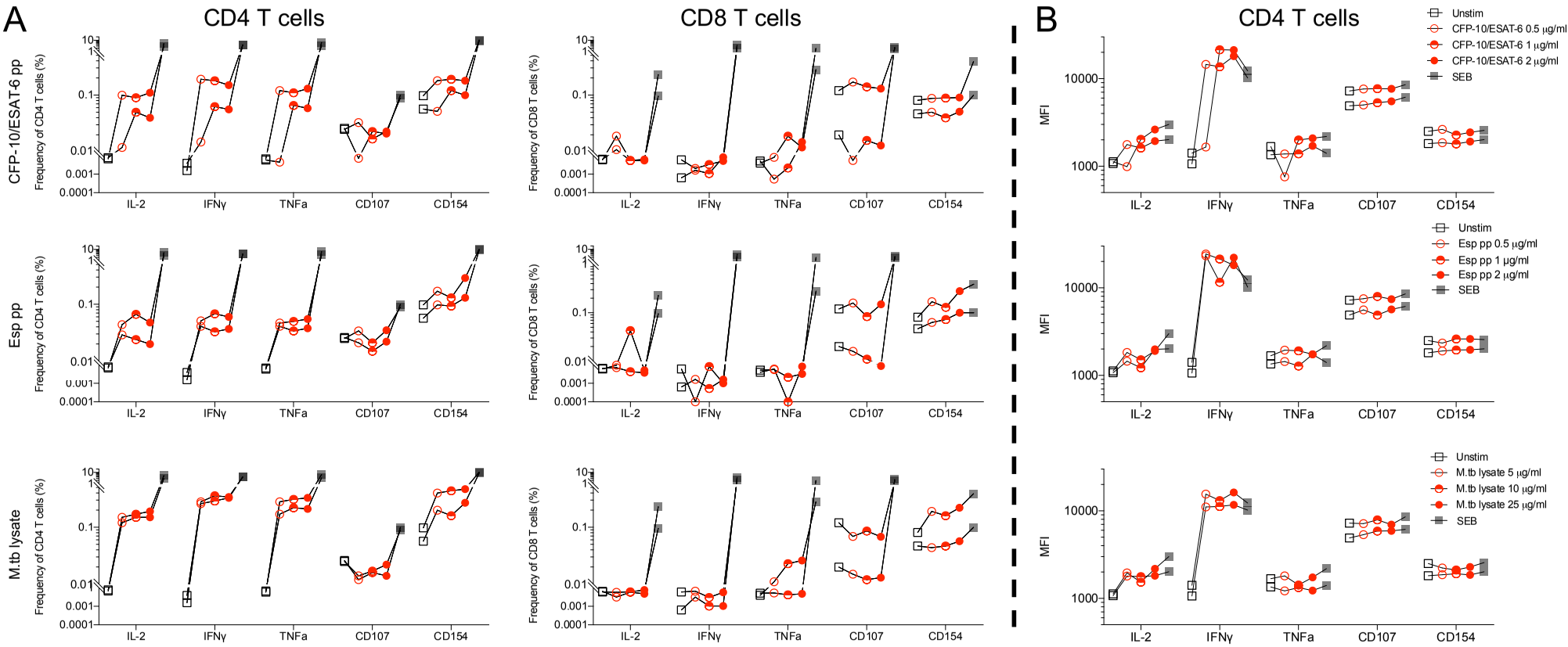

Figure 36: Frequencies of functional CD4 and CD8 T cells in response to different concentrations of M.tb antigens. Frequencies of (A) CD4 and CD8 T cells expressing functional markers: IFN-γ, TNF IL-2, CD154 and CD107 and (B) MFI of IFN-γ+, TNF+ and IL-2+, CD154+ and CD107+ CD4 T cells were measured in response to stimulation with varying concentrations of CFP-10/ESAT-6 peptide pools, Esp peptide pools and M.tb lysate. Immune responses reported here are not background subtracted *(n=2).*

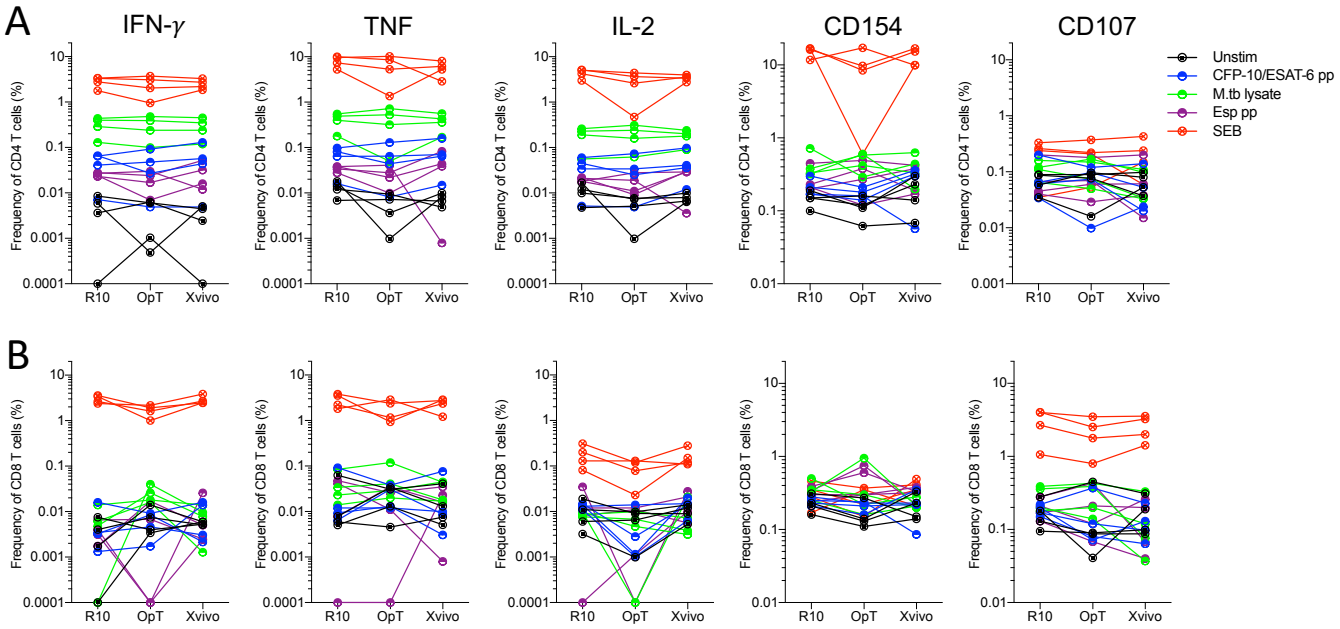

Figure 37: Stimulation in the presence of serum free media did not reduce detection of non-specific background responses nor increase detection of antigen-specific responses. Each graph depicts proportion of (A) CD4 and (B) CD8 T cells expressing IFN-γ, TNF, IL-2, CD154 and CD107 in unstimulated (Unstim, black), CFP-10/ESAT-6 peptide pools (blue), M.tb lysate (green), Esp peptide pools (purple) and SEB (red) stimulated PBMC (n=4) either in the presence of complete media (R10), OpT or XVIVO serum free media. Frequencies reported here are not background subtracted.

RPMI supplemented with antibody serum does not improve detection of cytokines compared to fetal bovine serum

Our complete media (R10) contained FBS as the source of serum, however, this provides heterologous (bovine) source of proteins which may induce non-specific functional responses and/or confound induction of antigen-specific functional responses (Mallone et al., 2011). To ensure that this was not the case, we compared the frequencies of mycobacteria-specific T cells in PBMC stimulated in the presence of either FBS or human AB serum as a supplement for complete medium. Interestingly, we observed similar or lower background Th1 cytokine production by CD4 T cells but higher background IFN-γ and TNF CD8 T cell responses when stimulated in the presence of AB/RPMI compared to complete media containing FBS (Figure 38). Overall, no differences in mycobacterial antigen-specific Th1 cytokine-producing CD4 T cells were detected. However, we did observe slightly higher CD8 T cell functional responses when stimulated with AB/RPMI compared to complete media containing FBS (Figure 38). These higher responses were partly due to non-specific activation since the frequencies of antigen-specific responses were in some cases similar or lower than non-specific functional

responses (when stimulation with AB/RPMI). This resulted in in higher background-subtracted antigen-specific frequencies of CD8+ T cells when cells were stimulated with complete media containing FBS compared to AB/RPMI. Based on these results, we opted to continue to use complete medium (R10) supplemented with FBS.

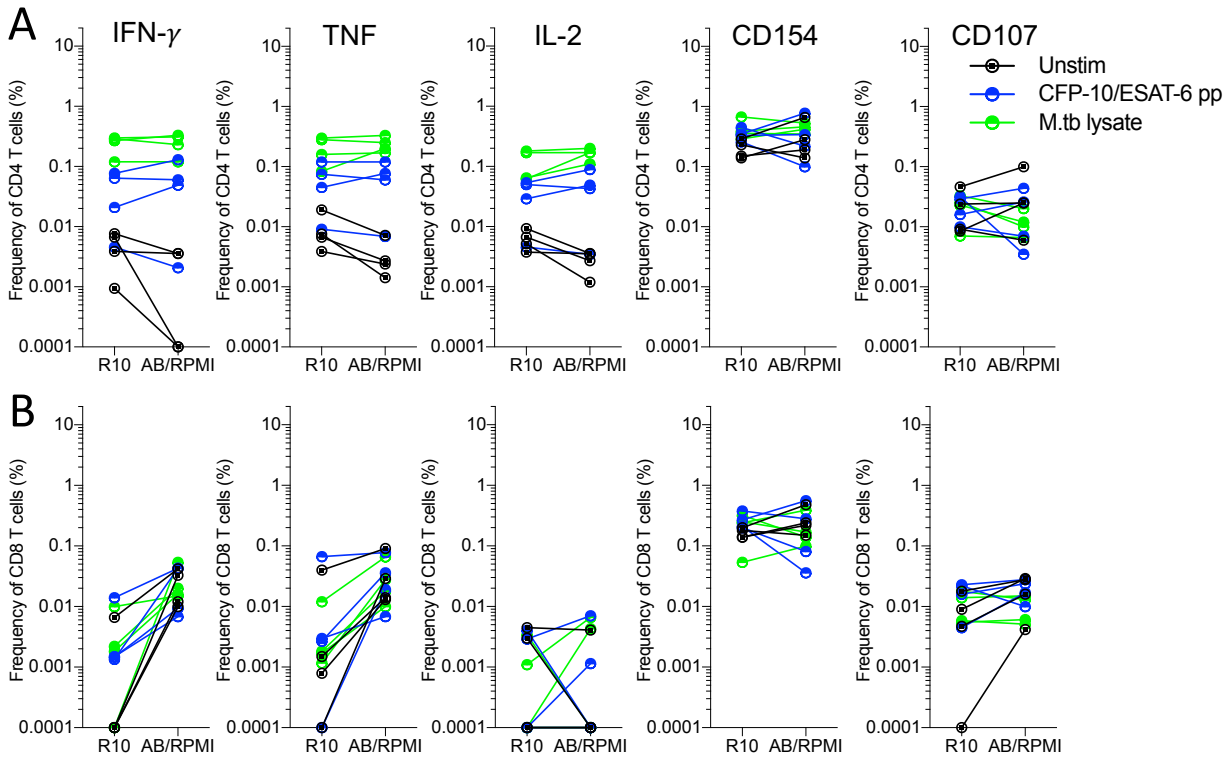

Figure 38: Use of AB serum does not improve detection of functional responses. Frequencies of (A) CD4 and (B) CD8 T cells producing IFN-γ, TNF, IL-2, CD154 and CD107 were measured in unstimulated (Unstim, black), CFP-10/ESAT-6 peptide pools (blue) and M.tb lysate (green) stimulated PBMC (n=4) either in the presence of complete media with FBS (R10) or AB serum. Frequencies reported here are not background subtracted.

Co-stimulatory molecules anti-CD28/CD49d do not improve induction of mycobacteria-specific functional responses in an 18 hour stimulation assay.

Our final optimisation experiment was to determine whether the use of co-stimulatory molecules anti-CD28/CD49d would improve induction of functional responses. T cell functional activity *in vivo* requires 3 signals, (1) HLA-antigen-T cell receptor interaction, (2) interaction between co-stimulatory molecules e.g. CD80/86 (on APCs) and CD28 (on T cells), and (3) cytokines such as IL-12, IL-4 to direct T cell differentiation. Since we were measuring functional activity of differentiated memory cells, we primarily relied on signal 1 to induce cell activation. This functional activity can be enhanced by using co-stimulatory molecules CD28/CD49d to also activate signal 2. Use of co-stimulatory molecules has been shown to improve induction of functional responses in short-term stimulations e.g. 6-12 hour

stimulations (Waldrop et al., 1998). Since we were stimulating for 18 hours, we hypothesised that this time frame was sufficient to induce functional activity without the need of co-stimulation. To determine if this was true, we then stimulated cells *in vitro* with or without costimulatory molecules. This experiment was conducted using PBMC from both QFT negative and positive individuals, to ensure that we were not missing the potential beneficial effect of co-stimulation in QFT negative individuals.

We first investigated whether co-stimulatory molecules increased non-specific activation of CD4 and CD8 T cells in unstimulated cells. Interestingly, we observed higher proportions of non-specific signal in unstimulated CD4 T cells in the presence of co-stimulatory molecules compared to without co-stimulation (Figure 39). This effect was not observed in CD8 T cells. Despite detection of higher responses, these background responses were still relatively low.

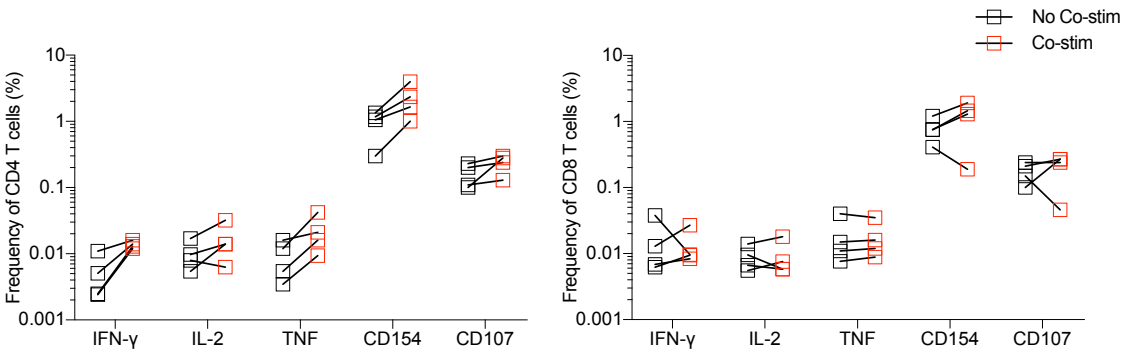

Figure 39: Use of co-stimulatory molecules suggestively increases CD4 T cell background functional activity. IFN-γ TNF and IL-2-, CD154 and CD107 expression was measured in unstimulated cells either in the absence or presence of co-stimulatory molecules (n=4).

Overall, frequencies of functional CD4+ and CD8+ T cells were not significantly higher when we used co-stimulatory molecules (Figure 40). Similar levels of functional activity regardless of addition of co-stimulatory molecules could be because we stimulated cells with peptide pools, which may require less co-stimulatory help than complex antigens. Additionally, the beneficial effect of co-stimulation could be more prominent for shorter stimulation durations (*i.e.* 6 hours) compared to our 18 hour incubation. This is similar to results observed by Horton and colleagues (Horton et al., 2007), who also did not observe a beneficial effect of addition of co-stimulation. Our stimulation protocol provided sufficient time for signal 1: MHC-antigen-TCR interaction to induce sufficient functional responses, which were not potentiated by addition of co-stimulatory molecules that would induce signal 2. Thus, based on these results we opted to not include co-stimulatory molecules, because it did not increase induction of functional markers while it suggestively increased non-specific T cell activation.

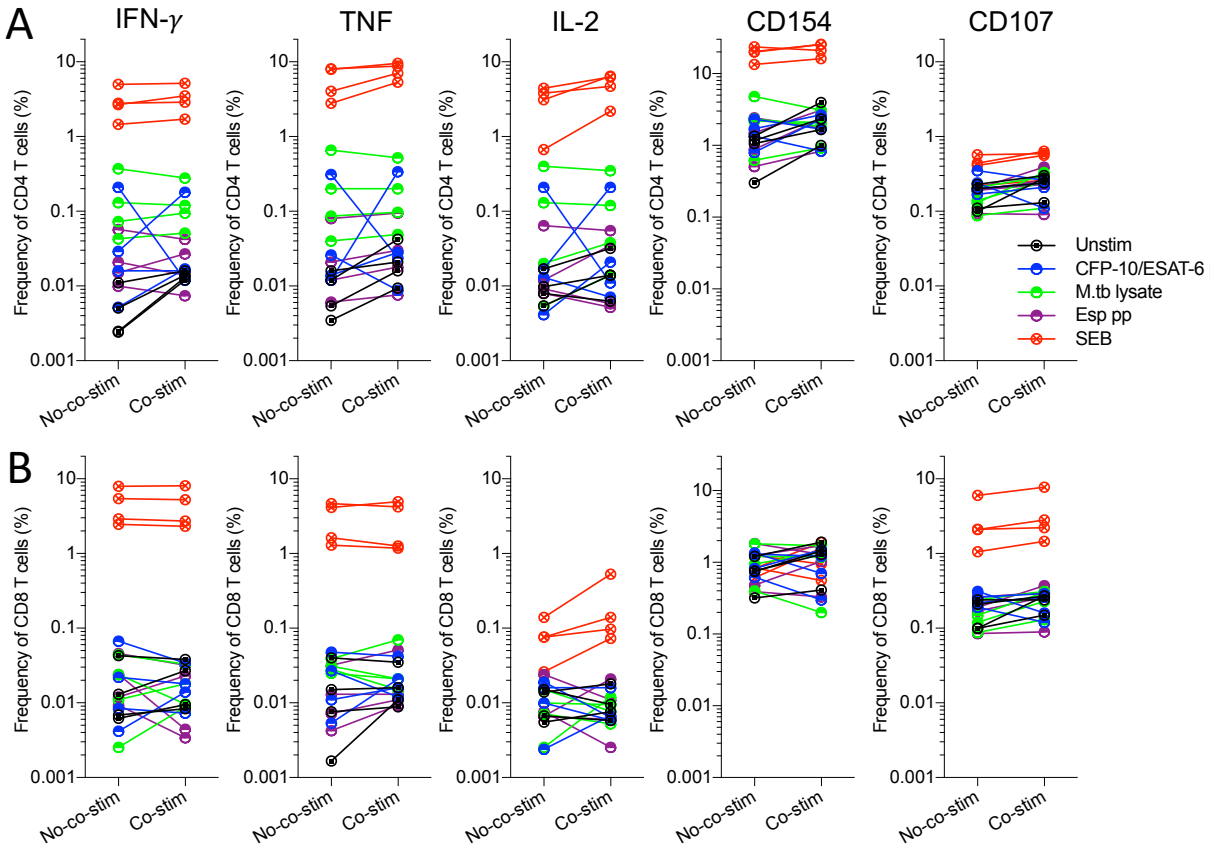

Figure 40: Use of co-stimulatory molecules did not significantly improve induction of functional responses. Frequencies of (A) CD4 and (B) CD8 T cells expressing functional markers: IFN-γ, TNF, IL-2, CD154 and CD107 were measured in response to stimulation with no-stimulant (Unstim), CFP-10/ESAT-6 peptide pools, M.tb lysate Esp peptide pools and SEB. Frequencies reported here are not background subtracted. (n=4).

Conclusion

We conducted multiple optimisations to determine the best PBMC stimulation and intracellular cytokine staining protocol for our specific experiment. We showed that stimulation of cells in the presence of serum free media, AB/RPMI and/or co-stimulatory molecules did not significantly reduce detection of non-specific background responses nor improved induction of functional activity of CD4+ and CD8+ T cells compared to stimulation in the presence of complete media with FBS. Samples used for these optimisation experiments were from the same cohort as the ones used for analyses presented in ***Chapters 5*** and ***6***, and were therefore ideal for developing a protocol suited to answer our scientific hypotheses. In addition to optimisation of our stimulation protocol, we demonstrated that staining cells using a protocol adapted from our qualified whole blood intracellular cytokine staining was not optimal for our PBMC intracellular cytokine staining protocol. Additionally, pre-staining of some lineage and phenotypic markers prior to stimulation in our PBMC

intracellular cytokine staining resulted in increased signal spread, which resulted in lower resolutions of markers such as HLA-DR, which are already expressed at low levels on CD4 and CD8 T cells. In summary, this chapter outlines steps we conducted to ensure that our protocol was optimal for detection of CD4 and CD8 T cell responses to mycobacterial antigens. Our final protocol is outlined in Chapter 5.

Chapter 5: Recent and remote TBI can be distinguished by T cell activation and less differentiated T cell memory phenotypes.

Results reported in this chapter were partially published in the following journals:

Journal: EBioMedicine

Title: Immune profiling of Mycobacterium tuberculosis-specific T cells in recent and remote infection

Authors: Cheleka A.M. Mpande, Virginie Rozot, Boitumelo Mosito, Munyaradzi Musvosvi, One B. Dintwe, Nicole Bilek, Mark Hatherill, Thomas J. Scriba, Elisa Nemes and ACS Study Team#

Year: 2021

Doi: 10.1016/j.ebiom.2021.103233

Journal: American Journal of Respiratory and Critical Care Medicine

Title: Antigen-specific T Cell Activation Distinguishes Between Recent and Remote Tuberculosis Infection

Authors: Cheleka A.M. Mpande, Munyaradzi Musvosvi, Virginie Rozot, Boitumelo Mosito, Timothy D Reid, Constance Schreuder, Tessa Lloyd, Nicole Bilek, Huang Huang, Gerlinde Obermoser, Mark M Davis, Morten Ruhwald, Mark Hatherill, Thomas J Scriba, Elisa Nemes , ACS Study Team#.

Year: 2021

Doi: 10.1164/rccm.202007-2686OC.

#: ACS Study Team: Hassan Mahomed, Willem A. Hanekom, Fazlin Kafaar, Leslie Workman, Humphrey Mulenga, Rodney Ehrlich, Mzwandile Erasmus, Deborah Abrahams, Anthony Hawkridge, E. Jane Hughes, Sizulu Moyo, Sebastian Gelderbloem, Ashley Veldsman, Michele Tameris, Hennie Geldenhuys, Gregory Hussey.

Introduction

A key strategy to alleviate the global burden of tuberculosis, promoted by the WHO, is to provide TPT to M.tb infected individuals, who are at risk of disease progression (Geneva: World Health Organization, 2020a; 2020c). In countries with low tuberculosis burden and/or

high income, TPT is standard of care for persons with clinical and epidemiological risk factors or TBI diagnosis and reduces the risk of tuberculosis (Erkens et al., 2016; Morán-Mendoza et al., 2010; Reichler et al., 2019). On the other hand, in many countries where tuberculosis is endemic as high as 80% of adults may already be infected (Andrews et al., 2015; Cohen et al., 2019; Houben and Dodd, 2016; Wood et al., 2010), making provision of TPT infeasible and unaffordable, especially without knowledge of exposure history and considering the high risk of reinfection after treatment completion in high transmission settings (Churchyard et al., 2017; Mathema et al., 2017). Importantly, given that only a minority (5-10%) of immunocompetent individuals infected with M.tb actually progress, provision of TPT to all those infected exposes many individuals to unnecessary side-effects.

Risk of disease progression is much higher in immunocompromised individuals who may have comorbidities such as HIV, diabetes, among others compared with immunocompetent individuals. Among immunocompetent individuals the highest risk of disease progression occurs within the first 1-2 years of primary infection [recent TBI; (Behr et al., 2018; Erkens et al., 2016; Morán-Mendoza et al., 2010; Trauer et al., 2016; Wiker et al., 2010)]. By contrast, established, remote (> 2 years) TBI is associated with much lower risk. In fact M.tb re-exposure of individuals with remote TBI has been associated with a significantly lower rate of disease progression compared with exposure of individuals without prior infection (Andrews et al., 2012), and there is evidence that most individuals with remote M.tb exposure may have cleared TBI (Behr et al., 2019; Emery et al., 2021). Similarly, a non-human primate tuberculosis model has demonstrated that TBI induces immunity that prevents re-infection or restricts bacterial growth upon re-infection (Cadena et al., 2018). A biomarker that could distinguish between recent and remote TBI would therefore allow targeted TPT to those with recent infection, regardless of setting (Organisation). Unfortunately, current diagnostic tests can identify persons with tuberculosis (sputum-based microbiological tests) and those with TBI (TST or IGRAs). However, these tests cannot distinguish who, among those with asymptomatic infection, are at high risk of progressing to active disease and should receive TPT. Improving tools for detecting TBI and testing for progression to disease is a key priority in the Global Plan to end tuberculosis (Geneva: World Health Organization, 2020a; Partnership, 2019).

Experimental tuberculosis animal models has demonstrated that an early peak in M.tb burden occurs during acute infection. This is followed by immune-mediated reduction of bacterial replication that can persist during chronic infection for very long periods (Lin et al., 2014;

North and Jung, 2004). We postulated that recent TBI in humans follows the same M.tb replication kinetic, albeit over a longer temporal period, resulting in a persisting "lifelong" low-grade infection in many individuals that facilitates maintenance of cellular immune responses or, alternatively, eventual clearance of infection despite persistent immunological sensitisation (Andersen et al., 2007; Behr et al., 2019). In contrast, failure to control bacterial replication results in high and persistent mycobacterial burden which are associated with disease progression. Since the magnitude and duration of *in vivo* T cell exposure to mycobacterial antigens are known to affect differentiation and functional capacity of CD4 T cells (Moguche et al., 2017; Seder et al., 2008), we propose that different states of TBI or disease will be associated with distinct T cell functional and differentiation states. Current TBI immunodiagnostics measure T cell memory responses to M.tb antigens. A major limitation of these tests is that they do not reveal the duration of infection and, as a consequence, most immunology studies of TBI have focused on remote TBI. Our current knowledge of T cell immunity in the context of TBI and disease is thus predominantly based on cross-sectional studies of individuals with remote TBI or recent tuberculosis diagnosis, and very little is known about the T cell features associated with recent TBI.

Upon antigen exposure, T cells become activated, differentiate and acquire functional properties. As discussed in the introduction (Chapter 1) studies have shown that disease, regardless of HIV status, is associated with significantly higher levels of T cell activation than TBI, and that activation is reduced upon successful antimicrobial treatment (Adekambi et al., 2015; Musvosvi et al., 2018; Riou et al., 2017, 2020; Silveira-Mattos et al., 2019; Wilkinson et al., 2016). Based on this, researchers hypothesise that antigen-specific T cell activation could be used as a biomarker of microbial burden, and potentially infer *in vivo* antigen exposure during different stages of infection and disease. In addition, upon exposure to high antigen load CD4 T cells predominantly express IFN-γ, which is mostly associated with an T_E cell phenotype. Conversely, expression of TNF and IL-2 in the absence of IFN-γ is associated with T_{SCM}/T_{CM} cell subsets and exposure to low antigen load or antigen clearance (Kirman et al., 2019; Seder et al., 2008). Further, chronic duration of antigen exposure is associated with upregulation of KLRG-1, T cell senescence marker, and T cell differentiation to a predominantly IFN-γ-monofunctional capacity (Moguche et al., 2017; Seder et al., 2008). These highly differentiated antigen-specific IFN-γ-monofunctional T cells have a lower

capacity to contribute to M.tb clearance than polyfunctional Th1 cells, and are positively correlated with an increase in bacterial burden (Sakai et al., 2014b; Sallin et al., 2017). Based on these cytokine co-expression profiles our research group defined a single measure, termed *functional differentiation score*, that aims to infer the degree of T cell differentiation (Moguche et al., 2017). We demonstrated that a higher M.tb-specific T cell functional differentiation score was associated with increased magnitude and duration of antigen exposure and T_E memory phenotypes (Moguche et al., 2017).

TST and IGRAs have a low predictive value for tuberculosis (Abubakar et al., 2018). Other functional assays that measure M.tb-specific T cell properties such as T cell activation (Adekambi et al., 2015; Musvosvi et al., 2018; Riou et al., 2017, 2020; Silveira-Mattos et al., 2019; Wilkinson et al., 2016), memory differentiation [CD27, (Petruccioli et al., 2015; Portevin et al., 2014)] and Th1 cytokine co-expression profiles (Harari et al., 2011; Rozot et al., 2015) have been proposed as new potential immunodiagnostic concepts that can distinguish between TBI and disease. In line with this principle, potential biomarkers of recent TBI based on proportions of TNF-only (IFN-γ-IL-2-) T_E (CD45RA-CCR7-CD127-) CD4 T cells (Halliday et al., 2017) or T cell proliferation (Borgström et al., 2020), as well as a blood transcriptomic signature (Ault et al., 2020), have been described. Halliday and colleagues demonstrated that the proportion of PPD-reactive TNF-only T_E CD4 T cells was highest in tuberculosis patients and lowest in individuals with remote TBI, and distinguished between recent and remote TBI with a sensitivity and specificity of 89% and 65%, respectively (Halliday et al., 2017). These studies all present evidence for potential biomarkers of tuberculosis risk. However, in-depth characterisation of immunological features associated with recent acquisition of infection that could contribute to an improved understanding of M.tb-specific immunobiology were not presented. The purpose of this chapter was to characterise the kinetics of M.tb-specific T cell features associated with recent and remote TBI.

Based on available evidence, we postulate that differential *in vivo* antigen exposure during recent and remote TBI is associated with distinct M.tb-specific T cell memory, functional and activation profiles. More specifically, we hypothesise *that recent TBI is associated with lower proportions of terminally differentiated T_E cells with IFN-γ-monofunctional activity, and higher proportions of activated (HLA-DR+) than remote TBI*. We thus, aimed to identify M.tb-specific T cell features that could distinguish between recent and remote TBI, as well as develop a

simplified assay that can identify individuals at high tuberculosis risk (recent TBI) and those with ongoing tuberculosis disease.

Objectives

I. **To determine T cell functional, activation and memory profiles associated with recent and remote TBI.**
II. **To identify potential biomarkers that could distinguish between recent and remote TBI.**
III. **Define a simplified biomarker that can identify individuals with recent TBI and on-going tuberculosis disease**

Materials and Methods

Study Design

To compare immune responses between recent and remote TBI, and tuberculosis, we retrieved stored PBMC from adolescents based on QFT status as defined below, and newly diagnosed adult tuberculosis patients.

Participant samples and ethics

Adolescent and adult participants were selected from the SATVI biorepository (HREC 045/2005, HREC 088/2008, HREC 102/2017). Detailed inclusion and exclusion criteria are described below.

Adolescents

Inclusion criteria for adolescents selected for the study were:

- Between 12 and 18 years old
- Live in the greater Worcester area, Western Cape, South Africa
- Attend public schools

Each adolescent participant provided written, informed assent and parents or legal guardians provided written, informed consent. Adolescents who were pregnant or lactating, and who reported acute or chronic medical conditions resulting in hospitalisation within 6 months

prior to enrolment were excluded. HIV testing was allowed only in participants diagnosed with tuberculosis during follow-up, none of which were included in this study.

Definition of recent TBI.

We defined two separate sub-cohorts of recent M.tb infected adolescents:

Tet+ Converters*:* this sub-cohort is described in Chapter 3 as participants used for the "Longitudinal natural M.tb infection studies". These adolescent participants, were QFT and TST negative at baseline, converted both their QFT and TST responses (which were sustained throughout follow-up) at 6 and 12 months post-follow up (Figure 14). Selected participants were also HLA-typed (see Chapter 2: HLA-typing), and M.tb-specific CD4 T cells were identified using tetramers [see Chapter 3: Flow Cytometry Staining Protocol (Panel 1) for methodology].

Recent QFT converters*:* adolescents in this group (referred to as recent TBI) were defined based on two negative QFT tests followed by two positive QFT tests 6 months apart (Figure 41). All participants had at least one positive and negative QFT test result out of the QFT uncertainty zone (0·2-0·7 IU/mL) defined by our research group (Nemes et al., 2017a). These participants also had TSTs performed annually, however, TST was not used to define TBI. Recently infected individuals were split into a biomarker discovery (n=30) and test (n=25) cohorts. PBMC from all four visits for the biomarker discovery cohort, while PBMC the first QFT**-** and the first QFT**+** visit (1 year apart) for the test cohorts were used for the experimental protocol defined below.

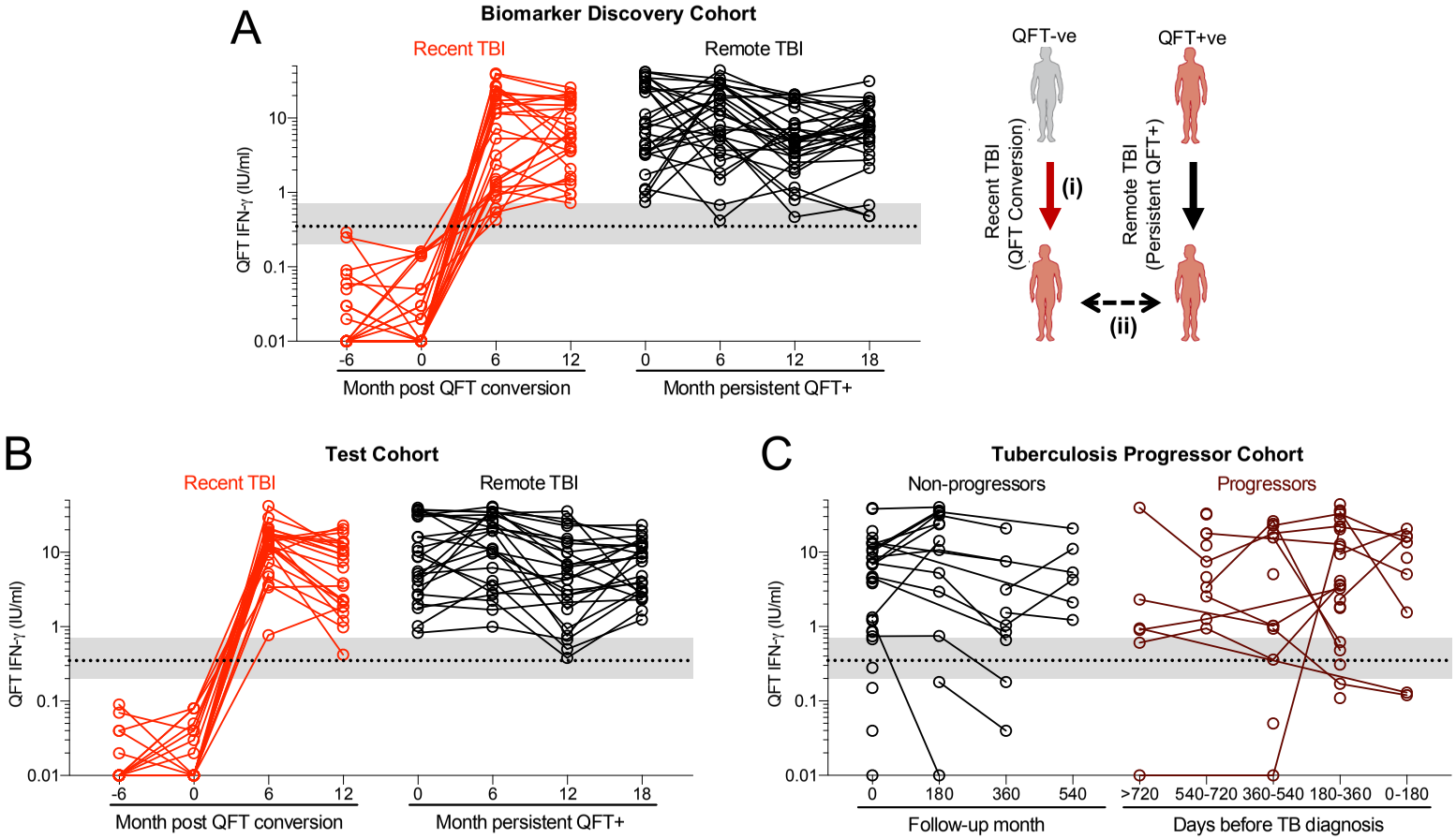

Figure 41: Cohort QFT Kinetics. TBI was defined using longitudinal QFT results for each participants in the (A) biomarker discovery, (B) test and (C) tuberculosis progressor cohorts. Dotted line and grey shading represents the QFT positivity threshold of 0.35 IU/mL and the QFT uncertainty zone criterion [0.2 IU/mL < QFT <0.7 IU/mL, *(Nemes et al., 2017a)*], respectively. Individuals selected for the recent TBI group (red symbols) in both the biomarker discovery (n=30) and test cohort (n=25) had at least one QFT negative visit <0.2 IU/mL and at least one QFT positive visit > 0.7 IU/mL, while individuals in the remote TBI group [black symbols; biomarker discovery (n=30) and test cohort (n=25)] had to have at least 2 QFT positive results > 0.7 IU/mL. Individuals in the tuberculosis progressor cohort (non-progressors n=39; progressors n=39) with a QFT negative test result had corresponding TST positive result (TST >5mm). We did not apply the QFT uncertainty zone criterion for participants in the tuberculosis progressor cohort because they were selected historically prior to definition of the metric (Zak et al., 2016). The image in (A) depicts comparisons that were performed on the biomarker discovery cohort: (i) pre- vs post- QFT conversion in recent M.tb infected individuals and (ii) recent vs remote TBI.

Definition of remote TBI.

Selection of adolescents for the remote TBI group was based on 4 consecutive QFT positive tests (two of which had to be > 0·7 IU/mL) 6 months apart (Figure 41). Remote TBI individuals were split into biomarker discovery (n=30) and test (n=25) cohorts. Remote TBI individuals were not matched to recent QFT converters. However, participants selected for the biomarker discovery cohort were part of a larger cohort of adolescents (described in Chapter 6) that were matched to QFT reverters, based on age, gender and school, as a proxy of M.tb exposure. As a result, demographics for recent and remote TBI adolescents in the biomarker discovery cohort were not different (Table 21), while no matching was performed on the test cohort.

Tuberculosis progressor cohort: definition of progressors and non-progressors

M.tb infected adolescents defined by a positive QFT test and/or a positive TST (induration >5mm), who developed microbiologically-confirmed, intrathoracic tuberculosis during the 2-year follow-up were included as progressors, while those who remained healthy were included as non-progressors (Figure 34C). Individuals included here were a sub-group of adolescents studied to identify a transcriptomic blood signature for tuberculosis risk, selected based on sample availability (Scriba et al., 2017; Zak et al., 2016). Tuberculosis was diagnosed by either two sputum samples positive on smear microscopy for acid-fast bacilli or one sputum sample positive for *M.tb* by liquid culture (Zak et al., 2016). Only samples collected before tuberculosis diagnosis were analysed.

Adults

Patients above 18 years old with recently diagnosed tuberculosis (positive XpertMTB/RIF, Cepheid), who provided written informed consent were recruited from the greater Worcester area clinics, Western Cape, South Africa, from January through August 2015. All adults with HIV-infection, anaemia (Haemoglobin <8.0d/dL), body mass index ≤17, with signs of other chronic illnesses that were not consistent with tuberculosis and those who had already started tuberculosis treatment were excluded from the study.

Table 21: Cohort demographics.

	Biomarker discovery Cohort		*Test Cohort*			*TB Progressor Cohort*	
	Remote TBI	**Recent TBI**	**Remote TBI**	**Recent TBI**	**Tuberculosis**	**Progressors**	**Non-progressors**
n	30	30	25	25	25	39	39
Gender (Female)	21	19	12	9	3	14	28
Age in years (IQR)	15 (14-16)	15 (14-16)	15 (14-16)	15 (14-16)	32 (21-42)	16 (15-17)	16 (14-17)
Ethnicity: Coloured	26	29	23	23	14	36	37
Ethnicity: Black	4	1	2	1	11	3	2
Ethnicity: Indian	0	0	0	1	0	0	0

PBMC stimulation and staining protocol

Biomarker discovery and test cohort protocol

PBMC stimulation: Cells were thawed, rested and enumerated as described in Chapter 4. Cells were then stimulated in tubes (biomarker discovery cohort) or 96 well plates (test cohort) in complete media containing anti-CD107a PE-CF594 (0.1μL, biomarker discovery cohort) with either no antigen (unstimulated), CFP-10/ESAT-6 peptide pools (15 mer peptides overlapping by 9-10 amino-acids, 1μg/mL), M.tb lysate (10μg/mL, biomarker discovery cohort), SEB (1μg/mL, biomarker discovery cohort) or phytohemagglutinin (5μg/mL, Remel, test cohort). Brefeldin A (5μg/mL) was added at the onset of the 18 hour stimulation in the test cohort. Cells from the biomarker discovery cohort were incubated for 3 hours at 37°C with 5% CO_2, after which Brefeldin A (5μg/mL) and monensin (2.5μg/mL) were added and incubated for a further 15 hours.

Phenotypic marker staining: After completion of stimulation incubation, cells were treated with 1mL (biomarker discovery cohort) or 20μL (test cohort) of 20mM EDTA, incubated for 10 minutes and washed by centrifugation at 930xg for 10 minutes and supernatant discarded. Cells were then stained with anti-CCR7 PE (3μL, Clone: 150503) and anti-CXCR3 PE-Cy5 (5μL) in a total volume of 50μL of PBS for 30 minutes at 37°C (biomarker discovery cohort). An antibody cocktail of viability, phenotypic and lineage markers (Table 22) was added to cells and incubated at RT for 30 minutes. Cells were then washed in FACS wash by centrifugation and supernatant discarded.

Table 22: Antibody clones and volumes for staining lineage and phenotypic markers.

Marker	Cohort	Clone	Manufacturer	Fluorochrome	Volume
CD3	Biomarker discovery cohort	UCHT1	BD Biosciences	BV650	1 μL
CD4		OKT4	BioLegend	BV785	0.75 μL
CD8		RPA-T8	BD Biosciences	BV711	0.5 μL
CD45RA		HI100	eBioscience	BV570	1.5 μL
CD27		L128	BD Biosciences	BV510	0.25 μL
HLA-DR		L243	BD Biosciences	FITC	1.25 μL
KLRG1		13F12F2	eBioscience	PerCP-eFluor 710	1 μL
Viability		N/A	Thermo-Fisher Scientific	FAR IR	0.2 μL
CD3	Test Cohort	UCHT1	BD Biosciences	BB 515	1.5 μL
HLA-DR		L243	BD Biosciences	PE	2 μL
Viability		N/A	Thermo-Fisher Scientific	FAR IR	0.15 μL
CD3	TB progressor cohort	SK7	BD Biosciences	BV786	2 μL
CD4		RPA-T4	Biolegend	BV605	3 μL
CD8		RPA-T8	BD Biosciences	Alexa Fluor 700	1 μL
TCRαβ		IP26	Biolegend	PE-Cy7	2 μL
CD69		L78	BD Biosciences	APC	0.2 μL
CD137		4B4-1	BD Biosciences	BV711	0.5 μL
CD26		BA5b	Biolegend	FITC	1 μL
HLA-DR		L243	Biolegend	BV421	1 μL
CD14		M5E2	Biolegend	BV510	1 μL
CD19		HIB19	Biolegend	BV510	1 μL

Note: Antibodies and viability marker used to stain the biomarker discovery and test cohorts were diluted in 50μL BS buffer or FACS Wash, respectively.

Permeabilisation and fixation of cells: After washing, cells were fixed and permeabilised in 100μL of CytoFix/CytoPerm solution and incubated for 20 minutes at RT, washed in 1mL of Perm/Wash by centrifugation and supernatant discarded.

Intracellular cytokine staining: Cells were then stained with an antibody cocktail of functional markers in a total volume of 50μL of Perm/Wash (Table 23) for 30 minutes at RT. Cells were washed in 2mL Perm/Wash by centrifugation, supernatant discarded, and cells resuspended in 100μL of 1% PFA and then acquired on BD LSR II.

Table 23: Antibody clones and volumes used for staining functional markers.

Marker	Cohort	Clone	Manufacturer	Fluorochrome	Volume
IFN-γ	Recent vs Remote	B27	BD Biosciences	Alexa Fluor700	1 μL
TNF		Mab11		PE-Cy 7	0.038 μL
IL-2		5344.111		APC	0.1 μL
CD154		TRAP-1		BV 421	0.5 μL
IFN-γ	Test Cohort	B27		APC	0.2 μL
TNF		Mab11		PE-Cy 7	0.025μL

Tuberculosis progressor cohort protocol

PBMC stimulation: Cells were thawed, rested for 6 hours, and stimulated in complete media for 12 hours with M.tb lysate (10µg/mL) in the presence of anti-CD49d antibody (1µg/mL, Clone L25, BD Biosciences), and anti-CD154-PE (10µL/mL; Clone TRAP1; BD Biosciences).

Phenotypic marker staining: Following stimulation cells were washed and stained with viability marker (LIVE/DEAD Fixable Aqua Stain, Invitrogen) for 30 minutes at 4°C. Next, cells were washed and stained with antibodies (Table 22) for 60 minutes at room temperature.

Cell sorting: Activated (i.e. CD69+CD137+ and/or CD69+CD154+) single T cells, gated according to gating strategy illustrated in Figure 42, were index-sorted (BD FACS Aria-II) into 96 well plates containing One-Step RT-PCR buffer (Qiagen) and a panel of primers specific for 20 mRNA transcripts (Table 24). Transcript-specific amplification was performed and further amplified in a nested PCR before sequencing on a MiSeq (Illumina) instrument using protocols defined by Glanville and colleagues (Glanville et al., 2017; Han et al., 2014). Data from the tuberculosis progressor cohort was collected as part of an unpublished single cell TCR sequencing (scTCRseq) study and shall not be reported in this thesis.

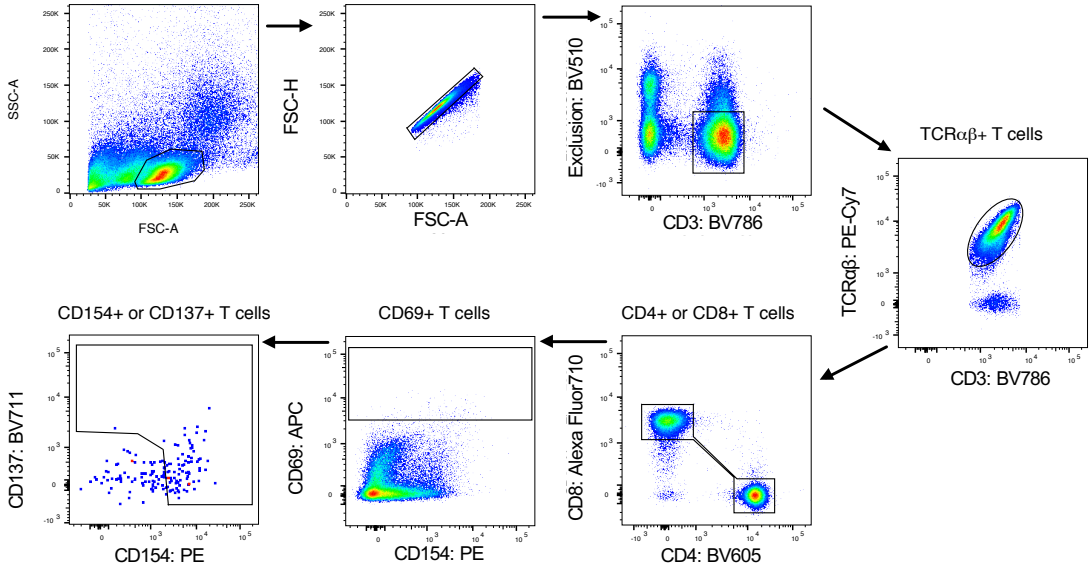

Figure 42: Gating strategy used to identify M.tb-lysate responsive T cells in the TB progressor cohort. Live, M.tb-responsive αβ T cells were defined as CD69+ cells co-expressing CD154 and/or CD137. M.tb-responsive T cells were index sorted into 96-well plates for single cell gene expression profiling.

Table 24: mRNA transcripts targeted by single cell phenotyping primers.

BCL6	*GZMB*	*IL13*	*IL4*	*RUNX3*
EOMES	*IFNG*	*IL17A*	*PERF*	*TBET*
FOXP3	*IL10*	*IL2*	*RORC*	*TGFB*
GATA3	*IL12A*	*IL21*	*RUNX1*	*TNF*

Biomarker discovery cohort data analysis pipeline

We detected mycobacteria-reactive CD4 T cell responses using flow cytometry and analysed flow cytometry data as described in Chapter 2-4. We focused our analyses on CD4+ T cells because frequencies of CD8+ T cell responses were undetectable or not different to background in most individuals (data not shown). Following flow cytometry analysis in FlowJo, we followed the analysis pipeline outlined in Figure 43. Briefly, expression of all possible combinations of functional responses (obtained by Boolean gates) were analysed using COMPASS (Lin et al., 2015), Pestle and SPICE (Roederer et al., 2011). In parallel, we utilised MIMOSA (Finak et al., 2013) to define responders. We identified differentially expressed T cell subsets (including all possible combinations of functional and phenotypic markers) between two groups using CITRUS analysis in Cytobank (Bruggner et al., 2014) on responders only. Following CITRUS analysis, we exported CITRUS cluster FCS files, concatenated files from all participants belonging to the same cluster and confirmed memory/cytokine cluster composition by manual re-gating in FlowJo.

Flow Cytometry Gating Strategy

We defined the following gating strategy to identify CD3+, CD4+ and CD8+ T cell functional responses in the biomarker discovery cohort, and CD3+ functional responses in the test cohort (Figure 44). Gating strategies used for biomarker discovery and test cohorts were similar. Total cells were first gated in B515, G610, V545 and R610 channels in parallel based on acquisition rate consistency and combined ("AND" expression) into one Boolean, to ensure we analysed cells acquired at the same acquisition consistency. This was followed by exclusion of cell doublets and antibody aggregates. We then gated on total lymphocytes and excluded additional staining artefacts. Due to a pronounced down-regulation of CD3 expression in IFN-γ producing T cells, we first gated on CD4+ and CD8+ T cells followed by gating on CD3+ T cells. Functional markers, IFN-γ, TNF, IL-2, CD154 and CD107, were then gated on CD4+CD3+ and CD8+CD3+ T cells. For the test cohort, we gated on total CD3+ T cells and included $CD3^{dim}$ IFN-γ+ in the total CD3+ cells gate. IFN-γ+, TNF+ and HLA-DR+ T cells were then gated on total CD3+ T cells

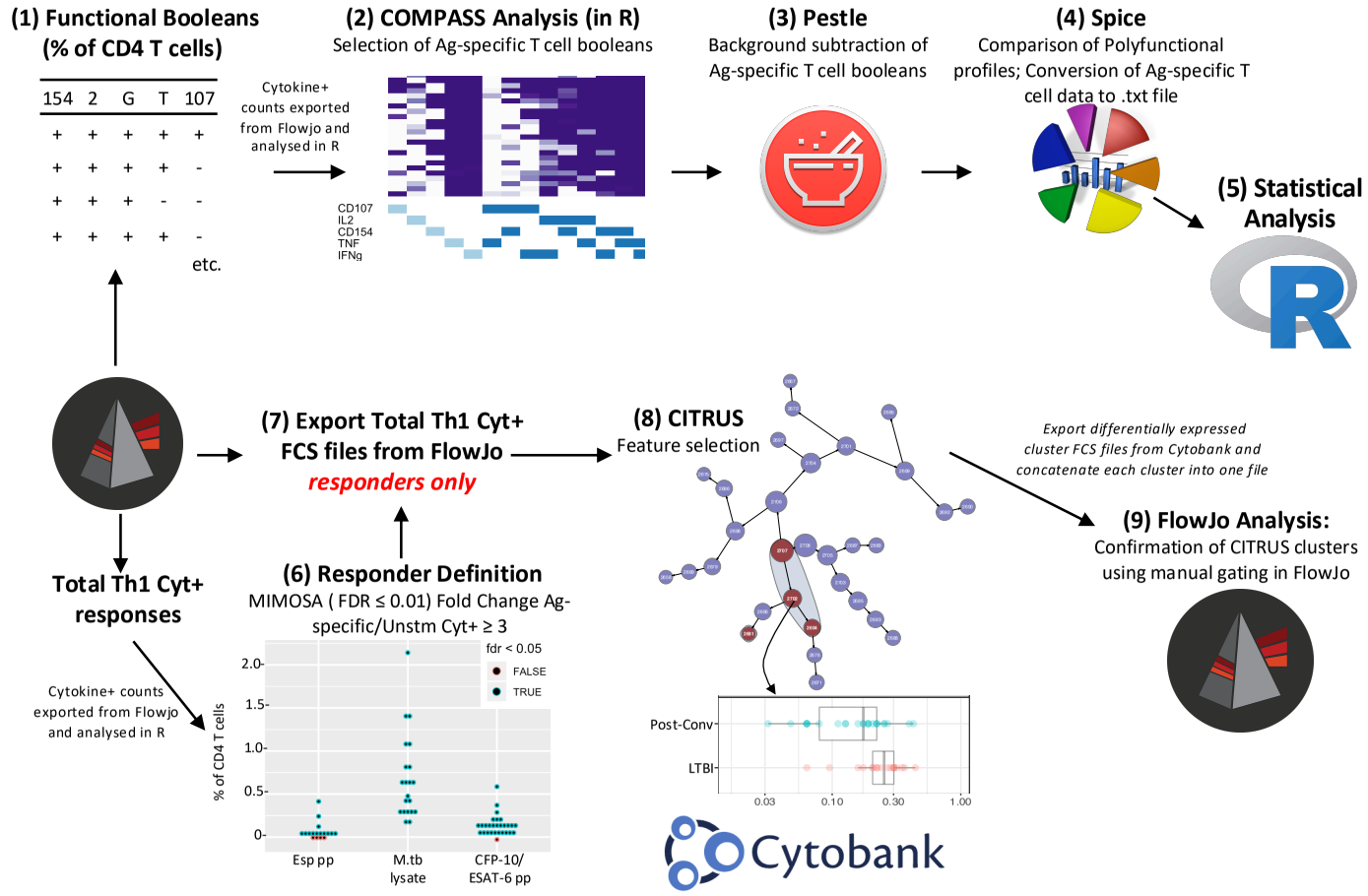

Figure 43: Analysis pipeline. (1) All combinations of functional subsets (Booleans of IFN-γ±TNF±IL-2±CD154±CD107±; n=31) were defined using Flowjo and (2) antigen-specific CD4 T cell subsets were identified using COMPASS in R. (3) To account for non-specific responses, we subtracted background (unstimulated) frequencies for each Boolean subset in Pestle. (4) The distribution of polyfunctional cell subsets (pie-charts) across groups were compared in SPICE. (5) Statistical comparisons of functional booleans were conducted in R. In parallel, (6) responders to antigenic stimulation were defined on total cytokine+ CD4+ T cells (expressing any combination of IFN-γ, TNF or IL-2) that passed a MIMOSA FDR threshold of ≤ 0.01 and had a ≥ 3-fold change of antigen-specific signal over unstimulated. (7) Total Th1 cytokine+ FCS files for responders only were exported from FlowJo and (8) imported into Cytobank to determine differentially expressed clusters between two groups using CITRUS. (9) Identity of clusters defined in CITRUS was confirmed using manual gating in FlowJo and the final gating strategy for each cluster was applied to individual responders.

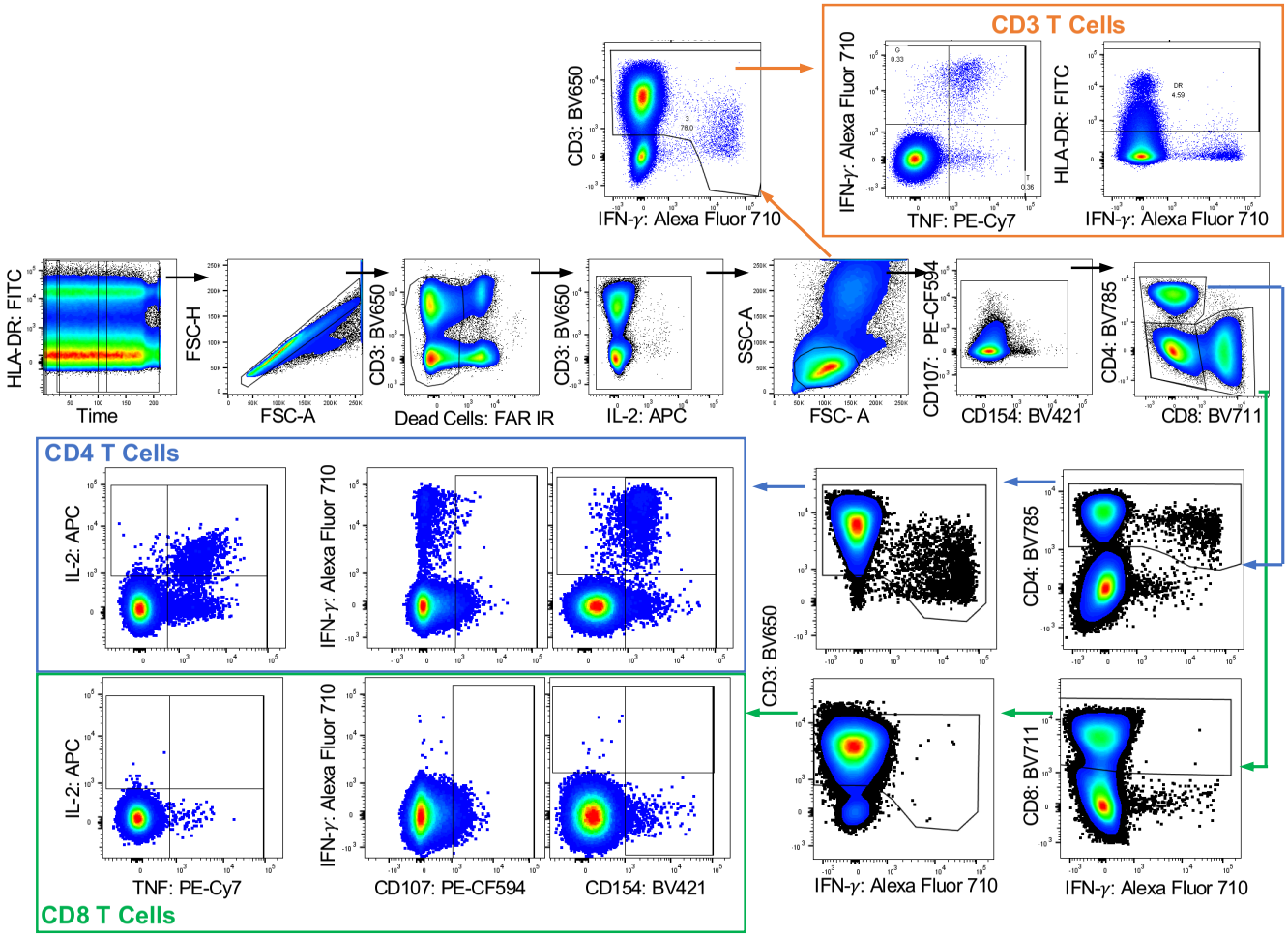

Figure 44: Gating strategy used to identify live M.tb-responsive CD3, CD4 and CD8 T cells. We first gated on total cells based on fluorescence consistency over acquisition time (time gate), followed by exclusion of cell doublets, dead cells and antibody aggregates. We then gated on total lymphocytes and excluded additional staining artefacts. Due to down-regulation of CD3 on cytokine-expressing M.tb-specific T cells upon stimulation with M.tb antigens, we also included cells that were $CD3^{dim}$ IFN-γ+ in the total CD3+ cells gate. To ensure that we correctly classified all cytokine+ CD4+ or CD8+ CD3+ T cells, we first gated on CD4+ (after excluding CD8+ cells) and CD8+ (after excluding CD4+ cells) T cells and then gated on CD3+ T cells. Functional markers (IFN-γ, TNF, IL-2, CD154 and CD107) were then gated independently on CD4+CD3+ (blue box) and CD8+CD3+ (green box) T cells, while HLA-DR+, IFN-γ+ and TNF+ were gated on CD3+ T cells (orange box).

COMPASS Analysis

We utilised flow cytometry to measure the expression of 5 functional markers, IFN-γ, TNF, IL-2, CD107 and CD154 by T cells in mycobacteria-stimulated PBMC. In addition to measuring expression of each functional marker, we also wanted to determine co-expression of every possible combination of these markers (n = 31). However, not all combinations would be expressed by M.tb-specific T cells nor present at frequencies higher than background. To determine which functional cell subsets were M.tb-specific, we utilised the COMPASS (**C**ombinatorial **p**olyfunctionality analysis of **a**ntigen-**s**pecific T-cell **s**ubsets; version 1.20.1; https://github.com/RGLab/COMPASS) R package using R version 3.6.1 and RStudio version 1.2.1335 (Lin et al., 2015). COMPASS uses a "*Bayesian hierarchical mixture model*" and defines antigen-specific responses across all identified T cell populations as T cell subsets with >5 counts and detectable in at least two participants. COMPASS computes the posterior probability of each cell subset co-expressing functional markers based on cell counts in stimulated *versus* unstimulated conditions for each individual. Posterior probability is the probability that an antigen-specific response is greater than a non-specific (unstimulated) response, where a higher posterior probability, indicates a greater probability that the response is greater than unstimulated. COMPASS also computes two scores, the functionality and polyfunctionality scores. The functionality score is defined as the proportion of antigen-specific subsets co-expressing functional markers detected among all possible ones. The polyfunctionality score is similar, but it weights the different subsets by their degree of functionality where subsets with higher degrees of functionality are favoured (Lin et al., 2015). We conducted COMPASS analysis of CFP-10/ESAT-6, M.tb lysate and SEB-specific CD4 T cell subsets at all study visits. We only analysed subsets expressing different combinations of cytokines if they had a posterior probability threshold of $\geq$ 0.1 in at least 10 participants/visit for recent and remote infection. This arbitrary cut-off was used to ensure that subsets that were further analysed were all antigen-specific, higher than background and to minimise experimental artefacts. Functional subsets (Booleans) that passed these criteria were then analysed after background subtraction using Pestle and SPICE. Regardless of posterior probability threshold, we calculated functionality and polyfunctionality scores for each participant.

Responder Definition

In addition to measuring functional markers, we also measured expression of memory and activation markers on the same cells. Since expression of phenotypic markers cannot be background subtracted, we identified responders and non-responders using MIMOSA (**Mi**xture **mo**dels for **s**ingle-cell **a**ssays, version 1.21.0; https://github.com/RGLab/MIMOSA) R package in R and RStudio. MIMOSA uses a *"Bayesian hierarchical framework based Markov chain Monte Carlo"* algorithm to determine if expression of a single marker or combination of markers is significantly higher than background and if so, classifies the participant as a responder to a specific stimuli MIMOSA analysis outputs a posterior probability and FDR, which it uses to classify a responder and non-responder (Finak et al., 2013). We defined responders as individuals whose frequencies of antigen-specific total Th1 cytokine+ (IFN-γ±TNF±IL-2±) CD4 T cells were significantly higher (FDR ≤0·01, calculated by MIMOSA, and at least 3-fold increase) than background. For the test cohort, responders were defined as individuals with relative counts of IFN-γ+TNF+ CD3+ T cells in the antigen-stimulated condition that were significantly higher ($p \leq 0.01$ by Fisher's Exact test, and at least 3-fold increase) than the background. In the tuberculosis progressor cohort, only samples with 10 or more *IFNG* and *TNF* co-expressing cells were analysed for HLA-DR expression. Non-responders were excluded from phenotypic marker expression analysis. We used this strict cut-off to ensure that cytokine responses in responders were truly antigen specific because analysis of activation, memory and/or functional phenotypes were performed using methods that could not account for non-specific signal using background subtraction.

CITRUS analysis

We included 5 functional (IFN-γ, TNF, IL-2, CD154 and CD107) and 6 phenotypic (CD45RA, CCR7, CD27, KLRG-1, CXCR3 and HLA-DR) markers in our analyses, amounting to a total of 2048 potential co-expression combinations. The majority of these marker combinations may not be expressed by mycobacteria-specific CD4 T cells. To determine which functional and phenotypic combinations changed upon recent TBI and which ones were different between recent and remote TBI, we utilised CITRUS analysis to identify subsets that were significantly different between two groups or to define the minimum number of markers that can predict differences between two groups (Bruggner et al., 2014).

Definition of CITRUS clusters: We utilised the significance analysis of microarrays association model to determine which co-expression patterns were significantly different between groups. We randomly down-sampled an equal number of events per participant and performed clustering characterisations based on marker abundance, which identifies differences based on the proportional contribution of each marker to the defined cluster. CITRUS clustering was performed based on memory markers, CD45RA, CCR7, CD27 and KLRG1, and Th1 cytokines IFN-γ, TNF and IL-2. CD107, CD154, CXCR3 and HLA-DR were not used to define the final CITRUS clusters because preliminary analysis showed that inclusion of these markers was not useful to further delineate the clusters in addition to the other 7 markers. CITRUS outputs data in the form of CITRUS trees, coloured by parameter abundance, highlights differentially expressed clusters that passed a defined FDR threshold of < 0.05 (Figure 45A-B) and depicts composition of clusters using histograms (Figure 45C).

Confirmation of CITRUS clusters in FlowJo: To confirm the memory and functional marker composition of clusters identified to be differentially abundant, we exported each CITRUS cluster that passed the FDR threshold of 0.05 and concatenated the FCS files belonging to the same cluster from all participants in FlowJo. Clusters were then manually reanalysed to determine the minimum set of markers whose combined expression "reproduced" each CITRUS cluster (Figure 46). Upon confirmation of cluster composition, we manually gated cell subsets representative of these clusters on individual responder FCS files and used this data to present the results described below.

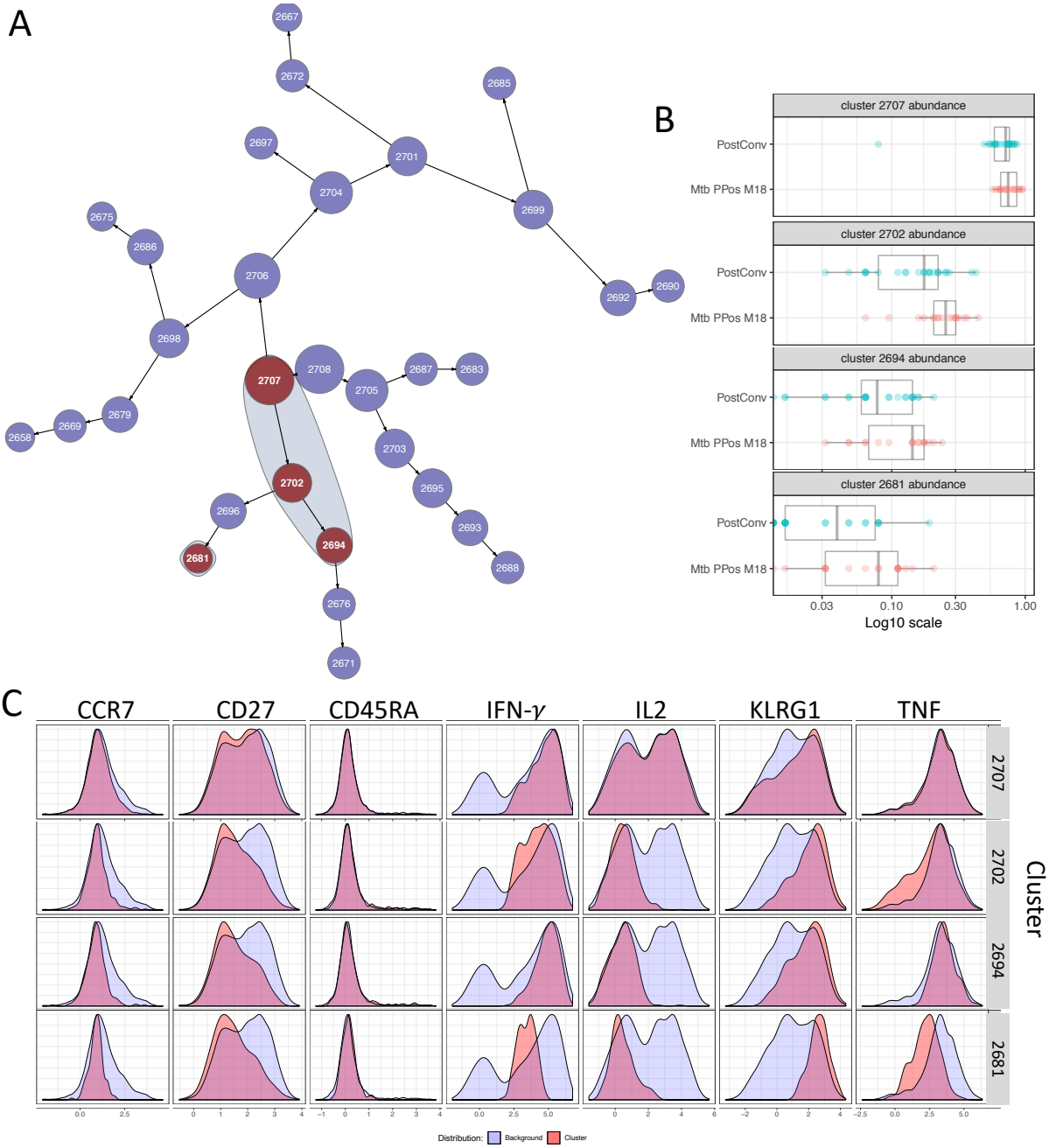

Figure 45: Recent vs remote TBI CITRUS analysis result. Representative example of CITRUS-defined clustering represented as a (A) CITRUS tree. Shaded clusters represent clusters that are differentially expressed with an FDR < 0.05 between recent and remote TBI. Differentially expressed clusters are also represented in (B) graphical format depicting expression by each participant. (C) Expression of each memory/functional marker used to define the cluster (salmon) compared to total Th1 cells (light purple) are depicted in overlaid histograms.

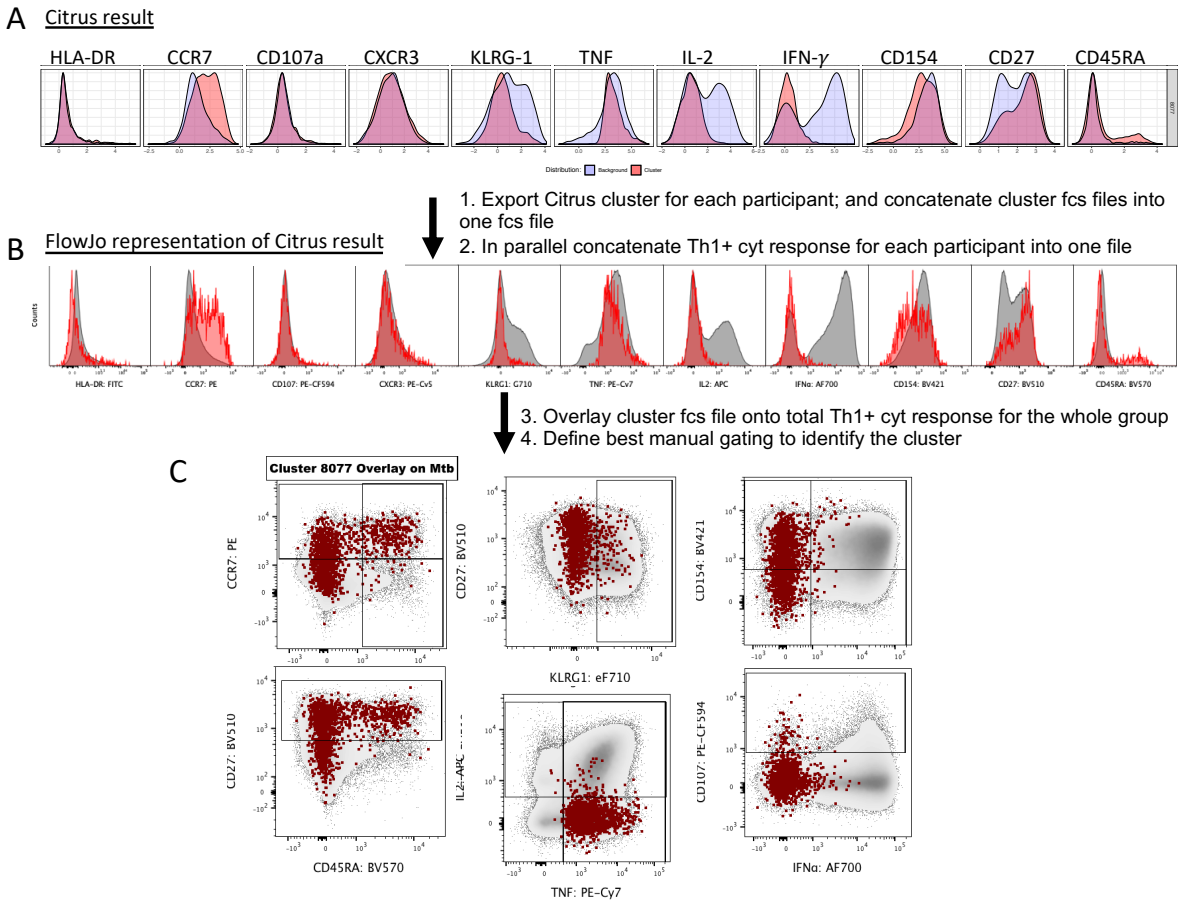

Figure 46: Analysis pipeline used to confirm CITRUS cluster co-expression profiles. (A) CITRUS clusters were exported from Cytobank and concatenated into one file using Flowjo. In parallel, total Th1+ cytokine (cyt) responses for each participant were also concatenated into one file (representing Th1+ cyt response for all participants). (B) Concatenated citrus cluster (red) was overlaid on total Th1+ cyt response (grey) to validate CITRUS modelling of marker expression. (C) Concatenated cluster events were overlaid on total Th1+ cyt, visualised by conventional bi-variate plots, and expression levels of memory markers and cytokines were used to define the best gating strategy to manually validate the clusters based on co-expression of CD45RA, CCR7, CD27, KLRG1, IFN-γ, TNF and IL-2.

Functional Differentiation Score

In addition to determining functional co-expression profiles, functionality and polyfunctionality scores, we also calculated the functional differentiation score [FDS; Equation 3; (Moguche et al., 2017)] for responders only.

Equation 3: Functional Differentiation Score calculation.

$$FDS = \frac{\boldsymbol{IFN-\gamma} + TNF \pm IL-2 \pm}{\boldsymbol{IFN-\gamma} - TNF \pm IL-2 \pm}$$

T cell activation biomarker definition

In the biomarker discovery and tuberculosis progressor cohorts, we explored different calculations to define the T cell activation biomarker: HLA-DR+ T cells as a percentage of total

IFN-γ+TNF+ T cells, HLA-DR MFI ratio (Equation 4) and Delta (Δ) HLA-DR MFI (Figure 47, Equation 5).

Equation 4: HLA-DR MFI ratio calculation.

$$\text{HLA} - \text{DR MFI Ratio} = \frac{\text{HLADR MFI on IFN}\gamma + \text{TNF} + \text{CD3} + \text{cells}}{\text{HLADR MFI on total CD3} + \text{cells}}$$

Equation 5: ΔHLADR MFI calculation.

ΔHLADR MFI = (HLADR MFI on IFN-γ+TNF+ CD3+ cells) – (HLADR MFI on total CD3+ cells)

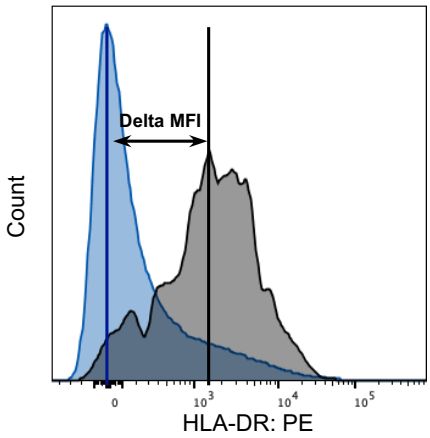

Figure 47: Representative flow cytometry histogram overlay of HLA-DR expression levels by IFN-γ+TNF+ CD3+ T cells (black) and total CD3 T cells (blue), and how Δ (Delta) HLA-DR MFI was calculated.

Progressor and non-progressors transcriptomic analysis

TCRαβ sequences were amplified using a panel of TCRαβ primers and further amplified in a nested PCR before sequencing on a MiSeq (Illumina) instrument, as described by Glanville and colleagues (Glanville et al., 2017; Han et al., 2014). Expression of 20 mRNA transcripts was detected within each sorted T cell, as described by Glanville and colleagues (Glanville et al., 2017; Han et al., 2014). Co-expression of IFNG+TNF+ was defined by 5 or more IFNG and TNF reads per cell.

Statistical analysis pipeline

Statistical analyses were performed using R, R Studio, GraphPad Prism v7 and/or SPICE version 5.2-6 (Roederer et al., 2011). We applied Wilcoxon signed-rank and Mann-Whitney U statistical tests for paired and unpaired comparisons, respectively. Differences in pie charts depicting co-expression profiles were calculated using nonparametric pair permutations comparing the overall distribution of functional or memory subsets between groups using SPICE (Roederer et al., 2011). Bonferroni or Benjamini-Hochberg (FDR <0·05) methods were

used to correct for up to 4 comparisons or more than 4 comparisons, respectively. In addition to this, functional, memory and activation features identified as significantly different between recent and remote TBI were tested for their diagnostic potential using receiver operating characteristic (ROC) curve analysis performed using the pROC package in R [version 1·15·3; https://web.expasy.org/pROC ;(Robin et al., 2011)].

We selected the ΔHLA-DR MFI threshold for the test cohort using remote TBI and tuberculosis groups, and then applied the same threshold to compare the performance of the biomarker between recent and persistent QFT+. The ΔHLA-DR MFI threshold for the TB progressor cohort was defined independently.

Results

M.tb-specific T cell activation peaks during acute M.tb infection.

In Chapter 3, we used tetramers to demonstrate that recent TBI is associated with induction of M.tb-specific CD4+ T_{SCM}, T_{CM} and T_E cell subsets. In addition to measuring memory subsets, we also wanted to determine T cell activation (HLA-DR expression) kinetics associated with recent TBI. Proportions of HLA-DR+ activated M.tb-tetramer+ CD4 T cells were highest at the first QFT+ time point (month 6 since last QFT negative test, when M.tb-tetramer+ cells were detectable) and markedly decreased by 18 months since QFT conversion (Figure 48). Notably, the activation status of bulk memory and T_N CD4+ T cells were unchanged during the follow-up period. M.tb-tetramer+ CD4 T cells were also significantly more activated than bulk memory CD4 T cells, and bulk naïve CD4 T cells were significantly less activated than bulk memory CD4 T cells (Figure 48).

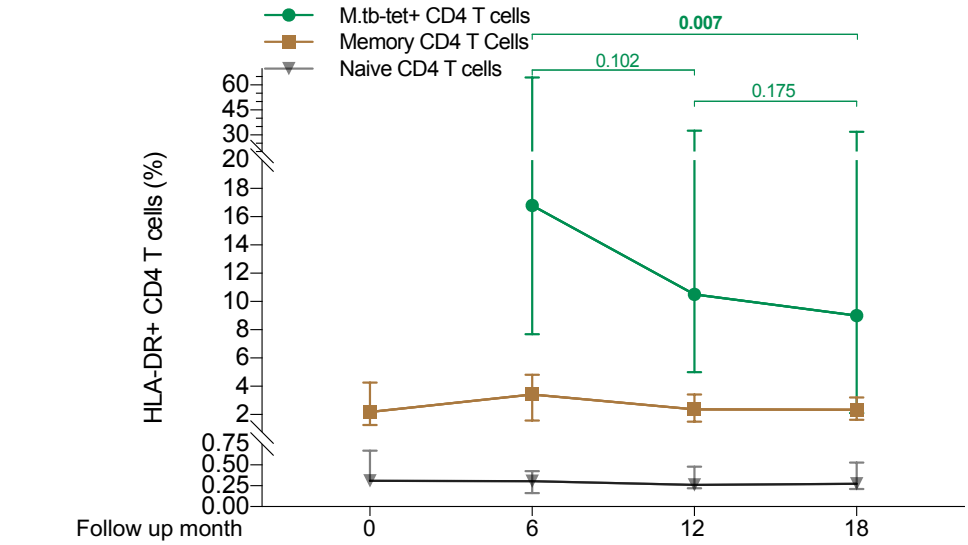

p -values				
M.tb tet+ vs Bulk Memory cells	-	**< 0.001**	**0.001**	**0.009**
M.tb tet+ vs Naïve cells	-	**< 0.001**	**0.001**	**0.002**
Bulk Memory vs Naïve cells	**0.001**	**< 0.001**	**0.001**	**< 0.001**

Figure 48: Acute TBI is associated with high proportions of activated M.tb-specific CD4 T cells which significantly decrease once TBI is established. Proportions of HLA-DR+ M.tb-specific tetramer+ (green), bulk naïve (grey, CD45RA+CCR7+CD27+CD95-) and bulk memory (brown, non-naïve T cells) CD4+ T cells are represented by median (symbol) and IQRs (bars) in recent M.tb infected individuals + (tetramer cohort, Month 0: n = 11; Month 6: n=12; Month 12: n=11; Month 18: n=12,) individuals. Some individuals were stained with more than one tetramer. P-values for were calculated with the Wilcoxon signed-rank test. P-values < 0·05 highlighted in **bold** were considered significant.

Since T cell activation has been suggested to track antigen load, these results suggest that M.tb antigen load is higher during the acute phase of infection compared to once infection is established and bacterial load is at least partially controlled. One limitation of this analysis, and analyses presented in Chapter 3, is the lack of a comparator group to determine how T cell activation and T cell memory subsets differ between recent and remote TBI. We therefore aimed to compare T cell activation and memory/functional subsets in an independent cohort of recent and remote M.tb infected adolescents. In the following experiments cryopreserved PBMC from recent (QFT converters) and remote TBI adolescents were stimulated with mycobacterial antigens, followed by measurement of M.tb-specific T cell functional, activation and memory responses.

Concordance of QFT and PBMC-ICS

To ensure that our methodology sufficiently induced functional responses, we compared detection of IFN-γ by ELISA (QFT assay) and flow cytometry. We observed a very good

correlation in the detection of IFN-γ using the two different sample types and protocols (Figure 49). This data demonstrates that our PBMC stimulation and intracellular cytokine staining protocol sufficiently detected M.tb-specific functional activity, even after 10 years of cryopreservation.

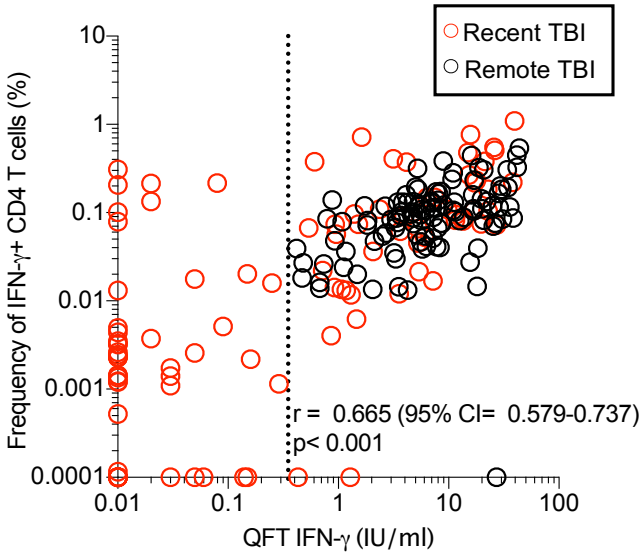

Figure 49: CFP-10/ESAT-6-specific IFN-γ+ CD4 T cells detected by flow cytometry correlate with QFT responses. Immune responses detected in recent (before and after infection) and remote M.tb infected individuals are illustrated by red and black symbols, respectively. Dotted line at 0.35 IU/ml represents the QFT cut-off. r represents the Spearman's correlation coefficient calculated in Prism 7.

Remote TBI is associated with maintenance of polyfunctional M.tb-specific CD4 T cells and a predominantly transitional and effector memory CD4 T cell phenotype.

Serial QFT testing has been a suggested tool for monitoring TBI rates in individuals with high M.tb-exposure such as medical health professionals (Christopher et al., 2011; Hill et al., 2007; Pai et al., 2012). To our knowledge, fluctuations of T cell immune properties such as functional, activation and memory profiles associated with serial testing have not been described. It is assumed that theses immune properties are stable once TBI is established, defined by persistent QFT positive responses. To determine if this is true, we compared T cell functional, activation and memory features in remotely infected, persistently QFT positive individuals (biomarker discovery cohort), a year apart (6 and 18 months during follow up). These individuals were predominantly TST positive throughout follow-up, with a concordance between TST and QFT of 94.55%. We chose 6 months during follow-up because we wanted to ensure that all participants were QFT positive for at least 6 months. As expected, we did not observe a difference in the proportion of CFP-10/ESAT-6- and M.tb lysate-specific IFN-γ+, IL-2+ and TNF+ CD4 T cells measured 1 year apart in remote M.tb infected individuals (Figure

50). In addition to measuring Th1 Cytokines, we also measured expression of CD154 and CD107. CD154, also known as CD40L, is upregulated in functionally reactive cells and can be used to identify antigen-specific cells in the absence of cytokine detection (Frentsch et al., 2005). CD107(a), LAMP-1, is expressed on the surface of cytotoxic cells upon fusion of cytotoxic granules with the outer cell membrane. As a result, CD107 expression is used as a proxy for cytotoxic capacity of cells (Betts et al., 2003). Similar to Th1 cytokine kinetics, frequencies of CD154+ CD4 M.tb-specific T cells were not different throughout the follow-up period. However, we consistently detected low to non-detectable levels of CD107-expressing M.tb-specific CD4 T cells throughout the study follow up (Figure 50). These results demonstrate that as observed with serial QFT positive test results, functionally reactive CD4 T cells, including IFN-γ-independent responses, are maintained at steady state during remote TBI.

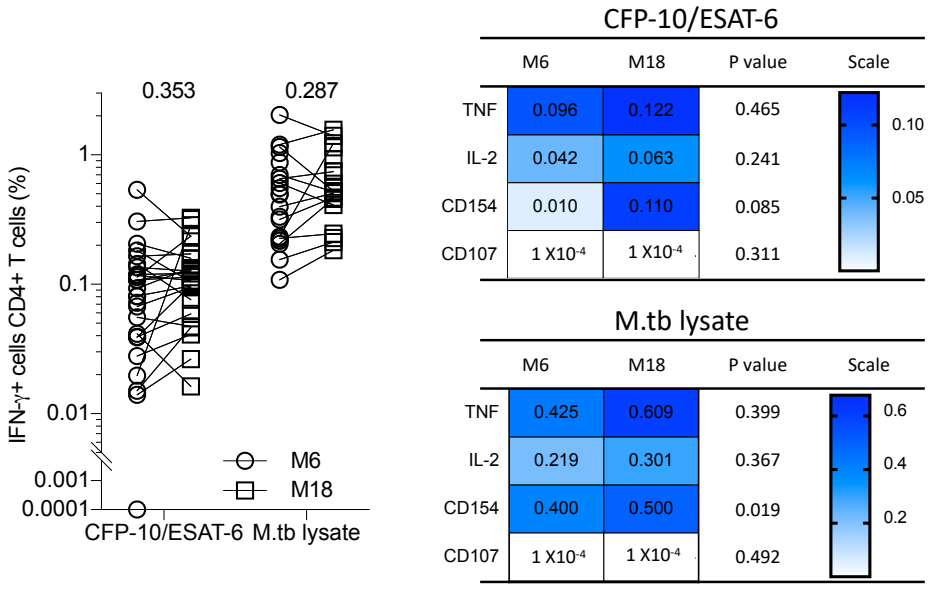

Figure 50: Remote TBI is associated with persistent detection of IFN-γ+ and IFN-γ-independent functional CD4 T cell responses. Graph depicts frequency of background subtracted IFN-γ+ CD4 T cells detected in responses to CFP-10/ESAT-6 pp (Month 6: n=27, Month 18: n=25) and M.tb lysate stimulation (Month 6: n=21, Month 18: n=19) in remote M.tb infected individuals. Tables depicts median frequencies of background subtracted TNF+, IL-2+, CD154+ and CD107+ M.tb-specific CD4 T cells. P-values were calculated with the Wilcoxon-signed rank test, p-values < 0.05 were considered significant.

Given these results, we wanted to determine if longitudinal M.tb-specific CD4 T cell polyfunctional co-expression patterns were also consistent in remote M.tb infected individuals. We utilised COMPASS to determine antigen-specific subsets, of the 31 potential cytokine co-expressing subsets, 14 and 21 of these were detectable in response to CFP-10/ESAT-6 and M.tb lysate stimulation, respectively (Figure 51). M.tb-specific polyfunctional

CD4 T cell responses were predominantly CD107-, however, we did detect CD107 only expressing M.tb lysate-specific CD4 T cells at Month 6 only but not in CFP-10/ESAT-6-specific CD4 T cells. We detected very low levels M.tb-specific CD154±IL-2+ CD4 T cells, with majority of cells (≥ 60%) co-expressing CD154+ IL-2± IFN-γ±TNF+ subsets (Figure 51).

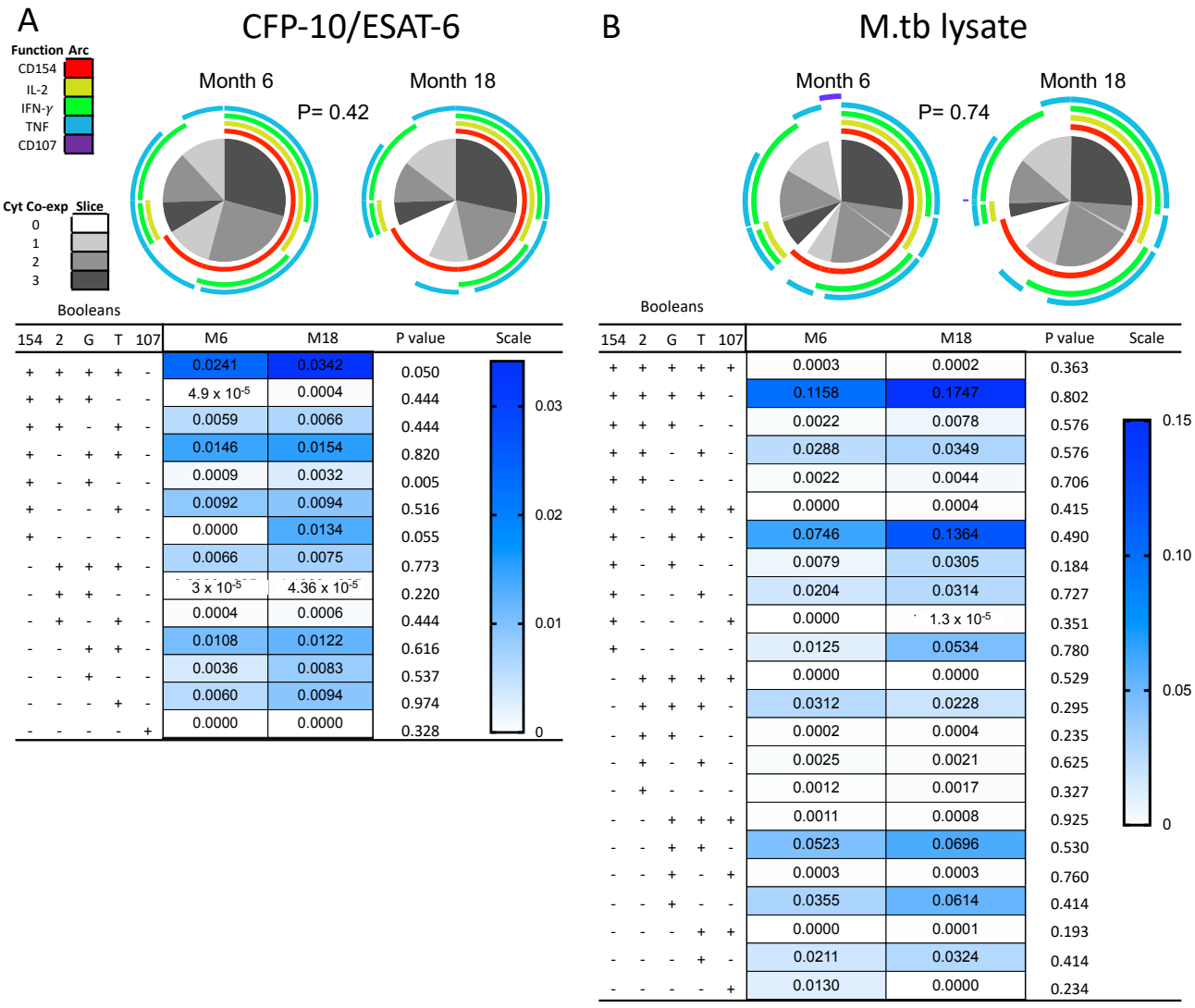

Figure 51: Polyfunctional cytokine co-expression capacity is stable during remote TBI. Pie and tables depict median CD154, IL-2, IFN-γ, TNF and CD107 co-expression of (A) CFP-10/ESAT-6-specific (Month 6: n=27, Month 18: n=25) and (B) M.tb lysate-specific (Month 6: n=21, Month 18: n=19) CD4 T cells. Arcs in the pie chart denote co-expression pattern for each pie slice. P-value for pies were calculated using nonparametric pairs permutations comparing the overall distribution between pies. Statistical analysis of individual function co-expression subset was conducted as in Figure 50.

To determine if the activation and memory profiles of M.tb-specific CD4 T cells were also stable during follow up, we compared expression of HLA-DR and co-expression of memory markers in responders only. Overall, M.tb-specific CD4 T cells consistently expressed low

levels of HLA-DR throughout follow up (Figure 52), suggesting that these individuals had stable low levels of mycobacterial replication, if any.

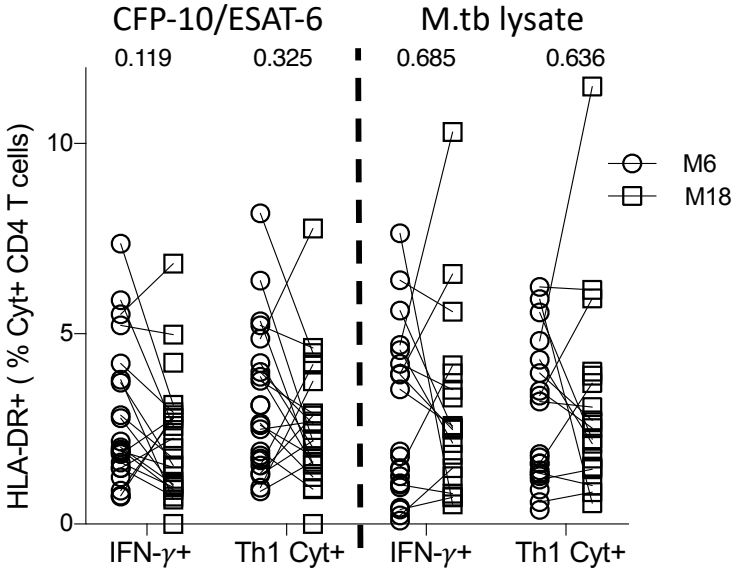

Figure 52: Remote TBI is associated with low levels of CD4 T cell activation. Proportions of HLA-DR+ IFN-γ+ or Th1 cytokine+ CD4 T cells were measured in response to CFP-10/ESAT-6 (Month 6: n=24, Month 18: n=22) or M.tb lysate stimulation (Month 6: n=21, Month 18: n=19) at 6 (circles) and 18 (boxes) months during follow up. Statistical analysis was conducted as in Figure 50.

Comparison of memory profiles demonstrated that CFP-10/ESAT-6-specific CD4 T cells were predominantly T_{TM} (CD45RA-CCR7-CD27+) and T_E (CD45RA-CCR7-CD27-) cells (Figure 53 A), with T_{TM} accounting for approximately half of total CFP-10/ESAT-6-specific CD4 T cells. Similar distribution of memory subsets were observed in M.tb lysate-specific CD4 T cells, however, we noted lower proportions of T_{SCM} and T_{TTM} subsets and higher proportions of T_E subsets that expressed KLRG1 compared to CFP-10/ESAT-6-specific CD4 T cells (Figure 53). Unlike CFP-10/ESAT-6 stimulation, M.tb lysate contains multiple antigens including those that are present in other *mycobacteria sp*.. Thus, detection of relatively high proportions of differentiated KLRG1+ T_E cells suggests that these individuals have had long term exposure to mycobacterial antigens, which may also include cross-reactive BCG responses resulting in increased T cell differentiation. Based on these results, we can conclude that remote or sustained TBI, defined by serial QFT positive tests is associated with a predominantly polyfunctional IFN-γ±TNF±, T_{TM} and T_E memory subsets. Minimal contribution of IL-2 only producing M.tb-specific CD4+ T cells and low sustained levels of T cell activation suggests a stable low level mycobacterial burden. For further comparisons, we shall utilise results obtained at Month 18 of follow up.

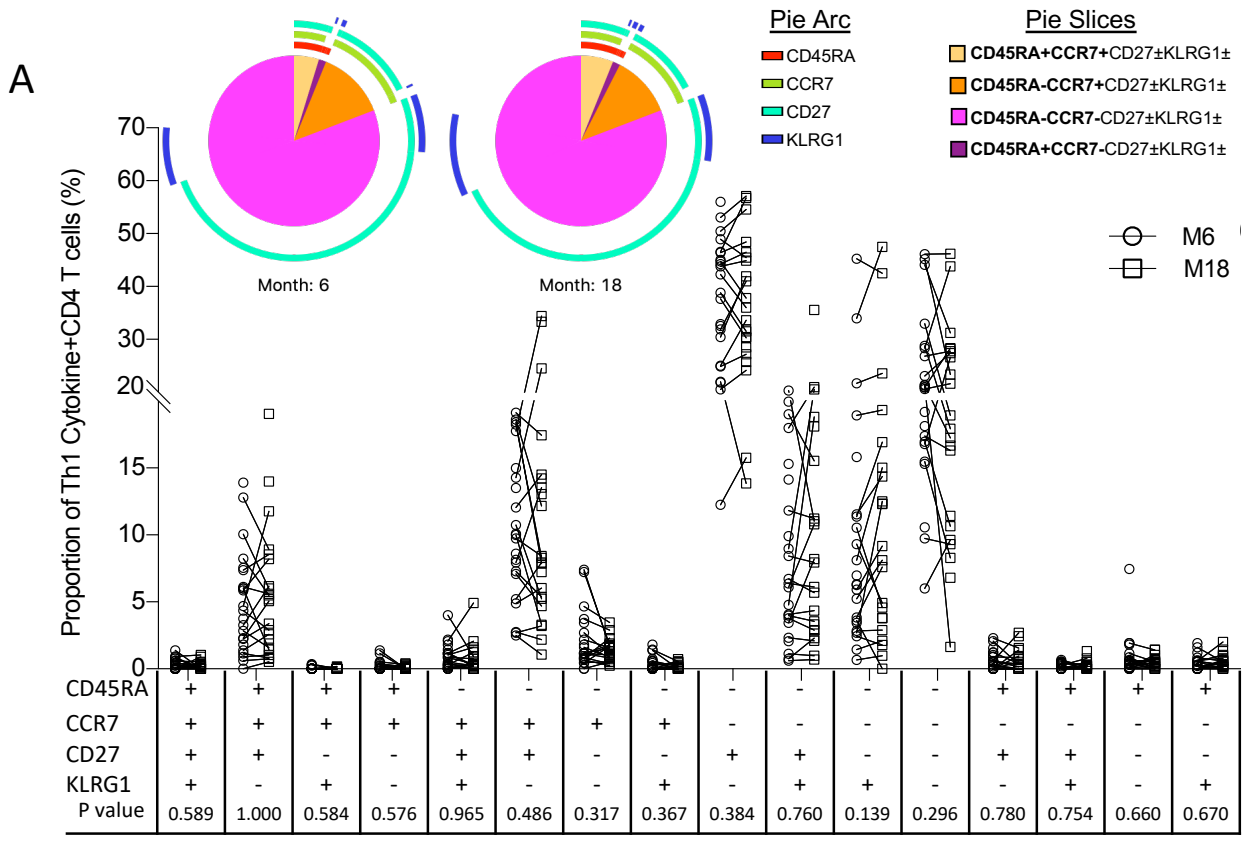

B

Booleans				M6	M18	P value
RA	R7	27	G1			
+	+	+	+	0.12	0.12	0.969
+	+	+	-	1.71	2.21	0.295
+	+	-	+	0.00	0.00	0.106
+	+	-	-	0.00	0.03	1.000
-	+	+	+	0.57	0.33	0.724
-	+	+	-	9.70	6.71	0.043
-	+	-	+	0.15	0.05	0.415
-	+	-	-	1.32	0.95	0.364
-	-	+	+	9.77	11.15	0.036
-	-	+	-	29.74	29.24	0.944
-	-	-	+	16.07	19.22	0.036
-	-	-	-	23.00	24.19	0.727
+	-	+	+	0.10	0.10	0.625
+	-	+	-	0.20	0.28	0.456
+	-	-	+	0.34	0.32	0.367
+	-	-	-	0.26	0.10	0.021

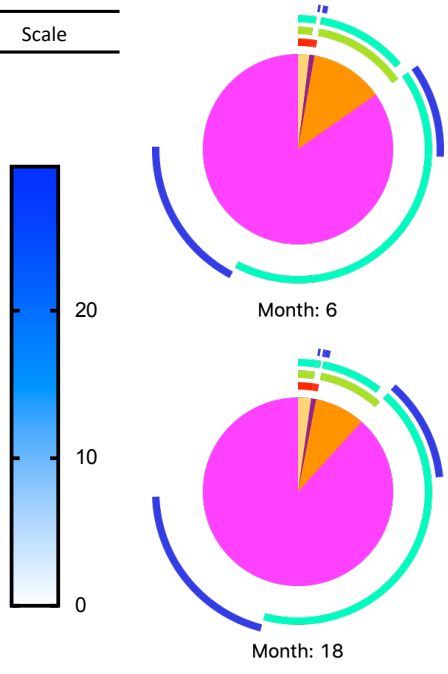

Figure 53: T_{TM} and T_E cells are the predominant memory phenotype during remote TBI. Pies and tables depict median co-expression of CD45RA (RA), CCR7 (R7), CD27 (27) and KLRG1 (G1) subsets by (A) CFP-10/ESAT-6-specific (Month 6: n=24, Month 18: n=22) and (B) M.tb lysate-specific (Month 6: n=21, Month 18: n=19) CD4 T cells in remote M.tb infected individuals during follow up. Arc in the pie chart denote co-expression pattern for each pie slice. (A) Graphical representation of CFP-10/ESAT-6 -specific CD4 T cell memory subsets detected in each participant at 6 (circles) and 18 (boxes) months during follow. Statistical analysis was conducted as in Figure 50.

Recent TBI is associated with higher T cell activation but lower T cell functional differentiation compared to remote TBI.

Before we compared how functional, memory and activation profiles changed upon TBI, we first wanted to confirm that QFT conversion was associated with an increase in IFN-γ specific CD4 T cell responses. Even though TST was not used to define recent TBI, TST and QFT responses were highly concordant (proportion of agreement = 88.14%; Kappa = 0.763).

Frequencies of CFP-10/ESAT-6-specific IFN-γ+ CD4 T cells were undetectable or very low prior to TBI, which significantly increased upon infection (Figure 54A). Few individuals who were TST negative showed relatively high frequencies of CFP-10/ESAT-6-specific IFN-γ+ CD4 T cells before QFT conversion, possibly suggesting that flow cytometry is more sensitive than QFT in detecting low responses. Frequencies of IFN-γ+ CD4+ M.tb-specific T cell responses in recent M.tb infected individuals were range with responses detected in remote M.tb infected individuals. (Figure 54 A). Similar IFN-γ+ CD4 T cell kinetics were also observed in response to M.tb lysate stimulation, with lowest detection prior to TBI, and similar levels of IFN-γ+ CD4 T cells detected in recent and remote TBI. As expected, we detected very low frequencies of IFN-γ-independent (TNF, IL-2 and CD154) responses prior to TBI, which significantly increased upon TBI and were observed in range with frequencies of M.tb-specific CD4 T cell responses detected in remote M.tb infected individuals (Figure 54A).

We next wanted to determine the kinetics of functionality and polyfunctionality scores associated with recent TBI. Consistent with individual cytokine expression profiles, CFP-10/ESAT-6 specific functionality and polyfunctionality scores were very low prior to TBI and increased significantly upon recent infection to levels that were similar to those in individuals with remote TBI (Figure 54B). We also observed similar functionality and polyfunctionality score kinetics in M.tb lysate-specific CD4 T cells as CFP-10/ESAT-6-specific CD4 T cells (Figure 54B).

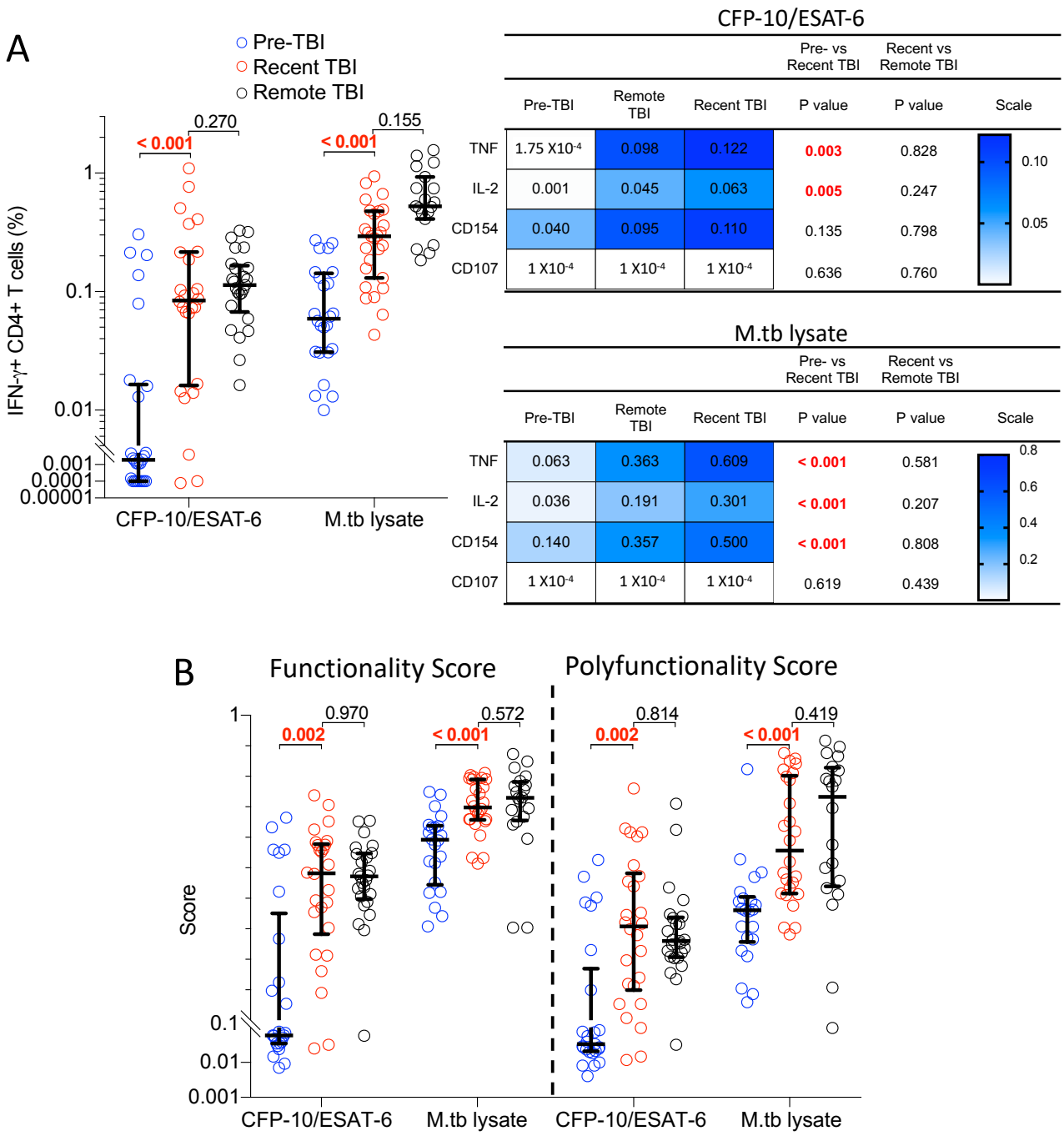

Figure 54: Recent TBI is associated with induction of functional responses which are observed in similar ranges as remote TBI. (A) Frequency of background subtracted functional CD4 T cells detected in response to CFP-10/ESAT-6 pp and M.tb lysate stimulation before (Pre-TBI, blue symbols, CFP-10/ESAT-6: n=26; M.tb lysate: n= 24), after (recent TBI, red symbols, CFP-10/ESAT-6: n=26; M.tb lysate: n= 27) and during remote TBI (black symbols, CFP-10/ESAT-6: n=25; M.tb lysate: n= 19) are shown for IFN-γ+ (graphs) and tables for TNF+, IL-2+, CD154+ and CD107+ CD4 T cell expression. Tables depicts median frequencies of cytokine-producing CD4 T cells. (B) CD4 T cell FS and PFS detected in response to CFP-10/ESAT-6 pp and M.tb lysate stimulation during Pre-TBI, recent TBI and remote TBI are shown. P-values were calculated with the Wilcoxon-signed rank test or Mann-Whitney test, for paired (Pre- vs Recent TBI) and unpaired (Recent vs Remote TBI) comparisons, respectively, and corrected for multiple comparison using the Benjamini–Hochberg method with a false discovery rate (FDR) of 0.05. P-values highlighted in **bold** and red were considered significant.

T cells are known to change their functional, memory and activation capacity depending on antigen burden, discussed in detail in the introduction. Our research group, recently defined a single measurement of functional differentiation, functional differentiation score, that we propose can distinguish between infection states associated with different levels of M.tb burden (Moguche et al., 2017). We thus compared the distribution of cytokine co-expressing Th1 subsets, functional differentiation score and memory T cell subsets in individuals in the biomarker discovery cohort. Since the majority of CFP-10/ESAT-6-specific CD4 T cells detected prior to M.tb infection were low and did not meet our responder criteria, we focused our longitudinal analyses of recent M.tb infected responders on M.tb lysate-specific CD4 T cells. On the other hand, cross-sectional comparison between recent and remote TBI responders was performed on both CFP-10/ESAT-6-specific and M.tb lysate-specific CD4 T cell responses. Relative proportions of M.tb lysate-specific CD4 T cells expressing only IL-2 or TNF were higher prior to than after TBI, while proportions of IFN-γ-TNF+IL-2+ and IFN-γ+TNF±IL-2± subsets were not different before and after TBI (Figure 55A). Higher proportions of IFN-γ-TNF+IL-2+ but lower proportions of IFN-γ+TNF+IL-2- M.tb lysate-specific CD4 T cells were detected in recent TBI compared to remote TBI. This resulted in lower Th1 functional differentiation, measured by functional differentiation score, in recent TBI compared with remote TBI (Figure 55A). In contrast, CFP-10/ESAT-6-specific Th1 cytokine co-expression profiles and functional differentiation scores were not different between recent and remote TBI, with IFN-γ+TNF+IL-2+ and IFN-γ+TNF+ accounting for just over half of the total Th1+ responses (Figure 55A).

Analysis of M.tb lysate-specific CD4 T cell memory subsets showed that recent TBI was associated with a decrease in KLRG-1- T_{SCM} and T_{CM} cells, and an increase in KLRG-1- T_E cells compared to the pre-infection (QFT-) time-point, indicative of increased antigen exposure (Figure 55B). Memory phenotypes of M.tb-specific responses, regardless of stimuli, were not different between recent and remote TBI, with T_{TM}/T_E cells being the predominant T cell memory subsets (Figure 55B).

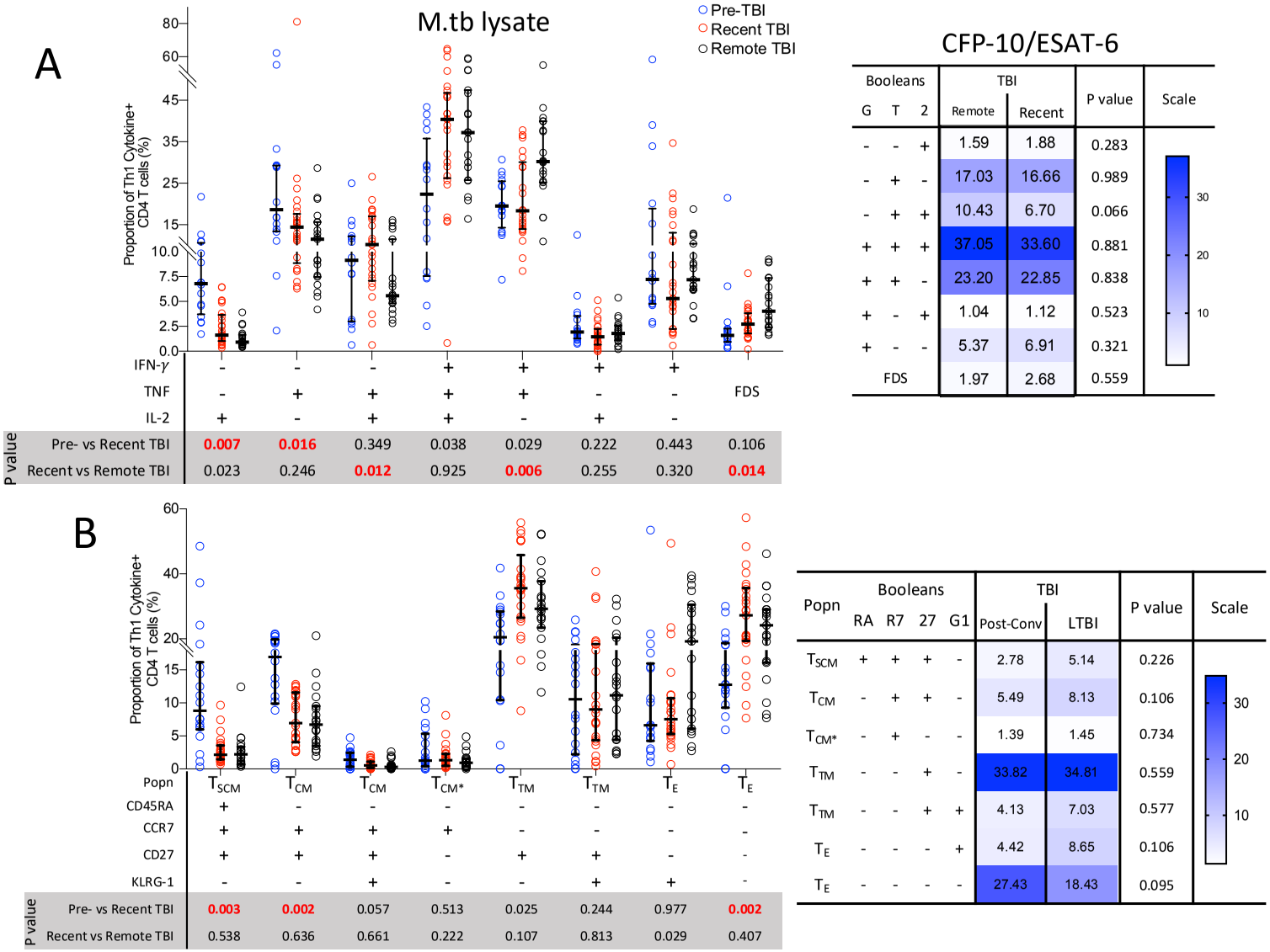

Figure 55: Recent TBI is associated with a decrease in less differentiated T cell subsets, and predominantly differentiated polyfunctional and memory T cell subsets which are similar between recent and remote TBI. Proportions of (A) M.tb lysate-specific (graph) and CFP-10-ESAT6-specific (table) Th1 polyfunctional and (B) memory profiles detected before (Pre-TBI, blue symbols, M.tb lysate, n= 16), after (recent TBI, red symbols, CFP-10/ESAT-6, n= 18; M.tb lysate, n=26), and during remote TBI (black symbols, CFP-10/ESAT-6, n= 22; M.tb lysate, n=19). Statistical analysis was conducted as in Figure 54.

Results above clearly illustrate a relationship between cytokine expression and memory phenotypes and suggest that combined analysis of these features may be informative. We therefore used CITRUS to identify cell subsets that were expressed at significantly different levels upon acquisition of TBI, and between recent and remote TBI, based on expression of CD45RA, CCR7, CD27, KLRG1, IFN-γ, TNF and IL-2. We did not include CD107 and CD154 in this analysis, due to high non-specific background expression of these markers. CXCR3 and HLA-DR were also excluded from this analysis because neither marker contributed to cell cluster definition during the optimisation of the CITRUS workflow.

CITRUS analyses identified 13 M.tb lysate-specific CD4 T cell clusters that were expressed at significantly different abundance levels upon recent TBI, and 4 M.tb lysate-specific and 3 CFP-10/ESAT-6-specific CD4 T cell clusters that were significantly different between recent and remote TBI (FDR < 0.05; Table 25; Appendix 1-3).

Table 25: Number of differentially expressed clusters identified between 2 groups using CITRUS.

Ag Specificity	TBI Comparison	Total Clusters	Differentially expressed (DE) clusters	DE distinct populations	Cell populations confirmed by Manual Gating in FlowJo
M.tb lysate	Pre- vs Recent	29	13	6	6
	Recent vs Remote	32	4	2	2
CFP-10/ESAT-6		32	3	3	2

Before confirming cluster identity by manual gating, we compared histogram expression patterns of differentially expressed clusters to ensure that there were no duplicate populations. This quality control step reduced the number of distinct differentially expressed populations that were confirmed using manual gating in Flow Jo (Table 26; Figure 56). Over 90% of cells in Cluster 2570 were CD45RA+ memory cells, however, proportions of CD45RA+ memory cells constitute <10% of total memory cells. We therefore separated cluster 2570 into CD45RA+ and CD45RA- cell subsets. We noted that clusters 2566 and 2559; and 2238 and 2219 had similar expression patterns and could be defined as the same populations (Table 26, Figure 56). Upon confirmation of CITRUS cluster composition, we manually gated cell subsets in all responders, and performed confirmatory statistical tests on manually gated data.

Table 26: Memory-cytokine expression profile of differentially expressed clusters between 2 groups.

Ag-specificity	TBI Comparison	Cluster	CD45RA	CCR7	CD27	KLRG1	IFN-γ	TNF	IL-2
M.tb lysate	Pre- vs Recent	2565	40.6	**82.7**	**81.2**	**8.27**	**8.27**	**14.3**	**99.2**
		2570	**94.8**	**99.3**	**97.4**	**10.5**	**28.8**	**85.6**	**17**
		2566	**0.6**	**15**	55.7	**3.59**	**90.4**	**98.2**	**93.4**
		2559	**0**	**2.79**	49.2	**0**	**100**	**96.6**	**82.7**
		2567	**0**	**4.78**	53	**3.04**	**95.7**	**91.3**	**3.04**
		2551	**0**	**3.33**	**73.8**	**74.8**	**100**	**100**	**98.1**
	Recent vs Remote	2694	**3.83**	**2.09**	36.6	50.2	**100**	**99.3**	**1.05**
		2681	**0**	**0**	**33.1**	**84.5**	**99.3**	**66.9**	**5.41**
CFP-10 /ESAT-6		2219	**0**	**9.46**	39.2	**0**	**0**	**100**	**9.46**
		2238	**0.51**	**13.1**	51	**8.08**	**8.08**	**99.5**	**4.55**
		2243	**0.28**	**33.8**	**70.2**	**4.55**	**4.55**	**99.7**	**3.12**

Numbers denote expression of each marker as percentage (%) of total M.tb-specific CD4 T cells in each cluster. Markers expressed in less than 35% and more than 65% of total M.tb-specific cells are denoted in **blue** and **red**, respectively, and were used to define the cluster using manual gating. These arbitrary cut-offs were chosen because it enabled manual gating of clusters that were most similar to the histogram depicting cluster composition.

Compared to the pre-infection (QFT-) timepoint, recent TBI was associated with a decrease in M.tb lysate-specific, early-differentiated IL-2-only T_{SCM}/T_{CM} (cluster 2565) and TNF-only T_{SCM}/T_{CM} (cluster 2570) cell subsets, and an increase in proportions of IFN-γ+TNF+IL-2+ (cluster 2559/66) and IFN-γ+TNF+ T_E (cluster 2567) cells (Figure 56 A). We also observed lower proportions of M.tb lysate-specific KLRG-1+IFN-γ+TNF+IL-2- (cluster 2681) T_E cells in recent TBI compared remote TBI (Figure 56A). Despite detecting differences in abundance levels of CITRUS clusters 2551 (pre- *versus* recent TBI) and 2219/43 (recent *versus* remote TBI), proportions of clusters were not different when manually gated (Figure 56).

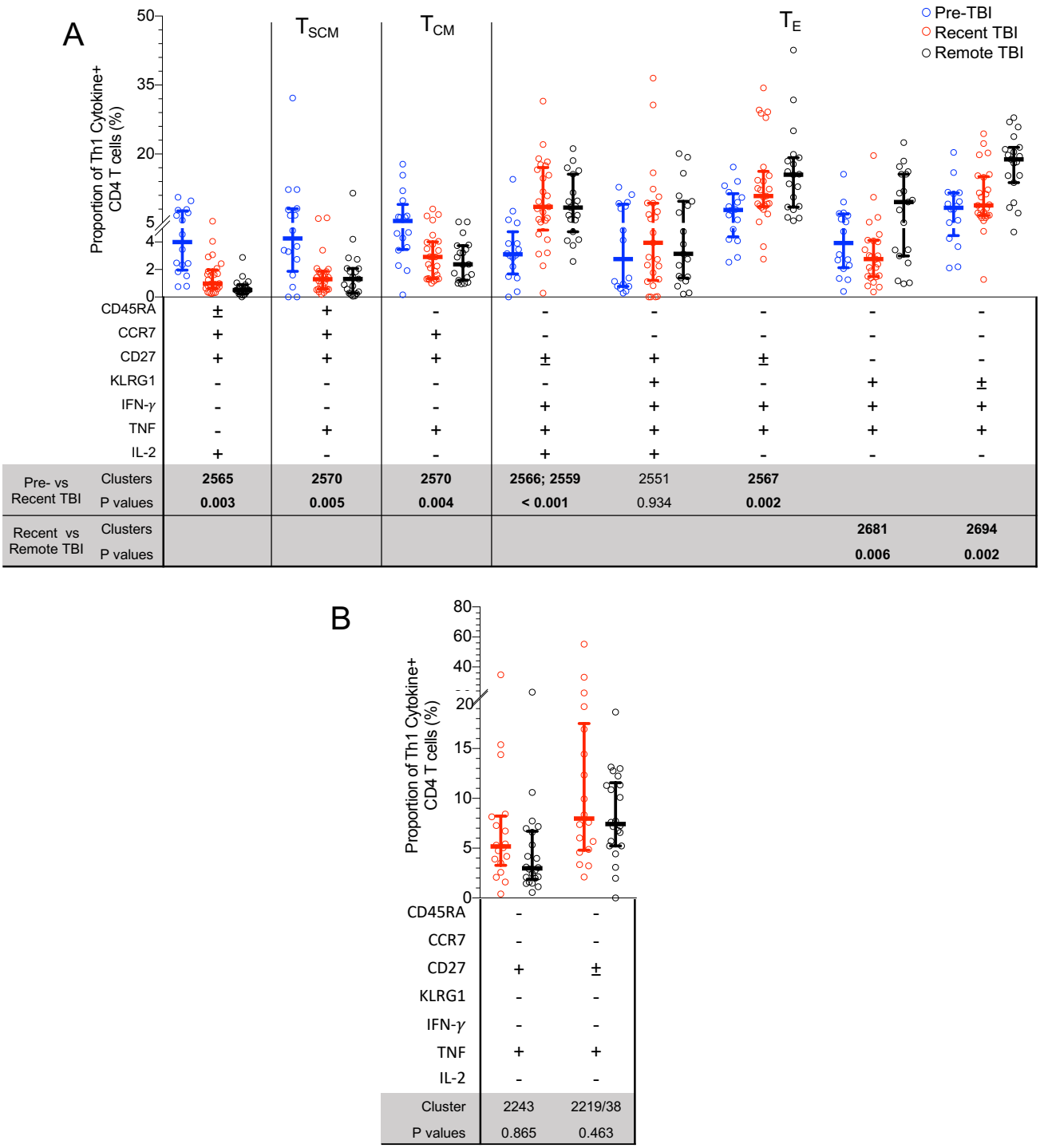

Figure 56: Recent TBI in associated with a decrease in less differentiated IFN-γ+-independent T_{SCM} and T_{CM} subsets, and an increase in T_E polyfunctional T cell subsets. Proportions of (A) M.tb lysate-specific and (B) CFP-10-ESAT6-specific memory/cytokine co-expression subsets before (Pre-TBI, blue symbols, M.tb lysate, n= 16), after (recent TBI, red symbols, CFP-10/ESAT-6, n= 18; M.tb lysate, n=26), and during remote TBI (black symbols, CFP-10/ESAT-6, n= 22; M.tb lysate, n=19). Statistical analysis was conducted as in Figure 54, clusters and p-values highlighted in **bold** were considered significantly different.

We next investigated T cell activation kinetics associated with acquisition of TBI and compared individuals with recent TBI to those with remote TBI. Acquisition of TBI (pre- *versus*

recent TBI) was associated with a significant increase in both activated (HLA-DR+) IFN-γ+ and total Th1 cytokine+ M.tb-specific CD4 T cells (Figure 57A), which were also higher in recent TBI than in remote TBI (Figure 57A). Longitudinal analysis of all available time points showed that CFP-10/ESAT-6-specific CD4 T cell activation significantly decreased by 12 months post QFT conversion (Figure 57B).

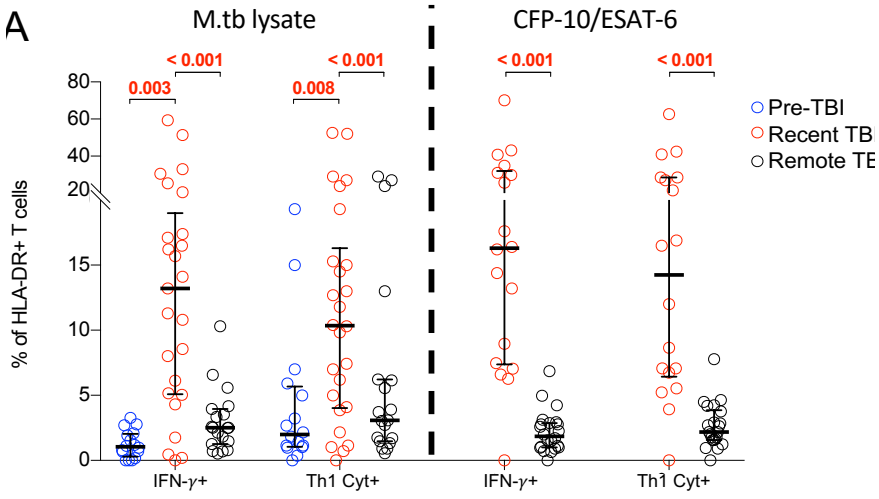

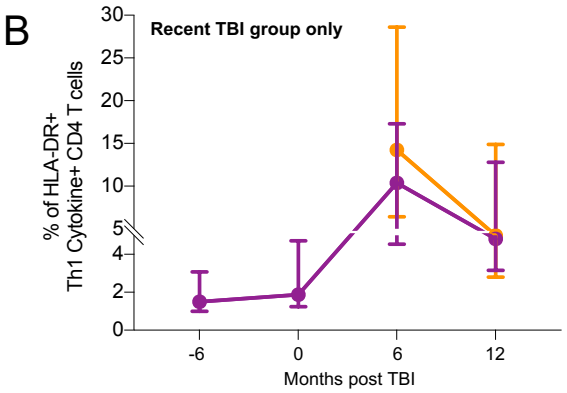

P-values

Pair-wise comparison	M.tb lysate	CFP-10/ESAT-6
-6 vs 0 months post TBI	0.791	-
0 vs +6 months post TBI	**0.002**	-
+6 vs +12 months post TBI	0.064	**0.002**

Figure 57: TBI is associated with higher levels T cell activation compared with remote TBI. (A) Graphs depict proportion of HLA-DR+ CFP-10/ESAT-6- and M.tb lysate-specific IFN-γ+ or Total Th1+ (IFN-γ±TNF±IL-2±) cytokine CD4 T cells before (Pre-TBI, blue symbols, M.tb lysate: n= 16), after (recent TBI, red symbols, CFP-10/ESAT-6: n=18; M.tb lysate: n= 26), and during remote TBI (black symbols, CFP-10/ESAT-6: n=22; M.tb lysate: n=19). Statistical analysis was conducted as in Figure 54. (B) Graphs depict proportions of HLA-DR+ M.tb-specific Total Th1 cytokine+ (IFN-γ±TNF±IL-2±) CD4 T cells represented by median (symbol) and IQRs (bars) in recent QFT+ (CFP-10/ESAT-6, orange, +6 months post TBI: n=18; +12 months post TBI: n=19; M.tb lysate, purple, -6 months post TBI: n=16, 0 months post TBI: n=17; +6 months post TBI: n=25; +12 months post TBI: n=23). P-values were calculated using the Wilcoxon signed-rank test. P-values were corrected for multiple comparison using the Bonferroni method with. P-values <0.0167 highlighted in **bold text** were considered significant.

Altogether, these results confirm that recent TBI was associated with lower proportions of CD4+ IFN-γ- T_{SCM}, T_{CM} and early differentiated memory cells, and higher proportions of polyfunctional IFN-γ+ T_E cells and activated CD4 T cells, compared to the respective QFT- time point in each individual. Memory and functional profiles induced upon early infection were sustained at stable proportions once M.tb infection is established, except for less abundant activated M.tb-specific CD4 T cells and more abundant highly differentiated KLRG-1+IFN-γ+TNF+ T_E CD4 T cells during remote TBI compared to recent TBI.

Potential biomarkers of recent M.tb infection

To the best of our knowledge, only one biomarker of recent TBI, relative proportions of TNF-only (IFN-γ-IL-2-) T_E (CD45RA-CCR7-CD127-) CD4 T cells, has previously been reported as a diagnostic biomarker for differentiating between recent and remote TBI (Halliday et al., 2017). We therefore aimed to evaluate the performance of this biomarker in our cohort. Because our flow cytometry panel did not include CD127, we defined this subset as TNF-only, CD45RA-CCR7- T_E memory cells. Acquisition of TBI (pre- *versus* recent TBI) was associated with an increase in proportions of TNF-only T_E memory cells, however, unlike results presented by Halliday and colleagues (Halliday et al., 2017), proportions of these cells, regardless of stimulus, were not different between recent and remote TBI (Figure 58A).

We next investigated the diagnostic performance of functional, memory and activation profiles that were significantly different between recent and remote TBI in our dataset. We performed ROC analysis to assess the performance of HLA-DR+ IFN-γ+ and Th1 cytokine+ M.tb-specific CD4 T cells (regardless of stimulus), M.tb-lysate-specific functional differentiation score, and proportions of KLRG-1+ IFN-γ+TNF+IL-2- T_E (CD45RA-CCR7-CD27-) CD4 T cells to discriminate between recent and remote TBI. We did not perform ROC analysis on differentially expressed CD4 T cell cytokine co-expression profiles (IFN-γ-TNF+IL-2+, IFN-γ+TNF+IL-2-, IFN-γ+TNF-IL-2-) because these were already included in the definition of either the functional differentiation score or KLRG-1+ IFN-γ+TNF+IL-2- T_E cell population. Proportions of HLA-DR+ M.tb-specific (IFN-γ+ or Th1 cytokine+) CD4 T cells demonstrated very good discrimination between recent and remote TBI, achieving area under the receiver operator curve (AUROCs) above 0·8 (Figure 58B). By comparison, the highly differentiated KLRG-1+ IFN-γ+TNF+IL-2- T_E cell population and functional differentiation score demonstrated

moderate discriminatory performance; AUROCs for these comparisons were below 0·8 (Figure 58C).

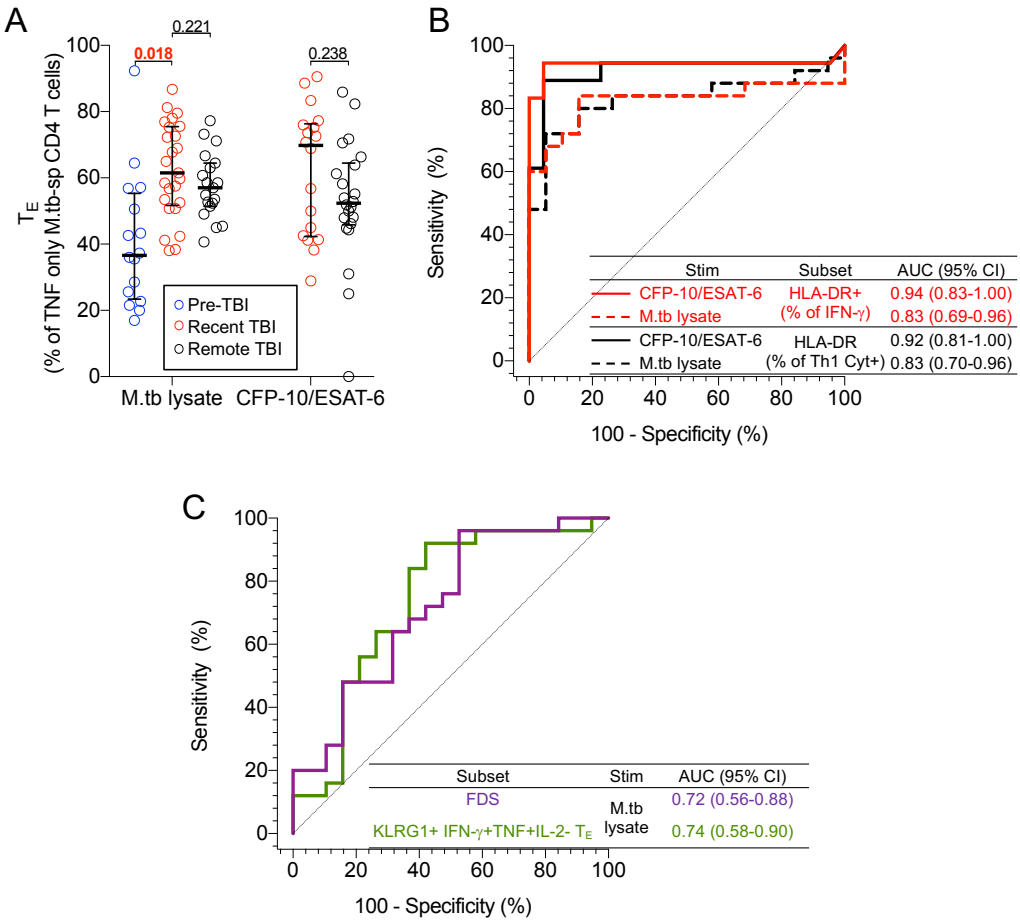

Figure 58: T cell activation is a potential biomarker of recent TBI. (A) Proportions of T_E TNF only M.tb lysate-specific and CFP-10/ESAT-6-specific CD4 T cells detected before (Pre-TBI, blue symbols, M.tb lysate , n= 16), after (recent TBI, red symbols, CFP-10/ESAT-6, n= 18; M.tb lysate, n=26) and during remote TBI (black symbols, CFP-10/ESAT-6, n=22; M.tb lysate, n=19). ROC analysis of the diagnostic potential of M.tb-specific CD4 T cells subsets: (B) IFN-γ+ and Th1+ cytokine+ T cell activation and (C) polyfunctional-memory subsets. All populations are significant defined by a $p < 0.05$ and 95% CI that do not cross 0.5.

We also compared the discriminatory performance between recent and remote TB of M.tb-specific HLA-DR+ IFN-γ+TNF+ CD4 T cells (Table 27), an adaptation of a previously published biomarker with excellent discrimination between tuberculosis cases and healthy controls and which also showed promise as a tuberculosis treatment monitoring biomarker since it decreased significantly upon successful tuberculosis therapy (Musvosvi et al., 2018). Biomarkers based on HLA-DR expression by CFP-10/ESAT-6-specific CD4 T cells had significantly higher AUROCs than those based on cytokine co-expression profiles or memory marker expression on M.tb lysate-specific CD4 T cells (Table 27). On the other hand, discriminatory AUROCs of biomarkers based on HLA-DR expression regardless of M.tb stimulus or M.tb-specific CD4 T cell denominator were not different (p-value > 0·05),

suggesting that neither subset had superior diagnostic potential over the other. Additionally, AUROCs of biomarkers defined on M.tb lysate-specific activation and functional differentiation were all similar (p-value > 0·05). Thus, based on these results, CFP-10/ESAT-6 antigen-specific T cell HLA-DR expression was identified as the best biomarker of recent M.tb infection in this dataset.

Table 27: AUROC comparison of potential biomarkers of recent TBI

CD4 T cell Subset 1			CD4 T cell Subset 2			Roc test p-value
Subset	***Stim***	***AUC (95% CI)***	***Subset***	***Stim***	***AUC (95% CI)***	
Significant AUC comparison results						
HLA-DR % of IFN-γ+	P10ES6	0·94 (0·83-1.00)	FDS	M.tbL	0·72 (0·56-0·88)	**0·018**
			KLRG- 1+ IFN-γ+TNF+IL-2- T_E		0·74 (0·58-0·90)	**0·035**
HLA-DR % of IFN-γ+TNF+		0·94 (0·84-1.00)	FDS		0·72 (0·56-0·88)	**0·014**
			KLRG- 1+ IFN-γ+TNF+IL-2- T_E		0·74 (0·58-0·90)	**0·030**
HLA-DR % of Th1 Cyt+		0·92 (0·81-1.00)	FDS		0·72 (0·56-0·88)	**0·039**
Non-significant AUC comparison results						
HLA-DR% of IFN-γ+	P10ES6	0.94 (0.83-1.00)	HLA-DR % of IFN-γ+	M.tbL	0.83 (0.69-0.96)	0.198
			HLA-DR % of IFN-γ+TNF+	P10ES6	0.94 (0.84-1.00)	0.332
			HLA-DR % of IFN-γ+TNF+	M.tbL	0.82 (0.68-096)	0.197
			HLA-DR % of Th1 Cyt+	P10ES6	0.92 (0.81-1.00)	0.227
			HLA-DR % of Th1 Cyt+	M.tbL	0.83 (0.70-0.96)	0.201
	M.tbL	0.83 (0.69-0.96)	HLA-DR % of IFN-γ+TNF+	P10ES6	0.94 (0.84-1.00)	0.180
			HLA-DR % of IFN-γ+TNF+	M.tbL	0.82 (0.68-096)	1.000
			HLA-DR % of Th1 Cyt+	P10ES6	0.92 (0.81-1.00)	0.295
			HLA-DR % of Th1 Cyt+	M.tbL	0.83 (0.70-0.96)	0.762
			IFN-γ+TNF+IL-2- KLRG- 1+ T_E	M.tbL	0.74 (0.58-0.90)	0.333
			FDS	M.tbL	0.72 (0.56-0.88)	0.272
HLA-DR % of IFN-γ+TNF+	P10ES6	0.94 (0.84-1.00)	HLA-DR % of IFN-γ+TNF+	M.tbL	0.82 (0.68-096)	0.197
			HLA-DR % of Th1 Cyt+	P10ES6	0.92 (0.81-1.00)	0.188
			HLA-DR % of Th1 Cyt+	M.tbL	0.83 (0.70-0.96)	0.182
	M.tbL	0.82 (0.68-096)	HLA-DR % of Th1 Cyt+	P10ES6	0.92 (0.81-1.00)	0.294
			HLA-DR % of Th1 Cyt+	M.tbL	0.83 (0.70-0.96)	0.767
			IFN-γ+TNF+IL-2- KLRG- 1+ T_E	M.tbL	0.74 (0.58-0.90)	0.339
			FDS	M.tbL	0.72 (0.56-0.88)	0.283
HLA-DR % of Th1 Cyt+	P10ES6	0.92 (0.81-1.00)	HLA-DR % of Th1+	M.tbL	0.83 (0.70-0.96)	0.302
			KLRG- 1+ IFN-γ+TNF+IL-2- T_E	M.tbL	0·74 (0·58-0·90)	0·062
HLA-DR % of Th1 Cyt+	M.tbL	0.83 (0.70-0.96)	IFN-γ+TNF+IL-2- KLRG- 1+ T_E	M.tbL	0.74 (0.58-0.90)	0.333
			FDS	M.tbL	0.72 (0.56-0.88)	0.252
IFN-γ+ TNF+IL-2- T_E		0.77 (0.62-0.92)	IFN-γ+TNF+IL-2- KLRG- 1+ T_E	M.tbL	0.74 (0.58-0.90)	0.636
			FDS	M.tbL	0.72 (0.56-0.88)	0.540
IFN-γ+TNF+IL-2- KLRG- 1+ T_E		0.74 (0.58-0.90)	FDS	M.tbL	0.72 (0.56-0.88)	0.818

Abbreviations: Stimulation: Stim; CFP-10/ESAT-6: P10ES6; M.tb lysate: M.tbL; FDS: functional differentiation score AUROC (AUC) comparisons that were considered significantly different based a ROC test p-value < 0.05 are highlighted in red.

T cell activation as a biomarker of recent TBI and TB

A study by Musvosvi and colleagues that compared the discriminatory ability of T cell activation and functional populations between remote TBI and tuberculosis suggested that activation (HLA-DR) defined on CFP-10/ESAT-6-specific CD3+IFN-γ+TNF+ is able to distinguish between these two clinical presentations, using a simplified 4-colour assay amenable for clinical translation (Musvosvi et al., 2018). We therefore aimed to determine if CD3+ T cell activation defined on CFP-10/ESAT-6-specific IFN-γ+TNF+ CD3 T cells can also distinguish between recent and remote TBI. We re-analysed our flow cytometry data to express functional markers IFN-γ and TNF as a proportion of total CD3+ T cells (Figure 59A). As observed for CD4+ T cells, acquisition of TBI was associated with an increase of CFP-10/ESAT-6-specific IFN-γ+TNF+ CD3 T cells, which were detectable at comparable frequencies in recent and remote TBI (Figure 59B). During re-analysis we experienced challenges with "placing" the HLA-DR gate on total CD3+ T cells for some of the samples. We therefore defined 2 additional T cell activation parameters: HLA-DR MFI ratio (Equation 4) and Δ HLA-DR MFI (Equation 5). As observed with our other activation profiles, proportions of HLA-DR+ M.tb-specific IFN-γ+TNF+ CD3 T cells, HLA-DR-MFI ratio and Δ HLA-DR MFI were all significantly higher in recent TBI compared with remote TBI (Figure 59C-E). All biomarkers yielded promising discriminatory potential with AUCROCs of 0.91 (95% CI: 0.81-1.00) for ΔHLA-DR MFI (Figure 2F), 0.93 (95% CI: 0.84-1.00) for % HLA-DR and 0.91 (95% CI: 0.80-1.00) for HLA-DR MFI ratio (Figure 59F). We selected ΔHLA-DR MFI for blinded confirmation in the test cohort because it does not require selection of a discrete HLA-DR-positive cell subset using a threshold or "gate", thus reducing operator bias, and avoids the issue of negative MFI values that can result from flow cytometric compensation, which would affect calculation of the ratio-based biomarker.

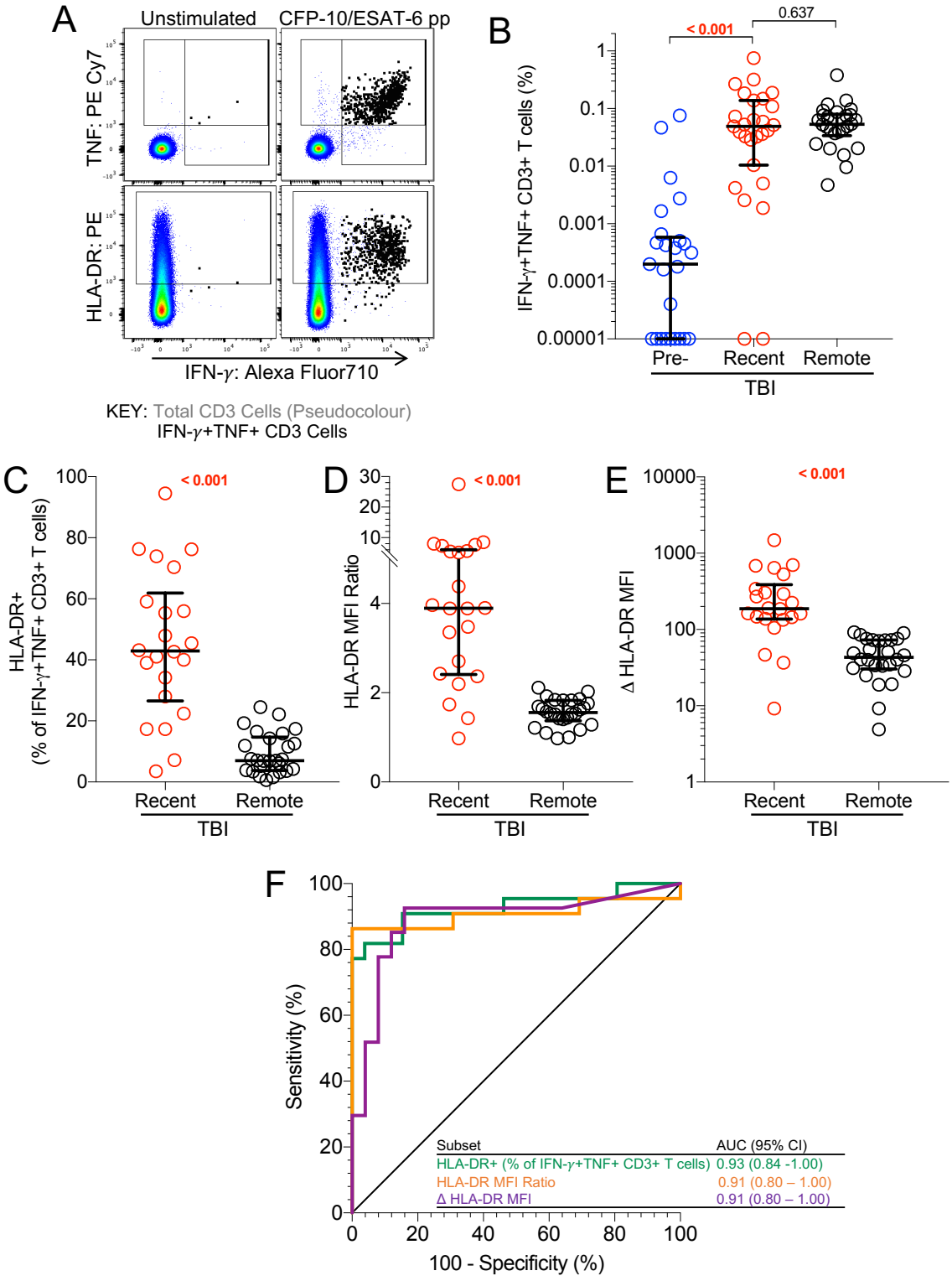

Figure 59: M.tb-specific IFN-γ+TNF+ CD3+ T cell activation biomarker distinguishes recent and remote TBI. (A) Representative flow cytometry plot depicting IFN-γ+, TNF+ and HLA-DR+ gates defined on CD3+ T cells. (B) Frequency of background subtracted M.tb-specific IFN-γ+TNF+ CD3+ T cells detected before (Pre-TBI, n=24), after (recent TBI, n=27) and during remote TBI (black symbols, n= 26). Graphs depicts (C) proportion of HLA-DR+ of IFN-γ+TNF+ CD3+ T cells, (D) HLA-DR MFI Ratio and (E) Δ HLA-DR MFI in recent (red symbols, n=22) and remote (black symbols, n=26) TBI responders. (F) ROC analysis of the diagnostic potential of M.tb-specific CD3 T cells activation biomarkers. Statistical analysis for B-E was conducted as in Figure 54.

Finally, we evaluated performance of the ΔHLA-DR MFI biomarker to distinguish between recent and remote TBI, recent TBI and tuberculosis, and remote TBI and tuberculosis in the test cohort. We developed a simplified version of the PBMC-intracellular cytokine assay and an algorithm to provide a framework for interpreting test results as a biomarker for potential M.tb infection states (Table 28). TBI was defined as a positive CFP-10/ESAT-6-specific IFN-γ+TNF+ CD3+ T cell response. In those with TBI, individuals were then classified into remote TBI and those with recent TBI or tuberculosis based on their ΔHLA-DR MFI.

Table 28: Interpretation of ΔHLA-DR MFI biomarker test results.

M.tb-specific Functional Response Definition			Responder Definition	Recent TBI or TB "definition"	
IFN-γ+TNF+ T cells E/C vs UNS (Fisher's Exact)	IFN-γ+TNF+ T cells PHA vs UNS (Fisher's Exact)	Interpretation	IFN-γ+TNF+ T cells E/C over UNS (Ratio)	ΔHLA-DR MFI (IFN-γ+TNF+) - (total T cells)	Interpretation
p ≤ 0.01	Any	TBI likely	≥3 fold	- (< 734) + (≥ 734)	Remote TBI likely Recent TBI or TB likely
			< 3 fold		
p > 0.01	p < 0.01	TBI unlikely			
p > 0.01	p > 0.01	Indeterminate			

Abbreviations: E/C: CFP-10/ESAT-6, UNS : Unstimulated

Frequencies of CFP-10/ESAT-6-specific IFN-γ+TNF+ CD3+ T cells induced by recent TBI were not different to those detected in individuals with remote TBI or with tuberculosis disease (Figure 60A). Importantly, we were able to discriminate QFT- individuals from those with recent or remote TBI with an AUCROC of 0.94 (95% CI: 0.87-1.00; Figure 60B), suggesting that this simple flow cytometry-based assay yields equivalent diagnostic information to QFT.

ΔHLA-DR MFI was significantly higher in recently infected individuals and tuberculosis patients compared to remotely infected individuals, however, individuals with recent TBI or tuberculosis disease had comparable ΔHLA-DR MFI (Figure 60C). Since measurement of MFI is panel-specific, and we used a different, simplified panel for the test cohort, we were unable to determine a ΔHLA-DR MFI cut-off for defining recent TBI in the biomarker discovery cohort that could be appropriately applied to the test cohort. We therefore report results of the biomarker in the test cohort, based on a threshold defined in the test cohort. Using a ΔHLA-DR MFI cut-off of 734, we were able to discriminate between recent and remote TBI with a specificity, sensitivity and AUCROC of 90%, 85% and 0.91 (95% CI: 0.83-1.00), respectively. We also observed excellent discrimination between remote TBI and tuberculosis, with high specificity (91%), sensitivity (100%) and AUCROC (0.99, 95% CI: 0.96-1.00). ΔHLA-DR MFI could

not accurately discriminate between recent TBI and tuberculosis (AUROC=0.67, 95% CI: 0.50-0.84; Figure 60C-D). Table 29 summarises the outcomes of the diagnostic algorithm described in Table 28 when applied to the test cohort.

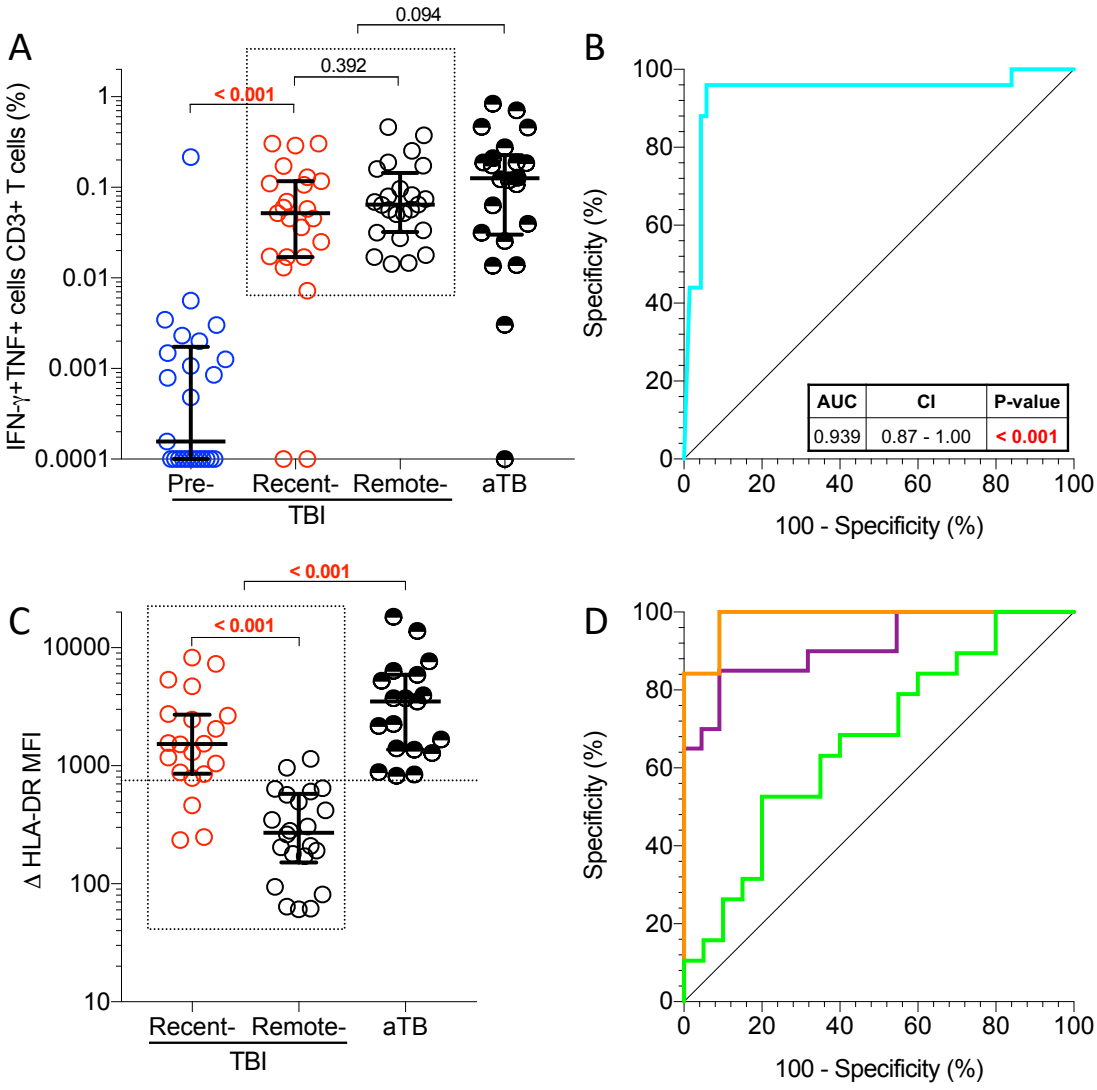

Comparison	Δ HLA-DR MFI Threshold = 750 Specificity	Sensitivity	AUC (95% CI)
Recent- vs Remote-TBI	90.21	85	0.91 (0.83- 1.00
Recent-TBI vs aTB	15.00	100	0.67 (0.50 – 0.84)
Remote-TBI vs aTB	90.91	100	0.99 (0.96 – 1.00

Figure 60: ΔHLA-DR MFI biomarker distinguishes remote TBI from recent TBI or tuberculosis. (A) Frequencies of background subtracted CFP-10/ESAT-6-specific IFN-γ+TNF+ CD3+ cells detected in before (pre-TBI, blue; n=25), and after (recent TBI, red, n=23) TBI, during remote TBI (black, n= 24) and in tuberculosis patients (aTB, half-filled circles, n = 22). (B) ROC analysis of illustrating the performance of CFP-10/ESAT-6-specific IFN-γ+TNF+ CD3 T cell to distinguish between samples taken before TBI (Pre-TBI) and those taken after (remote or recent) TBI. (C) ΔHLA-DR MFI responders with recent TBI (n=20), remote TBI (n=22) and tuberculosis (aTB, n=19). (D) ROC analysis depicting the performance of ΔHLA-DR MFI to discriminate between recent and remote TBI (purple), recent TBI and tuberculosis (green) and remote TBI and tuberculosis (orange). P-values were calculated using the Wilcoxon signed-rank test for paired (Pre-TBI vs recent TBI) or the Mann-Whitney test for unpaired (all other) comparisons. P-values highlighted in **bold** red are considered significant. Values < 0.0001 were set to 0.0001 to allow display on a logarithmic scale.

Table 29: Interpretation of Δ HLA-DR MFI biomarker on the test cohort.

Test interpretation		Pre-TBI (n=25)	Recent TBI (n=23)	Remote TBI (n = 24	TB (n=22)
Indeterminate	% of participants (n)	0	0	0	0
TBI unlikely		96% (24)	8.70% (2)	4.17% (1)	4.54% (1)
TBI likely		4% (1)	91.30% (21)	95.83% (23)	95.45% (21)
Responders (FE p ≤0.01 & FC >= 3)		4% (1)	86.96% (20)	91.67% (22)	86.36% (19)
Remote TBI likely	% of responders (n)	100% (1)	15% (3)	90.91% (20)	0% (0)
Recent TBI or TB disease likely		0	85% (17)	9.09% (2)	100% (19)

FE = Fisher's Exact test; FC = fold change stimulated over unstimulated

Our group previously reported a 6-gene blood transcriptomic signature, RISK6, that can identify QFT+ and/or TST+ individuals who are at risk of progressing to tuberculosis (Penn-Nicholson et al., 2020). We therefore tested the ability of the ΔHLA-DR MFI biomarker to distinguish between progressors (n=34) and non-progressors (n=34) in a longitudinal cohort of healthy, QFT+ and/or TST+ adolescents. Levels of ΔHLA-DR MFI were significantly higher in progressors up to 2 years before tuberculosis diagnosis compared to non-progressors (AUCROC of 0.75; 95% CI: 0.63-0.87; Figure 61). These results were consistent with the performance of RISK6 and suggest that the ΔHLA-DR MFI biomarker may also be useful to identify individuals at risk of disease progression.

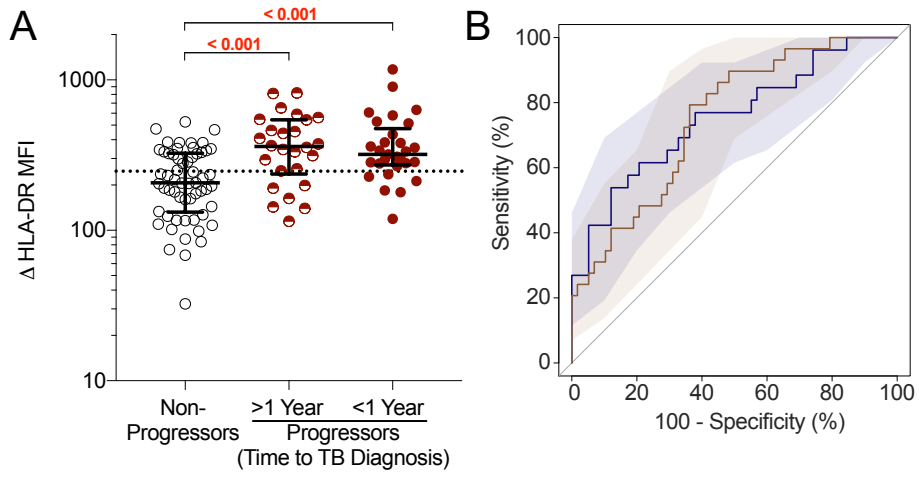

Figure 61: Mycobacteria-specific T cells in tuberculosis progressors are more activated than those in non-progressors. (A) ΔHLA-DR MFI on M.tb lysate-responsive T cells co-expressing IFNG and TNF mRNA transcripts in non-progressors (n=58 longitudinal data points from 34 participants) and progressors [in samples collected >1 year before tuberculosis diagnosis (> 1 Year, n=26 longitudinal data points from 19 participants) or in samples collected within 1 year of tuberculosis diagnosis (< 1 Year, n=29 longitudinal data points from 22 participants)]. P-values were computed by Mann–Whitney U test and were corrected for 2 comparisons as described in the methods. (B) ROC curve (AUC) depicting the performance of ΔHLA-DR MFI to discriminate between non-progressors and progressors in samples collected >1 year before tuberculosis or within 1 year of tuberculosis diagnosis.

Discussion

The risk of disease progression in M.tb infected individuals, identified by a positive IGRA or TST, is highest within the first 1-2 years after acquisition of TBI (Behr et al., 2018; Wiker et al., 2010). Identification of individuals who recently became infected, and who would thus benefit most from TPT, has only been possible with serial IGRA or TST testing. We performed in-depth analyses of M.tb-specific CD4 T cell function, memory and activation phenotypes to identify immunological differences between individuals who recently acquired infection and those with persistent (remote) infection. Four major points emerged from our study: 1) The acute response to TBI in humans was associated with highly activated M.tb-specific CD4 T cells that are moderately differentiated; 2) During remote infection M.tb-specific T cells were not activated but showed a phenotype consistent with long-term antigen exposure without evidence of exhaustion; 3) Among all the differences in M.tb-specific T cell phenotype and functions, HLA-DR expression had the highest diagnostic performance to distinguish between recent and remote infection; 4) T cell activation, detectable using a simplified 5 colour flow cytometry panel, can identify recent TBI, tuberculosis progressors and individuals with active tuberculosis, and could potentially guide provision of preventive or full tuberculosis treatment.

Firstly, we showed that recent acquisition of TBI (QFT conversion from negative to positive) was associated with an increase in frequencies of Th1 (IFN-γ, IL-2 and TNF) cytokine-expressing CD4 T cells to levels in range with those detectable during remote TBI. We did not observe marked differences in cytokine co-expression profiles between recent and remote infection and therefore focused our analysis on combinations of Th1 cytokine co-expression (polyfunctional) profiles and T cell differentiation. As typical for T cell responses during acute and chronic infection (Seder et al., 2008), we observed a predominance of M.tb-specific highly activated cells and T_{TM}/T_E cells upon recent acquisition of infection. The only distinguishing features between recent and remote TBI were higher M.tb-specific T cell activation and lower magnitude of M.tb lysate-specific KLRG-1+ IFN-γ+TNF+IL-2- T_E cells in recently compared to remotely infected individuals, while CFP-10/ESAT-6-specific T cell functional and memory profiles were not different between the two TBI states. In addition to being used as a proxy for T cell activation, HLA-DR expression by T cells has been suggested to facilitate antigen presentation to other T cells during times of high antigen burden (Aversa and Hall, 1991; Mangalam et al., 2006), thus providing an additional source of cells beyond professional APCs

that can induce *de novo* T cell priming. Here we present human evidence, in line with findings observed in murine models (North and Jung, 2004), that suggests M.tb antigen load is higher during the acute phase of infection compared to more established phases of infection, when bacterial load is at least partially controlled. However, in people who progress towards active tuberculosis, *in vivo* M.tb antigen exposure is likely high even before the onset of clinical symptoms.

Murine studies have demonstrated that chronic TBI is associated with differentiation of CD4 T cells to an exhausted T cell memory phenotype that expresses high levels of KLRG-1 and IFN-γ-monofunctional capacity, and poor ability to contribute to antigen clearance (Sakai et al., 2014b; Sallin et al., 2017). In contrast with these observations from mice, here we show that despite long-term QFT-positivity, M.tb-specific T cells in remotely infected individuals did not have a dominance of KLRG-1+ IFN-γ-monofunctional exhausted T cells, nor did they show elevated activation consistent with persistently high antigen load. Instead, the activation levels of M.tb lysate-specific CD4 T cells during remote TBI were not different to those observed before TBI, suggesting little or no *in vivo* antigen exposure during remote TBI. This may suggest that clearance of M.tb is rapid and usually occurs within 2 years in individuals who do not progress to disease. Under this scenario, immune responses detected in most remotely infected individuals represent immunological memory, and not necessarily ongoing M.tb replication (Behr et al., 2018). This is also consistent with our observation that the functional and memory differentiation profiles of CFP-10/ESAT-6-specific T cells were not different during recent and remote TBI, suggesting that these features are shaped during primary infection and remain relatively unchanged regardless of duration of antigen exposure. Alternatively, if remotely infected individuals truly harbour M.tb, as suggested by the higher functional differentiation of M.tb-specific T cells compared to recent infection, then levels of M.tb replication are likely low and stable, resulting in low T cell activation and a memory-functional phenotype not characteristic of T cell exhaustion. It is likely that persistent QFT+ status in humans represents a mixture of these scenarios.

We also showed that of all the immunological features that were different between recent and remote TBI, T cell activation was the best biomarker for differentiating between infection states. Overall, the T cell activation biomarker appears very robust, regardless of mycobacterial antigen specificity (M.tb lysate or CFP-10/ESAT-6) or the assay used for detection (PBMC intracellular cytokine, tetramer staining or gene-expression (after M.tb

stimulation) or, as previously reported, whole blood stimulation (Musvosvi et al., 2018; Riou et al., 2017, 2020; Wilkinson et al., 2016). Additionally, we described the development of a simplified assay and biomarker, ΔHLA-DR MFI, that measures M.tb-specific T cell frequencies and their activation levels, and can distinguish QFT- (presumably uninfected) individuals from QFT+ (presumably infected) individuals, and among the latter can discriminate between those with recent TBI, disease progression or active tuberculosis and remotely infected non-progressors. Results presented are a significant advance over current M.tb immunodiagnostics (TST and IGRA), which are unable to distinguish between different stages of TBI and identify individuals at risk of progression to disease. Since individuals with recent infection and high risk for disease progression would benefit from targeted TPT, this biomarker offers an opportunity to identify a group of asymptomatic individuals at particularly high risk of tuberculosis, while those with persistent QFT+ test and low risk of progression would derive less benefit from TPT. This is of particular importance in high incidence settings, where a large proportion of the population is already M.tb infected and identification of individuals at high risk of tuberculosis progression is challenging. Our findings build on previous studies that have shown that measurement of M.tb-specific T cell activation by flow cytometry has promising diagnostic potential to distinguish TBI from tuberculosis disease, regardless of HIV status, as well as to monitor treatment response (Adekambi et al., 2015; Musvosvi et al., 2018; Riou et al., 2017, 2020; Silveira-Mattos et al., 2019; Wilkinson et al., 2016).

The strengths of our study include unique and well-characterized clinical cohorts, blinded verification of our findings in a test cohort and translation of biological observations made with complex technology to a simple test that can be used for further validation.

Limitation of this study include convenience selection of participants based on sample availability, resulting in a small sample size, which could have introduced a bias that would have been avoided by random selection. Additionally, recently infected individuals selected were followed-up for a relatively short duration, none of whom progressed to disease during the study. This prevented us from demonstrating how immunity in recently infected individuals who either progress to disease or develop persistent TBI differ. Ideally, the M.tb-specific T cell activation biomarker should be prospectively validated on a cohort of individuals who acquire TBI and then progress to disease. This would be an extraordinarily large study to conduct, since on a population level only a minority of individuals who acquire

TBI progress to disease (Machingaidze et al., 2012). We tried to account for this by demonstrating the ΔHLA-DR MFI biomarker could distinguish between remotely infected non-progressors and tuberculosis progressors. Additionally, we were unable to formally validate our ΔHLA-DR MFI biomarker because the biomarker discovery, test and progressor cohorts were selected from the same epidemiological study and were thus not completely independent (Machingaidze et al., 2012). The control group of newly diagnosed tuberculosis included adults aged 21 - 42 years, therefore, we cannot exclude age-related differences. Further, experimental protocols, stimulants and reagents used to detect T cell activation were different between cohorts, thus preventing us from using the same assay and defining a ΔHLA-DR MFI threshold that could be uniformly applied to all 3 cohorts. However, the consistency of results points towards robustness of the biomarker. Unfortunately, due to the limited number of parameters that could be measured by the flow cytometer, we were unable to include additional activation markers, such as CD38 and Ki-67, in the initial panel used to compare recent and remote TBI. It is possible that inclusion of CD38 and/or Ki-67 could have enhanced the sensitivity and specificity of the biomarker based on ΔHLA-DR. Lastly, limited sample availability prevented us from testing other recently described biomarkers, such as those based on T cell proliferation (Borgström et al., 2020) or gene expression (Ault et al., 2020). Despite broad similarities between immune responses detected in our adolescent cohort and other cohorts of healthy M.tb-infected adults, showing a predominant of M.tb-specific CD4 Th1 polyfunctional profile and T_{EFF} phenotype (Adekambi et al., 2012; Harari et al., 2011; Jasenosky et al., 2015; Moguche et al., 2017; Riou et al., 2017; Rozot et al., 2015), the biomarker proposed by Halliday et al (Halliday et al., 2017) did not stratify recent and remote TBI in our study. Experimental differences may account for this discrepancy, including the different antigenic stimulation (purified protein derivative *versus* M.tb lysate) and the definition of T_{EFF} cells (which did not include CD127 expression in our panel).

In summary, we characterised changes in M.tb-specific T cell immunity in different phases of infection and present evidence of a peak in T cell activation, probably reflecting high M.tb burden, during recent infection followed by unexhausted T cell functional and memory phenotypes during remote, non-progressing infection, consistent with control or clearance of M.tb (Behr et al., 2018). We also described a blood-based T cell biomarker, ΔHLA-DR MFI, measured with a simple flow cytometry assay, that can be used to identify individuals with

recent TBI and those with tuberculosis progression, as well as clinical disease. Upon further validation and adaptation for use with whole blood, the ΔHLA-DR MFI biomarker has the potential to stratify individuals along the M.tb spectrum and could be considered as a screening test, to identify individuals at high risk of tuberculosis for further evaluation. If interpreted in association with clinical features and microbiological tests, this biomarker could identify individuals with tuberculosis who would benefit from standard treatment, those at high risk who should receive TPT, and those who would not currently benefit from TPT but may be re-tested in future.

Contributions

Experimental protocols and analysis of results generated for the tuberculosis progressor cohort were performed by Munyaradzi Musvosvi.

All methodology and statistical analyses were performed by Cheleka Anne-Marie Mpande, unless stated otherwise.

Chapter 6: QFT reversion is associated with M.tb-specific functional, memory and activation profiles suggestive of very low *in vivo* exposure M.tb.

Introduction and Rationale

Asymptomatic TBI is commonly thought to be chronic, however, longitudinal epidemiological and tuberculosis-HHC studies have demonstrated that this is not always the case. Upon longitudinal testing, TST and QFT have been observed to revert from a positive to a negative test in some individuals, a phenomenon known as reversion. In this chapter, we shall describe M.tb-specific functional, memory and activation kinetics associated with QFT reversion, as well as other TBI states: QFT non-conversion, recent TBI (QFT conversion) and remote TBI (persistent QFT+ responses).

Detection of memory immune responses that persist over long periods in M.tb infected individuals is assumed to result from sustained antigen exposure by chronic but low bacterial burden. This assumption is based on evidence from murine tuberculosis models that have demonstrated that persistent M.tb bacterial load is associated with maintenance of IFN-γ+ immune responses (Moguche et al., 2017; North and Jung, 2004). TBI diagnostics such as IGRAs and TSTs were designed and are clinically interpreted based on this premise: **detectable immune responses = viable TBI (bacterial persistence).** However, Behr and colleagues suggest that detection of M.tb-specific memory in many individuals is simply M.tb-specific reactivity and not indicative of bacterial burden, thus challenging this common assumption (Behr et al., 2019).

Though TBI immunodiagnostics quantifies M.tb-specific immune responses [IFN-γ concentration (IU/mL) or TST induration (mm)], results are clinically interpreted qualitatively i.e. positive or negative test result. Andersen and colleagues have suggested that the magnitude of IGRA responses correlates with antigen load, and analysis of quantitative IGRA results could contribute to improved clinical interpretation and utility of the test (Andersen et al., 2007). However, in practice this may not be easily implemented as other factors, such as age and local tuberculosis epidemiology, could impact the interpretation of quantitative IGRA results. Recent TBI is associated with an increase in quantitative IGRA/TST responses above the assay cut-off, which may decrease upon immune-mediated bacterial control during established TBI or increase to even higher levels upon uncontrolled bacterial burden, potentially indicating high risk of tuberculosis. In settings with low tuberculosis incidence,

IGRA/TST positivity regardless of age is likely due to recent M.tb exposure and indicative of recent conversion. In high incidence settings, house-hold and community transmission are responsible for TBI in infants/young children and adolescents/adults, respectively (Churchyard et al., 2017; Mathema et al., 2017). Further, since the force of infection is very high in high incidence settings, IGRA/TST positivity in adults could be due to recent or historical exposure. Studies have reported an association between high QFT responses (> 4.0 IU/mL) and increased tuberculosis risk suggestive of on-going TBI in adults from low incidence settings and infants/young children from high incidence settings (Andrews et al., 2017; Gupta et al., 2019a, 2019b, 2020c; Winje et al., 2018). While others have reported conflicting results that show no association between the two even in low incidence regions (Gupta et al., 2019a; Zellweger et al., 2015).

If a substantial increase of QFT responses is suggestive of increased tuberculosis risk, what does the inverse mean? TST and/or IGRA reversion has been widely reported (Adams et al., 1959; Dahlstrom, 1940; Hawn et al., 2014; Hill et al., 2007; Jenum et al., 2014; Medawar et al., 2019; Pai et al., 2009, 2012; Xin et al., 2019b; Zhang et al., 2019; Zyl-Smit et al., 2009), and could contribute to underestimation of the TBI burden in cross-sectional studies. In an observational adolescent cohort study conducted in our community (Worcester, Western Cape) ~55% of adolescents were TST+, with high annual risks of QFT conversion (14%) and QFT reversion (5.1%) (Andrews et al., 2015). TST and/or IGRA reversion in recent converters is inversely associated with the magnitude of IGRA or TST conversion response and M.tb-specific T cells responses, and is associated with IGRA results around the assay cut-off (Adams et al., 1959; Andrews et al., 2015; Hawn et al., 2014; Johnson et al., 2014; Joshi et al., 2014; Pai et al., 2009; Zanetti et al., 2012). These studies highlight the value of interpreting quantitative IGRA/TST responses as it could guide the correct interpretation of serial IGRA/TST results and improve the assessment of TBI dynamics and clinical management of highly exposed individuals (Brown et al., 2017; Joshi et al., 2014; Pai and O'Brien, 2007; Pai et al., 2007). It is therefore critical to understand the events underlying IGRA reversion, which could be due to diagnostic test variability or robust detection of transient T cell responses, which could be associated with clearance of TBI.

Studies conducted during the pre-antibiotic era reported detection of "*calcified nodules, presumably of tuberculous origin*" in TST reverters who had no history of disease (Dahlstrom, 1940), thus suggesting that some people can naturally sterilise TBI without antibiotic

treatment. Based on these findings researchers hypothesised that reversion could be associated with natural clearance, however, this is difficult to prove in humans. Fortunately, TBI studies in guinea pigs have provided evidence for this, by illustrating that TST reversion is associated with sterilising immunity (Dharmadhikari et al., 2011; Riley et al., 1959b). Furthermore, cases of antibiotic-associated IGRA (QFT) and/or TST reversion have also been documented in recent M.tb-exposed and/or M.tb-infected tuberculosis-HHC who received TPT (Ewer et al., 2006; Hill et al., 2007; Johnson et al., 2014; Zhang et al., 2019). Additionally, a recent BCG revaccination trial of M.tb-uninfected adolescents, who were BCG vaccinated at birth, demonstrated a vaccine induced partial protection against acquisition of sustained TBI defined as transient QFT conversion followed by a swift reversion (QFT- → QFT+ → QFT-) all within a 6 month period (Nemes et al., 2018). These findings support the **reversion-M.tb-clearance hypothesis**, and demonstrate that reversion can occur naturally, as well as in association with interventions such as TPT or BCG revaccination.

Two major caveats of the QFT test are the measurement of M.tb-specific IFN-γ-responses to only 3 M.tb-specific antigens (CFP-10, ESAT-6 and TB7.7) and the inability to detect IFN-γ-independent immunological readouts, which may reflect other aspects of immune responses against M.tb. Therefore, QFT reversion could be associated with a loss of recognition of QFT antigens, despite persistent TBI. To test this hypothesis, we shall measure IFN-γ expression in response to alternative M.tb immunodominant antigens absent in BCG and most NTMs. We selected Rv3615c (EspC) (Millington et al., 2011), Rv2348 and Rv3865 (EspF) (collectively referred to as Esp peptide pool) and M.tb lysate, which contains all M.tb antigens (including those present in the QFT). The Esp peptide pool has been used in combination with CFP-10 to develop an ESAT-6-free IGRA, to determine TBI status in clinical trials of candidate TB vaccines that contain ESAT-6 as one of the immunogens (Nemes et al., 2019; Ruhwald et al., 2017).

In Chapter 5, we showed that Th1 responses, including IFN-γ independent responses, are induced upon TBI, and are sustained throughout infection. A recent study of resisters, individuals with known M.tb exposure (tuberculosis-HHC) who appear to resist TBI characterised by sustained QFT and/or TST non-conversion, showed that these individuals have detectable M.tb-specific antibody responses and low levels of IFN-γ-CD154+TNF+IL-2+ CD4 T cell responses [discussed in detail in Chapter 1; (Lu et al., 2019)]. This suggests that TBI does not always result in generation of sustained IFN-γ+ responses, and further illustrates

limitations of the QFT test. If resistors were truly M.tb uninfected at the time of sampling, then it demonstrates that transient TBI can induce IFN-γ independent M.tb-specific immune responses that can be maintained long-term. CD154, TNF and/or IL-2 functional capacity is associated with quiescent T_{SCM} and T_{CM} memory phenotypes, which maintain long-lasting immunity in the absence of antigen (Lugli et al., 2013a; Seder et al., 2008). Thus, it was not surprising that resisters, who were QFT- or TST- at sampling, had detectable M.tb-specific cells with this functional profile. In Chapter 5, we demonstrated that mycobacteria-specific IL-2+ and TNF+ T_{SCM} and T_{CM} cells are preferentially enriched in QFT**-** compared to QFT**+** individuals, emphasising that low or no M.tb antigen burden is associated with higher abundance of early differentiated mycobacteria-specific T cell subsets. Therefore, if QFT reversion is associated with lower bacterial burden, we hypothesise an increase in the relative proportions of M.tb-specific cells with a T_{SCM} and T_{CM} phenotype, and IFN-γ-independent (CD154+, IL-2+ and/or TNF+) functional capacity compared to QFT+ M.tb infected individuals. Assuming that reversion is the "opposite" of conversion and is associated with antigen clearance, a reduced level of activation of M.tb-specific T cells may occur upon reversion. Tuberculosis is associated with higher expression of activation markers CD38, HLA-DR and Ki-67 by M.tb-specific IFN-γ+ T cells compared to TBI (Adekambi et al., 2015; Musvosvi et al., 2018; Riou et al., 2017). We have illustrated that recent TBI is associated with a peak in M.tb-specific T cell activation (HLA-DR+) during acute TBI (month 6) in QFT converters (chapter 3 and 5), which significantly decreases once TBI is established (month 12; Chapter 3). Additionally, recent M.tb-infected individuals have higher T cell activation levels than remote M.tb-infected individuals, who have persistently low levels of T cell activation. Further, studies have shown that successful tuberculosis treatment, which is thought to sterilise M.tb in most cases, is associated with a significant decrease in T cell activation compared to baseline (before treatment) (Adekambi et al., 2015; Musvosvi et al., 2018; Riou et al., 2017;2020). Taken together, these data suggest that levels of M.tb-specific T cell activation are likely associated with M.tb-antigen load, which in animal models peaks during primary infection, decreases to a plateau during established infection, and increases again during disease (Lin et al., 2014). Based on these results we shall measure T cell activation (HLA-DR) kinetics associated with QFT reversion, to determine if reversion is associated with a decrease in T cell activation.

We hypothesise that QFT reversion represents a true reduction in IFN-γ expression by M.tb-specific T cells rather than an artefact due to technical assay variability. Further, we hypothesise that QFT reversion is associated with a relative enrichment T_{SCM} and T_{CM} CD4+ T cells, memory subsets associated with low antigen load. To test our hypotheses, we aim to characterise functional, memory and activation profiles of M.tb-specific T cells in QFT persistent negatives, persistent positives, converters and reverters, to further elucidate the relationship between T cell memory, persistence and (inferred) mycobacterial burden. These data will supplement our current knowledge of kinetics and function of mycobacteria-specific memory phenotypes during different phases of M.tb infection.

Objectives

1. **To confirm that antigen-specific IFN-γ+ functional capacity significantly decreases during QFT reversion using PBMC intracellular cytokine staining and flow cytometry.**
2. **To determine whether IFN-γ-specific T cell responses directed to M.tb immunodominant antigens not included in the QFT assay are sustained in QFT reverters.**
3. **To ascertain whether M.tb-specific T cells from QFT reverters have an IFN-γ-independent functional capacity.**
4. **To determine whether QFT reversion is associated with an increase in the relative proportion of M.tb-specific cells with a T_{SCM} and T_{CM} memory phenotype.**
5. **To determine if QFT reversion is associated with a reduction of activated M.tb-specific memory T cells.**

<u>Methodology</u>

Study Design

We compared immune responses in recent QFT reverters to those from individuals at different stages of TBI, namely serial QFT negatives (QFT non-converters), recent QFT converters and serial QFT positive individuals. We retrieved stored PBMC from healthy adolescents based on serial QFT test results, as defined below, and sample availability. Inclusion criteria of adolescents selected for this study are described in Chapter 5: Participant samples and ethics.

Definition of Recent QFT reverters

Adolescents in this group had two positive QFT tests followed by two negative QFT tests 6 months apart (Figure 62). To ensure that at least one QFT positive and negative test result was outside the QFT uncertainty zone [0.2IU/mL-0.7IU/mL (Nemes et al., 2017a)] and reduce the likelihood of detecting immune responses associated with technical fluctuations around the assay cut-off, QFT reverters who had at least one positive QFT test that was > 0.7IU/mL (n=24) and one negative QFT test that was < 0.2IU/mL (n= 28) were selected when possible.

Definition of control sub-cohorts

Non-converters: Selection of QFT non-converters was based on 4 consecutive QFT negative tests (< 0.2 IU/mL) 6 months apart (Figure 62). We chose an upper limit of QFT response as 0.2IU/mL, below the QFT uncertainty zone, to increase the likelihood that these individuals were truly M.tb "unsensitised" at the time of sampling, and could represent a meaningful negative control group.

Recent QFT converters: this sub-cohort is described in Chapter 5: Definition of Recent TBI group (Figure 62).

Serial QFT positive individuals: this sub-cohort is described in Chapter 5: Definition of Remote TBI group (Figure 62) and for simplicity shall be referred to as remote TBI.

Matching of control groups to QFT reverters

Control groups (non-converters, QFT converters and remote TBI) were randomly selected from a pool of available samples and matched to QFT reverters based on age at enrolment (± 1 years), gender, ethnicity and school, which relates to socio-economic and M.tb exposure status (Mahomed et al., 2011a). However, due to sample availability we modified the age criterion for matching converters to reverters to be within ± 2 years (Table 30).

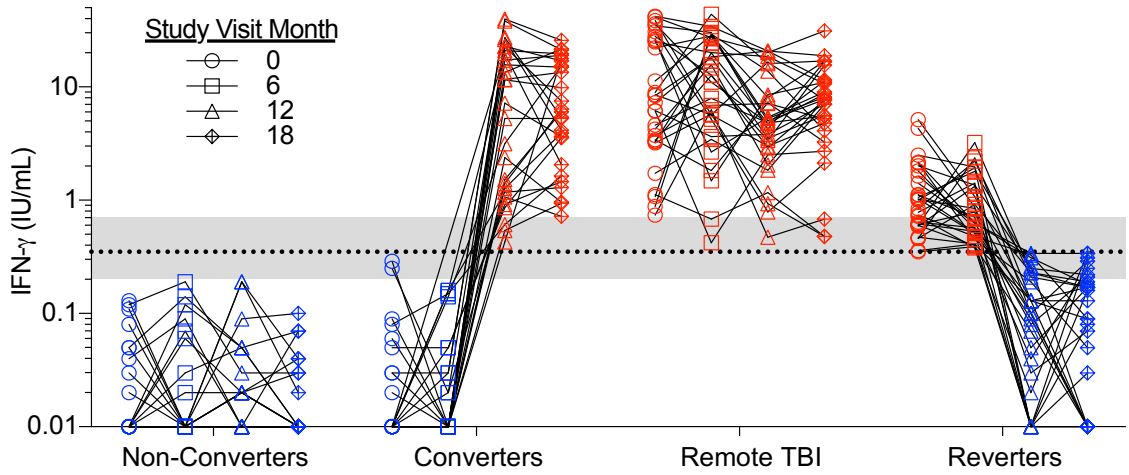

Figure 62: QFT results. Graphs illustrate QFT responses measured during follow-up in adolescent non-converters, converters, remote TBI and reverters. Positive and negative QFT responses are depicted by red and blue symbols, respectively. QFT tests were performed 0, 6, 12 and 18 months during follow up depicted by circle, square, triangle and diamond symbols respectively. To plot all data points on a log scale we set values equal to 0 to 0.01. Dotted line and shaded area represent the QFT assay threshold (0.35 IU/mL) and uncertainty zone (0.2-0.7IU/mL), respectively (Nemes et al., 2017a).

Table 30: Cohort Demographics.

	Non-converters	QFT converters	Remote TBI	QFT reverters
N	30	30	30	30
Gender (Female)	21	19	21	21
Median Age in years (IQR)	15 (14-16)	15 (14-16)	15 (14-16)	15 (14-16)
Ethnicity: Coloured	25	29	26	25
Ethnicity: Black	5	1	4	5
School 1	14	19	15	14
School 2	11	2	4	11
School 3	5	9	11	5

PBMC stimulation and intracellular cytokine staining protocol

PBMC stimulation and staining protocols were performed as outlined in Chapter 5: PBMC stimulation and staining protocol. In addition to stimulation with mycobacterial antigens CFP-10/ESAT-6 peptide pool (1μg/mL) and M.tb lysate (10μg/mL), we also stimulated cells with Esp-peptide pool [15 mer peptides overlapping by 10 amino-acids (1μg/mL, GenScript Biotechnology)], prepared as described in Chapter 4: Antigens, to determine functional and phenotypic characteristics of T cells specific for M.tb-antigens that are not in the QFT assay nor BCG vaccine.

Data analysis pipeline

Immune responses to mycobacterial antigens were predominantly analysed according to the Biomarker discovery cohort data analysis pipeline outlined in Chapter 5. Modifications to the analysis pipeline are outlined below.

Flow cytometry gating strategy

In addition to the gating strategy outlined in Chapter 5, we also measured expression of IFN-γ, TNF, IL-2, CD154 and CD107 by total lymphocytes from mycobacteria-stimulated PBMC (Figure 63).

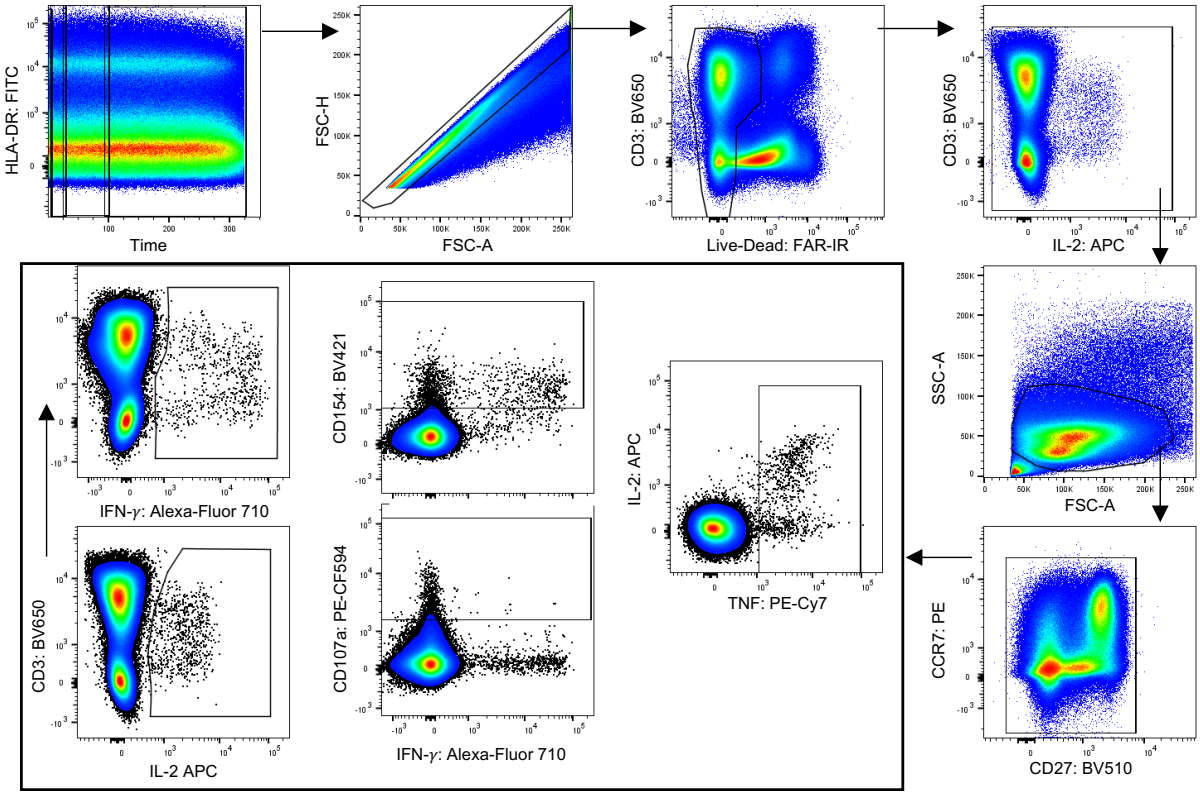

Figure 63: Gating strategy for detection of functional responses by lymphocytes. We used the same gating strategy illustrated in Chapter 5 for T cells. Modification to that strategy was the inclusion of functional gates on total live lymphocytes (black box) after we excluded antibody aggregates.

COMPASS analysis

We modified the analysis pipeline outlined in Chapter 5: Compass Analysis by including analysis of Esp-specific CD4 T cells subsets at all study visits, where possible. Additionally, we analysed subsets expressing different combinations of cytokines if they had a posterior probability threshold of ≥0.1 in at least 10 participants/visit for either converters or reverters.

Definition of participant functional responses and statistical approach

Experimental protocols were performed on all study participant visits where possible. To prevent the introduction of biases due to repeated sampling from the same donor, we calculated a representative functional response (frequencies of antigen-specific CD4 T cells, functionality scores, polyfunctionality scores etc.) based on QFT status for each individual.

Firstly, to determine if functional responses (single cytokine, functional booleans etc.) were significantly different between visits stratified by QFT status, we performed a Kruskal Wallis test to compare responses detected at all 4 QFT negative and positive visits in non-converters and remote TBI, respectively (Figure 64A). Wilcoxon signed-rank tests were used to compare functional responses detected at paired QFT negative and QFT positive visits in converters and reverters (Figure 64B). If functional responses were not significantly different ($p > 0.05$) between visits with the same QFT status, we calculated the median functional response for each participant based on QFT status (Figure 64C). We chose median instead of the mean because we wanted a representative figure that accounted for visit-to-visit variability, where the number of visits allowed. This resulted in a single value for each M.tb non-converter and remote TBI individual, and two values for QFT reverters and converters according to QFT status, which were then used for inter and intra group comparisons as outlined in Figure 64C. Statistical differences in expression levels of functional, memory and activation responses between groups were calculated using Mann-Whitney test for non-converters *versus* pre-converters, post-converters *versus* remote TBI, remote TBI *versus* pre-reverters and post-reverters *versus* non-converters comparisons (Figure 64C: black arrows), while Wilcoxon signed-rank test was used for paired pre- *versus* post- converter and pre- *versus* post- reverter comparisons (Figure 64C: orange arrows). Bonferroni and Benjamini-Hochberg (FDR <0.05) methods were used to correct for multiple comparisons for up to 4 comparisons or more than 4 comparisons, respectively.

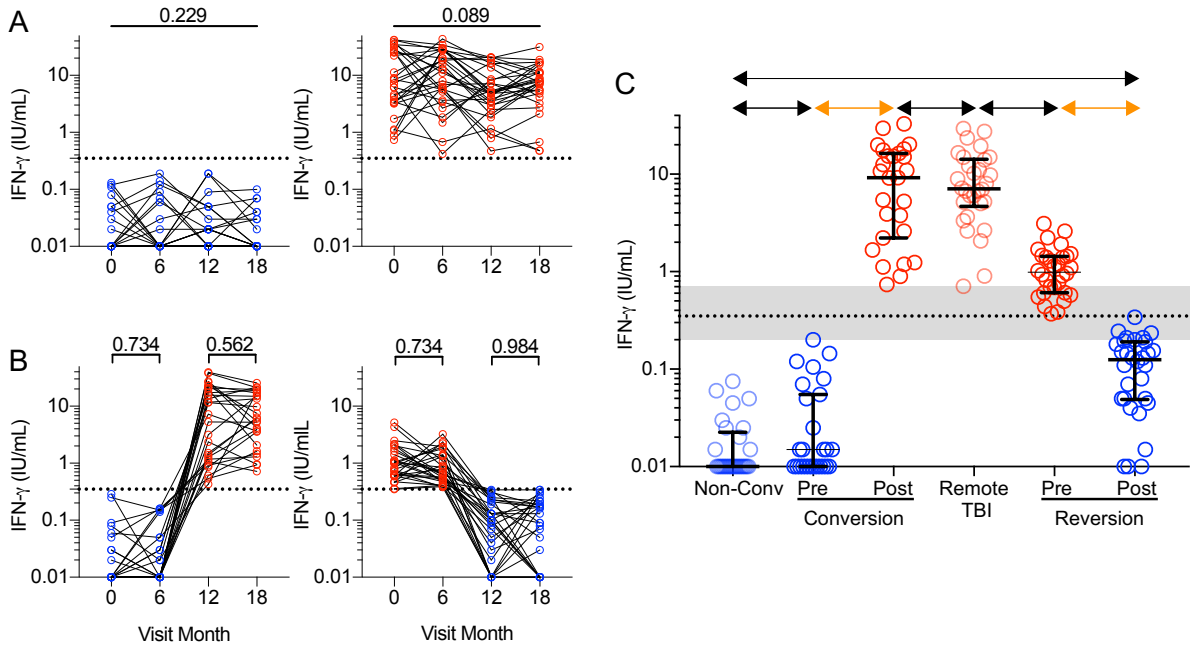

Figure 64: Calculation of median responses based on QFT status. (A) Kruskal-Wallis and (B) Wilcoxon-signed rank test were performed on (A) non-converters (Non-conv) and remote TBI; and (B) converters and reverters, respectively, to determine whether serial immune responses were significantly different based on QFT status (positive or negative). (C) Median functional responses were then compared between groups, as indicated by arrows, where black and orange arrows represent Mann-Whitney and Wilcoxon signed-rank tests, respectively. Dotted line and shaded area represent the QFT cut-off (0.35 IU/mL) and uncertainty zone, respectively.

Responder definition and longitudinal phenotypic analysis

Responders were defined as outlined in Chapter 5: Responder Definition, prior to phenotypic analysis of memory and activation kinetics, where background subtraction is not feasible. We defined responders as individuals whose IFN-γ+ lymphocyte and/or total Th1 cytokine CD4 T cell antigen-specific response had a MIMOSA FDR cut-off of ≤ 0.01 and a fold change of antigen-specific signal over background (unstimulated) of ≥ 3 (Figure 65). However, since we had longitudinal samples, we applied the responder definition to functional responses detected at each study visit for each participant. We then exported FCS files gated on IFN-γ+ lymphocytes or Th1 cytokine+ CD4 T cells from all visits that passed the responder criteria and concatenated FCS files based on QFT status to get a representative FCS file for each participant-QFT status combination (Figure 65). Concatenated FCS files of IFN-γ+ lymphocyte responses were used for tSNE analysis, while Th1 cytokine CD4 T cell responses were used CITRUS analysis and calculation of FDS (Figure 65).

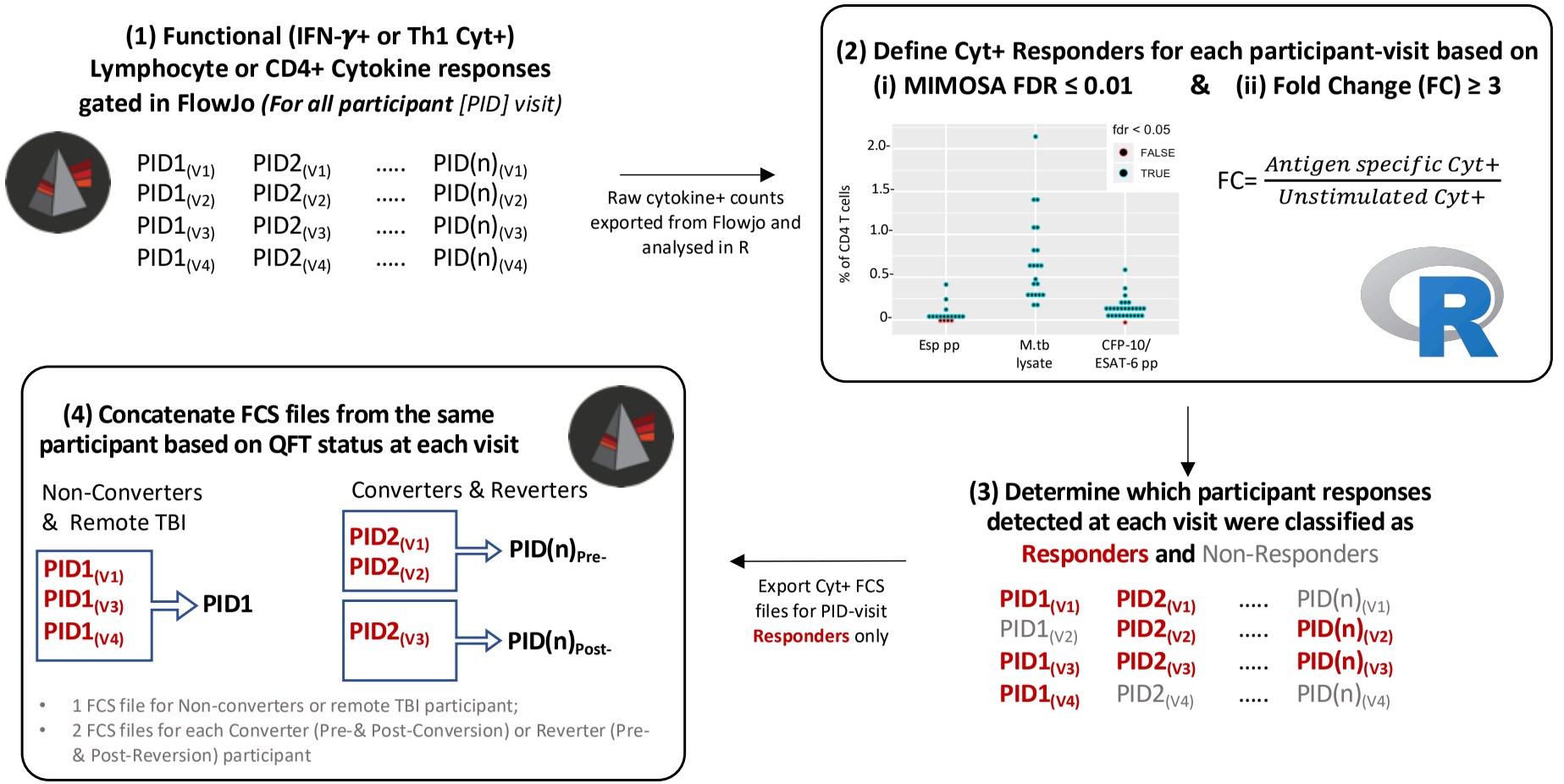

Figure 65: Analysis pipeline used to define a single FCS file per participant-QFT status. (1) Functional lymphocytes and CD4 cytokine responses were gated in FlowJo and cytokine+ counts exported to determine M.tb-specific responders. (2) Responders to antigenic stimulation were defined as IFN-γ+ lymphocytes and/or total Th1 cytokine+ CD4 T cell responses for each participant visit that had a MIMOSA FDR ≤ 0.01 and a fold change (FC) of antigen-specific signal over (unstimulated) of ≥ 3 (in R). (3) IFN-γ+ lymphocytes and/or total Th1 cytokine+ FCS files for all participant visits that passed the responder criteria were then exported, and (4) visits were concatenated based on the participant QFT group status.

tSNE analysis for IFN-γ+ lymphocyte responses

We performed tSNE analysis on IFN-γ+ lymphocytes from responders only to determine the main cellular source of IFN-γ (Figure 66A). To get one representative FCS file for each sub-group (i.e. non-converter, pre-converter, post-converter, etc.), we first set a maximum threshold count of 500 number of cells per participant and concatenated FCS files from each participant based on QFT status and group. To prevent the introduction of bias due to over or under-sampling each group, we down-sampled equal number of cells ($n \cong 7000$ counts) for each QFT status-group combination, concatenated all 6 (non-converters, pre- and post-converter, remote TBI, pre- and post-reverter) FCS files into one file and performed tSNE analysis on a single FCS file that included all responders from the entire cohort (Figure 66A).

CITRUS analysis of Th1 cyt+ CD4 T cell responses

To determine which T cell features were detectable at significantly different abundance levels between groups, we performed CITRUS analysis as defined in Chapter 5: CITRUS analysis & Functional differentiation score (Figure 66B). Memory and functional CD4 T cell features (CITRUS clusters) detected at significantly different abundance levels between groups with an FDR < 0.01 were identified using CITRUS. Composition of T cell features were then confirmed by manual gating in FlowJo and applied to individual participant samples to determine quantitative cellular expression (percentage of Th1 cytokine+ CD4 T cells) levels of each T cell feature per participant.

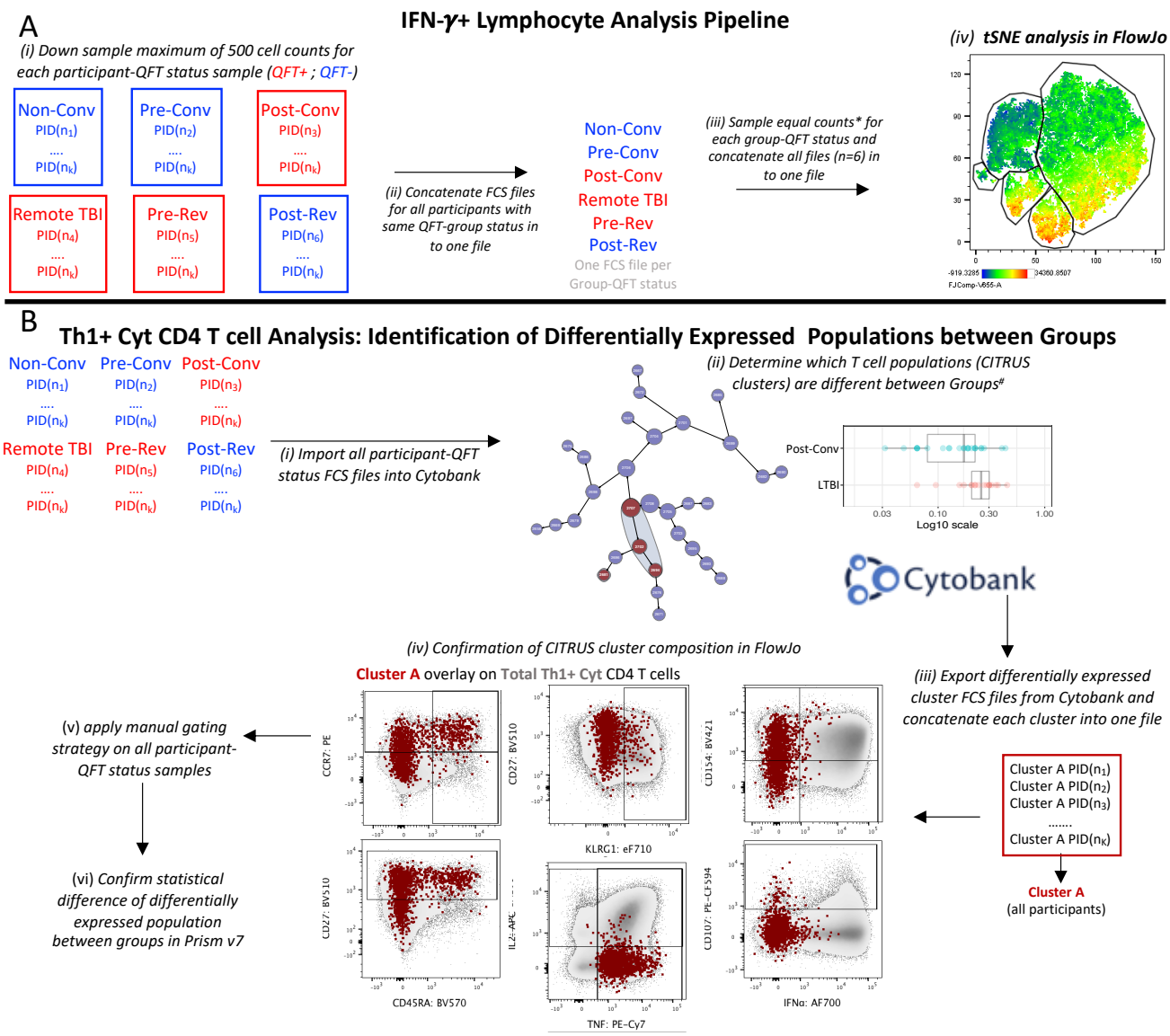

Figure 66: Lymphocyte and CD4 T cell Analysis Pipeline. (A) (i) IFN-γ+ lymphocyte FCS files were down-sampled to a maximum of 500 cell counts per participant-QFT status, (ii) followed by concatenation of all FCS files belonging to the same QFT-group in to one FCS file per group. (iii) Equal number of cells (n=7000) from each group, * except for pre-converters responses (n= 5500 cell counts) due to sample availability, were then concatenated into one file, (iv) and used to perform tSNE analysis. (B) (i) Total Th1 cytokine+ FCS files from all individuals were imported into Cytobank to conduct (ii) CITRUS analysis between groups (# 2 groups were compared for each CITRUS analysis as defined in Figure 63C). (iii) Differentially expressed clusters (FDR < 0.01) identified in CITRUS, were then exported from CITRUS and concatenated in to one file per cluster. (iv) To confirm the memory-functional phenotypic identity of each cluster, we manually gated these markers in FlowJo. (v) Final gating strategy of each cluster was then applied to individual responders, and (vi) confirmatory statistical analysis was performed on manually gated populations.

Results and Discussion

TST and QFT concordance

All participants in our study had QFT and TST performed biannually and annually, respectively. We defined TBI based on QFT only and not TST because TST responses are known to cross-react with BCG-induced immunity. We therefore determined the concordance between QFT

and TST for each group. Non-converters were predominantly TST negative, with only 5 out of the 28 individuals being TST+, 2 of which were persistently TST+ throughout the follow-up. (Figure 67). This resulted in a concordance of 87.93% between QFT and TST results. We also observed a very good concordance of 88.14% and 94.55% between QFT and TST in QFT converters and remote TBI, respectively. The majority of QFT reverters were persistently TST+ throughout follow up (Figure 67), which resulted in a poor concordance between QFT and TST tests, with a 45.28% agreement between the two immuno-diagnostics (Table 31).

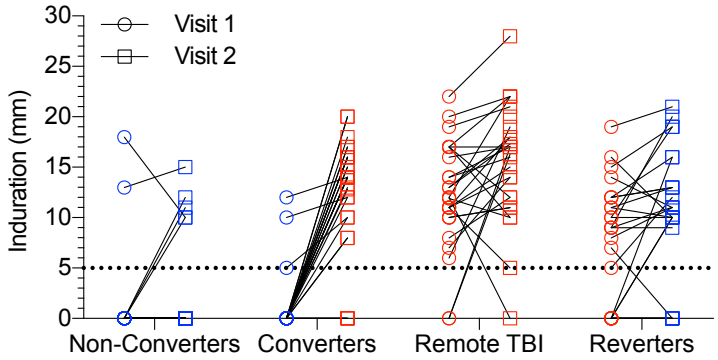

Figure 67: TST results. Graphs illustrate TST responses measured during follow-up in non-converters, converters, remote TBI and reverters. Positive and negative QFT responses are depicted by red and blue symbols, respectively. TST cut-off of 5mm as suggested by (Mahomed et al., 2011b) is represented by the dotted line.

Table 31: QFT and TST concordance.

	Non-converters	QFT converters	Remote TBI	QFT reverters
N	30	30	30	30
Baseline TST [Positive; (Unknown)]	2; (2)	3	26; (2)	17; (4)
1 year TST [Positive; (Unknown)]	5	25; (1)	26; (3)	20; (3)
TST vs QFT Concordance #	87.93%	88.14%	94.55%	45.28%
TST vs QFT Concordance: Kappa	0*	0.763	0*	-0.086

Note: #: Concordance calculated using QFT and TST test results obtained at the same study visit.
*: Kappa could not be calculated because all QFT responses were negative or positive for non-converters and remote TBI, respectively.

T cells are the main source of IFN-γ by mycobacteria-specific lymphocytes

QFT is an ELISA-based immunodiagnostic which measures IFN-γ production by all cells in CFP-10/ESAT-6/TB7.7 stimulated whole blood (http://www.quantiferon.com/wp-content/uploads/2017/04/English_QFT_ELISA_R04_082016.pdf). T cells are considered the main source of IFN-γ in QFT antigen-stimulated whole blood (Penn-Nicholson et al., 2015). However, they contribute less than 75% of BCG-specific IFN-γ production in recent BCG-vaccinees (Suliman et al., 2016). We thus aimed to determine which cell type out of total lymphocytes was responsible for most of the IFN-γ+ signal in our PBMC stimulation and intracellular cytokine staining assay. Based on our responder criteria only post-converters and

remotely infected individuals had sufficient CFP-10/ESAT-6 responders to perform tSNE analysis required to unbiasedly determine the main IFN-γ+ cell type. We therefore decided first performed initial tSNE analysis of CFP-10/ESAT-6 lysate-specific IFN-γ+ lymphocytes from post-converters and remotely infected individuals (Table 32). We then performed confirmatory tSNE analysis on M.tb lysate-specific IFN-γ+ lymphocytes from all groups as they had a minimum 33.33% responder rate (Table 32). M.tb lysate contains antigens that are also present in BCG and is the only stimulant we expected to detect antigen-specific responses in QFT-negative individuals. Thus, detection of M.tb lysate responders in all groups was not surprising.

Table 32: Proportions of M.tb-specific IFN-γ+ lymphocyte responders.

Group	CFP-10/ESAT-6			M.tb Lysate			Esp		
	Total (n)	Responders (n)	% of Responders	Total (n)	Responders (n)	% of Responders	Total (n)	Responders (n)	% of Responders
Non-Conv	28	6	21.43	28	17*	60.71*	27	3	11.11
Pre-Conv	27	4	14.81	26	12*	46.15*	25	3	12.00
Post-Conv	25	15*	60*	26	24*	92.31*	25	11*	44*
Remote TBI	29	21*	72.41*	30	30*	100*	30	13*	43.33*
Pre-Rev	30	5	16.67	28	20*	71.43*	26	4	15.38
Post-Rev	28	3	10.71	27	20*	74.07*	23	4	17.39

*Values highlighted in **bold red** are groups that had at least 10 responders and a responder rate of ≥33.33%.

We first used manually gated CD4, CD8 and CD4-CD8- T cells, CD3- (non T) and HLA-DR++ CD3- cells on total IFN-γ+ lymphocytes (Figure 68A). Using the tri-colour heat-map statistic in FlowJo, we were able to define 5 main cell clusters of IFN-γ producing lymphocytes based on the MFI of CD3-BV605, CD4-BV785, CD8-BV711 and HLA-DR-FITC (as a proxy for B cells) markers (Figure 68B). CD4 T cells accounted for a substantial proportion of CFP-10/ESAT-6-specific IFN-γ+ lymphocytes (post-converter = 66.4%; remote TBI= 70%; Figure 68C). As observed for CFP-10/ESAT-6, CD4+ T cells were the main source of IFN-γ and accounted for approximately 75% of IFN-γ expression post-conversion and during remote TBI, while they accounted for less than 50% of IFN-γ signal in non-converters (Figure 68D). Lower CD4 T cell (likely BCG-recall responses) but higher contribution of non-adaptive (CD4-CD8-) T cell and innate cell (non T cell) responses to the IFN-γ signal in non-converters compared to QFT+ individuals is further suggestive of uninfected nature of non-converters. QFT reverters (pre- and post-reversion) had similar T cell contribution to the IFN-γ signal as remote TBI (Figure 68D). Overall these results suggest that CD4 T cells were the main source of IFN-γ in QFT+

individuals, even post-reversion. We therefore decided to perform the rest of our analysis focusing on response kinetics observed in CD4+ T cells.

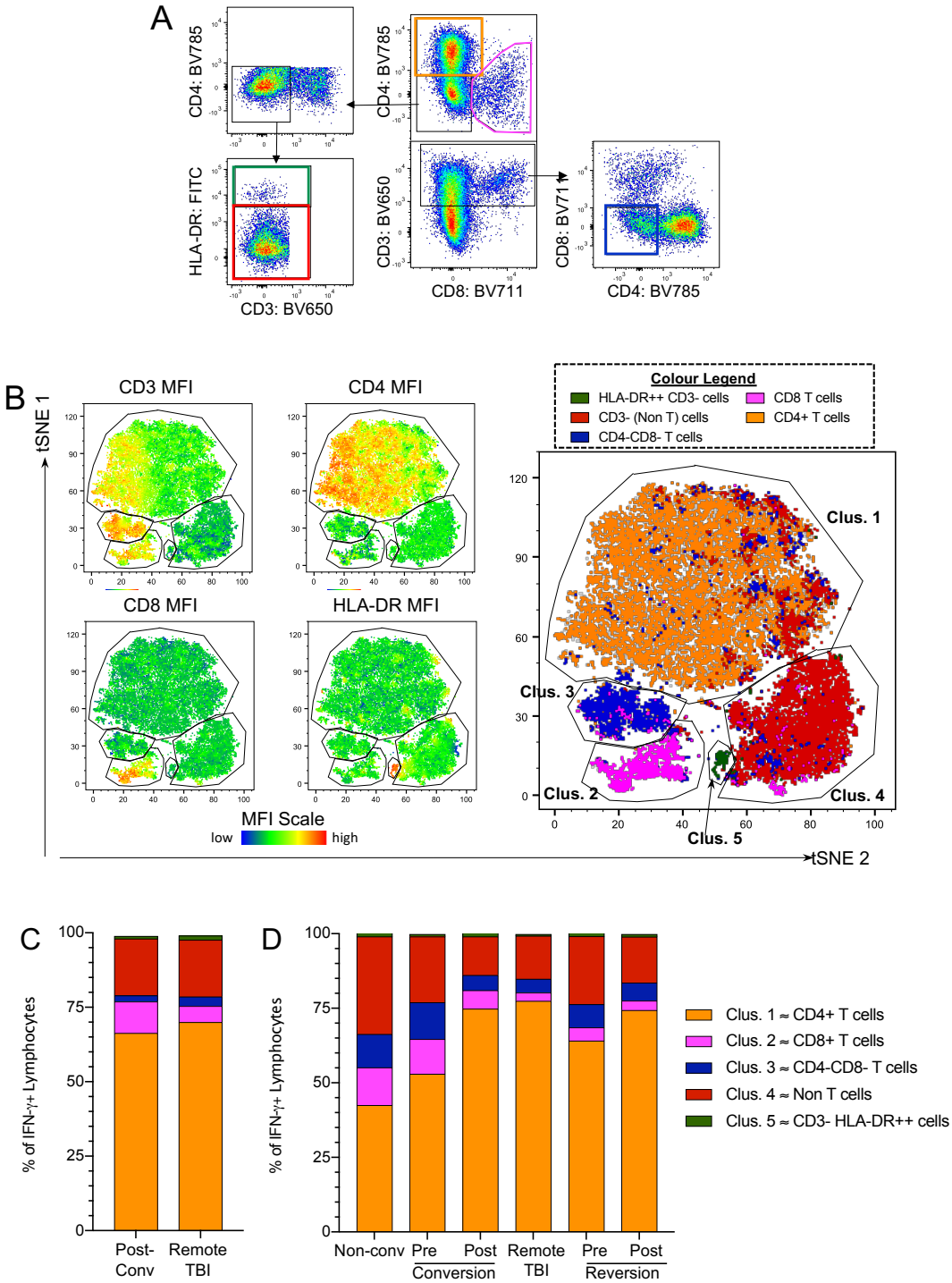

Figure 68: CD4 T cells are the main source of IFN-γ in QFT+ individuals. (A) Flow cytometry plots depict manual gating of CD4+ T cells (orange), CD8+ T cells (pink), CD4-CD8- T cells (blue), HLA-DR++ CD3- cells (green) and CD3-CD4-CD8- (non) T cells (red) on total IFN-γ+ lymphocytes. tSNE results (B) highlighting MFI of CD3-BV650, CD4-BV785, CD8-BV711 and HLA-DR-FITC, and 5 major clusters with cell populations manually defined in (A) highlighted. Graph depicts cellular contribution of each cluster defined in (B) [Cluster 1 ≈ CD4+ T cells (orange), Cluster 2 ≈ CD8+ T cells (pink), Cluster 3 ≈ CD4-CD8- T cells (blue), Cluster 4 ≈ non T cells and Cluster 5 ≈ CD3-HLA-DR++ cells (green)] to the total (C) CPF-10/ESAT-6 IFN-γ+ lymphocytes in post-converters and remote TBI and (D) M.tb lysate-specific IFN-γ+ lymphocytes in non-converters, pre- and post- conversion, remote TBI, pre- and post-reversion.

QFT reversion is not associated with decrease in IFN-γ production detected by flow cytometry

In Chapter 5, we showed that our experimental protocol sufficiently induced M.tb-specific IFN-γ-producing cells, the frequencies of which highly correlated with QFT responses, confirming that PBMC stimulation, intracellular cytokine staining and flow cytometry were suitable techniques to measure M.tb-specific immune responses associated with QFT reversion. We detected low levels of CFP-10/ESAT-6-specific IFN-γ+ CD4 T cells upon QFT reversion (month 12 and 18 of follow up, Figure 69A). This was not unexpected because M.tb-specific IFN-γ production is not bimodal around the QFT assay cut-off and can be detected even when an individual has a QFT negative test result (Adankwah et al., 2019; Penn-Nicholson et al., 2015). However, proportions of CFP-10/ESAT-6-specific IFN-γ+ CD4 T cells did not decrease upon QFT reversion and were maintained at similar levels throughout the study follow-up (Figure 69A). Additionally, we observed no correlation between QFT and CFP-10/ESAT-6-specific IFN-γ+ CD4 T cell responses in reverters (Figure 69B). Since we did not observe a difference in the frequencies of IFN-γ+ CD4 T cells during follow-up, we calculated median responses for each participant stratified by QFT status. As observed with immune responses detected at each visit, no significant difference in CFP-10/ESAT-6-specific IFN-γ+ CD4 T cells pre- and post-reversion (single value per QFT status) was observed (Figure 69C). Additionally, frequencies of IFN-γ+ CD8 T cells and lymphocytes were not significantly different pre- and post-reversion (Figure 69C). These results suggest that, at least in our cohort, QFT reversion is not associated with a decrease in CFP-10/ESAT6-specific IFN-γ+ responses detected by flow cytometry. QFT reversion observed in this cohort could be due to technical variability or detection of transient responses that decrease when measured upon fresh whole blood stimulation by ELISA but not by flow cytometry after M.tb antigen stimulation of cryopreserved PBMC.

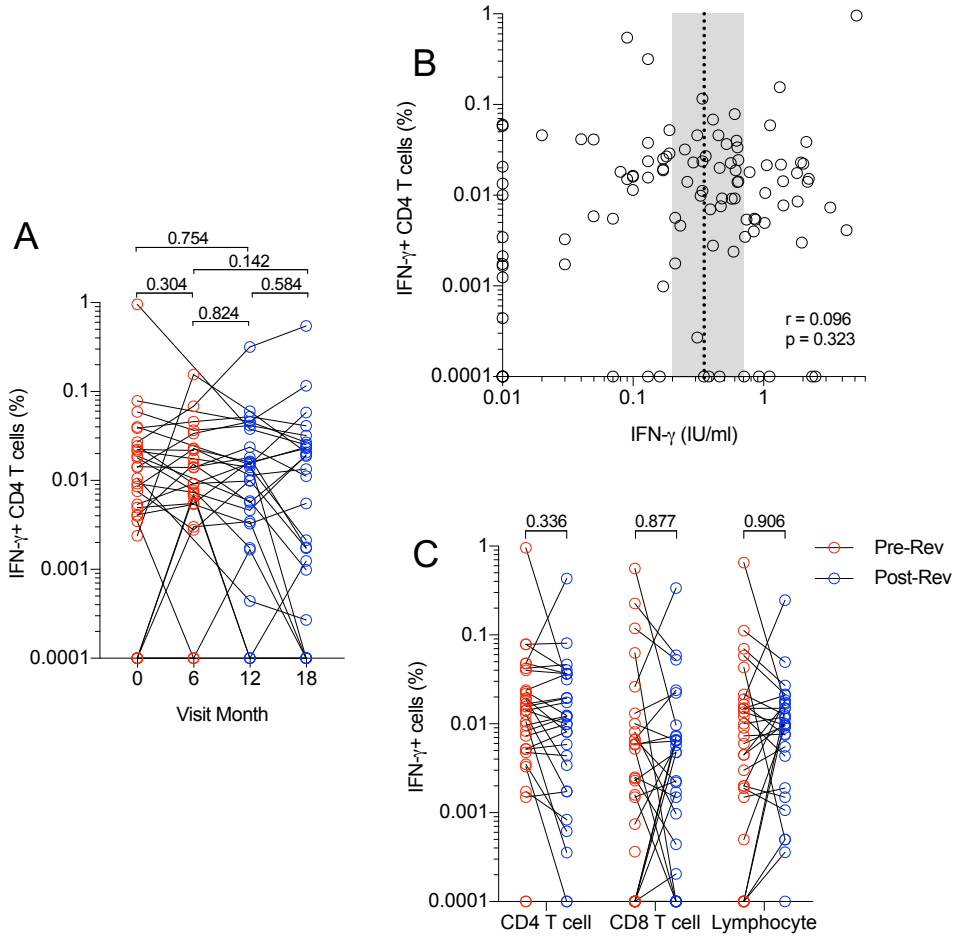

Figure 69: QFT reversion is not associated with a decrease in IFN-γ+ CD4 T cells detected by flow cytometry. Graph depicts (A) frequency of background subtracted CFP-10/ESAT-6-specific IFN-γ+ CD4 T cells detected in QFT reverters at Month 0: n=26 (red symbol), Month 6: n= 25 (red symbol), Month 12: n=28 (blue symbol) and Month 18: n=26 (blue symbol) study visits. (B) Immune responses detected before and after QFT reversion by flow cytometry (CFP-10/ESAT-6-specific IFN-γ+ CD4 T cells) and QFT-ELISA. Dotted line and shaded area represent the QFT cut-off (0.35 IU/mL) and uncertainty zone, respectively. r represents the Spearman's correlation coefficient. (C) Median CFP-10/ESAT-6-specific IFN-γ+ CD4 and CD8 T cells and total lymphocytes, measured pre- (red symbol) and post (blue symbol)- QFT reversion. P-values were calculated with the Wilcoxon-signed rank test, P-values < 0.0125 for (A) and < 0.05 (for B & C) were considered significant after correction for multiple comparisons.

Responses to immunodominant M.tb antigens are sustained in QFT reverters

We next wanted to determine how immune responses detected in QFT reverters compared to control groups. To reduce biases introduced by repeated sampling of each individual, we calculated median frequencies of cytokine+ (and other functional) antigen-specific responses, stratified by QFT status for each individual. CFP-10/ESAT-6-specific IFN-γ+ CD4 T cells detected pre-reversion were significantly lower than those detected in remote M.tb infected individuals, while those detected post-reversion were significantly higher than non-converters (Figure 70A). These results suggest that QFT reverters may potentially be exposed to lower mycobacterial burden than remotely infected individuals or have persistent memory

responses in the absence of exposure. Furthermore, CFP-10/ESAT-6-specific IFN-γ+ CD4 T cell responses pre-conversion were not significantly different to those in non-converters and significantly increased upon TBI (post-conversion) to levels in range with remote TBI (Figure 70A).

In the QFT assay whole blood is stimulated with CFP-10/ESAT-6/TB7.7 but M.tb expresses hundreds of antigens recognised by T cells (Arlehamn et al., 2016). We therefore determined if QFT reversion was associated with a decrease in M.tb-specific immune responses to other immunodominant antigens: Esp-peptide pool and M.tb lysate. As described in the introduction, EspC, EspF and Rv2348 proteins antigens are present in M.tb but absent in BCG and have been shown to correlate with QFT responses when combined with CFP-10 in an ESAT-6-free IGRA (Nemes et al., 2019; Ruhwald et al., 2017). Additionally, some individuals have been reported to have responses to Esp-peptide pool but not QFT antigens (Millington et al., 2010; Nemes et al., 2019; Ruhwald et al., 2017). As observed with CFP-10/ESAT-6-stimulation, Esp-specific IFN-γ+ CD4 T cells did not decrease upon QFT reversion (Figure 70B). However, immune responses detected pre- and post-QFT reversion were in range with those detected in remote TBI and non-converters, respectively (Figure 70B), probably due to high variability. Stimulation with M.tb lysate induced high levels of IFN-γ+ CD4 T cells in all study groups, including non-converters (Figure 70C), which could be due to a combination of BCG-recall responses, cross-reactivity with NTMs, or remote M.tb exposure which did not result in sustained QFT positivity. Overall, M.tb lysate-specific IFN-γ+ CD4 T cell kinetics were similar to those observed in response to CFP-10/ESAT-6, where immune responses did not decrease upon QFT reversion, and responses detected in reverters were of intermediate magnitude between non-converters and remote TBI (Figure 70C). These results further suggest that our cohort of QFT reverters maintain detectable M.tb-specific CD4 T cell responses, as suggested by the maintenance of TST reactivity, even after their QFT responses reverted to negative. However, persistent detection of functional responses in reverters, which were consistently of intermediate magnitude between non-converters and remote TBI, suggest that reverters may experience low levels of antigen exposure, consistent with contained infection. Alternatively, reverters may have cleared infection and maintain long-term memory albeit at lower levels than remotely infected individuals.

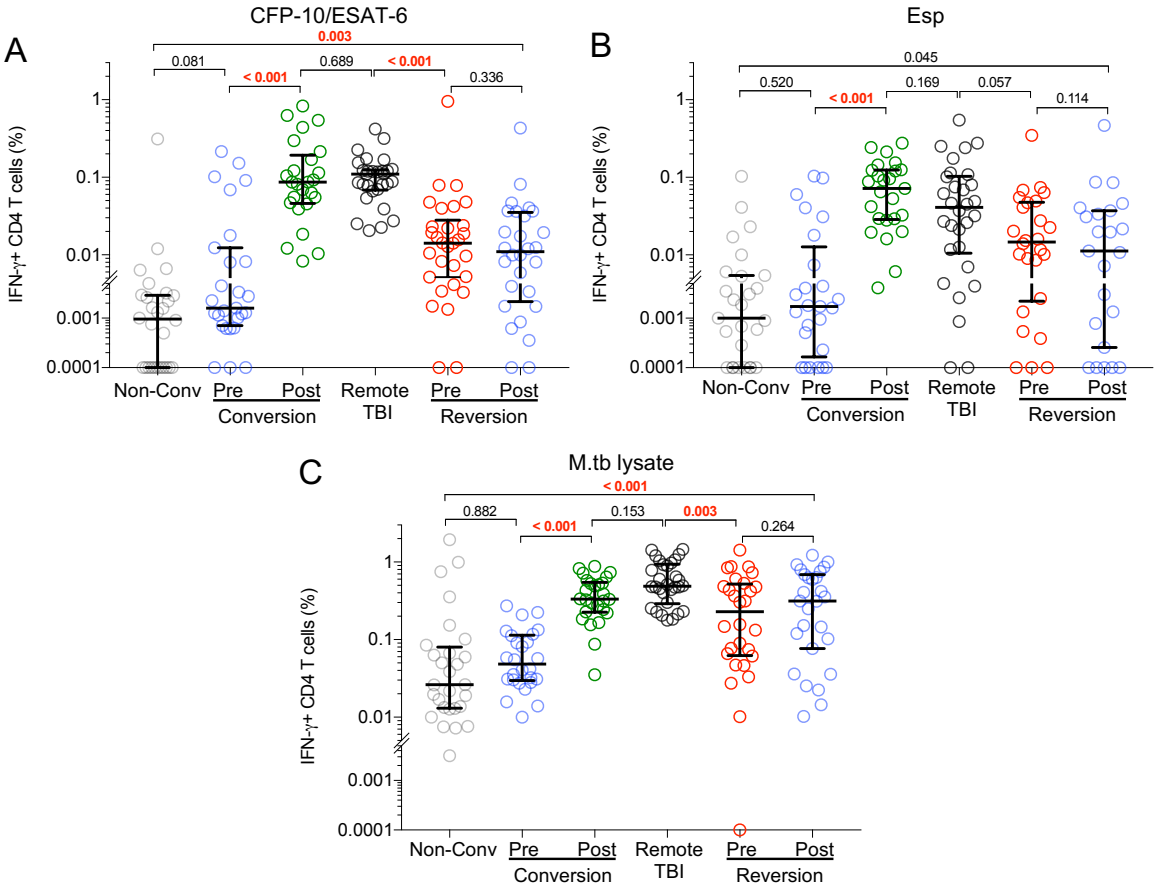

Figure 70: Immunodominant M.tb-specific IFN-γ+ CD4 T cells are maintained at similar frequencies during QFT reversion. Graphs depict (A) CFP-10/ESAT-6- (P10-ES6), (B) Esp- and (C) M.tb lysate- (M.tbL) specific IFN-γ+ CD4 T cells detected in non-converters (P10-ES6: n=28; Esp: n= 27; M.tbL: n= 28), pre-conversion (P10-ES6: n=27; Esp: n= 25; M.tbL: n= 26), post-conversion (P10-ES6: n=25; Esp: n= 25; M.tbL: n= 26), remote TBI (P10-ES6: n=29; Esp: n= 30; M.tbL: n= 30), pre-reversion (P10-ES6: n=30; Esp: n= 26; M.tbL: n= 28) and post-reversion (P10-ES6: n=28; Esp: n= 23; M.tbL: n= 27). P-values were calculated as defined in the methodology. P-values highlighted in **bold** red were considered significant after correction for multiple comparisons.

QFT reversion is associated with maintenance of functional M.tb-specific CD4+ T cells.

IFN-γ is not the only cytokine produced by M.tb-specific CD4 T cells and multiple studies have shown that these cells produce other Th1 associated cytokines, TNF and IL-2, as well as IL-17 and IL-22, among others (reviewed in Chapter 1: General introduction). We therefore aimed to determine whether M.tb-specific cells expressing Th1 cytokines, TNF and IL-2, are detectable in reverters. We detected robust levels of CFP-10/ESAT-6-specific TNF+ and IL-2+ CD4 T cells in reverters, that were sustained post-reversion (Figure 71A-B). As observed with CFP-10/ESAT-6-specific IFN-γ+ CD4 T cells, frequencies of TNF+ and IL-2+ CD4 T cells detected in reverters were lower than those detected in remote TBI but higher than non-converters. Again, no differences were observed between frequencies of TNF+ and IL-2+ CFP-10/ESAT-6-specific CD4 T cells between non-converters and pre-converters. Frequencies of CFP-10/ESAT-6-specific TNF+ and IL-2+ cells increased upon TBI, in range with those detected during remote

TBI. Additionally, we observed similar TNF+ and IL-2+ CD4+ T cells cohort differences in M.tb lysate specific CD4+ T cells (Figure 71C). Interestingly, Esp-specific CD4 T cells did not have similar functional differences as other immunodominant antigen responses, where Esp-specific-TNF+ and -IL-2+ CD4 T cells were only significantly different upon TBI (pre- *versus* post-conversion; Figure 71C). This could be because a few non-converters and pre-converters had robust detection of Esp-specific TNF+ and IL-2+ CD4 T cells, in range with those detected in post-converters, remote TBI and reverters, suggestive of historical M.tb exposure. Altogether, these results indicate that, as observed for IFN-γ, reverters maintain expression of M.tb-specific TNF and IL-2 at an intermediate magnitude between non-converters and remote TBI.

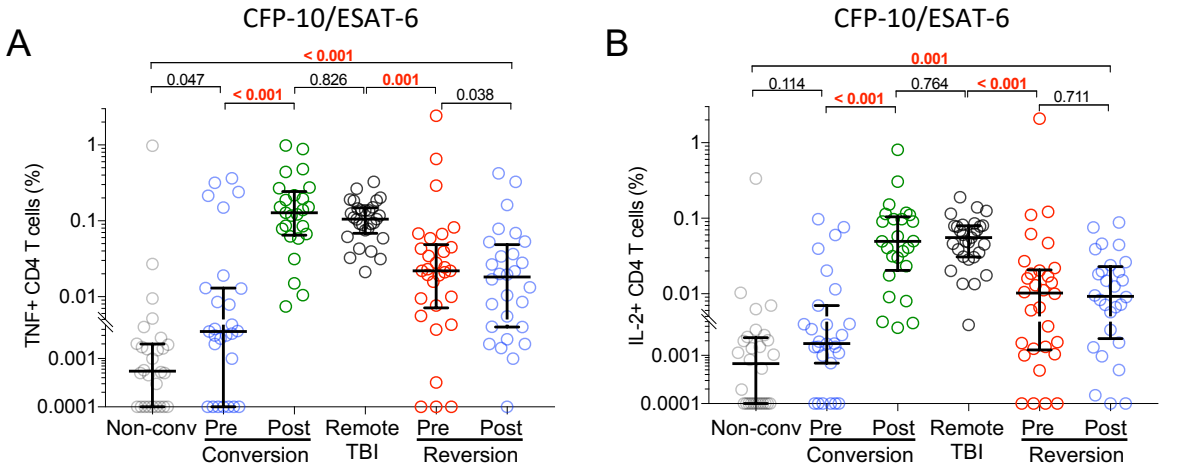

C

Cyt	Stim	Median (% of CD4 T cells) Non-Conv	Conversion Pre	Conversion Post	Remote TBI	Reversion Pre	Reversion Post	P-values Non-Conv vs Pre-Conv	Pre- vs Post-Conv	Post-Conv vs Remote TBI	Remote TBI vs Pre-Rev	Pre- vs Post-Rev	Post-Rev vs Non-Conv	Scale
TNF	M.tb lysate	0.043	0.071	0.439	0.518	0.249	0.251	0.924	**< 0.001**	0.534	**0.006**	0.958	**< 0.001**	0.4
	Esp	0.002	0.002	0.090	0.050	0.012	0.014	0.636	**< 0.001**	0.140	0.030	0.702	0.058	0.2
IL-2	M.tb lysate	0.013	0.035	0.233	0.264	0.124	0.114	0.801	**< 0.001**	0.655	0.015	1	**< 0.001**	
	Esp	0.001	0.002	0.025	0.017	0.004	0.009	0.635	**< 0.001**	0.130	0.037	0.838	0.035	

Figure 71: QFT reverters maintain expression of TNF and IL-2 cytokines. Graphs depict frequencies of CFP-10/ESAT-6-specific (A) TNF+ and (B) IL-2+ CD4 T cells, while (C) illustrates median expression of M.tb lysate- and Esp- specific TNF+ and IL-2+ CD4 T cells measured in non-converters, pre- and post-conversion, remote TBI, pre- and post-reversion. Number of participants and calculation of P-values is as in **Figure 70**. P-values highlighted in **bold** red were considered significant after correction for multiple comparisons.

Few studies have investigated immune responses, beyond IGRAs and TSTs, associated with QFT reversion, with only one study solely focused on investigating CD4 T cell immune responses. Similar to our QFT cohort dynamics, Medawar and colleagues (Gambian Cohort), demonstrated a decrease in M.tb-specific IFN-γ+ responses measured by Luminex upon reversion (Medawar et al., 2019). However, we observed no such difference when we utilised

flow cytometry to investigate M.tb-specific immune responses. This suggests that different protocols, technologies, and immunological read-outs have an impact on conclusions made. Alternatively, differences observed could be due to the reverter cohort definition, where Medawar and colleagues studied recently exposed tuberculosis-HHC who reverted, while we do not know when the initial M.tb-exposure occurred in our cohort of adolescent reverters. Additionally, baseline QFT responses in tuberculosis-HHC converters and reverters (before reversion) were similar, thus suggesting that the reversion signal observed was not due transient responses around the assay cut-off (Medawar et al., 2019). QFT reversion of tuberculosis-HHC was associated with a decrease in M.tb-specific IFN-γ, IL-2 and IL-22 responses, to similar levels as those observed in non-converters. Further, lower levels of IL-2 and IFN-γ could distinguish reverters from remote M.tb infected individuals. Based on these results, QFT reversion observed in the Gambian cohort could be suggestive of early antigen clearance upon recent exposure. Unlike observations made in the Gambian cohort (Medawar et al., 2019), we and others have detected significantly lower IFN-γ levels at QFT conversion in those who subsequently reverted, compared with sustained converters (Andrews et al., 2017; Xin et al., 2019a). Also, Xin and colleagues detected higher IGRA responses in discordant (QFT-TST+) reverters than concordant (QFT-TST-) reverters (Xin et al., 2019a). Additionally, they observed lower serum levels of MCP-1 and IL-8 in concordant QFT reverters (but not discordant reverters) compared with remote TBI (Xin et al., 2019a). These results highlight the spectrum of functional M.tb-specific immune responses associated with reversion, which could be different in individuals with recent or remote M.tb exposure.

In addition to measuring Th1 cytokine expression, we also measured expression of CD154 and CD107. CD154 is a functional marker that is upregulated when cells are activated through interaction with its ligand CD40 on antigen-presenting cells and is also involved in providing T cell help to B cells. CD107 is a marker of cytotoxic molecule degranulation, that is expressed on the cell membrane of cells that have recently released cytotoxic molecules. We included these markers because we wanted to detect Th1 cytokine-independent functional responses and potential T cell cytotoxic ability of reverters. We detected high levels of non-specific CD154+ and CD107+ CD4 T cells in all individuals regardless of QFT status. Overall, M.tb-specific-CD154+ and CD107+ CD4 T cells were detected in the majority of individuals from all groups, including 15 non-converters (Figure 72). Frequencies of CD154+ and CD107+ cells were predominantly not different between groups, regardless of stimulation, with the

exception of a significant increase in M.tb lysate-specific CD154+ CD4 T cells upon recent TBI (QFT conversion) (Figure 72C).

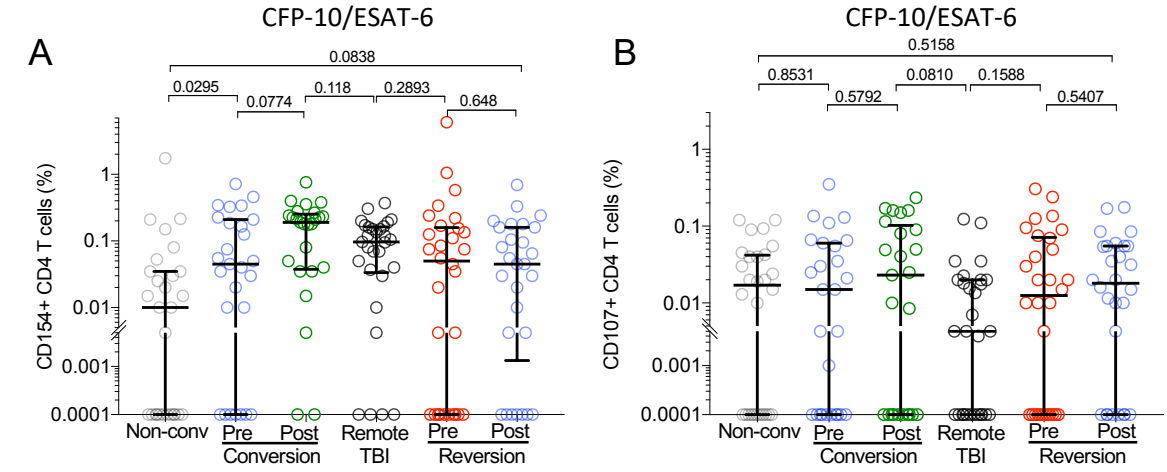

C

Function	Stim	Median (% of CD4 T cells) Non-Conv	Conversion Pre	Conversion Post	Remote TBI	Reversion Pre	Reversion Post	P-values Non-Conv vs Pre-Conv	Pre- vs Post-Conv	Post-Conv vs Remote TBI	Remote TBI vs Pre-Rev	Pre- vs Post-Rev	Pre-Rev vs Non-Conv	Scale
CD154	M.tb lysate	0.115	0.135	0.415	0.405	0.230	0.275	0.952	**< 0.006**	0.752	0.014	0.658	0.102	0.4
	Esp	0.060	0.070	0.140	0.070	0.088	0.150	0.831	0.090	0.207	0.846	0.216	0.201	0.3
CD107	M.tb lysate	0.011	0.008	0.016	0.012	0.023	0.010	0.800	0.182	0.325	0.431	0.676	0.747	0.2
	Esp	0.004	0.000	0.001	0.002	0.010	0.012	0.477	0.489	0.743	0.403	0.940	0.911	0.1
														0

Figure 72: M.tb-specific CD154+ and CD107+ responses are detected similar levels regardless of stage of M.tb infection. Graphs depict frequencies of CFP-10/ESAT-6-specific (A) CD154+ and (B) CD107+ CD4 T cells, while (C) illustrates median frequencies of M.tb lysate- and Esp-specific-CD154+ and CD107+ CD4 T cells measured in non-converters, pre- and post-conversion, remote TBI, pre- and post-reversion. Number of participants, and calculation of P-values is as in **Figure 70**. P-values highlighted in **bold** red were considered significant after correction for multiple comparisons.

Next, we investigated polyfunctional cytokine expression patterns associated with QFT-reversion. Polyfunctionality scores (computed by COMPASS) summarise the polyfunctional ability of T cells, where higher scores are associated with the ability to produce multiple functional molecules at a single-cell level (Darrah et al., 2007; Lin et al., 2015; Seder et al., 2008). M.tb-specific CD4+ T cell polyfunctionality scores were not significantly different pre- and post-reversion, regardless of antigenic stimulation, with highest scores observed in M.tb lysate-specific CD4+ T cells (Figure 73A-C). Group comparisons confirmed previous observations, where polyfunctionality scores in reverters were higher than non-converters but lower than remote M.tb infected individuals (Figure 73A-C). The only exception to this were comparable M.tb lysate-specific polyfunctionality scores between remote TBI and pre-reversion (Figure 73B). These results suggest that once M.tb infected, the polyfunctionality of M.tb-specific memory cells is maintained, even upon QFT reversion.

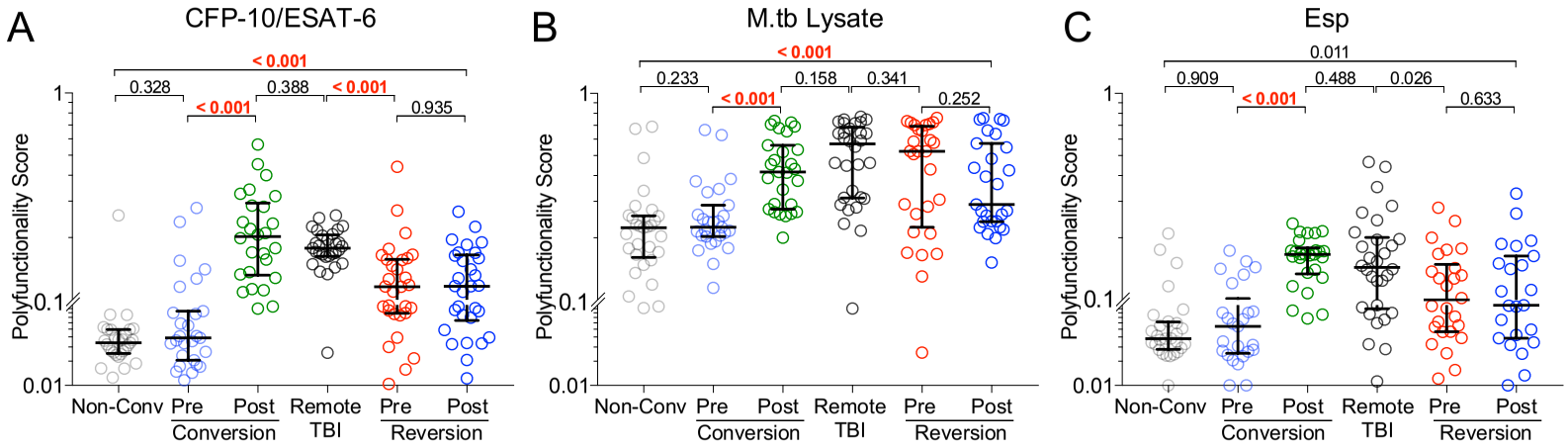

D

	CD154	IL-2	TNF	IFN-γ	CD107	Median (% of CD4 T cells) Non-Conv	Conversion Pre	Conversion Post	Remote TBI	Reversion Pre	Reversion Post	P-values Non-Conv vs Pre-Conv	Pre- vs Post-Conv	Post-Conv vs Remote TBI	Remote TBI vs Pre-Rev	Pre- vs Post-Rev	Post-Rev vs Non-Conv
Early Differentiation	+	-	-	-	-	0.0084	0.0420	0.0996	0.0148	0.0492	0.0305	0.048	0.943	0.032	0.244	0.959	0.065
	-	-	-	-	+	0.0163	0.0112	0.0217	0.0050	0.0164	0.0246	0.907	0.897	0.103	0.129	0.955	0.302
	+	-	+	-	-	0.0003	0.0006	0.0119	0.0077	0.0029	0.0037	0.052	**0.002**	0.041	0.190	0.168	**< 0.001**
	-	-	+	-	-	0.0010	0.0019	0.0127	0.0061	0.0022	0.0023	**0.016**	**0.007**	0.033	0.056	0.489	0.024
	+	+	+	-	-	2.98 e-05	0.0006	0.0094	0.0058	0.0024	0.0023	0.035	**0.003**	0.087	0.101	0.622	**< 0.001**
	-	+	+	-	-	0.0000	0.0002	0.0019	0.0005	0.0002	0.0001	**0.001**	**< 0.001**	**0.006**	0.162	0.149	0.031
Late Differentiation	+	+	+	+	-	0.0000	0.0002	0.0268	0.0292	0.0047	0.0035	0.036	**< 0.001**	0.886	**< 0.001**	0.089	**< 0.001**
	-	+	+	+	-	0.0000	0.0000	0.0113	0.0078	0.0009	0.0006	0.304	**< 0.001**	0.704	**< 0.001**	0.063	**< 0.001**
	+	-	+	+	-	0.0000	0.0002	0.0143	0.0159	0.0027	0.0027	**0.004**	**< 0.001**	0.953	**< 0.001**	0.936	**< 0.001**
	-	-	+	+	-	0.0001	0.0003	0.0162	0.0145	0.0009	0.0011	0.430	**< 0.001**	0.833	**< 0.001**	0.793	**0.009**
	+	+	-	+	-	0.0000	0.0001	0.0004	0.0005	0.0003	0.0003	0.108	0.031	0.571	0.190	0.402	**0.004**
	-	+	-	+	-	0.0000	1.64 e-05	0.0001	0.0001	5.83 e-06	1.89 e-07	0.189	**0.004**	0.800	**< 0.001**	0.271	0.640
	+	-	-	+	-	0.0000	0.0007	0.0011	0.0017	0.0006	0.0002	**0.001**	0.706	0.820	0.030	0.334	0.194
	-	-	-	+	-	0.0006	0.0011	0.0077	0.0065	0.0013	0.0014	0.045	**0.001**	0.966	**< 0.001**	0.846	0.027

Scale: 0.08, 0.06, 0.04, 0.02, 0

Figure 73: Polyfunctionality score and polyfunctional profiles are not significantly different between pre- and post- reversion. Graphs depict (A) CFP-10/ESAT-6- (B) M.tb lysate and (C) Esp- specific polyfunctionality scores, while (D) represent median frequencies of CFP-10/ESAT-6-specific polyfunctional CD4 T cell subsets measured in non-converters, pre- and post-conversion, remote TBI, pre- and post-reversion. Number of participants, and calculation of P-values is as in **Figure 70**. P-values <0.025 and < 0.0125 for paired and unpaired comparisons for A-C, and P < values with an FDR of < 0.05 for D, highlighted in **bold** red were considered significantly different.

Expression of IFN-γ-independent polyfunctional profiles is associated with lower antigen exposure and early T cell differentiation (Seder et al., 2008), as well as resistance to M.tb infection, as observed in resisters (Lu et al., 2019). We therefore aimed to determine if QFT reversion is associated with preferential maintenance of IFN-γ-independent cytokine co-expressing T cells compared to control groups, specifically enrichment of CD154+TNF+IL-2+ CD4 T cells. As expected, the magnitude of cytokine co-expressing T cells was highest in post-converters and during remote TBI, with most cells expressing CD154 only and TNF+ IFN-γ+ cells (Figure 73D). Higher frequencies of CFP-10/ESAT-6-specific IL-2+TNF+ (early differentiated) CD4+ T cells were observed post-conversion compared to remote TBI, characteristic of lower duration of antigen exposure. Polyfunctional CD4 T cell subsets were not different pre- and post-reversion, with no enrichment of CD154+TNF+IL-2+ CD4 T cells (Figure 73D). Frequencies of CFP-10/ESAT-6-specific IFN-γ-independent TNF+IL-2± subsets were not significantly different between reverters and remote TBI. However, we observed significantly lower frequencies of CFP-10/ESAT-6 TNF+IFN-γ+ polyfunctional subsets in reverters than remote TBI (Figure 73D). Results described here relate to frequencies of CD4 T cell polyfunctional responses. However, approximately a third of reverters had CFP-10/EAST-6-specific Th1 cytokine co-expressing frequencies that were less than 0.01% of total CD4 T cells. We further wanted to investigate if Th1 functional profiles were significantly different upon reversion, as well as between reverters and controls in responders only. This analysis ignored expression of CD154 and CD107 because expression of these functional markers had high background responses and were predominantly not different between groups (Figure 72). Thus, we only analysed Th1 cytokine co-expression (IFN-γ±TNF±IL-2±) profiles in groups that had a minimum responder rate of 33.33% and/or at least 10 responder participants per group (Table 33). Based on this responder criterion less than half of the reverters were classified as responders to CFP-10/ESAT-6 stimulation. This further encouraged us to investigate Th1 cytokine co-expression profiles in responders only.

Table 33: Antigen-specific Th1+ CD4 T cell responders.

Group	CFP-10/ESAT-6			M.tb Lysate			Esp		
	Total (n)	Responders (n)	% of Responders	Total (n)	Responders (n)	% of Responders	Total (n)	Responders (n)	% of Responders
Non-Conv	29	4	13.79	29	24*	82.76*	28	5	17.86
Pre-Conv	27	6	22.22	26	20*	76.92*	25	5	20.00
Post-Conv	26	24*	88.46*	26	26*	100*	26	19*	69.23*
Remote TBI	29	28*	96.55*	30	30*	100*	30	16*	53.33*
Pre-Rev	30	11*	36.67*	27	22*	81.48*	26	8	30.77
Post-Rev	29	12*	41.38*	27	25*	92.59*	23	6	26.09

*Values highlighted in **bold** red are groups that had at least 10 responders and a responder rate of ≥ 33.33%.

We detected a heterogeneous population of both IFN-γ+ and IFN-γ- M.tb lysate-specific cytokine co-expression subsets in non-converters and pre-converters, where IFN-γ-TNF±IL-2± accounted for almost 40% of total M.tb-specific CD4 T cells, compared to less than a third of total cells in post-converters, remote TBI and reverters (Figure 74A). M.tb lysate-specific immune profiles were not different between remote TBI and pre-reverters, while post-reversion was associated with lower proportions of TNF+ only cells and a higher FDS compared with non-converters (Figure 74A). Recent TBI (post-conversion) was associated with higher proportions of M.tb lysate IFN-γ-TNF+IL-2+ CD4 T cells compared to remote TBI, which resulted in a significantly lower FDS (Figure 74B). As observed in Chapter 5, CFP-10/ESAT-6- and Esp-specific functional profiles were not significantly different between recent-converters and remote TBI. Interestingly, more than half of CFP-10/ESAT-6-specific responses in reverters were IFN-γ-TNF±IL-2±. Additionally, pre-reverters exhibited higher proportions of M.tb-lysate TNF only and IFN-γ-TNF+IL-2+ CD4 T cells, but lower FDS and proportions of IFN-γ+TNF+IL-2+ and IFN-γ+TNF+IL-2- M.tb-lysate CD4+ T cell compared with remote TBI (Figure 74). These results contradict findings by Jenum and colleagues that showed that QFT reversion (in TST-negative adolescents) was associated with non-significant differences in M.tb-specific Th1 polyfunctional profiles compared with remote TBI (Jenum et al., 2014). However, this study had a limited sample size: 14 remote TBI and 6 reverters. Therefore, their inability to detect significant differences between the two groups could be due to low statistical power.

Overall, our functional analysis indicates that QFT reverters maintain M.tb-specific polyfunctional responses, that are not restricted to CFP-10/ESAT-6. Based on this, reversion could be associated with lower antigen burden and indicative of M.tb clearance as suggested by a predominantly similar distribution of Th1 cytokine co-expression profiles between

reverters and non-converters, and detection of higher CFP-10/ESAT-6-specfic IFN-γ-independent responses but lower CFP-10/ESAT-6-specfic functional differentiation scores in reverters compared to remote TBI.

A

Stim	IFN-γ	TNF	IL-2	Median (% of Th1 Cytokine+ CD4 T cells) Non-Conv	Conversion Pre	Conversion Post	Remote TBI	Reversion Pre	Reversion Post	P values Non-Conv vs Pre-Conv	Pre- vs Post-Conv	Post-Conv vs Remote TBI	Remote TBI vs Pre-Rev	Pre- vs Post-Rev	Post-Rev vs Non-Conv
M.tb lysate	-	-	+	4.2	5.8	1.6	1.2	2.0	2.5	0.058	< 0.001	0.141	0.013	0.614	0.03
	-	+	-	26.1	21.9	12.4	10.8	11.0	10.7	0.795	0.012	0.052	0.097	0.104	0.003
	-	+	+	7.6	8.9	11.7	6.0	9.9	7.1	0.612	0.021	< 0.001	0.044	0.013	0.849
	+	+	+	20.1	17.6	41.2	37.3	38.0	33.7	0.564	< 0.001	0.475	0.65	0.514	0.021
	+	+	-	19.7	21.8	16.9	29.1	24.5	26.8	0.502	0.560	0.001	0.198	0.131	0.02
	+	-	+	1.4	1.6	1.5	1.7	1.2	1.9	0.733	0.112	0.155	0.146	0.012	0.406
	+	-	-	9.2	6.8	4.4	9.0	6.1	7.9	0.733	< 0.001	0.007	0.036	0.076	0.912
CFP-10/ESAT-6	-	-	+			2.1	3.3	5.4	6.2			0.09	0.156	0.683	
	-	+	-			20.4	17.1	35.1	25.0			0.293	< 0.001	0.067	
	-	+	+			11.2	7.4	20.5	19.1			0.02	0.003	0.76	
	+	+	+			37.9	35.8	11.3	17.6			0.932	0.003	0.359	
	+	+	-			18.3	19.4	9.3	13.4			0.311	< 0.001	0.025	
	+	-	+			1.3	2.4	1.9	1.3			0.048	0.255	0.919	
	+	-	-			4.2	8.9	3.7	5.8			0.018	0.02	0.185	
Esp	-	-	+			3.6	2.3					0.345			
	-	+	-			15.6	9.6					0.214			
	-	+	+			7.5	4.4					0.132			
	+	+	+			37.9	29.8					0.540			
	+	+	-			17.8	27.0					0.076			
	+	-	+			1.3	2.2					0.074			
	+	-	-			4.1	7.2					0.150			

Scale: 40, 30, 20, 10, 0

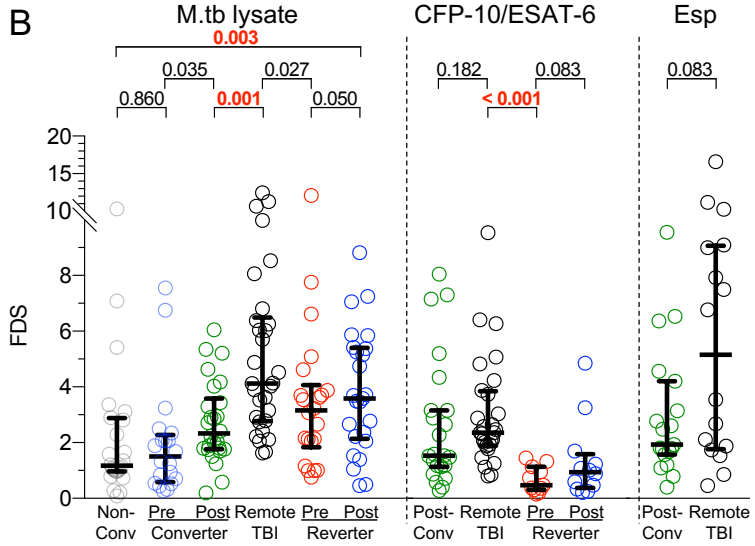

Figure 74: Reverters have lower CFP-10/ESAT-6-specific functional differentiation than remote M.tb infected individuals. (A) Median proportions of polyfunctional CD4 T cells and (B) functional differentiation scores of M.tb-specific CD4 T cells in non-converters (M.tbL: n= 24), pre-conversion (M.tbL: n= 20), post-conversion (P10-ES6: n=23; M.tbL: n= 26 ; Esp: n= 20), remote TBI (P10-ES6: n=28; M.tbL: n= 30 ; Esp: n= 19), pre-reversion (P10-ES6: n=11; M.tbL: n= 22) and post-reversion (P10-ES6: n=12; M.tbL: n= 25). P-values were calculated and corrected as described in the methodology. P-values highlighted in **bold** red were considered significantly different.

Reversion is associated with the maintenance of predominantly T_{TM} and T_E cells.

Less differentiated T cell memory and IFN-γ- functional phenotypes have been associated with lower antigen load (Seder et al., 2008). To determine if this is also true for M.tb-specific CD4 T cells during QFT reversion, we measured the kinetics of memory subsets in our cohort. We defined memory subsets based on co-expression of CD45RA (RA), CCR7 (R7), CD27 (27) and KLRG-1 (G1). Of the 16 potential memory combinations, we focused our analysis on 6 memory subsets: T_{SCM} (RA+R7+27+G1-), T_{CM} (RA-R7+27+G1-), T_{TM} (RA-R7-27+G1±) and T_E (RA-R7-27-G1±) because these subsets comprised ≥ 2% of antigen-specific responses in all groups regardless of stimulation (Figure 75). As observed in Chapter 5, the predominant memory subsets in post-converters and remote TBI, as well as reverters were T_{TM} and T_E cells (Figure 75). Despite detecting high levels T_{TM} and T_E cells in non-converters and pre-converters, these individuals also had sizeable (≥ 20%) proportions of both T_{SCM} and T_{CM} cell subsets. Further, we observed significantly lower proportions of T_{SCM}/T_{CM} subsets in post-reverters than non-converters (Figure 75). Proportions of these less differentiated T_{SCM} and T_{CM} cells also decreased upon TBI, confirming that higher proportions of these memory phenotypes are associated with lower antigen burden (Figure 75).

Following the results above, we aimed to determine if a combination of memory and functional markers could be used to identify subsets that were significantly different between groups using an unbiased approach, CITRUS. We excluded HLA-DR, CD107, CD154 and CXCR3 from CITRUS analysis because these markers did not contribute to the definition of any differentially expressed subset. Additionally, CXCR3 expression was not significantly different between groups, with a median expression of less than 25% of M.tb-specific CD4 T cells regardless of group (Figure 76).

Stim	RA	R7	27	G1	Popn	Median (% of Th1 Cytokine+ CD4 T cells)						P values						Scale
						Non-Conv	Conversion		Remote TBI	Reversion		Non-Conv vs Pre-Conv	Pre- vs Post-Conv	Post-Conv vs Remote TBI	Remote TBI vs Pre-Rev	Pre- vs Post-Rev	Post-Rev vs Non-Conv	
							Pre	Post		Pre	Post							
M.tb lysate	+	+	+	-	T_{SCM}	9.8	7.3	2.2	2.1	2.1	1.7	0.860	**0.001**	0.465	0.279	0.401	**0.001**	
	-	+	+	-	T_{CM}	12.5	16.6	7.5	8.2	9.4	8.3	0.444	**0.001**	0.824	0.313	0.185	0.023	
	-	-	+	-	T_{TM}	25.9	22.1	35.0	29.5	31.0	28.4	0.972	**< 0.001**	0.106	0.788	0.695	0.177	
	-	-	+	+	T_{TM}	6.3	12.6	9.4	10.6	8.9	10.7	0.075	0.507	0.736	0.69	0.121	0.201	
	-	-	-	-	T_E	18.6	14.6	29.3	23.0	24.9	21.2	0.161	**0.004**	0.297	0.598	0.271	0.787	
	-	-	-	+	T_E	8.5	8.9	8.9	18.9	13.3	13.9	0.878	0.305	**0.005**	0.146	0.032	0.131	
CFP-10/ESAT-6	+	+	+	-	T_{SCM}			3.4	4.8	5.0	6.0			0.244	0.743	0.683		
	-	+	+	-	T_{CM}			4.8	7.8	16.3	12.1			0.182	0.004	0.541		
	-	-	+	-	T_{TM}			32.9	38.5	36.9	35.0			0.201	0.543	0.61		
	-	-	+	+	T_{TM}			6.9	9.1	4.8	5.6			0.813	0.326	1		
	-	-	-	-	T_E			26.9	18.4	20.5	17.4			0.06	0.289	1		
	-	-	-	+	T_E			8.1	8.5	5.4	7.1			0.466	0.185	0.154		
Esp	+	+	+	-	T_{SCM}			2.8	4.3					0.136				
	-	+	+	-	T_{CM}			7.3	5.7					0.289				
	-	-	+	-	T_{TM}			29.1	30.4					0.778				
	-	-	+	+	T_{TM}			6.8	4.7					0.150				
	-	-	-	-	T_E			35.6	29.6					0.728				
	-	-	-	+	T_E			6.5	9.6					0.345				

Figure 75: Reversion is not associated with a shift in T cell memory composition. Table depicts median proportions of T_{SCM} (RA+R7+27+G1-), T_{CM} (RA-R7+27+G1-), T_{TM} (RA-R7-27+G1±) and T_E (RA-R7-27-G1±) memory cells in M.tb lysate-, CFP-10/ESAT-6- and Esp- specific Th1 cytokine+ CD4 T cells in non-converters, pre- and post-conversion, remote TBI, pre- and post-reversion. Number of participants and p-values calculations is as in **Figure 74.** P-values highlighted in **bold** red were considered significantly different after Benjamin-Hochberg correction for multiple comparisons.

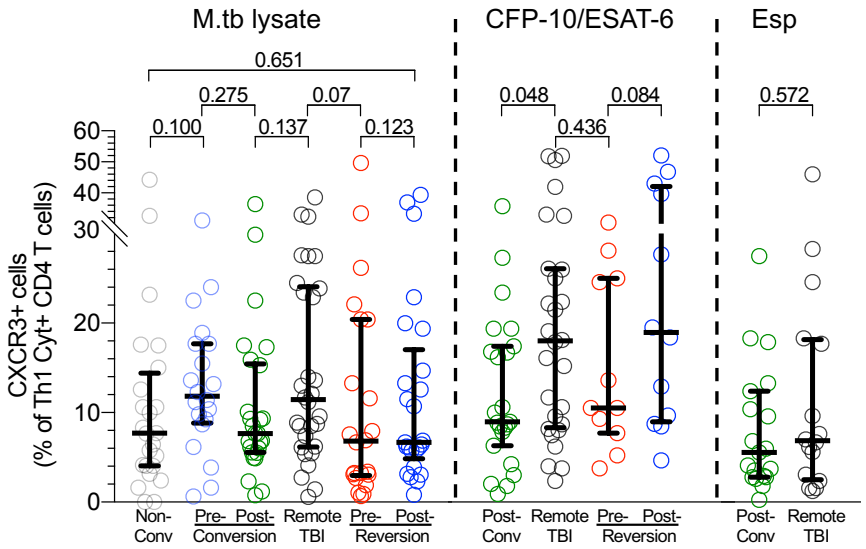

Figure 76: M.tb-specific CXCR3 expression levels are not different between groups. Graphs depict proportions of CXCR3+ M.tb lysate, CFP-10/ESAT-6- and Esp- specific Th1 cytokine+ CD4 T cells in non-converters, pre- and post-converters, remote TBI, pre- and post-reverters. Number of participants and p-values calculations is as in **Figure 74**.

Independent CITRUS analyses were performed on total Th1 cyt+ CD4 T cells (from responders only), for all pre-defined group comparisons possible: (i) non-converters *versus* pre-converter,

(ii) pre- *versus* post-converter, (iii) post-converter *versus* remote TBI, (iv) remote TBI *versus* pre-reverter, (v) pre- *versus* post-reverter and (vi) post-reverter *versus* non-converter. CITRUS analyses did not identify any differences in T cell cluster abundance levels between M.tb lysate-specific T cells from non-converters and pre-converters, pre- and post-reverters, and Esp-specific T cells from post-converters and remote TBI. We identified M.tb lysate-specific T cell clusters expressed at significantly different abundance between pre- and post-converters (12 clusters), post-converters and remote TBI (11 clusters), remote TBI and pre-reverters (6 clusters), and post-reverters and non-converters (5 clusters). While CFP-10/ESAT-6-specific CITRUS analysis identified T cell clusters expressed at significantly different abundance levels between post-converters and remote TBI (3 clusters), remote TBI and pre-reverters (11 clusters), and pre- and post-reverters (1 cluster). Before confirming cluster identity by manual gating, we compared histogram expression patterns of differentially expressed CITRUS clusters to ensure that there were no duplicate populations (Appendix 4-11). This is because in some cases the cluster composition of smaller secondary clusters that branch off the primary cluster differ by minor variations but are not sufficiently different to be defined as a distinct cluster upon comparison of histogram composition. Further, T cell clusters that had the same expression pattern but branched off different nodes of the CITRUS tree were considered identical populations. These quality control steps reduced the number of unique differentially expressed populations that were confirmed using manual gating in Flow Jo (Table 34). The composition of each unique differentially expressed T cell cluster between 2 groups is illustrated in Appendix 12. Upon confirmation of CITRUS cluster composition, we manually gated cell subsets in all responders, and performed confirmatory statistical tests on manually gated populations that comprised ≥ 2% of antigen-specific responses in all responders. As a result, the final number of cell clusters that were confirmed to exist by manual gating for some the of the comparisons were less than the number of distinct populations identified in CITRUS.

Table 34: Number of differentially expressed clusters identified between 2 groups using CITRUS.

Ag Specificity	TBI Comparison	Total Clusters	Differentially expressed (DE) clusters	Unique DE populations	Cell populations confirmed by Manual Gating in FlowJo
M.tb lysate	Non-Converter vs Pre-Converter	31	0	0	0
	Pre- vs Post Converter	29	12	6	5
	Post-Converter vs Remote TBI	30	11	4	3
	Remote TBI vs Pre-Reverter	31	6	3	3
	Pre- vs Post-Reverter	30	0	0	0
	Post-Reverter vs Non-converter	32	5	2	1
CFP-10/ ESAT-6	Post-Converter vs Remote TBI	30	3	1	1
	Remote TBI vs Pre-Reverter	31	21	7	6
	Pre- vs Post-Reverter	31	1	1	1
Esp	Post-Converter vs Remote TBI	29	0	0	0

Composition of DE distinct population is illustrated in Appendix 4-11

As expected, acquisition of TBI (pre- vs post-conversion) was associated with a decrease in T_{SCM}/T_{CM} IL-2 only (cluster 6335), $T_{CM/TM}$ TNF only (cluster 6320/40) and $T_{TM/TE}$ IFN-γ only (cluster 6334), and an increase in T_E IFN-γ+TNF+IL-2+ (cluster 6326) M.tb-lysate specific CD4 T cells (Figure 77A). Additionally, we identified higher proportions of IFN-γ-TNF+IL-2+ early differentiated cells (cluster 12425) but lower proportions of IFN-γ+TNF+IL-2- (cluster 12426) and IFN-γ only T_E (cluster 12417) M.tb-lysate specific CD4 T cells in post-converters compared to remote TBI (Figure 77B). Despite detecting differences in cellular composition using CITRUS, proportions of manually gated early differentiated CD45RA-CD27+TNF+IL-2± (cluster 9813/20) and T_E IFN-γ+TNF+IL-2- (cluster 9823) T cells were not different ($p > 0.05$) between pre-reverters and remote TBI (Figure 77C). This could because manually gated clusters were defined using Boolean combinations, while CITRUS analysis does not use such binary definitions, which resulted in slightly different cell populations that were not different. We also detected lower proportions of less differentiated TNF only T_{SCM} (cluster 2662) M.tb-lysate specific CD4 T cells in post-reverters compared to non-converters (Figure 77D). Overall, the majority of M.tb lysate-specific memory/functional subsets induced upon recent TBI, maintained during remote TBI and detectable upon reversion did not differ significantly.

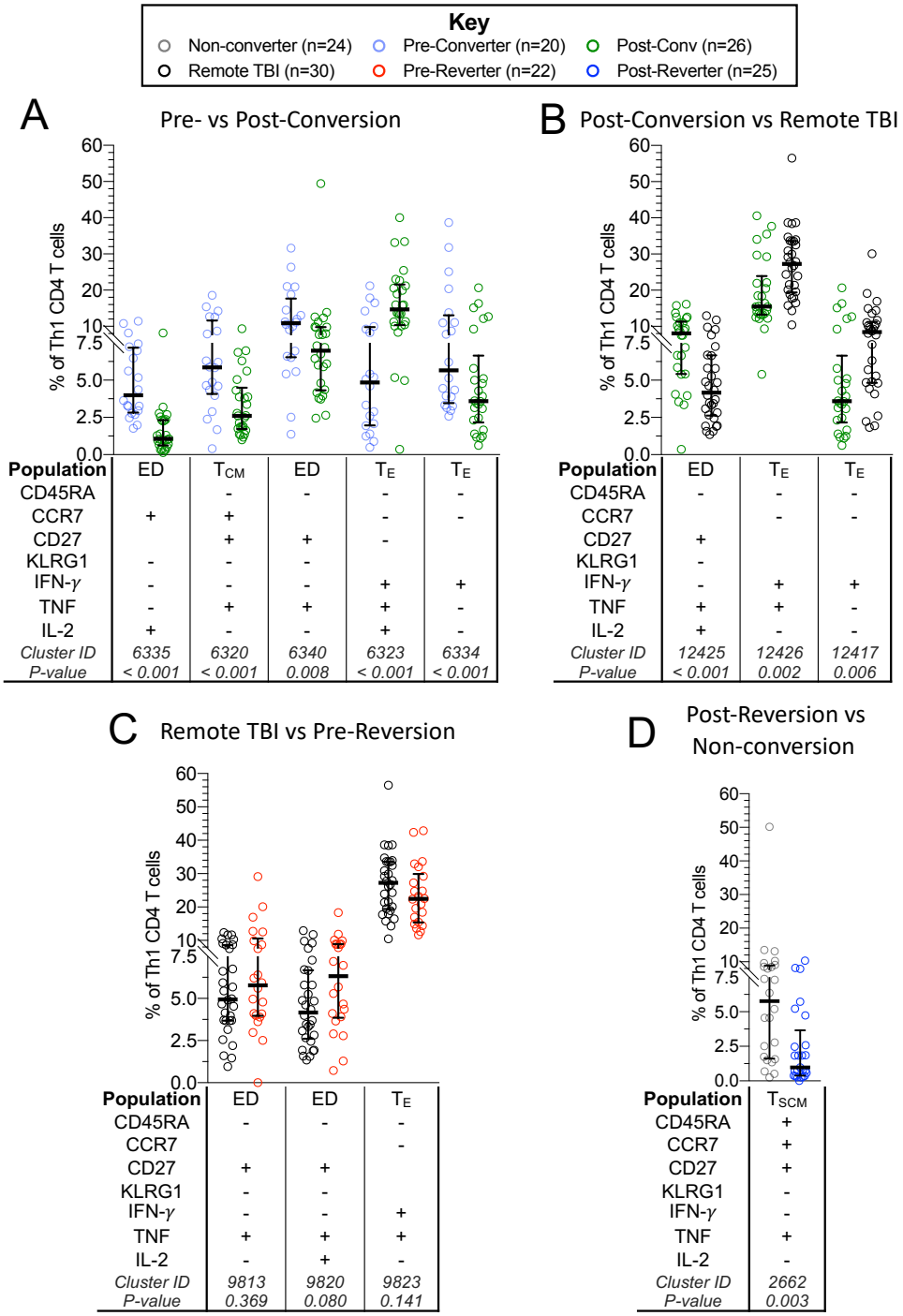

Figure 77: M.tb lysate-specific memory/functional profiles induced upon M.tb infection are sustained once TBI is established even upon QFT reversion. Box and whisker plots of differentially expressed memory (RA, R7, 27, G1) and functional (IL-2, TNF, IFN-γ) markers among M.tb lysate-specific CD4 T cells between (A) Pre- vs Post converters (B) Post-Converters vs Remote TBI, (C) Remote TBI vs Pre-Reversion and (D) Post-Reversion vs Non-conversion. Number of participants, confirmatory statistical analysis and p-value calculations is as in **Figure 74**.

CITRUS analysis identified CFP-10/ESAT-6-specific CD4 T cells that express TNF only with an effector-like memory phenotype (cluster 3651) as significantly different between post-converters and remote TBI (Appendix 8). However, when we manually gated this subset, TNF only T_E memory cells were not significantly different (p-value > 0.05) between post-converters

and remote TBI (Figure 78A). We detected higher proportions of $T_{CM/TM}$ TNF only (cluster 3718/25) and TNF+IL-2+ (cluster 3714) co-expressing CFP-10/ESAT-6-specific CD4 T cells but lower proportions IFN-γ+TNF+IL-2± $T_{TM/E}$ (clusters 3707/11/17/19) CFP-10/ESAT-6-specific CD4 T cells in pre-reverters compared with remote TBI (Figure 78B). Lastly, despite CITRUS analysis identifying higher proportions of TNF only T_{CM}/T_{TM} (cluster 932) CFP-10/ESAT-6-specific CD4 T cell, manual gating of this population did not yield in a significant difference ($p > 0.05$) in the abundance levels of this population between pre- and post-reversion (Figure 78C). Based on these results, we can conclude that although QFT reversion is not associated with a decrease in the magnitude of IFN-γ+ nor other Th1 cytokine+ cells, combined memory/functional phenotyping confirms that M.tb-specific CD4+ T cells from QFT reverters are less differentiated compared to remote TBI, consistent with much lower antigen exposure. Further, reverters may have actually cleared TBI as suggested by largely indistinguishable differentiation profile compared to non-converters.

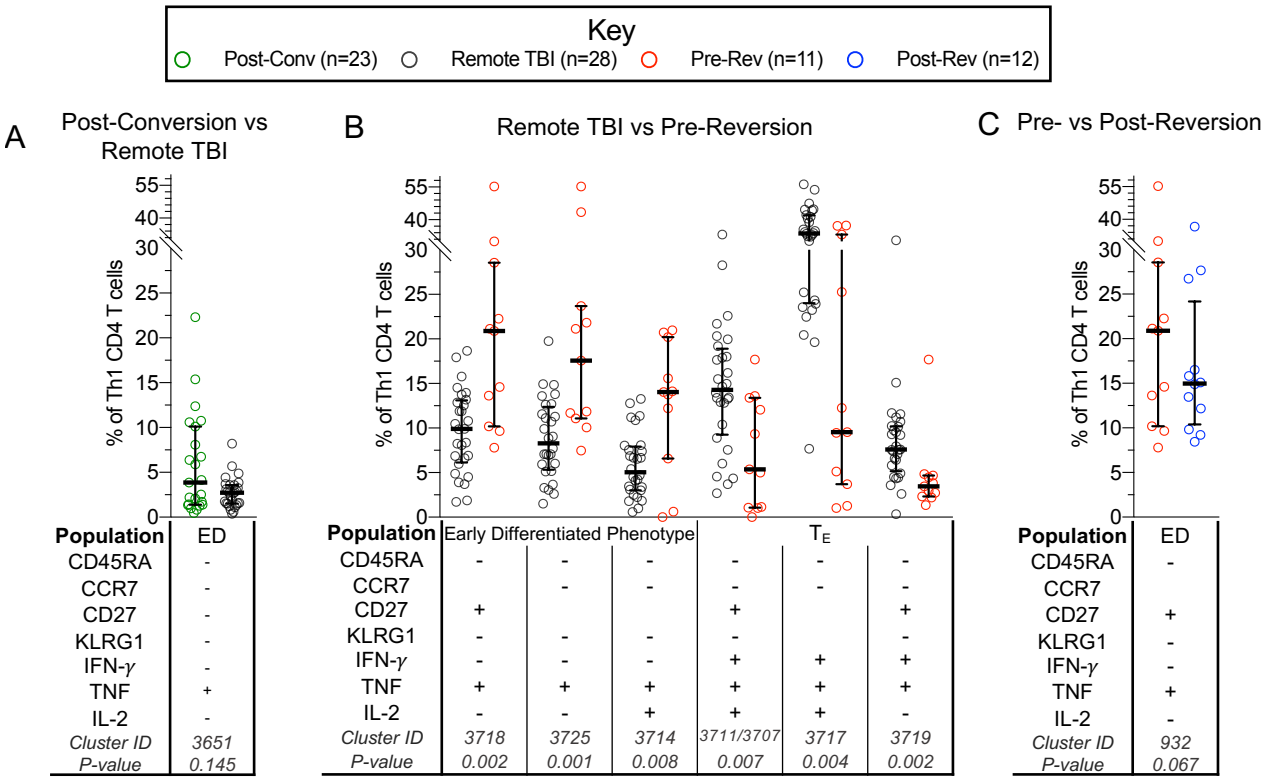

Figure 78: CFP-10/ESAT-6-specific memory/functional co-expression patterns are different between LTBI and reverters. Box and whisker plot of differentially expressed memory (RA, R7, 27, G1) and functional (IL-2, TNF, IFN-γ) markers among CFP-10/ESAT-6-specific CD4 T cells between (A) Post-conversion vs Remote TBI, (B) Remote TBI vs Pre-reversion and (C) Pre- vs Post-Reversion. Number of participants, confirmatory statistical analysis and p-value calculations is as in **Figure 74**.

Reversion is not associated with a decrease in T cell activation

In Chapter 5, we showed that T cell activation can distinguish between recent and remote TBI, where recent TBI and tuberculosis diseases is associated with higher proportions of activated T cells than remote TBI, thus suggesting that T cell activation may correlate with M.tb bacterial burden. Since reversion is hypothesised to be associated with M.tb clearance, we aimed to determine if QFT reversion was associated with a decrease in T cell activation. Overall, similar proportions of activated (HLA-DR+) M.tb-specific (Th1 cytokine+) CD4 T cells were detected pre- and post-reversion, as well as in non-converters and remote TBI (Figure 79).

Based on these results, we are unable to unequivocally demonstrate that reverters may be exposed to less M.tb antigen *in vivo* because their activation status was similar to both non-converters and remote TBI. However, these observations suggest that remote M.tb infected individuals may also experience very low or no M.tb-antigen exposure, which is insufficient to trigger higher levels of T cell activation as observed in recent TBI.

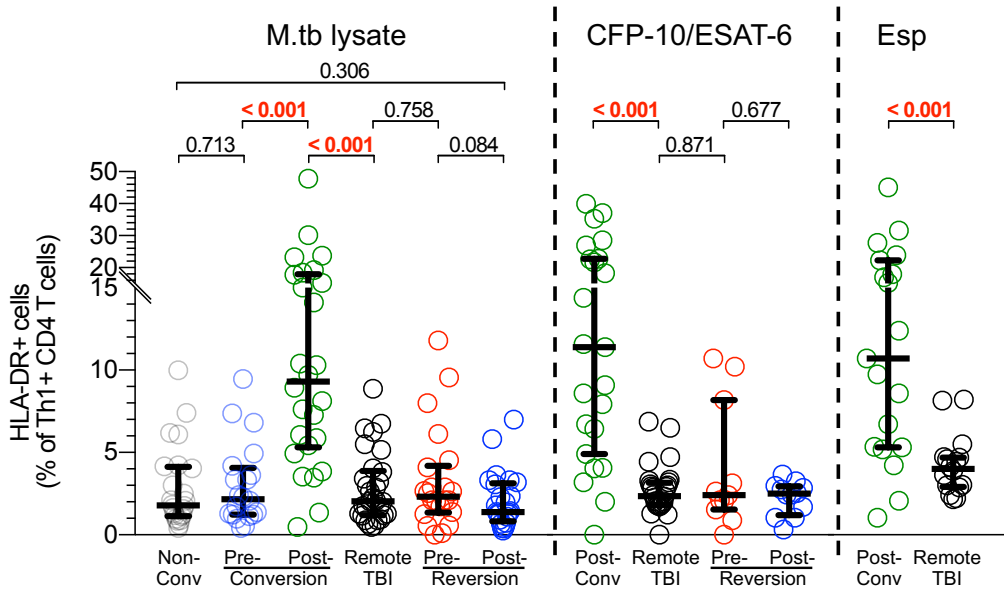

Figure 79: Reverters have low T cell activation. Graphs depict proportions of HLA-DR+ M.tb lysate, CFP-10/ESAT-6- and Esp- specific Th1 cytokine+ CD4 T cells in non-converters (M.tbL: n= 24), pre-conversion (M.tbL: n= 20), post-conversion (P10-ES6: n=23; M.tbL: n= 26 ; Esp: n= 20), remote TBI (P10-ES6: n=28; M.tbL: n= 30 ; Esp: n= 19), pre-reversion (P10-ES6: n=11; M.tbL: n= 22) and Post-reversion (P10-ES6: n=12; M.tbL: n= 25). Number of participants, confirmatory statistical analysis and p-value calculations is as in **Figure 74**.

Conclusion

Based on TST reversion studies in humans and guinea pig animal models, researchers hypothesise that QFT and/or TST reversion is associated with M.tb clearance or a reduction

of bacterial burden. To our knowledge, few studies have interrogated immune features associated with QFT reversion beyond a decrease in quantitative M.tb-specific-IFN-γ responses measured by IGRAs (Jenum et al., 2014; Medawar et al., 2019; Xin et al., 2019a). We aimed to expand on this literature by measuring M.tb-specific functional, memory, and activation kinetics associated with QFT reversion, as well as comparing these responses to control groups (non-converters, recent QFT converters, remote TBI).

We hypothesised that QFT reversion was associated with a decrease in frequencies of M.tb-specific IFN-γ+ functional CD4 T cells responses and T cell activation levels, and a shift to a predominantly early differentiated phenotypes and IFN-γ-independent functional responses, features associated with low antigen load. We demonstrate that, at least in our cohort of QFT reverters, functional and memory M.tb-specific CD4 T cell profiles did not change upon QFT reversion in response to a variety of M.tb immunodominant antigens. However, less than half of the reverters, before and after reversion, were classified as responders to CFP-10/ESAT-6 stimulation. This highlights the heterogeneous nature of QFT reverters, which includes individuals who have low M.tb-specific immune responses which fluctuate around the QFT cut-off, and individuals who have low but detectable M.tb-specific responses despite a QFT-result. Functional responses detected in reverters were of intermediate magnitude that fell between response magnitudes observed in non-converters and remote TBI, and surprisingly T cell activation levels detected in reverters, non-converters and remote TBI were very low and not significantly different. Based on these results, we found no clear evidence against the *reversion = clearance* hypothesis, in fact persistent low level of activation in all groups except post-converters suggests that even remotely infected individuals are exposed to lower bacterial burden that does not trigger high T cell activation. We detected higher levels of CFP-10/ESAT-6-specific T_{TM} and early differentiated IFN-γ-TNF+IL-2± memory subsets, but lower levels of IFN-γ+TNF+ T_E cells and functional differentiation in reverters compared with remote TBI. Further, majority of memory/functional subsets were not significantly different between reverters and non-converters. These findings suggest that reverters likely have a controlled low-grade TBI or may have even potentially cleared infection, prior to detection of the reversion signal. Thus, highlighting that once an infection is established, immunological memory, consisting of both effector and T_{SCM}/T_{CM} cell subsets, is sustained even upon QFT reversion.

Observations described here may not be directly informative to the interpretation of the BCG revaccination trial results (Nemes et al., 2018), where all the recently M.tb infected BCG vaccinees who reverted did so within 6 months of acquiring TBI, while we don't know when the cohort of reverters studied in the thesis acquired infection, as they were selected to be QFT+ for >6 months before reversion. As a result, immune memory phenotypes detected post-reversion are clearly indicative of a previous established infection which has likely cleared, whereas T cell features associated with reversion in the BCG revaccination trial could be associated with short-lived T cell immunity characteristic of transient acquisition of recent infection, as described by others (Medawar et al., 2019).

We acknowledge that this study has limitations, some of which include discordance between QFT and TST responses in reverters, with the majority of reverters being persistently TST positive during follow-up. This result suggests that TST may be a more sensitive test to detect low mycobacteria-reactive responses than QFT. This could be due to the long-time frame (48-72 hours) between administration and measurement of TST results. This time frame likely allows recruitment of tissue-resident memory cells from the lung and lymphoid tissue to the administration site and for early differentiated cells to proliferate and induce a reaction, compared to QFT, a shorter *ex vivo* assay that is designed to detect circulating effector IFN-γ+ T cell responses. Persistence of TST responses suggests that these individuals indeed have mycobacteria-specific memory responses. Therefore, persistent detection of Th1 functional responses and memory phenotypes similar to those detected in remote TBI was not entirely surprising as majority of reverters were persistence of TST+. We may have observed different M.tb-specific memory and functional kinetics if we had concordant QFT and TST reverters. Unfortunately, not enough individuals in our ACS cohort with this phenotype had sufficient PBMC available. This discordant phenotype of reverters could be a more representative cohort of reversion in our setting, and reflects cohorts observed by others (Xin et al., 2019a). We measured M.tb-specific responses to CFP-10/ESAT-6 and Esp, M.tb proteins that share sequence homology and are secreted by the same ESAT-6 system 1 (Esx-1) secretion system (Millington et al., 2011). To obtain more information about immune features associated with reversion, we could have expanded our stimulation panel to include Ag85 complex (Ag85A-C) or latency-associated antigens, which have different expression kinetics than RD-1 proteins. In the mouse model of TBI, Ag85 complex is highly expressed during early stages of bacterial replication, and decrease over time (Rogerson et al., 2006; Shi et al., 2003). Additionally,

functional and memory phenotypes have been shown to be different between ESAT-6- and Ag85-specific CD4 T cell responses (Moguche et al., 2017). Thus, if we had measured Ag85 complex- or latency associated antigen -specific responses we may have observed different memory/functional markers kinetics compared to CFP-10/ESAT-6-specific CD4 T cells, and potentially differences upon QFT reversion and/or between reverters and controls. We tried to circumvent the need for multiple antigenic stimulations by using M.tb lysate, which contains all antigens expressed with different kinetics. However, we detected similar functional, memory and activation M.tb lysate-specific CD4 T cell kinetics to those detected in response to CFP-10/ESAT-6 stimulation, suggesting that M.tb antigen expression kinetics may not play a significant role in the maintenance of functional phenotype in reverters. Alternatively, the additive effect of multiple antigens in M.tb lysate, some of which are shared with BCG and NTM and thus responses may include T cells that respond to M.tb, NTM or BCG, may have confounded results observed by masking differentially expressed responses upon reversion and/or between reverters and controls.

Lastly, we did not measure expression of other cytokines or functions known to contribute to M.tb control, such as IL-17 and IL-10, cytokines that might be associated with protective immunity in non-human primates (Darrah et al., 2020; Dijkman et al., 2019). We did not include IL-17 in our panel because mycobacterial stimulation of PBMC induces very low IL-17 production by T cells (Scriba et al., 2008), which would have been too low to allow phenotyping of these cells. Even though IL-10 was not included in our flow cytometry panel, we have preliminary data (from the same cohort) suggesting that frequencies of IL-10-expressing CD3+ T cells do not change upon recent QFT conversion nor reversion. We thus propose that future studies that aim to immuno-phenotype QFT and/or TST reverters should consider addressing some of these limitations.

In summary, results described here demonstrate the heterogeneous nature of immune responses associated with QFT reversion. It includes individuals who do not have robust responses that are detectable by flow cytometry but are detectable by QFT, likely due to technical variability, and those with robust T cell responses who have a less differentiated phenotype suggestive of lower antigen exposure, if any, than remote TBI, either before or after QFT reversion. Lower antigen exposure may enable maintenance of memory and functional immune responses that are induced upon TBI.

Chapter 7: General Discussion and Concluding Remarks

QFT is one of the most widely used immuno-diagnostics for TBI. Despite its wide use in well-resourced settings, we have a limited understanding of immunological features associated with different stages of TBI (defined by a positive QFT test) and discordant serial QFT results such as QFT reversion. The main objective of this study was to gain a better understanding of classical T cell immunity associated with serial QFT test results including QFT conversion, defined as a transition from negative to positive test results (acquisition of TBI) and reversion, from positive to negative test results. To achieve this objective, we first performed an in-depth characterisation of M.tb-specific T cell memory subsets, including the first description of T_{SCM} cells, in remotely infected individuals. We then investigated M.tb-specific functional, memory and activation kinetics associated with recent TBI (QFT conversion). Finally, we investigated whether T cell functional and phenotypic features induced by remote infection are maintained upon recent QFT reversion. Through the studies reported here, we defined M.tb-specific functional, memory and activation profiles associated with the full spectrum of TBI defined by QFT (Figure 80). *For simplicity, we shall use QFT when referring to results presented in the thesis and IGRA when making generalised discussion statements.*

We demonstrated that in the absence of M.tb exposure, as suggested by persistent QFT negative results in BCG-vaccinated non-converters, mycobacteria-specific CD4 T cell responses consisted of both IFN-γ producing effector and less-differentiated TNF+ and IL-2+ T_{SCM}/T_{CM} memory cells with a lower proportion of highly differentiated IFN-γ+TNF±IL-2± cytokine co-expressing cells compared to remote TBI (Figure 80A). These results indicate that BCG-induced immune responses do not greatly wane and remain detectable during adolescence. These results confirm other findings by our group, showing that M.tb-specific adaptive immune responses between pre-adolescents (8 years olds; who have a low incidence of disease) and young adults (18 year olds; with much higher incidence) are not significantly different (Baguma et al., 2017). Thus other factors, not necessarily related to memory T cells, are likely associated with the increase in tuberculosis incidence in young adults (Orme, 2010).

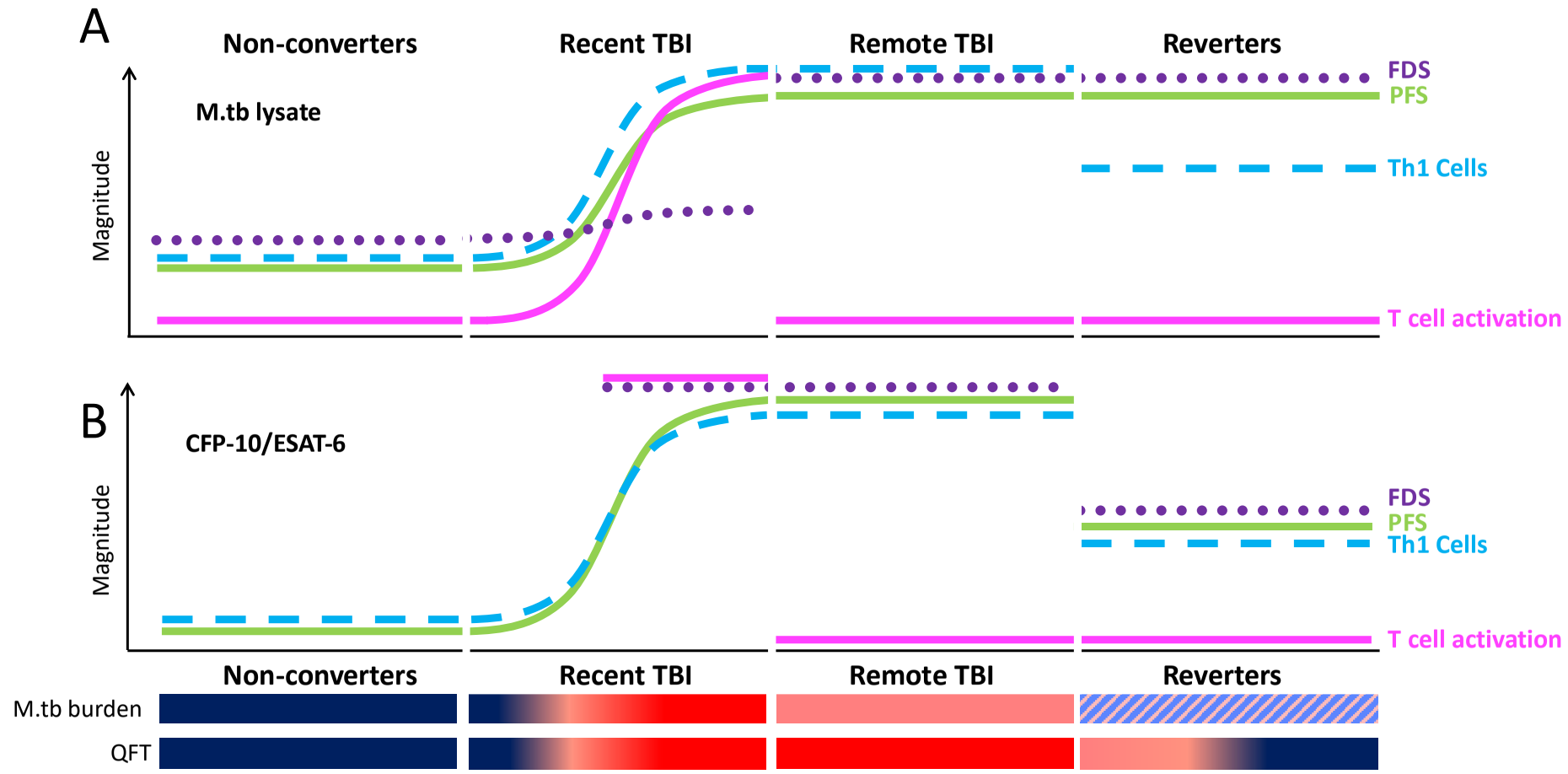

Figure 80: Magnitude and duration of M.tb exposure shape M.tb-specific immune responses. Graphical illustration of (A) M.tb lysate- and (B) CFP-10/ESAT-6- specific **functional differentiation scores (FDS, which depicts the ratio of IFN-γ+TNF±IL-2± : IFN-γ-TNF±IL-2± cells)**, **T cell activation**, **frequencies of Th1 cytokines** and **polyfunctionality scores (PFS)** associated with different states of TBI i.e. non-conversion, recent TBI, remote TBI and QFT reversion in BCG vaccinated adolescents. Hypothesised M.tb bacterial burden and observed QFT kinetics are illustrated as a gradient blue to red which represents no M.tb burden/QFT responses to high M.tb burden/ quantitative QFT responses, respectively.

Th1 functional/memory CD4 T cell responses detected in non-converters partly contradict the functional differentiation model proposed by Seder and colleagues, which suggests that in the absence of (viral) antigen exposure, IFN-γ-independent T_{SCM}/T_{CM} cells are the predominant cell types. Our results thus highlight key differences in viral- and bacterial-memory profiles associated with antigen exposure. Further, it underscores the robustness of mycobacteria-specific immune responses, which maintain a long-lasting effector-like memory phenotype, even in the absence of antigen exposure and after successful anti-M.tb therapy (Essone et al., 2014; Ewer et al., 2006; Higuchi et al., 2008; Kumar et al., 2016). Alternatively, detection of robust mycobacterial immune responses in non-converters could be due to historical TBI which did not result in persistent QFT/TST positivity. A few of the non-converters could be similar to the resistor phenotype described by Lu and colleagues (Lu et al., 2019). However, without records of known exposure to mycobacteria (e.g. tuberculosis HHC or NTM) and since the majority (86.2%) of non-converters did not have robust detectable CFP-10/ESAT-6 specific CD4 T cell responses, we shall not speculate on other factors that might contribute to the detection of effector-like mycobacterial responses in non-converters.

Our understanding of M.tb-specific CD4 T cell memory development is still very limited, and most studies focus on Th1 cells only. Our first major finding was demonstrating that M.tb-specific CD4+ T_{SCM} cells are induced by recent TBI (< 6 months post QFT conversion) and maintained during established TBI (>18 months post QFT conversion). By using MHC class II tetramers, we showed that, like other M.tb-specific memory subsets, these T_{SCM} cells expressed CXCR3, CCR6, CCR5, granzymes A and K, in addition to Th1 cytokines (Mpande et al., 2018). Detection of this memory subset at low levels was not surprising, because they potentially undergo asymmetric cell division which maintains both a T_{SCM} cell memory pool and gives rise to other memory subsets (Ciocca et al., 2012; Graef et al., 2014; Oliveira et al., 2015). This pluripotent differentiation capacity of T_{SCM} cells and their preferential maintenance in the absence of antigen, make them important players in maintaining long-lasting immunity (Fuertes Marraco et al., 2015; Gattinoni et al., 2017; Lugli et al., 2013a). We also identified differences in the T cell memory compartment between recent and established TBI, which were dominated by T_E and T_{CM} cells, respectively (Figure 81). Moreover, the transition of T cells through the differentiation pathway (T_{SCM} → T_{CM} → T_{CM*} → T_{TM} →T_E) was associated with an increase in chemokine receptor and cytotoxic molecule

co-expression, thus confirming our proposed linear differentiation model (Figure 81B). However, detection of a small proportion of T_{SCM} cells that co-expressed CXCR3+CCR6+CCR5+ and GrnA+GrnK+ suggests that even at early stages of T cell differentiation M.tb-specific cells acquire functions typically associated with long-term antigen exposure.

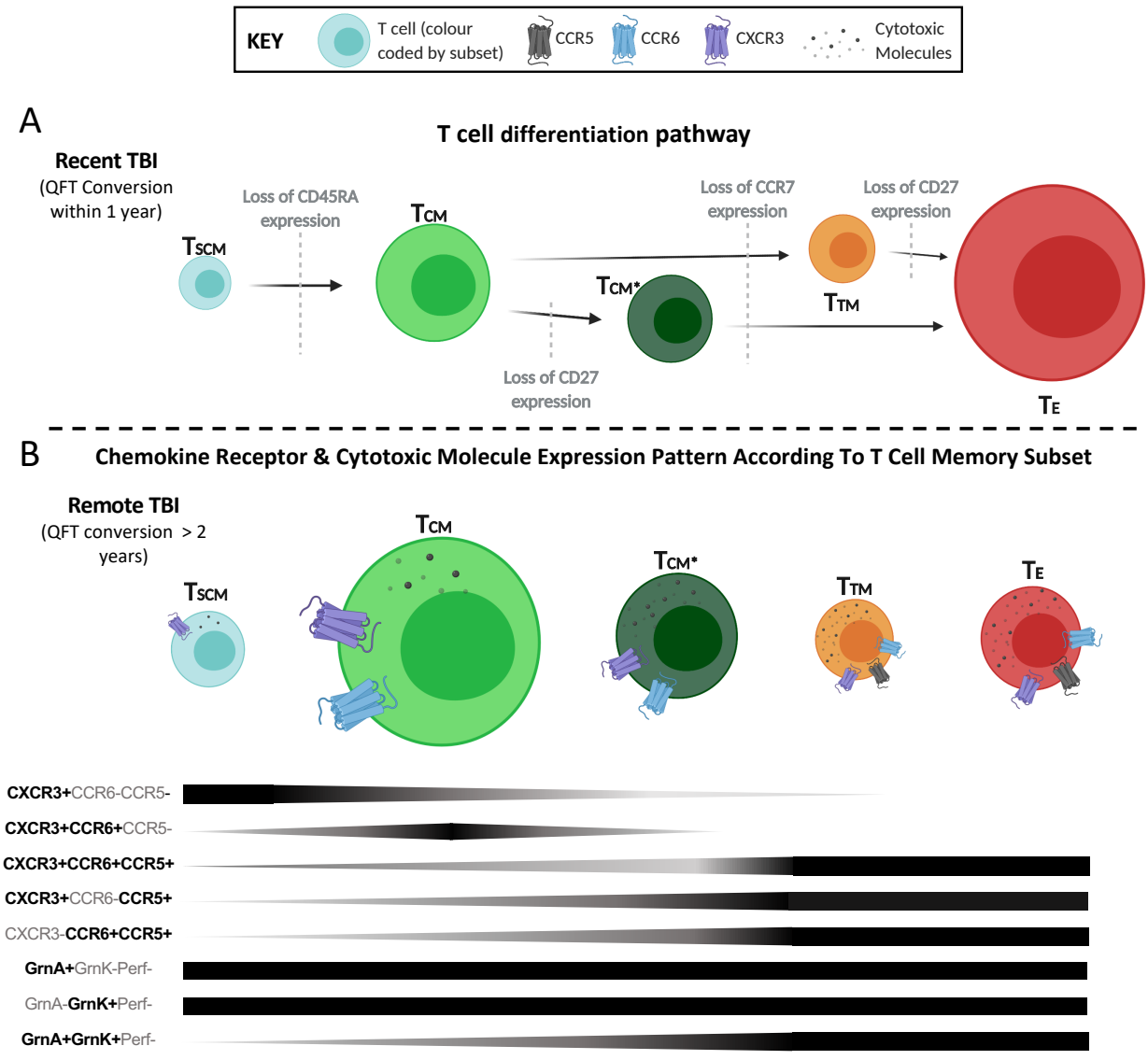

Figure 81: Length of M.tb-exposure governs the composition of M.tb-specific memory subsets, which follows a predominantly linear T cell differentiation model. (A) Visual illustration of the potential differentiation pathway of M.tb-specific CD4 T cells upon recent bacterial exposure. (B) M.tb-specific T_{SCM}, T_{CM}, T_{CM*}, T_{TM} and T_E cells co-expression of chemokine receptors (CCR5, CCR6, CXCR3) and cytotoxic molecules (granzyme A, granzyme K and perforin) during remote TBI. The proportional contribution of each memory subset to the total M.tb-specific T cell compartment is depicted by the approximate size of the cell. (Graphical schematic was created using BioRender.com).

The second major finding of this work was the discovery and validation of biomarkers of recent TBI, based on differential expression of T cell functional, memory and activation profiles between recent and remote TBI. Recent TBI is associated with a higher risk of disease

progression than remote TBI (Behr et al., 2018; Wiker et al., 2010). The Global Tuberculosis Report 2020 highlighted the need to "*dramatically scale up provision of tuberculosis preventive treatment*" as one of the top 10 priorities to accelerate progress needed to achieve the tuberculosis elimination targets (Organization, 2020a). Unfortunately, current immunodiagnostics such as QFT and TST are unable to distinguish between the two TBI states, differentiate TBI from disease, nor identify individuals at high risk of disease progression, making provision of preventive therapy challenging in under-resourced settings. Multiple studies have identified potential biomarkers of disease progression, predominantly based on *ex vivo* transcriptomic biomarkers that measure genes associated with increased inflammation, IFN stimulation, complement activation and cell signalling (Penn-Nicholson et al., 2020; Scriba et al., 2017; Suliman et al., 2018; Zak et al., 2016). However, few studies have described potential biomarkers of recent TBI or M.tb exposure that can distinguish between recent and remote TBI (Ault et al., 2020; Borgström et al., 2020; Halliday et al., 2017). In our cohort, acquisition of recent TBI was associated with a striking increase in activation of M.tb-specific CD4 T cells and induction of M.tb-specific T cells with both effector-like (IFN-γ+) and less-differentiated TNF+ and IL-2+ T_{SCM}/T_{CM} cells properties. In contrast, remote TBI was associated with preferential maintenance of polyfunctional cells with low T cell activation levels and a T_{TM}/T_E memory profile. These results contradict the memory kinetics described in Chapter 3, where the predominant memory subsets of M.tb-tetramer+ CD4 T cells during remote TBI were T_{CM}/T_{CM*} cells, a finding also observed by others (Lindestam Arlehamn et al., 2013; Strickland et al., 2017). Differences in the dominant M.tb-specific memory subsets detected by these different studies are probably due to the different methods used to detect antigen-specific T cells: tetramers (chapter 3) *versus* PBMC intracellular cytokine staining assay (chapter 5). While tetramers detect T cells directly *ex vivo* by binding to the TCR without activating the T cell, antigenic stimulation in the PBMC intracellular cytokine staining assay predominantly activates cells that have an effector-like profile and can readily produce Th1 cytokines. Further, stimulation may also affect expression of memory and phenotypic markers. This finding highlights the confounding effect experimental protocols may have on the detection of memory and functional subsets, which may not reflect and potentially misrepresent *in vivo* T cell memory subsets (Strickland et al., 2017). Even though identification of T cells using tetramers may give a better representation of *in vivo* responses, T cell specificity is based on a single epitope, thus stimulating PBMC with multiple antigens provides

broader detection of the M.tb- specific memory repertoire. Thus based on potential biases associated with stimulation and intracellular cytokine staining, we primarily used tetramer data to define the proposed M.tb-specific T cell differentiation model described in Figure 81. Interestingly, M.tb lysate- and CFP-10/ESAT-6-specific polyfunctionality scores, which reflect the ability to produce more than one cytokine, were not different between recent and remote TBI, suggesting that duration of infection has no impact on the ability to produce multiple cytokines. Although no differences in CFP-10/ESAT-6-specific functional and memory T cell features were observed between recent and remote TBI, M.tb lysate-specific functional and memory responses were more distinct between the two TBI states. Specifically, we detected lower proportions of highly differentiated IFN-γ+ and KLRG-1+ T_E subsets and higher proportions of less differentiated IFN-γ-TNF+IL-2+ T_{CM}/T_{TM} M.tb lysate-specific T cells in recent TBI compared to remote TBI. These results suggest that functional differentiation of CFP-10/ESAT-6-specific T cells remains relatively unchanged throughout TBI, consistent with persistent expression of these antigens (Moguche et al., 2017; Rogerson et al., 2006; Shi et al., 2004). Indeed, while CFP-10 and ESAT-6 are expressed at high levels during all phases of TBI, M.tb lysate theoretically contains the full complement of M.tb antigens, including those expressed by BCG and NTMs. Therefore, differences in T cell differentiation observed in response to M.tb lysate are possibly driven by CD4 T cell subsets recognising different antigens expressed at different levels during recent or remote TBI. Additionally, stimulation with CFP-10/ESAT-6 likely results in the measurement of immune responses specific for M.tb, while M.tb lysate stimulation results in the detection of M.tb-specific and BCG/NTM cross-reactive immune responses. Unfortunately, due to limited sample availability, we were unable to identify the antigens driving the functional differences in Th1 cytokine co-expression profiles differentiation observed in response to M.tb lysate but not CFP-10/ESAT-6. Overall, T cell memory, functional and activation features described here suggest that persistent TBI is not associated with chronic high M.tb burden that leads to T cell exhaustion, as suggested by murine models (Sakai et al., 2014b; Sallin et al., 2017). Instead, the data suggests that immune responses detected in most remotely infected individuals represents immunological memory and not ongoing M.tb replication, as hypothesised by others (Behr et al., 2019; Emery et al., 2021). Alternatively, if remotely infected individuals do harbour replicating M.tb then their M.tb-specific functional and memory differentiation profiles are suggestive of low antigen burden that does not lead to T cell exhaustion nor high T cell

activation. These results clearly indicate that differences in functional differentiation and activation states between recent and remote TBI are likely associated with the differential impact bacterial burden and duration of infection have on T cell immunity. While long-term exposure to a supposedly low bacterial burden (*i.e.* remote TBI) drives M.tb-specific CD4 T cells to a more differentiated but not exhausted T_E phenotype, short-term exposure to a high bacterial burden, likely experienced during recent TBI, is instead associated with less functional differentiation, demonstrated by detection of both IFN-γ+ dependent and independent Th1 cytokine co-expressing cells and high T cell activation. Thus, persistent low level chronic infection that maintains T_E cells likely confers protection against re-infection, as demonstrated in the leishmaniasis animal model (Peters et al. 2014). This suggestively explains, why remotely infected (TST positive) individuals have lower risk of disease compared with uninfected (TST negative) individuals (Andrews et al., 2012).

We showed that out of all the immunological features that were different between recent and remote TBI, T cell activation was the most accurate biomarker of recent TBI. Overall, the T cell activation biomarker appears robust with regards to mycobacterial antigen specificity (M.tb lysate, CFP-10/ESAT-6 or Esp peptide pool) and the method used to detect activated T cells (tetramer staining, PBMC or whole blood stimulation followed by intracellular cytokine staining). Additionally, T cell activation [defined as ΔHLA-DR MFI, the difference in HLA-DR MFI between M.tb-specific IFN-γ+TNF+ and total CD3+ T cells] could also identify individuals who progress to disease and those who currently have disease from individuals with remote TBI [(Mpande et al., 2021), Appendix 13]. Further, successful tuberculosis treatment, determined by bacterial clearance in tuberculosis patients, is associated with significant decrease in M.tb-specific T cell activation levels compared to baseline (tuberculosis diagnosis) (Adekambi et al., 2015; Musvosvi et al., 2018; Riou et al., 2020; Vickers et al., 2020). Therefore, in addition to inferring risk of disease, the ΔHLA-DR biomarker could potentially be used as an immunological marker of treatment success and bacterial clearance (Riou et al., 2020). Taken together, T cell activation likely reflects the antigen burden, which is highest during recent *in vivo* antigen exposure (TBI), progression to and during disease, and lowest during remote TBI and successfully treated disease (Adekambi et al., 2015; Musvosvi et al., 2018; Riou et al., 2017, 2020; Silveira-Mattos et al., 2019; Wilkinson et al., 2016). We propose that upon adaptation to a whole blood-intracellular cytokine staining assay and further large-scale validation, the ΔHLA-DR MFI biomarker in conjunction with clinical examinations could

be used to delineate the full spectrum of tuberculosis from recent TBI, progression to disease, active disease and finally treatment response and identify individuals who should receive preventive or full tuberculosis therapy (Figure 82) (Organisation, 2020; Organization, 2020b). Results described here provide evidence that could contribute to achieving one of the top 10 priorities required to reach the global tuberculosis elimination targets.

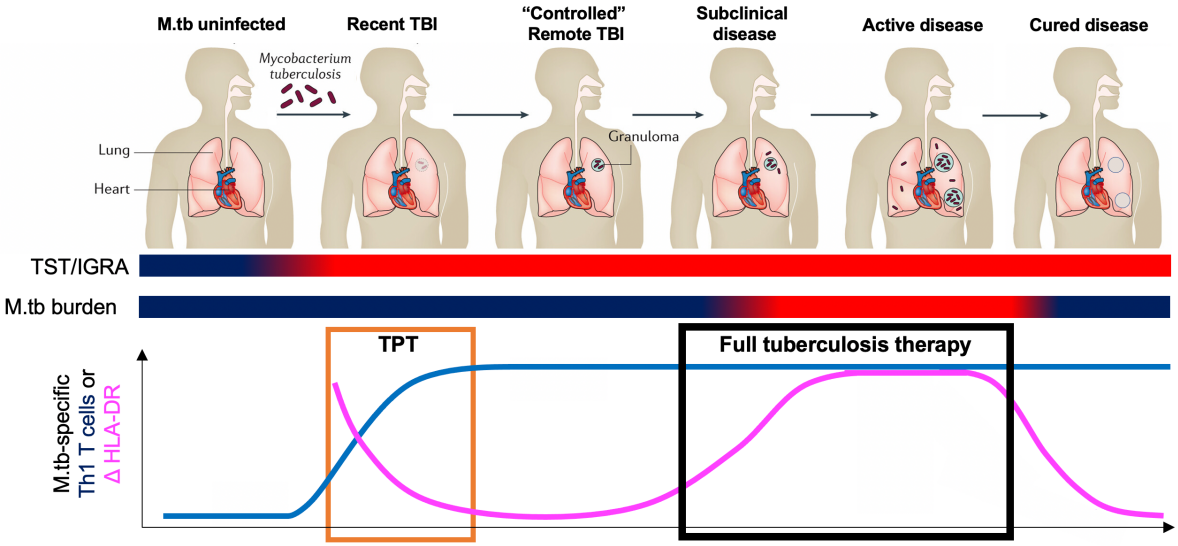

Figure 82: M.tb-specific T cell activation tracks the tuberculosis spectrum. Visual and graphical illustration of TST/IGRA, M.tb burden, M.tb-specific Th1 (blue line) and ΔHLA-DR (magenta line) kinetics during the full spectrum of tuberculosis [adapted from (Pai et al., 2016)] following exposure to M.tb, progression to disease and cured disease. Gradient blue to red represents negative to positive diagnostic results. M.tb infection induces Th1 responses which remain detectable even after tuberculosis is cured. T cell activation levels (ΔHLA-DR) are highest during recent M.tb exposure, subclinical and active disease, and are detected at much lower levels during "controlled" TBI and after successful disease therapy. Boxes indicate potential preventive (TPT) or full tuberculosis therapy that could be administered based on ΔHLA-DR biomarker, clinical and microbiological outcomes.

Results described thus far suggest that not all M.tb sensitised (QFT/TST+) individuals have on-going *in vivo* M.tb exposure. Unfortunately, not much is known about M.tb-specific immune responses associated with bacterial clearance. An improved understanding of this phenomenon, as well as protective immunity, could lead to the development of vaccines and tests that can diagnose M.tb clearance, innovations required to achieve the tuberculosis elimination targets. Based on data from observational studies conducted during the pre-antibiotic era and guinea pig tuberculosis models, TST reversion is the only TBI state in humans hypothesised to be associated with spontaneous (natural) clearance of M.tb infection (Dahlstrom, 1940; Dharmadhikari et al., 2011; Riley et al., 1959a). Since TST and IGRA both measure immunological sensitisation to M.tb, it is likely that IGRA reversion could also be

associated with M.tb clearance. In spite of multiple reports of natural or antibiotic-associated IGRA and/or TST reversion, immunological features associated with reversion, beyond a decrease in M.tb-specific IFN-γ responses, have not been well characterised. Clearance of viral infections is associated with a shift from a predominantly effector memory profile to a quiescent T_{SCM}/T_{CM} cell memory profile, which maintains long-lasting immunity in the absence of antigen (Bajwa et al., 2017; Lugli et al., 2013a; Seder et al., 2008). An important question is *whether IGRA reversion is associated with similar T cell memory kinetics.* Our third major finding showed that QFT reversion was not associated with a decrease in IFN-γ+ responses (detected by flow cytometry) and T cell activation, nor an increase in quiescent T_{SCM}/T_{CM} memory subsets. Instead, reversion was associated with low levels of M.tb-specific T cell activation, maintenance of predominantly T_{TM}/T_E subsets and both IFN-γ dependent and independent Th1 cytokine co-expressing cells (Bajwa et al., 2017; Lugli et al., 2013; Riou et al., 2020; Seder et al., 2008). These results are in line with findings in other infection models, which showed that chronic leishmaniasis infection that results in low antigen burden or is subsequently cleared is associated with long-term maintenance of both effector and central memory cells (Pacheco-Fernandez et al., 2021).

Overall, CD4 T cell responses to CFP-10/ESAT-6 in reverters were of intermediate magnitude between non-converters and remotely infected individuals (Figure 80). These responses were very low in most reverters (regardless of QFT status), which may explain fluctuations around the QFT assay cut-off resulting in reversion of the test. In the reverters who had low but robustly detectable responses, CFP-10/ESAT-6-specific CD4 T cells showed low levels of M.tb-specific T cell activation, maintenance of both IFN-γ dependent and independent Th1 cytokine co-expressing profiles and a predominantly T_{TM}/T_E phenotype. Memory and functional profiles detected in reverters in response to M.tb lysate shared more characteristics with non-converters than persistently QFT+ individuals. Based on these results, we conclude that QFT reverters represent a heterogenous population in the tuberculosis spectrum who may experience very low or no *in vivo* antigen exposure. However, it remains to be determined whether reversion is associated with a lower risk of tuberculosis diseases and M.tb re-infection (IGRA conversion).

The reverter phenotype observed here could also share some immunological characteristics with resistors, individuals with known (high) M.tb exposure who appear to resist M.tb infection, as determined by QFT/TST non-conversion and absence of TB disease (Lu et al., 2019; Ma et al., 2014; Stein et al., 2018b). Despite being QFT/TST negative, detection of M.tb (including CFP-10/ESAT-6) -specific-IFN-γ-independent T cell and antibody responses demonstrated that resistors were at the very least transiently infected but likely cleared infection rapidly without maintaining or inducing an IFN-γ+ effector-like phenotype (Lu et al., 2019). The reverter phenotype described here is probably representative of individuals who were infected, as suggested by the detection of IFN-γ+ cells by QFT and flow cytometry, and it remains unclear whether reverters share immunological similarities with resistors.

Whether ongoing *in vivo* antigen exposure is required to maintain memory responses against M.tb remains to be determined. It is possible that key features of T cell responses against M.tb, including magnitude and differentiation, are shaped by the antigen load experienced during primary infection, regardless of whether infection is subsequently cleared. Our analysis of mycobacteria-specific immune responses demonstrated that once infection is established (defined by QFT/TST positivity) memory responses are imprinted and do not change even upon reversion (Figure 80A). This is not unique to TBI, and has also been observed in leishmaniasis infection model, whereby the overall quality of the functional memory responses is maintained even after parasitic clearance (Seder & Sacks 2004, Zaph 2004, Peters et al. 2014). Instead, differences in T cell immunity between remote TBI and reversion are probably best explained when focusing on constitutively expressed M.tb antigens, e.g. CFP-10/ESAT-6, which are likely indicative of the level of M.tb exposure (Figure 80B). Specifically, we detected CFP-10/ESAT-6-specific Th1 cells with a lower proportion of IFN-γ co-expressing cells (depicted by FDS) in reverters compared with remote TBI. Additionally, significantly lower quantitative QFT responses in reverters compared to recently and remotely infected individuals suggest that initial *in vivo* M.tb exposure during TBI was not high enough to induce IFN-γ+ responses that were consistently detected above the QFT assay cut-off. These findings suggest a spectrum of initial TBI and *in vivo* antigen exposure. Under this scenario, we propose that remote TBI (defined by persistent QFT+ responses) is likely associated with initial infection by a “high” M.tb inoculum that drives the maintenance of long-lived, predominantly effector-like IFN-γ+ responses. Conversely, initial M.tb infection in reverters is likely

associated with a “low” initial M.tb burden, which is insufficient to induce robust levels of IFN-γ+ and drive T cells to a more differentiated state. Thus, we are likely measuring different degrees of memory responses shaped by either high (remote TBI) or low (reversion) M.tb burden during primary TBI.

Detection of similar T cell memory profiles between reverters and non-converters is also indicative of low M.tb burden in reverters. Moreover, T cell activation levels in remotely infected individuals were in range with T cell activation levels detected in non-converters and reverters. This suggests that other than in recently infected individuals, majority of M.tb infected individuals have likely cleared M.tb infection or at the very least controlled M.tb burden to very low levels that do not induce high T cell activation, as suggested by others (Behr et al., 2019; Emery et al., 2021).

It is important to note that the majority of the reverters were still TST+, despite the detection of a QFT reversion signal. This suggests that TST has a higher sensitivity for detecting M.tb-specific memory responses than QFT. This is likely due to the “long” time interval (48-72 hours) between TST administration and measurement of results, which provides sufficient time for low-grade memory responses to be activated, proliferate, exit lymphoid organs and induce a detectable hypersensitivity reaction *in vivo*. On the other hand, the “short” duration of the *in vitro* QFT assay (16-24 hrs) may not provide sufficient time for early differentiated T cells to mount a robust IFN-γ expression, resulting in a potential underestimation of T cell immunity besides detection of effector cells. Additionally, memory cells may not be in circulation and could be residing in tissues, and as such were not sampled during blood draw. Thus, based on persistent TST detection, it is likely that M.tb exposure in reverters could have induced T cell memory responses that resulted in initial QFT and/or TST conversion, but eventually decreased to low levels which were undetectable by QFT (resulting in reversion) but were still detectable by TST and flow cytometry, which may be more sensitive than QFT. These nuances may explain the intermediate phenotype of reverters that is between non-converters and remote TBI.

A major limitation of this study is selection bias, which we were unable to circumvent. Our selection criteria of QFT reverters were very strict (2 positive QFT test results followed by 2 negative QFT test results), and we were also restricted by sample availability. QFT reverters had much lower quantitative QFT IFN-γ responses than recent and remote TBI, which were

expressed at similar ranges. However, QFT reversion has been associated with lower IFN-γ levels compared to persistent QFT+ in this and other cohorts (Andrews et al., 2015, 2017; Pai et al., 2009; Zhang et al., 2018) and it was simply not possible to select enough QFT reverters with higher IFN-γ levels among the available ~3300 adolescents. Low IFN-γ levels observed in reverters may be biologically relevant, as discussed above, but can also result in false positive or false negative QFT results, purely due to technical variability affecting values around the assay qualitative cut-off. Our results suggest that this reverter cohort included a mix of both scenarios.

Another limitation was that results presented here predominantly focused on characterising functional, activation and memory capacity of Th1 CD4 T cells, cell subsets known to play an important role in immunity against M.tb infection. Recent pre-clinical vaccine studies have demonstrated that Th17 cells likely play a critical role in protective immunity together with Th1 cells (Darrah et al., 2020; Dijkman et al., 2019). Unfortunately, we did not measure IL-17 in our PBMC intracellular staining cytokine assay because, in our experience, stimulation of PBMC, unlike whole blood, induces such low levels of IL-17+ cells that these cannot be reliably immunophenotyped. We did however detect high proportions of CXCR3+CCR6+ M.tb-specific T cells during remote TBI, which is suggestive of Th1/Th17 functional capacity, providing evidence that natural infection does induce Th1/17 cells as reported by others (Lindestam Arlehamn et al., 2013). Further, due to time constraints and the scope of my PhD, we did not assess the humoral and innate immune responses associated with QFT reversion. However, this research project is part of a larger study which is investigating these responses. Preliminary results on innate immunity also suggest that reversion is not associated with a decrease of IFN-γ expression by NK cells or donor unrestricted T cells, nor does it result in differences in monocyte functional capacity. Overall, innate responses detected in reverters were very similar to both non-converters and remote TBI (Pia Steigler, personal communication).

Future studies based on results presented here include the validation ΔHLA-DR MFI biomarker in several independent cohorts, including a prospective South African paediatric cohort of household contacts of patients with tuberculosis. We are also investigating mucosal immune responses in bronchoalveolar lavage samples collected from sustained converters and reverters in the BCG-revaccination study. Lastly, we are also conducting epidemiological

analysis of the prevalence and historical incidence of tuberculosis diseases in reverters studied in thesis, as well as the whole ACS study.

In conclusion, our data provides compelling evidence that current models of T cell differentiation conceptualised primarily in viral infection scenarios may not entirely apply to M.tb-specific T cell immunity, and that M.tb-specific T cell immunity models conceptualised on mouse studies may not entirely apply to humans. We showed that M.tb-specific memory responses persists even in the absence (or very low) *in vivo* exposure (QFT reversion). Additionally, we showed that remote TBI is not associated with T cell exhaustion and terminal differentiation. We further showed that M.tb-specific T cell immune responses, which seem mostly imprinted after initial infection, are sustained even upon QFT reversion in remotely infected individuals, albeit at a lower magnitude. Finally, we demonstrated that differences in T cell activation levels between recent and remote TBI, which are likely driven by magnitude and duration of *in vivo* M.tb burden, can be harnessed to develop novel immunodiagnostics of recent TBI and active disease. Overall, our data support the recent hypothesis that the majority of individuals sensitised to M.tb antigens may not harbour ongoing infection (Behr et al., 2019; Emery et al., 2021).

References

Abubakar, I., Pimpin, L., Ariti, C., et al. (2013). Systematic review and meta-analysis of the current evidence on the duration of protection by bacillus Calmette-Guérin vaccination against tuberculosis. Health Technol Asses *17*, 1–372, v–vi.

Abubakar, I., Drobniewski, F., Southern, J., et al. (2018). Prognostic value of interferon-γ release assays and tuberculin skin test in predicting the development of active tuberculosis (UK PREDICT TB): a prospective cohort study. Lancet Infect Dis *18*, 1077–1087.

Abu-Raddad, L.J., Sabatelli, L., Achterberg, J.T., et al. (2009). Epidemiological benefits of more-effective tuberculosis vaccines, drugs, and diagnostics. Proc National Acad Sci *106*, 13980–13985.

Achkar, J.M., Chan, J., and Casadevall, A. (2015). B cells and antibodies in the defense against Mycobacterium tuberculosis infection. Immunol Rev *264*, 167–181.

Acosta-Rodriguez, E.V., Rivino, L., Geginat, J., et al. (2007). Surface phenotype and antigenic specificity of human interleukin 17–producing T helper memory cells. Nat Immunol *8*, 639–646.

Adams, J.M., Kalajan, V.A., Mork, B.O., et al (1959). Reversal of Tuberculin Reaction in Early Tuberculosis. Dis Chest *35*, 348–356.

Adankwah, E., Lundtoft, C., Güler, A., et al (2019). Two-Hit in vitro T-Cell Stimulation Detects Mycobacterium tuberculosis Infection in QuantiFERON Negative Tuberculosis Patients and Healthy Contacts From Ghana. Front Immunol *10*, 1518.

Adekambi, T., Ibegbu, C.C., Kalokhe, A.S., et al. (2012). Distinct Effector Memory CD4+ T Cell Signatures in Latent Mycobacterium tuberculosis Infection, BCG Vaccination and Clinically Resolved Tuberculosis. Plos One *7*, e36046.

Adekambi, T., Ibegbu, C.C., Cagle, S., et al. (2015). Biomarkers on patient T cells diagnose active tuberculosis and monitor treatment response. J Clin Invest *125*, 1827 1838.

Aerts, L., Selis, E., Corbière, V., et al. (2019). HBHA-Induced Polycytotoxic CD4+ T Lymphocytes Are Associated with the Control of Mycobacterium tuberculosis Infection in Humans. J Immunol *202*, 421–427.

Agizew, T., Boyd, R., Auld, A.F., et al. (2019). Treatment outcomes, diagnostic and therapeutic impact: Xpert vs. smear. A systematic review and meta-analysis. Int J Tuberc Lung Dis *23*, 82–92.

Ai, J.W., Ruan, Q.L., Liu, Q.H., et al. (2019). Updates on the risk factors for latent tuberculosis reactivation and their managements. Emerg Microbes Infec *5*, 1–8.

Akbar, A.N., and Henson, S.M. (2011). Are senescence and exhaustion intertwined or unrelated processes that compromise immunity? Nat Rev Immunol *11*, 289 295.

Algood, H.M.S., Lin, P.L., and Flynn, J.L. (2005). Tumor Necrosis Factor and Chemokine Interactions in the Formation and Maintenance of Granulomas in Tuberculosis. Clin Infect Dis *41*, S189–S193.

Altman, J.D., Moss, P.A.H., Goulder, P.J.R., et al. (1996). Phenotypic Analysis of Antigen-Specific T Lymphocytes. Science *274*, 94–96.

Andersen, P., and Smedegaard, B. (2000). CD4+ T-Cell Subsets That Mediate Immunological Memory to Mycobacterium tuberculosis Infection in Mice. Infect Immun *68*, 621–629.

Andersen, P., and Urdahl, K.B. (2015). TB vaccines; promoting rapid and durable protection in the lung. Curr Opin Immunol *35*, 55–62.

Andersen, P., Doherty, T.M., Pai, M., et al. (2007). The prognosis of latent tuberculosis: can disease be predicted? Trends Mol Med *13*, 175 182.

Anderson, M.K. (2013). Changing course by lymphocyte lineage redirection. Nat Immunol *14*, 1 4.

Andrews, J.R., Noubary, F., Walensky, R.P., et al. (2012). Risk of Progression to Active Tuberculosis Following Reinfection With Mycobacterium tuberculosis. Clin Infect Dis *54*, 784 791.

Andrews, J.R., Hatherill, M., Mahomed, H., et al. (2015). The dynamics of QuantiFERON-TB gold in-tube conversion and reversion in a cohort of South African adolescents. Am J Resp Crit Care *191*, 584 591.

Andrews, J.R., Nemes, E., Tameris, M., et al. (2017). Serial QuantiFERON testing and tuberculosis disease risk among young children: an observational cohort study. Lancet Respir Medicine *5*, 282 290.

Appay, V., Lier, R.A.W. van, Sallusto, F., et al. (2008). Phenotype and function of human T lymphocyte subsets: consensus and issues. Cytom Part A *73*, 975 983.

Arlehamn, C.S.L., McKinney, D.M., Carpenter, C., et al. (2016). A Quantitative Analysis of Complexity of Human Pathogen-Specific CD4 T Cell Responses in Healthy M. tuberculosis Infected South Africans. Plos Pathog *12*, e1005760.

Ault, R.C., Headley, C.A., Hare, A.E., et al. (2020). Blood RNA signatures predict recent tuberculosis exposure in mice, macaques and humans. Sci Rep-Uk *10*, 16873.

Aversa, G.G., and Hall, B.M. (1991). Cell surface markers of T-cell activation. Transplant Rev *5*, 9–30.

Bachelerie, F., Ben-Baruch, A., Burkhardt, A.M., et al. (2013). International Union of Pharmacology. LXXXIX. Update on the Extended Family of Chemokine Receptors and Introducing a New Nomenclature for Atypical Chemokine Receptors. Pharmacol Rev *66*, 1 79.

Baena, A., and Porcelli, S.A. (2009). Evasion and subversion of antigen presentation by Mycobacterium tuberculosis. Tissue Antigens *74*, 189–204.

Baguma, R., Penn-Nicholson, A., Smit, E., et al. (2017). Application of a whole blood mycobacterial growth inhibition assay to study immunity against Mycobacterium tuberculosis in a high tuberculosis burden population. Plos One *12*, e0184563.

Bajwa, M., Vita, S., Vescovini, R., et al. (2017). CMV-specific T-cell responses at older ages: broad responses with a large central memory component may be key to long-term survival. J Infect Dis *215*, 1212–1220.

Barreto, M.L., Pereira, S.M., Pilger, D., et al. (2011). Evidence of an effect of BCG revaccination on incidence of tuberculosis in school-aged children in Brazil: Second report of the BCG-REVAC cluster-randomised trial. Vaccine *29*, 4875–4877.

Barry, C.E., Boshoff, H.I., Dartois, V., et al. (2009). The spectrum of latent tuberculosis: rethinking the biology and intervention strategies. Nat Rev Microbiol *7*, nrmicro2236.

Bean, A.G., Roach, D.R., Briscoe, H., et al. (1999). Structural deficiencies in granuloma formation in TNF gene-targeted mice underlie the heightened susceptibility to aerosol Mycobacterium tuberculosis infection, which is not compensated for by lymphotoxin. J Immunol Baltim Md 1950 *162*, 3504–3511.

Becattini, S., Latorre, D., Mele, F., et al. (2015). Functional heterogeneity of human memory $CD4^+$ T cell clones primed by pathogens or vaccines. Sci New York N Y *347*, 400–406.

Behr, M.A., Edelstein, P.H., and Ramakrishnan, L. (2018). Revisiting the timetable of tuberculosis. BMK *362*, k2738.

Behr, M.A., Edelstein, P.H., and Ramakrishnan, L. (2019). Is Mycobacterium tuberculosis infection life long? BMJ Clin Res Ed *367*, l5770.

Berhanu, D., Mortari, F., Rosa, S.C.D., et al. (2003). Optimized lymphocyte isolation methods for analysis of chemokine receptor expression. J Immunol Methods *279*, 199 207.

Betts, M.R., and Koup, R.A. (2004). Methods in Cell Biology. Methods Cell Biol *75*, 497–512.

Betts, M.R., Brenchley, J.M., Price, D.A., et al. (2003). Sensitive and viable identification of antigen-specific CD8+ T cells by a flow cytometric assay for degranulation. J Immunol Methods *281*, 65 78.

Biasco, L., Scala, S., Ricci, L.B., et al. (2015). In vivo tracking of T cells in humans unveils decade-long survival and activity of genetically modified T memory stem cells. Science Translational Medicine *7*, 273ra13.

Bonecchi, R., Bianchi, G., Bordignon, P.P., et al. (1998). Differential Expression of Chemokine Receptors and Chemotactic Responsiveness of Type 1 T Helper Cells (Th1s) and Th2s. J Exp Medicine *187*, 129–134.

Borgström, E.W., Fröberg, G., Correia-Neves, M., et al. (2020). CD4+ T cell proliferative responses to PPD and CFP-10 associate with recent M. tuberculosis infection. Tuberculosis *123*, 101959.

Boyman, O., and Sprent, J. (2012). The role of interleukin-2 during homeostasis and activation of the immune system. Nat Rev Immunol *12*, 180 190.

Brodie, T., Brenna, E., and Sallusto, F. (2013). OMIP-018: Chemokine receptor expression on human T helper cells. Cytom Part A *83A*, 530 532.

Brown, D.M. (2010). Cytolytic CD4 cells: Direct mediators in infectious disease and malignancy. Cell Immunol *262*, 89 95.

Brown, J., Kumar, K., Reading, J., et al. (2017). Frequency and significance of indeterminate and borderline QuantiFERON Gold TB IGRA results. Eur Respir J *50*, 1701267.

Bruggner, R.V., Bodenmiller, B., Dill, D.L., et al. (2014). Automated identification of stratifying signatures in cellular subpopulations. Proc National Acad Sci *111*, E2770–E2777.

Bustamante, J., Boisson-Dupuis, S., Abel, L., et al.. (2014). Mendelian susceptibility to mycobacterial disease: Genetic, immunological, and clinical features of inborn errors of IFN-γ immunity. Semin Immunol *26*, 454–470.

Caccamo, N., and Dieli, F. (2012). Are Polyfunctional Cells Protective in M. tuberculosis Infection? Undefined.

Cadena, A.M., Hopkins, F.F., Maiello, P., et al. (2018). Concurrent infection with Mycobacterium tuberculosis confers robust protection against secondary infection in macaques. Plos Pathog *14*, e1007305.

Canaday, D.H., Wilkinson, R.J., Li, Q., et al. (2001). CD4+ and CD8+ T Cells Kill Intracellular Mycobacterium tuberculosis by a Perforin and Fas/Fas Ligand-Independent Mechanism. J Immunol *167*, 1 10.

Castellino, F., Huang, A.Y., Altan-Bonnet, G., et al. (2006). Chemokines enhance immunity by guiding naive CD8+ T cells to sites of CD4+ T cell-dendritic cell interaction. Nature *440*, 890 895.

Chattopadhyay, P.K., Melenhorst, J.J., Ladell, K., et al. (2008). Techniques to improve the direct ex vivo detection of low frequency antigen-specific CD8+ T cells with peptide-major histocompatibility complex class I tetramers. Cytom Part A *73A*, 1001–1009.

Chawla, K.S., Kanyama, C., Mbewe, A., et al. (2016). Policy to practice: impact of GeneXpert MTB/RIF implementation on the TB spectrum of care in Lilongwe, Malawi. T Roy Soc Trop Med H *110*, 305–311.

Cheroutre, H., and Husain, M.M. (2013). CD4 CTL: Living up to the challenge. Semin Immunol *25*, 273 281.

Christopher, D.J., James, P., Michael, J.S., et al. (2011). Serial testing using IGRAs in a cohort of Indian nursing students. European Respiratory Journal *38*, p2654.

Churchyard, G., Kim, P., Shah, N.S., et al. (2017). What We Know About Tuberculosis Transmission: An Overview. J Infect Dis *216*, S629–S635.

Churchyard, G.J., Stevens, W.S., Mametja, L.D., et al. (2015). Xpert MTB/RIF versus sputum microscopy as the initial diagnostic test for tuberculosis: a cluster-randomised trial embedded in South African roll-out of Xpert MTB/RIF. Lancet Global Heal *3*, e450–e457.

Ciocca, M.L., Barnett, B.E., Burkhardt, J.K., et al. (2012). Cutting Edge: Asymmetric Memory T Cell Division in Response to Rechallenge. J Immunol *188*, 4145–4148.

Cohen, A., Mathiasen, V.D., Schön, T., et al. (2019). The global prevalence of latent tuberculosis: a systematic review and meta-analysis. Eur Respir J *54*, 1900655.

Colditz, G.A., Brewer, T.F., Berkey, C.S., et al. (1994). Efficacy of BCG Vaccine in the Prevention of Tuberculosis: Meta-analysis of the Published Literature. Jama *271*, 698 702.

Colditz, G.A., Berkey, C.S., Mosteller, F., et al. (1995). The efficacy of bacillus Calmette-Guérin vaccination of newborns and infants in the prevention of tuberculosis: meta-analyses of the published literature. Pediatrics *96*, 29 35.

Conradie, F., Diacon, A.H., Ngubane, N., et al. (2020). Treatment of Highly Drug-Resistant Pulmonary Tuberculosis. New Engl J Med *382*, 893–902.

Cooper, A.M., and Khader, S.A. (2008). The role of cytokines in the initiation, expansion, and control of cellular immunity to tuberculosis. Immunol Rev *226*, 191–204.

Cruz, A., Fraga, A.G., Fountain, J.J., Rangel-Moreno, J., et al. (2010). Pathological role of interleukin 17 in mice subjected to repeated BCG vaccination after infection with Mycobacterium tuberculosis. J Exp Medicine *207*, 1609 1616.

Cruz, A., Torrado, E., Carmona, J., Fraga, A.G., et al. (2015). BCG vaccination-induced long-lasting control of Mycobacterium tuberculosis correlates with the accumulation of a novel population of CD4+IL-17+TNF+IL-2+ T cells. Vaccine *33*, 85 91.

Dahlstrom, A.W. (1940). The Instability of the Tuberculin Reaction Observations on Dispensary Patients, with Special Reference to the Existence of Demonstrable Tuberculous Lesions and the Degree of Exposure to Tubercle Bacilli. Am Rev Tuberc Pulm Dis *42*, 471–487.

Darboe, F., Mbandi, S.K., Thompson, E.G., et al. (2018). Diagnostic performance of an optimized transcriptomic signature of risk of tuberculosis in cryopreserved peripheral blood mononuclear cells. Tuberculosis *108*, 124–126.

Darrah, P.A., Patel, D.T., Luca, P.M.D., et al. (2007). Multifunctional TH1 cells define a correlate of vaccine-mediated protection against Leishmania major. Nat Med *13*, 843–850.

Darrah, P.A., Zeppa, J.J., Maiello, P., et al. (2020). Prevention of tuberculosis in macaques after intravenous BCG immunization. Nature *577*, 95–102.

Day, C.L., Abrahams, D.A., Lerumo, L., et al. (2011). Functional capacity of Mycobacterium tuberculosis-specific T cell responses in humans is associated with mycobacterial load. J Immunol *187*, 1 12.

Dharmadhikari, A.S., Basaraba, R.J., Walt, M.L.V.D., et al. (2011). Natural infection of guinea pigs exposed to patients with highly drug-resistant tuberculosis. Tuberculosis *91*, 329 338.

Dijkman, K., Sombroek, C.C., Vervenne, R.A.W., et al. (2019). Prevention of tuberculosis infection and disease by local BCG in repeatedly exposed rhesus macaques. Nat Med *25*, 255 262.

Dintwe, O. (2014). Characterisation of Mycobacterium tuberculosis specific T cell immunity with HLA class II tetramers.

Dintwe, O.B., Day, C.L., Smit, E., et al. (2013). Heterologous vaccination against human tuberculosis modulates antigen-specific CD4+ T-cell function. Eur J Immunol *43*, 2409 2420.

Dolton, G., Tungatt, K., Lloyd, A., et al. (2015). More tricks with tetramers: a practical guide to staining T cells with peptide–MHC multimers. Immunology *146*, 11–22.

Domingo-Gonzalez, R., Prince, O., Cooper, A., et al. (2017). Cytokines and Chemokines in Mycobacterium tuberculosis Infection. Microbiol Spectr (*4*) 5.

Ehlers, S., and Schaible, U.E. (2013). The Granuloma in Tuberculosis: Dynamics of a Host–Pathogen Collusion. Front Immunol *3*, 411.

Elias, G., Ogunjimi, B., and Tendeloo, V.V. (2019). Activation-induced surface proteins in the identification of antigen-responsive CD4 T cells. Immunol Lett *219*, 1–7.

Ellis, R.D., Hatherill, M., Tait, D., et al. (2015). Innovative clinical trial designs to rationalize TB vaccine development. Tuberculosis *95*, 352 357.

Emery, J.C., Richards, A.S., Dale, K.D., et al. (2021). Self-clearance of Mycobacterium tuberculosis infection: implications for lifetime risk and population at-risk of tuberculosis disease. Proc Royal Soc B *288*, 20201635.

Erkens, C.G.M., Slump, E., Verhagen, M., et al. (2016). Risk of developing tuberculosis disease among persons diagnosed with latent tuberculosis infection in the Netherlands. Eur Respir J *48*, 1420–1428.

Esmail, H., Lai, R.P., Lesosky, M., et al. (2016). Characterization of progressive HIV-associated tuberculosis using 2-deoxy-2-[18F]fluoro-D-glucose positron emission and computed tomography. Nat Med *22*, 1090–1093.

Essone, P.N., Kalsdorf, B., Chegou, N.N., et al. (2014). Bifunctional T-Cell-Derived Cytokines for the Diagnosis of Tuberculosis and Treatment Monitoring. Respiration *88*, 251–261.

Ewer, K., Millington, K.A., Deeks, J.J., et. al. (2006). Dynamic Antigen-specific T-Cell Responses after Point-Source Exposure to Mycobacterium tuberculosis. Am J Resp Crit Care *174*, 831–839.

Finak, G., McDavid, A., Chattopadhyay, P., et al. (2013). Mixture models for single-cell assays with applications to vaccine studies. Biostatistics *15*, 87 101.

Fletcher, H.A., Snowden, M.A., Landry, B., et al. (2016). T-cell activation is an immune correlate of risk in BCG vaccinated infants. Nat Commun *7*, 11290.

Flynn, J.L., Goldstein, M.M., Chan, J., et al. (1995). Tumor necrosis factor-α is required in the protective immune response against mycobacterium tuberculosis in mice. Immunity *2*, 561–572.

Flynn, J.L., Chan, J., and Lin, P.L. (2011). Macrophages and control of granulomatous inflammation in tuberculosis. Mucosal Immunol *4*, 271 278.

Frascella, B., Richards, A.S., Sossen, B., et al. (2020). Subclinical tuberculosis disease - a review and analysis of prevalence surveys to inform definitions, burden, associations and screening methodology. Clin Infect Dis ciaa1402.

Frentsch, M., Arbach, O., Kirchhoff, D., et al. (2005). Direct access to CD4+ T cells specific for defined antigens according to CD154 expression. Nat Med *11*, 1118–1124.

Fritsch, R.D., Shen, X., Sims, G.P., et al. (2005). Stepwise Differentiation of CD4 Memory T Cells Defined by Expression of CCR7 and CD27. J Immunol *175*, 6489–6497.

Fuertes Marraco, S.A., Soneson, C., Cagnon, L., et al. (2015). Long-lasting stem cell-like memory CD8+ T cells with a naïve-like profile upon yellow fever vaccination. Science Translational Medicine *7*, 282ra48.

Gattinoni, L., Lugli, E., Ji, Y., et al. (2011). A human memory T cell subset with stem cell-like properties. Nat Med *17*, 1290 1297.

Gattinoni, L., Speiser, D.E., Lichterfeld, M., et al. (2017). T memory stem cells in health and disease. Nature Medicine *23*, 18 27.

Geginat, J., Paroni, M., Facciotti, F., et al. (2013). The CD4-centered universe of human T cell subsets. Semin Immunol *25*, 252 262.

Geginat, J., Paroni, M., Maglie, S., et al. (2014). Plasticity of Human CD4 T Cell Subsets. Front Immunol *5*, 630.

Geneva: World Health Organization. (1979). Trial of BCG vaccines in south India for tuberculosis prevention: first report--Tuberculosis Prevention Trial. Bull World Health Organ *57*, 819–827.

Geneva: World Health Organization (2014). The End TB Strategy. Undefined.

Geneva: World Health Organization ,SAGE Working Group on BCG vaccination on Immunisation. (2017). Report on BCG vaccine use for protection against mycobacterial infections including tuberculosis, leprosy, and other nontuberculous mycobacteria (NTM) infections.

Geneva: World Health Organization. World Health Organization. (2017). Consensus meeting report: development of a target product profile (TPP) and a framework for evaluation for a test for predicting progression from tuberculosis infection to active disease. World Health Organization. https://apps.who.int/iris/handle/10665/259176. License: CC BY-NC-SA 3.0 IGO

Geneva: World Health Organization. (2019a). Global tuberculosis report 2019.

Geneva: World Health Organization. (2019b). Lateral flow urine lipoarabinomannan assay (LF-LAM) for the diagnosis of active tuberculosis in people living with HIV.

Geneva: World Health Organization. (2020a). Global tuberculosis report 2020.

Geneva: World Health Organization. (2020b). Framework for the evaluation of new tests for tuberculosis infection (World Health Organization).

Geneva: World Health Organization. (2020c). WHO consolidated guidelines on tuberculosis: tuberculosis preventive treatment.

Gerdes, J., Lemke, H., Baisch, H., et al. (1984). Cell cycle analysis of a cell proliferation-associated human nuclear antigen defined by the monoclonal antibody Ki-67. J Immunol Baltim Md 1950 *133*, 1710–1715.

Glanville, J., Huang, H., Nau, A., et al. (2017). Identifying specificity groups in the T cell receptor repertoire. Nature *547*, 94–98.

Glatman-Freedman, A., and Casadevall, A. (1998). Serum Therapy for Tuberculosis Revisited: Reappraisal of the Role of Antibody-Mediated Immunity against Mycobacterium tuberculosis. Clin Microbiol Rev *11*, 514–532.

Gold, M.C., Napier, R.J., and Lewinsohn, D.M. (2015). MR1-restricted mucosal associated invariant T (MAIT) cells in the immune response to Mycobacterium tuberculosis. Immunol Rev *264*, 154 166.

Grace, A.G., Mittal, A., Jain, S., et al. (2018). Shortened treatment regimens versus the standard regimen for drug-sensitive pulmonary tuberculosis. Cochrane Db Syst Rev.

Graef, P., Buchholz, V.R., Stemberger, C., et al. (2014). Serial transfer of single-cell-derived immunocompetence reveals stemness of CD8(+) central memory T cells. Immunity *41*, 116 126.

Griffith, J.W., Sokol, C.L., and Luster, A.D. (2014). Chemokines and Chemokine Receptors: Positioning Cells for Host Defense and Immunity. Immunology *32*, 659 702.

Gupta, R., Lipman, M., Jackson, C., et al. (2019a). Do higher quantitative interferon gamma release assay or tuberculin skin test results help to predict incident tuberculosis? Data from the UK PREDICT study. OA3822.

Gupta, R.K., Lipman, M., Jackson, C., et al. (2019b). Quantitative IFN-γ Release Assay and Tuberculin Skin Test Results to Predict Incident Tuberculosis. A Prospective Cohort Study. Am J Resp Crit Care *201*, 984–991.

Gupta, R.K., Turner, C.T., Venturini, C., (2020a). Concise whole blood transcriptional signatures for incipient tuberculosis: a systematic review and patient-level pooled meta-analysis. Lancet Respir Medicine.

Gupta, R.K., Kunst, H., Lipman, M., et al. (2020b). Evaluation of QuantiFERON-TB Gold Plus for Predicting Incident Tuberculosis among Recent Contacts: A Prospective Cohort Study. Ann Am Thorac Soc *0*.

Gupta, R.K., Calderwood, C.J., Yavlinsky, A., et al. (2020c). Discovery and validation of a personalized risk predictor for incident tuberculosis in low transmission settings. Nat Med 1–9.

Halliday, A., Whitworth, H., Kottoor, S.H., et al. (2017). Stratification of Latent Mycobacterium tuberculosis Infection by Cellular Immune Profiling. J Infect Dis *215*, 1480 1487.

Han, A., Glanville, J., Hansmann, L., et al. (2014). Linking T-cell receptor sequence to functional phenotype at the single-cell level. Nat Biotechnol *32*, 684–692.

Harari, A., Rozot, V., Enders, F.B., et al. (2011). Dominant TNF-α+ Mycobacterium tuberculosis–specific CD4+ T cell responses discriminate between latent infection and active disease. Nat Med *17*, 372 376.

Harris, R.C., Sumner, T., Knight, G.M., et al. (2020). Potential impact of tuberculosis vaccines in China, South Africa, and India. Sci Transl Med *12*, eaax4607.

Hatherill, M., White, R.G., and Hawn, T.R. (2020). Clinical Development of New TB Vaccines: Recent Advances and Next Steps. Front Microbiol *10*, 3154.

Hawn, T.R., Day, T.A., Scriba, T.J., et al. (2014). Tuberculosis Vaccines and Prevention of Infection. Microbiol Mol Biol R *78*, 650–671.

Henao-Tamayo, M., Ordway, D.J., and Orme, I.M. (2014). Memory T cell subsets in tuberculosis: What should we be targeting? Tuberculosis *94*, 1 7.

Henson, S.M., and Akbar, A.N. (2009). KLRG1--more than a marker for T cell senescence. Age *31*, 285 291.

Henson, S.M., Franzese, O., Macaulay, R., et al. (2009). KLRG1 signaling induces defective Akt (ser473) phosphorylation and proliferative dysfunction of highly differentiated CD8+ T cells. Blood *113*, 6619–6628.

Hermans, S.M., Zinyakatira, N., Caldwell, J., et al. (2020). High rates of recurrent TB disease: a population-level cohort study. Clin Infect Dis.

Higuchi, K., Harada, N., and Mori, T. (2008). Interferon-γ responses after isoniazid chemotherapy for latent tuberculosis. Respirology *13*, 468–472.

Hill, P.C., Brookes, R.H., Fox, A., et al. (2007). Longitudinal Assessment of an ELISPOT Test for Mycobacterium tuberculosis Infection. Plos Med *4*, e192.

Hoft, S.G., Sallin, M.A., Kauffman, K.D., et al. (2019). The Rate of CD4 T Cell Entry into the Lungs during Mycobacterium tuberculosis Infection Is Determined by Partial and Opposing Effects of Multiple Chemokine Receptors. Infect Immun *87*.

Hong, H., Gu, Y., Sheng, S.Y., et al. (2016). The Distribution of Human Stem Cell-like Memory T Cell in Lung Cancer. Journal of Immunotherapy (Hagerstown, Md. : 1997) *39*, 233 240.

Horton, H., Thomas, E.P., Stucky, J.A., et al. (2007). Optimization and validation of an 8-color intracellular cytokine staining (ICS) assay to quantify antigen-specific T cells induced by vaccination. J Immunol Methods *323*, 39 54.

Houben, R.M.G.J., and Dodd, P.J. (2016). The Global Burden of Latent Tuberculosis Infection: A Re-estimation Using Mathematical Modelling. Plos Med *13*, e1002152.

Knowledge HUB (2021). The First National TB Prevalence Survey - South Africa 2018 (South African National Department of Health).

Irmler, M., Hertig, S., and MacDonald, H.R. (1995). Granzyme A is an interleukin 1 beta-converting enzyme. The Journal of ….

Jacobs, A.J., Mongkolsapaya, J., Screaton, G.R., et al. (2016). Antibodies and tuberculosis. Tuberculosis *101*, 102–113.

Jaleco, S., Swainson, L., Dardalhon, V., et al. (2003). Homeostasis of Naive and Memory CD4+ T Cells: IL-2 and IL-7 Differentially Regulate the Balance Between Proliferation and Fas-Mediated Apoptosis. J Immunol *171*, 61 68.

Jankovic, D., Kugler, D.G., and Sher, A. (2010). IL-10 production by CD4+ effector T cells: a mechanism for self-regulation. Mucosal Immunol *3*, 239–246.

Jasenosky, L.D., Scriba, T.J., Hanekom, W.A., et al. (2015). T cells and adaptive immunity to Mycobacterium tuberculosis in humans. Immunol Rev *264*, 74 87.

Jenum, S., Grewal, H.M.S., Hokey, D.A., et al. (2014). The Frequencies of IFNγ+IL2+TNFα+ PPD-Specific CD4+CD45RO+ T-Cells Correlate with the Magnitude of the QuantiFERON® Gold In-Tube Response in a Prospective Study of Healthy Indian Adolescents. Plos One *9*, e101224.

Joeckel, L.T., Wallich, R., Martin, P., et al. (2011). Mouse granzyme K has pro-inflammatory potential. Cell Death Differ *18*, 1112 1119.

Johnson, D.F., Malone, L.L., Zalwango, S., et al. (2014). Tuberculin Skin Test Reversion following Isoniazid Preventive Therapy Reflects Diversity of Immune Response to Primary Mycobacterium tuberculosis Infection. Plos One *9*, e96613.

Jones, B.E., Young, S.M.M., Antoniskis, D., et al. (1993). Relationship of the Manifestations of Tuberculosis to CD4 Cell Counts in Patients with Human Immunodeficiency Virus Infection. Am Rev Respir Dis *148*, 1292–1297.

Joshi, M., Monson, T.P., Joshi, A., et al. (2014). IFN-γ Release Assay Conversions and Reversions. Challenges with Serial Testing in U.S. Health Care Workers. Ann Am Thorac Soc *11*, 296–302.

Juno, J.A., Bockel, D. van, Kent, S.J., et al. (2017). Cytotoxic CD4 T Cells—Friend or Foe during Viral Infection? Front Immunol *8*, 19.

Jurado, J.O., Pasquinelli, V., Alvarez, I.B., et al. (2012). IL-17 and IFN- expression in lymphocytes from patients with active tuberculosis correlates with the severity of the disease. J Leukocyte Biol *91*, 991 1002.

Kagina, B.M., Mansoor, N., Kpamegan, E.P., et al. (2015). Qualification of a whole blood intracellular cytokine staining assay to measure mycobacteria-specific CD4 and CD8 T cell immunity by flow cytometry. J Immunol Methods *417*, 22 33.

Kagina, B.M.N., Abel, B., Bowmaker, M., et al. (2009). Delaying BCG vaccination from birth to 10 weeks of age may result in an enhanced memory CD4 T cell response. Vaccine *27*, 5488 5495.

Kagina, B.M.N., Abel, B., Scriba, T.J., et al. (2010). Specific T cell frequency and cytokine expression profile do not correlate with protection against tuberculosis after bacillus Calmette-Guérin vaccination of newborns. Am J Resp Crit Care *182*, 1073 1079.

Kara, E.E., Comerford, I., Fenix, K.A., et al. (2014). Tailored Immune Responses: Novel Effector Helper T Cell Subsets in Protective Immunity. Plos Pathog *10*, 1 15.

Kaufmann, S.H.E. (2001). How can immunology contribute to the control of tuberculosis? Nat Rev Immunol *1*, 20–30.

Keane, J. (2005). TNF-blocking agents and tuberculosis: new drugs illuminate an old topic. Rheumatology *44*, 714–720.

Khader, S.A., and Cooper, A.M. (2008). IL-23 and IL-17 in tuberculosis. Cytokine *41*, 79–83.

Khader, S.A., Bell, G.K., Pearl, J.E., et al. (2007). IL-23 and IL-17 in the establishment of protective pulmonary CD4+ T cell responses after vaccination and during Mycobacterium tuberculosis challenge. Nat Immunol *8*, ni1449.

Kipnis, A., Irwin, S., Izzo, A.A., et al. (2005). Memory T lymphocytes generated by Mycobacterium bovis BCG vaccination reside within a CD4 CD44lo CD62 ligand(hi) population. Infect Immun *73*, 7759 7764.

Kirman, J.R., Quinn, K.M., and Seder, R.A. (2019). Immunological memory. Immunol Cell Biol *97*, 615–616.

Klenerman, P., Cerundolo, V., and Dunbar, P.R. (2002). Tracking T cells with tetramers: new tales from new tools. Nat Rev Immunol *2*, 263–272.

Kobayashi, T., Okamoto, S., Iwakami, Y., et al. (2007). Exclusive increase of CX3CR1+ CD28− CD4+ T cells in inflammatory bowel disease and their recruitment as intraepithelial lymphocytes. Inflamm Bowel Dis *13*, 837–846.

Kumar, N.P., Moideen, K., Viswanathan, et al. (2016). Effect of standard tuberculosis treatment on naive, memory and regulatory T-cell homeostasis in tuberculosis–diabetes co-morbidity. Immunology *149*, 87–97.

Kunkel, E.J., Boisvert, J., Murphy, K., et al. (2002). Expression of the chemokine receptors CCR4, CCR5, and CXCR3 by human tissue-infiltrating lymphocytes. Am J Pathology *160*, 347 355.

Kwan, C.K., and Ernst, J.D. (2011). HIV and Tuberculosis: a Deadly Human Syndemic. Clin Microbiol Rev *24*, 351–376.

Lamoreaux, L., Roederer, M., and Koup, R. (2006). Intracellular cytokine optimization and standard operating procedure. Nat Protoc *1*, 1507–1516.

Lechner, F., Cuero, A.L.V., Kantzanou, M., et al. (2001). Studies of human antiviral CD8+ lymphocytes using class I peptide tetramers. Rev Med Virol *11*, 11–22.

Leeuwen, E.M.M. van, Remmerswaal, E.B.M., Vossen, M.T.M., et al. (2004). Emergence of a CD4+CD28− Granzyme B+, Cytomegalovirus-Specific T Cell Subset after Recovery of Primary Cytomegalovirus Infection. J Immunol *173*, 1834–1841.

Lewinsohn, D.A., Lewinsohn, D.M., and Scriba, T.J. (2017). Polyfunctional CD4+ T Cells As Targets for Tuberculosis Vaccination. Front Immunol *8*, 1262.

Li, H., and Javid, B. (2018). Antibodies and tuberculosis: finally coming of age? Nat Rev Immunol *18*, 591–596.

Liao, W., Lin, J.-X., and Leonard, W.J. (2013). Interleukin-2 at the Crossroads of Effector Responses, Tolerance, and Immunotherapy. Immunity *38*, 13–25.

Libero, G.D., Singhal, A., Lepore, M., et al. (2014). Nonclassical T Cells and Their Antigens in Tuberculosis. Csh Perspect Med *4*, a018473.

Lin, L., Finak, G., Ushey, K., et al. (2015). COMPASS identifies T-cell subsets correlated with clinical outcomes. Nat Biotechnol *33*, 610–616.

Lin, P.L., Ford, C.B., Coleman, M.T., et al. (2014). Sterilization of granulomas is common in active and latent tuberculosis despite within-host variability in bacterial killing. Nat Med *20*, 75 79.

Lindestam Arlehamn, C.S., Gerasimova, A., Mele, F., et al. (2013). Memory T cells in latent Mycobacterium tuberculosis infection are directed against three antigenic islands and largely contained in a CXCR3+CCR6+ Th1 subset. Plos Pathog *9*, e1003130.

Liu, C.H., Liu, H., and Ge, B. (2017). Innate immunity in tuberculosis: host defense vs pathogen evasion. Cell Mol Immunol *14*, 963–975.

Lu, L.L., Chung, A.W., Rosebrock, T.R., et al. (2016). A Functional Role for Antibodies in Tuberculosis. Cell *167*, 433-443.e14.

Lu, L.L., Smith, M.T., Yu, K.K.Q., et al. (2019). IFN-γ-independent immune markers of Mycobacterium tuberculosis exposure. Nat Med 1–11.

Luabeya, A.K.K., Kagina, B.M.N., Tameris, M., et al. (2015). First-in-human trial of the post-exposure tuberculosis vaccine H56:IC31 in Mycobacterium tuberculosis infected and non-infected healthy adults. Vaccine *33*, 4130 4140.

Lugli, E., Pinti, M., Nasi, M., et al. (2007). Subject classification obtained by cluster analysis and principal component analysis applied to flow cytometric data. Cytom Part A *71A*, 334 344.

Lugli, E., Dominguez, M.H., Gattinoni, L., et al. (2013a). Superior T memory stem cell persistence supports long-lived T cell memory. J Clin Invest *123*, 594–599.

Lugli, E., Gattinoni, L., Roberto, A., et al. (2013b). Identification, isolation and in vitro expansion of human and nonhuman primate T stem cell memory cells. Nat Protoc *8*, 33 42.

Lyadova, I., and Nikitina, I. (2019). Cell Differentiation Degree as a Factor Determining the Role for Different T-Helper Populations in Tuberculosis Protection. Front Immunol *10*, 972.

Lyadova, I.V., and Panteleev, A.V. (2015). Th1 and Th17 Cells in Tuberculosis: Protection, Pathology, and Biomarkers. Mediat Inflamm *2015*, 854507 13.

Ma, N., Zalwango, S., Malone, L.L., et al. (2014). Clinical and epidemiological characteristics of individuals resistant to M. tuberculosis infection in a longitudinal TB household contact study in Kampala, Uganda. Bmc Infect Dis *14*, 352.

MacArthur, G.J., Wilson, A.D., Birchall, M.A., et al. (2007). Primary CD4+ T-Cell Responses Provide both Helper and Cytotoxic Functions during Epstein-Barr Virus Infection and Transformation of Fetal Cord Blood B Cells. J Virol *81*, 4766 4775.

Machingaidze, S., Verver, S., Mulenga, H., et al. (2012). Predictive Value of Recent QuantiFERON Conversion for Tuberculosis Disease in Adolescents. Am J Resp Crit Care *186*, 1051 1056.

Mahan, C.S., Zalwango, S., Thiel, B.A., et al. (2012). Innate and Adaptive Immune Responses during Acute M. tuberculosis Infection in Adult Household Contacts in Kampala, Uganda. Am J Tropical Medicine Hyg *86*, 690 697.

Mahnke, Y.D., Brodie, T.M., Sallusto, F., et al. (2013). The who's who of T-cell differentiation: human memory T-cell subsets. Eur J Immunol *43*, 2797 2809.

Mahomed, H., Hawkridge, T., Verver, S., et al. (2011a). The tuberculin skin test versus QuantiFERON TB Gold® in predicting tuberculosis disease in an adolescent cohort study in South Africa. Plos One *6*, e17984.

Mahomed, H., Hawkridge, T., Verver, S., et al. (2011b). Predictive factors for latent tuberculosis infection among adolescents in a high-burden area in South Africa. Int J Tuberc Lung Dis Official J Int Union Against Tuberc Lung Dis *15*, 331–336.

Mallone, R., Mannering, S.I., Brooks-Worrell, B.M., et al. (2011). Isolation and preservation of peripheral blood mononuclear cells for analysis of islet antigen-reactive T cell responses: position statement of the T-Cell Workshop Committee of the Immunology of Diabetes Society. Clin Exp Immunol *163*, 33–49.

Mami-Chouaib, F., Echchakir, H., Dorothee, G., et al. (2002). Antitumor cytotoxic T-lymphocyte response in human lung carcinoma: identification of a tumor-associated antigen. Immunol Rev *188*, 114–121.

Mangalam, A., Rodriguez, M., and David, C. (2006). Role of MHC class II expressing CD4+ T cells in proteolipid protein91–110-induced EAE in HLA-DR3 transgenic mice. Eur J Immunol *36*, 3356–3370.

Mangtani, P., Abubakar, I., Ariti, C., et al. (2014). Protection by BCG Vaccine Against Tuberculosis: A Systematic Review of Randomized Controlled Trials. Clin Infect Dis *58*, 470–480.

Marrack, P., Bender, J., Hildeman, D., et al. (2000). Homeostasis of αβ TCR+ T cells. Nat Immunol *1*, 107–111.

Martirosyan, A., Bargen, K.V., Gorvel, V.A., et al. (2013). In Vivo Identification and Characterization of CD4. Plos One *8*, 1 10.

Mateus, J., Lasso, P., Pavia, P., et al. (2015). Low frequency of circulating CD8+ T stem cell memory cells in chronic chagasic patients with severe forms of the disease. PLoS Neglected Tropical Diseases *9*, e3432.

Mathema, B., Andrews, J.R., Cohen, T., et al. (2017). Drivers of Tuberculosis Transmission. J Infect Dis *216*, S644–S653.

Medawar, L., Tukiman, H.M., Mbayo, G., et al. (2019). Analysis of cellular and soluble profiles in QuantiFERON nonconverters, converters, and reverters in the Gambia. Immun Inflamm Dis *7*, 260–270.

Mendelsohn, S.C., Fiore-Gartland, A., Penn-Nicholson, A., et al. (2021). Prospective Validation of a Host Blood Transcriptomic Biomarker for Pulmonary Tuberculosis in People Living with HIV: A Diagnostic and Prognostic Accuracy Study. Available at SSRN: https://ssrn.com/abstract=3750013

Menzies, D. (1999). Interpretation of Repeated Tuberculin Tests. Am J Resp Crit Care *159*, 15–21.

Metkar, S.S., Menaa, C., Pardo, J., et al. (2008). Human and mouse granzyme A induce a proinflammatory cytokine response. Immunity *29*, 720 733.

Millington, K.A., Gooding, S., Hinks, T.S.C., et al. (2010). Mycobacterium tuberculosis-Specific Cellular Immune Profiles Suggest Bacillary Persistence Decades after Spontaneous Cure in Untreated Tuberculosis. J Infect Dis *202*, 1685–16849.

Millington, K.A., Fortune, S.M., Low, J., et al. (2011). Rv3615c is a highly immunodominant RD1 (Region of Difference 1)-dependent secreted antigen specific for Mycobacterium tuberculosis infection. Proc National Acad Sci *108*, 5730 5735.

Mitra, D.K., Rosa, S.C.D., Luke, A., et al. (1999). Differential representations of memory T cell subsets are characteristic of polarized immunity in leprosy and atopic diseases. Int Immunol *11*, 1801–1810.

Moguche, A.O., Musvosvi, M., Penn-Nicholson, A., et al. (2017). Antigen Availability Shapes T Cell Differentiation and Function during Tuberculosis. Cell Host Microbe *21*, 695 706.e5.

Mogues, T., Goodrich, M.E., Ryan, L., et al. (2001). The Relative Importance of T Cell Subsets in Immunity and Immunopathology of Airborne Mycobacterium tuberculosis Infection in Mice. J Exp Med *193*, 271–280.

Mølhave, M., and Wejse, C. (2020). Historical review of studies on the effect of treating latent tuberculosis. Int J Infect Dis *92*, S31–S36.

Moore, K.W., Malefyt, R. de W., Coffman, R.L., et al. (2001). Interleukin-10 and the Interleukin-10 Receptor. Annual Review of Immunology *19*, 683–765.

Morán-Mendoza, O., Marion, S.A., Elwood, K., et al. (2010). Risk factors for developing tuberculosis: a 12-year follow-up of contacts of tuberculosis cases. Int J Tuberc Lung Dis Official J Int Union Against Tuberc Lung Dis *14*, 1112–1119.

Morgan, D., Ruscetti, F., and Gallo, R. (1976). Selective in vitro growth of T lymphocytes from normal human bone marrows. Science *193*, 1007–1008.

Mori, T., Sakatani, M., Yamagishi, F., et al. (2004). Specific Detection of Tuberculosis Infection: An Interferon-γ–based Assay Using New Antigens. Am J Resp Crit Care *170*, 59–64.

Mousset, C.M., Hobo, W., Woestenenk, R., et al. (2019). Comprehensive Phenotyping of T Cells Using Flow Cytometry. Cytom Part A.

Mpande, C.A.M., Dintwe, O.B., Musvosvi, M., et al. (2018). Functional, Antigen-Specific Stem Cell Memory (T_{SCM}) CD4+ T Cells Are Induced by Human Mycobacterium tuberculosis Infection. Front Immunol *9*, 324.

Mpande, C.A.M., Musvosvi, M., Rozot, V., et al. (2021). Antigen-specific T Cell Activation Distinguishes Between Recent and Remote Tuberculosis Infection. Am J Resp Crit Care *148*, 1292–1297.

Mpande, C.A.M., Rozot, V., Mosito, B., et al.(2021). Immune profiling of Mycobacterium tuberculosis-specific T cells in recent and remote infection. Ebiomedicine 64, 103233.

Mucida, D., Husain, M.M., Muroi, S., et al. (2013). Transcriptional reprogramming of mature CD4 + helper T cells generates distinct MHC class II-restricted cytotoxic T lymphocytes. Nature Immunology *14*, 281 289.

Mueller, H., Faé, K.C., Magdorf, K., et al. (2011). Granulysin-Expressing CD4+ T Cells as Candidate Immune Marker for Tuberculosis during Childhood and Adolescence. Plos One *6*, 1 10.

Mulenga, H., Bunyasi, E.W., Mbandi, S.K., et al. (2019). Performance of host blood transcriptomic signatures for diagnosing and predicting progression to tuberculosis disease in HIV-negative adults and adolescents: a systematic review protocol. Bmj Open *9*, e026612.

Musvosvi, M., Duffy, D., Filander, E., et al. (2018). T-cell biomarkers for diagnosis of tuberculosis: candidate evaluation by a simple whole blood assay for clinical translation. Eur Respir J *51*, 1800153.

Naidoo, P., Theron, G., Rangaka, M.X., et al. (2017). The South African Tuberculosis Care Cascade: Estimated Losses and Methodological Challenges. J Infect Dis *216*, S702–S713.

Nakajima, C., Mukai, T., Yamaguchi, N., et al. (2002). Induction of the chemokine receptor CXCR3 on TCR-stimulated T cells: dependence on the release from persistent TCR-triggering and requirement for IFN-γ stimulation. Eur J Immunol *32*, 1792.

Ndiaye, B.P., Thienemann, F., Ota, M., et al. (2015). Safety, immunogenicity, and efficacy of the candidate tuberculosis vaccine MVA85A in healthy adults infected with HIV-1: a randomised, placebo-controlled, phase 2 trial. Lancet Respir Medicine *3*, 190 200.

Ndlovu, H., and Marakalala, M.J. (2016). Granulomas and Inflammation: Host-Directed Therapies for Tuberculosis. Front Immunol *7*, 434.

Neel, N.F., Schutyser, E., Sai, J., et al. (2005). Chemokine receptor internalization and intracellular trafficking. Cytokine Growth F R *16*, 637–658.

Nemes, E., Rozot, V., Geldenhuys, H., et al. (2017a). Optimization and Interpretation of Serial QuantiFERON Testing to Measure Acquisition of Mycobacterium tuberculosis Infection. Am J Resp Crit Care *196*, 638 648.

Nemes, E., Hesseling, A.C., Tameris, M., et al. (2017b). Safety and Immunogenicity of Newborn MVA85A Vaccination and Selective, Delayed Bacille Calmette-Guerin (BCG) for Infants of HIV Infected Mothers: A Phase 2 Randomized Controlled Trial. Clin Infect Dis.

Nemes, E., Geldenhuys, H., Rozot, V., et al. (2018). Prevention of M. tuberculosisInfection with H4:IC31 Vaccine or BCG Revaccination. New Engl J Med *379*, 138 149.

Nemes, E., Abrahams, D.A., Scriba, T.J., et al. (2019). Diagnostic accuracy of ESAT-6 free IGRA compared to QuantiFERON-TB Gold In-tube. Clin Infect Dis.

Nepom, G.T. (2012). MHC Class II Tetramers. J Immunol *188*, 2477 2482.

Nepom, G.T., Buckner, J.H., Novak, E.J., et al. (2002). HLA class II tetramers: Tools for direct analysis of antigen-specific CD4+ T cells. Arthritis Rheumatism *46*, 5–12.

Nguyen, R., Perfetto, S., Mahnke, Y.D., et al. (2013). Quantifying spillover spreading for comparing instrument performance and aiding in multicolor panel design. Cytom Part A *83A*, 306 315.

Nicol, M.P., and Zar, H.J. (2020). Advances in the diagnosis of pulmonary tuberculosis in children. Paediatr Respir Rev *36*, 52–56.

Nicol, M.P., Schumacher, S.G., Workman, L., et al. (2020). Accuracy of a Novel Urine Test, Fujifilm SILVAMP Tuberculosis Lipoarabinomannan, for the Diagnosis of Pulmonary Tuberculosis in Children. Clin Infect Dis.

Nienhaus, A., Ringshausen, F.C., Costa, J.T., et al. (2014). IFN-γ release assay versus tuberculin skin test for monitoring TB infection in healthcare workers. Expert Rev Anti-Infe *11*, 37–48.

Nikitina, I.Y., Panteleev, A.V., Kosmiadi, G.A., et al. (2018). Th1, Th17, and Th1Th17 Lymphocytes during Tuberculosis: Th1 Lymphocytes Predominate and Appear as Low-Differentiated CXCR3+CCR6+Cells in the Blood and Highly Differentiated CXCR3+/−CCR6−Cells in the Lungs. J Immunol *200*, 2090–2103.

North, R.J., and Jung, Y.-J. (2004). Immunity to Tuberculosis. Immunology *22*, 599–623.

Nyasha, M.M. (2016). Systems analysis of the CD4 T cell response induced bythe novel subunit tuberculosis vaccine, H1:IC31.

Okada, R., Kondo, T., Matsuki, F., Takata, H., et al. (2008). Phenotypic classification of human CD4+ T cell subsets and their differentiation. Int Immunol *20*, 1189–1199.

Oliveira, G., Ruggiero, E., Stanghellini, M.T.L., et al. (2015). Tracking genetically engineered lymphocytes long-term reveals the dynamics of T cell immunological memory. Science Translational Medicine *7*, 317ra198.

Orlando, V., Manna, M.P.L., Goletti, D., et al. (2018). Human CD4 T-Cells With a Naive Phenotype Produce Multiple Cytokines During Mycobacterium Tuberculosis Infection and Correlate With Active Disease. Front Immunol *9*, 1119.

Orme, I.M. (2010). The Achilles heel of BCG. Tuberculosis *90*, 329 332.

Orme, I.M., and Henao-Tamayo, M.I. (2018). Trying to See the Forest through the Trees: Deciphering the Nature of Memory Immunity to Mycobacterium tuberculosis. Front Immunol *9*, 461.

Ouyang, W., Kolls, J.K., and Zheng, Y. (2008). The Biological Functions of T Helper 17 Cell Effector Cytokines in Inflammation. Immunity *28*, 454–467.

Pacheco-Fernandez, T. , Volpedo, G., Gannavaram, S., et al. (2021). Revival of Leishmanization and Leishmanin. Front Cell Infect Mi 11, 639801

Pagán, A.J., and Ramakrishnan, L. (2015). Immunity and Immunopathology in the Tuberculous Granuloma. Csh Perspect Med *5*, a018499.

Pai, M., and O'Brien, R. (2007). Serial Testing for Tuberculosis: Can We Make Sense of T Cell Assay Conversions and Reversions? Plos Med *4*, e208.

Pai, M., Dheda, K., Cunningham, J., et al. (2007). T-cell assays for the diagnosis of latent tuberculosis infection: moving the research agenda forward. Lancet Infect Dis *7*, 428–438.

Pai, M., Joshi, R., Dogra, S., et al. (2009). T-cell assay conversions and reversions among household contacts of tuberculosis patients in rural India. Int J Tuberc Lung Dis Official J Int Union Against Tuberc Lung Dis *13*, 84–92.

Pai, M., Joshi, R., Dogra, S., et al. (2012). Serial Testing of Health Care Workers for Tuberculosis Using Interferon-γ Assay. Am J Resp Crit Care *174*, 349–355.

Pai, M., Behr, M.A., Dowdy, D., et al. (2016). Tuberculosis. Nat Rev Dis Primers *2*, nrdp201676.

Papagno, L., Almeida, J.R., Nemes, E., et al. (2007). Cell permeabilization for the assessment of T lymphocyte polyfunctional capacity. J Immunol Methods *328*, 182 188.

Partnership, S.T. (2019). The Paradigm Shift 2018-2022.

Penn-Nicholson, A., Nemes, E., Hanekom, W.A., et al. (2015). Mycobacterium tuberculosis-specific CD4 T cells are the principal source of IFN-γ in QuantiFERON assays in healthy persons. Tuberculosis *95*, 350 351.

Penn-Nicholson, A., Mbandi, S.K., Thompson, E., et al. (2020). RISK6, a 6-gene transcriptomic signature of TB disease risk, diagnosis and treatment response. Sci Rep-Uk *10*, 8629.

Perfetto, S.P., Ambrozak, D., Nguyen, R., et al. (2012). Quality assurance for polychromatic flow cytometry using a suite of calibration beads. Nat Protoc *7*, 2067 2079.

Peters, N.C., Pagán, A.J., Lawyer, P.G., et al. (2014). Chronic Parasitic Infection Maintains High Frequencies of Short-Lived Ly6C+CD4+ Effector T Cells That Are Required for Protection against Re-infection. Plos Pathog 10, e1004538.

Peters, W., Scott, H.M., Chambers, H.F., et al. (2001). Chemokine receptor 2 serves an early and essential role in resistance to Mycobacterium tuberculosis. Proc National Acad Sci *98*, 7958–7963.

Petruccioli, E., Petrone, L., Vanini, V., et al. (2015). Assessment of CD27 expression as a tool for active and latent tuberculosis diagnosis. J Infection *71*, 1 8.

Petruccioli, E., Chiacchio, T., Pepponi, I., et al. (2016). First characterization of the CD4 and CD8 T-cell responses to QuantiFERON-TB Plus. J Infection *73*, 588 597.

Petruccioli, E., Vanini, V., Chiacchio, T., et al.(2017). Analytical evaluation of QuantiFERON- Plus and QuantiFERON- Gold In-tube assays in subjects with or without tuberculosis. Tuberculosis *106*, 38–43.

Portevin, D., Moukambi, F., Clowes, P., et al. (2014). Assessment of the novel T-cell activation marker–tuberculosis assay for diagnosis of active tuberculosis in children: a prospective proof-of-concept study. Lancet Infect Dis *14*, 931–938.

Prezzemolo, T., Guggino, G., Manna, M.P.L., et al.(2014). Functional Signatures of Human CD4 and CD8 T Cell Responses to Mycobacterium tuberculosis. Front Immunol *5*, 180.

Qin, S., Rottman, J.B., Myers, P., et al. (1998). The chemokine receptors CXCR3 and CCR5 mark subsets of T cells associated with certain inflammatory reactions. J Clin Invest *101*, 746 754.

Rakshit, S., Ahmed, A., Adiga, V., et al. (2019). BCG revaccination boosts adaptive polyfunctional Th1/Th17 and innate effectors in IGRA+ and IGRA- Indian adults. Jci Insight *4*.

Ramachandran, H., Laux, J., Moldovan, I., et al. (2012). Optimal thawing of cryopreserved peripheral blood mononuclear cells for use in high-throughput human immune monitoring studies. Cells *1*, 313–324.

Ramakrishnan, L. (2012). Revisiting the role of the granuloma in tuberculosis. Nat Rev Immunol *12*, 352 366.

Redford, P.S., Murray, P.J., and Garra, A.O. apos (2011). The role of IL-10 in immune regulation during M. tuberculosis infection. Mucosal Immunol *4*, 261 270.

Reichler, M.R., Khan, A., Sterling, T.R., et al. (2019). Risk Factors for Tuberculosis and Effect of Preventive Therapy Among Close Contacts of Persons with Infectious Tuberculosis. Clin Infect Dis *70*, 1562–1572.

Riley, R.L., Mills, C.C., Nyka, W., et al. (1959a). Aerial dissemination of pulmonary tuberculosis a two-year study of contagion in a tuberculosis ward. Am J Epidemiol *70*, 185–196.

Riley, R.L., Mills, C.C., Nyka, W., et al. (1959b). Aerial dissemination of pulmonary tuberculosis: a two-year study of contagion in a tuberculosis ward1. Am J Hygiene *142*, 3–14.

Riley, R.L., Mills, C.C., O'Grady, F., et al. (1962). Infectiousness of Air from a Tuberculosis Ward. Am Rev Respir Dis *85*, 511–525.

Ringshausen, F.C., Nienhaus, A., Schablon, A., et al. (2010). Predictors of persistently positive Mycobacterium-tuberculosis-specific interferon-gamma responses in the serial testing of health care workers. Bmc Infect Dis *10*, 220.

Ringshausen, F.C., Schablon, A., and Nienhaus, A. (2012). Interferon-gamma release assays for the tuberculosis serial testing of health care workers: a systematic review. J Occup Med Toxicol *7*, 1.

Riou, C., Berkowitz, N., Goliath, R., et al (2017). Analysis of the Phenotype of Mycobacterium tuberculosis-Specific CD4+ T Cells to Discriminate Latent from Active Tuberculosis in HIV-Uninfected and HIV-Infected Individuals. Front Immunol *8*, 968.

Riou, C., Bruyn, E.D., Ruzive, S., et al. (2020). Disease extent and anti-tubercular treatment response correlates with Mycobacterium tuberculosis-specific CD4 T-cell phenotype regardless of HIV-1 status. Clin Transl Immunol *9*.

Rivino, L., Messi, M., Jarrossay, D., et al. (2004). Chemokine Receptor Expression Identifies Pre–T Helper (Th)1, Pre–Th2, and Nonpolarized Cells among Human CD4 +Central Memory T Cells. J Exp Medicine *200*, 725 735.

Robbins, S.H., Terrizzi, S.C., Sydora, B.C., et al. (2003). Differential Regulation of Killer Cell Lectin-Like Receptor G1 Expression on T Cells. J Immunol *170*, 5876–5885.

Robin, X., Turck, N., Hainard, A., et al. (2011). pROC: an open-source package for R and S+ to analyze and compare ROC curves. Bmc Bioinformatics *12*, 77.

Roederer, M., Nozzi, J.L., and Nason, M.C. (2011). SPICE: Exploration and analysis of post-cytometric complex multivariate datasets. Cytom Part A *79A*, 167–174.

Rogerson, B.J., Jung, Y.-J., LaCourse, R., et al. (2006). Expression levels of Mycobacterium tuberculosis antigen-encoding genes versus production levels of antigen-specific T cells during stationary level lung infection in mice. Immunology *118*, 195 201.

Rosa, S.C.D., Herzenberg, L.A., Herzenberg, L.A., et al. (2001). 11-color, 13-parameter flow cytometry: Identification of human naive T cells by phenotype, function, and T-cell receptor diversity. Nat Med *7*, 245–248.

Roy, A., Eisenhut, M., Harris, R.J., et al. (2014). Effect of BCG vaccination against Mycobacterium tuberculosis infection in children: systematic review and meta-analysis. Bmj Br Medical J *349*, g4643.

Rozot, V., Vigano, S., Mazza-Stalder, J., et al. (2013). Mycobacterium tuberculosis-specific CD8+ T cells are functionally and phenotypically different between latent infection and active disease. Eur J Immunol *43*, 1568 1577.

Rozot, V., Patrizia, A., Vigano, S., et al. (2015). Combined Use of Mycobacterium tuberculosis–Specific CD4 and CD8 T-Cell Responses Is a Powerful Diagnostic Tool of Active Tuberculosis. Clin Infect Dis *60*, 432–437.

Rozot, V., Nemes, E., Geldenhuys, H., et al. (2020). Multidimensional analyses reveal modulation of adaptive and innate immune subsets by tuberculosis vaccines. Commun Biology *3*, 563.

Ruhwald, M., Thurah, L. de, Kuchaka, D., et al. (2017). Introducing the ESAT-6 free IGRA, a companion diagnostic for TB vaccines based on ESAT-6. Sci Rep-Uk *7*, 45969.

Ruibal, P., Voogd, L., Joosten, S.A., et al. (2021). The role of donor-unrestricted T-cells, innate lymphoid cells, and NK cells in anti-mycobacterial immunity. Immunol Rev.

Sakai, S., Kauffman, K.D., Schenkel, J.M., et al. (2014a). Cutting Edge: Control of Mycobacterium tuberculosis Infection by a Subset of Lung Parenchyma–Homing CD4 T Cells. J Immunol *192*, 2965–2969.

Sakai, S., Mayer-Barber, K.D., and Barber, D.L. (2014b). ScienceDirect Defining features of protective CD4 T cell responses to Mycobacterium tuberculosis. Curr Opin Immunol *29*, 137 142.

Sakai, S., Kauffman, K.D., Sallin, M.A., et al. (2016). CD4 T Cell-Derived IFN-γ Plays a Minimal Role in Control of Pulmonary Mycobacterium tuberculosis Infection and Must Be Actively Repressed by PD-1 to Prevent Lethal Disease. Plos Pathog *12*, e1005667.

Sallin, M.A., Sakai, S., Kauffman, K.D., et al. (2017). Th1 Differentiation Drives the Accumulation of Intravascular, Non-protective CD4 T Cells during Tuberculosis. Cell Reports *18*, 3091–3104.

Sallusto, F., Lenig, D., Förster, R., et al. (1999). Two subsets of memory T lymphocytes with distinct homing potentials and effector functions. Nature *401*, 708 712.

Sargentini, V., Mariotti, S., Carrara, S., et al. (2009). Cytometric detection of antigen-specific IFN-γ/IL-2 secreting cells in the diagnosis of tuberculosis. Bmc Infect Dis *9*, 99.

Sarkar, S., Kalia, V., Haining, W.N., et al. (2008). Functional and genomic profiling of effector CD8 T cell subsets with distinct memory fates. J Exp Medicine *205*, 625–640.

Scanga, C.A., Mohan, V.P., Yu, K., et al. (2000). Depletion of Cd4+ T Cells Causes Reactivation of Murine Persistent Tuberculosis despite Continued Expression of Interferon γ and Nitric Oxide Synthase 2. J Exp Medicine *192*, 347–358.

Scholzen, T., and Gerdes, J. (2000). The Ki-67 protein: From the known and the unknown. J Cell Physiol *182*, 311–322.

Scriba, T.J., and Nemes, E. (2019). Protection against tuberculosis by mucosal BCG administration. Nat Med *25*, 199 201.

Scriba, T.J., Purbhoo, M., Day, C.L., et al. (2005). Ultrasensitive Detection and Phenotyping of CD4 + T Cells with Optimized HLA Class II Tetramer Staining. J Immunol *175*, 6334–6343.

Scriba, T.J., Kalsdorf, B., Abrahams, D.A., et al. (2008). Distinct, Specific IL-17- and IL-22-Producing CD4+ T Cell Subsets Contribute to the Human Anti-Mycobacterial Immune Response. J Immunol *180*, 1962–1970.

Scriba, T.J., Penn-Nicholson, A., Shankar, S., et al. (2017). Sequential inflammatory processes define human progression from M. tuberculosis infection to tuberculosis disease. Plos Pathog *13*, e1006687.

Scriba, T.J., Fiore-Gartland, A., Penn-Nicholson, A., et al. (2021). Biomarker-guided tuberculosis preventive therapy (CORTIS): a randomised controlled trial. Lancet Infect Dis.

Seder, R.A., Darrah, P.A., and Roederer, M. (2008). T-cell quality in memory and protection: implications for vaccine design. Nat Rev Immunol *8*, nri2274.

Seder, R.A., and Sacks, D.L. (2004). Memory may not need reminding. Nat Med 10, 1045–1047.

Serbina, N.V., and Flynn, J.L. (1999). Early emergence of CD8(+) T cells primed for production of type 1 cytokines in the lungs of Mycobacterium tuberculosis-infected mice. Infect Immun *67*, 3980–3988.

Shafiani, S., Tucker-Heard, G., Kariyone, A., et al. (2010). Pathogen-specific regulatory T cells delay the arrival of effector T cells in the lung during early tuberculosis. J Exp Medicine *207*, 1409 1420.

Shi, L., Jung, Y.-J., Tyagi, S., et al. (2003). Expression of Th1-mediated immunity in mouse lungs induces a Mycobacterium tuberculosis transcription pattern characteristic of nonreplicating persistence. Proc National Acad Sci *100*, 241–246.

Shi, L., North, R., and Gennaro, M.L. (2004). Effect of Growth State on Transcription Levels of Genes Encoding Major Secreted Antigens of Mycobacterium tuberculosis in the Mouse Lung. Infect Immun *72*, 2420–2424.

Sia, J.K., and Rengarajan, J. (2019). Immunology of Mycobacterium tuberculosis Infections. Microbiol Spectr *7*.

Sia, J.K., Georgieva, M., and Rengarajan, J. (2015). Innate Immune Defenses in Human Tuberculosis: An Overview of the Interactions between Mycobacterium tuberculosisand Innate Immune Cells. J Immunol Res *2015*, 1 12.

Sidney, J., Southwood, S., Oseroff, C., et al. (1999). Measurement of MHC/Peptide Interactions by Gel Filtration. Curr Protoc Immunol *31*, 18.3.1-18.3.19.

Silva, D.R., Mello, F.C. de Q., and Migliori, G.B. (2020). Shortened tuberculosis treatment regimens: what is new? J Bras Pneumol *46*, e20200009.

Silveira-Mattos, P.S., Barreto-Duarte, B., Vasconcelos, B., et al. (2019). Differential expression of activation markers by Mycobacterium tuberculosis-specific CD4+ T-cell distinguishes extrapulmonary from pulmonary tuberculosis and latent infection. Clin Infect Dis *71*, 1905–1911.

Simmons, J.D., Stein, C.M., Seshadri, C., et al. (2018). Immunological mechanisms of human resistance to persistent Mycobacterium tuberculosis infection. Nat Rev Immunol *18*, 575 589.

Sims, S., Willberg, C., and Klenerman, P. (2014). MHC–peptide tetramers for the analysis of antigen-specific T cells. Expert Rev Vaccines *9*, 765–774.

Singh, S.P., Zhang, H.H., Foley, J.F., et al. (2008). Human T Cells That Are Able to Produce IL-17 Express the Chemokine Receptor CCR6. J Immunol *180*, 214 221.

Smith, S.G., Smits, K., Joosten, S.A., et al. (2015). Intracellular Cytokine Staining and Flow Cytometry: Considerations for Application in Clinical Trials of Novel Tuberculosis Vaccines. Plos One *10*, e0138042.

Soares, A., Govender, L., Hughes, J., et al. (2010). Novel application of Ki67 to quantify antigen-specific in vitro lymphoproliferation. J Immunol Methods *362*, 1 8.

Soares, A.P., Scriba, T.J., Joseph, S., et al. (2008). Bacillus Calmette-Guérin Vaccination of Human Newborns Induces T Cells with Complex Cytokine and Phenotypic Profiles. J Immunol *180*, 3569–3577.

Soares, A.P., Chung, C.K.C.K., Choice, T., et al. (2013). Longitudinal changes in CD4(+) T-cell memory responses induced by BCG vaccination of newborns. J Infect Dis *207*, 1084 1094.

Sower, L.E., Froelich, C.J., Allegretto, N., et al. (1996). Extracellular activities of human granzyme A: Monocyte activation by granzyme A versus α-thrombin. Journal of Immunology *156*, 2585 2590.

Spencer, C.T., Abate, G., Sakala, I.G., et al. (2013). Granzyme A Produced by γ9δ2 T Cells Induces Human Macrophages to Inhibit Growth of an Intracellular Pathogen. Plos Pathog *9*, e1003119 8.

Stein, C.M., Nsereko, M., Malone, L.L., et al. (2018a). Long-term Stability of Resistance to Latent Mycobacterium tuberculosis Infection in Highly Exposed Tuberculosis Household Contacts in Kampala, Uganda. Clin Infect Dis *68*, 1705–1712.

Stein, C.M., Zalwango, S., Malone, L.L., et al. (2018b). Resistance and Susceptibility to Mycobacterium Tuberculosis Infection and Disease in Tuberculosis Households in Kampala, Uganda. Am J Epidemiol.

Strickland, N., Müller, T.L., Berkowitz, N., et al. (2017). Characterization ofMycobacterium tuberculosis–Specific Cells Using MHC Class II Tetramers Reveals Phenotypic Differences Related to HIV Infection and Tuberculosis Disease. J Immunol *199*, 2440–2450.

Suliman, S., Geldenhuys, H., Johnson, J.L., et al. (2016). Bacillus Calmette–Guérin (BCG) Revaccination of Adults with Latent Mycobacterium tuberculosis Infection Induces Long-Lived BCG-Reactive NK Cell Responses. J Immunol *197*, 1100–1110.

Suliman, S., Thompson, E.G., Sutherland, J., et al. (2018). Four-Gene Pan-African Blood Signature Predicts Progression to Tuberculosis. Am J Resp Crit Care *197*, 1198 1208.

Sun, Q., Burton, R.L., and Lucas, K.G. (2002). Cytokine production and cytolytic mechanism of CD4+ cytotoxic T lymphocytes in ex vivo expanded therapeutic Epstein-Barr virus-specific T-cell cultures. Blood *99*, 3302 3309.

Tait, D.R., Hatherill, M., Meeren, O.V.D., et al. (2019). Final Analysis of a Trial of M72/AS01E Vaccine to Prevent Tuberculosis. New Engl J Med *381*, 2429–2439.

Tameris, M., Hatherill, M., Landry, B.S., et al. (2013). Safety and efficacy of MVA85A, a new tuberculosis vaccine, in infants previously vaccinated with BCG: a randomised, placebo-controlled phase 2b trial. Lancet *381*, 1021 1028.

Tanna, G.L.D., Khaki, A.R., Theron, G., et al. (2019). Effect of Xpert MTB/RIF on clinical outcomes in routine care settings: individual patient data meta-analysis. Lancet Global Heal *7*, e191–e199.

Tena-Coki, N.G., Scriba, T.J., Peteni, N., et al. (2010). CD4 and CD8 T-cell responses to mycobacterial antigens in African children. Am J Resp Crit Care *182*, 120 129.

Theron, G., Zijenah, L., Chanda, D., et al. (2014). Feasibility, accuracy, and clinical effect of point-of-care Xpert MTB/RIF testing for tuberculosis in primary-care settings in Africa: a multicentre, randomised, controlled trial. Lancet *383*, 424–435.

Torrado, E., and Cooper, A.M. (2010). IL-17 and Th17 cells in tuberculosis. Cytokine Growth F R *21*, 455–462.

Trauer, J.M., Moyo, N., Tay, E.-L., et al. (2016). Risk of Active Tuberculosis in the Five Years Following Infection . . . 15%? Chest *149*, 516–525.

Turner, C.T., Gupta, R.K., Tsaliki, et al. (2020). Blood transcriptional biomarkers for active pulmonary tuberculosis in a high-burden setting: a prospective, observational, diagnostic accuracy study. Lancet Respir Medicine *8*, 407–419.

UN General Assembly, (2015). Transforming our world : the 2030 Agenda for Sustainable Development (UN General Assembly).

Verrall, A.J., Netea, M.G., Alisjahbana, B., et al. (2014). Early clearance of Mycobacterium tuberculosis : a new frontier in prevention. Immunology *141*, 506–513.

Vickers, M.A., Darboe, F., Muefong, C.N., et al. (2020). Monitoring Anti-tuberculosis Treatment Response Using Analysis of Whole Blood Mycobacterium tuberculosis Specific T Cell Activation and Functional Markers. Front Immunol *11*, 572620.

Waldrop, S.L., Davis, K.A., Maino, V.C., et al. (1998). Normal human CD4+ memory T cells display broad heterogeneity in their activation threshold for cytokine synthesis. J Immunol Baltim Md 1950 *161*, 5284–5295.

Wang, P., Sidney, J., Dow, C., et al. (2008). A Systematic Assessment of MHC Class II Peptide Binding Predictions and Evaluation of a Consensus Approach. Plos Comput Biol *4*, e1000048.

Warsinske, H., Vashisht, R., and Khatri, P. (2019). Host-response-based gene signatures for tuberculosis diagnosis: A systematic comparison of 16 signatures. Plos Med *16*, e1002786.

Wiker, H.G., Mustafa, T., Bjune, G.A., et al. (2010). Evidence for waning of latency in a cohort study of tuberculosis. Bmc Infect Dis *10*, 37.

Wilkinson, K.A., Oni, T., Gideon, H.P., et al. (2016). Activation Profile of Mycobacterium tuberculosis–Specific CD4+ T Cells Reflects Disease Activity Irrespective of HIV Status. Am J Resp Crit Care *193*, 1307–1310.

Winje, B.A., White, R., Syre, H., et al. (2018). Stratification by interferon-γ release assay level predicts risk of incident TB. Thorax *73*, 652.

Wood, R., Liang, H., Wu, H., et al. (2010). Changing prevalence of tuberculosis infection with increasing age in high-burden townships in South Africa. Int J Tuberc Lung Dis Official J Int Union Against Tuberc Lung Dis *14*, 406–412.

Woodworth, J.S., Cohen, S.B., Moguche, A.O., et al. (2016). Subunit vaccine H56/CAF01 induces a population of circulating CD4 T cells that traffic into the Mycobacterium tuberculosis-infected lung. Mucosal Immunol *10*, 555–564.

Wu, C., Kirman, J.R., Rotte, M.J., et al. (2002). Distinct lineages of TH1 cells have differential capacities for memory cell generation in vivo. Nat Immunol *3*, ni832.

Xin, H., Zhang, H., Cao, X., et al. (2019a). Serum level of IL-8 is associated with reversion of QuantiFERON-TB gold in-tube tests. J Infect *78*, 292–298.

Xin, H., Zhang, H., Yang, S., et al. (2019b). 5-Year Follow-up of Active Tuberculosis Development From Latent Infection in Rural China. Clin Infect Dis.

Yamamoto, J., Adachi, Y., Onoue, Y., et al. (2000). Differential expression of the chemokine receptors by the Th1- and Th2-type effect or populations within circulating CD4+ T cells. J Leukocyte Biol *68*, 568–574.

Yoshikawa, T.T. (1992). Tuberculosis in Aging Adults. J Am Geriatr Soc *40*, 178–187.

Yuan, J., Tenant, J., Pacatte, T., et al. (2019). A Subset of Mycobacteria-Specific CD4+ IFN-γ+ T Cell Expressing Naive Phenotype Confers Protection against Tuberculosis Infection in the Lung. J Immunol Baltim Md 1950 *203*, 972–980.

Zak, D.E., Penn-Nicholson, A., Scriba, T.J., et al. (2016). A blood RNA signature for tuberculosis disease risk: a prospective cohort study. Lancet *387*, 2312 2322.

Zanetti, C., Peracchi, M., Zorzi, et al. (2012). Outbreak of Transient Conversions of the QuantiFERON-TB Gold In-Tube Test in Laboratory Health Care Worker Screenings. Clin Vaccine Immunol *19*, 954–960.

Zaph, C., Uzonna, J., Beverley, S.M., et al. (2004). Central memory T cells mediate long-term immunity to Leishmania major in the absence of persistent parasites. Nat Med 10, nm1108.

Zellweger, J.-P., Sotgiu, G., Block, M., et al. (2015). Risk Assessment of Tuberculosis in Contacts by IFN-γ Release Assays. A Tuberculosis Network European Trials Group Study. Am J Resp Crit Care *191*, 1176–1184.

Zhang, H., Xin, H., Li, X., et al. (2018). Reversion of QuantiFERON-TB Gold In-Tube test in individuals with and without prophylactic treatment for latent tuberculosis infection: A systematic review and meta-analysis. J Infection *77*, 276–282.

Zhang, H., Xin, H., Wang, D., et al. (2019). Serial Testing of Mycobacterium Tuberculosis Infection in Chinese Village Doctors by QuantiFERON-TB Gold Plus, QuantiFERON-TB Gold In-Tube and T-SPOT.TB. J Infection *78*, 305–310.

Zhu, J., Yamane, H., and Paul, W.E. (2010). Differentiation of Effector CD4 T Cell Populations*. Annu Rev Immunol *28*, 445–489.

Zielinski, C.E., Mele, F., Aschenbrenner, D., et al. (2012). Pathogen-induced human TH17 cells produce IFN-γ or IL-10 and are regulated by IL-1β. Nature *484*, 514–518.

Zyl-Smit, R.N. van, Pai, M., Peprah, K., et al. (2009). Within-Subject Variability and Boosting of T-Cell Interferon-γ Responses after Tuberculin Skin Testing. Am J Resp Crit Care *180*, 49–58.

(1980). Trial of BCG vaccines in south India for tuberculosis prevention. Indian J Medical Res *72 (Su)*, 349–363.

Appendix

Legend for Appendix 1-11: CITRUS Analysis results: (A) tree, (B) graphs and (C) histogram (blue total cells, salmon cluster specific cells) depicting expression of each memory/functional marker used to define differentially expressed M.tb-specific CD4 T cell clusters between 2 M.tb infection states (as defined per appendix). Black circles highlight unique differentially expressed T cell clusters that were selected for manual gating confirmation.

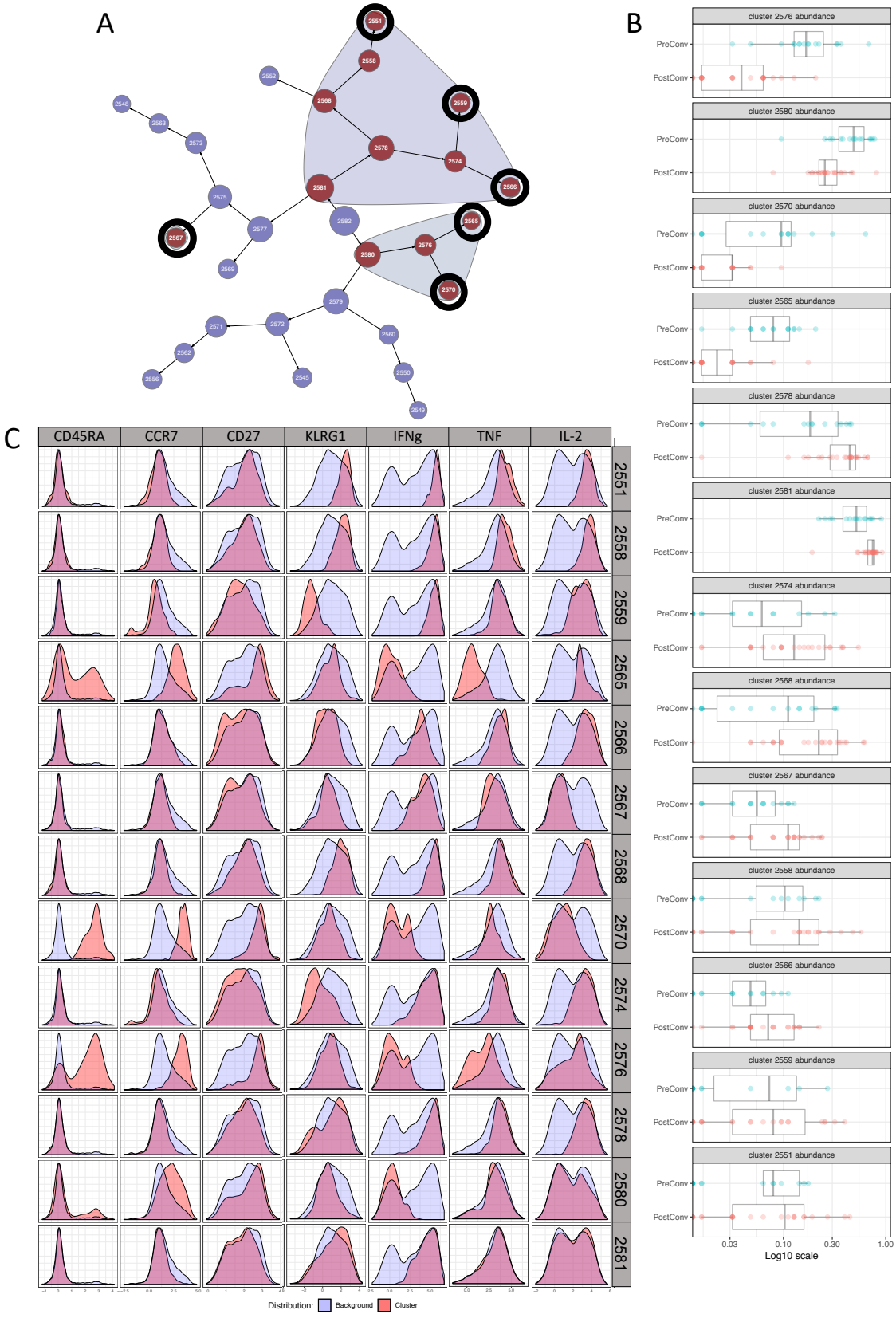

Appendix 1: M.tb lysate Pre-(PreConv) vs Post- (PostConv) TBI CITRUS analysis result

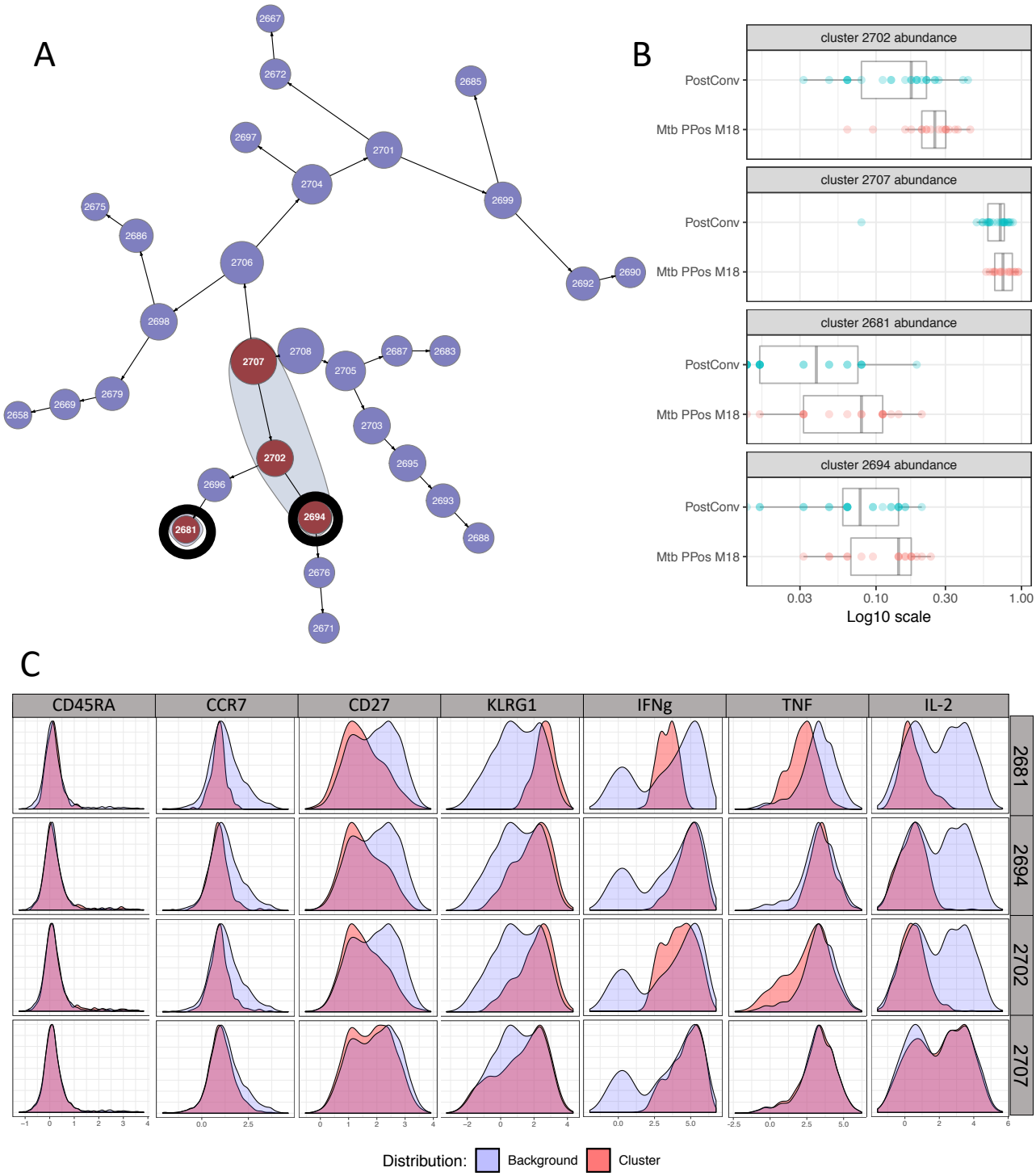

Appendix 2: M.tb lysate Recent TBI (Post-Conv) vs Remote TBI (M.tb PPos M18) CITRUS analysis result

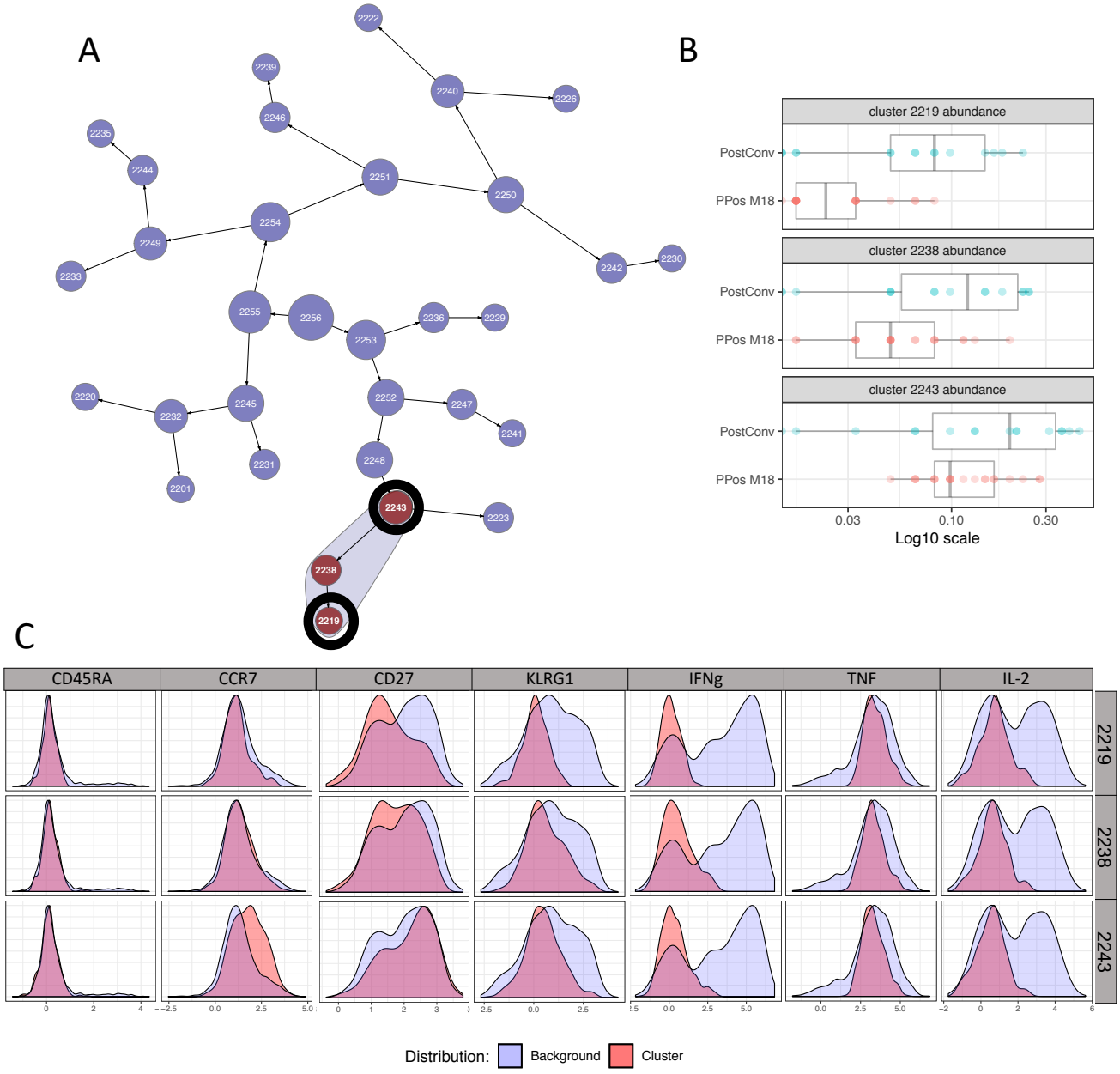

Appendix 3: CFP-10/ESAT-6 Recent TBI (PostConv) vs Remote TBI (PPos M18) CITRUS analysis result

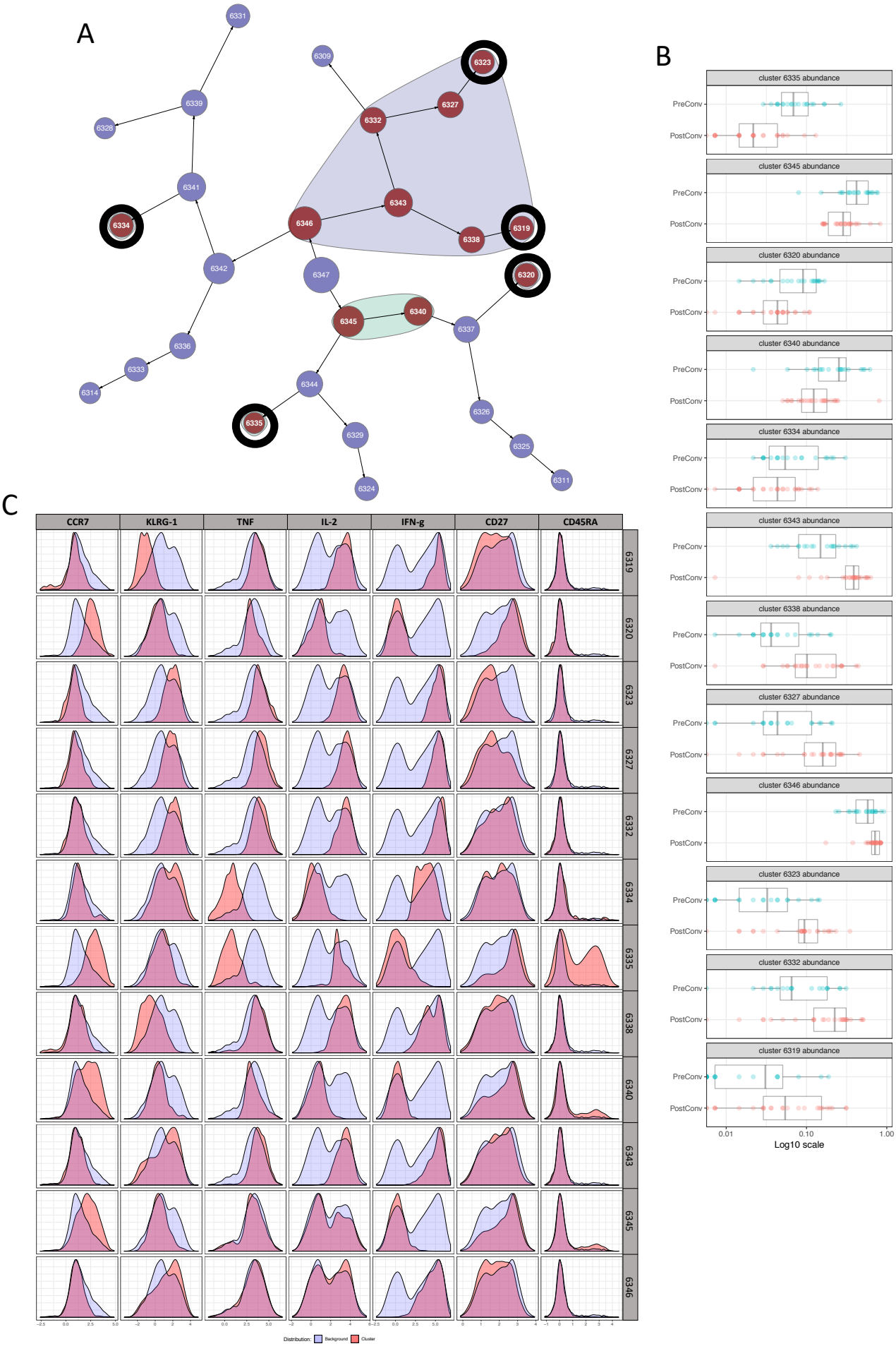

Appendix 4: M.tb lysate Pre- (PreConv) vs Post- (PostConv) Converter CITRUS analysis result .

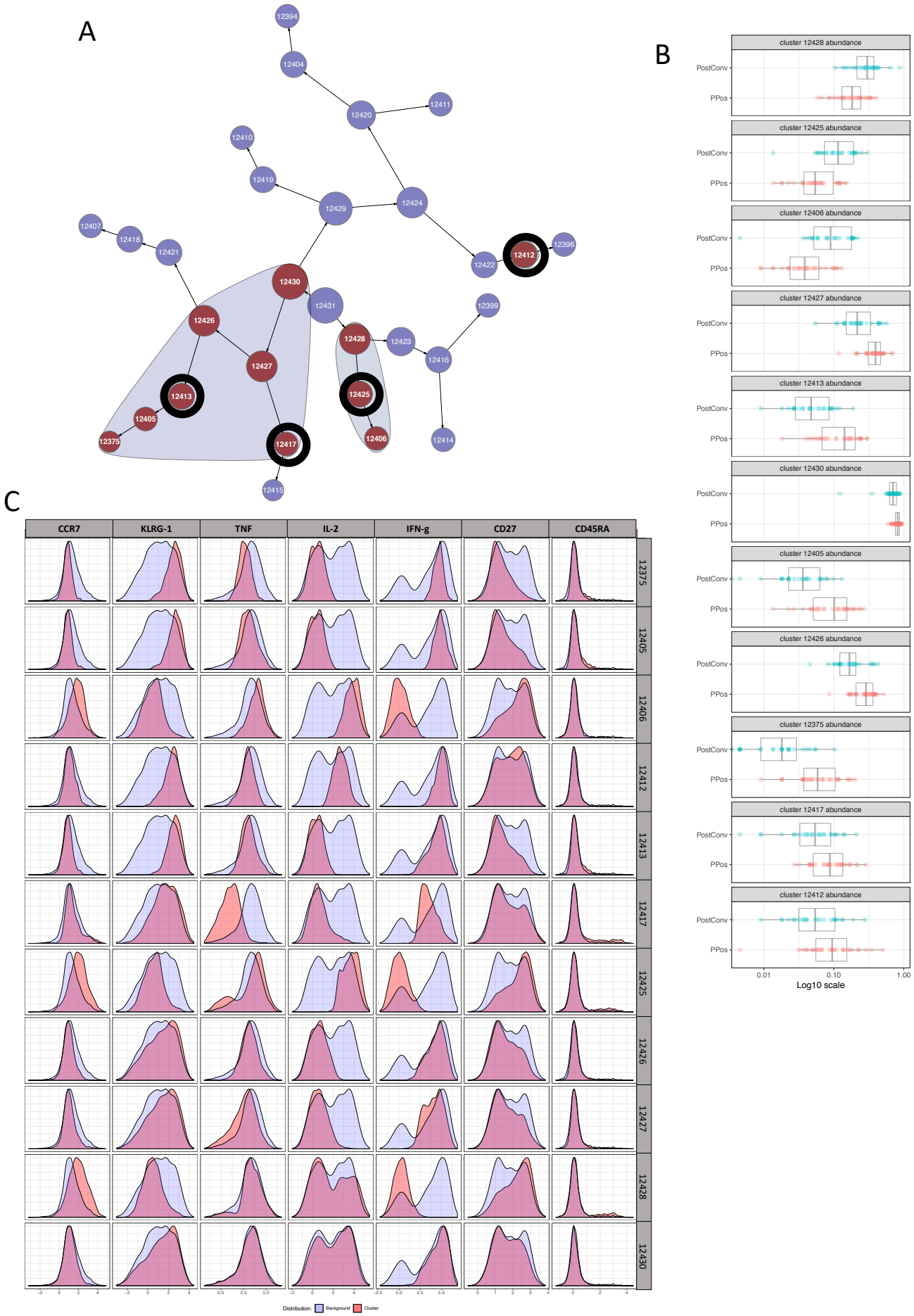

Appendix 5: M.tb lysate Post-Converter (PostConv) vs Remote TBI (PPos) CITRUS analysis result for Chapter 6

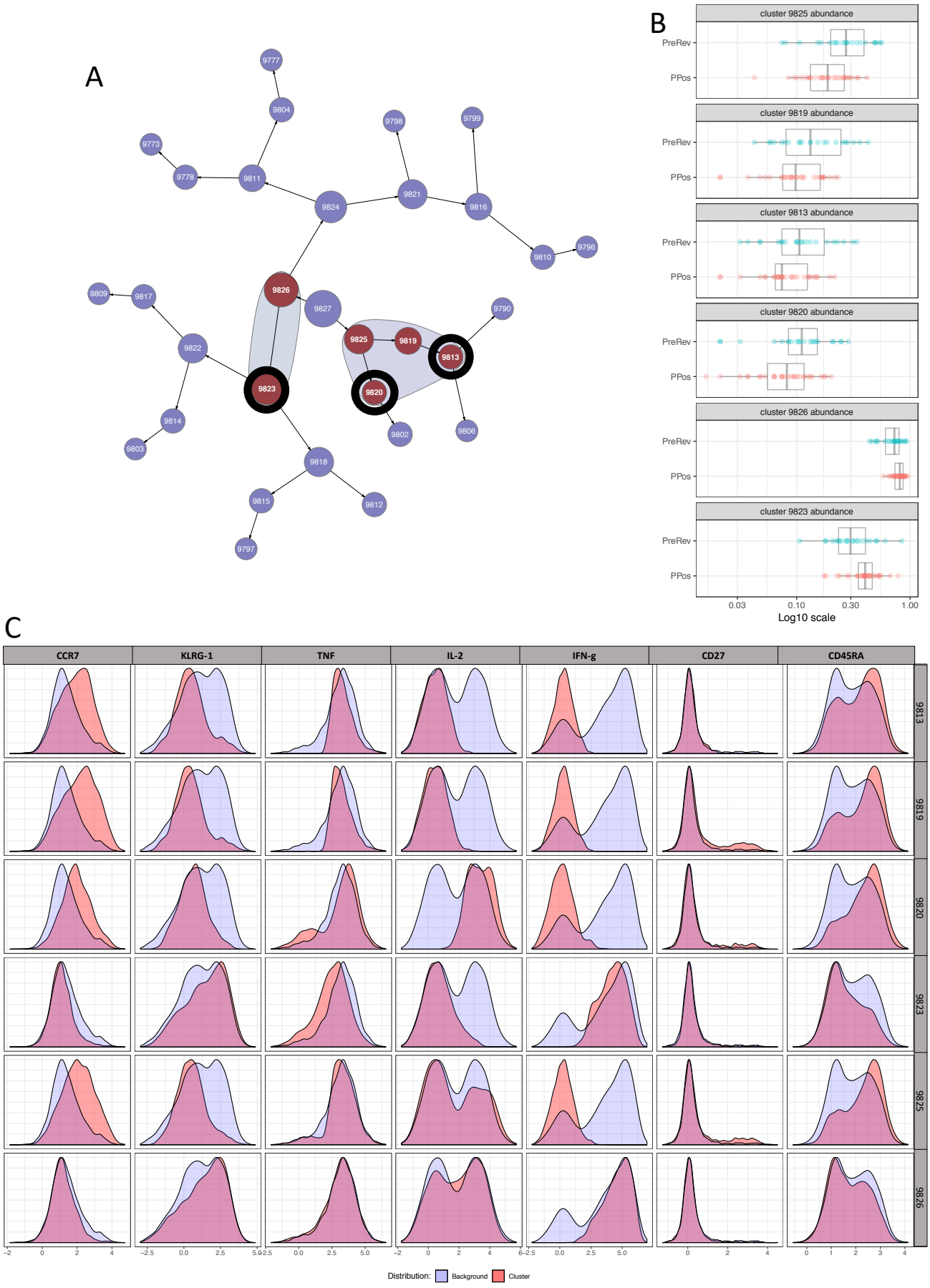

Appendix 6: M.tb lysate Remote TBI (PPos) vs Pre-Reverter (PreRev) CITRUS analysis result.

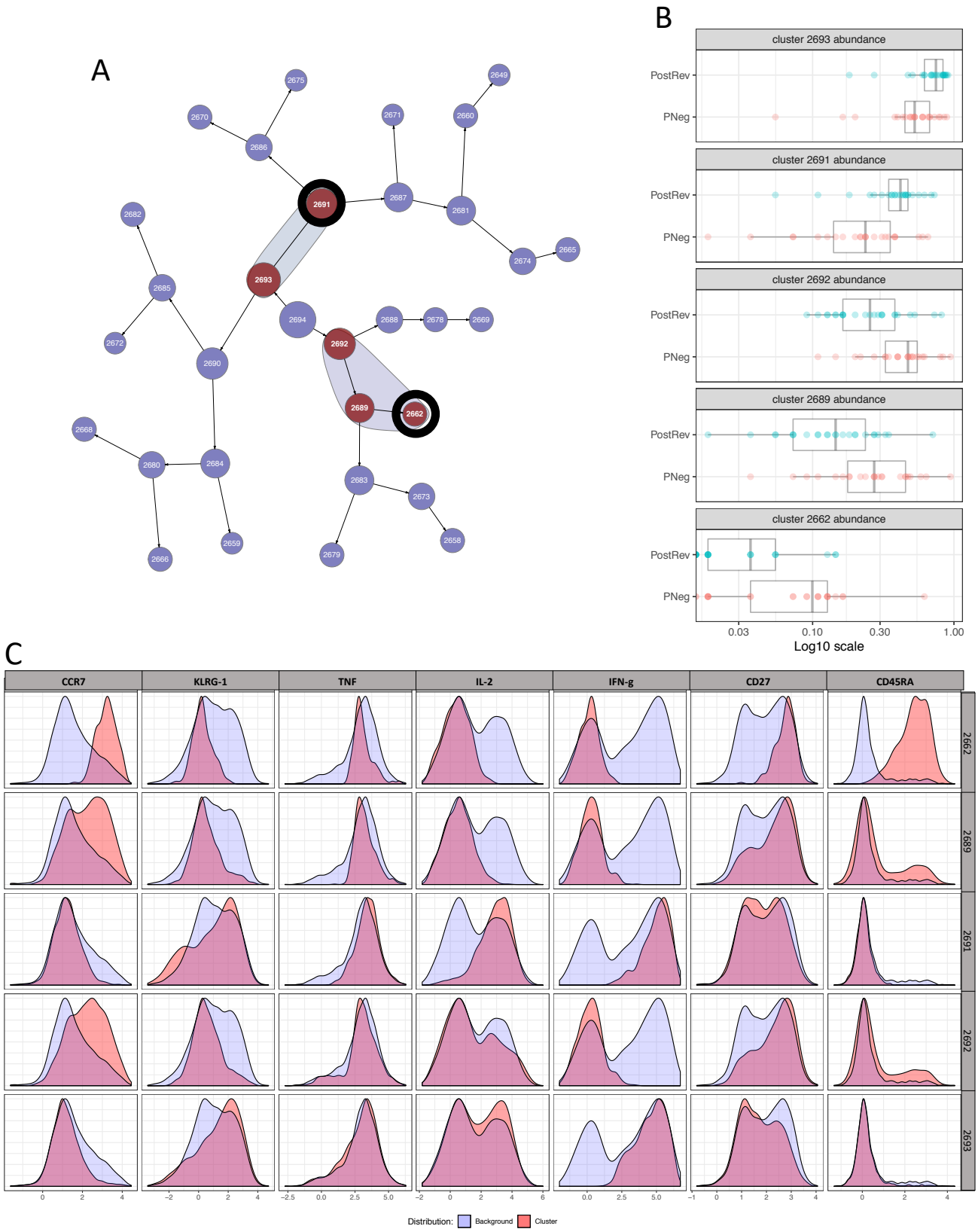

Appendix 7: M.tb lysate Post-Reverters (PostRev) vs Non-converter (PNeg) CITRUS analysis result.

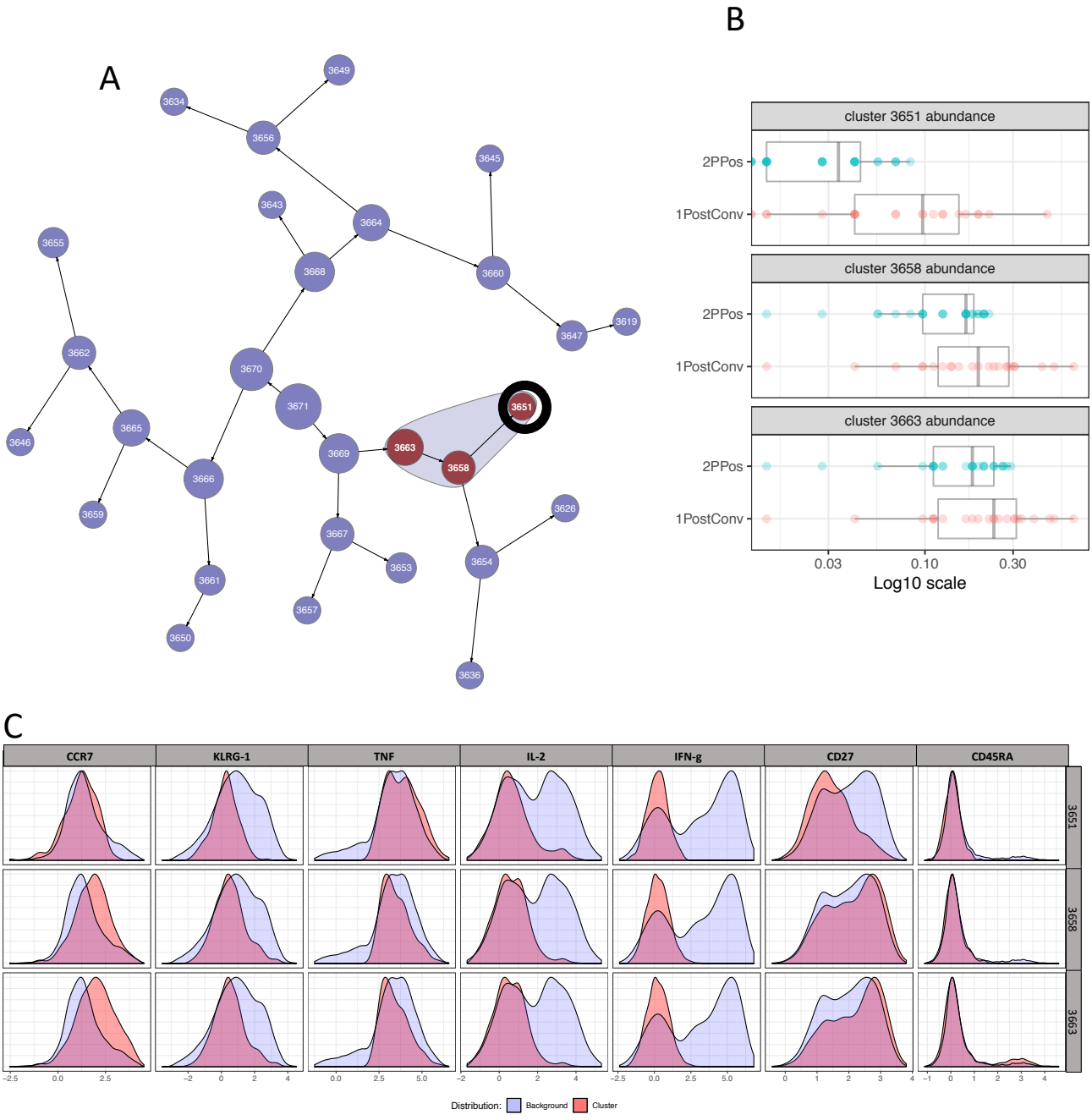

Appendix 8: CFP-10/ESAT-6 Post-Converter (1PostConv) vs Remote TBI (2PPos) CITRUS analysis result .

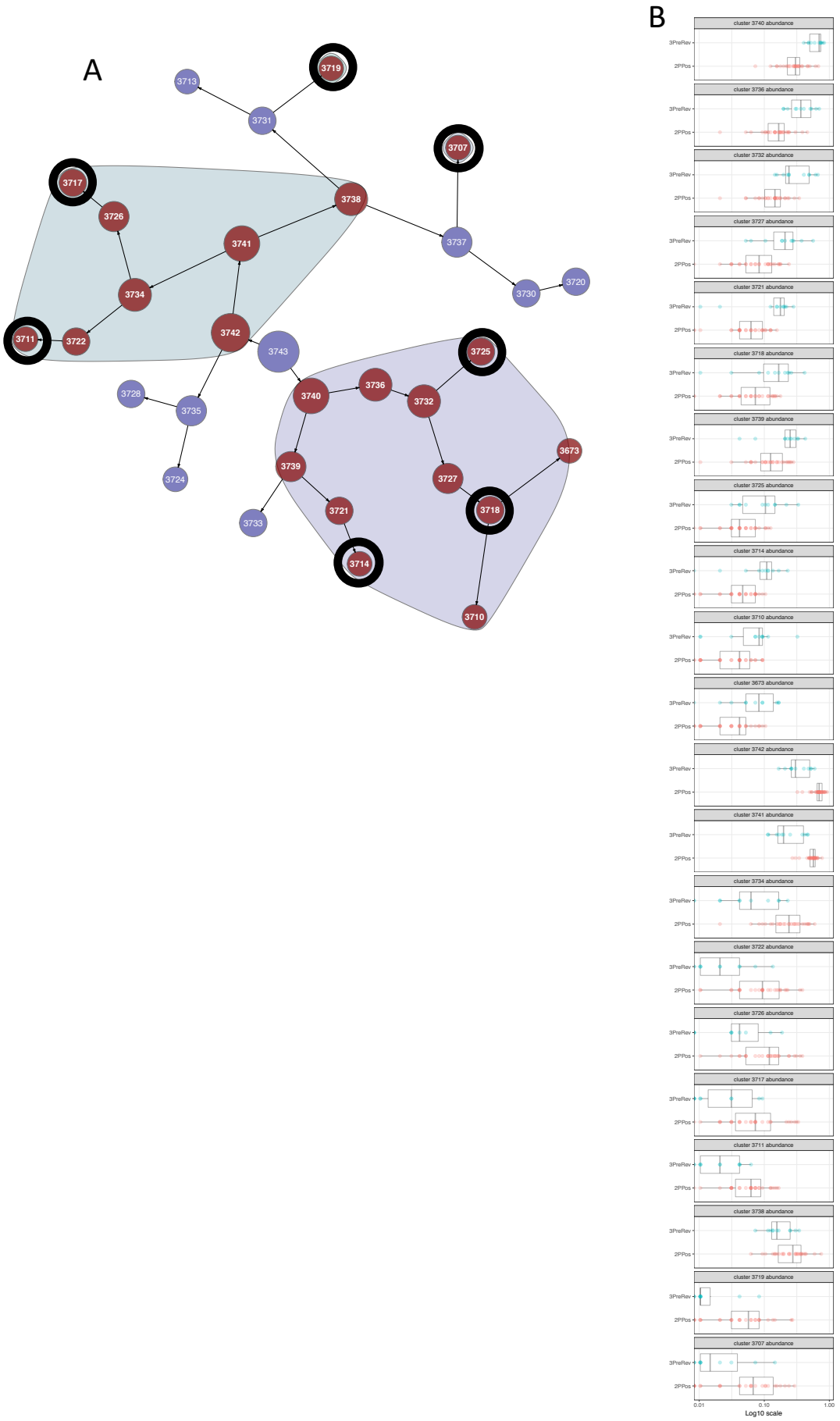

Appendix 9: CFP-10/ESAT-6 Remote TBI (2PPos) vs Pre-Reverter (3PreRev) CITRUS analysis [(A) CITRUS Tree and (B) graphs] result.

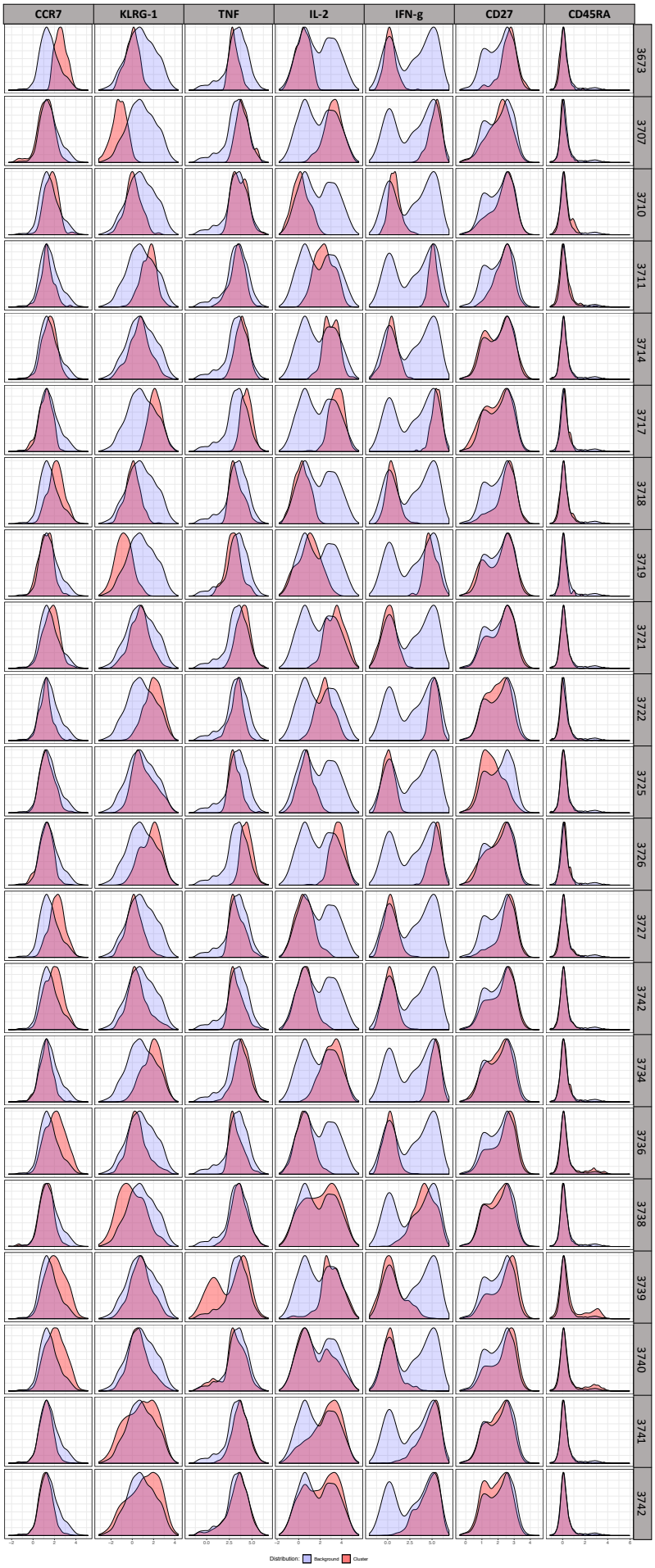

Appendix 10: CFP-10/ESAT-6 Remote TBI (2PPos) vs Pre-Reverter (3PreRev) CITRUS analysis (histograms only) result.

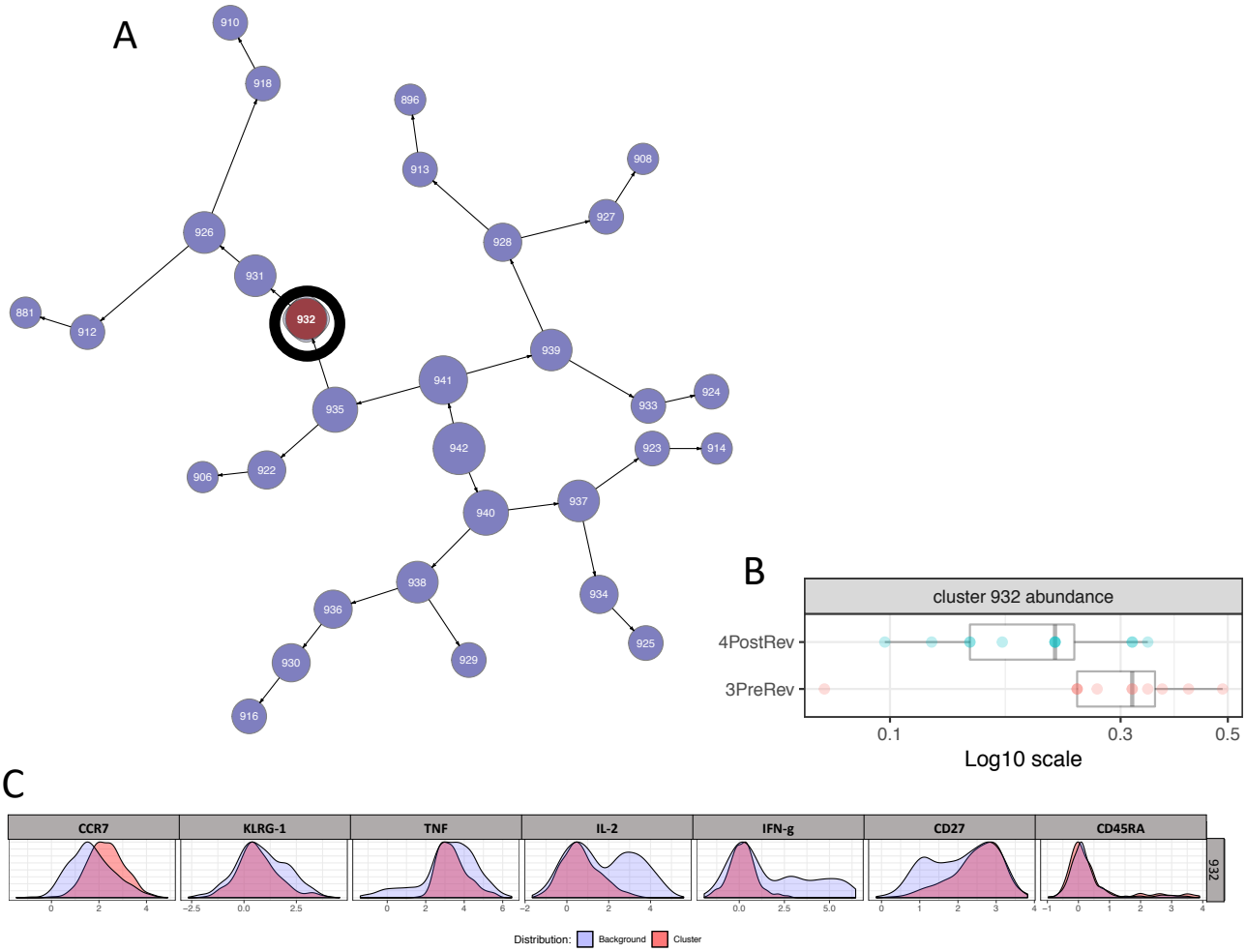

Appendix 11: CFP-10/ESAT-6 Pre- (3PreRev) vs Post- (4PostRev) Reverter CITRUS analysis.

Appendix 12: Memory-cytokine expression profiles of differentially expressed CITRUS clusters per TBI comparison.

TBI Comparison	Ag-specificity	Cluster	CD45RA	CCR7	CD27	KLRG-1	IFN-γ	TNF	IL-2
Pre- vs Post-Converter	M.tb lysate	6335	45.9	78.4	64.9	18.9	10.8	16.2	97.3
		6320	0.24	71.8	91.5	1.94	1.46	99.3	4.13
		6340	21.7	49.8	72.1	4.89	0.93	98.3	4.19
		6319	0	3.17	50.7	0	100	99.8	96.1
		6323	0.2	1	28.9	47	100	100	98
		6334	8.33	12.7	61.3	39.4	99.8	9.72	3.7
Post-Converter vs Remote TBI	M.tb lysate	12425	10.6	39.8	77.5	5.41	3.74	78.1	99.7
		12412	0.16	3.33	57.4	68.4	100	90.5	86.7
		12426	1.1	3.12	40.8	37.3	98.1	91	4.72
		12417	14.1	14.5	47.3	41	98.4	19	9.51
	CFP-10/ESAT-6	3651	0	9.87	33.5	0.86	0	100	11.2
Remote TBI vs Pre-Reverter	CFP-10/ESAT-6	3718	0.51	48	85.2	0.51	3.57	100	0.51
		3725	0	12.4	42.7	21	0	99.3	4.87
		3714	0.43	13.7	62.4	11.1	1.28	100	95.3
		3711	2.8	7.48	86.9	23.4	100	94.9	67.3
		3707	0.43	6.01	70.4	0	100	100	91.8
		3717	0.33	1	60.5	58.5	100	100	99
		3719	1.05	5.26	65.8	0	100	90	17.4
	M.tb lysate	9813	0.37	41.4	66	10.1	0.84	100	1.96
		9820	11.2	36.7	78.2	7.2	4.03	79.1	96.8
		9823	4.1	5.98	40	41	98.3	70.8	10.8
Pre vs Post- Reverter	CFP-10/ESAT-6	932	12.5	55	86.2	9.17	2.92	99.6	10.8
Post-reverters vs Non-Converter	M.tb lysate	2662	84.8	98.9	98.9	0.56	0	100	3.37
		2691	0.44	7.52	54.3	32.3	99.3	95.1	82.5

Numbers denote expression of each memory and functional marker as percentage (%) of total cells in the CITRUS cluster. Markers expressed in less than 35% and more than 65% of total cells denoted in **blue** and **red**, respectively, were used to define the manual gating booleans applied on all participants.

frontiers in Immunology

ORIGINAL RESEARCH
published: 01 March 2018
doi: 10.3389/fimmu.2018.00324

Functional, Antigen-Specific Stem Cell Memory (T_{SCM}) CD4$^+$ T Cells Are Induced by Human *Mycobacterium tuberculosis* Infection

Cheleka A. M. Mpande†, One B. Dintwe†, Munyaradzi Musvosvi, Simbarashe Mabwe, Nicole Bilek, Mark Hatherill, Elisa Nemes†, Thomas J. Scriba† and The SATVI Clinical Immunology Team*

South African Tuberculosis Vaccine Initiative, Institute of Infectious Disease and Molecular Medicine, Division of Immunology, Department of Pathology, University of Cape Town, Cape Town, South Africa

OPEN ACCESS

Edited by:
Jesús Gonzalo-Asensio, University of Zaragoza, Spain

Reviewed by:
Enrico Lugli, National Institutes of Health (NIH), United States
Ian Orme, Colorado State University, United States

***Correspondence:**
Thomas J. Scriba
thomas.scriba@uct.ac.za

†These authors have contributed equally to this work.

Specialty section:
This article was submitted to Microbial Immunology, a section of the journal Frontiers in Immunology

Received: *21 December 2017*
Accepted: *06 February 2018*
Published: *01 March 2018*

Citation:
Mpande CAM, Dintwe OB, Musvosvi M, Mabwe S, Bilek N, Hatherill M, Nemes E, Scriba TJ and The SATVI Clinical Immunology Team (2018) Functional, Antigen-Specific Stem Cell Memory (T_{SCM}) CD4$^+$ T Cells Are Induced by Human Mycobacterium tuberculosis Infection. Front. Immunol. 9:324. doi: 10.3389/fimmu.2018.00324

Background: Maintenance of long-lasting immunity is thought to depend on stem cell memory T cells (T_{SCM}), which have superior self-renewing capacity, longevity and proliferative potential compared with central memory (T_{CM}) or effector (T_{EFF}) T cells. Our knowledge of T_{SCM} derives primarily from studies of virus-specific CD8$^+$ T_{SCM}. We aimed to determine if infection with *Mycobacterium tuberculosis* (*M. tb*), the etiological agent of tuberculosis, generates antigen-specific CD4$^+$ T_{SCM} and to characterize their functional ontology.

Methods: We studied T cell responses to natural *M. tb* infection in a longitudinal adolescent cohort of recent QuantiFERON-TB Gold (QFT) converters and three cross-sectional QFT$^+$ adult cohorts; and to bacillus Calmette–Guerin (BCG) vaccination in infants. *M. tb* and/or BCG-specific CD4 T cells were detected by flow cytometry using major histocompatibility complex class II tetramers bearing Ag85, CFP-10, or ESAT-6 peptides, or by intracellular cytokine staining. Transcriptomic analyses of *M. tb*-specific tetramer$^+$ CD4$^+$ T_{SCM} (CD45RA$^+$ CCR7$^+$ CD27$^+$) were performed by microfluidic qRT-PCR, and functional and phenotypic characteristics were confirmed by measuring expression of chemokine receptors, cytotoxic molecules and cytokines using flow cytometry.

Results: *M. tb*-specific T_{SCM} were not detected in QFT-negative persons. After QFT conversion frequencies of T_{SCM} increased to measurable levels and remained detectable thereafter, suggesting that primary *M. tb* infection induces T_{SCM} cells. Gene expression (GE) profiling of tetramer$^+$ T_{SCM} showed that these cells were distinct from bulk CD4$^+$ naïve T cells (T_N) and shared features of bulk T_{SCM} and *M. tb*-specific tetramer$^+$ T_{CM} and T_{EFF} cells. These T_{SCM} were predominantly CD95$^+$ and CXCR3$^+$, markers typical of CD8$^+$ T_{SCM}. Tetramer$^+$ T_{SCM} expressed significantly higher protein levels of CCR5, CCR6, CXCR3, granzyme A, granzyme K, and granulysin than bulk T_N and T_{SCM} cells. *M. tb*-specific T_{SCM} were also functional, producing IL-2, IFN-γ, and TNF-α upon antigen stimulation, and their frequencies correlated positively with long-term BCG-specific CD4$^+$ T cell proliferative potential after infant vaccination.

Conclusion: Human infection with *M. tb* induced distinct, antigen-specific CD4+ T_{SCM} cells endowed with effector functions, including expression of cytotoxic molecules and Th1 cytokines, and displayed chemokine receptor profiles consistent with memory Th1/17 cells. Induction of CD4+ T_{SCM} should be considered for vaccination approaches that aim to generate long-lived memory T cells against *M. tb*.

Keywords: T_{SCM}, *Mycobacterium tuberculosis*, memory T cells, QuantiFERON conversion, LTBI

INTRODUCTION

Memory T cells have been classified into subsets, according to their phenotypes, functions and homing potential (1). Antigen-specific central memory T cells (T_{CM}, CD45RA$^-$ CCR7$^+$) have been considered the main mediators of maintenance and expansion of T cell immunity, following secondary antigen exposure, due to their ability to differentiate into effector T cells (T_{EFF}, CD45RA$^-$ CCR7$^-$), as well as their increased proliferative capacity and longevity compared with T_{EFF} cells. This ontology of memory T cells has recently been revised to include a new subset termed stem cell memory T cells (T_{SCM}). T_{SCM} typically express CD45RA, CCR7, and CD27, and thus phenotypically resemble naïve T cells, but their co-expression of memory markers, such as CD95 and CXCR3, distinguish them from naïve T cells (2, 3). Functional characterization of antigen-specific T_{SCM} has predominantly focused on viral, parasitic, and tumor-specific CD8 T cells, identified by major histocompatibility complex (MHC) class I tetramers, or by non-specific and/or antigen specific stimulation (2–6). These studies showed that T_{SCM} characteristically possess excellent self-renewing capacity, longevity, proliferative capacity, relative to T_{CM} and T_{EFF}. Importantly, T_{SCM} can also differentiate into T_{CM} and/or T_{EFF} cells (2). CD8+ T_{SCM} are preferentially enriched in the absence of antigen (3), non-chronic states of infection (6) and among long-lived T cells induced by vaccination (7). CD8+ T_{SCM} were also essential for the re-establishment of Ag-specific memory responses after T cell depletion in cancer patients (8, 9). As a result, T_{SCM} T cells are considered as a potential target for vaccination against infectious diseases and T cell therapy for autoimmunity, that aim at inducing and maintaining long-lasting T cell immunity capable of replenishing all T cell memory subsets.

Animal models of tuberculosis (TB) and human studies show that CD4 T cells, and especially those that have differentiated into antigen-specific Th1 cells, are necessary for immunological control of the intracellular bacterium, *Mycobacterium tuberculosis* (*M. tb*) [reviewed in Ref. (10)]. Newborn vaccination against TB with the bacillus Calmette–Guerin (BCG) vaccine is efficacious against severe forms of TB, such as milliary and meningitic TB, in young children (11, 12). Efficacy of BCG against pulmonary disease after childhood is variable and mostly poor (13, 14). As a consequence, it has been proposed that waning of mycobacteria-specific T cell memory responses and insufficient maintenance of protective CD4+ T cells may underlie the limited durability of BCG-induced protection (15, 16).

Newborn BCG vaccination induces antigen-specific T_{CM} and T_{EFF} CD4+ T cell responses (17), but the role of CD4+ T_{SCM} cells in immune responses induced by vaccination against TB, or by natural *M. tb* infection, in humans has not been explored. In fact, there is very limited knowledge about the functional capacity and persistence of CD4+ T_{SCM} that are specific for bacterial antigens. We and others have reported that a considerable proportion of cytokine-expressing or tetramer+ mycobacteria-specific CD4+ T cells, in humans, displayed a memory phenotype characteristic of naïve T cells (CD45RA+ CCR7+), and termed them naïve-like CD4+ T cells (17–22). In a clinical trial that tested boosting of mycobacteria-specific responses with the TB vaccine candidate, MVA85A, low but detectable Ag85A-specific CD45RA+ CCR7+ CD27+ naive-like CD4+ T cell responses were observed before MVA85A vaccination and frequencies of these cells remained unchanged after vaccination (23). In addition, a murine study demonstrated that BCG-induced naïve-like (CD44^{lo} CD62L^{hi}) memory cells played a role in the control of *M. tb* infection, where these cells were capable of replenishing effector (CD44^{hi} CD62L^{lo}) T cells with superior functional activity and protective potential against *M. tb* infection, compared with those originating from effector T cells (24). The characteristics of such mycobacteria-specific naïve-like CD4+ T cells are thus consistent with those of CD4+ T_{SCM} cells.

We hypothesized that *M. tb*-specific CD4+ T_{SCM} are induced by primary infection with *M. tb* in humans and aimed to determine the kinetics of their generation and to characterize gene expression (GE), homing potential and functional profiles of mycobacteria-specific CD4+ T_{SCM}. Phenotypic and functional properties of *M. tb*-specific T_{SCM} were compared with those of *M. tb*-specific T_{CM} and T_{EFF}, to determine their ontology. Our findings contribute to the current knowledge of the *M. tb*-specific T cell memory repertoire and highlight the need for a better understanding of CD4+ T_{SCM} cells in natural *M. tb* infection, TB disease and vaccine-induced immune responses.

MATERIALS AND METHODS

Study Participants

Consent forms and study protocols were approved by the Human Research Ethics Committee of the University of Cape Town (UCT HREC 126/2006, 045/2008, 179/2011, 013/2012, 753/2014). Healthy adults with a positive QuantiFERON Gold In-Tube (QFT) test (IFN-γ > 0.35 IU/mL) were recruited from the community living in the Worcester region of Western Cape, South Africa. All participants provided written informed consent. Inclusion criteria included age above 18 years, QFT-positive, HIV-seronegative, and no prior (*self-reported*) or current signs or symptoms suggestive of TB disease.

We also retrieved cryopreserved peripheral blood mononuclear cells (PBMC) from a subset of 12- to 18-year-old adolescent

participants with evidence of newly acquired *M. tb* infection, from the longitudinal Adolescent Cohort Study (25). Parents or legal guardians of adolescents provided written informed consent and adolescents provided written informed assent. New *M. tb* infection was defined as a negative Tuberculin Skin Test (TST) (induration = 0 mm) and negative QFT test (IFN-γ < 0.35 IU/mL), followed by at least three positive QFT tests 6, 12, and 18 months later and a positive TST (induration > 10 mm) at 12 months.

We also performed new analyses of existing immune response data from healthy HIV-exposed but uninfected infant participants of a recently published clinical trial [see Ref. (26) for details; http://ClinicalTrials.gov NCT01650389]. Participants of this trial received either MVA85A vaccination or placebo (Candin®, AllerMed) at birth and, if confirmed HIV-PCR negative, BCG vaccination at 8 weeks of age, after which they were followed up for 44 weeks. Analyses reported here include only infants who received placebo at birth.

Blood Processing and Stimulation for Intracellular Cytokine Staining Assay

Peripheral blood mononuclear cells from adults were isolated by density gradient centrifugation (Ficoll histopaque, Lonza) from blood collected in sodium (Na)-heparin tubes (Greiner Bio-one) or heparinized blood bags. PBMC were analyzed fresh or cryopreserved in RPMI 1640 media (RPMI, Lonza) with 10% v/v dimethyl sulfoxide (DMSO, Sigma-Aldrich) and 45% v/v fetal bovine serum (Biochrom).

Whole blood intracellular cytokine staining (WB-ICS) assays were performed as described previously (26–28). Briefly, 1 mL whole blood was either left unstimulated (negative control) or stimulated with phytohemagglutinin (at 10 μg/mL, positive control), peptide pools of Ag85B, ESAT-6, or CFP-10 (all 15mer peptides, overlapping by 10 aa at 2 μg/mL, GenScript) or BCG (≈1.2×10^6 CFU/mL, Statens Serum Institut) for 12 h or 7 days (BCG only, used at 1×10^5 CFU/mL). Thereafter, red cells were lysed and white cells fixed using FACS-Lysing solution (BD Biosciences), before cryopreservation in 10% DMSO in fetal calf serum.

Flow Cytometry

Multiparameter flow cytometry panels were designed (Table S1 in Supplementary Material) to sort memory subsets as bulk or *M. tb*-tetramer+ CD4+ T cells (panel 1, Figure S1A in Supplementary Material), measure *M. tb*-specific CD4+ T cell kinetics after *M. tb* infection (panel 2, Figure S1B in Supplementary Material), determine *M. tb*-specific CD4+ T cell chemokine receptor (panel 3, Figure S1C in Supplementary Material), cytotoxic molecule (panel 4, Figure S1D in Supplementary Material), and cytokine [panel 5, Figure S6A in Supplementary Material, see Ref. (28)] expression profiles. In addition, BCG vaccine-induced cytokine expression profiles [panel 6, see Ref. (26)] and proliferative capacity [panel 7, see Ref. (26)] of mycobacteria-specific CD4+ T cells were measured.

MHC Class II Tetramers

Major histocompatibility complex class II tetramers conjugated to PE and/or APC were kindly provided by the National Institutes of Health (NIH) tetramer core facility. To exclude detection of non-specific MHC class II tetramer binding to B cells, CD8 T cells, monocytes, and dead cells, we gated CD4+ T cells on CD8−, CD14−, CD19−, live cells by including antibodies conjugated to the same fluorochrome to these markers (collectively termed a dump channel) (Figure S1A–D in Supplementary Material). *M. tb*-tetramer+ CD4+ T cells were detected using MHC class II tetramers conjugated to the following mycobacterial peptides: Ag85 [DPB1*04:01-Ag85B$_{128–144}$ (GKAGCQTYKWETFLTSE), DRB1*03:01-Ag85A$_{56–75}$ (VPSPSMGRDIKVQFQSGGAN)], CFP-10 [DRB1*04:01-CFP-10$_{71–85}$ (EISTNIRQAGVQYSR), DRB5*01:01-CFP-10$_{51–65}$ (AQAAVVRFQEAANKQ)], and ESAT-6 [DQB1*06:02-ESAT6$_{31–45}$ (EGKQSLTKLAAAWGG)]. Non-specific tetramer staining was detected using MHC class II tetramers conjugated to human CLIP self-peptide, [DPB1*04:01-CLIP$_{81–101}$ (PVSKMRMATPLLMQA), DQB1*06:02-CLIP$_{81–101}$, DRB1*03:01-CLIP$_{81–101}$, DRB1*04:01-CLIP$_{81–101}$, and DRB5*01:01-CLIP$_{81–101}$].

Flow Cytometry Staining Protocol for Sorting (Flow Cytometry Panel 1)

Cryopreserved PBMC were thawed into medium containing DNAse (50 IU/mL, Sigma-Aldrich), washed and stained with Violet or Aqua LIVE/DEAD Fixable Dead Cell Stain (ThermoFisher Scientific). Cells were then stained with anti-CCR7 antibody at 37°C for 20 min, washed and then stained with 2 μg/mL MHC class II-CFP10 tetramers (DRB1*04:01-CFP-10$_{71–85}$, DRB5*01:01-CFP-10$_{51–65}$) at room temperature (RT) for 1 h. Cells were washed and stained with surface marker antibodies, according to Table S1 in Supplementary Material, for 40 min at RT in a total volume of 100 μL. Samples were acquired and sorted on a BD Bioscience FACS Aria I sorter using FACS DIVA software (Version 6).

Flow Cytometry Staining Protocol for PBMC (Panels 2–4)

Chemokine Receptor Staining

Cryopreserved or fresh PBMC were stained with antibodies to chemokine receptors (Table S1 in Supplementary Material) for 30 min at 37°C.

MHC Class II Tetramers Staining

During optimization experiments we noted that MHC class II tetramer staining of some samples yielded artifactual labeling which appeared to be fluorochrome-dependent. As a consequence, when necessary, PBMC were stained with two preparations of the identical tetramer, one conjugated to PE and the other to APC. This identified PE and APC double-positive cells, allowing rigorous identification of tetramer+ CD4+ T cells. Tetramer staining was performed using mycobacteria-specific tetramers at a concentration of 2 μg/mL per tetramer preparations for 1 h at RT.

Phenotypic Marker Staining

Peripheral blood mononuclear cells were stained with fluorescently labeled antibodies to phenotypic markers and viability dye, according to Table S1 in Supplementary Material, for 30 min at RT, before washing and fixation with 1% paraformaldehyde (Kimix).

Intracellular Cytotoxic Molecule Staining

To stain for cytotoxic molecules, PBMC were fixed and permeabilized using the BD CytoxFix/Perm (BD Biosciences) according to the manufacturer's protocol. Permeabilized PBMC were then stained with fluorescently labeled antibodies to cytotoxic molecules, according to Table S1 in Supplementary Material, for 30 min at RT. This was followed by washing and fixation. Samples were acquired on a BD Bioscience LSRFortessa using FACS DIVA software (Version 8).

Flow Cytometry Staining Protocol for Whole Blood Intracellular Cytokine (WB-ICS) Assay (Panels 5–7)

Cryopreserved, fixed cells from the whole blood stimulation were thawed, permeabilized using Perm/Wash Solution (BD Biosciences), washed and stained with anti-CCR7 at 37°C for 20 min, followed by addition of the remaining antibodies, and staining on ice for 40 min.

High Throughput Microfluidic RT-qPCR on Sorted T Cells

Thirty cells (MHC class II tetramer+ or bulk CD4+ T cells from each memory subset) were sorted into PCR tubes containing 5 µL CellsDirect 2× reaction mix, 0.5 µL SuperScript™ III RT/Platinum® Taq mix, 2.5 µL of pooled TaqMan GE primer-probe assays (at a concentration of 0.2× per assay), and 1 µL TE buffer (10 mM Tris, pH 8.0, and 0.1 mM EDTA). Selection of TaqMan assays was based on published literature of transcriptional profiles of T cell memory subsets (Table S2 in Supplementary Material). The amplification efficiency of each TaqMan GE assay was assessed as previously described (29) and found to be close to 100% (±10%, data not shown). Specific transcript amplification (STA) was performed using the following thermal profile: 20 min at 50°C to lyse cells and perform cDNA synthesis, followed by 2 min at 95°C, then 18 cycles of 95°C for 15 s and 60°C for 4 min. STA-cDNA samples were diluted fivefold and loaded onto a 96.96 Dynamic Array chip (Fluidigm) with TaqMan GE assays for qPCR using a BioMark HD System (Fluidigm) according to the manufacturer's protocol.

Data Analysis

Flow cytometry data was analyzed using FlowJo (Tree Star) versions v9.7 to v10.1r.1, Pestle version 1.8, and SPICE version 5.2–5.3 (30).

Threshold cycle (Ct) values were determined by the BioMark Real-time PCR Analysis software using linear derivative background correction and an amplification curve quality threshold of 0.65. We excluded data from sorted CD4+ T cells with undetectable levels (i.e., Ct = 40) of *CD4* and/or *B2M* from our analyses. For ease of interpretation, Ct values were transformed to Et values (40 − Ct), because a higher Et value indicates higher mRNA levels. Relative mRNA transcript levels (delta Et) in tetramer+ CD4+ T cells were derived by subtracting the B2M Et value from the Et values of the genes of interest, and average delta Et values were calculated from duplicate STA-cDNA samples.

The lower detection limit for tetramer+ CD4 T cells measured by flow cytometry panels 2–4 (0.0021% of CD4+ T cells) was calculated as the median frequency of negative control tetramer+ CD4 T cells plus the 95% confidence interval of the median absolute deviation of negative control tetramer proportions. In addition, frequencies of tetramer+ CD4+ T cells had to be at least fivefold higher than frequencies of the corresponding control tetramer+ CD4+ T cells. Chemokine and cytotoxic molecule expression profiles were assessed for cell subsets comprising 20 or more cells (e.g., tetramer+ T_{CM} or T_{EFF} cells).

Antigen-specific cytokine+ cells expressing a T_{SCM} (CD45RA+ CCR7+) phenotype detected in the WB-ICS assay (panel 5) were typically very infrequent, and in some donors less than 10 cells of this subset were detected per sample upon background subtraction. As a result, we did not perform in-depth cytokine co-expression or Boolean analyses, and we report frequencies of CD4+ T_{SCM} cells that express IFN-γ, TNF-α, and IL-2 in unstimulated and antigen-stimulated samples.

Statistical analyses were performed using GraphPad Prism v6/7, R version 3.0.1 or SPICE version 5.2–5.3 (30). Specific statistical analyses are clearly defined where applicable. Differences in mRNA transcript expression between CD4+ T cell populations were computed using the Kruskal–Wallis or Mann–Whitney tests at a *p*-value threshold of 0.05 and a false discovery rate (FDR) threshold of 0.05 [Benjamini–Hochberg method (31)]. Principal component analysis (PCA) plots and heat maps were generated using the prcomp and heatmap.2 functions in R. Differences in protein expression were computed using Kruskal–Wallis or Mann–Whitney tests. The Bonferroni and Benjamini–Hochberg (FDR < 0.05) methods were used to correct for multiple comp-arisons for up to four comparisons or more than four comparisons, respectively. Differences in pie charts depicting chemokine receptor and cytotoxic molecule co-expression profiles were calculated using non-parametric permutation test comparing the overall distribution between subset proportions using SPICE (30).

RESULTS

CD45RA+ CCR7+ CD27+*M. tb*-Tetramer+ CD4 T Cells Are Not Naïve CD4 T Cells

We previously observed mycobacteria-specific CD4+ T cells that expressed a CD45RA+ CCR7+ naïve phenotype but exhibited features not consistent with T_N, which we termed "naïve-like" CD4+ T cells. In four studies, we showed that these "naïve-like" CD4+ T cells expressed Th1 cytokines (17–20), functions characteristic of antigen-experienced T cells. Also, in another study (23), we detected "naïve-like" CD4+ T cells by MHC class II tetramer staining at frequencies that exceeded those typical of T_N, at 1–5 cells/million CD4 T cells (32–34). We hypothesized that such mycobacteria-specific naïve-like CD4+ T cells are T_{SCM} cells and performed GE profiling of sorted CFP10-specific tetramer+ CD4 T cells that displayed such a naive memory phenotype (CD45RA+ CCR7+ CD27+, naïve-like memory cells, T_{NLM}) from seven healthy, *M. tb*-infected donors with HLA alleles that corresponded to our tetramer reagents. Refer to Supplementary

Information for the rationale for using MHC class II tetramers. We also sorted and profiled GE of tetramer+ T_{CM} (CD45RA− CCR7+ CD27+) and T_{EFF} (CD45RA− CCR7−) CD4 T cells as well as bulk naïve, T_{SCM}, T_{CM} and T_{EFF} CD4 T cells (Figure S1A in Supplementary Material). Because less than 50% of the tetramer+ T_{NLM} CD4 T cells expressed CD95, as also shown previously (23), we focused on CD95- tetramer+ T_{NLM} cells. One participant did not have detectable tetramer+ T_{NLM} CD4 T cells.

Twenty-two mRNA transcripts were differentially expressed between the bulk (not *M. tb*-specific) T_N, T_{SCM}, T_{CM}, and T_{EFF} CD4+ T cell subsets at a *p*-value of <0.05 and FDR of ≤0.05 (data not shown). These bulk memory subsets could readily be distinguished from each other by PCA (**Figure 1A**) of these 22 transcripts. When the component loadings from principal components 1 and 2 were applied to the *M. tb*-specific tetramer+ cell subset data, CFP10-tetramer+ T_{NLM} cells clustered with bulk CD4+ T_{SCM} cells and were distinct from bulk CD4+ T_N cells (**Figure 1A**). Unsupervised hierarchical clustering based on expression of these 22 transcripts also showed that CFP10-tetramer+ T_{NLM} cells clustered with bulk CD4+ T_{SCM} cells, and expressed transcripts associated with antigen-experienced cells, such as TNF-α, IFN-γ, perforin, granulysin, granzyme A and K, CCL5 (RANTES), CCR4, and CCR5. By contrast, bulk CD4+ T_N cells did not express these transcripts and formed a discrete cluster (**Figure 1B**).

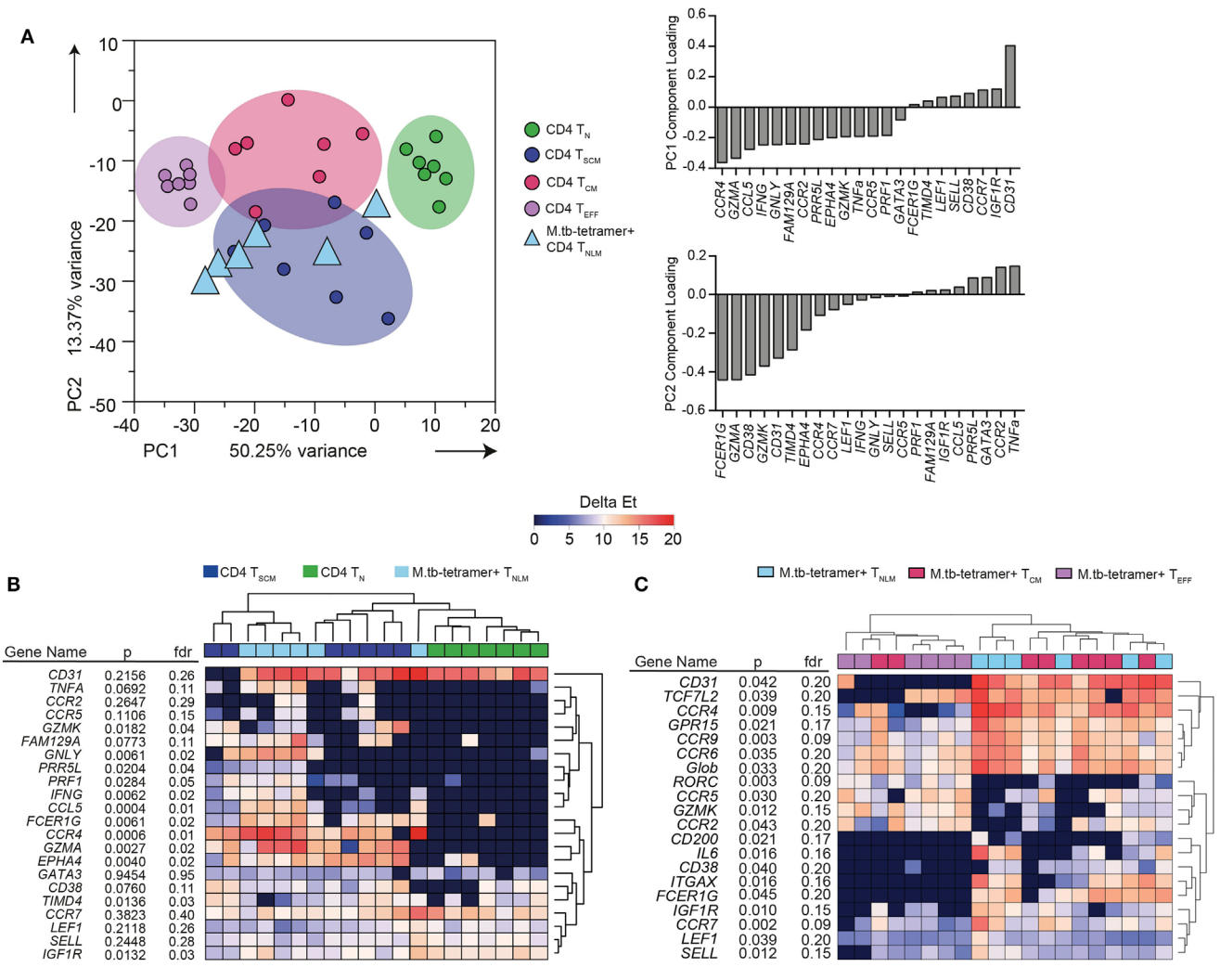

FIGURE 1 | Transcriptional profile of *Mycobacterium tuberculosis* (*M. tb*)-specific T_{SCM}. Expression of 96 genes was measured by microfluidic qRT-PCR on bulk or *M. tb*-tetramer+ CD4+ T cells expressing a naïve (T_N, CD45RA+ CCR7+ CD27+ CD95−, labeled as naïve-like memory T_{NLM} for *M. tb*-tetramer+), T_{SCM} (CD45RA+ CCR7+ CD27+ CD95+, bulk CD4+ cells only), T_{CM} (CD45RA− CCR7+ CD27+), or T_{EFF} (CD45RA− CCR7−) phenotype, sorted from *M. tb*-infected adults ($n = 7$). Analyses shown in this figure were built on transcripts (22 mRNA) that were differentially expressed [Kruskal–Wallis *H* test $p < 0.05$ and false discovery rate (FDR) < 0.05] between bulk CD4+ T_N, T_{SCM}, T_{CM}, and T_{EFF} cells. **(A)** Principal component analysis (PCA) of sorted bulk T_N (green), T_{SCM} (indigo), T_{CM} (magenta), and T_{EFF} (purple). PCA loadings—PC1 and PC2—defined on bulk CD4+ subsets were applied to *M. tb*-tetramer+ T_{NLM} (light blue triangles) CD4+ T cells. **(B)** Unsupervised heat map of 22 transcripts differentially expressed between bulk T_N, T_{SCM}, T_{CM}, and T_{EFF} subsets. Bulk T_N, T_{SCM}, and *M. tb*-tetramer+ T_{NLM} represented as green, indigo, and light blue, respectively. Gene expression (GE) is reported as delta Et values [40 − threshold cycle (Ct) values]. **(C)** Supervised heat map of 20 transcripts differentially expressed (Kruskal–Wallis *H* test $p < 0.05$ and FDR < 0.2) between *M. tb*-tetramer+ T_{NLM} (light blue), T_{CM} (magenta), and T_{EFF} (purple) CD4 T cell subsets. GE is reported as delta Et values (40 − Ct values).

Next, we determined whether CFP10-tetramer+ T_{NLM} exhibited a transcriptional profile distinct from *M. tb*-specific tetramer+ CD4+ T_{CM} and T_{EFF} memory subsets. We compared the mRNA expression between the three *M. tb*-specific tetramer+ CD4+ T cell subsets and selected 20 mRNA transcripts ($p < 0.05$ and FDR ≤ 0.2) for cluster analysis (**Figure 1C**). Unsupervised hierarchical clustering (**Figure 1C**) and PCA analysis (Figure S2 in Supplementary Material) revealed substantial overlap in GE between the CFP10-tetramer+ cell subsets, although CFP10-tetramer+ T_{NLM} appeared to cluster more closely with T_{CM} cells than T_{EFF} cells.

Since the GE profiles of *M. tb*-specific CD4+ cells with a naïve phenotype (CD45RA+ CCR7+ CD27+) were distinct from T_N cells and consistent with antigen-experienced, bulk T_{SCM}, we concluded that these cells are *M. tb*-specific CD4+ T_{SCM} cells.

M. tb-Specific T_{SCM} Cells Are Induced by Primary *M. tb* Infection

We next determined whether antigen-specific CD4+ T_{SCM} cells are induced during primary *M. tb* infection. We retrieved stored PBMC collected from adolescents before and after *M. tb* infection, as determined by negative QFT and TST tests, with subsequent test conversion at 6- and 12-month intervals, respectively (**Figure 2A**). To track *M. tb*-specific CD4 T cells during acquisition of *M. tb* infection, we utilized MHC class II tetramers loaded with peptides of the *M. tb* complex-specific antigens, CFP-10 and ESAT-6. Dual staining with PE and APC-conjugated tetramers improved staining specificity (**Figure 2B**; Figure S3A in Supplementary Material). Frequencies of *M. tb*-tetramer+ CD4+ T cells were below the limit of reliable detection before *M. tb* infection in 11 out of 12 participants and increased significantly upon QFT conversion 6 months later, when this response also peaked. Thereafter, frequencies of *M. tb*-tetramer+ CD4+ T cells decreased but were maintained at detectable levels throughout established *M. tb* infection, at months 12 and 18 (Figure S3B in Supplementary Material).

Frequencies of *M. tb*-specific tetramer+ T_{SCM} (CD45RA+ CCR7+ CD27+), T_{CM} (CD45RA− CCR7+), and T_{EFF} (CD45RA− CCR7−) were below the limit for reliable detection at enrollment (month 0), demonstrating that circulating *M. tb*-specific T_N are too rare to detect by direct *ex vivo* tetramer staining (**Figures 2C–D**). After *M. tb* infection all three *M. tb*-specific memory subsets increased to detectable levels and remained detectable throughout established infection (**Figure 2D**). Interestingly, frequencies of *M. tb*-specific T_{SCM} and T_{CM} remained relatively consistent throughout primary and established *M. tb* infection, while *M. tb*-specific T_{EFF} peaked during the primary *M. tb* infection phase (month 6) and thereafter steadily decreased (**Figure 2D**). These data suggest that *M. tb*-specific T_{SCM} are induced by *M. tb* infection and maintained at low but consistent levels in the peripheral blood once *M. tb* infection has been established.

M. tb-Specific T_{SCM} Express Chemokine Receptor and Cytotoxic Profiles Distinct from Bulk T_N and T_{SCM} CD4 T Cells

Our transcriptomic analysis showed that bulk CD4+ T_{SCM} and *M. tb*-specific T_{SCM} cells expressed chemokine receptor and cytotoxic molecule transcripts, which were mostly undetectable in bulk T_N cells (**Figure 1B**). Chemokine receptors mediate tissue homing and allow classification of memory CD4 cells into Th1, Th2, and Th17 lineages (35–37). Expression of cytotoxic mediators by CD4+ T cells indicates highly differentiated cells typically associated with high antigen exposure and effector T cell properties (38). We sought to validate our transcriptomic findings by measuring protein expression in an independent cohort of *M. tb*-infected (QFT+) adults. Expression of CCR4, CCR5, CCR6, and CXCR3 and cytotoxic molecules granzyme A, B, and K, granulysin, and perforin by *M. tb*-specific T_{SCM} (CD45RA+ CCR7+ CD27+) cells was compared with bulk T_N (CD45RA+ CCR7+ CD27+ CD95−) and T_{SCM} (CD45RA+ CCR7+ CD27+ CD95+) cells (**Figure 3**; Figures S1C,D in Supplementary Material).

Virtually, all *M. tb*-tetramer+ CD4+ cells expressed CXCR3 (median and IQR: 96.2 and 86.2–97.8%), with relatively high proportions also expressing CCR5 and CCR6 (**Figure 3A**). A very small proportion of tetramer+ CD4 T cells expressed CCR4 (**Figure 3A**). By contrast, expression of these chemokine receptors was negligible or not detected on bulk T_N as expected of naïve cells (**Figure 3B**), while CXCR3, CCR6, and CCR5 were expressed by a small proportion of bulk T_{SCM} (**Figure 3B**). Co-expression of these chemokine receptors by bulk T_{SCM} and *M. tb*-specific T_{SCM} revealed interesting patterns. Bulk T_{SCM} cells mostly expressed only a single chemokine receptor, whereas *M. tb*-specific T_{SCM} displayed more diverse co-expression profiles with single (CXCR3+), double (CCR5+ CXCR3+ or CCR6+ CXCR3+) and a small proportion of triple (CCR5+ CCR6+ CXCR3+) positive cells (**Figure 3C**). Importantly, a small subset of *M. tb*-specific T_{SCM} and >50% of bulk T_{SCM} did not express any of the chemokine receptors (**Figure 3C**), a profile suggesting early T cell differentiation (36). Virtually, all *M. tb*-specific CD4 T_{SCM} cells expressed CXCR3, while CD95, a typical marker of CD8 T_{SCM} cells (4, 39), was expressed by approximately 75% of tetramer+ CD4+ T_{SCM} cells (**Figure 3C**)—refer to Supplementary Material for factors that affected CD95 expression in our experiments (Figure S4 in Supplementary Material).

Approximately 40% (range: 4.38–86.9%) of *M. tb*-tetramer+ CD4 T cells expressed granzyme A and/or K. Very few *M. tb*-tetramer+ CD4 T cells expressed granzyme B, granulysin, or perforin (**Figure 3D**). Interestingly, about a quarter of *M. tb*-specific CD4+ T_{SCM} expressed cytotoxic molecules, also dominated by granzyme A and K. These were generally not co-expressed by *M. tb*-specific CD4+ T_{SCM}. By contrast, bulk T_{SCM} expressed very low levels of cytotoxic molecules (**Figures 3E,F**).

Increased expression of some chemokine receptors and cytotoxic molecules by *M. tb*-specific T_{SCM} compared with bulk T_{SCM} suggested that *M. tb*-specific T_{SCM} are more phenotypically differentiated than bulk T_{SCM}. We thus also compared chemokine receptor and cytotoxic molecule expression patterns by *M. tb*-specific T_{SCM} with bulk T_{CM} (CD45RA− CCR7+ CD27+) and T_{EFF} (CD45RA− CCR7−CD27−) cells (Figures S5A,B in Supplementary Material). *M. tb*-specific T_{SCM} expressed higher levels of CXCR3 than both bulk T_{CM} and T_{EFF} cells, further supporting their T_{SCM} identity. Surprisingly, *M. tb*-specific T_{SCM} had similar expression levels of CCR5 and CCR6 to bulk T_{EFF} cells, but significantly lower expression of CCR4 than bulk T_{CM} or T_{EFF} cells (Figure S5A in Supplementary Material).

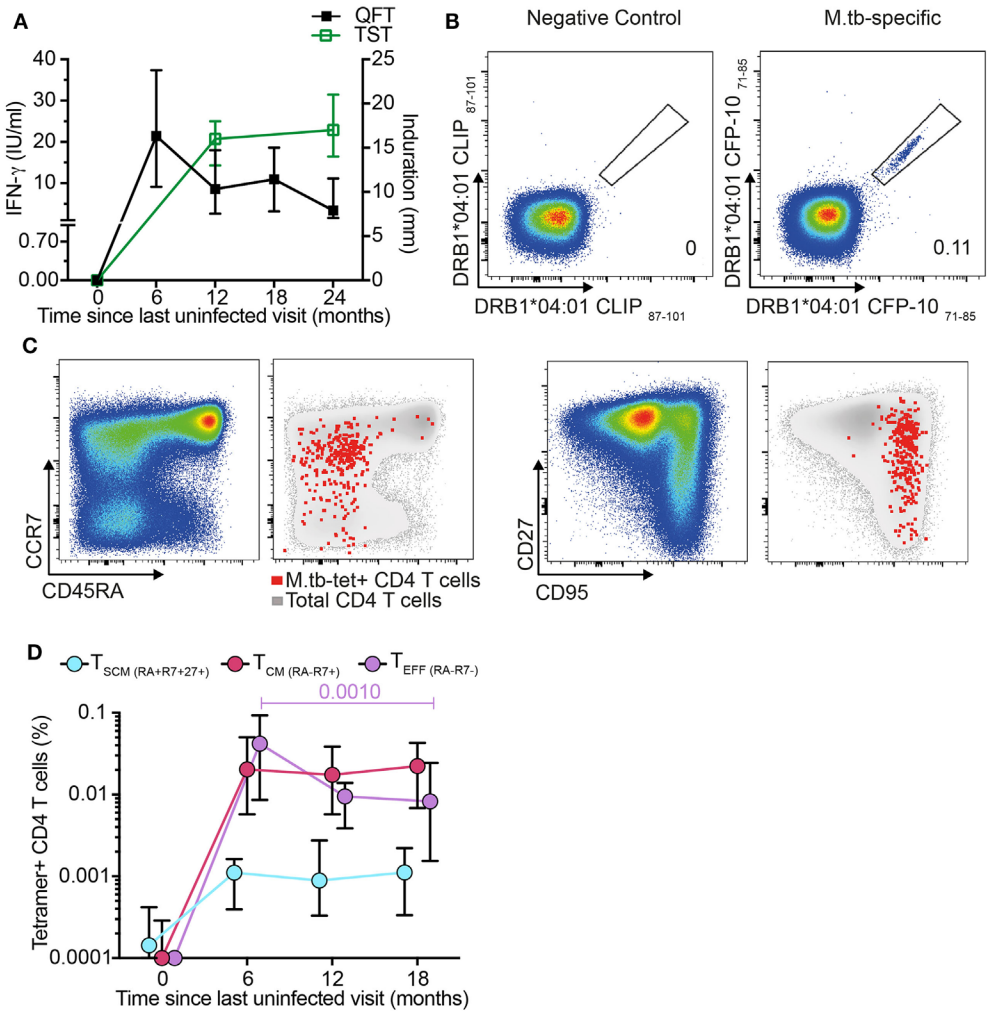

FIGURE 2 | *Mycobacterium tuberculosis* (*M. tb*)-specific T_{SCM} are detected in recently *M. tb*-infected adolescents. **(A)** Median (error bars denote IQR) of Tuberculin Skin Test (TST) and QuantiFERON-TB Gold In-Tube (QFT) performed at the indicated time points. A 5 mm and 0.35 IU/ml cutoff were used to define positive TST and QFT, respectively (n = 19 participants). **(B)** Representative flow cytometry plots showing peripheral blood mononuclear cells staining with two identical major histocompatibility complex (MHC) class II tetramers conjugated to PE and APC to detect CD4+ T cells specific for CFP-10. Tetramers matched by MHC allele but loaded with a self-peptide were used as negative control. Number indicates percentage of tetramer+ CD4 T cells. **(C)** Representative flow cytometry plots for memory markers CD45RA, CCR7, CD27, and CD95 gated on bulk (pseudo-color and gray) and *M. tb*-specific CD4+ T cells (red dots). **(D)** Median (error bars denote IQR) frequencies of *M. tb*-specific T_{SCM} (CD45RA+ CCR7+ CD27+, light blue), T_{CM} (CD45RA− CCR7+, magenta), and T_{EFF} (CD45RA− CCR7−, purple) during primary *M. tb* infection (n = 12 participants).

M. tb-specific T_{SCM} also expressed significantly higher levels of granzyme A and K than bulk T_{CM} (Figure S5B in Supplementary Material). However, T_{SCM} expressed lower levels of all cytotoxic molecules except granzyme K than bulk T_{EFF} cells. These data further support the finding that *M. tb*-specific T_{SCM} cells are antigen-experienced memory cells with unique phenotypic and functional attributes that distinguish them from bulk T_{SCM} cells, and are more similar to highly differentiated bulk T_{CM} and T_{EFF} cells.

M. tb-Specific CD4 T_{SCM} Are Less Differentiated than *M. tb*-Specific T_{CM} and T_{EFF} CD4 T Cells

We then compared the expression of chemokine receptors and cytotoxic molecules between *M. tb*-specific tetramer+ CD4+ T_{SCM} cells and the other tetramer+ CD4+ T cell memory subsets. Virtually all cells among the three *M. tb*-specific memory subsets expressed CXCR3, as has been previously reported for *M. tb*-specific CD4+ T cells, although T_{CM} displayed the highest proportion of CXCR3+ cells, compared with *M. tb*-specific T_{SCM} and T_{EFF} cells (**Figure 4A**). A significantly lower proportion of *M. tb*-specific T_{SCM} expressed CCR6 than either *M. tb*-specific T_{CM} or T_{EFF} cells, while a minority of *M. tb*-specific T_{SCM} and T_{CM} expressed CCR5 or CCR4. As expected, virtually all *M. tb*-specific T_{EFF} cells were CCR5+ and CCR4−. An increase from single to triple chemokine receptor co-expression profiles was observed when *M. tb* memory cells were ordered according to their expected differentiation sequence, from T_{SCM} to T_{CM} to T_{EFF} cells (**Figure 4B**; Figure S5A in Supplementary Material).

This was also observed when expression of the cytotoxic molecules granzyme A and K was assessed. Proportions of *M. tb*-specific T_{SCM} cells expressing granzyme A and/or K were lower than T_{CM} expressing these cytotoxic molecules, which in turn were lower than *M. tb*-specific T_{EFF} cells (**Figure 4C**). Proportions of *M. tb*-specific T_{EFF} expressing both granzyme A and K were also higher than those observed in *M. tb*-specific T_{CM} and T_{SCM} CD4+ T cells (**Figure 4D**; Figure S5B in Supplementary Material).

Taken together, these data show that *M. tb*-specific T_{SCM} possess the least differentiated *M. tb*-specific phenotypic and functional profile, and suggest that *M. tb*-specific T_{CM} cells appear as an intermediate subset before cells differentiate into *M. tb*-specific T_{EFF} CD4+ T cells.

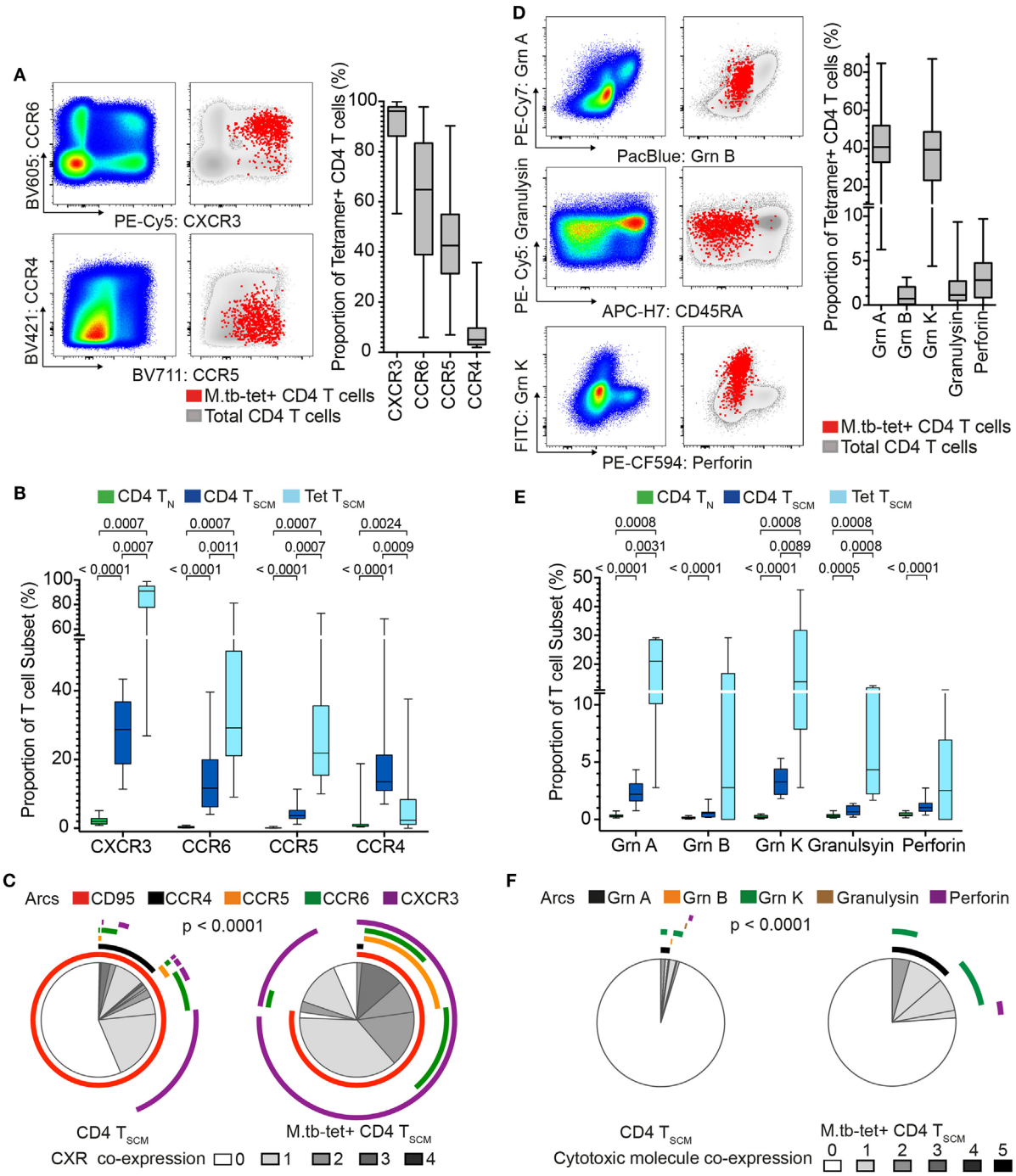

FIGURE 3 | Continued

FIGURE 3 | *Mycobacterium tuberculosis* (*M. tb*)-specific T_{SCM} are not T_N and express distinct homing and cytotoxic profiles from bulk T_{SCM}. Expression of chemokine receptors and cytotoxic molecules was measured in remotely *M. tb*-infected (QFT+) adults (n = 28) when at least 20 events were detected in each tetramer+ memory subset. **(A)** Representative flow cytometry plots of chemokine receptor expression on bulk (pseudo-color and gray) and *M. tb*-specific (red dots) CD4+ T cells. Box and whisker plots represent the median proportion, IQR, and range of expression of chemokine receptor (n = 28). **(B)** Box and whisker plot depicting the proportion of chemokine receptor-expressing bulk T_N (CD45RA+ CCR7+ CD27+ CD95−, n = 28, green), T_{SCM} (CD45RA+ CCR7+ CD27+ CD95+, n = 28, blue), and *M. tb*-specific T_{SCM} (CD45RA+ CCR7+ CD27+, n = 15, light blue) CD4+ T cells. p-Values were calculated using Wilcoxon signed-rank test and corrected for multiple comparison using the Benjamini–Hochberg method with an false discovery rate (FDR) of 0.05. Adjusted p-values <0.05 were considered significant. **(C)** Pie chart showing the median proportions (slices) of bulk T_{SCM} (n = 28) and *M. tb*-specific T_{SCM} (n = 15) CD4+ T cells co-expression of CD95, CCR4, CCR5, CCR6, and/or CXCR3, denoted by arcs. p-Value was calculated using non-parametric permutation test comparing the overall distribution between pies. **(D)** Representative flow cytometry plots of cytotoxic molecule expression on total (pseudo-color and gray) and *M. tb*-specific (red dots) CD4+ T cells. Box and whisker plots represent the median proportion, IQR, and range of expression of cytotoxic molecules (n = 20). **(E)** Proportion of granzyme (grn) A, grnB, grnK, granulysin, and perforin expression in bulk T_N (n = 20, green), T_{SCM} (n = 20, blue), and *M. tb*-specific T_{SCM} (n = 5, light blue) CD4+ T cells. p-Values were calculated with the Mann–Whitney test, corrected for multiple comparisons with the Benjamini–Hochberg method with an FDR of 0.05. Adjusted p-values <0.05 were considered significant. **(F)** Pie chart showing the median proportions (slices) of bulk T_{SCM} (n = 20) and *M. tb*-specific T_{SCM} (n = 5) CD4+ T cells co-expression grnA, grnB, grnK, granulysin, and/or perforin, denoted by arcs. p-Value was calculated using non-parametric permutation test comparing the overall distribution between pies.

M. tb-Specific T_{SCM} CD4 T Cells Express Th1 Cytokines

Studies of CD8+ (and CD4+) T_{SCM} have shown that T_{SCM} have limited cytokine expression capacity that is dominated by IL-2 and TNF-α in responses to non-specific stimulation (2, 3, 5). To determine if this is also true for mycobacteria-specific T_{SCM}, we re-analyzed available data from stimulated whole blood (WB-ICS, Figure S6A in Supplementary Material) from a previously published cohort of QFT+ adults (28). Significantly higher frequencies of IFN-γ, TNF-α, or IL-2 cytokine-expressing CD4 T_{SCM} cells, defined as CD45RA+ CCR7+, were detected in blood stimulated with BCG, or peptide pools spanning either Ag85B or CFP-10, compared with unstimulated blood (**Figure 5**)—refer to Supplementary Information for the justification for using CD45RA+ CCR7+ as a marker for T_{SCM} by cytokine-expressing CD4+ T cells (Figure S7 in Supplementary Material). This was, however, not observed in blood stimulated with ESAT-6.

In summary, cytokine production by mycobacteria-specific CD4+ T_{SCM} cells is not restricted to IL-2 but includes TNF-α and IFN-γ.

BCG-Specific T_{SCM} Cell Frequencies Are Associated with CD4+ T Cell Proliferative Capacity

A key feature of T_{SCM} is long-term maintenance of proliferative capacity in the absence of antigenic stimulation (2). To determine whether vaccine-induced CD4+ T_{SCM} contribute to T cell long-term proliferative potential, we analyzed available data from a recently completed clinical trial in infants, who received BCG vaccination (26). Frequencies of BCG-specific CD4+ T_{SCM} and T_{CM} cells, but not T_{EFF} cells, positively correlated with proliferative potential of BCG-stimulated CD4+ T cells 10 months after BCG vaccination (**Figure 6**). These results suggest that vaccine-induced T_{SCM} contribute to long-term memory and proliferative capacity of the vaccine-induced T cell response to mycobacteria.

DISCUSSION

We performed in-depth analyses of the kinetics, phenotype and functional characteristics of *M. tb*-specific CD4+ T_{SCM} cells during natural *M. tb* infection. Our data show that CD4+ T_{SCM} induced by *M. tb* infection in humans, predominantly express CD95 and CXCR3, are distinct from naïve T cells and possess phenotypic and functional profiles consistent with *M. tb*-specific CD4+ T cells at an early stage of differentiation (36). These data supplement our current knowledge of T_{SCM} cells, which has primarily been derived from studies of virus-specific CD8 T cells (2–4, 7).

CD4+ *M. tb*-specific T_{SCM} were induced during primary *M. tb* infection and maintained throughout established *M. tb* infection at low frequencies. This phenomenon is highly characteristic of the stem cell nature of long-term memory cells such as T_{CM} and potentially T_{SCM} cells, where asymmetrical cell division maintains both the overall proportions of these memory cells and the pool of more differentiated effector memory subsets (40, 41).

The transcriptomic profile of *M. tb*-specific T_{SCM} cells overlapped substantially with bulk CD4+ T_{SCM}. However, protein expression of chemokine receptors and cytotoxic molecules distinguished bulk from *M. tb*-specific T_{SCM}. Our data show that *M. tb*-specific T_{SCM} cells possess unique phenotypic and functional profiles that share more similarities with bulk T_{CM} and T_{EFF} memory cells than bulk T_{SCM} cells. This might suggest that *M. tb*-specific T_{SCM} are exposed to chronic antigen stimulation, which is probably not the case for all T_{SCM} specific for other pathogens, resulting in a more differentiated chemokine and cytotoxic molecules expression pattern. Whether this increased phenotypic differentiation profile is unique to *M. tb*-specific CD4 T_{SCM} cells requires further investigation. Consistent with published findings (21), we found that *M. tb*-specific cells were predominantly CXCR3+, a Th1 associated chemokine receptor (42). This was accompanied with relatively high CCR5 and CCR6 expression, chemokine receptors associated with activation (43) and Th1/17 T cells (44), respectively, but low expression of the Th2 associated CCR4 (42). The predominant CXCR3 expression by *M. tb*-specific T_{SCM} is suggestive of Th1 lineage, which we confirmed on a functional level by showing that mycobacteria-specific T_{SCM} not only produced, IL-2 but also TNF-α and IFN-γ and, to a lower extent, cytotoxic molecules.

Our data suggested that *M. tb*-specific T_{SCM} had different cytokine expression patterns depending on the *M. tb* antigen recognized. For example, Ag85B-specific T_{SCM} produced only

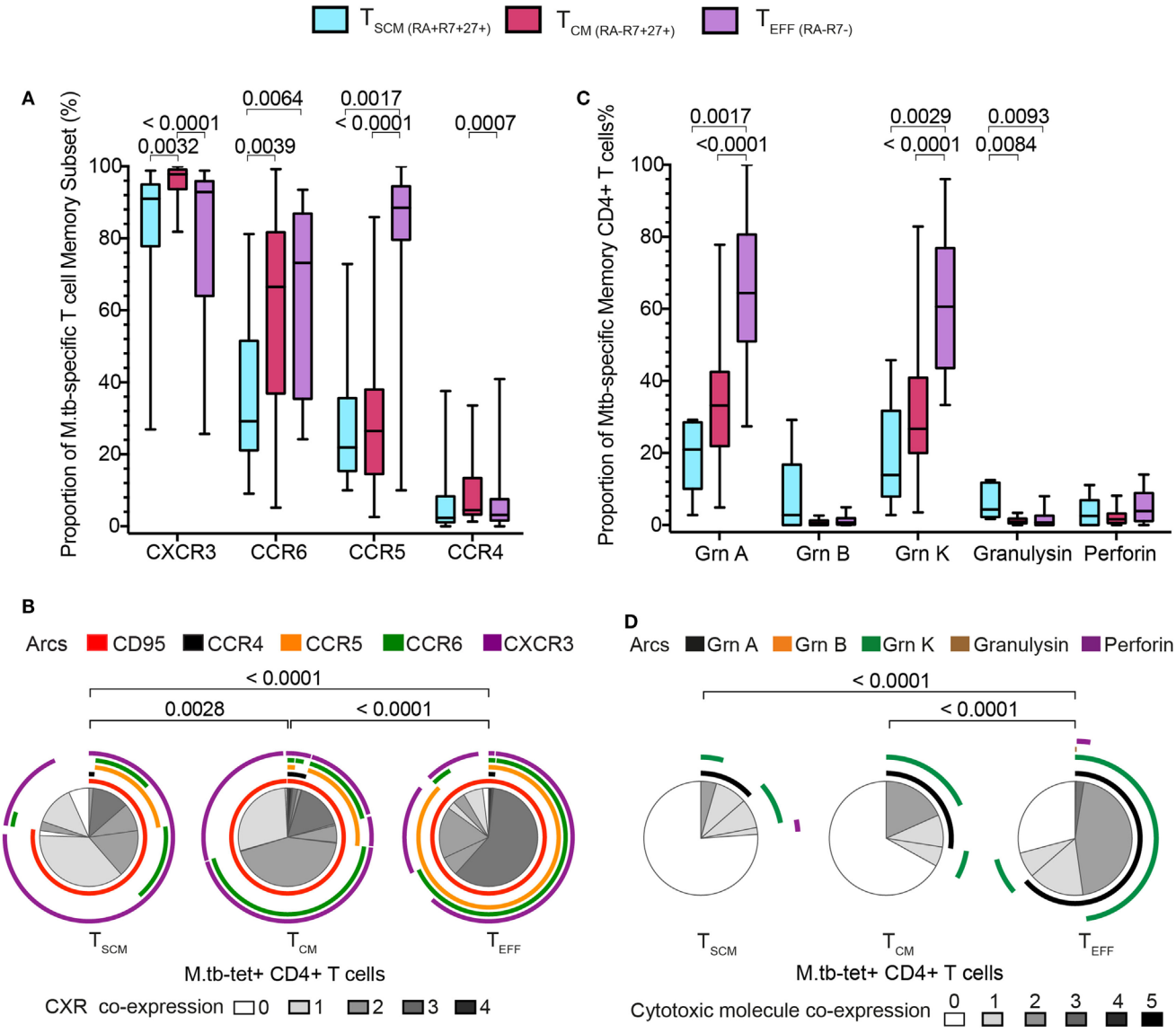

FIGURE 4 | *Mycobacterium tuberculosis* (*M. tb*)-specific T_{SCM} display early memory tissue homing and cytotoxic profiles. Expression of chemokine receptors and cytotoxic molecules was measured in remotely *M. tb*-infected (QFT+) adults (n = 28) when at least 20 events were detected in each tetramer+ memory subset. **(A)** Box and whiskers plots depicting the proportion of chemokine receptors expression of *M. tb*-specific T_{SCM} (n = 15, light blue), T_{CM} (n = 27, magenta), and T_{EFF} (n = 23, purple) CD4+ T cells. p-Values were calculated using Wilcoxon signed-rank test and corrected for multiple comparison using the Benjamini–Hochberg method with a false discovery rate (FDR) of 0.05. Adjusted p-values <0.05 were considered significant. **(B)** Pie chart showing the median proportions (slices) of *M. tb*-specific T_{SCM} (n = 15), T_{CM} (n = 27), and T_{EFF} (n = 23) CD4+ T cells co-expression of CD95, CCR4, CCR5, CCR6, and/or CXCR3, denoted by arcs. p-Values were calculated using non-parametric permutation test comparing the overall distribution between pies. **(C)** Box and whiskers plots depicting the proportion of grnA, grnB, grnK, granulysin, and perforin expression in *M. tb*-specific T_{SCM} (n = 5, light blue), T_{CM} (n = 19, magenta), and T_{EFF} (n = 17, purple) CD4+ T cells. p-Values were calculated using Mann–Whitney test and corrected for multiple comparison using the Benjamini–Hochberg method with an FDR of 0.05. Adjusted p-values <0.05 were considered significant. **(D)** Pie chart showing the median proportions (slices) of *M. tb*-specific T_{SCM} (n = 5), T_{CM} (n = 19), and T_{EFF} (n = 17) CD4+ T cells co-expression of grnA, grnB, grnK, granulysin, and/or perforin, denoted by arcs. p-Values were calculated using non-parametric permutation test comparing the overall distribution between pies.

IL-2, while BCG- and CFP-10-specific T_{SCM} produced TNF-α and IFN-γ in addition to IL-2. Despite the early stage of T cell memory differentiation of T_{SCM} these findings may reflect different degrees of antigen exposure *in vivo*. A murine study showed that Ag85B mRNA expression peaks during early stages of *M. tb* infection and significantly reduces during established infection, whereas ESAT-6 mRNA was maintained at high levels throughout these infection stages (45). We also recently showed differential degrees of T cell differentiation of Ag85B and ESAT-6-specific CD4 T cells in *M. tb*-infected mice and humans (46). Expression of only IL-2, a cytokine associated with homeostatic proliferation and early T cell differentiation, by Ag85B-specific T_{SCM} thus may

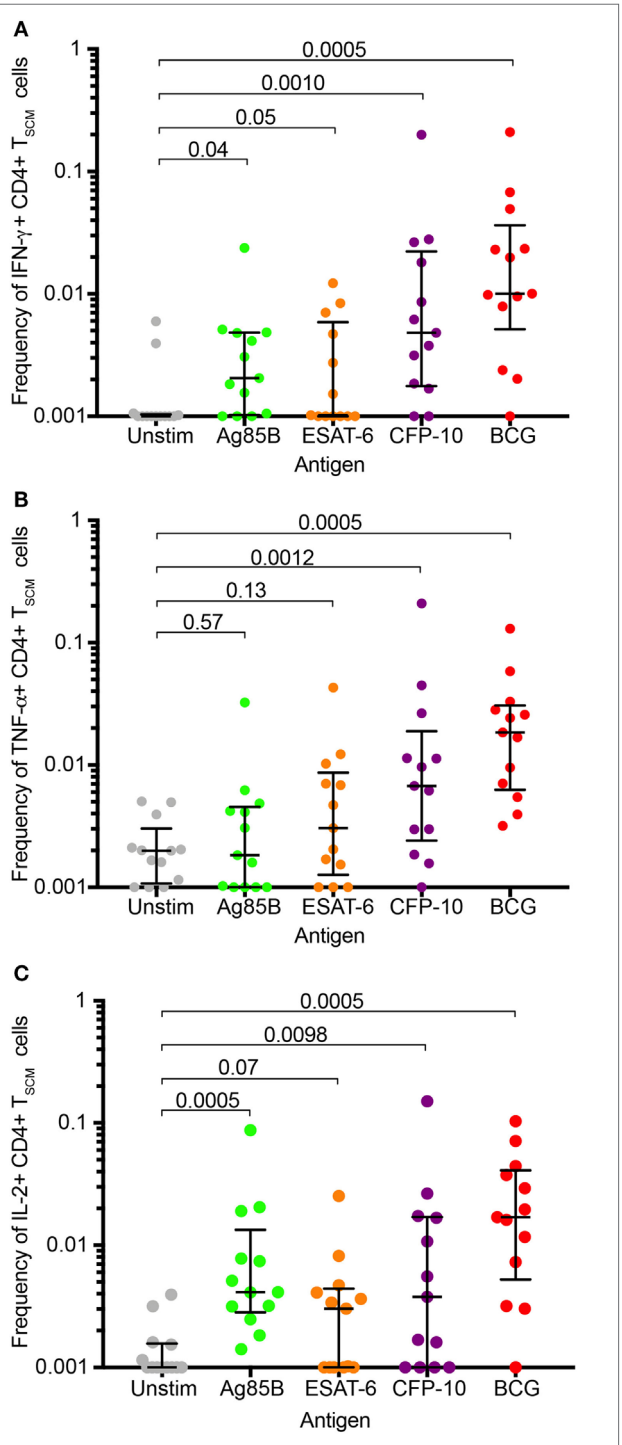

FIGURE 5 | *Mycobacterium tuberculosis* (*M. tb*)-specific T_{SCM} express Th1 cytokines. Fresh whole blood from remotely *M. tb*-infected (QFT+) adults (n = 13) was left unstimulated (gray) or stimulated with peptide pools spanning *M. tb* antigens, Ag85B (green), ESAT-6 (orange), or CFP-10 (purple), or whole bacillus Calmette–Guerin (red) for 12 h. Box and whisker plots depict frequencies of CD4+ T_{SCM} (RA+ R7+) T cells expressing IFN-γ **(A)**, TNF-α **(B)**, or IL-2+ **(C)**. p-Values were calculated using the Wilcoxon matched pairs test, and p-values <0.0125 were considered significant (corrected for multiple testing using the Bonferroni method).

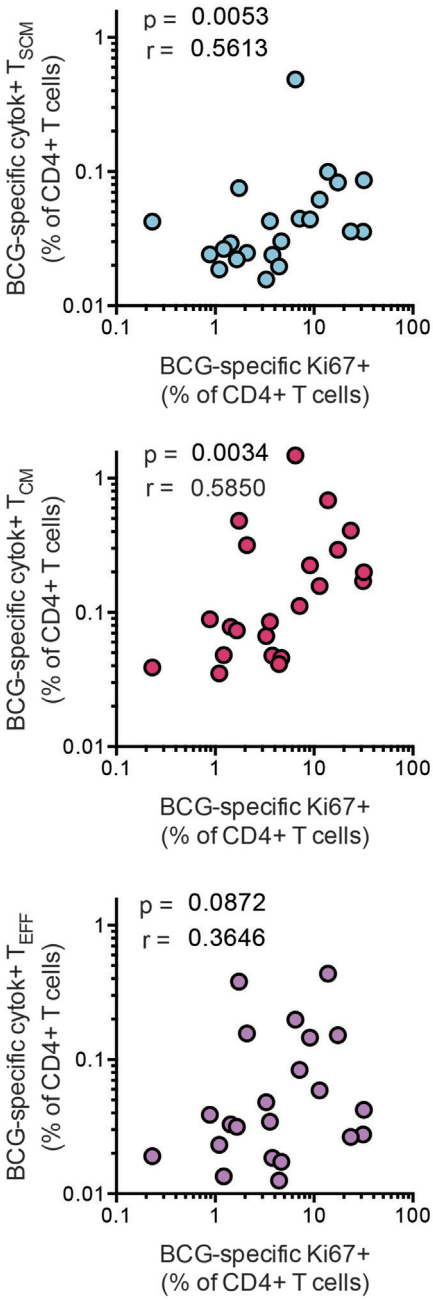

FIGURE 6 | Bacillus Calmette–Guerin (BCG)-specific T_{SCM} are associated with long-term CD4+ T cell proliferation after vaccination. Whole blood from 1-year-old infants (n = 23) was stimulated with BCG for 12 h to measure the frequencies of cytokine-producing T_{SCM} (CD45RA+, CCR7+), T_{CM} (CD45RA−, CCR7+), and T_{EFF} (CD45RA−, CCR7−). In parallel, whole blood was stimulated with BCG for 7 days, and the frequency of proliferating CD4+ cells was assessed by upregulation of Ki-67. Correlations between the frequencies of BCG-specific CD4+ memory T cell subsets and those of proliferating CD4+ T cells were calculated by Spearman test 10 months postvaccination.

reflect lower exposure of T cells to this antigen. By contrast, expression of TNF-α and IFN-γ, cytokines typically produced by more differentiated T cells, by CFP-10 and BCG-specific

T_{SCM} is consistent with higher *in vivo* recognition or exposure to these antigens (36). However, in light of the low frequencies of *M. tb*-specific T_{SCM} these data on functional profiles should be interpreted conservatively. The nature of cytokine expression by *M. tb*-specific T_{SCM} cells requires more attention in future studies. In addition, co-expression of CCR6, observed in about a third of *M. tb*-specific T_{SCM}, might indicate early polarization toward Th1/Th17 lineage, which has been described as the major CD4+ T cell subset responding to *M. tb* (21). Finally, CCR5 expression, observed in about 20% of *M. tb*-specific T_{SCM}, suggests that at least some *M. tb*-specific T_{SCM} may have the potential to migrate to sites of infection (47, 48) and are not confined to the lymphoid compartment, despite CCR7 expression.

The ability of CD4+ T cells to produce cytotoxic molecules has been associated with high antigen exposure resulting in increased MHC-antigen-T cell receptor interaction and is mostly associated with late differentiated T cells with increased effector functions (38, 49, 50). Cytotoxic CD4+ T cells have been well characterized in contexts of viral infections, where cytotoxic CD4+ T cells either utilize granzyme B and perforin or Fas–FasL interactions to mediate killing of infected cells (49, 50). Surprisingly, we found that CD4+ *M. tb*-specific T cells, including *M. tb*-specific T_{SCM} cells, predominantly expressed granzyme A and/or K. Unlike granzyme B and perforin that mediate cytotoxic killing of infected cells, granzymes A and K, have been described as pro-inflammatory and cytokine-inducing cytotoxic molecules (51–54). In fact, expression of granzyme A by γδ T cells mediated increased *M. tb* killing by macrophages (55). Thus, expression of these cytotoxic molecules by *M. tb*-specific T_{SCM}, T_{CM}, and T_{EFF}, in absence of granzyme B and perforin, may induce pro-inflammatory responses in macrophages at the site of infection, rather than mediate direct killing of *M. tb*-infected macrophages, which would require perforin to mediate entry of granzymes into infected cells.

We primarily employed MHC class II tetramers loaded with *M. tb*-epitopes to identify *M. tb*-specific CD4+ T cells directly *ex vivo* for transcriptional and phenotypic profiling (Figures S1A–D in Supplementary Material). MHC tetramers provide a method for detecting antigen-specific T cells directly *ex vivo* without the need for antigen stimulation, which can alter the function, phenotype and GE profiles of T cells. However, an important limitation to using MHC class II tetramers is that only T cells that bear the cognate TCR for a single peptide in the context of a single MHC allele can be studied. To address this, we employed several tetra-mers that allowed detection of CFP-10, ESAT-6, and Ag85-specific CD4+ T cells restricted by DRB1*0301, DRB1*0401, DRB5*0101, DPB1*0401, or DQB*0602, providing adequate coverage of the *M. tb*-specific CD4 T cell response and cohort. Another limita-tion of our study was our inability to characterize the proliferation and differentiation potential of purified *M. tb*-specific CD4+ T_{SCM} cells, because very large number of cells (approximately 500 million PBMC per participant) would be required to sort at least 1,000 *M. tb*-specific tetramer+ CD4 T_{SCM} cells. This is only achievable by leukapheresis, which was not available at our clinical site, where study visits were performed. We provided indirect evidence for this by showing that the precursor frequencies of BCG-specific T_{SCM} and T_{CM} CD4+ T cells correlated with proliferative potential of BCG-specific CD4+ T cells 10 months post infant BCG vaccination. Further studies measuring vaccine-induced T_{SCM} and long-term persistence of memory T cells are required to define the role of antigen-specific CD4+ T_{SCM} after vaccination.

In summary, we have shown that *M. tb*-specific CD4+ T_{SCM} are induced by primary *M. tb* infection and exhibit transcriptional, phenotypic and functional features that are distinct from bulk CD4+ T_N and T_{SCM} and consistent with early differentiation of *M. tb*-specific CD4+ T cells, possibly shaped by antigen exposure. Our findings have important implications in the study of the *M. tb*-specific T cell memory repertoire and raise numerous unanswered questions. For example, determining the functional role of *M. tb*-specific T_{SCM} in long-term immune responses, how their features differ between asymptomatic *M. tb* infection and TB disease, as well as during TB treatment. In addition, future work should determine whether long-lived CD4+ T_{SCM} can be induced by vaccination, and whether they are associated with long-term memory responses and protection, as observed for CD8+ T_{SCM} upon yellow fever vaccination (7) as well as in adoptive immune-therapy (4, 8, 9).

THE SATVI CLINICAL IMMUNOLOGY TEAM

Cynthia Ontong, **Elizabeth Filander**, **Fadia Alexander**, **Hadn Africa**, **Janelle Botes**, **Lebohang Makhethe**, **Lungisa Jaxa**, **Marcia Steyn**, **Noncedo Xoyana**, **Rachel Oelfose**, **Sindile Matiwane**, South African Tuberculosis Vaccine Initiative, Institute of Infectious Disease and Molecular Medicine, Division of Immunology, Department of Pathology, University of Cape Town, Cape Town, South Africa.

ETHICS STATEMENT

Consent forms and study protocols were approved by the Human Research Ethics Committee of the University of Cape Town (UCT HREC 126/2006, 045/2008, 179/2011, 013/2012, 753/2014). All adult participants provided written informed consent. Parents or legal guardians of adolescents provided written informed consent and adolescents provided written informed assent.

AUTHOR CONTRIBUTIONS

CAMM, OBD, MH, EN, and TJS contributed to conception and design of the study. CAMM and OBD performed experimental work. SM, NB, EN, and TJS contributed to execution and oversight of experimental work. CM and MM performed statistical analyses. CAMM, OBD, MM, EN, and TJS contributed to data interpretation and drafted the manuscript. All the authors read, revised, and approved the final version of the manuscript.

ACKNOWLEDGMENTS

The authors thank the volunteers for participating in this study and acknowledge the contributions of clinical research workers

at the South African Tuberculosis Vaccine Initiative. EN is an ISAC Marylou Ingram Scholar.

FUNDING

This study was funded by grants to TJS from the South African Medical Research Council and from the European Commission funded TBVAC2020 Consortium (H2020-PHC-643381). CAMM was funded by the University of Cape Town and the South African National Research Foundation. OBD and MM were funded by the Carnegie Corporation PhD Schol-arship.

SUPPLEMENTARY MATERIAL

The Supplementary Material for this article can be found online at http://www.frontiersin.org/articles/10.3389/fimmu.2018.00324/full#supplementary-material.

REFERENCES

1. Sallusto F, Lenig D, Förster R, Lipp M, Lanzavecchia A. Two subsets of memory T lymphocytes with distinct homing potentials and effector functions. *Nature* (1999) 401:708–12. doi:10.1038/44385
2. Gattinoni L, Lugli E, Ji Y, Pos Z, Paulos CM, Quigley MF, et al. A human memory T cell subset with stem cell-like properties. *Nat Med* (2011) 17: 1290–7. doi:10.1038/nm.2446
3. Lugli E, Dominguez MH, Gattinoni L, Chattopadhyay PK, Bolton DL, Song K, et al. Superior T memory stem cell persistence supports long-lived T cell memory. *J Clin Invest* (2013) 123:594–9. doi:10.1172/JCI66327
4. Gattinoni L, Speiser DE, Lichterfeld M, Bonini C. T memory stem cells in health and disease. *Nat Med* (2017) 23:18–27. doi:10.1038/nm.4241
5. Hong H, Gu Y, Sheng SY, Lu CG, Zou JY, Wu CY. The distribution of human stem cell-like memory T cell in lung cancer. *J Immunother* (2016) 39:233–40. doi:10.1097/CJI.0000000000000128
6. Mateus J, Lasso P, Pavia P, Rosas F, Roa N, Valencia-Hernández CA, et al. Low frequency of circulating CD8+ T stem cell memory cells in chronic chagasic patients with severe forms of the disease. *PLoS Negl Trop Dis* (2015) 9:e3432. doi:10.1371/journal.pntd.0003432
7. Fuertes Marraco SA, Soneson C, Cagnon L, Gannon PO, Allard M, Abed Maillard S, et al. Long-lasting stem cell-like memory CD8+ T cells with a naïve-like profile upon yellow fever vaccination. *Sci Transl Med* (2015) 7:282ra48. doi:10.1126/scitranslmed.aaa3700
8. Biasco L, Scala S, Basso Ricci L, Dionisio F, Baricordi C, Calabria A, et al. In vivo tracking of T cells in humans unveils decade-long survival and activity of genetically modified T memory stem cells. *Sci Transl Med* (2015) 7:273ra13. doi:10.1126/scitranslmed.3010314
9. Oliveira G, Ruggiero E, Stanghellini MT, Cieri N, D'Agostino M, Fronza R, et al. Tracking genetically engineered lymphocytes long-term reveals the dynamics of T cell immunological memory. *Sci Transl Med* (2015) 7:317ra198. doi:10.1126/scitranslmed.aac8265
10. Jasenosky LD, Scriba TJ, Hanekom WA, Goldfeld AE. T cells and adaptive immunity to *Mycobacterium tuberculosis* in humans. *Immunol Rev* (2015) 264:74–87. doi:10.1111/imr.12274
11. Colditz GA, Berkey CS, Mosteller F, Brewer TF, Wilson ME, Burdick E, et al. The efficacy of bacillus Calmette-Guérin vaccination of newborns and infants in the prevention of tuberculosis: meta-analyses of the published literature. *Pediatrics* (1995) 96:29–35.
12. Roy A, Eisenhut M, Harris RJ, Rodrigues LC, Sridhar S, Habermann S, et al. Effect of BCG vaccination against *Mycobacterium tuberculosis* infection in children: systematic review and meta-analysis. *BMJ* (2014) 349:g4643. doi:10.1136/bmj.g4643
13. Colditz GA, Brewer TF, Berkey CS, Wilson ME, Burdick E, Fineberg HV, et al. Efficacy of BCG vaccine in the prevention of tuberculosis: meta-analysis of the published literature. *JAMA* (1994) 271:698–702. doi:10.1001/jama.1994.03510330076038
14. Mangtani P, Abubakar I, Ariti C, Beynon R, Pimpin L, Fine PE, et al. Protection by BCG vaccine against tuberculosis: a systematic review of randomized controlled trials. *Clin Infect Dis* (2014) 58:470–80. doi:10.1093/cid/cit790
15. Orme IM. The Achilles heel of BCG. *Tuberculosis* (2010) 90:329–32. doi:10.1016/j.tube.2010.06.002
16. Henao-Tamayo M, Ordway DJ, Orme IM. Memory T cell subsets in tuberculosis: what should we be targeting? *Tuberculosis* (2014) 94:455–61. doi:10.1016/j.tube.2014.05.001
17. Soares AP, Scriba TJ, Joseph S, Harbacheuski R, Murray RA, Gelderbloem SJ, et al. Bacillus Calmette-Guérin vaccination of human newborns induces T cells with complex cytokine and phenotypic profiles. *J Immunol* (2008) 180:3569–77. doi:10.4049/jimmunol.180.5.3569
18. Soares AP, Kwong Chung CKC, Choice T, Hughes EJ, Jacobs G, van Rensburg EJ, et al. Longitudinal changes in CD4+ T-cell memory responses induced by BCG vaccination of newborns. *J Infect Dis* (2013) 207:1084–94. doi:10.1093/infdis/jis941
19. Kagina BM, Abel B, Bowmaker M, Scriba TJ, Gelderbloem S, Smit E, et al. Delaying BCG vaccination from birth to 10 weeks of age may result in an enhanced memory CD4 T cell response. *Vaccine* (2009) 27:5488–95. doi:10.1016/j.vaccine.2009.06.103
20. Tena-Coki N, Scriba TJ, Peteni N, Eley B, Wilkinson RJ, Andersen P, et al. CD4 and CD8 T-cell responses to mycobacterial antigens in African children. *Am J Respir Crit Care Med* (2010) 182:120–9. doi:10.1164/rccm.200912-1862OC
21. Lindestam Arlehamn CS, Gerasimova A, Mele F, Henderson R, Swann J, Greenbaum JA, et al. Memory T cells in latent *Mycobacterium tuberculosis* infection are directed against three antigenic islands and largely contained in a CXCR3+CCR6+ Th1 subset. *PLoS Pathog* (2013) 9:e1003130. doi:10.1371/journal.ppat.1003130
22. Strickland N, Müller TL, Berkowitz N, Goliath R, Carrington MN, Wilkinson RJ, et al. Characterization of mycobacterium tuberculosis-specific cells using MHC Class II tetramers reveals phenotypic differences related to HIV infection and tuberculosis disease. *J Immunol* (2017) 199:2440–50. doi:10.4049/jimmunol.1700849
23. Dintwe OB, Day CL, Smit E, Nemes E, Gray C, Tameris M, et al. Heterologous vaccination against human tuberculosis modulates antigen-specific CD4+ T-cell function. *Eur J Immunol* (2013) 43:2409–20. doi:10.1002/eji.201343454
24. Kipnis A, Irwin S, Izzo AA, Basaraba RJ, Orme IM. Memory T lymphocytes generated by *Mycobacterium bovis* BCG vaccination reside within a CD4 $CD44^{lo}$ CD62 $Ligand^{hi}$ population. *Infect Immun* (2005) 73:7759–64. doi:10.1128/IAI.73.11.7759-7764.2005
25. Mahomed H, Hawkridge T, Verver S, Abrahams D, Geiter L, Hatherill M, et al. The tuberculin skin test versus QuantiFERON TB Gold® in predicting tuberculosis disease in an adolescent cohort study in South Africa. *PLoS One* (2011) 6:e17984. doi:10.1371/journal.pone.0017984
26. Nemes E, Hesseling AC, Tameris M, Mauff K, Downing K, Mulenga H, et al. Safety and immunogenicity of newborn MVA85A vaccination and selective, delayed Bacille Calmette-Guerin (BCG) for infants of HIV infected mothers: a phase 2 randomized controlled trial. *Clin Infect Dis* (2017) 66(4):554–63. doi:10.1093/cid/cix834
27. Kagina BM, Mansoor N, Kpamegan EP, Penn-Nicholson A, Nemes E, Smit E, et al. Qualification of a whole blood intracellular cytokine staining assay to measure mycobacteria-specific CD4 and CD8 T cell immunity by flow cytometry. *J Immunol Methods* (2015) 417:22–33. doi:10.1016/j.jim.2014.12.003
28. Luabeya AK, Kagina BM, Tameris MD, Geldenhuys H, Hoff ST, Shi Z, et al. First-in-human trial of the post-exposure tuberculosis vaccine H56:IC31 in *Mycobacterium tuberculosis* infected and non-infected healthy adults. *Vaccine* (2015) 33:4130–40. doi:10.1016/j.vaccine.2015.06.051
29. Dominguez MH, Chattopadhyay PK, Ma S, Lamoreaux L, McDavid A, Finak G, et al. Highly multiplexed quantitation of gene expression on single cells. *J Immunol Methods* (2013) 391:133–45. doi:10.1016/j.jim.2013.03.002

30. Roederer M, Nozzi JL, Nason MC. SPICE: exploration and analysis of post-cytometric complex multivariate datasets. *Cytometry A* (2011) 79A(2):167–74. doi:10.1002/cyto.a.21015
31. Benjamini Y, Yosef H. Controlling the false discovery rate: a practical and powerful approach to multiple testing. *J R Stat Soc B Methodol* (1995) 57:289–300.
32. Moon JJ, Chu HH, Pepper M, McSorley SJ, Jameson SC, Kedl RM, et al. Naive CD4+ T cell frequency varies for different epitopes and predicts repertoire diversity and response magnitude. *Immunity* (2007) 27:203–13. doi:10.1016/j.immuni.2007.07.007
33. Kwok WW, Tan V, Gillette L, Littell CT, Soltis MA, LaFond RB, et al. Frequency of epitope-specific naive CD4(+) T cells correlates with immunodominance in the human memory repertoire. *J Immunol* (2012) 188:2537–44. doi:10.4049/jimmunol.1102190
34. Su LF, Kidd BA, Han A, Kotzin JJ, Davis MM. Virus-specific CD4+ memory-phenotype T cells are abundant in unexposed adults. *Immunity* (2013) 38:373–83. doi:10.1016/j.immuni.2012.10.021
35. Acosta-Rodriguez EV, Rivino L, Geginat J, Jarrossay D, Gattorno M, Lanzavecchia A, et al. Surface phenotype and antigenic specificity of human interleukin 17-producing T helper memory cells. *Nat Immunol* (2007) 8:639–46. doi:10.1038/ni1467
36. Mahnke YD, Brodie TM, Sallusto F, Roederer M, Lugli E. The who's who of T-cell differentiation: human memory T-cell subsets. *Eur J Immunol* (2013) 43:2797–809. doi:10.1002/eji.201343751
37. Becattini S, Latorre D, Mele F, Foglierini M, De Gregorio C, Cassotta A, et al. T cell immunity. Functional heterogeneity of human memory CD4+ T cell clones primed by pathogens or vaccines. *Science* (2015) 347:400–6. doi:10.1126/science.1260668
38. Cheroutre H, Husain MM. CD4 CTL: living up to the challenge. *Semin Immunol* (2013) 25:273–81. doi:10.1016/j.smim.2013.10.022
39. Lugli E, Gattinoni L, Roberto A, Mavilio D, Price DA, Restifo NP, et al. Identification, isolation and in vitro expansion of human and nonhuman primate T stem cell memory cells. *Nat Protoc* (2013) 8:33–42. doi:10.1038/nprot.2012.143
40. Ciocca ML, Barnett BE, Burkhardt JK, Chang JT, Reiner SL. Cutting edge: asymmetric memory T cell division in response to rechallenge. *J Immunol* (2012) 188:4145–8. doi:10.4049/jimmunol.1200176
41. Graef P, Buchholz VR, Stemberger C, Flossdorf M, Henkel L, Schiemann M, et al. Serial transfer of single-cell-derived immunocompetence reveals stemness of CD8(+) central memory T cells. *Immunity* (2014) 41:116–26. doi:10.1016/j.immuni.2014.05.018
42. Rivino L, Messi M, Jarrossay D, Lanzavecchia A, Sallusto F, Geginat J. Chemokine receptor expression identifies pre–T helper (Th)1, Pre–Th2, and nonpolarized cells among human CD4+ central memory T cells. *J Exp Med* (2004) 200:725–35. doi:10.1084/jem.20040774
43. Castellino F, Huang AY, Altan-Bonnet G, Stoll S, Scheinecker C, Germain RN. Chemokines enhance immunity by guiding naive CD8+ T cells to sites of CD4+ T cell-dendritic cell interaction. *Nature* (2006) 440:890–5. doi:10.1038/nature04651
44. Singh SP, Zhang HH, Foley JF, Hedrick MN, Farber JM. Human T cells that are able to produce IL-17 express the chemokine receptor CCR6. *J Immunol* (2008) 180:214–21. doi:10.4049/jimmunol.180.1.214
45. Shi L, North R, Gennaro ML. Effect of growth state on transcription levels of genes encoding major secreted antigens of *Mycobacterium tuberculosis* in the mouse lung. *Infect Immun* (2004) 72:2420–4. doi:10.1128/IAI.72.4.2420-2424.2004
46. Moguche AO, Musvosvi M, Penn-Nicholson A, Plumlee CR, Mearns H, Geldenhuys H, et al. Antigen availability shapes T cell differentiation and function during tuberculosis. *Cell Host Microbe* (2017) 21:695–706. doi:10.1016/j.chom.2017.05.012
47. Qin S, Rottman JB, Myers P, Kassam N, Weinblatt M, Loetscher M, et al. The chemokine receptors CXCR3 and CCR5 mark subsets of T cells associated with certain inflammatory reactions. *J Clin Invest* (1998) 101:746–54. doi:10.1172/JCI1422
48. Kunkel EJ, Boisvert J, Murphy K, Vierra MA, Genovese MC, Wardlaw AJ, et al. Expression of the chemokine receptors CCR4, CCR5, and CXCR3 by human tissue-infiltrating lymphocytes. *Am J Pathol* (2002) 160:347–55. doi:10.1016/S0002-9440(10)64378-7
49. Brown DM. Cytolytic CD4 cells: Direct mediators in infectious disease and malignancy (2010). *Cell Immunol* (2010) 262:89–95. doi:10.1016/j.cellimm.2010.02.008
50. Juno AJ, van Bockel D, Kent SJ, Kelleher AD, Zaunders JJ, Mee Ling Munier C. Cytotoxic CD4 T cells – friend or foe during viral infection? *Front Immunol* (2017) 8:19. doi:10.3389/fimmu.2017.00019
51. Irmler M, Hertig S, MacDonald HR, Sadoul R, Becherer JD, Proudfoot A, et al. Granzyme A is an interleukin 1 beta-converting enzyme. *J Exp Med* (1995) 181:1917–22. doi:10.1084/jem.181.5.1917
52. Sower LE, Froelich CJ, Allegretto N, Rose PM, Hanna WD, Klimpel GR. Extracellular activities of human granzyme A: monocyte activation by granzyme A versus α-thrombin. *J Immunol* (1996) 156:2585–90.
53. Metkar SS, Menaa C, Pardo J, Wang B, Wallich R, Freudenberg M, et al. Human and mouse granzyme A induce a proinflammatory cytokine response. *Immunity* (2008) 29:720–33. doi:10.1016/j.immuni.2008.08.014
54. Joeckel LT, Wallich R, Martin P, Sanchez-Martinez D, Weber FC, Martin SF, et al. Mouse granzyme K has pro-inflammatory potential. *Cell Death Differ* (2011) 18:1112–9. doi:10.1038/cdd.2011.5
55. Spencer CT, Abate G, Sakala IG, Xia M, Truscott SM, Eickhoff CS, et al. Granzyme A produced by γ9δ2 T cells induces human macrophages to inhibit growth of an intracellular pathogen. *PLoS Pathog* (2013) 9:e1003119. doi:10.1371/journal.ppat.1003119

Conflict of Interest Statement: The authors declare that the research was conducted in the absence of any commercial or financial relationships that could be construed as a potential conflict of interest.

Copyright © 2018 Mpande, Dintwe, Musvosvi, Mabwe, Bilek, Hatherill, Nemes, Scriba and The SATVI Clinical Immunology Team. This is an open-access article distributed under the terms of the Creative Commons Attribution License (CC BY). The use, distribution or reproduction in other forums is permitted, provided the original author(s) and the copyright owner are credited and that the original publication in this journal is cited, in accordance with accepted academic practice. No use, distribution or reproduction is permitted which does not comply with these terms.

EBioMedicine 64 (2021) 103233

Contents lists available at ScienceDirect

EBioMedicine

journal homepage: www.elsevier.com/locate/ebiom

Research paper

Immune profiling of *Mycobacterium tuberculosis*-specific T cells in recent and remote infection

Cheleka A.M. Mpande, Virginie Rozot, Boitumelo Mosito, Munyaradzi Musvosvi, One B. Dintwe, Nicole Bilek, Mark Hatherill, Thomas J. Scriba, Elisa Nemes*, ACS Study Team

South African Tuberculosis Vaccine Initiative, Institute of Infectious Disease and Molecular Medicine, Division of Immunology, Department of Pathology, University of Cape Town, South Africa

ARTICLE INFO

Article History:
Received 17 November 2020
Revised 7 January 2021
Accepted 19 January 2021
Available online xxx

Keywords:
Tuberculosis
Recent infection
T cell activation
Biomarker
T cell differentiation

ABSTRACT

Background: Recent *Mycobacterium tuberculosis* (M.tb) infection is associated with a higher risk of progression to tuberculosis disease, compared to persistent infection after remote exposure. However, current immunodiagnostic tools fail to distinguish between recent and remote infection. We aimed to characterise the immunobiology associated with acquisition of M.tb infection and identify a biomarker that can distinguish recent from remote infection.

Methods: Healthy South African adolescents were serially tested with QuantiFERON-TB Gold to define recent (QuantiFERON-TB conversion <6 months) and persistent (QuantiFERON-TB+ for >1.5 year) infection. We characterised M.tb-specific CD4 T cell functional (IFN-γ, TNF, IL-2, CD107, CD154), memory (CD45RA, CCR7, CD27, KLRG-1) and activation (HLA-DR) profiles by flow cytometry after CFP-10/ESAT-6 peptide pool or M.tb lysate stimulation. We then assessed the diagnostic performance of immune profiles that were differentially expressed between individuals with recent or persistent QuantiFERON-TB+.

Findings: CFP-10/ESAT-6-specific CD4 T cell activation but not functional or memory phenotypes distinguished between individuals with recent and persistent QuantiFERON-TB+. In response to M.tb lysate, recent QuantiFERON-TB+ individuals had lower proportions of highly differentiated IFN-γ+TNF+ CD4 T cells expressing a KLRG-1+ effector phenotype and higher proportions of early differentiated IFN-γ-TNF+IL-2+ and activated CD4 T cells compared to persistent QuantiFERON-TB+ individuals. Among all differentially expressed T cell features CFP-10/ESAT-6-specific CD4 T cell activation was the best performing diagnostic biomarker of recent infection.

Interpretation: Recent M.tb infection is associated with highly activated and moderately differentiated functional M.tb-specific T cell subsets, that can be used as biomarkers to distinguish between recent and remote infection.

Funding: US National Institutes of Health (NIH), Bill and Melinda Gates Foundation, South African National Research Foundation, South African Medical Research Council, and Aeras.

© 2021 The Author(s). Published by Elsevier B.V. This is an open access article under the CC BY license (http://creativecommons.org/licenses/by/4.0/)

1. Introduction

Tuberculosis remains a major global health problem, causing approximately 1.4 million deaths annually [1]. Despite being responsible for the most deaths due to a single infectious agent, only a minority (5–10%) of immunocompetent individuals infected with M.tb actually progress to disease. The risk of disease progression is not uniform in immunocompetent M.tb infected individuals, with the highest risk occurring within the first 2 years of primary (recent) M.tb infection [2–6]. By comparison, risk of tuberculosis in established, remote infection that has persisted for > 2 years is much lower [7]. Re-exposure of individuals with remote M.tb infection has been associated with a significantly lower rate of disease progression compared with exposure of individuals without prior infection [7,8]. Similarly, a non-human primate tuberculosis model has demonstrated that primary M.tb infection induces immunity that prevents re-infection or restricts bacterial growth upon re-infection [9].

Experimental M.tb infection in animal models has demonstrated that an early peak in M.tb burden occurs during acute infection. This is followed by immune-mediated reduction of bacterial replication that can persist during chronic infection for very long periods [10,11]. We postulated that recent M.tb infection in humans follows the same M.tb replication kinetic, albeit over a longer temporal

* Corresponding author.
E-mail address: elisa.nemes@uct.ac.za (E. Nemes).

https://doi.org/10.1016/j.ebiom.2021.103233
2352-3964/© 2021 The Author(s). Published by Elsevier B.V. This is an open access article under the CC BY license (http://creativecommons.org/licenses/by/4.0/)

Research in Context

Evidence before this study

Recent M.tb infection is associated with a higher risk of disease progression than remote infection. Unfortunately, current immunodiagnostics such as QFT and TST are unable to distinguish the two infection states, differentiate M.tb infection from tuberculosis disease, or identify individuals at risk of disease progression. A few studies have described immune features, such as gene expression, T cell proliferation capacity, M.tb-specific T cell functional and memory subsets associated with recent M.tb infection or M.tb exposure, that can distinguish between recent and remote infection, one of which reported high accuracy. These studies did not provide an in-depth description of M.tb-specific immune features associated with acquisition of recent M.tb infection, which is needed to guide the development of novel immunodiagnostics to identify recently infected individuals, who are at high risk of disease progression.

Added value of this study

Our findings add novel evidence that M.tb-specific T cells from healthy individuals with recently acquired M.tb infection are highly activated. By contrast, M.tb-specific T cells from those with remote M.tb infection are not activated. We demonstrate that M.tb-specific CD4 T cells from recently infected individuals are less functionally differentiated than T cells from remotely infected individuals. Further, biomarkers based on T cell activation out-performed those defined on cytokine and/or memory co-expression profiles and showed excellent performance to discriminate between recent and remote M.tb infection. A previously described biomarker of recent M.tb infection proposed by Halliday and colleagues did not significantly discriminate between recent and remote M.tb infection in our study.

Implications of all the available evidence

The T cell activation biomarker could potentially be developed as a rule-in test to identify individuals at high risk of disease, who should receive further clinical evaluation prior to the administration of tuberculosis preventive therapy. Further, M.tb-specific T cell responses in individuals with remote M.tb infection are consistent with *in vivo* exposure to very low antigen load, which may question the risk/benefit ratio associated with provision of tuberculosis preventive therapy to these individuals.

period, resulting in a persisting "lifelong" low-grade infection in many individuals that facilitates maintenance of cellular immunity or, alternatively, eventual clearance of infection despite persistent immunological sensitisation [12]. In contrast, failure to control bacterial replication results in high and persistent mycobacterial burden which are associated with disease progression. Since the magnitude and duration of *in vivo* T cell exposure to mycobacterial antigens are known to affect differentiation and functional capacity of CD4 T cells [13,14], we propose that different states of M.tb infection or disease will be associated with distinct T cell functional and differentiation states. Current tests for M.tb infection status such as tuberculin skin tests (TST) or IFN-γ release assays (IGRAs) measure T cell memory responses to M.tb antigens. A major limitation of these tests is that they do not reveal the duration of infection and, as a consequence, most immunology studies of M.tb infection have focused on remote M.tb infection. Our current knowledge of T cell immunity in the context of M.tb infection and disease is thus predominantly based on cross-sectional studies of individuals with remote M.tb infection or recent tuberculosis diagnosis, and very little is known about the T cell features associated with recent M.tb infection.

Upon antigen exposure, T cells become activated, differentiate and acquire functional properties. Expression of HLA-DR, a member of the MHC class II family typically expressed by antigen-presenting cells, is often used as a marker of T cell activation [15,16]. In the context of tuberculosis, studies have shown that disease, regardless of HIV status, is associated with significantly higher levels of T cell activation than M.tb infection, and that activation is reduced upon successful antimicrobial treatment [17–22]. These studies suggest that antigen-specific T cell activation could be used as a biomarker of microbial burden, and potentially infer *in vivo* antigen exposure during different stages of infection and disease. In addition, upon exposure to high antigen load CD4 T cells predominantly express IFN-γ, which is mostly associated with an effector memory T (T_E) cell phenotype. Conversely, expression of TNF and IL-2 in the absence of IFN-γ is associated with stem cell memory (T_{SCM}) and central memory (T_{CM}) T cell subsets and exposure to low antigen load or antigen clearance [13,23]. Further, chronic duration of antigen exposure is associated with upregulation of the T cell senescence marker, KLRG-1, and T cell differentiation to a predominantly IFN-γ-monofunctional capacity [13,14]. These highly differentiated antigen-specific IFN-γ-monofunctional T cells have a lower capacity to contribute to M.tb clearance than polyfunctional Th1 cells, and are positively correlated with an increase in bacterial burden [24,25]. Based on these cytokine co-expression profiles we defined a single measure, which we termed *functional differentiation score* (FDS), that aims to infer the degree of T cell differentiation [14]. A higher M.tb-specific T cell FDS was associated with increased magnitude and duration of antigen exposure and T_E memory phenotypes [14].

TST and IGRAs have a low predictive value for tuberculosis [26]. Other functional assays that measure M.tb-specific T cell properties such as Th1 cytokine co-expression profiles [27,28], T cell differentiation (CD27, [29,30]) and T cell activation [17–22] have been proposed as new potential immunodiagnostic concepts that can distinguish between M.tb infection and disease. In line with this principle, potential biomarkers of recent M.tb infection based on proportions of TNF-only (IFN-γ-IL-2-) T_E (CD45RA-CCR7-CD127-) CD4 T cells or T cell proliferation, as well as a blood transcriptomic signature, have been described [31–33]. Halliday and colleagues demonstrated that the proportion of PPD-reactive TNF-only T_E CD4 T cells was highest in tuberculosis patients and lowest in individuals with remote M.tb infection, and distinguished between recent and remote M.tb infection with a sensitivity and specificity of 89% and 65%, respectively [31]. These studies all present evidence for potential biomarkers of tuberculosis risk. However, in-depth characterisation of immunological features associated with recent acquisition of infection that could contribute to an improved understanding of M.tb-specific immunobiology were not presented. The purpose of our study was to characterise the kinetics of M.tb-specific T cell features associated with recent and remote M.tb infection.

We *postulated that differential in vivo antigen exposure during recent and remote M.tb infection is associated with distinct M.tb-specific T cell memory, functional and activation profiles*. More specifically, *we hypothesised that recent infection is associated with lower T cell differentiation and higher T cell activation compared to remote infection*. We thus aimed to identify *M.tb-specific T cell features that could distinguish between recent and remote M.tb infection*.

2. Methods

2.1. Study design

We designed a retrospective study in adolescents to compare immune responses between recent and remote M.tb infection using cryopreserved peripheral blood mononuclear cells (PBMC).

2.2. Participants

South African adolescent participants were enrolled in observational studies approved by the University of Cape Town Human Research Ethics Committee (protocol references: 045/2005, 102/2017). Adolescents provided written, informed assent and their parents or legal guardians provided written, informed consent. IGRA testing with QuantiFERON-TB Gold In-Tube (QFT; Qiagen) was performed to measure M.tb infection and PBMC were collected at enrolment and at 6-monthly intervals during a 2-year follow-up in a subset of the cohort. See supplementary methods for detailed inclusion and exclusion criteria.

2.3. Definition of recent and remote M.tb infection

We defined two adolescent cohorts of recent M.tb infection based on serial QFT (and TST) results (Supplementary Table 1). Adolescents selected for the *biomarker discovery cohort* were defined as healthy participants with two negative QFT tests (IFN-γ < 0.35 IU/mL; assay performed and interpreted according to the manufacturer's specifications) followed by two positive QFT tests (IFN-γ ≥0.35 IU/mL) 6 months apart over 1.5 years (Fig. 1a). Recent QFT+ individuals (n=30) selected for this cohort had at least one positive and negative QFT test result out of the QFT uncertainty zone (0.2–0.7 IU/mL) defined by our research group [34]. All data on functional and differentiation profiles reported in this manuscript was generated from this cohort.

Recently M.tb infected adolescents selected for the *tetramer cohort* (n=11) were defined by a negative QFT (IFN-γ < 0.35 IU/mL) and TST negative (induration < 5 mm) at baseline, followed by at least three positive QFT tests and one positive TST result (Fig. 1b) [35]. All participant had quantitative QFT responses outside of the QFT uncertainty zone. Only the data reporting tetramer staining (Fig. 5b) was generated from this cohort.

Remote (persistent) M.tb infection was defined in healthy participants (n=30) by 4 consecutive QFT positive tests (two of which had to be > 0.7 IU/mL) 6 months apart over 1.5 years (*biomarker discovery cohort*, Fig. 1).

Here we included results from all visits from the tetramer cohort, while results presented for the biomarker discovery cohort were from the first QFT– and the first QFT+ visit (1 year apart) for recent QFT+ participants, and fourth QFT+ visit for persistent QFT+ participants (Fig. 1).

2.4. Protocols used to detect M.tb-specific CD4 T cells

M.tb-specific CD4 T cells were detected using either PBMC intracellular cytokine staining (ICS) or major histocompatibility complex (MHC) class II tetramer staining and flow cytometry. Detailed PBMC-ICS stimulation protocol is outlined in the *Supplementary Methods*. Briefly, cryopreserved PBMC were stimulated with peptide pools spanning full length CFP-10/ESAT-6, M.tb-specific antigens used in

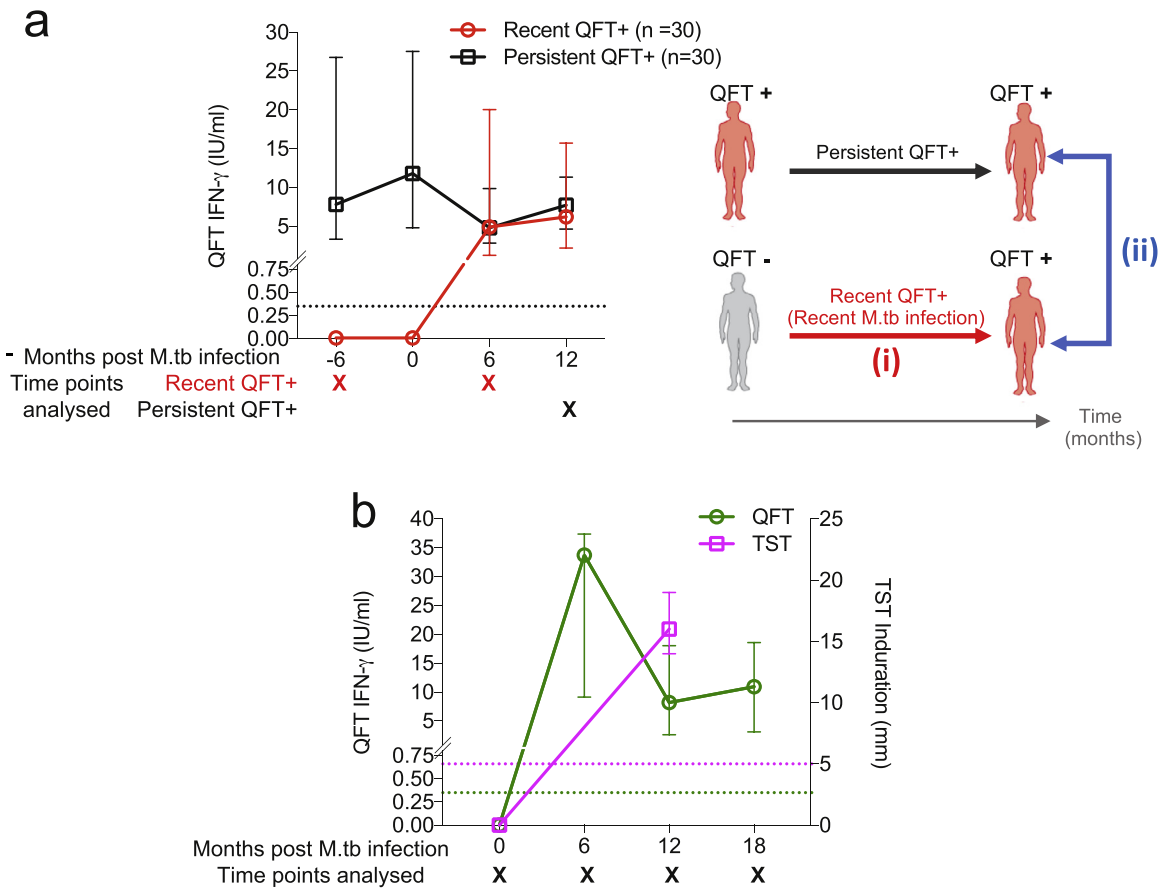

Fig. 1. Longitudinal QFT (and TST) kinetics in the biomarker discovery and tetramer cohorts. M.tb infection was defined using longitudinal (a) QFT (only) results for the biomarker discovery cohort [recent QFT+ (red symbols, n=30 for all time points) and persistent QFT+ (black symbols, n= 30 for all time points)], and (b) both QFT (green) and TST (magenta) results for the tetramer cohort (n=11 for all time points). Longitudinal QFT+ and TST results are depicted as median with an interquartile range (IQR). Dotted lines indicate the assay positivity cut-offs. Only samples collected at time points marked with "X" were analysed in this study. The image in (a) depicts comparisons that were performed on the biomarker discovery cohort: (i) QFT– vs recent QFT+ and (ii) recent vs persistent QFT+.

the QFT assay, or M.tb lysate (H37Rv) for 18 h (biomarker discovery cohort). Cells were then stained with antibodies (Supplementary Table 2) and analysed by flow cytometry. For the ICS assay M.tb-specific cells were defined by cytokine expression (Supplementary Fig. 1 A).

For the tetramer cohort, human leukocyte antigen (HLA)-typing was performed to determine which tetramers could be used to measure M.tb-specific T cells. Briefly, DNA was extracted from PBMC to determine high resolution HLA class I and II genotypes by polymerase chain reaction (PCR) using sequence-specific primers [36]. HLA allele ambiguities were resolved by allele-specific DNA sequencing [14,37]. For M.tb-specific MHC class II tetramer staining the previously described protocol was followed [35]. Briefly, thawed cryopreserved PBMC were stained with anti-CCR7 for 30 min at 37 °C, washed and then stained with 2 μg/mL MHC class II tetramers (Supplementary Table 3) for 1 h at room temperature. Cells were then washed and stained with surface marker antibodies (Supplementary Table 4) and analysed by flow cytometry (Supplementary Fig. 1b).

2.5. Data analysis

2.5.1. Biomarker discovery cohort analysis pipeline

We focused our analyses on CD4 T cells because frequencies of CD8 T cell responses were undetectable or not different to background in most individuals (data not shown). After conventional gating performed in FlowJo (Supplementary Fig. 1), we followed the analysis pipeline outlined in Supplementary Fig. 2 and described in the online methods. Briefly, expression of all possible combinations of functional responses (obtained by Boolean gates) were analysed using COMPASS [38], Pestle and SPICE [39]. In parallel, we utilised MIMOSA [40] to define responders (see below). We identified differentially expressed T cell subsets (including all possible combinations of functional and phenotypic markers) between two groups using CITRUS analysis (Supplementary Figs. 3 and 4) in Cytobank on responders only [41]. Following CITRUS analysis, we exported CITRUS cluster FCS files, concatenated the files from all participants belonging to the same cluster and confirmed memory/cytokine cluster composition by manual re-gating in FlowJo.

2.5.2. Biomarker discovery cohort responder definition

Responders were defined as individuals with frequencies of antigen-specific total Th1 cytokine+ (IFN-$\gamma\pm$TNF$\pm$IL-2$\pm$) CD4 T cells that were significantly higher [false discovery rate (FDR) $\leq$0.01, calculated by MIMOSA in R, version 1.21.0; https://github.com/RGLab/MIMOSA; [40] and at least 3-fold increase] than background. Non-responders were excluded from phenotypic marker expression analysis. We used this strict cut-off to ensure that cytokine responses in responders were truly antigen specific because analysis of activation, memory and/or functional phenotypes were performed using methods that would not account for non-specific signal using background subtraction.

2.5.3. Functional differentiation score

All possible cytokine co-expression T cell subsets were computed as posterior probabilities or summarised as a single functionality score (FS) or polyfunctionality score (PFS) for each individual using COMPASS [38]. We also calculated the FDS (Equation 1 [14]) for responders only.

Equation 1: Functional differentiation score calculation.

$$FDS = \frac{IFN\gamma + TNF \pm IL-2 \pm}{IFN\gamma - TNF \pm IL-2 \pm}$$

2.5.4. Statistical analysis

Statistical analyses were performed using R, R Studio or GraphPad Prism v7. We applied Wilcoxon signed-rank and Mann–Whitney *U* statistical tests for paired and unpaired comparisons, respectively. Bonferroni or Benjamini–Hochberg (FDR $<$0.05) methods were used to correct for up to 4 comparisons or more than 4 comparisons, respectively. In addition to this, functional, memory and activation features identified as significantly different between recent and persistent QFT+ individuals were tested for their diagnostic potential using receiver operating characteristic (ROC) curve analysis performed using the pROC package in R [version 1.15.3; https://web.expasy.org/pROC/;[42]].

2.6. Role of the funding source

The funders had no role in study design, data collection, analysis and interpretation, writing and submission of the manuscript. CM, TJS and EN had complete access to the data, EN had final responsibility for the decision to submit for publication.

3. Results

3.1. TST dynamics in the biomarker discovery cohort

M.tb infection status of individuals in the biomarker discovery cohort, on which the ICS assay was performed, was based on QFT only. However, we also had access to TST results for most of these individuals and observed 100% concordance between QFT and TST results in recent QFT+ individuals, and an equally high concordance between QFT and TST results in persistent QFT+ individuals: proportion of agreement = 88.14%; Kappa = 0.763 (data not shown).

3.2. Recent QFT+ is associated with lower T cell functional differentiation compared to persistent QFT+

We aimed to determine functional properties associated with acquisition of infection, and how they compare to persistent QFT+. Frequencies of CFP-10/ESAT-6-specific CD4 T cells expressing IFN-γ, TNF, IL-2 or CD107 were undetectable or very low before QFT conversion, as expected (Fig. 2a). By contrast, CD154-expresisng CD4 T cells were detected in more than half of the individuals at this time point (Fig. 2a). QFT conversion was associated with a significant increase in frequencies of M.tb-specific IFN-γ, TNF or IL-2-expressing CD4 T cell responses (Fig. 2a). CD107 or CD154-expresisng CD4 T cells did not change significantly after QFT conversion.

We then utilised COMPASS analysis to determine FS, PFS and posterior probabilities of antigen-specific responses for all possible cytokine co-expression subsets associated with acquisition of M.tb infection (Fig. 2b). As observed above, FS, PFS and probabilities of antigen-specific responses of CFP-10/ESAT-6-specific CD4 T cells were very low prior to M.tb infection (QFT–) in most individuals. These outcomes increased significantly upon recent QFT conversion to levels that were similar to those in individuals with persistent QFT+ reactivity (Fig. 2). Probabilities of antigen-specific responses in persistent QFT+ individuals were universally high for subsets that co-expressed two, three or four functions among IFN-γ, TNF, IL-2 and CD154, but not CD107. We next investigated M.tb lysate-specific CD4 T cell responses kinetics associated with acquisition of infection. M.tb lysate contains antigens that cross-react with bacille Calmette–Guérin (BCG) vaccine and other non-tuberculous mycobacteria *sp.*, facilitating detection of mycobacterial responses in BCG-vaccinated M.tb uninfected individuals (QFT–) and comparisons of T cell features before and after M.tb infection. Prior to M.tb infection we detected robust levels of M.tb lysate-specific CD4 T cells with relatively high FS and PFS, which increased to even higher levels upon infection (recent QFT+) that were in a similar range to those detected in persistent QFT+ individuals (Fig. 2b).

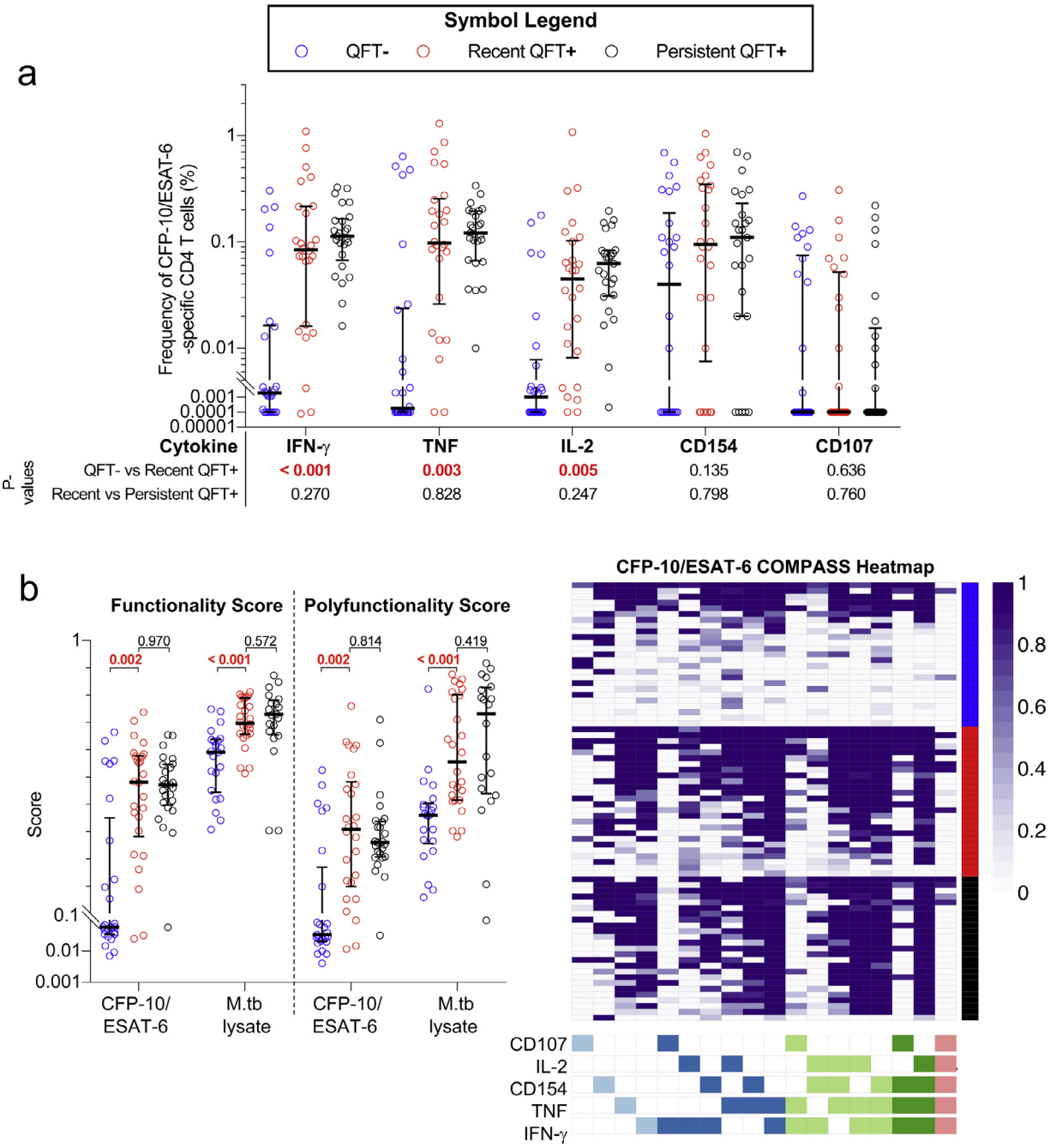

Fig. 2. Recent QFT conversion induces similar CFP-10/ESAT-6-specific CD4 T cell cytokine co-expression profiles as in persistent QFT+ individuals. (a) Frequencies of background subtracted CFP-10/ESAT-6-specific IFN-γ+, TNF+, IL-2+, CD154+ and CD107+ CD4 T cells and (b) COMPASS analysis results [functionality scores, polyfunctionality scores and posterior probability heat map (CFP-10-ESAT-6 stimulation)] of M.tb-specific CD4 T cells detected before (QFT−, blue, CFP-10/ESAT-6, *n*=26; M.tb lysate, *n*=22), after (recent QFT**+**, red, CFP-10/ESAT-6, *n*=26; M.tb lysate, *n*=26) and during persistent M.tb infection (persistent QFT**+**, black, CFP-10/ESAT-6, *n*=25; M.tb lysate, *n*=20). *P*-values were calculated using the Wilcoxon-signed rank test for paired (QFT− *versus* recent QFT**+**) or the Mann−Whitney *U* test for unpaired (recent *versus* persistent QFT+) comparisons and corrected for multiple comparison using the Benjamini−Hochberg method with a false discovery rate (FDR) of 0.05. *P*-values highlighted in **red, bold text** were considered significant.

T cells are known to change their functional capacity depending on antigen burden. We recently defined a single measurement of functional differentiation, FDS, that we propose can distinguish between infections states associated with different levels of M.tb burden [14]. We thus compared the distribution of cytokine co-expressing Th1 subsets and FDS in individuals in the biomarker discovery cohort. Since the majority of CFP-10/ESAT-6-specific CD4 T cells detected prior to M.tb infection were low and did not meet our responder criteria, we focused our longitudinal analyses of functional changes on M.tb lysate-specific CD4 T cells (Supplementary Fig. 5). Relative proportions of M.tb lysate-specific CD4 T cells expressing only IL-2 or TNF were higher prior to than after M.tb infection, while proportions of IFN-γ-TNF+IL-2+ and IFN-γ+TNF±IL-2± subsets were not different before and after M.tb infection (Fig. 3a). Higher proportions of IFN-γ-TNF+IL-2+ but lower proportions of IFN-γ+TNF+IL-2- M.tb lysate-specific CD4 T cells were detected in recent QFT+ compared to persistent QFT+ individuals. This resulted in lower Th1 functional differentiation, measured by FDS, in recent QFT+ compared with persistent QFT+ individuals (Fig. 3b). FDS of CFP-10/ESAT-6-specific CD4 T cells between the two M.tb infection states were not different (Fig. 3b).

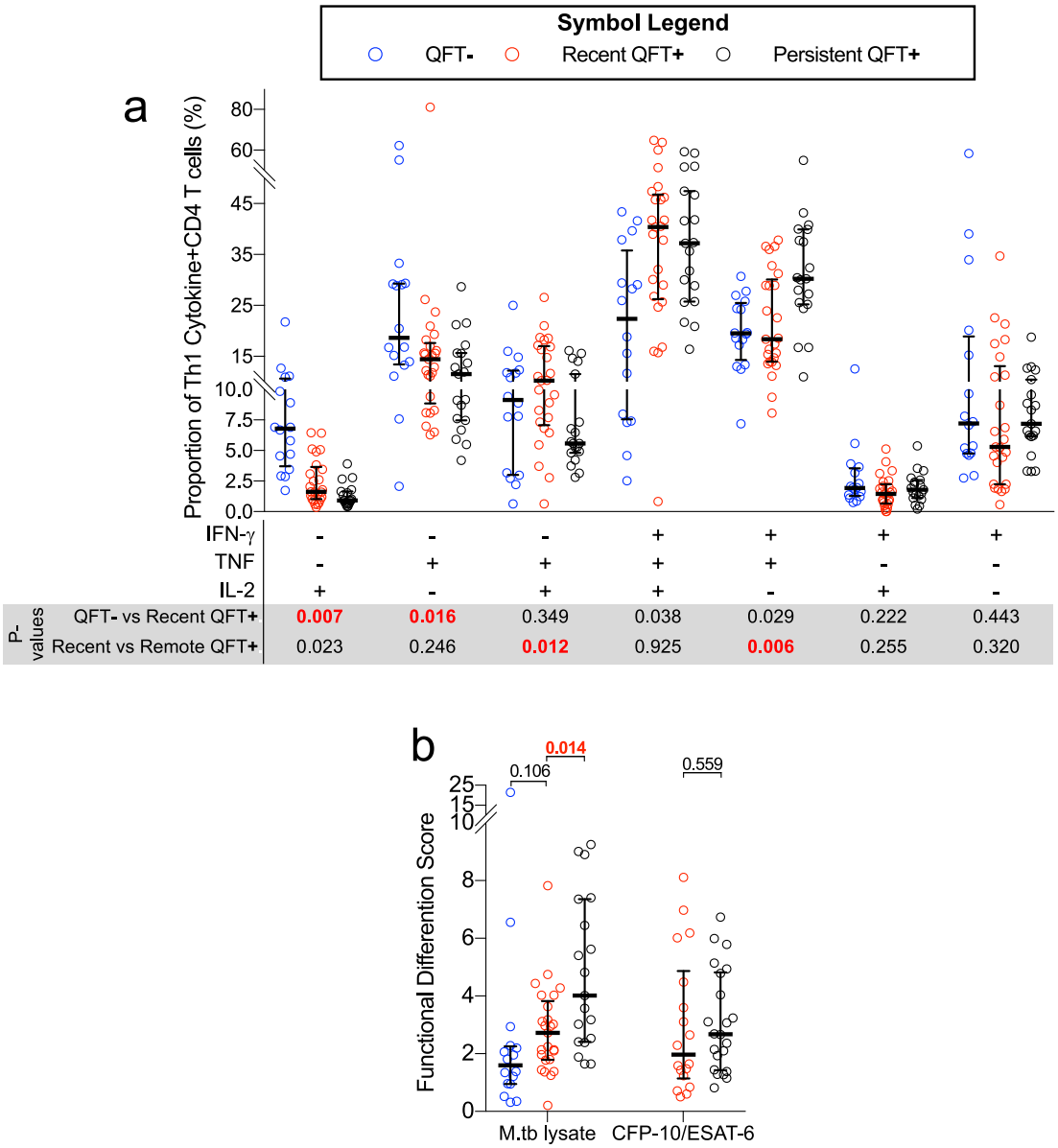

Fig. 3. Recent QFT+ is associated with lower proportions of M.tb lysate-specific functionally differentiated CD4 T cell subsets than persistent QFT+. (a) Proportions of M.tb lysate-specific Th1 polyfunctional profiles detected before (QFT−, *n*= 16), after (recent QFT+, *n*=25) and during persistent M.tb infection (persistent QFT+, *n*=22) in responders only. (b) Functional differentiation scores of M.tb-specific CD4 T cells before (QFT−, M.tb lysate, *n*= 16), after (recent QFT+, CFP-10/ESAT-6, *n*= 18; M.tb lysate, *n*=25), and during persistent M.tb infection (black symbols, CFP-10/ESAT-6, *n*= 22; M.tb lysate, *n*=19) in responders only. *P*-values were calculated using the Wilcoxon-signed rank test for paired (QFT− *versus* recent QFT+) or the Mann−Whitney *U* test for unpaired (recent *versus* persistent QFT+) comparisons and corrected for multiple comparison using the Benjamini−Hochberg method with a false discovery rate (FDR) of 0.05. *P*-values highlighted in **red, bold text** were considered significant.

3.3. CFP-10/ESAT-6-specific memory T cell subsets induced by recent QFT conversion are maintained in persistent QFT+ individuals

We next aimed to determine if acquisition of M.tb infection is associated with a shift in M.tb-specific T cell memory phenotypes, as well as compare the distribution of M.tb-specific memory phenotypes between recent and persistent QFT+ individuals. Analysis of T cell memory markers expressed by M.tb lysate-specific CD4 T cells showed that recent QFT conversion was associated with a decrease in KLRG-1- T_{SCM} (CD45RA+CCR7+CD27+) and T_{CM} (CD45RA-CCR7+CD27+) cells, and an increase in KLRG-1- T_E (CD45RA-CCR7-CD27-) cells compared to the pre-infection (QFT−) time-point, indicative of increased antigen exposure (Supplementary Fig. 6a). Memory phenotypes of M.tb-specific responses, regardless of stimuli, were not different between recent and persistent QFT+ individuals, with transitional memory (T_{TM}, CD45RA-CCR7-CD27+) and T_E cells being the predominant T cell memory subsets (Supplementary Fig. 6b).

Results above clearly illustrate a relationship between cytokine expression and memory phenotypes and suggest that combined analysis of these features may be informative. We therefore used CITRUS to identify cell subsets that were expressed at significantly different levels upon acquisition of M.tb infection, and between recent and persistent QFT+ individuals, based on expression of CD45RA, CCR7, CD27, KLRG1, IFN-γ, TNF and IL-2. We did not include CD107 and CD154 in this analysis, due to high non-specific, background expression of these markers. CXCR3 and HLA-DR were also excluded from this analysis because neither marker contributed to cell cluster definition during the optimisation of the CITRUS workflow. Composition of each differentially expressed T cell cluster, identified by CITRUS

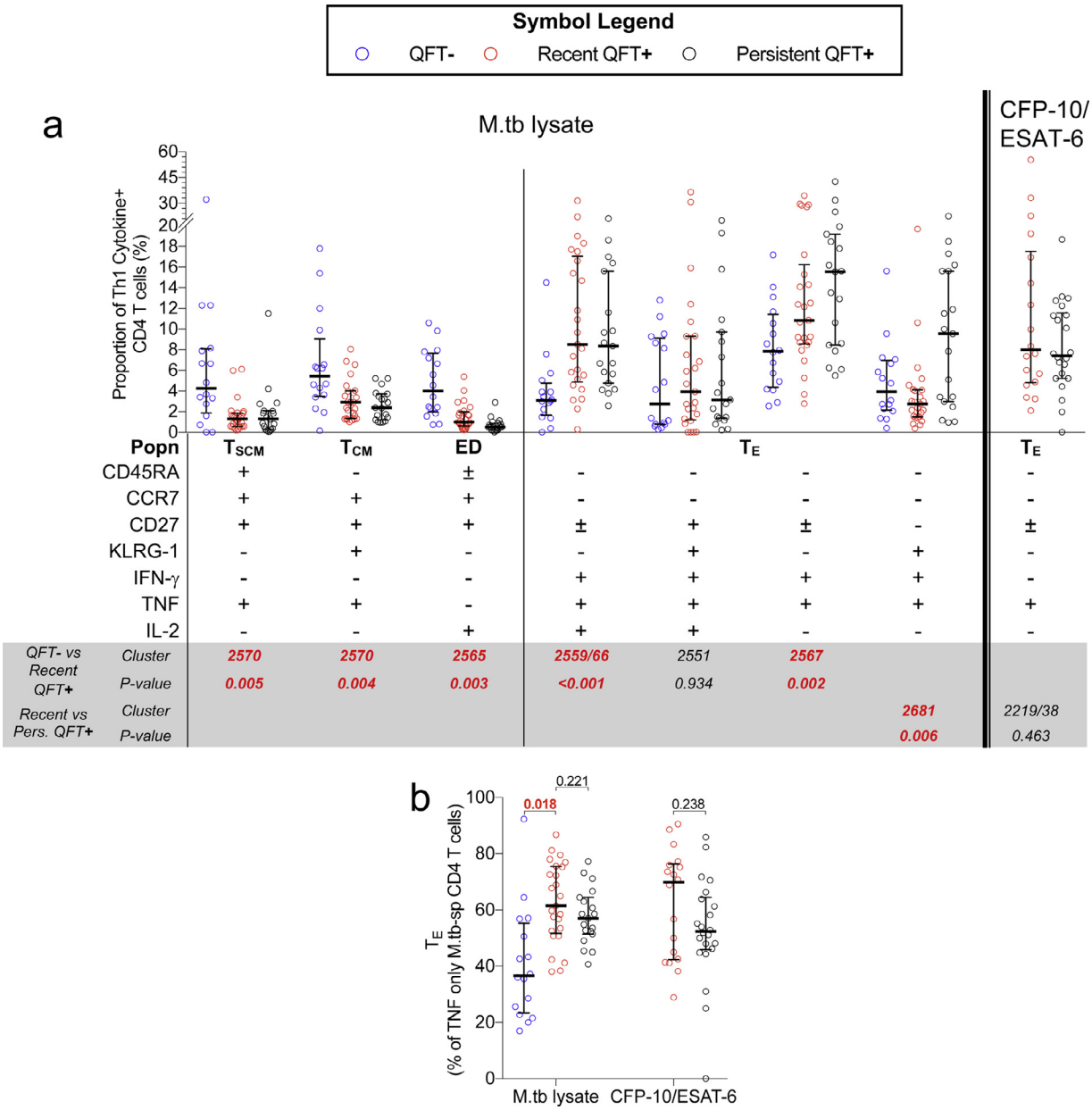

Fig. 4. Induction of highly differentiated polyfunctional T_E cells upon recent QFT conversion at the expense of less differentiated IFN-γ-independent T_{SCM} and T_{CM} subsets. Proportions of (a) M.tb lysate-specific and CFP-10/ESAT6-specific memory/cytokine co-expression subsets before (QFT−, blue, M.tb lysate, *n*= 16), after (recent QFT+, red, CFP-10/ESAT-6, *n*= 18; M.tb lysate, *n*=25), and during persistent M.tb infection (persistent QFT+, black, CFP-10/ESAT-6, *n*= 22; M.tb lysate, *n*=19). The CITRUS cluster number corresponding to the manually gated populations is shown. (b) Proportions of T_E TNF only M.tb lysate-specific and CFP-10/ESAT-6-specific CD4 T cells detected before, after and during persistent M.tb infection (number of participants is as in A). Statistical analysis was conducted as in Fig. 2, clusters and *p*-values highlighted in **red, bold text** were considered significantly different.

(*supplementary methods*), was confirmed by manual gating in all responders.

Compared to the pre-infection (QFT−) timepoint, recent QFT+ conversion was associated with a decrease in M.tb lysate-specific, early-differentiated IL-2-only T_{SCM}/T_{CM} (cluster 2565) and TNF-only T_{SCM}/T_{CM} (cluster 2570) cell subsets, and an increase in proportions of IFN-γ+TNF+IL-2+ (cluster 2559/66) and IFN-γ+TNF+ T_E (cluster 2567) cells (Fig. 4a). We also observed lower proportions of M.tb lysate-specific KLRG-1+IFN-γ+TNF+IL-2- (cluster 2681) T_E cells in recent QFT+ compared to persistent QFT+ individuals (Fig. 4a). Despite detecting differences in abundance levels of CITRUS clusters 2551 (QFT− *versus* recent QFT+) and 2219/43 (recent *versus* persistent QFT+), proportions of clusters were not different when manually gated (Fig. 4a).

To the best of our knowledge, only one biomarker of recent M.tb infection, relative proportions of TNF-only (IFN-γ-IL-2-) T_E (CD45RA-CCR7-CD127-) CD4 T cells, has previously been reported as a diagnostic biomarker for differentiating between recent and remote M.tb infection [31]. We therefore aimed to evaluate the performance of this biomarker in our cohort. Because our flow cytometry panel did not include CD127, we defined this subset as TNF-only, CD45RA-CCR7- T_E memory cells. Acquisition of M.tb infection (QFT− *versus* recent QFT+) was associated with an increase in proportions of TNF-only T_E memory cells, however, unlike results presented by Halliday and colleagues [31], proportions of these cells, regardless of stimulus, were not different between recent and persistent QFT+ individuals (Fig. 4b).

These results confirm that recent QFT+ was associated with lower proportions of CD4+ IFN-γ- T_{SCM}, T_{CM} and early differentiated memory cells, and higher proportions of activated and polyfunctional IFN-γ+ T_E cells, compared to the respective QFT− time point in each

individual. Memory and functional profiles induced upon early infection were sustained at stable proportions once M.tb infection is established, with the exception of highly differentiated KLRG-1+IFN-γ+TNF+ T_E cells, which were more abundant during persistent QFT+ compared to recent QFT conversion.

3.4. Higher levels of T cell activation in recent QFT+ than persistent QFT+ individuals

We next investigated T cell activation kinetics associated with acquisition of M.tb infection, and compared individuals with recent QFT conversion to those with persistent QFT+ status. Acquisition of M.tb infection (QFT− *versus* recent QFT+) was associated with a significant increase in both activated (HLA-DR+) IFN-γ+ and total Th1 cytokine+ M.tb-specific CD4 T cells (Fig. 5a), which were also higher in recent QFT+ than in persistent QFT+ individuals (Fig. 5a). Longitudinal analysis of all available time points showed that CFP-10/ESAT-6-specific CD4 T cell activation significantly decreased by 12 months post QFT conversion (Supplementary Fig. 7).

Since *in vitro* stimulation may affect expression of activation markers, we aimed to confirm T cell activation kinetics using MHC class II tetramer staining, which detects antigen-specific cells directly *ex vivo* and does not require stimulation, on a different cohort of recently M.tb infected individuals [35]. Proportions of HLA-DR+ activated M.tb-tetramer+ CD4 T cells were highest at the first QFT+ time point (month 6 since last QFT negative test, when M.tb-tetramer+ cells were detectable) and markedly decreased by 18 months post QFT conversion (Fig. 5b). Notably, the activation status of bulk memory and naïve CD4+ T cells were unchanged during the follow-up period. M.tb-tetramer+ CD4 T cells were also significantly more activated than bulk memory CD4 T cells, and bulk naïve CD4 T cells were significantly less activated than bulk memory CD4 T cells (Fig. 5b). These results demonstrate the robustness of T cell activation as a potential biomarker to distinguish between recent and persistent QFT+ individuals.

3.5. T cell activation is a superior biomarker of recent M.tb infection than T cell differentiation

Finally, we investigated the diagnostic performance of functional, memory and activation profiles that were significantly different between recent and persistent QFT+ individuals in our dataset. We performed ROC analysis to assess the performance of HLA-DR+ IFN-γ+ and Th1 cytokine+ M.tb-specific CD4 T cells (regardless of stimulus), M.tb-lysate-specific FDS, and proportions of KLRG-1+ IFN-γ+TNF+IL-2- T_E (CD45RA-CCR7-CD27-) CD4 T cells to discriminate between recent and persistent QFT+ individuals. We did not perform ROC analysis on differentially expressed CD4 T cell cytokine co-expression profiles (IFN-γ-TNF+IL-2+, IFN-γ+TNF+IL-2-, IFN-γ+TNF-IL-2-) because these were already included in the definition of either the FDS or KLRG-1+ IFN-γ+TNF+IL-2- T_E cell population. Proportions of HLA-DR+ M.tb-specific (IFN-γ+ or Th1 cytokine+) CD4 T cells demonstrated very good discrimination between recent and persistent QFT+ individuals, achieving AUCs above 0.8 (Fig. 6a). By comparison, the highly differentiated KLRG-1+ IFN-γ+TNF+IL-2- T_E cell population and FDS demonstrated moderate discriminatory performance; AUCs for these comparisons were below 0.8 (Fig. 6b).

We also compared the discriminatory performance between recent and persistent QFT+ of CFP-10/ESAT-6-specific or M.tb lysate-specific HLA-DR+ IFN-γ+TNF+ CD4 T cells (Supplementary Table 7), an adaptation of a previously published biomarker with excellent discrimination between tuberculosis cases and healthy controls and which also showed promise as a tuberculosis treatment monitoring biomarker, since it decreased significantly upon successful tuberculosis therapy [20]. Biomarkers based on HLA-DR expression by CFP-10/ESAT-6-specific CD4 T cells had significantly higher AUCs than those based on cytokine co-expression profiles or memory marker expression on M.tb lysate-specific CD4 T cells (Table 1). On the other hand, discriminatory AUCs of biomarkers based on HLA-DR expression regardless of M.tb stimulus or M.tb-specific CD4 T cell denominator were not different (p-value > 0.05), suggesting that neither subset had superior diagnostic potential over the other (Supplementary Table 7). Additionally, AUCs of biomarkers defined on M.tb lysate-specific activation and functional differentiation were all similar (p-value > 0.05). Thus, based on these results, M.tb antigen-specific T cell HLA-DR expression was identified as the best biomarker of recent M.tb infection in this dataset.

4. Discussion

The risk of disease progression in M.tb infected individuals, identified by a positive IGRA or TST, is highest within the first 1-2 years after acquisition of M.tb infection [2,6]. Identification of individuals who recently became infected, and who would thus benefit most from tuberculosis preventive therapy, has only been possible with serial IGRA or TST testing. We performed in-depth analyses of M.tb-specific CD4 T cell function, activation and memory phenotypes to identify immunological differences between individuals who recently acquired infection and those with persistent (remote) infection. Three major points emerged from our study: 1) The acute response to M.tb-infection in humans was associated with highly activated M.tb-specific CD4 T cells that are moderately differentiated; 2) During remote infection M.tb-specific T cells were not activated but showed a phenotype consistent with long-term antigen exposure without evidence of exhaustion; 3) Among all the differences in M.tb-specific T cell phenotype and functions, HLA-DR expression had the highest diagnostic performance to distinguish between recent and remote infection.

We showed that recent acquisition of M.tb infection (QFT conversion from negative to positive) was associated with an increase in frequencies of Th1 (IFN-γ, IL-2 and TNF) cytokine-expressing CD4 T cells to levels in range with those detected in individuals with remote M.tb infection. We did not observe marked differences in cytokine co-expression profiles between recent and remote infection and therefore focused our analysis on combinations of Th1 cytokine co-expression (polyfunctional) profiles and T cell differentiation. As typical for T cell responses during acute and chronic infection [13], we observed a predominance of M.tb-specific highly activated cells and T_E cells upon recent acquisition of infection. The only distinguishing features between recent and remote infection were higher M.tb-specific T cell activation and lower proportions of M.tb lysate-specific KLRG-1+ IFN-γ+TNF+IL-2- T_E cells in recently compared to remotely infected individuals, while CFP-10/ESAT-6-specific T cell functional and memory profiles were very similar. In addition to being used as a proxy for T cell activation, HLA-DR expression by T cells has been suggested to facilitate antigen presentation to other T cells during times of high antigen burden [15,16], thus providing an additional source of cells beyond professional antigen presenting cells that can induce *de novo* T cell priming. Here we present human evidence, in line with findings observed in murine models [10], that suggests M.tb antigen load is higher during the acute phase of infection compared to more established phases of infection, when bacterial load is at least partially controlled.

Murine studies have also demonstrated that chronic M.tb infection is associated with differentiation of CD4 T cells to an exhausted T cell memory phenotype that expresses high levels of KLRG-1 and IFN-γ-monofunctional capacity, and poor ability to contribute to antigen clearance [24,25]. In contrast with these observations from mice, here we show that despite long-term QFT-positivity, M.tb-specific T cells in remotely infected individuals did not have a dominance of KLRG-1+ IFN-γ-monofunctional exhausted T cells, nor did they show elevated activation consistent with persistently high antigen

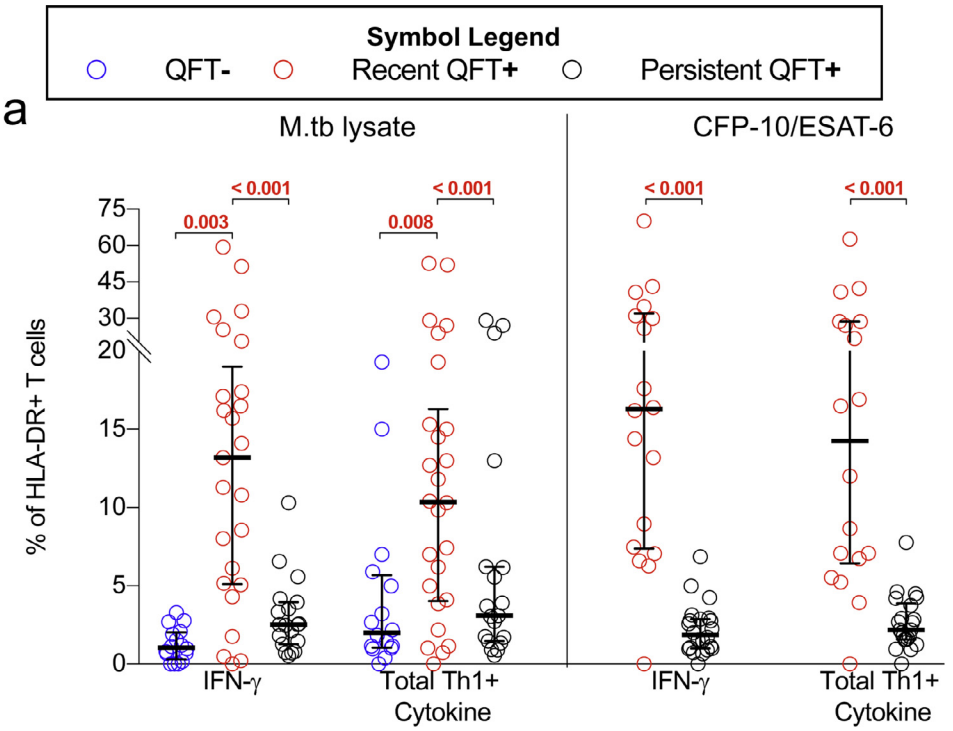

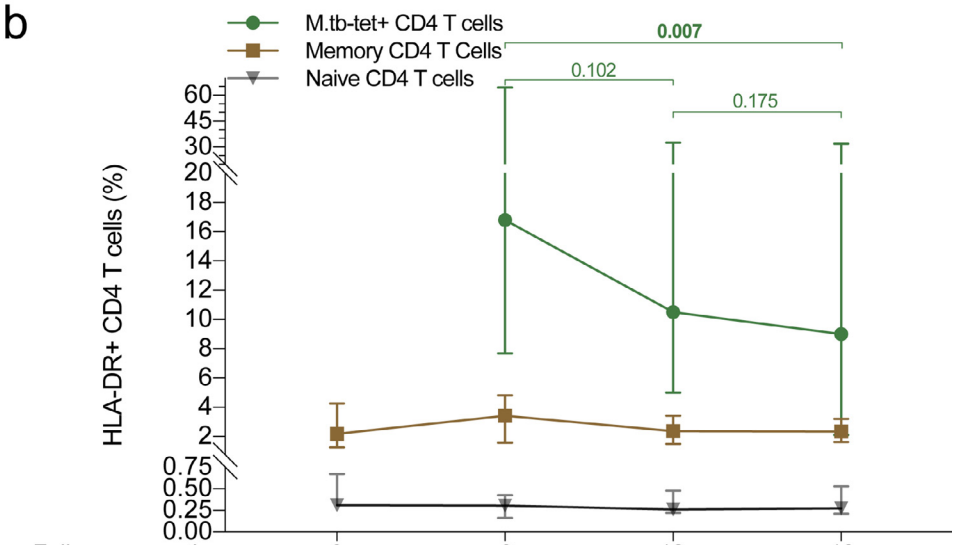

Follow up month	0	6	12	18
QFT	-	+	+	+
n	11	12	11	12
p -values				
M.tb tet+ vs Bulk Memory cells	-	**< 0.001**	**0.001**	**0.009**
M.tb tet+ vs Naïve cells	-	**< 0.001**	**0.001**	**0.002**
Bulk Memory vs Naïve cells	**0.001**	**< 0.001**	**0.001**	**< 0.001**

Fig. 5. Recent QFT+ is associated with higher levels of T cell activation than persistent QFT+. (a) Graphs depict proportions of HLA-DR+ CFP-10/ESAT-6- and M.tb lysate-specific IFN-γ+ or Total Th1 cytokine+ (IFN-$\gamma\pm$TNF$\pm$IL-2$\pm$) CD4 T cells before (QFT−, blue, M.tb lysate: n= 16), after (recent QFT+, red, CFP-10/ESAT-6: n=18; M.tb lysate: n= 25), and during persistent M.tb infection (persistent QFT+, black, CFP-10/ESAT-6: n=22; M.tb lysate: n=19). Statistical analysis was conducted as in Fig. 2. (b) Proportions of HLA-DR+ M.tb-specific tetramer+ (green), bulk naïve (grey, CD45RA+CCR7+CD27+CD95-) and bulk memory (brown, non-naïve T cells) CD4+ T cells are represented by median (symbol) and IQRs (bars) in recent QFT+ (tetramer cohort, Month 0: n = 11; Month 6: n=12; Month 11: n=17; Month 18: n=12) individuals. Some individuals were stained with more than one tetramer. P-values for (b) were calculated with the Wilcoxon signed-rank test. P-values <0.016 (for a) and < 0.05 (for b), highlighted in **bold** were considered significant.

load. Instead, the activation levels of M.tb lysate-specific CD4 T cells during remote M.tb infection were not different to those observed before M.tb infection, suggesting little or no *in vivo* antigen exposure during remote M.tb infection. This may suggest that clearance of M.tb is rapid and usually occurs within 2 years in individuals who do not progress to disease. Under this scenario, immune responses detected

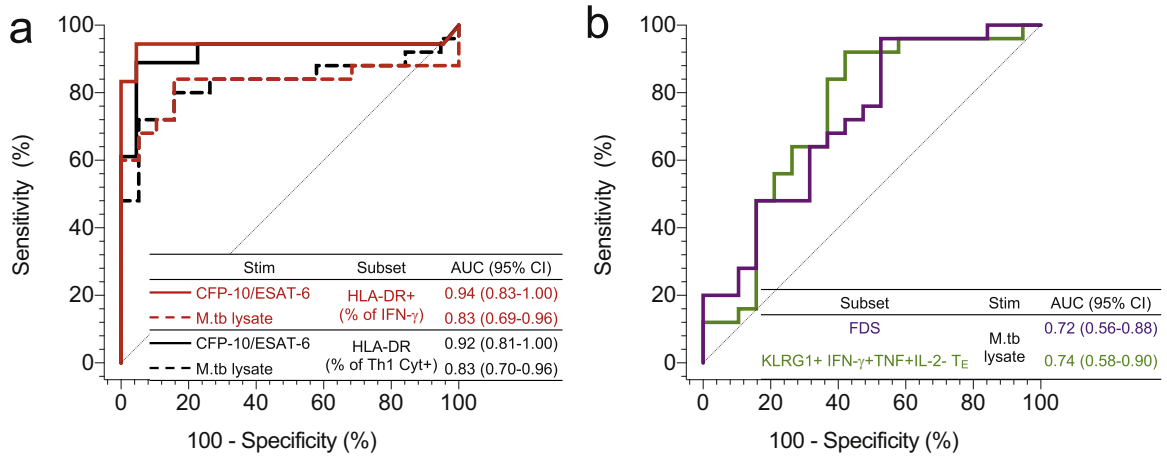

Fig. 6. T cell activation is a biomarker of recent M.tb infection. ROC analysis of the diagnostic potential of M.tb-specific CD4 T cells subsets: (a) IFN-γ+ and Th1 cytokine+ T cell activation and (b) polyfunctional/memory subsets. All populations are significant based on 95% confidence intervals (CI) that do not cross 0.5.

in most remotely infected individuals represent immunological memory, and not necessarily ongoing M.tb replication [2]. This is also consistent with our observation that the functional and memory differentiation profiles of CFP-10/ESAT-6-specific T cells were not different during recent and remote M.tb infection, suggesting that these features are shaped during primary infection and remain relatively unchanged regardless of duration of antigen exposure. Alternatively, if remotely infected individuals truly harbour M.tb, as suggested by the higher functional differentiation of M.tb-specific T cells compared to recent infection, then levels of M.tb replication are likely low and stable, resulting in low T cell activation and a memory-functional phenotype not characteristic of T cell exhaustion. It is likely that persistent QFT+ status in humans represents a mixture of these scenarios.

Finally, we showed that of all the immunological features that were different between recent and remote M.tb infection, T cell activation was the best biomarker for differentiating between infection states. Overall, the T cell activation biomarker appears very robust, regardless of mycobacterial antigen specificity (M.tb lysate or CFP-10/ESAT-6) or the assay used for detection (PBMC-ICS, tetramer staining or, as previously reported, whole blood stimulation [17–22]). This study focused on understanding T cell immunobiology during acquisition of M.tb infection and the discovery of potential biomarkers to distinguish between recent and remote M.tb infection. Development of a simplified assay to identify such individuals in clinical settings, including validation in a test cohort and performance as a marker of disease progression, are beyond the scope of this paper and were reported separately [43]. In this follow-up study [43], we showed that levels of HLA-DR expression on CFP-10/ESAT-6-specific T cells were not significantly different in TB patients compared to recently infected individuals. This observation further supports the hypothesis that T cell activation may track levels of *in vivo* antigen exposure, which is expected to be higher during recent M.tb infection and active disease compared to remote asymptomatic infection. This biomarker has the potential to identify individuals who are at high risk of progression and should receive tuberculosis preventive treatment, a key priority highlighted in the recent Global Tuberculosis Report [1], and differentiate them from those who are at low risk of progression and could be spared from treatment.

A limitation of this study was the small sample size and relatively short duration of follow-up of recently infected individuals, none of whom progressed to disease during the study. This prevented us from demonstrating how immunity in recently infected individuals who either progress to disease or develop persistent M.tb infection differ. Ideally, the M.tb-specific T cell activation biomarker should be prospectively validated on a cohort of individuals who acquire M.tb infection and then progress to disease. This would be an extraordinarily large study to conduct, since on a population level only a minority of individuals who acquire M.tb infection progress to disease [44]. Further, limited sample availability prevented us from testing other recently described biomarkers, such as those based on T cell proliferation [32] or gene expression [33]. Finally, despite broad similarities between immune responses detected in our adolescent cohort and other cohorts of healthy M.tb-infected adults, showing a predominant Th1 polyfunctional profile and T_{EFF} phenotype [14,19,27,28,45,46] of M.tb-specific CD4 T cells, the biomarker proposed by Halliday et al. [31] did not stratify recent and remote infection in our study. Experimental differences may account for this

Table 1
AUCROC comparison of potential biomarkers of recent M.tb infection.

CD4 T cell Subset 1			CD4 T cell Subset 2			Roc test *p*-value
Subset	*Stim*	*AUCROC (95% CI)*	*Subset*	*Stim*	*AUCROC (95% CI)*	
HLA-DR % of IFN-γ+	CFP-10/ESAT-6	0.94 (0.83–1.00)	FDS	M.tb lysate	0.72 (0.56–0.88)	**0.018**
			KLRG- 1+ IFN-γ+TNF+IL-2- T_E		0.74 (0.58–0.90)	**0.035**
HLA-DR % of IFN-γ+TNF+		0.94 (0.84–1.00)	FDS		0.72 (0.56–0.88)	**0.014**
			KLRG- 1+ IFN-γ+TNF+IL-2- T_E		0.74 (0.58–0.90)	**0.030**
HLA-DR % of Th1 Cyt+		0.92 (0.81–1.00)	FDS		0.72 (0.56–0.88)	**0.039**
			KLRG- 1+ IFN-γ+TNF+IL-2- T_E		0.74 (0.58–0.90)	0.062

We only report AUC comparisons that had a ROC test *p*-value < 0.10, all other comparisons are reported in **Supplementary Table 7.** *P*-values highlighted in **red, bold** text were considered significant.

discrepancy, including the different antigenic stimulation (purified protein derivative *versus* M.tb lysate) and the definition of T_{EFF} cells (which did not include CD127 expression in our panel).

In summary, we characterised changes in M.tb-specific T cell immunity in different phases of infection and present evidence of a peak in T cell activation, probably reflecting high M.tb burden, during recent infection followed by unexhausted T cell functional and memory phenotypes during remote, non-progressing infection, consistent with control or clearance of M.tb [2].

Declaration of Interests

EN reports grants to the University of Cape Town from AERAS, Bill & Melinda Gates Foundation and NIH during the conduct of the study. TJS reports grants to the University of Cape Town from AERAS, Bill & Melinda Gates Foundation, and NIH during the conduct of the study.

All other authors declare no competing interests.

Acknowledgements

We are grateful to the study participants and their families; the Cape Winelands East district communities, the Department of Education and the Department of Health; the SATVI clinical and laboratory teams; Thomas Hawn, Morten Ruhwald and Jason Andrews for valuable input on the study design. US NIH (R21AI127121) funded the study. This work was also supported by Global Health Grant OPP1066265 from the Bill & Melinda Gates Foundation and South African Medical Research Council. The South African National Research Foundation and the University of Cape Town funded scholarships to CM. The ACS study was supported by Aeras and BMGF GC12 (grant 37885) for QFT testing.

Data sharing statement

Data presented in this manuscript is available at Figshare URL: https://doi.org/10.25375/uct.13490901.v1.

Supplementary materials

Supplementary material associated with this article can be found in the online version at doi:10.1016/j.ebiom.2021.103233.

References

[1] World Health Organisation. Global tuberculosis report 2020. Licence: CC BY-NC-SA 3.0 IGO. Available from: https://www.who.int/tb/publications/global_report/en/ (Accessed October 15 2020).
[2] Behr MA, Edelstein PH, Ramakrishnan L. Revisiting the timetable of tuberculosis. BMJ 2018;362:k2738. doi: 10.1136/bmj.k2738.
[3] Erkens CGM, Slump E, Verhagen M, Schimmel H, Cobelens F, Hof S van den. Risk of developing tuberculosis disease among persons diagnosed with latent tuberculosis infection in the Netherlands. Eur Respir J 2016;48:1420–8. doi: 10.1183/13993003.01157-2016.
[4] Morán-Mendoza O, Marion SA, Elwood K, Patrick D, FitzGerald JM. Risk factors for developing tuberculosis: a 12-year follow-up of contacts of tuberculosis cases. Int J Tuberc Lung Dis Off J Int Union Against Tuberc Lung Dis 2010;14:1112–9.
[5] Trauer JM, Moyo N, Tay E-L, Dale K, Ragonnet R, McBryde ES, et al. Risk of active tuberculosis in the five years following infection . . . 15%? Chest 2016;149:516–25. doi: 10.1016/j.chest.2015.11.017.
[6] Wiker HG, Mustafa T, Bjune GA, Harboe M. Evidence for waning of latency in a cohort study of tuberculosis. BMC Infect Dis 2010;10:37. doi: 10.1186/1471-2334-10-37.
[7] Andrews JR, Noubary F, Walensky RP, Cerda R, Losina E, Horsburgh CR. Risk of progression to active tuberculosis following reinfection with mycobacterium tuberculosis. Clin Infect Dis 2012;54:784–91. doi: 10.1093/cid/cir951.
[8] Behr MA, Edelstein PH, Ramakrishnan L. Is Mycobacterium tuberculosis infection life long? Bmj Clin Res Ed 2019;367:l5770. doi: 10.1136/bmj.l5770.
[9] Cadena AM, Hopkins FF, Maiello P, Carey AF, Wong EA, Martin CJ, et al. Concurrent infection with Mycobacterium tuberculosis confers robust protection against secondary infection in macaques. Plos Pathog 2018;14:e1007305. doi: 10.1371/journal.ppat.1007305.
[10] North RJ, Jung Y-J. Immunity to tuberculosis. Immunology 2004;22:599–623. doi: 10.1146/annurev.immunol.22.012703.104635.
[11] Lin PL, Ford CB, Coleman MT, Myers AJ, Gawande R, Ioerger T, et al. Sterilization of granulomas is common in active and latent tuberculosis despite within-host variability in bacterial killing. Nat Med 2014;20:75–9. doi: 10.1038/nm.3412.
[12] Andersen P, Doherty TM, Pai M, Weldingh K. The prognosis of latent tuberculosis: can disease be predicted? Trends Mol Med 2007;13:175–82. doi: 10.1016/j.molmed.2007.03.004.
[13] Seder RA, Darrah PA, Roederer M. T-cell quality in memory and protection: implications for vaccine design. Nat Rev Immunol 2008;8:nri2274. doi: 10.1038/nri2274.
[14] Moguche AO, Musvosvi M, Penn-Nicholson A, Plumlee CR, Mearns H, Geldenhuys H, et al. Antigen availability shapes T cell differentiation and function during tuberculosis. Cell Host Microbe 2017;21:695–706.e5. doi: 10.1016/j.chom.2017.05.012.
[15] Aversa GG, Hall BM. Cell surface markers of T-cell activation. Transpl Rev 1991;5:9–30. doi: 10.1016/s0955-470x(10)80024-2.
[16] Mangalam A, Rodriguez M, David C. Role of MHC class II expressing CD4+ T cells in proteolipid protein91−110-induced EAE in HLA-DR3 transgenic mice. Eur J Immunol 2006;36:3356–70. doi: 10.1002/eji.200636217.
[17] Adekambi T, Ibegbu CC, Cagle S, Kalokhe AS, Wang YF, Hu Y, et al. Biomarkers on patient T cells diagnose active tuberculosis and monitor treatment response. J Clin Invest 2015;125:1827–38. doi: 10.1172/jci77990.
[18] Wilkinson KA, Oni T, Gideon HP, Goliath R, Wilkinson RJ, Riou C. Activation profile of mycobacterium tuberculosis−specific CD4+ T cells reflects disease activity irrespective of HIV status. Am J Resp Crit Care 2016;193:1307–10. doi: 10.1164/rccm.201601-0116le.
[19] Riou C, Berkowitz N, Goliath R, Burgers WA, Wilkinson RJ. Analysis of the phenotype of mycobacterium tuberculosis-specific CD4+ T cells to discriminate latent from active tuberculosis in HIV-uninfected and HIV-infected individuals. Front Immunol 2017;8:968. doi: 10.3389/fimmu.2017.00968.
[20] Musvosvi M, Duffy D, Filander E, Africa H, Mabwe S, Jaxa L, et al. T-cell biomarkers for diagnosis of tuberculosis: candidate evaluation by a simple whole blood assay for clinical translation. Eur Respir J 2018;51:1800153. doi: 10.1183/13993003.00153-2018.
[21] Silveira-Mattos PS, Barreto-Duarte B, Vasconcelos B, Fukutani KF, Vinhaes CL, Oliveira-de-Souza D, et al. Differential expression of activation markers by Mycobacterium tuberculosis-specific CD4+ T-cell distinguishes extrapulmonary from pulmonary tuberculosis and latent infection. Clin Infect Dis 2019;71:1905–11. doi: 10.1093/cid/ciz1070.
[22] Riou C, Bruyn ED, Ruzive S, Goliath RT, Arlehamn CSL, Sette A, et al. Disease extent and anti-tubercular treatment response correlates with Mycobacterium tuberculosis-specific CD4 T-cell phenotype regardless of HIV-1 status. Clin Transl Immunol 2020;9:e1176. doi: 10.1002/cti2.1176.
[23] Kirman JR, Quinn KM, Seder RA. Immunological memory. Immunol Cell Biol 2019;97:615–6. doi: 10.1111/imcb.12280.
[24] Sallin MA, Sakai S, Kauffman KD, Young HA, Zhu J, Barber DL. Th1 differentiation drives the accumulation of intravascular, non-protective CD4 T cells during tuberculosis. Cell Rep 2017;18:3091–104. doi: 10.1016/j.celrep.2017.03.007.
[25] Sakai S, Mayer-Barber KD, Barber DL. ScienceDirect defining features of protective CD4 T cell responses to Mycobacterium tuberculosis. Curr Opin Immunol 2014;29:137–42. doi: 10.1016/j.coi.2014.06.003.
[26] Abubakar I, Drobniewski F, Southern J, Sitch AJ, Jackson C, Lipman M, et al. Prognostic value of interferon-γ release assays and tuberculin skin test in predicting the development of active tuberculosis (UK PREDICT TB): a prospective cohort study. Lancet Infect Dis 2018;18:1077–87. doi: 10.1016/s1473-3099(18)30355-4.
[27] Harari A, Rozot V, Enders FB, Perreau M, Stalder JM, Nicod LP, et al. Dominant TNF-α+ Mycobacterium tuberculosis−specific CD4+ T cell responses discriminate between latent infection and active disease. Nat Med 2011;17:372–6. doi: 10.1038/nm.2299.
[28] Rozot V, Patrizia A, Vigano S, Mazza-Stalder J, Idrizi E, Day CL, et al. Combined use of mycobacterium tuberculosis−specific CD4 and CD8 T-cell responses is a powerful diagnostic tool of active tuberculosis. Clin Infect Dis 2015;60:432–7. doi: 10.1093/cid/ciu795.
[29] Petruccioli E, Petrone L, Vanini V, Cuzzi G, Navarra A, Gualano G, et al. Assessment of CD27 expression as a tool for active and latent tuberculosis diagnosis. J Infect 2015;71:1–8. doi: 10.1016/j.jinf.2015.07.009.
[30] Portevin D, Moukambi F, Clowes P, Bauer A, Chachage M, Ntinginya NE, et al. Assessment of the novel T-cell activation marker−tuberculosis assay for diagnosis of active tuberculosis in children: a prospective proof-of-concept study. Lancet Infect Dis 2014;14:931–8. doi: 10.1016/s1473-3099(14)70884-9.
[31] Halliday A, Whitworth H, Kottoor SH, Niazi U, Menzies S, Kunst H, et al. Stratification of latent mycobacterium tuberculosis infection by cellular immune profiling. J Infect Dis 2017;215:1480–7. doi: 10.1093/infdis/jix107.
[32] Borgström EW, Fröberg G, Correia-Neves M, Atterfelt FB, Bellbrant J, Szulkin R, et al. CD4+ T cell proliferative responses to PPD and CFP-10 associate with recent M. tuberculosis infection. Tuberculosis 2020;123:101959. doi: 10.1016/j.tube.2020.101959.
[33] Ault RC, Headley CA, Hare AE, Carruthers BJ, Mejias A, Turner J. Blood RNA signatures predict recent tuberculosis exposure in mice, macaques and humans. Sci Rep 2020;10:16873. doi: 10.1038/s41598-020-73942-z.
[34] Nemes E, Rozot V, Geldenhuys H, Bilek N, Mabwe S, Abrahams D, et al. Optimization and interpretation of serial QuantiFERON testing to measure acquisition of mycobacterium tuberculosis infection. Am J Resp Crit Care 2017;196:638–48. doi: 10.1164/rccm.201704-0817oc.

[35] Mpande CAM, Dintwe OB, Musvosvi M, Mabwe S, Bilek N, Hatherill M, et al. Functional, antigen-specific stem cell memory (TSCM) CD4+ T cells are induced by human mycobacterium tuberculosis infection. Front Immunol 2018;9:324. doi: 10.3389/fimmu.2018.00324.
[36] Sidney J, Southwood S, Oseroff C, Guercio M, Sette A, Grey HM. Measurement of MHC/peptide interactions by gel filtration. Curr Protoc Immunol 2001;31 18.3.1-18.3.19. doi: 10.1002/0471142735.im1803s31.
[37] Wang P, Sidney J, Dow C, Mothé B, Sette A, Peters B. A systematic assessment of MHC class II peptide binding predictions and evaluation of a consensus approach. PLoS Comput Biol 2008;4:e1000048. doi: 10.1371/journal.pcbi.1000048.
[38] Lin L, Finak G, Ushey K, Seshadri C, Hawn TR, Frahm N, et al. COMPASS identifies T-cell subsets correlated with clinical outcomes. Nat Biotechnol 2015;33:610–6. doi: 10.1038/nbt.3187.
[39] Roederer M, Nozzi JL, Nason MC. SPICE: exploration and analysis of post-cytometric complex multivariate datasets. Cytom Part A 2011;79A:167–74. doi: 10.1002/cyto.a.21015.
[40] Finak G, McDavid A, Chattopadhyay P, Dominguez M, Rosa SD, Roederer M, et al. Mixture models for single-cell assays with applications to vaccine studies. Biostatistics 2013;15:87–101. doi: 10.1093/biostatistics/kxt024.
[41] Bruggner RV, Bodenmiller B, Dill DL, Tibshirani RJ, Nolan GP. Automated identification of stratifying signatures in cellular subpopulations. Proc Natl Acad Sci 2014;111:E2770–7. doi: 10.1073/pnas.1408792111.
[42] Robin X, Turck N, Hainard A, Tiberti N, Lisacek F, Sanchez J-C, et al. pROC: an open-source package for R and S+ to analyze and compare ROC curves. BMC Bioinform 2011;12:77. doi: 10.1186/1471-2105-12-77.
[43] Mpande CAM, Musvosvi M, Rozot V, Mosito B, Reid TD, Schreuder C, et al. Antigen-specific T cell activation distinguishes between recent and remote tuberculosis infection. Am J Resp Crit Care 2021 [in production]. doi: 10.1164/rccm.202007-2686oc.
[44] Machingaidze S, Verver S, Mulenga H, Abrahams D-A, Hatherill M, Hanekom W, et al. Predictive value of recent QuantiFERON conversion for tuberculosis disease in adolescents. Am J Resp Crit Care 2012;186:1051–6. doi: 10.1164/rccm.201206-1134oc.
[45] Jasenosky LD, Scriba TJ, Hanekom WA, Goldfeld AE. T cells and adaptive immunity to Mycobacterium tuberculosis in humans. Immunol Rev 2015;264:74–87. doi: 10.1111/imr.12274.
[46] Adekambi T, Ibegbu CC, Kalokhe AS, Yu T, Ray SM, Rengarajan J. Distinct effector memory CD4+ T cell signatures in latent mycobacterium tuberculosis infection, BCG vaccination and clinically resolved tuberculosis. PLoS One 2012;7:e36046. doi: 10.1371/journal.pone.0036046.

Check for updates

ORIGINAL ARTICLE

Antigen-Specific T-Cell Activation Distinguishes between Recent and Remote Tuberculosis Infection

Cheleka A. M. Mpande[1], Munyaradzi Musvosvi[1], Virginie Rozot[1], Boitumelo Mosito[1], Timothy D. Reid[1], Constance Schreuder[1], Tessa Lloyd[1], Nicole Bilek[1], Huang Huang[2], Gerlinde Obermoser[2], Mark M. Davis[2], Morten Ruhwald[3,4], Mark Hatherill[1], Thomas J. Scriba[1]*, Elisa Nemes[1]*, and the ACS Study Team

[1]South African Tuberculosis Vaccine Initiative, Institute of Infectious Disease and Molecular Medicine, Division of Immunology, Department of Pathology, University of Cape Town, Cape Town, South Africa; [2]Institute for Immunity, Transplantation and Infection, Stanford University School of Medicine, Stanford, California; [3]Statens Serum Institute, Copenhagen, Denmark; and [4]Foundation of Innovative New Diagnostics, Geneva, Switzerland

ORCID IDs: 0000-0003-3438-2214 (C.A.M.M.); 0000-0003-1662-4961 (E.N.); 0000-0002-0641-1359 (T.J.S.)

Abstract

Rationale: Current diagnostic tests fail to identify individuals at higher risk of progression to tuberculosis disease, such as those with recent *Mycobacterium tuberculosis* infection, who should be prioritized for targeted preventive treatment.

Objectives: To define a blood-based biomarker, measured with a simple flow cytometry assay, that can stratify different stages of tuberculosis infection to infer risk of disease.

Methods: South African adolescents were serially tested with QuantiFERON-TB Gold to define recent (QuantiFERON-TB conversion <6 mo) and persistent (QuantiFERON-TB+ for >1 yr) infection. We defined the ΔHLA-DR median fluorescence intensity biomarker as the difference in HLA-DR expression between IFN-γ^+ TNF^+ *Mycobacterium tuberculosis*–specific T cells and total $CD3^+$ T cells. Biomarker performance was assessed by blinded prediction in untouched test cohorts with recent versus persistent infection or tuberculosis disease and by unblinded analysis of asymptomatic adolescents with tuberculosis infection who remained healthy (nonprogressors) or who progressed to microbiologically confirmed disease (progressors).

Measurements and Main Results: In the test cohorts, frequencies of *Mycobacterium tuberculosis*–specific T cells differentiated between QuantiFERON-TB− ($n = 25$) and QuantiFERON-TB+ ($n = 47$) individuals (area under the receiver operating characteristic curve, 0.94; 95% confidence interval, 0.87–1.00). ΔHLA-DR significantly discriminated between recent ($n = 20$) and persistent ($n = 22$) QuantiFERON-TB+ (0.91; 0.83–1.00); persistent QuantiFERON-TB+ and newly diagnosed tuberculosis ($n = 19$; 0.99; 0.96–1.00); and tuberculosis progressors ($n = 22$) and nonprogressors ($n = 34$; 0.75; 0.63–0.87). However, ΔHLA-DR median fluorescent intensity could not discriminate between recent QuantiFERON-TB+ and tuberculosis (0.67; 0.50–0.84).

Conclusions: The ΔHLA-DR biomarker can identify individuals with recent QuantiFERON-TB conversion and those with disease progression, allowing targeted provision of preventive treatment to those at highest risk of tuberculosis. Further validation studies of this novel immune biomarker in various settings and populations at risk are warranted.

Keywords: tuberculosis infection; QuantiFERON-TB Gold; biomarker; tuberculosis risk; recent tuberculosis infection

(Received in original form July 6, 2020; accepted in final form January 6, 2021)

This article is open access and distributed under the terms of the Creative Commons Attribution Non-Commercial No Derivatives License 4.0 (https://creativecommons.org/licenses/by-nc-nd/4.0/). For commercial usage and reprints, please contact Diane Gern (dgern@thoracic.org).

A complete list of the ACS Study Team may be found before the beginning of the References.

*Co–senior authors.

Supported by the U.S. NIH (R21AI127121), Bill and Melinda Gates Foundation (OPP1066265, OPP1113682, GC 6-74 Grant 37772, and GC12 Grant 37885), Aeras, and the Strategic Health Innovation Partnerships Unit of the South African Medical Research Council with funds received from the South African Department of Science and Technology. Carnegie Corporation of New York funded scholarships to M.M.; South African National Research Foundation and the University of Cape Town funded C.A.M.M. The funding sources had no role in study design, data collection, analysis and interpretation, writing, and submission of the manuscript.

Author Contributions: M.M.D., M.R., M.H., T.J.S., and E.N. designed the study and raised funding. C.A.M.M., M.M., B.M., T.D.R., C.S., N.B., H.H., and G.O. generated the data. C.A.M.M., M.M., V.R., T.L., and H.H. analyzed the data. C.A.M.M., M.M., V.R., M.M.D., M.R., M.H., T.J.S., and E.N. interpreted the results. C.A.M.M., M.M., V.R., T.J.S., and E.N. wrote the manuscript. All authors revised and approved the manuscript and are accountable for the work.

Data are available on the zivahub UCT platform (https://zivahub.uct.ac.za), DOI: 10.25375/uct.14761596.

Correspondence and requests for reprints should be addressed to Elisa Nemes, Ph.D., Faculty of Health Sciences, University of Cape Town, Room S2.02, Wernher-Beit South Building, Anzio Road, 7925 Observatory, Cape Town, South Africa. E-mail: elisa.nemes@uct.ac.za.

This article has a related editorial.

This article has an online supplement, which is accessible from this issue's table of contents at www.atsjournals.org.

Am J Respir Crit Care Med Vol 203, Iss 12, pp 1556–1565, Jun 15, 2021

Copyright © 2021 by the American Thoracic Society

Originally Published in Press as DOI: 10.1164/rccm.202007-2686OC on January 6, 2021
Internet address: www.atsjournals.org

At a Glance Commentary

Scientific Knowledge on the Subject: Preventive treatment of individuals with *Mycobacterium tuberculosis* (*M.tb*) infection who are at high risk of progressing to active tuberculosis is a key strategy to reduce the global tuberculosis burden. Current diagnostic tests can identify persons with tuberculosis and those with *M.tb* infection; however, these tests cannot distinguish who, among those with asymptomatic *M.tb* infection, are most likely to progress to tuberculosis and would therefore benefit most from preventive treatment.

What This Study Adds to the Field: We present novel evidence that *M.tb*-specific T cells from healthy individuals with recently acquired *M.tb* infection and individuals progressing to active disease are highly activated but *M.tb*-specific T cells from those with remote *M.tb* infection and nonprogressors are not. The ΔHLA-DR median fluorescent intensity biomarker has utility as a screening test to identify individuals who would warrant further clinical investigation and microbiological tests to guide the administration of either tuberculosis preventive therapy or a full course of tuberculosis treatment. Further large-scale validation of the ΔHLA-DR median fluorescent intensity biomarker is warranted.

Tuberculosis (TB) is an ongoing global threat causing an estimated 10 million incident cases and approximately 1.4 million deaths (1) and was the leading cause of death due to a single infectious agent in 2019. A key strategy to alleviate the global burden of TB, promoted by the World Health Organization, is to provide TB preventive therapy (TPT) to individuals with *Mycobacterium tuberculosis* (*M.tb*) infection who are at risk of disease progression (1, 2). Current diagnostic tests can identify persons with TB (sputum-based microbiological tests) and those with infection (tuberculin skin test [TST] or IFN-γ release assays [IGRAs]). However, these tests cannot distinguish who, among those with asymptomatic infection, are at high risk of progressing to active disease and should receive TPT.

In countries with low TB burden and/or high income, TPT is standard of care for persons with clinical and epidemiological risk factors or a diagnosis of *M.tb* infection, and it reduces the risk of TB (3, 4). On the other hand, in many countries where *M.tb* is endemic, >50% of adults may already be infected (5), making the provision of TPT infeasible and unaffordable, especially without knowledge of exposure history and considering the high risk of reinfection after treatment completion in high transmission settings (6, 7). Furthermore, given the small proportion of individuals with *M.tb* infection who are actually at risk of TB progression, the provision of TPT to all those infected exposes many individuals to unnecessary side effects.

The highest risk of TB progression occurs within the first 1–2 years after primary infection (8–10). By contrast, more remote or persistent infection is associated with a lower risk of TB (8, 9). In fact, remote *M.tb* infection has been associated with a significantly lower risk of disease progression compared with recent infection (11, 12), and there is evidence that many individuals with remote *M.tb* exposure may actually have cleared *M.tb* (13). A blood-based biomarker that could distinguish between recent and remote infection would therefore allow targeted TPT to those with recent infection and could potentially transform the clinical management of TB, regardless of setting (14). Unfortunately, current diagnostic tests for *M.tb* infection only measure immunological sensitization to *M.tb* and cannot distinguish between recent and remote infection. Improving tools for detecting *M.tb* infection and testing for progression to TB is a key priority in the Global Plan to End TB (15).

M.tb-specific T-cell features, such as activation (16–20), differentiation (21, 22) and cytokine coexpression profiles (23, 24), have shown promising diagnostic applications to distinguish *M.tb* infection from TB, and to monitor treatment response. The underlying hypothesis is that all these biomarkers reflect *M.tb* antigen load, which is higher during TB compared with controlled infection, and that treatment effectively reduces *M.tb* load (16, 20). We postulated that recent *M.tb* infection is associated with a high initial *M.tb* load that is ultimately controlled by immune responses in those with remote infection who do not progress to disease. We also postulated that progression from *M.tb* infection to disease is associated with an increase in *M.tb* load (25). This is supported by our previous study in progressors, which showed increased inflammation and activation of bulk CD4 T cells before clinical onset (26). In line with this principle, Halliday and colleagues discovered that proportions of *M.tb*-specific TNF^{+} IFN-γ^{-} $IL\text{-}2^{-}$ CD4 T cells with an effector phenotype distinguished between recent and remote *M.tb* infection (27).

In this study, we hypothesized that individuals with high-risk *M.tb* infection, associated with recent QuantiFERON-TB Gold (QFT) conversion, and progressors to TB disease have higher levels of *M.tb*-specific T-cell activation in peripheral blood compared with individuals with persistently QFT-positive results at low risk of progression. We aimed to develop a simplified assay that could stratify, for the first time, the entire spectrum of *M.tb* from acquisition of infection to clinical disease and through treatment response that is amenable to clinical translation and further large-scale clinical validation.

Some of the results of these studies have been previously reported in the form of abstracts (28–33) and a preprint (medRxiv [29 June 2020] https://doi.org/10.1101/2020.06.26.20135665).

Methods

Study Participants

Different groups of adolescents and adults enrolled in observational studies approved by the University of Cape Town Human Research Ethics Committee (protocol references: 045/2005, 088/2008, and 102/2017) were included the training, test, and TB progressor cohorts (Figure 1 and Table 1). Detailed inclusion and exclusion criteria are described in the online supplement.

Adolescents were selected on the basis of QFT (Cellestis) and/or TST results and sample availability from a large epidemiological study conducted in the

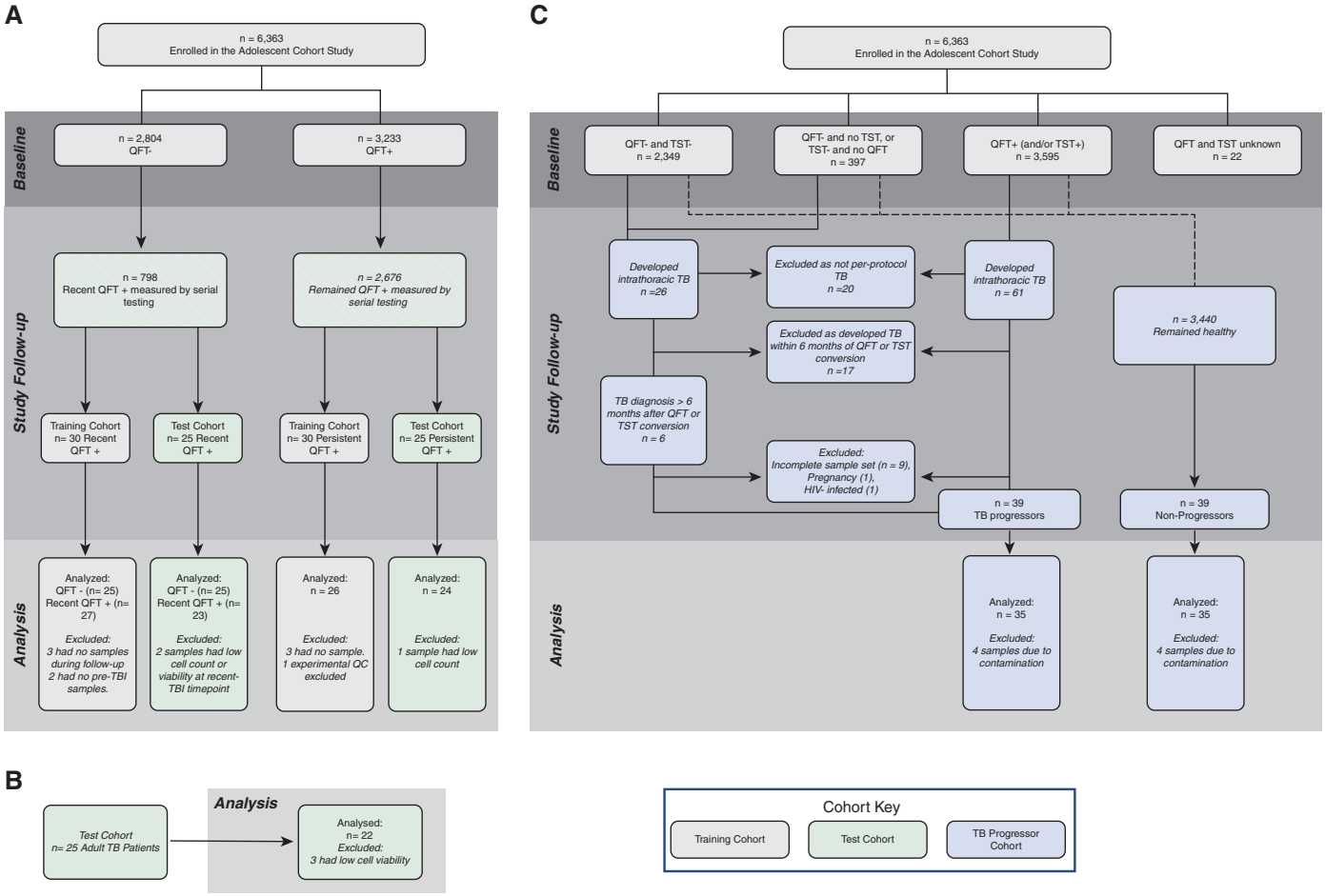

Figure 1. Study design. Adolescent participants were selected on the basis of peripheral blood mononuclear cell sample availability from a larger epidemiological study, the Adolescent Cohort Study (10). (*A*) Inclusions and exclusions for recent and remote QFT+ individuals in the training and test cohorts. (*B*) Adults with tuberculosis diagnosis sampled cross-sectionally (40). (*C*) Reasons for inclusion and exclusion of participants in progressor and nonprogressor cohorts. QC = quality control; QFT = QuantiFERON-TB Gold; TB = tuberculosis; TBI = tuberculosis infection; TST = tuberculin skin test.

Worcester Area, Western Cape, South Africa (2005–2009), a region with high TB incidence (10). Recent *M.tb* infection (recent QFT+) was defined in healthy participants by two negative QFT tests (IFN-γ <0.35 IU/ml with at least one test <0.2 IU/ml) followed by two positive QFT tests (IFN-γ ⩾0.35 IU/ml with at least one test >0.7 IU/ml) 6 months apart over 1.5 years (Figures E1A and E1B in the online supplement) (34). Remote *M.tb* infection (persistent QFT+) was defined in healthy participants by four consecutive positive QFT tests 6 months apart over 1.5 years with at least two QFT-positive results >0.7 IU/ml (Figures E1A and E1B). Clinical definitions for the adolescents selected for TB nonprogressors and progressors in the TB progressor cohort have been described (26, 35) and are available in the online supplement.

Adults with recently diagnosed pulmonary TB by positive Xpert MTB/RIF (Cepheid) were recruited before treatment initiation.

Peripheral Blood Mononuclear Cell Stimulation and Staining Protocols

Cryopreserved peripheral blood mononuclear cells (PBMCs) were thawed and stimulated with peptide pools spanning the full length of CFP-10 (10-kDa culture filtrate protein)/ESAT-6 (6-kDa early secretory antigenic target), antigens used in the QFT assay, for 18 hours (training and test cohorts) or *M.tb* lysate (H37Rv) for 12 hours (TB progressor cohort). Cells were stained and analyzed by flow cytometry (Tables E1–E3). *M.tb*-specific cells were defined by cytokine expression, detected either by intracellular cytokine staining (ICS; test and training cohorts), or gene expression from sorted single $CD69^+$ $CD137^+$ and/or $CD69^+$ $CD154^+$ T cells (TB progressor cohort). Different stimulation and detection protocols were used because data from the TB progressor cohort were from an unpublished study that aimed to perform single-cell T-cell receptor sequencing and measurement of selected transcripts. CD3 and HLA-DR expression were measured by flow cytometry, whereas *IFNG* and *TNF* mRNA expression in sorted single *M.tb*-specific cells were quantified by RNA sequencing using Illumina MiSeq, as previously described (36, 37). Detailed information about protocols used is provided in the online supplement.

Data Analysis

Responder definition. In the training and test cohorts, we identified responders as individuals with relative counts of IFN-γ^+ TNF^+ $CD3^+$ T cells in the antigen-

stimulated condition that were significantly higher ($P \leq 0.01$ by Fisher exact test) than in the unstimulated condition and had a fold change of antigen-specific T-cell frequencies of three or more. In the TB progressor cohort, only samples with 10 or more *IFNG* and *TNF* coexpressing cells were analyzed for HLA-DR expression (see below).

T-cell activation biomarker definition. In the training and TB progressor cohorts, we explored different calculations to define the T-cell activation biomarker: HLA-DR$^+$ T cells as a percentage of total IFN-γ^+ TNF$^+$ T cells, HLA-DR median fluorescent intensity (MFI) ratio (Equation 1) and ΔHLA-DR MFI (Equation 2, Figure 2D).

$$\text{HLA-DR MFI Ratio} = \frac{\text{HLA-DR MFI on IFN-}\gamma^+\ \text{TNF}^+\ \text{CD3}^+\ \text{cells}}{\text{HLA-DR MFI on total CD3}^+\text{cells}} \quad (1)$$

$$\Delta\text{HLA-DR MFI} = (\text{HLA-DR MFI on IFN-}\gamma^+\ \text{TNF}^+\ \text{CD3}^+\ \text{cells}) - (\text{HLA-DR MFI on total CD3}^+\ \text{cells}) \quad (2)$$

Statistical Analysis

Statistical analyses were performed using R and GraphPad Prism v7. We performed Wilcoxon signed-rank and Mann-Whitney *U* tests for paired and unpaired analyses, respectively. We corrected for multiple comparisons using the Bonferroni method as appropriate for the numbers of groups compared for each hypothesis/experiment. Biomarker selection was performed in the training cohort and was tested in a blinded fashion in the test cohort. Receiver operating characteristic (ROC) curve analysis and selection of the ΔHLA-DR MFI threshold were performed using the pROC package in R (version 1.15.3; https://web.expasy.org/pROC/) (38). We selected the ΔHLA-DR MFI threshold for the test cohort using persistent QFT+ and TB groups and then applied the same threshold to compare the performance of the biomarker between recent and persistent QFT+. The ΔHLA-DR MFI threshold for the TB progressor cohort was defined independently.

Results

To identify potential biomarkers of recent *M.tb* infection, we first evaluated a training cohort of adolescents with recent ($n = 30$) and persistent ($n = 30$) QFT+ responses (Figure 1A and Table 1) and compared T-cell polyfunctional, memory, and activation profiles between the two *M.tb* infection states. Results from these comprehensive immunological analyses, which inform immune responses and biological pathways associated with recent and remote infection, are presented elsewhere (39). Here we focused on developing a single candidate biomarker that distinguished between recent and persistent QFT+ individuals with the highest accuracy (39). With a simplified assay, we then tested the T-cell activation biomarker in a blinded test cohort of recent ($n = 25$) and persistent ($n = 25$) QFT+ adolescents and adults with TB disease ($n = 25$) (Figures 1A and 1B).

In the training cohort, we measured the expression of HLA-DR, IFN-γ, and TNF in live CD3$^+$ T cells upon PBMC stimulation with CFP-10/ESAT-6 (Figures 2A and E2A and E3A). IFN-γ concentrations measured by QFT and flow cytometry were strongly correlated (Figure E3B). Activation was measured on cytokine-producing T cells as HLA-DR MFI; thus, the contribution of nonspecific signal from the unstimulated control cannot be subtracted. We defined antigen-specific T cells as IFN-γ^+ TNF$^+$ CD3$^+$ cells, on the basis of previous observations that activation measured on CFP-10/ESAT-6–specific IFN-γ^+ TNF$^+$ could yield better diagnostic accuracy than IFN-γ^+ T cells (20). The IFN-γ^+ TNF$^+$ subset was also associated with lower responses than IFN-γ^+ CD3 T cells in unstimulated control subjects (Figure E3A).

QFT conversion was associated with an increase of CFP-10/ESAT-6–specific IFN-γ^+ TNF$^+$ and IFN-γ^+ CD3 T cells, which were detectable at comparable frequencies in recent and persistent QFT+ individuals (Figures 2B and E3C). Similar to the QFT assay, frequencies of CFP-10/ESAT-6–specific IFN-γ^+ TNF$^+$ CD3 T cells allowed discrimination between QFT− and recent QFT+, with an area under the ROC curve (AUROC) of 0.89 (95% confidence interval [CI], 0.79–0.99), but not recent and persistent QFT+ (AUROC, 0.54; 95% CI, 0.38–0.70, Figure 2C). Results for IFN-γ^+ CD3 T cells were similar (Figures E3C and E3D).

Analysis of T-cell activation in CFP-10/ESAT-6–stimulated samples (Figure 2D) was restricted to samples that passed our responder criteria (*see* Methods). ΔHLA-DR MFI (Figure 2E), proportions of HLA-DR$^+$ IFN-γ^+ TNF$^+$ CD3$^+$ T cells (Figure E4A), and HLA-DR MFI ratio (Figure E4B) were significantly higher in recent QFT+ individuals compared with persistent QFT+ individuals. All biomarkers yielded promising discriminatory potential with AUROCs of 0.91 (95% CI, 0.81–1.00) for ΔHLA-DR MFI (Figure 2F), 0.93 (95% CI, 0.84–1.00) for percentage HLA-DR, and 0.91 (95% CI, 0.80–1.00) for HLA-DR MFI ratio (Figure E4D). We also evaluated a published candidate biomarker for recent *M.tb* infection, namely proportions of TNF only–expressing effector

Table 1. Demographics

	Training Cohort		Test Cohort			TB Progressor Cohort	
	Persistent QFT+	Recent QFT+	Persistent QFT+	Recent QFT+	TB	Progressors	Nonprogressors
n	30	30	25	25	25	39	39
Sex, F	21	19	12	9	3	14	28
Age, median (IQR), yr	15 (14–16)	15 (14–16)	15 (14–16)	15 (14–16)	32 (21–42)	16 (15–17)	16 (14–17)
Ethnicity: colored, *n*	26	29	23	23	14	36	37
Ethnicity: Black, *n*	4	1	2	1	11	3	2
Ethnicity: Indian, *n*	0	0	0	1	0	0	0

Definition of abbreviations: IQR = interquartile range; QFT = QuantiFERON-TB Gold In-Tube; TB = tuberculosis.

(CD45RA−CCR7−) $CD4^+$ T cells (27), and found similar concentrations in recent and persistent QFT+ individuals, with poor diagnostic performance (AUROC, 0.61; 95% CI, 0.42–0.80; Figures E4C and E4D). We selected ΔHLA-DR MFI for blinded confirmation in the test cohort because it does not require the selection of a discrete HLA-DR–positive cell subset using a threshold or "gate," thus reducing operator bias, and also avoids the issue of negative MFI values that can result from flow cytometric compensation, which would affect calculation of the ratio-based biomarker.

Next, we evaluated the performance of the ΔHLA-DR MFI biomarker to distinguish between recent and persistent QFT+, recent QFT+ and TB, and persistent QFT+ and TB in the test cohorts. We developed a simplified version of the PBMC-ICS assay and an algorithm to provide a framework for interpreting test results as a biomarker for potential *M.tb* infection states (Table 2). *M.tb* infection was defined as a positive CFP-10/ESAT-6–specific IFN-γ^+ TNF^+ $CD3^+$ T-cell response. In those with *M.tb* infection, individuals were then classified as those with persistent QFT+ and those with recent QFT+ or TB on the basis of their ΔHLA-DR MFI.

CFP-10/ESAT-6–specific IFN-γ^+ TNF^+ $CD3^+$ T cells induced by recent QFT conversion in the test cohort were detected at

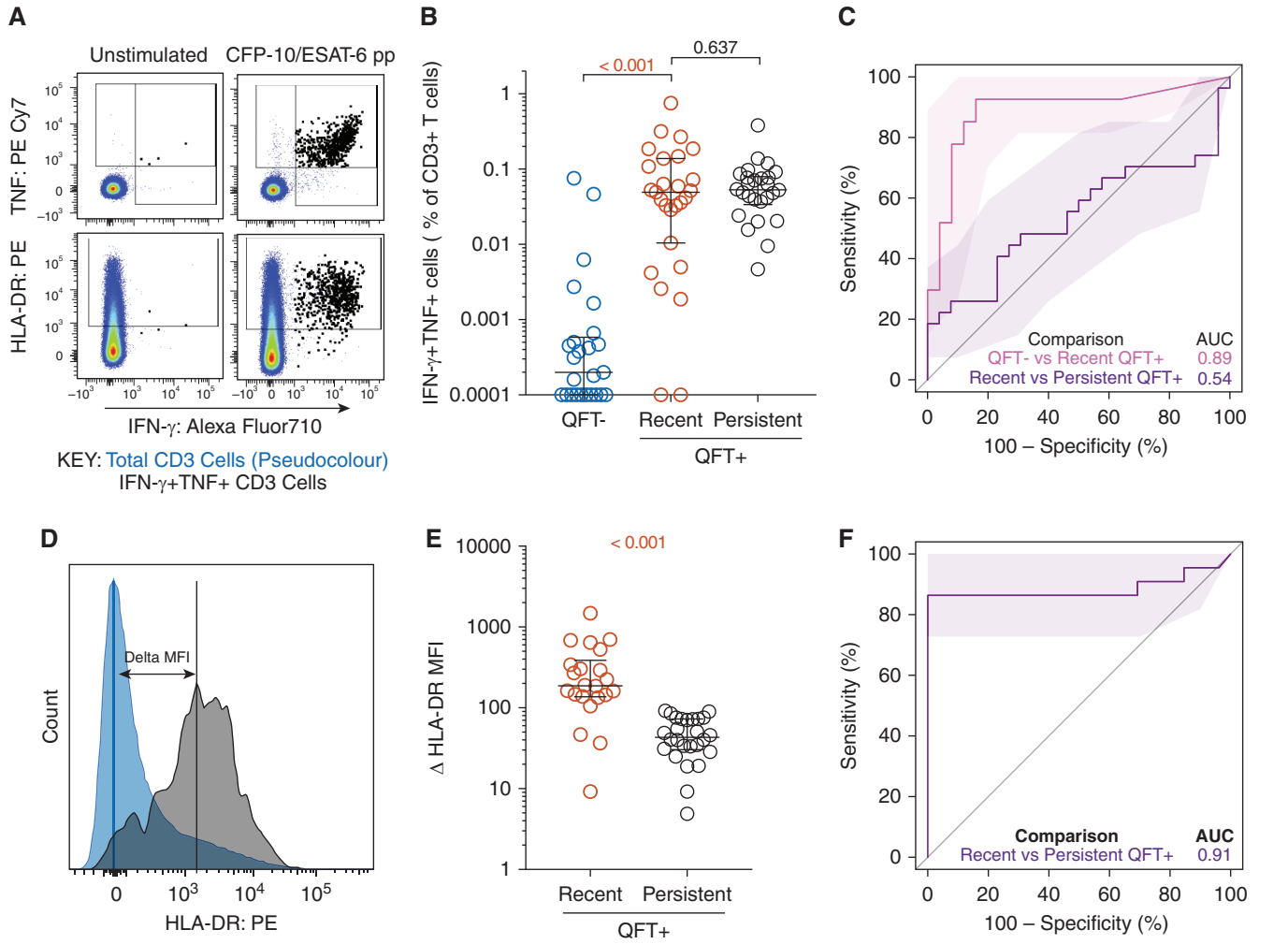

Figure 2. Recent QuantiFERON-TB Gold (QFT)+ conversion is associated with higher T-cell activation than persistent QFT+ results. (*A*) Representative flow cytometry plots depicting IFN-γ, TNF, and HLA-DR expression in $CD3^+$ T cells. IFN-γ^+ TNF^+ and total $CD3^+$ T cells are depicted by black and pseudocolor dots, respectively. (*B*) Frequencies of background subtracted CFP-10/ESAT-6–specific IFN-γ^+ TNF^+ $CD3^+$ T cells detected before (QFT−; blue; $n = 25$) and after (recent QFT+; red; $n = 27$) infection, and in persistent QFT+ (black; $n = 26$) individuals in the training cohort. (*C*) Area under the receiver operating characteristic curve (AUROC) showing performance of CFP-10/ESAT-6–specific IFN-γ^+ TNF^+ $CD3^+$ T cells to discriminate between QFT− and recent QFT+ individuals and between recent and persistent QFT+ individuals. (*D*) Representative flow cytometry histogram overlay of HLA-DR expression levels by IFN-γ^+ TNF^+ $CD3^+$ T cells (black) and total $CD3^+$ T cells (blue) and how ΔHLA-DR median fluorescent intensity (MFI) is calculated. (*E*) ΔHLA-DR MFI in recent ($n = 22$) and persistent ($n = 26$) QFT+ responders in the training cohort. (*F*) Performance of ΔHLA-DR MFI to discriminate between recent and persistent QFT+ individuals. *P* values were calculated using the Wilcoxon signed-rank test for paired (QFT− vs. recent QFT+) or Mann-Whitney *U* test for unpaired (recent vs. persistent QFT+) comparisons. Where appropriate, we corrected for multiple comparison as described in the Methods. *P* values highlighted in red are considered significant. Shaded areas in AUROC plots depict 95% confidence intervals. Values <0.0001 were set to 0.0001 to allow display on a logarithmic scale. AUC = area under the curve; pp = peptide pool.

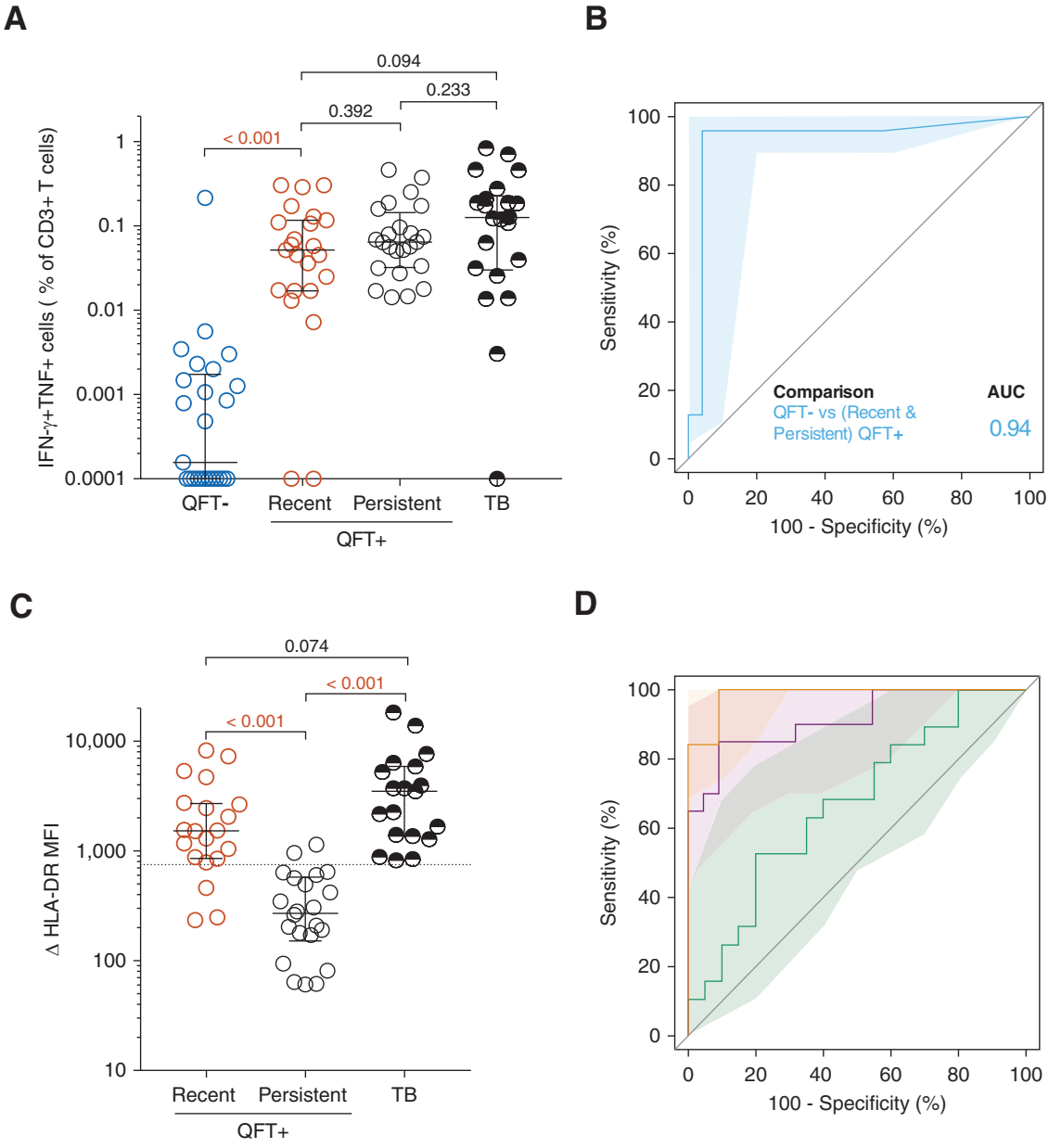

ΔHLA-DR MFI Threshold = 734	Specificity (%)	Sensitivity (%)	AUC
Recent vs Persistent QFT+	85.00	90.91	0.91
Recent QFT+ vs. TB	15.00	100.00	0.67
Persistent QFT+ vs. TB	90.91	100.00	0.99

Figure 3. T-cell activation biomarker can distinguish between recent and persistent QuantiFERON-TB Gold (QFT)+ individuals as well as between persistent QFT+ individuals and individuals with tuberculosis (TB). (*A*) Frequencies of background subtracted CFP-10/ESAT-6–specific IFN-γ^+ TNF^+ $CD3^+$ T cells detected before (QFT−; blue; $n = 25$) and after (recent QFT+; red; $n = 23$) QFT conversion, during persistent QFT+ (black open symbols, $n = 24$), and in patients with TB (black half-filled symbols; $n = 22$) in the test cohort. (*B*) Area under the receiver operating characteristic curve (AUROC) analysis illustrating the performance of CFP-10/ESAT-6–specific IFN-γ^+ TNF^+ $CD3^+$ T cells to distinguish between samples taken before (QFT−) and after QFT conversion (recent or persistent QFT+ combined). (*C*) ΔHLA-DR median fluorescent intensity (MFI) in responders with recent QFT+ conversion ($n = 20$), persistent QFT+ results ($n = 22$), or TB ($n = 19$). (*D*) AUROC analysis depicting the performance of ΔHLA-DR MFI to discriminate between recent and persistent QFT+, between recent QFT+ and TB and between persistent QFT+ and TB. *P* values were calculated using the Wilcoxon signed-rank test for paired (QFT− vs. recent QFT+) or the Mann-Whitney *U* test for unpaired (all other) comparisons. Where appropriate, we corrected for multiple comparisons as described in the Methods. *P* values highlighted in red are considered significant. Shaded areas in AUROC plots depict 95% confidence intervals. Values <0.0001 were set to 0.0001 to allow display on a logarithmic scale. AUC = area under the curve.

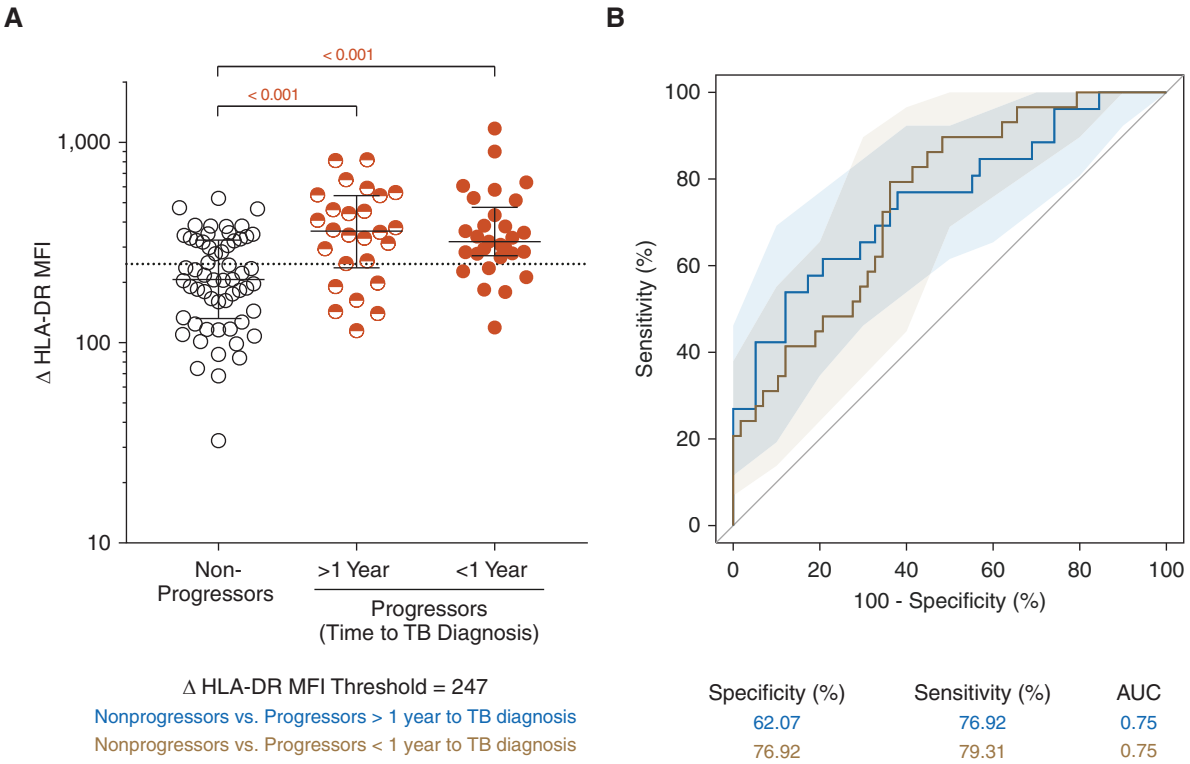

Figure 4. Mycobacteria-specific T cells in tuberculosis (TB) progressors are more activated than those in nonprogressors. (*A*) ΔHLA-DR median fluorescent intensity (MFI) on *Mycobacterium tuberculosis* lysate–responsive T cells coexpressing IFNG and TNF mRNA transcripts in nonprogressors ($n = 58$ longitudinal data points from 34 participants) and progressors (in samples collected >1 yr before TB diagnosis [>1 yr, $n = 26$ longitudinal data points from 19 participants] or in samples collected within 1 yr of tuberculosis diagnosis [<1 yr, $n = 29$ longitudinal data points from 22 participants]). *P* values were computed by Mann-Whitney *U* test and were corrected for two comparisons as described in the Methods. (*B*) Area under the receiver operating characteristic curve depicting the performance of ΔHLA-DR MFI to discriminate between nonprogressors and progressors in samples collected >1 year before TB or within 1 year of TB diagnosis. AUC = area under the curve.

similar frequencies to those with persistent QFT+ reactivity or with TB (Figure 3A). Importantly, we were able to discriminate QFT– individuals from those with recent or persistent QFT+ with an AUROC of 0.94 (95% CI, 0.87–1.00; Figure 3B), suggesting that this simple flow cytometry–based assay yields equivalent diagnostic information to QFT.

ΔHLA-DR MFI was significantly higher in patients with recent QFT+ and TB compared with persistent QFT+ individuals (Figure 3C), however, individuals with recent QFT+ or TB disease showed similar ΔHLA-DR MFI. Using a ΔHLA-DR MFI cutoff of 734, we were able to discriminate between recent and persistent QFT+ with a specificity, sensitivity, and AUROC of 90%, 85%, and 0.91 (95% CI, 0.83–1.00), respectively. We also observed excellent discrimination between persistent QFT+

Table 2. Interpretation of the T-Cell Activation Biomarker Test Results

M.tb-Specific Response Definition			Responder Definition	Recent *M.tb* Infection or TB Definition	
IFN-γ^+ TNF$^+$ T Cells ESAT-6/CFP-10 vs. UNS (Fisher Exact Test)	IFN-γ^+ TNF$^+$ T Cells PHA vs. UNS (Fisher Exact Test)	Interpretation	IFN-γ^+ TNF$^+$ T Cells ESAT-6/CFP-10 over UNS (Ratio)	Δ HLA-DR MFI (IFN-γ^+ TNF$^+$) – (Total T Cells)	Interpretation
$P \leq 0.01$	Any	*M.tb* infection likely	Threefold or greater	– (<734)	Persistent *M.tb* infection likely
				+ (≥734)	Recent *M.tb* infection or TB likely
			Less than threefold	N/A	N/A
$P > 0.01$	$P < 0.01$	*M.tb* infection unlikely	N/A	N/A	N/A
$P > 0.01$	$P > 0.01$	Indeterminate	N/A	N/A	N/A

Definition of abbreviations: MFI = median fluorescent intensity; *M.tb* = *Mycobacterium tuberculosis*; N/A = not applicable; PHA = phytohemagglutinin positive control; TB = tuberculosis; UNS = unstimulated control.

and TB, with high specificity (91%), sensitivity (100%), and AUROC (0.99; 95% CI, 0.96–1.00). ΔHLA-DR MFI could not accurately discriminate between recent QFT+ and TB (AUC, 0.67; 95% CI, 0.50–0.84; Figures 3C and 3D). Table E5 summarizes the outcomes of the diagnostic algorithm described in Table 2 when applied to the test cohort.

Our group previously reported a six-gene blood transcriptomic signature, RISK6, that can identify QFT+ and/or TST+ individuals who are at risk of progressing to TB (40). We therefore tested the ability of the ΔHLA-DR MFI biomarker to distinguish between progressors ($n = 34$) and nonprogressors ($n = 34$) in a longitudinal cohort of healthy QFT+ and/or TST+ adolescents (Figure 1C). Levels of ΔHLA-DR MFI were significantly higher in progressors up to 2 years before TB diagnosis compared with nonprogressors (AUROC, 0.75; 95% CI, 0.63–0.87; Figure 4). These results were consistent with the performance of RISK6 and suggest that the ΔHLA-DR MFI biomarker may also be useful for identifying individuals at risk of disease progression.

Discussion

We describe a simple biomarker, ΔHLA-DR MFI, that measures *M.tb*-specific T-cell frequencies and their activation levels, can distinguish QFT− (presumably uninfected) individuals from QFT+ (presumably infected) individuals, and, among the latter, can discriminate between those with recent QFT conversion, disease progression, or active TB and persistent QFT+ nonprogressors. This is a significant advance over current *M.tb* immunodiagnostics (TST and IGRA), which are unable to distinguish between different stages of *M.tb* infection and identify individuals at risk of progression to disease. Consistent with this limitation, we demonstrated that measuring *M.tb*-specific T-cell functions by flow cytometry can distinguish between QFT− and QFT+ individuals but not between QFT+ individuals and individuals with TB or recent and remote QFT conversion. Because individuals with recent QFT conversion and high risk for disease progression would benefit from targeted TPT, this biomarker offers an opportunity to identify a group of asymptomatic individuals at particularly high risk of TB, whereas those with persistent QFT+ test and low risk of progression would derive less benefit from TPT. This is of particular importance in high incidence settings, where a large proportion of the population is already *M.tb* infected and identification of individuals at high risk of TB progression is challenging. Our findings build on previous studies that have shown that measurement of *M.tb*-specific T-cell activation by flow cytometry has promising diagnostic potential to distinguish *M.tb* infection from TB disease, regardless of HIV status, as well as to monitor treatment response (16–20).

The immunological speculation that underpins our observations is that peripheral blood T-cell activation is driven by *in vivo* exposure to *M.tb* antigens and that these concentrations peak during primary infection and then drop in most people with remote infection, likely because of containment of bacterial replication. However, in people who progress toward active TB, *in vivo M.tb* antigen exposure is likely high even before the onset of clinical symptoms. Our measurements of T-cell activation during the different stages of infection provide evidence that supports this hypothesis. Specifically, we showed that a recent *M.tb* exposure (initial peak in *M.tb* burden) as well as a high bacterial load in progressors (before symptom onset) are associated with much higher levels of T-cell activation than those observed during presumed containment of *M.tb* replication (persistent QFT+ and nonprogressors). Furthermore, our findings suggest that remote infection is associated with low and stable amounts of *M.tb*-specific T-cell activation, consistent with control or perhaps even clearance of *M.tb*. This supports the hypothesis promulgated recently by Behr and colleagues that TB has a short incubation period (<2 yr) and that *M.tb*-specific T-cell responses detected with IGRAs in most individuals with remote *M.tb* exposure represent immunological memory, not ongoing *M.tb* replication (13). Indeed, a minority of individuals with remote *M.tb* exposure may harbor replicating *M.tb* and are at high risk of TB progression, as suggested by detection of high T-cell activation in progressors compared with nonprogressors. Therefore, our biomarker has utility to distinguish the majority of individuals with persistent QFT+ results and low risk of TB progression, who would be spared TPT, from the minority who harbor replicating *M.tb*, are at high risk of progression, and would benefit from further clinical investigation and TPT. Our inability to distinguish between recent QFT conversion and disease using the ΔHLA-DR MFI biomarker further supports the utility of T-cell activation as an indirect marker for *M.tb* antigen load, which is supposedly high in both these TB stages. To the best of our knowledge, whether TPT-mediated reduction of bacterial load would result in decreased HLA-DR expression on *M.tb*-specific T cells has not yet been shown; however, successful TB treatment is associated with a decrease in T-cell activation (16, 19, 20). We acknowledge that antibiotic regimens used for TPT and full course of treatment may differ and may have distinct impact on T-cell activation kinetics, and this should be addressed in future studies.

The strengths of our study include unique and well-characterized clinical cohorts, blinded verification of our findings in a test cohort, and translation of biological observations made with complex technology to a simple test that can be used for further validation.

Limitations of our study include convenience selection of participants on the basis of sample availability, which could have introduced a bias that would have been avoided by random selection. However, the finding that biomarker performance was reproduced in two cohorts (training and test) suggests that the effects of this bias are not significant. We were unable to formally validate our ΔHLA-DR MFI biomarker because the test, training, and progressor cohorts were selected from the same epidemiological study and were thus not completely independent (10). The control group of individuals with newly diagnosed TB included adults aged 21–42 years; therefore, we cannot exclude age-related differences. Furthermore, experimental protocols, stimulants, and reagents used to detect T-cell activation were different between cohorts, thus preventing us from using the same assay and defining a ΔHLA-DR MFI threshold that could be uniformly applied to all three cohorts. However, the consistency of results points toward robustness of the biomarker. Our cohort design did not include *M.tb*-uninfected individuals from low TB burden countries, nor do we have access to samples from such individuals; thus, we were unable to test the false positivity rate of our proposed biomarker in *M.tb*-unexposed individuals. We did, however, test the biomarker in

individuals before QFT conversion and reported that only 1 of 25 QFT− participants was classified as likely infected.

The candidate biomarker proposed by Halliday and colleagues (TNF only–expressing T effector cells) (27) did not discriminate between recent and remote QFT conversion in our study. Compared with the original biomarker description, we used a different flow cytometry panel that lacked CD127, and therefore the cell subset definition was not identical.

Finally, experimental protocols described here were performed on cryopreserved PBMCs, a sample type that is not be ideal for clinical purposes but was the only one available for this retrospective study. Although this is not a point-of-care assay, we have shown that it can be adapted to a whole blood assay (such as QFT) with a simple four-color flow cytometry panel as readout (20), using basic technology that is widespread even in resource-limited settings and is suitable for automated analysis. It will be necessary to validate this simplified assay in large prospective field studies to estimate its true performance characteristics. Preferred performance characteristics of a test that can differentiate between recent and remote *M.tb* infection are currently not defined and would need to be developed to provide benchmarks for test performance. A validation is currently underway in a prospective South African pediatric cohort of household contacts of patients with TB.

In summary, we describe a blood-based T-cell biomarker, ΔHLA-DR MFI, measured with a simple flow cytometry assay, that can be used to identify individuals with recent QFT conversion and those with TB progression as well as clinical disease. Upon further validation, the ΔHLA-DR MFI biomarker has the potential to stratify individuals along the *M.tb* spectrum and could be considered as a screening test to identify individuals at high risk of TB for further evaluation. If interpreted in association with clinical features and microbiological tests, this biomarker could identify individuals with TB who would benefit from standard treatment, those at high risk who should receive TPT, and those who would not currently benefit from TPT but may be retested in the future. ■

Author disclosures are available with the text of this article at www.atsjournals.org.

Acknowledgment: The authors thank the study participants and their families; the Cape Winelands East district communities, the Department of Education and the Department of Health; the South African Tuberculosis Vaccine Initiative (SATVI) clinical and laboratory teams; Thomas Hawn and Jason Andrews for valuable input on the study design.

ACS Study Team: Hassan Mahomed, Willem A. Hanekom, Fazlin Kafaar, Leslie Workman, Humphrey Mulenga, Rodney Ehrlich, Mzwandile Erasmus, Deborah Abrahams, Anthony Hawkridge, E. Jane Hughes, Sizulu Moyo, Sebastian Gelderbloem, Michele Tameris, Hennie Geldenhuys, and Gregory Hussey.

References

1. World Health Organization. Global tuberculosis report 2020 [accessed 2020 Oct 15]. Available from: https://www.who.int/tb/publications/global_report/en/.
2. World Health Organization. WHO consolidated guidelines on tuberculosis: tuberculosis preventive treatment. 2020 [accessed 2020 Jun 18]. Available from: https://www.who.int/publications-detail/who-consolidated-guidelines-on-tuberculosis-module-1-prevention-tuberculosis-preventive-treatment.
3. Erkens CGM, Slump E, Verhagen M, Schimmel H, Cobelens F, van den Hof S. Risk of developing tuberculosis disease among persons diagnosed with latent tuberculosis infection in the Netherlands. *Eur Respir J* 2016;48:1420–1428.
4. Reichler MR, Khan A, Sterling TR, Zhao H, Chen B, Yuan Y, *et al*.; Tuberculosis Epidemiologic Studies Consortium Task Order 2 Team. Risk factors for tuberculosis and effect of preventive therapy among close contacts of persons with infectious tuberculosis. *Clin Infect Dis* 2020;70:1562–1572.
5. Cohen A, Mathiasen VD, Schön T, Wejse C. The global prevalence of latent tuberculosis: a systematic review and meta-analysis. *Eur Respir J* 2019;54:1900655.
6. Mathema B, Andrews JR, Cohen T, Borgdorff MW, Behr M, Glynn JR, *et al*. Drivers of tuberculosis transmission. *J Infect Dis* 2017;216:S644–S653.
7. Churchyard G, Kim P, Shah NS, Rustomjee R, Gandhi N, Mathema B, *et al*. What we know about tuberculosis transmission: an overview. *J Infect Dis* 2017;216:S629–S635.
8. Wiker HG, Mustafa T, Bjune GA, Harboe M. Evidence for waning of latency in a cohort study of tuberculosis. *BMC Infect Dis* 2010;10:37.
9. Behr MA, Edelstein PH, Ramakrishnan L. Revisiting the timetable of tuberculosis. *BMJ* 2018;362:k2738.
10. Machingaidze S, Verver S, Mulenga H, Abrahams D-A, Hatherill M, Hanekom W, *et al*. Predictive value of recent QuantiFERON conversion for tuberculosis disease in adolescents. *Am J Respir Crit Care Med* 2012;186:1051–1056.
11. Andrews JR, Noubary F, Walensky RP, Cerda R, Losina E, Horsburgh CR. Risk of progression to active tuberculosis following reinfection with *Mycobacterium tuberculosis*. *Clin Infect Dis* 2012;54:784–791.
12. Cadena AM, Hopkins FF, Maiello P, Carey AF, Wong EA, Martin CJ, *et al*. Concurrent infection with *Mycobacterium tuberculosis* confers robust protection against secondary infection in macaques. *PLoS Pathog* 2018;14:e1007305.
13. Behr MA, Edelstein PH, Ramakrishnan L. Is *Mycobacterium tuberculosis* infection life long? *BMJ* 2019;367:l5770.
14. World Health Organization. FIND. Consensus Meeting Report: Development of a Target Product Profile (TPP) and a framework for evaluation for a test for predicting progression from tuberculosis infection to active disease. 2017 [accessed 2020 Jun 18]. Available from: https://apps.who.int/iris/handle/10665/259176.
15. STOP TB Partnership. Global Plan to End TB: 2018-2022. [accessed 2020 Jun 18]. Available from: http://www.stoptb.org/assets/documents/global/plan/GPR_2018-2022_Digital.pdf.
16. Riou C, Du Bruyn E, Ruzive S, Goliath RT, Lindestam Arlehamn CS, Sette A, *et al*. Disease extent and anti-tubercular treatment response correlates with *Mycobacterium tuberculosis*-specific CD4 T-cell phenotype regardless of HIV-1 status. *Clin Transl Immunology* 2020;9:e1176.
17. Riou C, Berkowitz N, Goliath R, Burgers WA, Wilkinson RJ. Analysis of the phenotype of *Mycobacterium tuberculosis*-specific CD4+ T cells to discriminate latent from active tuberculosis in HIV-uninfected and HIV-infected individuals. *Front Immunol* 2017;8:968.
18. Wilkinson KA, Oni T, Gideon HP, Goliath R, Wilkinson RJ, Riou C. Activation profile of *Mycobacterium tuberculosis*-specific CD4(+) T cells reflects disease activity irrespective of HIV status. *Am J Respir Crit Care Med* 2016;193:1307–1310.
19. Adekambi T, Ibegbu CC, Cagle S, Kalokhe AS, Wang YF, Hu Y, *et al*. Biomarkers on patient T cells diagnose active tuberculosis and monitor treatment response. *J Clin Invest* 2015;125:1827–1838.
20. Musvosvi M, Duffy D, Filander E, Africa H, Mabwe S, Jaxa L, *et al*. T-cell biomarkers for diagnosis of tuberculosis: candidate evaluation by a simple whole blood assay for clinical translation. *Eur Respir J* 2018;51:1800153.
21. Portevin D, Moukambi F, Clowes P, Bauer A, Chachage M, Ntinginya NE, *et al*. Assessment of the novel T-cell activation marker-tuberculosis assay for diagnosis of active tuberculosis in children: a prospective proof-of-concept study. *Lancet Infect Dis* 2014;14:931–938.

22. Petruccioli E, Petrone L, Vanini V, Cuzzi G, Navarra A, Gualano G, *et al*. Assessment of CD27 expression as a tool for active and latent tuberculosis diagnosis. *J Infect* 2015;71:526–533.
23. Rozot V, Patrizia A, Vigano S, Mazza-Stalder J, Idrizi E, Day CL, *et al*. Combined use of *Mycobacterium tuberculosis*-specific CD4 and CD8 T-cell responses is a powerful diagnostic tool of active tuberculosis. *Clin Infect Dis* 2015;60:432–437.
24. Harari A, Rozot V, Bellutti Enders F, Perreau M, Stalder JM, Nicod LP, *et al*. Dominant TNF-α+ *Mycobacterium tuberculosis*-specific CD4+ T cell responses discriminate between latent infection and active disease. *Nat Med* 2011;17:372–376.
25. Andersen P, Doherty TM, Pai M, Weldingh K. The prognosis of latent tuberculosis: can disease be predicted? *Trends Mol Med* 2007;13:175–182.
26. Scriba TJ, Penn-Nicholson A, Shankar S, Hraha T, Thompson EG, Sterling D, *et al*.; other members of the ACS cohort study team. Sequential inflammatory processes define human progression from *M. tuberculosis* infection to tuberculosis disease. *PLoS Pathog* 2017;13:e1006687.
27. Halliday A, Whitworth H, Kottoor SH, Niazi U, Menzies S, Kunst H, *et al*. Stratification of latent *Mycobacterium tuberculosis* infection by cellular immune profiling. *J Infect Dis* 2017;215:1480–1487.
28. Mpande CAM. Memory, activation and functional profiles of *Mycobacterium tuberculosis*-specific CD4 T cells in recent QFT converters. Presented at the 5th Global Forum on TB Vaccines. February 21, 2018, New Delhi, India.
29. Mpande CAM. *Mycobacterium tuberculosis* (*M.tb*) -specific CD4 T cell memory repertoire in recently and remotely *M.tb*-infected Individuals. Presented at the 33rd Congress of the International Society for Advancement of Cytometry. April 29, 2018, Prague, Czech Republic.
30. Mpande CAM. Investigating the *Mycobacterium tuberculosis*-specific CD4 T cell memory profiles: a comparison of immune responses between primary and established *M.tb* infection. Presented at the 17th International Congress of Immunology. October 22, 2019, Beijing, China.
31. Musvosvi M. Determining the role of TB-specific TCR clonotypes in disease progression: the Collaboration for TB Vaccine Discovery (CTVD) Presented at the 5th Annual Meeting. June 19, 2019, Seattle, WA.
32. Nemes E. Antigen-specific T cell activation distinguishes between recent and remote tuberculosis infection. Presented at the 51st Union World Conference on Lung Health (Virtual). October 22, 2020.
33. Nemes E. *Mycobacterium tuberculosis*-specific CD4 T cell activation distinguishes primary from remote, established infection. Presented at the Keystone Symposia on Tuberculosis: Immunity and Immune Evasion. January 20, 2020, Santa Fe, NM.
34. Nemes E, Rozot V, Geldenhuys H, Bilek N, Mabwe S, Abrahams D, *et al*.; C-040-404 Study Team and the Adolescent Cohort Study Team. Optimization and Interpretation of Serial QuantiFERON testing to measure acquisition of *Mycobacterium tuberculosis* infection. *Am J Respir Crit Care Med* 2017;196:638–648.
35. Zak DE, Penn-Nicholson A, Scriba TJ, Thompson E, Suliman S, Amon LM, *et al*.; ACS and GC6-74 cohort study groups. A blood RNA signature for tuberculosis disease risk: a prospective cohort study. *Lancet* 2016;387:2312–2322.
36. Han A, Glanville J, Hansmann L, Davis MM. Linking T-cell receptor sequence to functional phenotype at the single-cell level. *Nat Biotechnol* 2014;32:684–692.
37. Glanville J, Huang H, Nau A, Hatton O, Wagar LE, Rubelt F, *et al*. Identifying specificity groups in the T cell receptor repertoire. *Nature* 2017;547:94–98.
38. Robin X, Turck N, Hainard A, Tiberti N, Lisacek F, Sanchez J-C, *et al*. pROC: an open-source package for R and S+ to analyze and compare ROC curves. *BMC Bioinformatics* 2011;12:77.
39. Mpande CAM, Rozot V, Mosito B, Musvosvi M, Dintwe OB, Bilek N, *et al*.; Immune profiling of *Mycobacterium tuberculosis*-specific T cells in recent and remote infection. *Ebiomedicine* 2021;64:103233.
40. Penn-Nicholson A, Mbandi SK, Thompson E, Mendelsohn SC, Suliman S, Chegou NN, *et al*.; Adolescent Cohort Study team; GC6-74 Consortium; SATVI Clinical and Laboratory Team; ScreenTB Consortium; AE-TBC Consortium; RePORT Brazil Team; Peruvian Household Contacts Cohort Team; CAPRISA IMPRESS team. RISK6, a 6-gene transcriptomic signature of TB disease risk, diagnosis and treatment response. *Sci Rep* 2020;10:8629.